

Instytut Chemii Organicznej
Polskiej Akademii Nauk

**Kataliza witaminą B₁₂ –
generowanie rodników alkilowych i acylowych**

mgr Aleksandra Potrząsaj

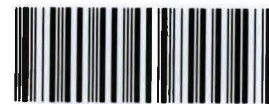
Monotematyczny cykl publikacji wraz z komentarzem przedstawiony
Radzie Naukowej Instytutu Chemii Organicznej Polskiej Akademii Nauk
w celu uzyskania stopnia doktora

A-21-6
K-g-172
K-C-125
K-g-153

Promotor: prof. dr hab. Dorota Gryko

Biblioteka Instytutu Chemii Organicznej PAN

O-B.436/22



10000000109960



Warszawa 2022

Praca doktorska wykonana w ramach projektu:



„Bioinspired catalysis for sustainable light-induced processes”

Realizowanego w ramach programu **TEAM**

Fundacji na rzecz Nauki Polskiej

Numer grantu: POIR.04.04.00-00-4232/17-00

W tym miejscu chciałabym serdecznie podziękować wszystkim osobom, które pośrednio lub bezpośrednio przyczyniły się do powstania niniejszej rozprawy doktorskiej, w szczególności:

Prof. Dorocie Gryko, za ogromną cierpliwość, cenne porady merytoryczne, wiarę we mnie i w moje możliwości. Dziękuję za okazane wsparcie (również te w słodkiej postaci) oraz zaufanie na każdym etapie mojej pracy naukowej.

Dr Maciejowi Giedykowi, za wprowadzenie w świat chemii witaminy B₁₂, nieocenioną pomoc w trakcie realizacji projektów oraz za ogromną motywację do działania.

Dr Michałowi Ociepie, za współpracę w projektach.

Byłym i obecnym członkom najwspanialszego i najlepszego zespołu na świecie, w szczególności Oli W., Dżoanie, Orłowi, KRJ, Lolo, Agnieszce, Uszce, Maksowi, Klaudii, Kitty, Joe, Joao, Martynie, Łukaszowi, Krzyškowi, Kubie, Krzyškowi G., Tomkowi, Wojtkowi, Kacprowi oraz Keithowi.

Laseczkom XV, za wspólnie spędzony czas przy lampce wina i rozmowach o wszystkim i o niczym.

Maćkowi, za bycie najwspanialszym Przyjacielem i Narzeczonym na świecie. Dziękuję Ci za wsparcie w trudnych chwilach i za to, że zawsze mogę na Ciebie liczyć !

Rodzicom i siostrze, za wsparcie i wiarę w moje możliwości.

SPIS TREŚCI

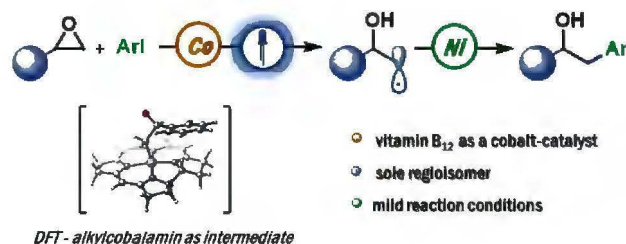
1. SPIS PUBLIKACJI WCHODZĄCYCH W SKŁAD ROZPRAWY DOKTORSKIEJ	9
2. SPIS WYSTĄPIEŃ KONFERENCYJNYCH.....	11
3. PRZEWODNIK PO ROZPRAWIE DOKTORSKIEJ.....	13
3.1 Cel i założenia pracy.....	13
3.2 Wstęp literaturowy	17
3.2.1 Witamina B ₁₂ : budowa i właściwości katalityczne	18
3.2.2 Katalizowane witaminą B ₁₂ reakcje z udziałem rodnika alkilowego.....	20
3.2.2.1 Dehalogenowanie	20
3.2.2.2 Dimeryzacja.....	24
3.2.2.3 Reakcje addycji do wiązań wielokrotnych.....	27
3.2.2.4 Inne reakcje	35
3.2.3 Generowanie rodników acylowych katalizowane witaminą B ₁₂	39
3.3 Podsumowanie.....	42
4. BADANIA WŁASNE	43
4.1 Regioselektywne otwieranie epoksydów katalizowane witaminą B ₁₂	43
4.2 Regioselektywna metoda otwierania oksetanów w obecności pochodnej witaminy B ₁₂	48
4.3 Generowanie rodnika acylowego i alkilowego z jednego reagenta.....	52
4.4 Podsumowanie.....	57
4.5 Bibliografia.....	58
5. STRESZCZENIE W JĘZYKU POLSKIM.....	63
6. STRESZCZENIE W JĘZYKU ANGIELSKIM / ABSTRACT IN ENGLISH.....	64
7. PUBLIKACJE ORYGINALNE.....	65
8. OŚWIADCZENIA AUTORÓW PUBLIKACJI.....	378

1. SPIS PUBLIKACJI WCHODZĄCYCH W SKŁAD ROZPRAWY DOKTORSKIEJ

Publikacje oryginalne:

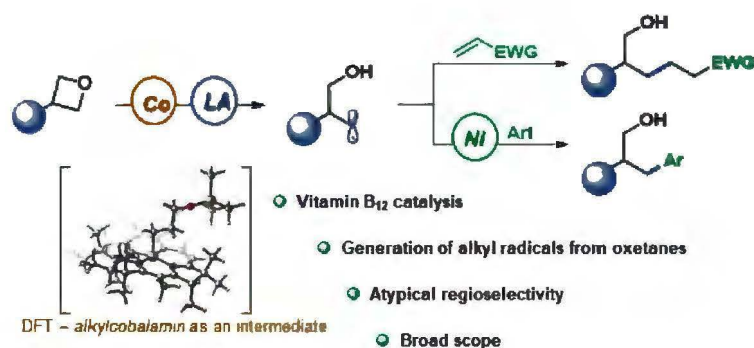
1. **A. Potrząsaj**, M. Musiejuk, W. Chaładaj, M. Giedyk, D. Gryko, *J. Am. Chem. Soc.*, **2021**, 143, 25, 9368–9376

Cobalt Catalyst Determines Regioselectivity in Ring Opening of Epoxides with Aryl Halides



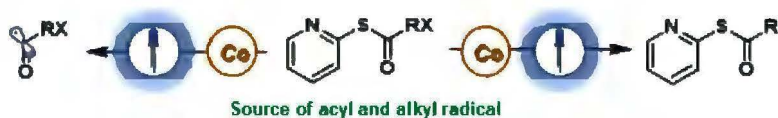
2. **A. Potrząsaj**, M. Ociepa, W. Chaładaj, D. Gryko, *Org. Lett.*, **2022**, 10.1021/acs.orglett.2c00355

Bioinspired Cobalt-Catalysis Enables Generation of Nucleophilic Radicals from Oxetanes



3. **A. Potrząsaj**, M. Ociepa, O. Baka, G. Spólnik, D. Gryko, *Eur. J. Org. Chem.*, **2020**, 1567–1571

Vitamin B₁₂ Enables Consecutive Generation of Acyl and Alkyl Radicals from One Reagent



2. SPIS WYSTĄPIEŃ KONFERENCYJNYCH

Wyniki przedstawione w niniejszej pracy zostały zaprezentowane na konferencji:

1. Exploratory Photochemistry: Light Creates Structure; Halle, Niemcy, 2021:
Cobalt-catalysis enables photogeneration of alkyl radicals from strained molecules
prezentacja posterowa

3. PRZEWODNIK PO ROZPRAWIE DOKTORSKIEJ

3.1 Cel i założenia pracy

Kataliza metalami przejściowymi jest potężnym narzędziem w chemii organicznej. Na przestrzeni ostatniej dekady umożliwiła ona syntezę wielu ważnych produktów w sposób wydajny i selektywny. Duża liczba reakcji tworzenia wiązań C-C i C-heteroatom wymaga wykorzystania katalizy metalami przejściowymi bloku 4d i 5d układu okresowego. Niestety, są to rozwiązania bardzo kosztowne i nieprzyjazne środowisku. W związku z tym, stale poszukuje się nowych rozwiązań. Alternatywą mogą być katalizatory oparte na naturalnych, a co za tym idzie tańszych, kompleksach metali przejściowych bloku 3d. W rezultacie zastosowanie ich w procesach tworzenia nowych wiązań C-C jest coraz bardziej pożądane. Wśród nich można wyróżnić, m.in. te, zawierające w swojej budowie jon kobaltu.

Za początek ery katalizy kobaltem uważa się pionierskie odkrycie Kharasha i Fieldsa, którzy w 1941 roku w obecności 2 mol% chlorku kobaltu(II) przeprowadzili pierwszą reakcję dimeryzacji bromku fenylo-magnezowego. Kolejne siedemdziesiąt lat badań sprawiło, że katalizatory kobaltowe stały się jednymi z częściej wykorzystywanych w reakcjach homo- a później również heterosprzęgania.

Katalizatorem kobaltowym, który zasługuje na wyróżnienie, ze względu na jego znaczenie biologiczne jak i chemiczne, jest witamina B₁₂. Jest to wysoce sfunekjonalizowany związek organiczny, zawierający wewnątrz pierścienia korynowego jon kobaltu na +3 stopniu utlenienia. W wyniku redukcji przyjmuje formy Co(II) oraz Co(I), mające charakter odpowiednio rodnikowy i nukleofilowy. Kompleks kobaltu na +1 stopniu utlenienia reaguje z elektrofilami tworząc alkilokobalaminy. Związki te, na drodze termo- bądź fotolizy ulegają homolitycznemu rozpadowi tworząc rodniki alkilowe. Jeszcze do niedawna, najczęściej stosowanymi w tym celu elektrofilami były halogenki alkilowe.

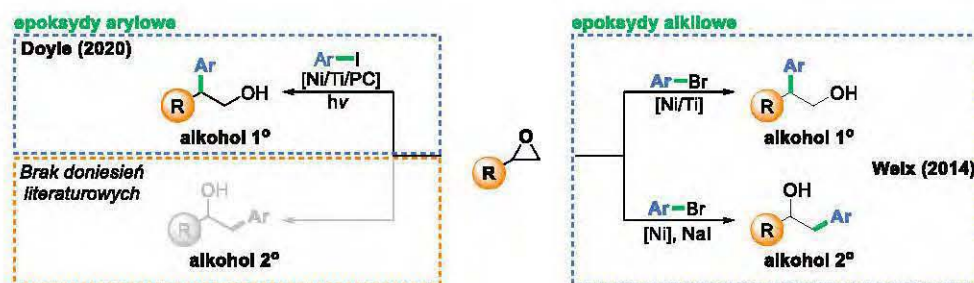
Celem mojej pracy było rozszerzenie grupy prekursorów rodników użytecznych w katalizie witaminą B₁₂, które stanowiłyby dopelnienie aktualnie istniejącej grupy substratów.

W 2020 roku nasz zespół wykazał, że w reakcjach katalizowanych witaminą B₁₂ można generować rodniki z naprężonych bicyklobutanów. Rodniki te wstępowały w reakcje z SOMOfilami lub halogenkami aryłowymi w obecności katalizatora niklowego.

Założyłam, że możliwe będzie wykorzystanie również innych naprężonych pierścieni, które z udziałem witaminy B₁₂ prowadziłyby do powstania rodników nukleofilowych.

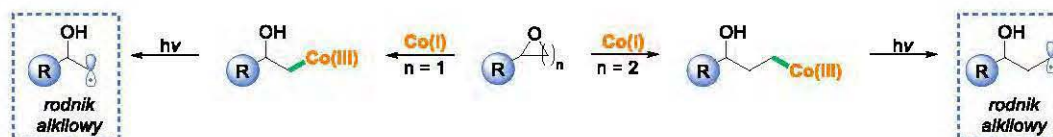
Swoje badania rozpoczęłam od przetestowania epoksydów, jako najmniejszych cyklicznych eterów. W ostatnich latach pojawiło się wiele metod pozwalających na generowanie rodników alkilowych z epoksydów, przy czym regioselektywność reakcji zależna jest od podstawnika występującego przy pierścieniu heterocyklicznym. Znane są selektywne metody otwierania epoksydów zawierających podstawnik alkilowy od strony mniej lub bardziej zatłoczonej sterycznie prowadząc tym samym do utworzenia odpowiednich alkoholi pierwszo- lub drugorzędowych (*Schemat 1*). Niestety problem pojawia się w przypadku epoksydów z podstawnikiem aryłowym. Ze względu na wysoką stabilność

rodników benzytowych, preferowane podejście, bez względu na typ katalizatora, (fotokatalizator bądź kompleksy tytanu) następuje od strony bardziej zatłoczonej sterycznie, co prowadzi jedynie do utworzenia pierwszorzędowych alkoholi. W oparciu o aktualne doniesienia literaturowe, nie było metody pozwalającej na otwarcie tego typu epoksydów od strony mniej zatłoczonej sterycznie, narzucającej tym samym generowanie rodnika alkilowego.



Schemat 1 Rodnikowe reakcje otwarcia pierścienia epoksydu

Założyłam, że zastosowanie porfirynoidowych kompleksów kobaltu (głównie witaminy B₁₂ i jej pochodnych) jako katalizatorów, które w warunkach redukujących ulegają reakcji z elektrofilami, pozwoli na rozwiązanie powyższego problemu. Witamina B₁₂ jako sterycznie zatłoczona molekula powinna mieć wpływ na regioselektywność powyższego procesu. Ponadto, przypuszczałam, że powstały rodnik na drodze homolitycznego rozpadu wiązania Co-C będzie ulegał dalszym przemianom, np. wstępował w cykl niklowy i uczestniczył w reakcji tworzenia wiązania C_{sp3}-C_{sp2}. W dalszej części swoich badań postanowiłam sprawdzić, czy możliwe będzie przeprowadzenie analogicznych transformacji również dla czterocłonowych pierścieni heterocyklicznych, oksetanów (Schemat 2).



Schemat 2 Regioselektywne otwarcie epoksydów i oksetanów katalizowane witaminą B₁₂

Druga część moich badań dotyczyła jednoczesnego generowania rodników alkilowych i acylowych w reakcjach katalizowanych witaminą B₁₂. Warto podkreślić, że tworzenie rodników acylowych z udziałem witaminy B₁₂ było do niedawna oparte tylko na reakcjach elektrochemicznych przy zastosowaniu symetrycznych bezwodników. Dużym postępem w tej tematyce była opracowana przez nasz zespół fotokatalityczna metoda oparta na zastosowaniu tioestrów jako prekursorów w tworzeniu rodników acylowych, katalizowana pochodną hydrofobową witaminy B₁₂. Tak zaproponowane rozwiązanie nie tylko znacząco poprawiło wydajność i efektywność procesu ale także zwiększyło tolerancję grup funkcyjnych (Schemat 3).



Schemat 3 Generowanie rodników alkilowych i acylowych z jednego reagenta

W oparciu o te informacje, postanowiłam więc zaprojektować taki związek, który umożliwiłby wytworzenie obu typów rodników: alkilowego i acylowego. Nawiązując do danych literaturowych założyłam, że powinien on mieć ugrupowanie tioestru oraz halogenek.

3.2 Wstęp literaturowy

Natura jest niewyczerpanym źródłem inspiracji dla naukowców wszystkich dyscyplin. To ona, wykorzystując polimery (białka), stworzyła ogromną liczbę katalizatorów (enzymów), które determinują procesy metaboliczne i biochemiczne związane z funkcjonowaniem organizmów żywych. Obecnie potrzebne są również reakcje chemiczne, które nie zawsze mogą być prowadzone z wykorzystaniem katalizy enzymatycznej. W związku z tym, na przestrzeni lat, opracowano i przebadano wiele nowych, syntetycznych katalizatorów, tak aby mogły promować transformacje chemiczne w sposób wydajny i selektywny. Podejmowane przez uczonych wysiłki mają na celu opracowanie metod, które choć w nieznacznym stopniu mogłyby dorównać naturalnie zachodzącym przemianom enzymatycznym. Niestety, wiele z nich wymaga zastosowania metali ciężkich (Pd, Ru, Ir), które charakteryzuje niska stabilność i selektywność, a także toksyczność.

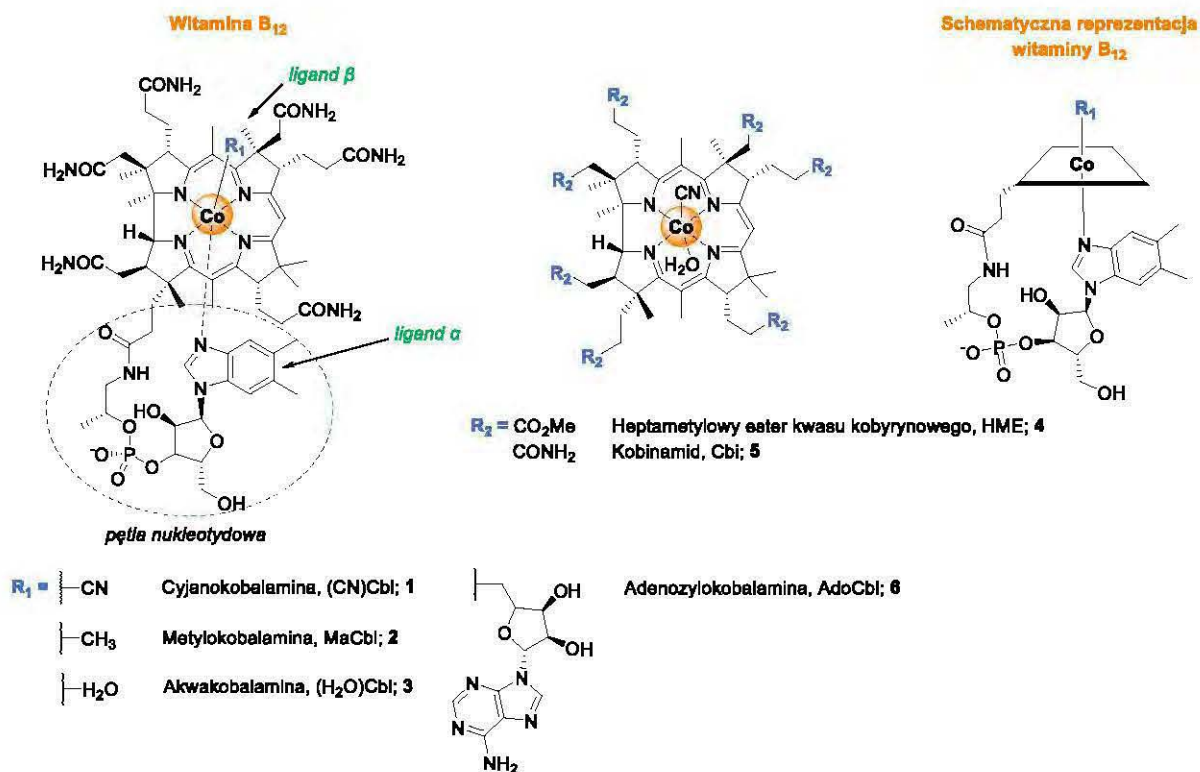
W 1948 roku, grupy Folkersa i Smitha po raz pierwszy wyizolowały krystaliczną formę witaminy B₁₂, zwaną również kobalaminą.¹ Jest ona składnikiem niezbędnym do prawidłowego funkcjonowania organizmów żywych, m.in bierze udział w tworzeniu czerwonych krwinek, których niedobór może prowadzić do anemii. Ponadto, odpowiedzialna jest za prawidłowe funkcjonowanie układu nerwowego i pokarmowego. W komórkach eukariotycznych przekształcana jest w metaloorganiczne kofaktory, których rolą jest katalizowanie szeregu reakcji biochemicznych, do których należą między innymi izomeryzacja, transfer grupy metylowej czy dehalogenowanie.²⁻⁷ Zdolność witaminy B₁₂ do przeprowadzania tych wymagających pod względem termodynamicznym reakcji zwróciła uwagę chemików syntetyków, co w efekcie doprowadziło do odkrycia wielu nowych, użytecznych reakcji z jej udziałem.

Aktualnie chemia witaminy B₁₂ przeżywa swój renesans. Wykorzystywana jest ona jako bezpieczny i „zielony” katalizator kobaltowy, transporter leków czy sensor mRNA i cyjanków.

Poniższy przegląd literaturowy nie jest wyczerpujący, z założenia ma tylko zademonstrować potencjał możliwości wykorzystania witaminy B₁₂ jako katalizatora reakcji chemicznych.

3.2.1 Witamina B₁₂: budowa i właściwości katalityczne

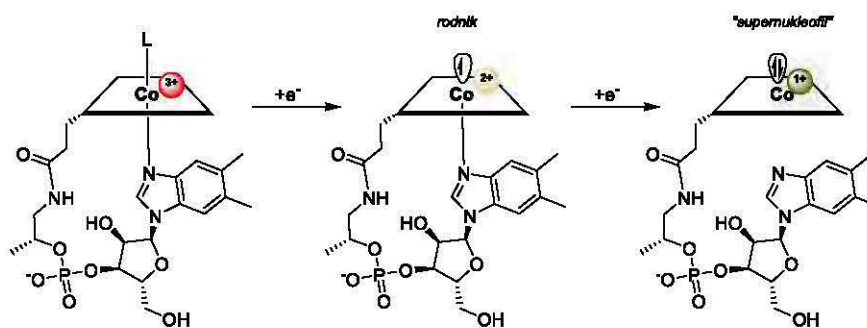
Witamina B₁₂ (1) jest to wysoce sfunkcjonalizowany tetrapirolowy związek tworzący pierścień makrocykliczny, wewnątrz którego ulokowany jest jon kobaltu będący na +3 stopniu utlenienia (Rysunek 1).⁸⁻¹¹ Kation ten jest skoordynowany z czterema pirolowymi atomami azotu oraz dwoma ligandami usytuowanymi po obu stronach pierścienia korynowego. Ligandem α (aksjalnym) jest 5,6-dimetylobenzimidazol, natomiast ligand β zależny jest od formy kobalaminy, i tak cyjanokobalamina ($L_{\beta} = \text{CN}$), metylokobalamina ($L_{\beta} = \text{CH}_3$), akwakobalamina ($L_{\beta} = \text{H}_2\text{O}$), adenozylokobalamina ($L_{\beta} = \text{adenozyna}$). Wszystkie je określa się mianem witaminy B₁₂. Niestety, dużą niedogodnością w powszechnym stosowaniu ich jako katalizatorów jest hydrofilowość, która znacząco ogranicza wykorzystanie popularnych w chemii organicznej rozpuszczalników (acetonitryl, aceton, czy chlorek metylenu). Problem ten pojawia się również przy zastosowaniu pochodnej witaminy B₁₂, kobinamidu (5), który pozbawiony jest pętli nukleotydowej. Rozwiązaniem tego problemu jest heptametylowy ester kwasu kobyrinowego (4) powstały na drodze kwasowej metanolizy. Ze względu na jego hydrofobowy charakter z powodzeniem może być stosowany w reakcjach prowadzonych w rozpuszczalnikach, które były ograniczeniem w przypadku katalizy witaminą B₁₂.



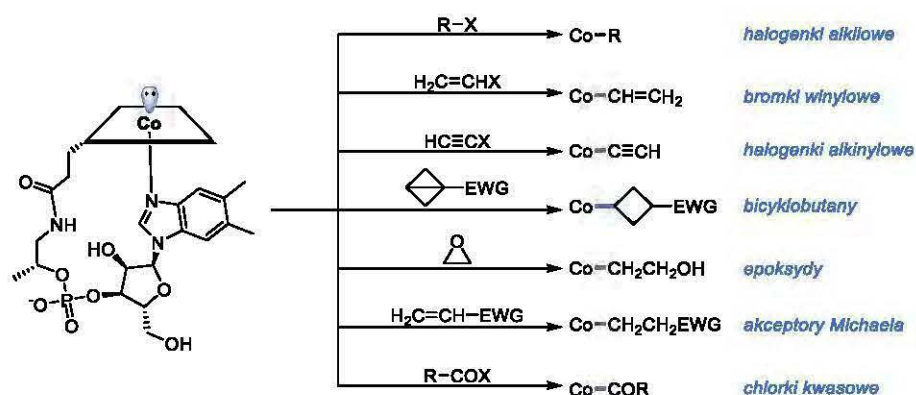
Rysunek 1 Witamina B₁₂ i jej pochodne

Procesy katalizowane witaminą B₁₂ ściśle zależą od właściwości redukująco-utleniających jonu Co(III), który pod wpływem działania czynnika redukującego może przyjąć formę Co(II) lub Co(I) o charakterze odpowiednio: rodnikowym i nukleofilowym (Schemat 4).¹²⁻¹⁴ Formy te mają różne

barwy, a ich zmiana pomocna jest przy wizualnym określeniu stopnia utlenienia jonu kobaltu. Witamina B₁₂, której centralny jon kobaltu jest na +3 stopniu utlenienia jest czerwona, w wyniku redukcji do Co(II) przybiera barwę brązowobrunatną, natomiast forma z jonem Co(I) jest zielona.

Schemat 4 Procesy redukcji witaminy B₁₂

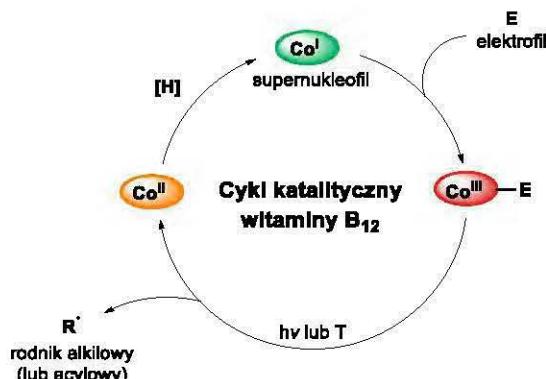
Większość syntetycznie użytecznych reakcji chemicznych katalizowanych witaminą B₁₂ przebiega z udziałem jonu Co(I).¹³ Zredukowana forma witaminy B₁₂ na +1 stopniu utlenienia jest diamagnetycznym kompleksem przejawiającym silne właściwości nukleofilowe. Często też nazywana jest supernukleofilem i jako taka bierze udział w wielu reakcjach substytucji nukleofilowej S_N2. Kobalamina na +1 stopniu utlenienia reaguje z elektrofilami tworząc odpowiednio alkilo- lub acylokobalaminy(III). Do elektrofilów, które do tej pory były wykorzystane w reakcjach katalizowanych witaminą B₁₂ należą, m.in. halogenki alkilowe, winylowe i alkinyłowe, bicyklobutany, epoksydy, akceptory Michaela, chlorki i bezwodniki kwasowe (Schemat 5).^{2,15-33}



Schemat 5 Przykłady elektrofilów wchodzących w reakcje z Co(I)

Typowy mechanizm reakcji chemicznych katalizowanych witaminą B₁₂ zakłada, w pierwszym etapie redukcję katalizatora Co(III) do Co(I) (Schemat 6). Najczęściej stosowanym układem redukującym, jest Zn/NH₄Cl, ale można stosować również związki tytanu, NaBH₄, Mn lub układy fotokatalityczne.^{13,31,34} Powstała kobalamina na +1 stopniu utlenienia, jako nukleofil, reaguje z elektrofilowym substratem tworząc alkilokobalaminy (lub acylokobalaminy). Na skutek działania temperatury lub promieniowania świetlnego następuje homoliza wiązania Co(III)-elektrofil, w wyniku której generowany jest rodnik alkilowy (lub acylowy) oraz Co(II). Wysoka efektywność tego procesu

przypisywana jest stosunkowo słabemu wiązaniu Co-C, którego energia dysocjacji wynosi zaledwie ~ 126 kJ/mol.³⁵⁻³⁸ Cykl katalityczny zamyka się w wyniku ponownej redukcji Co(II) do Co(I).



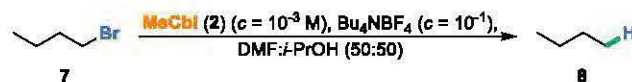
Schemat 6 Ogólny cykl katalityczny reakcji przebiegających w obecności witaminy B₁₂

3.2.2 Katalizowane witaminą B₁₂ reakcje z udziałem rodnika alkilowego

W reakcjach katalizowanych witaminą B₁₂, rodniki alkilowe generowane są z alkilokobalamin na drodze foto- lub termolizy. Stabilność otrzymanych indywiduów w dużej mierze zależy od rodzaju podstawnika alkilowego (efekty steryczne i indukcyjne), konformacji pierścienia i obecności pętli nukleotydowej. Energie (BDE) dysocjacji wiązania Co-C w tych pochodnych zmniejszają się w kolejności Me > Et > *i*Pr > *t*Bu. Zatem najstabilniejsze są alkilokobalaminy, których atom kobaltu połączony jest z pierwszorzędowym atomem węgla.

3.2.2.1 Dehalogenowanie

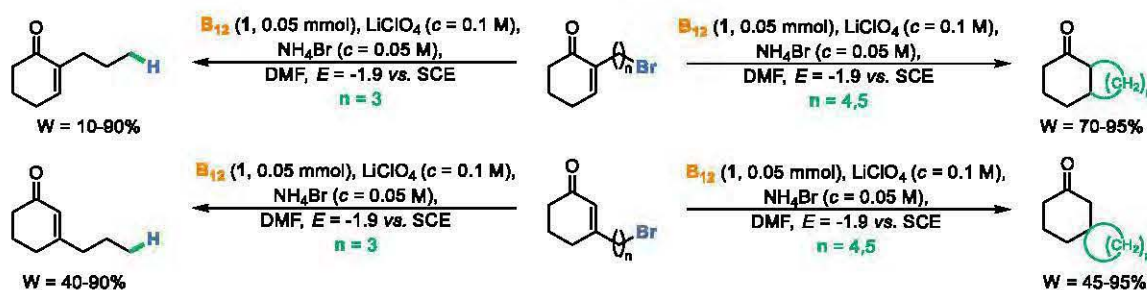
W reakcjach dehalogenowania katalizowanych witaminą B₁₂ i jej pochodnymi najczęściej stosowanymi prekursorami są halogenki alkilowe. W 1979 roku Soufflet, jako jeden z pionierów opracował elektrochemiczną metodę dehalogenowania bromku butylu (7) katalizowaną pochodną witaminy B₁₂ (Schemat 7).³⁹



Schemat 7 Elektrochemiczna metoda dehalogenowania bromku butylu

Wykazał on, że przy kontrolowanym potencjale możliwa jest redukcja kobalaminy i utworzenie rodnika alkilowego. Proces katalityczny tak zaproponowanej przemiany rozpoczyna się od utworzenia formy Co(I) powstałej na drodze dwuelektronowej redukcji metylokobalaminy (2) przy potencjale -1.0 V, która następnie reagując z bromkiem butylu (7) daje odpowiednią butylokobalaminę. Związek ten ulega elektrolizie przy -1.0 V do -1.5 V prowadzącej do powstania kobalaminy z jonem kobaltu na +2 stopniu utlenienia i rodnika butylowego, którego redukcja prowadzi do alkanu 8.

Elektrochemiczną metodę generowania rodników wykorzystał również Foote w wewnątrzcząsteczkowej cyklizacji odpowiednio zaprojektowanych bromków alkilowych (Schemat 8).⁴⁰



Schemat 8 Elektrochemiczna metoda wewnątrzcząsteczkowej cyklizacji opisana przez Foote

W toku badań, wykazał on zależność struktury powstającego produktu od długości łańcucha alifatycznego halogenku. Bromki alkilowe zawierające cztero- i pięciowęglowy łańcuch alifatyczny selektywnie ulegają wewnątrzcząsteczkowej cyklizacji. Natomiast, związki z trzema atomami węgla, dla których cyklizacje 5-endo-trig nie są uprzywilejowane; dają, podobnie jak u Souffleta, produkty dehalogenowania.

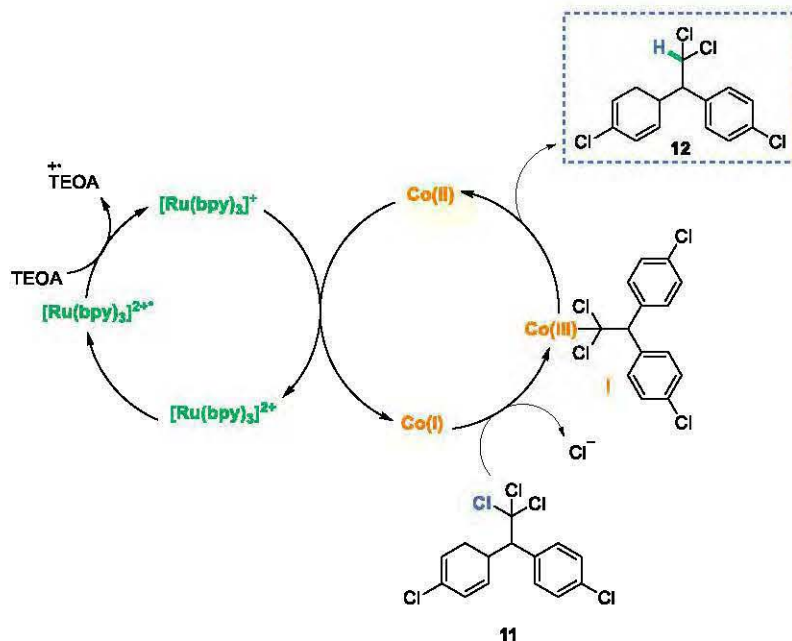
Halogenki alkilowe ze względu na swoją wysoką reaktywność oraz podatność na tworzenie rodników bardzo często ulegają różnym przekształceniom, które czasami mogą być przydatne. Jedną z najczęściej obserwowanych jest reakcja dehalogenowania, która na przestrzeni ostatniej dekady jest bardzo intensywnie badana przez zespoły van der Donka i Hisaedy. Hisaeda, przeprowadził, zakrojone na szeroką skalę, badania nad dehalogenowaniem di(chlorofenylo)trichloroetanu (DDT, **11**), który należy do grupy silnych insektycydów.^{11,31} Wykazał on, że w obecności pochodnej witaminy B_{12} i odpowiedniego reduktora tworzy się di(chlorofenylo)dichloroetan (DDD, **12**) z wydajnością 71% (Schemat 9). W reakcji tej można stosować różne czynniki redukujące, w tym $NaBH_4$ oraz metody elektrochemiczne. Ostatnio opisano zastosowanie $[Ru(bpy)_3]Cl_2$, w roli fotokatalizatora i aminy jako „sacrificial reductant”.⁴¹



Schemat 9 Dehalogenowanie DDT katalizowane pochodną witaminy B_{12}

Ponadto, w oparciu o wcześniejsze dane literaturowe, Hisaeda ze współpracownikami zaproponował mechanizm tej reakcji (Schemat 10). W pierwszym etapie $[Ru(bpy)_3]^{2+}$ w stanie wzbudzonym utlenia trietanolaminę (TEOA) do kationorodnika, sam redukując się do $[Ru(bpy)_3]^+$. Tak powstały kompleks redukuje katalizator kobaltowy do formy Co(I), jednocześnie zamykając I cykl katalityczny. Zredukowana forma katalizatora, reaguje z DDT (**11**) tworząc wiązanie Co-C. Dehydrokobaltowanie daje pożądany produkt DDD (**12**). Należy nadmienić, że katalizator rutenowy jest w stanie

zredukować wyłącznie kompleks kobaltu na +2 stopniu utlenienia, a zatem wymaga on wcześniejszego przygotowania.



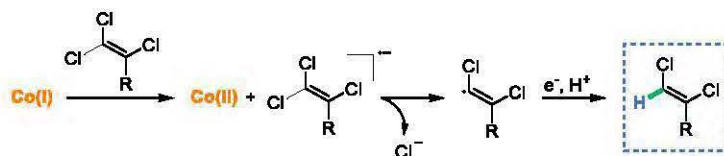
Schemat 10 Mechanizm reakcji dehalogenowania DDT

Innym, równie niebezpiecznym i toksycznym związkiem jak DDT zawierającym atomy chloru jest tetrachloroetylen (PCE). Alken ten należy do grupy związków zagrażających zdrowiu i życiu organizmów żywych. Jak wynika z przeprowadzonych badań, jest odpowiedzialny, m.in. za występowanie nowotworów wątroby i nerek wśród zwierząt, a także został sklasyfikowany jako prawdopodobny czynnik rakotwórczy u ludzi. Zatem sposoby jego utylizacji są niezmiernie istotne. W 2002 roku, van der Donk przedstawił fotokatalityczną metodę dehalogenowania polichloroetylenów (Schemat 11).⁴²



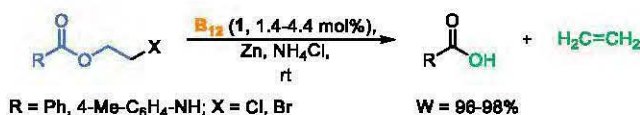
Schemat 11 Fotokatalityczna metoda dehalogenowania van der Donka

Na podstawie przeprowadzonych badań eksperymentalnych, van der Donk zaproponował mechanizm powyższej transformacji (Schemat 12). Analogicznie, jak w poprzednio opisanych pracach, reakcja rozpoczyna się od redukcji kobaltu do jonu Co(I), który jako nukleofil reagując z trichloroetylenem tworzy wiązanie Co-C. Ze względu na niską energię tego wiązania, pod wpływem światła widzialnego następuje jego rozerwanie generując rodnik winylowy, a następnie jego redukcja prowadzi do powstania finalnego produktu.



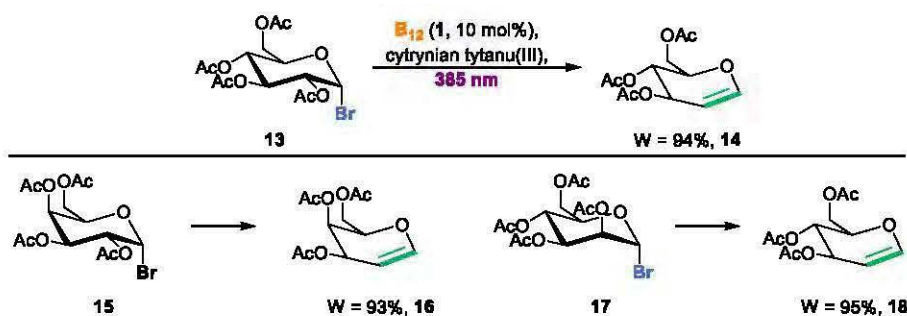
Schemat 12 Mechanizm reakcji dehalogenowania opisana przez van der Donka

W 1980 roku Scheffold wykorzystał reakcję dehalogenowania katalizowaną witaminą B₁₂ w przemianie β -haloestrów do kwasów karboksylowych (Schemat 13).⁴³

Schemat 13 Metoda tworzenia kwasów karboksylowych z β -haloestrów

Opracowana metoda bardzo dobrze sprawdza się dla estrów kwasu benzoowego, pożądane produkty otrzymuje się z bardzo wysokimi wydajnościami (90-98%) niezależnie od użytego halogenku (Cl, Br). Niestety, w pracy zabrakło informacji na temat reaktywności alifatycznych kwasów karboksylowych. Mechanizm opracowanej metody zakłada reakcję Co(I) z β -haloestrem, która prowadzi do odpowiedniej alkilokobalaminy. Kończącym etapem jest dwuelektronowa redukcja kompleksu, w wyniku której powstaje odpowiedni kwas karboksylowy oraz etylen jako produkt uboczny.

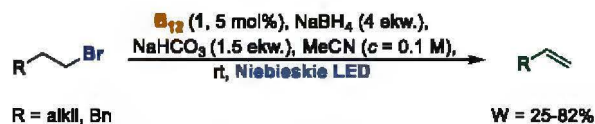
Nawiązując do badań opisanych powyżej, w 1999 roku Franck zaprezentował fotochemiczną metodę tworzenia podstawionych glikali z bromoheksoz (Schemat 14).⁴⁴ Udowodnił on, że stosując witaminę B₁₂ oraz Zn i NH₄Cl, w sposób selektywny, można utworzyć wiązanie C=C. Kluczowe etapy mechanizmu są analogiczne do tych, opisanych przez Scheffolda.



Schemat 14 Fotochemiczna metoda tworzenia glikali

Analogiczna reakcja prostych bromków alkilowych daje terminalne alkeny z dobrymi wydajnościami (Schemat 15).⁴⁵ Opisane przez Westa podejście selektywnie prowadzi do utworzenia terminalnych alkenów. Warto podkreślić, że reakcje eliminacji bardzo często charakteryzuje brak chemo- i regioselektywności, a dodatkowo stosowanie mocnej zasady skutkuje ograniczeniem wprowadzanych grup funkcyjnych. Co ważne, metody eliminacji sprzyjają powstawaniu termodynamicznie stabilnych olefin, w których wiązanie podwójne występuje wewnątrz łańcucha cząsteczki, zgodnie z regułą Zajcewa. West wykazał natomiast, że przy zastosowaniu zatłoczonej

sterycznie witaminy B₁₂ oraz NaBH₄, w obecności słabej zasady (NaHCO₃) możliwe jest selektywne utworzenie terminalnego wiązania C=C z bardzo dobrą wydajnością.



Schemat 15 Fotochemiczna metoda generowania wiązania C=C katalizowana witaminą B₁₂

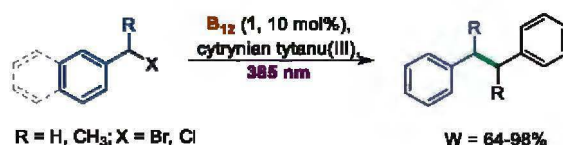
Opracowane warunki sprawdzają się dobrze nie tylko dla bromków, ale również i pseudohalogenków, dając produkty 26-32 z wydajnościami 54-87% (Tabela 1). W reakcji tej, bromek adamantyłu okazał się całkowicie niereaktywny, przede wszystkim, ze względu na niezdolność do wstępowania w reakcje S_N2 oraz hipotetyczną niestabilność produktu końcowego. Co ciekawe, przetestowane w badaniach mesylany (24-25), również dawały terminalne olefiny (31-32) z wydajnością 88% i 53% (wiersze 6 i 7).

Tabela 1 Zakres stosowalności metody tworzenia alkenów z pseudohalogenków alkilowych

L.p.	Substrat	Produkt	Wydajność [%]
1			87
2			54
3			56
4			56
5			75
6			88
7			53

3.2.2.2 Dimeryzacja

Zdolność witaminy B₁₂ do generowania rodników alkilowych z halogenków wykorzystał van der Donk w fotokatalitycznej metodzie dimeryzacji halogenków benzylowych, zarówno bromków jak i chlorków (Schemat 16).



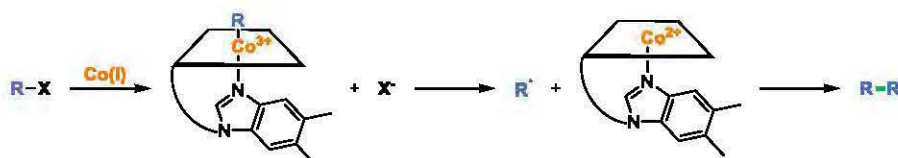
Schemat 16 Fotokatalityczna metoda tworzenia dimerów

Pozwala ona na otrzymanie pożądanego produktu **37** z wydajnością odpowiednio 98% i 68% (Tabela 2, wiersze 1 i 2). Niewiele niższą wydajność obserwuje się dla drugorzędowych halogenków (**35** i **36**). Produkty te powstały z wydajnością 64% i 75% (wiersze 3 i 4).

Tabela 2 Zakres stosowalności i ograniczenia fotokatalitycznej reakcji dimeryzacji opracowanej przez van der Donka

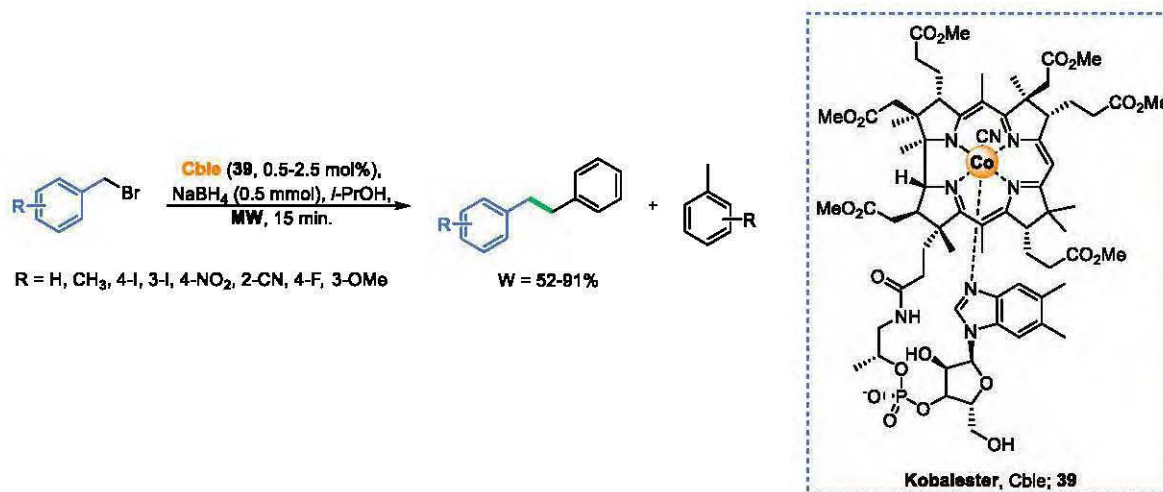
L.p	Substrat	Produkt	Wydajność [%]
1			98
2			68
3			64
4			75

W tym wypadku jako reduktor został zastosowany cytrynian tytanu(III). Wytworzona benzylokobalamina, w wyniku homolizy wiązania Co-C, doprowadziła do powstania rodnika benzyłowego, który na drodze homosprzęgania daje finalny produkt (dimer) (Schemat 17).



Schemat 17 Mechanizm dimeryzacji halogenków benzylu opisany przez van der Donka

Niewątpliwą wadą przedstawionej metody jest zastosowanie aż 10 mol% katalizatora. W 2014 roku, nasz zespół wykazał, że reakcję tę można prowadzić w obecności kobalestru (**39**) i NaBH₄ jako reduktora (Schemat 18).⁴⁶ Kobalester to pochodna witaminy B₁₂, w której grupy amidowe zostały zastąpione estrowymi, dzięki temu związek przejawia charakter amfifilowy i rozpuszcza się również w rozpuszczalnikach organicznych. W tym przypadku, zastosowanie jedynie 0.5 mol% katalizatora kobaltowego oraz ogrzewania mikrofalowego efektywnie wpłynęło na selektywność reakcji, pożądane dimery powstawały z wysokimi wydajnościami (74-91%, Tabela 3).



Schemat 18 Reakcja dimeryzacji katalizowana kobalestem w obecności NaBH₄

Niestety, w reakcji tej bromki benzylove posiadające grupy elektronoakceptorowe są mniej reaktywne i ulegają jedynie dehalogenowaniu (wiersz 4). Zwiększenie ilości katalizatora do 2.5 mol% oraz podwyższenie temperatury (120 °C) znacząco poprawiły selektywność, a tym samym wydajność pożądaných produktów (56-90%).

Tabela 3 Zakres stosowalności i ograniczenia metody

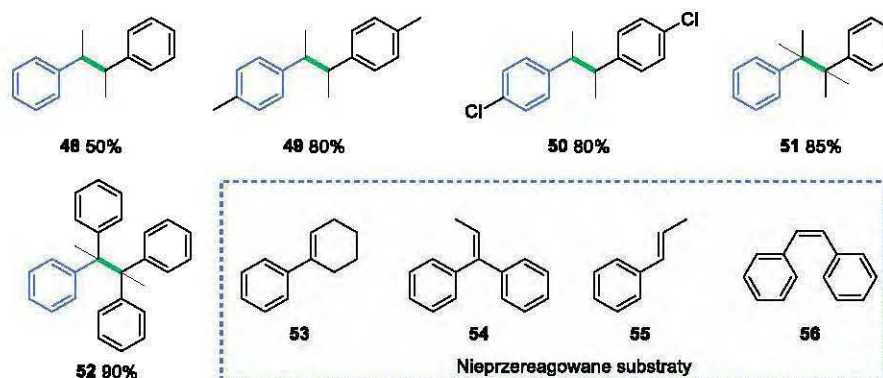
L.p.	R	Ilość katalizatora [mol%]	T [°C]	Produkt	Wydajność dimerów [%]
1	H	0.5	90	40	84
2	4-I	0.5	90	41	74
3	3-I	0.5	90	42	70
4	4-NO ₂	0.5	90	43	Śladowe ilości
5	4-NO ₂	2.5	120	44	56
6	2-CN	2.5	120	45	52
7	4-F	0.5	90	46	90
8	3-OMe	0.5	90	47	91

Zdolność witaminy B₁₂ do generowania rodników alkilowych nie ogranicza się tylko do stosowania halogenków alkilowych. W 2002 roku van der Donk wykazał, że do tego celu można wykorzystać również alkeny (*Schemat 19*).⁴⁷



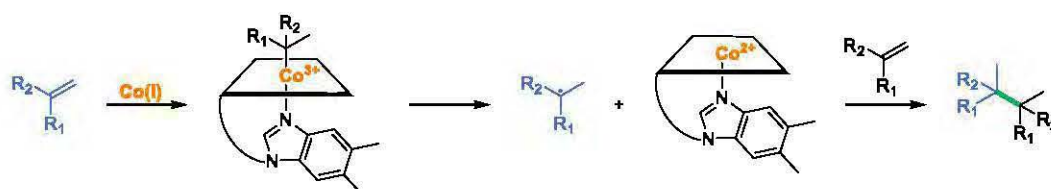
Schemat 19 Dimeryzacja alkenów opisana przez van der Donka

Opracowana metoda jest użyteczna jedynie dla mono- i 1,1-dipodstawionych styrenów i prowadzi do utworzenia dimerów (*Rysunek 2*). Natomiast brak konwersji obserwuje się w przypadku 1,2-dipodstawionych alkenów, najprawdopodobniej ze względów sterycznych.



Rysunek 2 Zakres stosowności i ograniczenia metody dimeryzacji alkenów

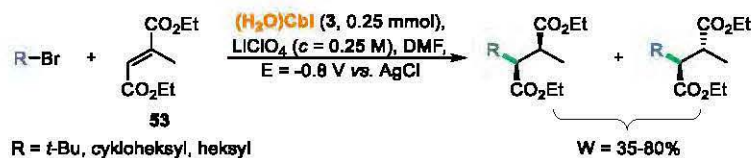
Postulowany przez van der Donka mechanizm dimeryzacji jest analogiczny do opisanych powyżej (Schemat 20). Powstały rodnik ulega reakcji z drugą cząsteczką olefiny, a wytworzony produkt pośredni w wyniku redukcji daje dimer.



Schemat 20 Mechanizm dimeryzacji alkenów opracowany przez van der Donka

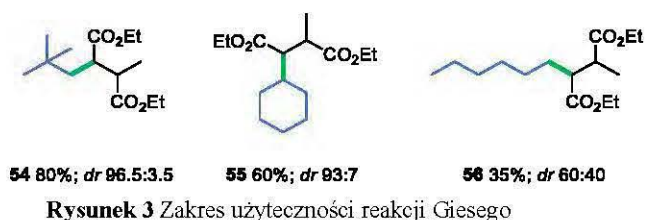
3.2.2.3 Reakcje addycji do wiązań wielokrotnych

Oprócz reakcji homosprzęgania, na znaczeniu zyskują reakcje sprzęgań krzyżowych. Powstające w tych przemianach niesymetryczne produkty są o wiele bardziej przydatne dla chemików organicznych, m.in. z uwagi na ich użyteczność w syntezach związków, np. biologicznie czynnych. Jednym z pierwszych takich przykładów jest opisana przez Giesego fotoelektrokatalityczna funkcjonalizacja monopodstawionego maleinianu dietylu **53** (Schemat 21).⁴⁸



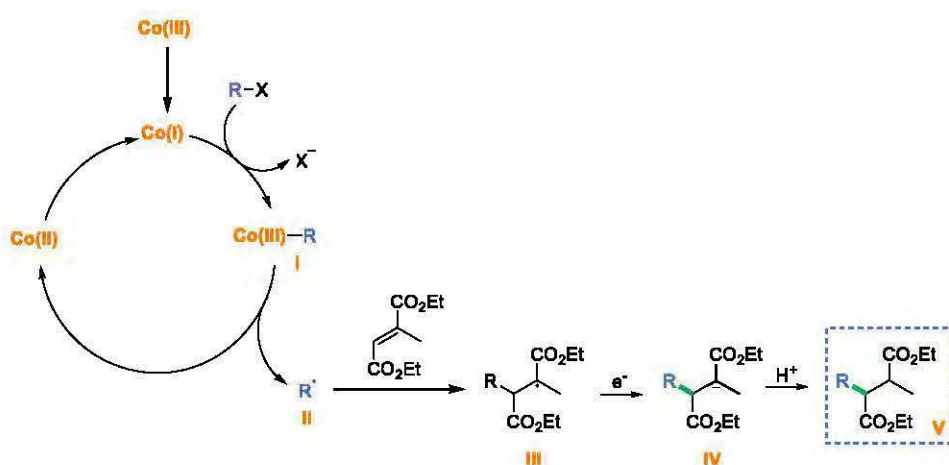
Schemat 21 Fotoelektrochemiczna metoda tworzenia wiązania C-C z bromków alkilowych i akceptorów Michaela

Wykazał on, że rodnik wygenerowany z bromku alkilowego w obecności akwakobalaminy (**3**) w sposób selektywny tworzy wiązanie C-C z tripodstawionym alkenem. Przetestowane bromki alifatyczne: I-, II- oraz III-rzędowe prowadziły do pożądaných produktów z wydajnościami 35-80% (Rysunek 3). Niestety, autorzy pracy ograniczyli się tylko do przetestowania jednego, bardzo reaktywnego akceptora Michaela, i nie pokusili się o zbadanie jaki wpływ na reakcje mogą mieć inne podstawniki elektrono-akceptorowe obecne w strukturze tego substratu.



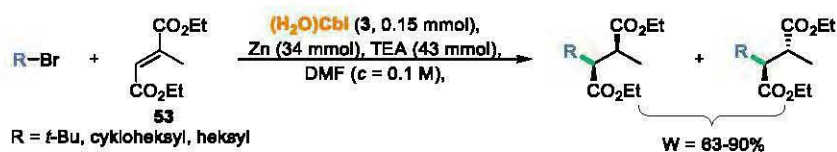
Rysunek 3 Zakres użyteczności reakcji Giese'go

Zaproponowany przez autorów mechanizm zakłada generowanie rodnika alkilowego na drodze homolizy wiązania Co-C, który następnie reaguje z olefiną tworząc produkt pośredni I (Schemat 22). Finalnym etapem jest protonowanie karboanionu do produktu końcowego V. Zaproponowany mechanizm poparty jest eksperymentami mechanistycznymi, do których należy, m.in. reakcja z deuterowanym odczynnikiem (D_2O), która potwierdza obecność karboanionu, powstałego w wyniku redukcji rodnika.



Schemat 22 Mechanizm addycji bromków alkilowych do akceptorów Michaela

Ponadto, Giese wraz ze współpracownikami zaproponowali alternatywną metodę prowadzenia tej reakcji i zamiast elektrochemicznej redukcji katalizatora kobaltowego zastosowano Zn/ Et_3N (trietyloamina). Wyniki jakie uzyskali były analogiczne do tych, które otrzymano w reakcji prowadzonej na drodze elektrochemicznej (Schemat 23).



Schemat 23 Funkcjonalizacja olefin za pomocą bromków alkilowych

Analogią do generowania rodników alkilowych z halogenków alkilowych, jest zastosowanie pseudohalogenków. Przykładowo, grupa Komeyama przedstawiła metodę tworzenia wiązania C-C na drodze fotokatalitycznej reakcji tosyłanu alkilu z akceptorem Michaela (Schemat 24).⁴⁹



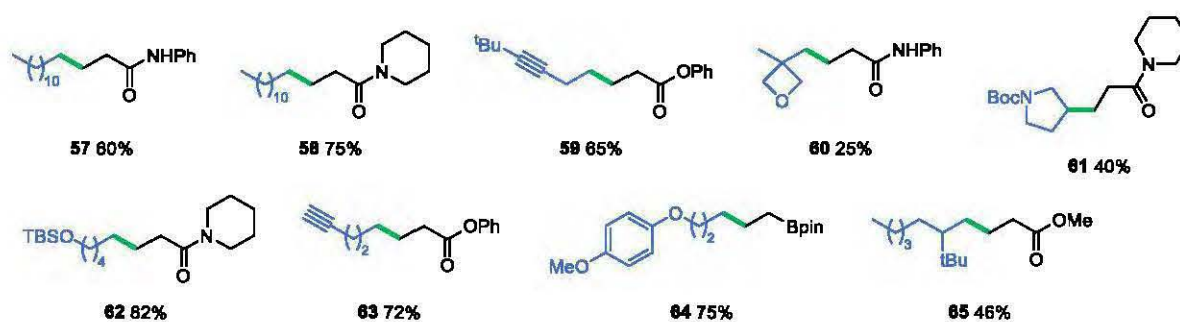
Schemat 24 Fotokatalityczna metoda tworzenia wiązania C-C z tosylanu alkilu i akceptora Michaela

Eksperymenty optymalizacyjne, wykazały że zastosowanie witaminy B₁₂ w obecności manganu jako reduktora oraz światła niebieskiego pozwala na syntezę pożądanego produktu w sposób selektywny i wydajny. W przypadku braku któregoś z komponentów, obserwowane były jedynie śladowe ilości produktów, bądź ich całkowity brak (Tabela 4).

Tabela 4 Optymalizacja warunków reakcji tworzenia wiązania C-C z tosylanu alkilu i akceptora Michaela

L.p.	Zmiany warunków reakcji w stosunku do zoptymalizowanych	Wydajność [%]
1	brak	61
2	bez udziału TEA·HCl	10
3	CoCl(dmgh) ₂ Py zamiast witaminy B ₁₂	śladowe ilości
4	Zn zamiast Mn	51
5	bez udziału światła	5

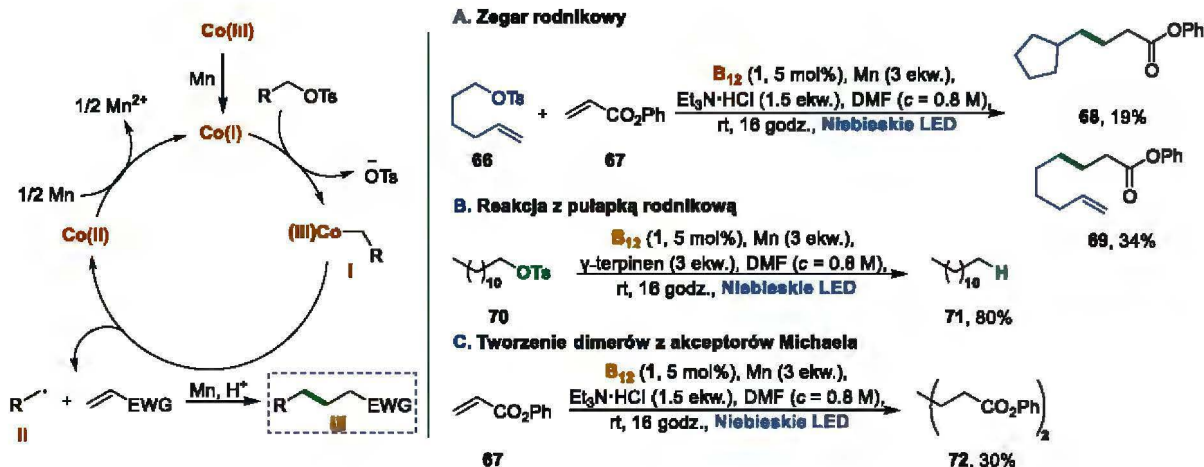
W zoptymalizowanych warunkach sprawdzono zakres stosowalności i ograniczenia metody (Rysunek 4). Alkilowe pseudohalogenki w reakcjach z akrylanem fenylu prowadziły do odpowiednich produktów z dobrymi wydajnościami. Przetestowane akceptory Michaela z podstawnikiem amidowym w reakcji z pierwszorzędowymi tosylanami dawały produkty (57-58) z wydajnościami odpowiednio 60% i 75%. Zastosowanie drugorzędowych pseudohalogenków spowodowało obniżenie wydajności do 40%. Podobne wydajności były obserwowane również w przypadku zastosowania winyloboranu pinakolu oraz akrylanu metylu.



Rysunek 4 Zakres stosowalności fotokatalitycznej metody tworzenia wiązania C-C z pseudohalogenków i akceptorów Michaela

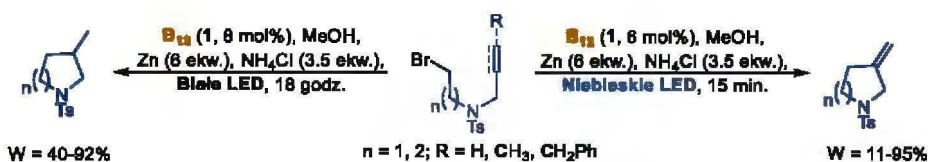
Osaka ze współpracownikami, zaproponowali również mechanizm tej reakcji, jest on analogiczny do tych, prezentowanych przez Scheffolda i van der Donka w odniesieniu do halogenków alkilowych (Schemat 25). Zakłada on tworzenie rodnika alkilowego powstałego na drodze homolizy wiązania Co-alkil, który następnie reagując z akceptorem Michaela daje produkt końcowy. W celu potwierdzenia mechanizmu zostały przeprowadzone niezbędne badania mechanistyczne. Charakter rodnikowy reakcji udowodniono stosując zegar rodnikowy (Schemat 25A) oraz γ -terpinen, powszechnie stosowany jako donor wodoru (Schemat 25B). Co więcej, reakcja prowadzona bez

udziału tosyłanu alkilu daje dimer akceptora Michaela **72** z wydajnością 30% przy konwersji 60% (Schemat 25C).



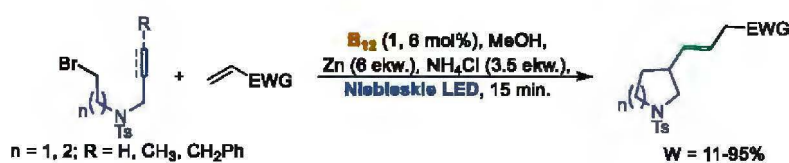
Schemat 25 Postulowany mechanizm Osaki wraz z badaniami mechanistycznymi

Kolejnym przykładem jest fotokatalityczna metoda tworzenia pochodnych pirolidyny na drodze wewnątrzcząsteczkowej cyklizacji odpowiednio zaprojektowanego bromku alkilowego (Schemat 26).⁵⁰



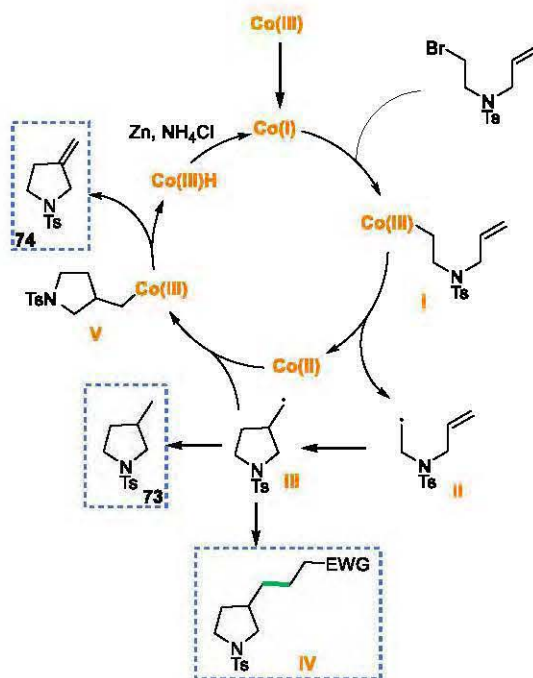
Schemat 26 Fotokatalityczna metoda wewnątrzcząsteczkowej cyklizacji katalizowana witaminą B₁₂

W obecności witaminy B₁₂ jako katalizatora oraz układu redukującego Zn/NH₄Cl generowany jest rodnik alkilowy, który w następnym etapie reaguje z terminalnym wiązaniem wielokrotnym prowadząc do powstania określonego produktu. Struktura produktu zależy od warunków reakcji, w tym zastosowanego światła. 3-Metylopirolidyna tworzy się w reakcji naświetlanej światłem białym, podczas gdy pirolidyna z egzocyklicznym wiązaniem podwójnym powstaje pod wpływem światła niebieskiego. Ograniczeniem metody jest konieczność zastosowania bromków alkilowych; jodki, chlorki bądź pseudohalogenki prowadziły do powstania jedynie śladowych ilości produktu. Ponadto grupa aminowa obecna w substracie wymaga zabezpieczenia. Wykazano, że tylko grupa tosyłowa była odpowiednia w powyższej transformacji. Co więcej, opracowana metodologia bardzo dobrze sprawdza się w reakcji tandemowej, która zachodzi w obecności akceptora Michaela (Schemat 27).



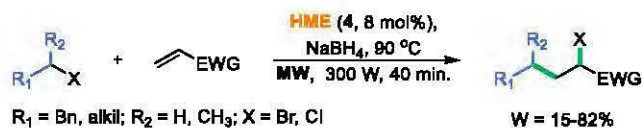
Schemat 27 Fotokatalityczna metoda otrzymywania podstawionych pirolidyn

Większość z przetestowanych ubogich w elektrony alkenów (zawierające ugrupowania estrowe, amidowe, karbonylowe czy sulfonowe) prowadzi do powstania oczekiwanych produktów z satysfakcjonującymi wydajnościami. Postulowany mechanizm, zakłada tworzenie alkilokobalaminy I, która pod wpływem światła widzialnego wiązanie Co-C ulega homolizie generując rodnik alkilowy II. W wyniku wewnątrzcząsteczkowej cyklizacji powstaje produkt pośredni III, który może, a) zostać zredukowany do produktu 73, b) reagować z kobalaminą na +2 stopniu utlenienia lub c) reagować z akceptorem Michaela tworząc wysoce sfunkcjonalizowane pochodne pirolidynowe IV (Schemat 28).



Schemat 28 Mechanizm reakcji cyklizacji oraz następczej addycji akceptora Michaela

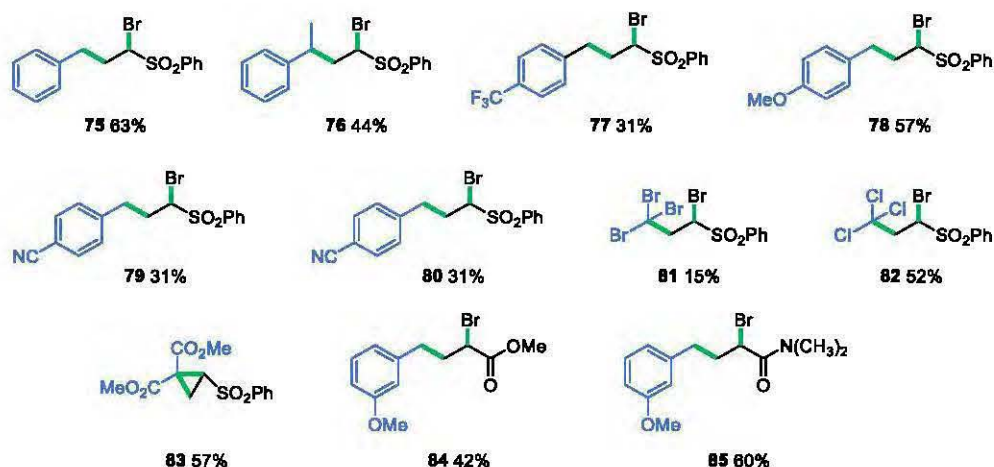
Od czasu jej odkrycia przez Kharasha w 1937 roku, addycja rodnikowa z przeniesieniem atomu (*Atom Transfer Radical Addition* - ATRA) jest przedmiotem wielu badań, mających na celu opracowanie wydajnych i selektywnych metod jednoczesnego tworzenia wiązań C-C i C-halogen. Większość z opracowanych metod opiera się na wykorzystaniu toksycznych katalizatorów oraz dodatków w postaci nadtlenków, odczynników cynoorganicznych lub boranów, a także często reakcje te prowadzi się w wysokich temperaturach. Wychodząc naprzeciw tym problemom, nasz zespół opracował metodę, która w sposób selektywny pozwoliła otrzymać szereg α -bromopochodnych z prostych bromków alkilowych i akceptorów Michaela (Schemat 29).⁵¹



Schemat 29 Addycja rodnikowa z przeniesieniem atomu (ATRA)

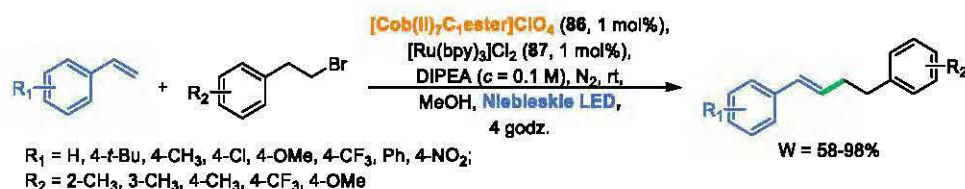
Zastosowanie katalizatora kobaltowego w obecności NaBH_4 i ogrzewania mikrofalowego może być doskonałą alternatywą do wcześniej opisanych metod, a jednocześnie stanowić ich dopełnienie. Badania zakresu stosowności i ograniczeń metody wykazały, że w reakcji z sulfonem

fenylo-winylovym, bromki i chlorki benzylove zawierające podstawniki elektronodonorowe lub elektronoakceptorowe w pierścieniu aromatycznym, a także I- i II-rzędowe bromki alkilowe dają pożądane produkty z dobrymi wydajnościami (Rysunek 5). W przypadku akceptorów Michaela, oprócz sulfonu, dobrymi substratami są również estry i amidy. Co ciekawe, w reakcji 2-bromomalonianu metylu z sulfonem fenylo-winylovym tworzy się cyklopropan **83** z wydajnością 57%. Tak powstały produkt najprawdopodobniej jest wynikiem deprotonowania produktu ATRA w obecności zasady (Cs_2CO_3), który w konsekwencji indukuje cyklizację.



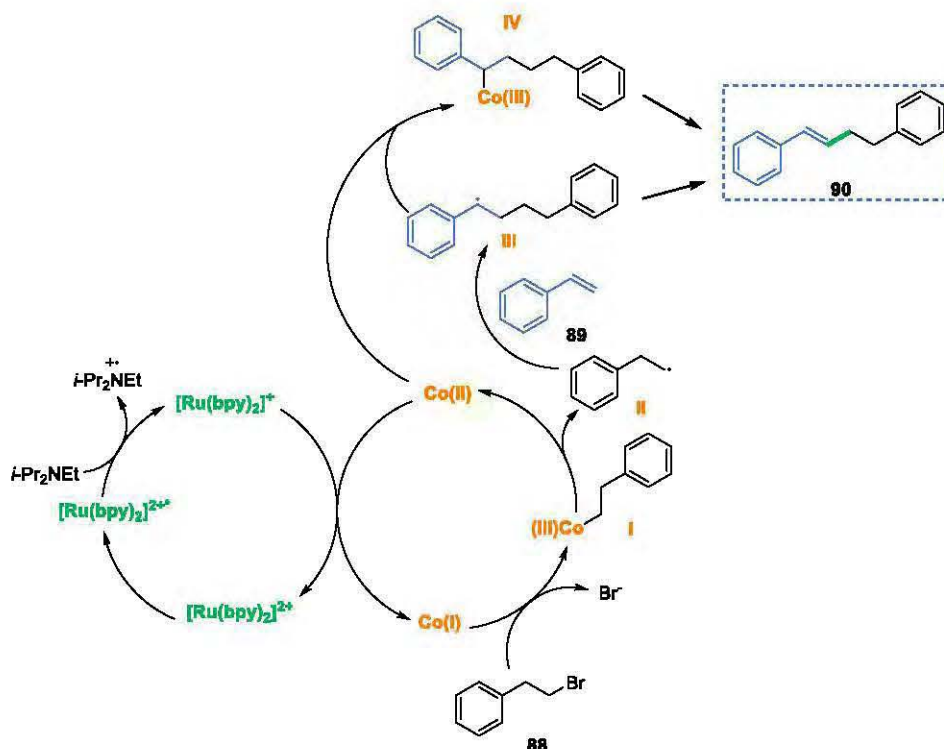
Rysunek 5 Zakres użyteczności reakcji ATRA

Metodę tworzenia rodników alkilowych z halogenków organicznych w obecności witaminy B₁₂ wykorzystała grupa Hisaedy w syntezie podstawionych olefin ze styrenów (Schemat 30).⁵² Przedstawili oni, alternatywną do reakcji Hecka, metodę funkcjonalizacji wiązania C=C. Wykazali, że zastosowanie fotokatalizatora $[\text{Ru}(\text{bpy})_3]\text{Cl}_2$ jako reduktora oraz hydrofobowej, stabilnej pochodnej witaminy B₁₂ z jonem kobaltu na +2 stopniu utlenienia jest efektywnym układem katalitycznym w syntezie alkilowanych olefin.



Schemat 30 Metoda tworzenia wiązania C=C ze styrenów i bromków alkilowych

W reakcji tej fotokatalizator w stanie wzbudzonym utlenia trzeciorzędową aminę - *N,N*-diizopropyletyloaminę (DIPEA) do kationorodnika, a sam redukuje się do $[\text{Ru}(\text{bpy})_2]^+$ (Schemat 31). Tak powstały kompleks $[\text{Ru}(\text{bpy})_3]^+$ redukuje jon $\text{Co}(\text{II})$ do jonu $\text{Co}(\text{I})$. Nukleofilowa forma katalizatora kobaltowego reaguje z bromkiem alkilowym tworząc alkilokobalaminę, która w wyniku homolitycznego rozerwania wiązania Co-C prowadzi do utworzenia rodnika II. W kolejnym etapie rodnik II reagując z olefiną **89** tworzy produkt pośredni III. Powstały rodnik benzylovej z $\text{Co}(\text{II})$ tworzy kompleks IV. Finalnym etapem jest β -eliminacja prowadząca do produktu **90**.



Schemat 31 Mechanizm reakcji sprzęgania styrenu z bromkiem alkilu

W reakcji tej możliwe jest również zastosowanie terminalnych alkinów jako substratów, które dają dipodstawione alkiny (Schemat 32).⁵³ Tym razem jako fotokatalizator wykorzystano Ir[(dtbbpy)(ppy)₂]₂PF₆. Postulowany, na podstawie badań eksperymentalnych mechanizm jest analogiczny do zaproponowanego powyżej.



Schemat 32 Fotokatalityczna reakcja sprzęgania alkinów z bromkami alkilowymi

Wśród grupy związków, zdolnych generować rodniki alkilowe w obecności witaminy B₁₂ są diazozwiązki. Przykładowo, Gryko wraz ze współpracownikami opracowała fotokatalityczną metodę C-H funkcjonalizacji olefin katalizowaną pochodną witaminy B₁₂, kobalestem 39 (Schemat 33).⁵⁴

Schemat 33 C-H funkcjonalizacja olefin katalizowana witaminą pochodną witaminy B₁₂

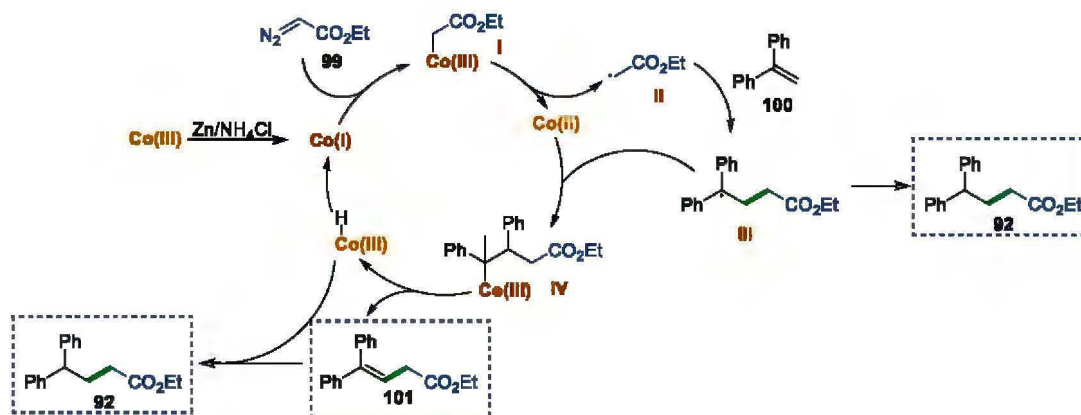
Zoptymalizowane łagodne warunki reakcji (zaledwie 2 mol% katalizatora kobaltowego, układ Zn/NH₄Cl jako czynnik redukujący oraz światło widzialne) prowadziły do otrzymania produktów z dobrymi wydajnościami (16-91%). Niestety utrudnieniem, wynikającym z cyklu katalitycznego było

powstawanie mieszaniny dwóch produktów: olefiny oraz jej zredukowanej formy. Rozwiązaniem tego problemu była następcza reakcja wodorowania w obecności palladu na węglu aktywnym (Pd/C), w celu otrzymania tylko związków nasyconych. Opracowana metoda została przetestowana pod kątem jej użyteczności. 1,1-Dipodstawione olefiny dawały pożądane produkty z dobrymi wydajnościami (Tabela 5). Obecność podstawników elektrono-donorowych w pierścieniu fenylovym jest dobrze tolerowana. Natomiast ubogie w elektrony olefiny są niereaktywne w tej reakcji.

Tabela 5 Zakres stosowalności i ograniczenia metody

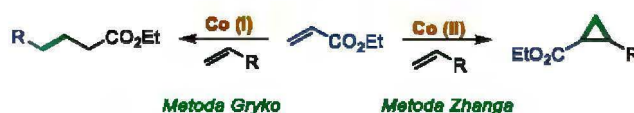
L.p.	R ₁	R ₂	R ₃	Czas [h]	Produkt	Wydajność [%]
1	Ph	Ph	Et	18	92	91
2	Ph	Ph	<i>t</i> -Bu	18	93	67
3	Ph	Ph	(CH ₂) ₃ Ph	18	94	60
4	4-FC ₆ H ₄	H	Et	6	95	16
5	4-BrC ₆ H ₄	H	Et	6	96	28
6	4-MeOC ₆ H ₄	H	Et	6	97	38
7	4-CO ₂ MeC ₆ H ₄	H	Et	6	98	0

Badania mechanistyczne wykazały, że reakcja ta ma charakter rodnikowy (Schemat 34). Zredukowana postać Co(I) działając jako supernukleofil reaguje z elektrofilowym diazozwiązkiem 99 tworząc wiązanie Co-alkil. Na drodze homolizy wygenerowany rodnik II ulega reakcji addycji do wiązania podwójnego a dalsza redukcja prowadzi do produktu końcowego (92).



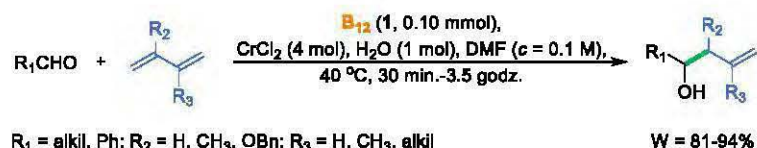
Schemat 34 Mechanizm C-H funkcjonalizacji olefin opracowany przez zespół Gryko

Warto podkreślić, że jest to pierwsze doniesienie literaturowe, w którym z diazozwiązku generowany jest rodnik. Dotychczasowe reakcje oparte były bowiem na tworzeniu z nich karbenów, które prowadziły do cyklopropanów (Schemat 35).⁵⁵ Taką reaktywność w reakcji katalizowanej witaminą B₁₂ opisał Zhang.

Schemat 35 Porównanie reaktywności diazozwiązków w reakcjach katalizowanych witaminą B₁₂

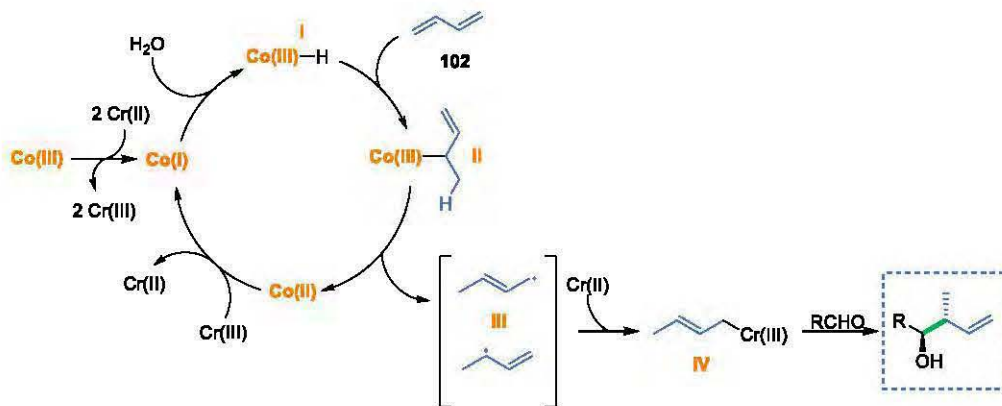
3.2.2.4 Inne reakcje

Witamina B₁₂, oprócz powszechnie stosowanego cynku jako reduktora, ulega również redukcji chlorkiem chromu(II), co wykazano w termicznej reakcji aldehydów z 1,3-dienami katalizowanej witaminą B₁₂ (Schemat 36).⁵⁶ W procesie tym chlorek chromu(II) jest nie tylko reduktorem, ale wstępnie w reakcji z rodnikiem dając związek chromoorganiczny.



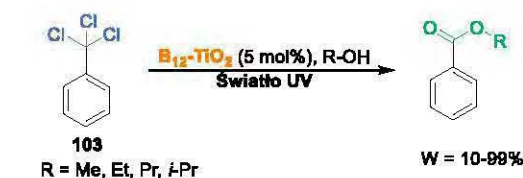
Schemat 36 Termiczna metoda funkcjonalizacji 1,3-dienów

W opracowanej przez zespół Takai metodzie, zostały przetestowane różne aldehydy alifatyczne oraz aromatyczne, wszystkie prowadziły do powstania pożądanego produktu z bardzo dobrymi wydajnościami. Podobne rezultaty otrzymano w przypadku różnie podstawionych 1,3-dienów. W tym przypadku, Co(III) zostaje zredukowany za pomocą CrCl_2 do formy Co(I), która w reakcji z wodą tworzy wodorek kobalaminy I (Schemat 37). Tak powstały kompleks ulega reakcji hydrokobaltowania z dienem tworząc allilokobalaminę II. Na drodze homolizy wiązania Co-C generuje się rodnik allilowy III, który reagując z Cr(II) tworzy związek chromoorganiczny IV. Finalnym etapem jest jego reakcja z aldehydem dająca produkt końcowy.



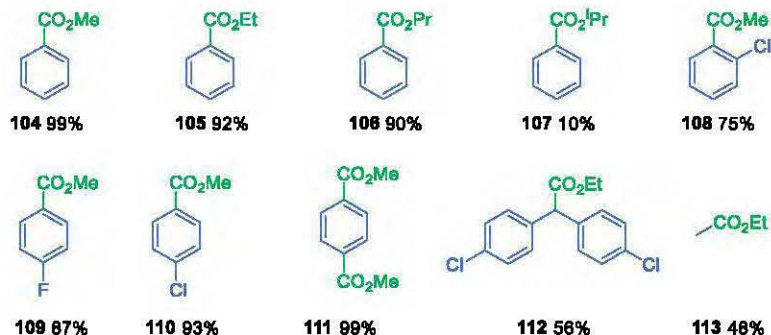
Schemat 37 Mechanizm funkcjonalizacji 1,3-dienów

W podrozdziale 3.2.2.1 zostały opisane reakcje dehalogenowania DDT. Zespół Hisaedy, opracował również inne metody wykorzystania trichloropodstawionych związków. W 2016 roku zaproponował syntezę estrów benzylowych, katalizowaną pochodną witaminy B₁₂ immobilizowaną na TiO_2 (Schemat 38).⁵⁷



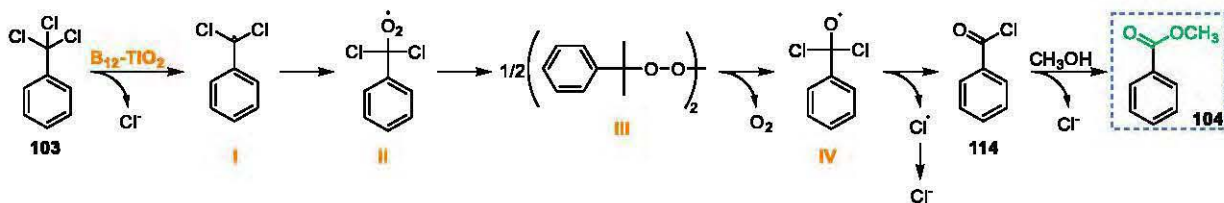
Schemat 38 Metoda tworzenia estrów z trichlorotoluenu

Wykazał on, że pod wpływem działania światła UV możliwe jest utworzenie odpowiedniego chlorku benzoilu, który w reakcji z alkoholem (pełni on również rolę rozpuszczalnika) daje produkt końcowy – ester. Opracowane warunki reakcji z powodzeniem zostały wykorzystane do syntezy szeregu różnie podstawionych estrów (104-113) z dobrymi wydajnościami (10-99%, Rysunek 6).



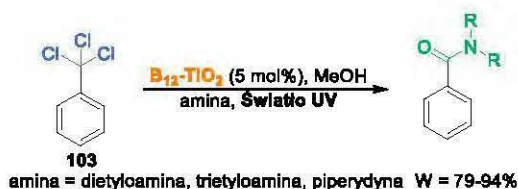
Rysunek 6 Zakres stosowalności i ograniczenia tworzenia estrów z trichlorpodstawionych arenów

Wyjątkiem była reakcja z *i*-propanolem, która prowadziła jedynie do śladowych ilości benzoesu *i*-propylu (107), najprawdopodobniej ze względu na zatłoczone steryczne cząsteczki. Ponadto przetestowane halogenki, zarówno alifatyczne jak i aromatyczne również prowadziły do odpowiednich produktów z dobrymi wydajnościami (Rysunek 6). Mechanizm powyższego procesu, ze względu na obecność tlenu, jest inny od tych prezentowanych powyżej (Schemat 39). W pierwszym etapie zakłada on generowanie rodnika benzyloвого I, który reagując z tlenem cząsteczkowym tworzy rodnik nadtlenkowy II. Następuje reakcja eliminacji oraz dysproporcjonowania prowadzi do powstania chlorku benzoilu (114), który ulega reakcji z alkoholem finalnie dając ester 104.



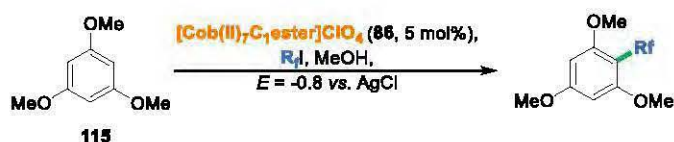
Schemat 39 Mechanizm reakcji tworzenia estrów w warunkach tlenowych

Hisaeda i współpracownicy, w swoich badaniach wykazali, że opracowana metoda może posłużyć do syntezy amidów (Schemat 40). Postulowany mechanizm jest analogiczny do opisanego powyżej; z tym że powstały chlorek benzoilu (114) reagując z odpowiednią aminą prowadzi do powstania amidów.



Schemat 40 Metoda tworzenia amidów z trichlorotoluenu z udziałem $B_{12}-TiO_2$

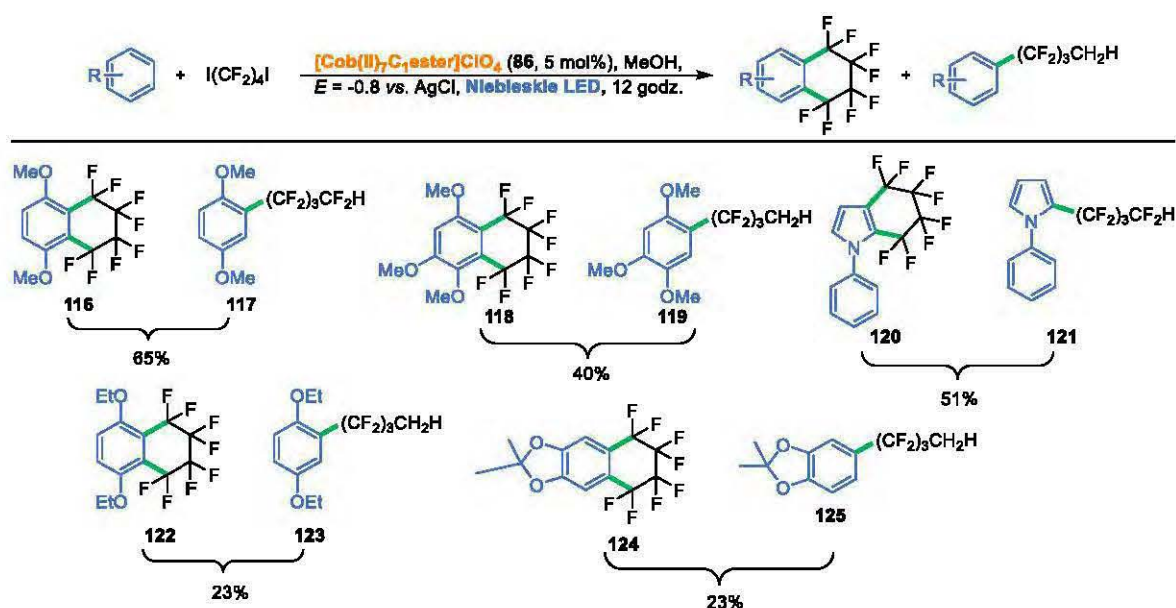
Związki fluoroalkilowe odgrywają znaczącą rolę w wielu dziedzinach życia, m.in. w przemyśle farmaceutycznym, rolnictwie oraz w materiałach organicznych. Ze względu na ich stabilność, lipofilowość, a także ze względu na występowanie podstawnika elektrono-akceptorowego, największą popularnością cieszą się te, zawierające podstawniki $-CF_3$ lub perfluoroalkilowe. Do tej pory, znane metody syntezy tej klasy związków w dużej mierze opierały się na stosowaniu katalizatorów palladowych oraz miedziowych, co pozwalało na wprowadzenie tych grup do pierścienia aromatycznego. Niestety, ich dużym ograniczeniem była przede wszystkim, konieczność zastosowania grupy kierującej (elektrofilowej lub nukleofilowej), halogenku lub podstawnika boranowego. Rozwiązaniem jest przeprowadzenie tych reakcji na drodze rodnikowej. Opracowane przez Barana,⁵⁸ MacMillana,⁵⁹ Rittera⁶⁰ czy Blackmonda⁶¹ metody wymagają jednak zastosowania niekiedy kosztownych, trujących lub potencjalnie wybuchowych odczynników. Dlatego, wyzwaniem było opracowanie nietoksycznej, taniej, ekologicznej a przede wszystkim bezpiecznej metody, która w sposób selektywny prowadziłaby do powstania fluorowanych pochodnych. Hisaeda wraz ze współpracownikami w 2017 roku opisał fotoelektrochemiczne perfluoroalkilowanie arenów katalizowaną hydrofobową pochodną witaminy B₁₂ (Schemat 41).⁵⁹



Schemat 41 Fotoelektrochemiczna metoda perfluoroalkilowania arenów

W toku optymalizacji reakcji 1,3,5-trimetoksybenzenu (115) z jodkiem perfluoropropylu przetestowano różne rozpuszczalniki oraz potencjały elektrolizy. Następnie w optymalnych warunkach sprawdzono zakres i ograniczenia opracowanej metody. Metoksybenzeny w reakcjach z różnymi perfluoroalkilowymi jodkami dawały pożądane produkty z dobrymi wydajnościami (48-84%). Analogiczne rezultaty, otrzymano dla związków heterocyklicznych; produkty powstawały z wydajnościami w zakresie 35-61%.

Ponadto, autorzy wykazali, że te same warunki reakcji mogą prowadzić do wewnątrzcząsteczkowej cyklizacji, pod warunkiem użycia 1,4-dijodopochodnych jako substratów (Schemat 42). Niewątpliwą wadą było otrzymywanie mieszanin dwóch produktów: powstałego w wyniku wewnątrzcząsteczkowej cyklizacji oraz perfluoroalkilowania arenów.

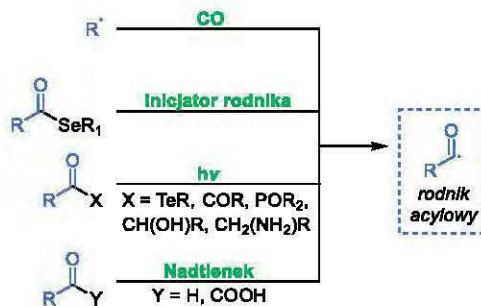


Schemat 42 Wewnątrzcząsteczkowa cyklizacja arenów związkami perfluoroalkilującymi katalizowana pochodną witaminy B₁₂

W zaprezentowanych w powyższym rozdziale reakcjach katalizowanych witaminą B₁₂ oraz jej pochodnymi w dużej mierze jako substraty wykorzystywane są halogenki alkiłowe. Związki te ze względu na wysoką reaktywność stosowane są na dużą skalę, nie tylko w reakcjach homosprzęgań ale stały się również popularne w reakcjach heterosprzęgania. Istotnym ich zastosowaniem są intensywnie prowadzone przez Hisaedę badania nad reakcjami dehalogenowania, które przede wszystkim mają na celu przekształcenie szkodliwych dla organizmów żywych, związków (pestycydy) do ich bezpieczniejszych odpowiedników.

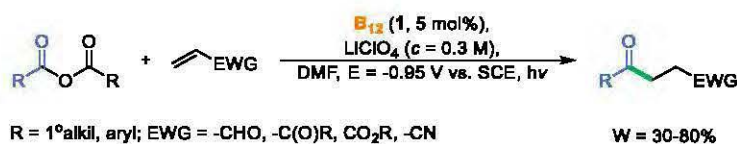
3.2.3 Generowanie rodników acylowych katalizowane witaminą B₁₂

Rodniki acylowe ze względu na ich nukleofilowy charakter są reaktywnymi indywidualami często stosowanymi w chemii syntetycznej i organicznej.⁶² Biorą udział m.in. w rodnikowych reakcjach addycji typu Giese'go do aktywowanych alkenów,⁶³⁻⁶⁵ acylowaniu heteroarenow typu Minisci,⁶⁶ czy też w procesach otrzymywania szerokiej gamy naturalnych i biologicznie aktywnych cząsteczek.^{67,68} Standardowe metody ich generowania, w dużej mierze wymagają zastosowania drastycznych warunków reakcji, do których niewątpliwie należy promieniowanie UV czy wysoka temperatura (Schemat 43).⁶⁹ Innym sposobem ich otrzymywania jest wstępne wygenerowanie rodników alkiłowych z ogólnodostępnych jodków alkiłowych na drodze fotochemicznej bądź termicznej i ich następcza reakcja z tlenkiem węgla (CO). W alternatywnych metodach stosowane są inicjatory rodnikowe (azobis(izobutyronitryl) - AIBN) lub nadtlenek wodoru, który w wyniku homolitycznej abstrakcji atomu wodoru z aldehydów lub α -oksokwasów prowadzi do utworzenia pożądanych rodników acylowych.⁶²



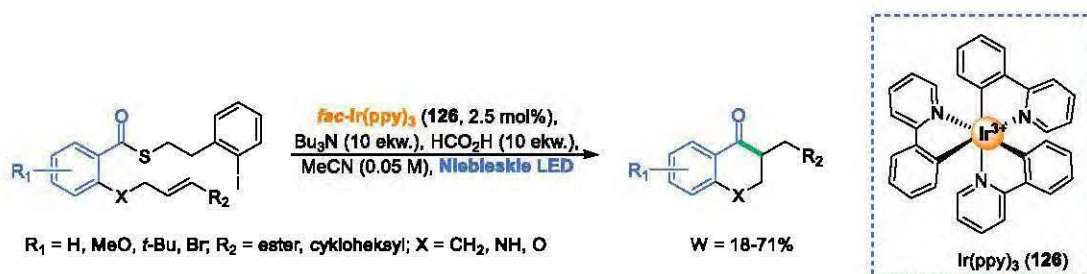
Schemat 43 Metody generowania rodników acylowych

Jednakże, z syntetycznego punktu widzenia użyteczność tych metod jest nieco ograniczona z uwagi na wymóg stosowania wysokich temperatur podczas prowadzenia reakcji lub stechiometrycznych ilości toksycznych reagentów czy utleniaczy. Scheffold wykorzystał symetryczne bezwodniki kwasowe w fotoelektrochemicznej metodzie acylowania elektrofilowych olefin w obecności witaminy B₁₂ (Schemat 44).⁷⁰ Wykazał on, że zastosowanie elektrolizy przy kontrolowanym potencjale pozwala na otrzymanie szeregu pożądaných produktów, również tych z grupami podatnymi na redukcję (np. grupa karbonylowa).

Schemat 44 Acylowanie olefin katalizowane witaminą B₁₂

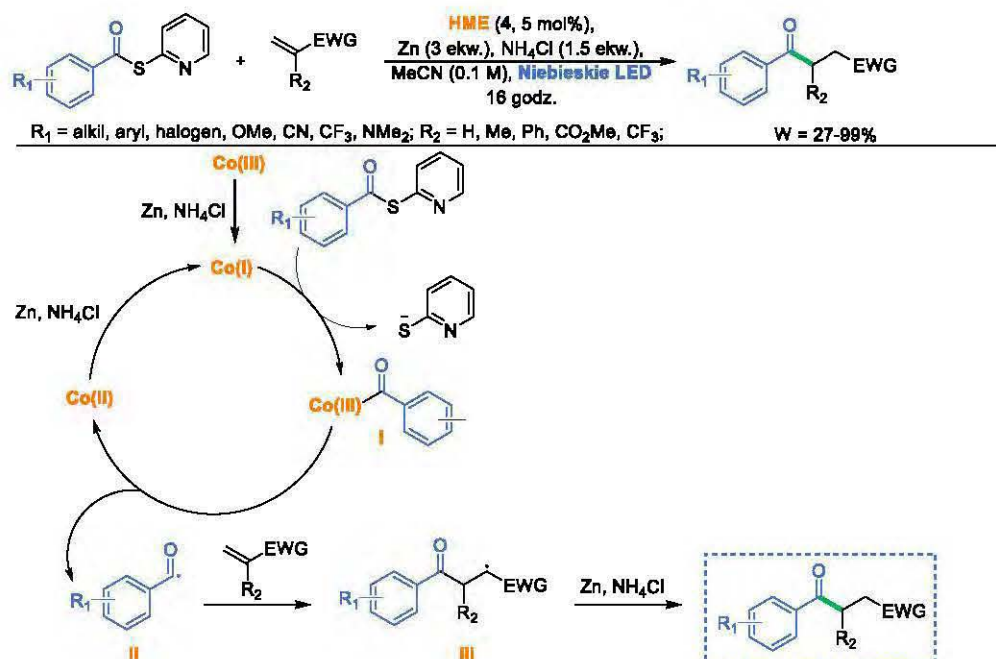
Wykorzystanie bezwodników kwasowych w syntezie niesie ze sobą wiele trudności. Z uwagi na ich niestabilność i podatność na hydrolizę najczęściej wytwarzane są *in situ*, w reakcji kwasów karboksylowych z DMDC (diwęglan dimetylu) lub Boc₂O (diwęglan di-*tert*-butylu). Na podstawie mechanizmu fragmentacji, połowa cząsteczki bezwodnika rozpada się do karboksylanu, co z punktu widzenia wieloetapowych syntez totalnych bądź syntezy leków jest mało ekonomiczne. Alternatywą może być zastosowanie bezwodników niesymetrycznych, ale w ich przypadku dużym problemem jest nieselektywna fragmentacja cząsteczki, która prowadzi do powstania jednego z dwóch możliwych rodników acylowych. Lepszym rozwiązaniem jest zastosowanie stabilniejszej pochodnej kwasu karboksylowego, która znacząco ograniczyłaby powstawanie produktów ubocznych. Takim przykładem są tioestry, z których w sposób wydajny można generować rodniki acylowe. Tioestry charakteryzują się mniejszą energią wiązania C-S, w porównaniu do wiązania C-O występującego w estrach, dzięki czemu są one o wiele bardziej podatne na homolityczną dysocjację prowadzącą do utworzenia rodnika acylowego, co pozwala na zastosowanie łagodniejszych warunków reakcji. Związki te najczęściej stosowane były w fotokatalitycznych reakcjach wewnątrzcząsteczkowych. Na przykład, w obecności kompleksów irydu, McErlean ze współpracownikami wykorzystał te prekursorzy jako źródło rodników acylowych w wewnątrzcząsteczkowej reakcji cyklizacji typu 6-*exo*-trig dającej pochodne chromanonu i indanonu z dobrymi wydajnościami (18-71%) (Schemat

45).⁷¹ Warto podkreślić, że próby zastosowania opracowanych warunków w międzycząsteczkowej reakcji prowadziły do uzyskania tylko śladowych ilości produktów.



Schemat 45 Wewnątrzcząsteczkowa reakcja cyklizacji pomiędzy tioestrami i olefinami katalizowana *fac*-Ir(ppy)₃

Po raz pierwszy międzycząsteczkową reakcję tioestrów z akceptorami Michaela katalizowaną pochodną witaminy B₁₂ opisał nasz zespół w 2017 roku (Schemat 46).⁷² Mechanizm tego procesu zakłada w pierwszym etapie redukcję Co(III) do Co(I), który jako nukleofil na drodze substytucji nukleofilowej typu S_N2 reaguje z tioestrem tworząc acylokobalaminę(III) I. W wyniku działania światła widzialnego następuje homolityczne rozerwanie wiązania Co-C. Utworzony rodnik acylowy II, reaguje z olefiną dając produkt III, którego redukcja prowadzi do ketonu. Cykl katalityczny zostaje zamknięty w wyniku redukcji Co(II) do Co(I). Opracowana metoda bardzo dobrze sprawdza się w przypadku zastosowania szeregu różnych akceptorów Michaela. Najwyższe wydajności obserwowane są w przypadku estrów i akrylonitrylu, produkty tworzą się z wydajnością 83-99%. Reakcja zachodzi efektywnie również dla ketonów i 1,1-dipodstawionych olefin, natomiast 1,2-dipodstawione olefiny są mniej reaktywne (27-40%).



Schemat 46 Fotokatalityczna reakcja tioestrów z akceptorami Michaela

Autorzy pracy przetestowali i porównali aktywność różnych tioestrów arylowych i alkilowych z podstawnikami elektrono-donorowymi jak i elektrono-akceptorowymi. Reakcje prowadziły do pożądaných produktów z bardzo dobrymi wydajnościami.

Metod tworzenia jak również wykorzystania rodników acylowych z udziałem witaminy B₁₂ jest naprawdę niewiele. Tematyka ta nie jest aż tak dokładnie przebadana jak w przypadku opisanych wcześniej rodników alkilowych. Z tego powodu, aktualnie poszukiwane są alternatywne metody ich tworzenia oraz poszerzanie zastosowania już istniejących.

3.3 Podsumowanie

Od momentu wyizolowania krystalicznej formy witaminy B₁₂ przez Folkersa i Smitha w 1948 roku, aż do chwili obecnej opracowano szereg reakcji katalizowanych zarówno kobalaminą jak i jej hydrofobowymi pochodnymi. Większość z nich oparta jest na wykorzystaniu formy Co(I) powstałej na drodze redukcji chemicznej bądź elektrochemicznej i przejawiającej właściwości supernukleofilowe. Z uwagi na jej charakter, może wstępować w reakcje ze związkami elektrofilowymi, które prowadzą do alkilokobalamin (lub acylokobalamin). Następnie, na drodze termo- bądź fotolizy, wiązanie Co-C ulega homolitycznemu rozpadowi, w wyniku czego generowany jest rodnik alkilowy (lub acylowy), który może ulegać dalszym przemianom. Warto jednak pamiętać, że atom kobaltu w witaminie B₁₂, może przyjmować trzy stopnie utlenienia, z czego dwa mogą uczestniczyć w reakcjach katalitycznych: Co(I) oraz Co(II). Obie formy przejawiają odmienne właściwości fizykochemiczne, a rezultatem mogą być inne produkty powstałe z tych samych substratów. Za przykład mogą posłużyć prace Zhanga i Gryko. Zastosowany w obu rozważaniach diazozwiązek w reakcji z Co(II) prowadził do utworzenia cyklopropanów przez karbeny, natomiast po redukcji pochodnej witaminy B₁₂ do formy Co(I) dawał on selektywnie produkty liniowe, a zaproponowany mechanizm miał charakter typowo rodnikowy.

Aktualne doniesienia literaturowe obszernie opisują metody tworzenia rodników alkilowych poczynając od prostych halogenków i pseudohalogenków alkilowych do bardziej złożonych struktur. I choć wydawałoby się, że opracowane metodologie są efektywne, to dalsze badania mają na celu poprawę ich selektywności, wydajności czy efektywności. Inaczej wygląda sytuacja w przypadku rodników acylowych. W literaturze odnotowano tylko dwie procedury ich tworzenia: z symetrycznych bezwodników kwasowych oraz z tioestrów. Obie katalizowane są witaminą B₁₂.

Rozwiązanie niektórych problemów oraz poszerzenie tematyki związanej z katalizą witaminy B₁₂ znajduje się w dalszej części dysertacji: krótkim opisie każdego zrealizowanego przeze mnie projektu oraz załączonych publikacji.

4. BADANIA WŁASNE

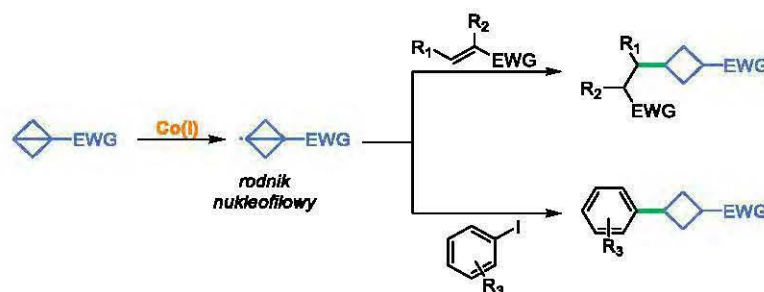
Kataliza kompleksami kobaltu na przełomie ostatnich kilkudziesięciu lat jest prężnie rozwijającą się tematyką w zakresie chemii organicznej. Ze względu na możliwość prowadzenia reakcji chemicznych w warunkach redukujących lub utleniających stwarza chemikom organiczom doskonały warsztat do pracy. I choć kompleksy kobaltu do niedawna były jedynie alternatywą wielu przemian chemicznych, aktualne koszty związane z pozyskiwaniem surowców naturalnych sprawiło, że związki te stosowane są na szeroką skalę.

Witamina B₁₂ jako jeden z przedstawicieli katalizatorów kobaltowych uważana jest za nietoksyczną, bezpieczną i ekonomiczną alternatywę fotokatalizatorów. I choć jej złożona budowa oraz ograniczenia w stosowaniu niektórych substratów, z uwagi na warunki redukujące, niekiedy mogą być przeszkodą, to wciąż katalizator ten jest stale badany a możliwości jego wykorzystania nieustannie się poszerzają.

W poniższym rozdziale opisałam nowe metody tworzenia rodników alkilowych z naprężonych pierścieni heterocyklicznych, w których kluczową rolę odegrała witamina B₁₂. Ponadto zaprezentowane wyniki, uzupełniają aktualne doniesienia w zakresie generowania rodników acylowych i wykorzystania ich w reakcji Giese'go.

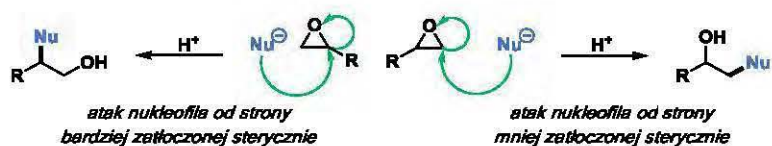
4.1 Regioselektywne otwieranie epoksydów katalizowane witaminą B₁₂

W 2020 roku w naszym zespole wykazano, że rodniki alkilowe mogą być generowane z naprężonych bicyklobutanów. Powstałe rodniki wstępowały w reakcje z SOMOfilami i elektrofilami (Schemat 47).⁷³ Na podstawie tego doniesienia założyłam, że analogicznej reakcji powinny ulegać również inne naprężone związki. Na tej podstawie, w celu poszerzenia grupy substratów, które mogą być aktywowane witaminą B₁₂ postanowiłam wykorzystać do tego celu epoksydy.



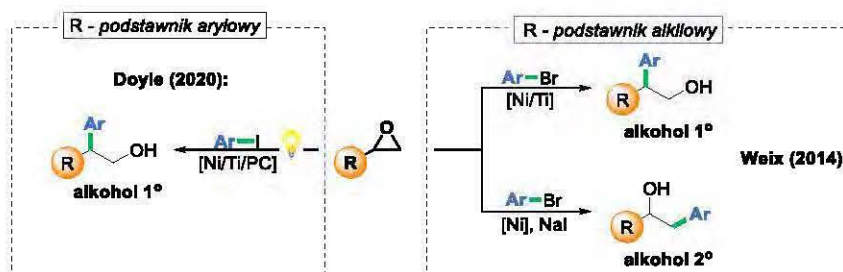
Schemat 47 Generowanie rodników alkilowych z bicyklobutanów katalizowane pochodną witaminy B₁₂

Epoksydy, stanowią ważną grupę elektrofilu w chemii organicznej. Z uwagi na ich dostępność, powszechnie stosowane są w syntezie złożonych cząsteczek organicznych.^{74,75} Ze względu na naprężenie pierścienia trójczłonowego (112 kJ/mol) z łatwością ulegają one otwarciu różnymi czynnikami nukleofilowymi, a powstałe alkohole odgrywają znaczącą rolę w chemii syntetycznej i medycznej (Schemat 48).^{76,77}



Schemat 48 Możliwe podejścia nukleofila do pierścienia epoksydu

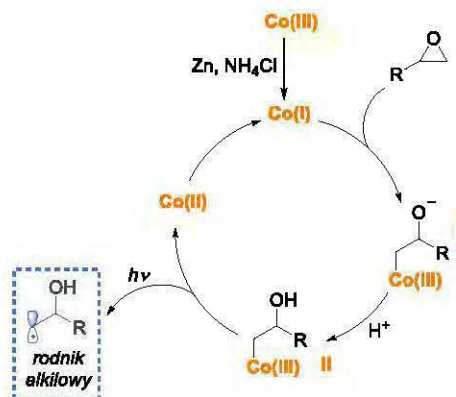
W 2014 roku Weix wykazał, że możliwe jest selektywne generowanie rodników alkilowych z epoksydów, które w katalizowanej nikiem reakcji z jodkami aryłowymi dają drugorzędowe alkohole (Schemat 49).⁷⁸ Metoda ta doskonale sprawdza się jedynie dla epoksydów z podstawnikami alkilowymi zarówno liniowymi jak i cyklicznymi. Natomiast reakcje epoksydów posiadających ugrupowania aryłowe prowadzą do mieszaniny dwóch regioizomerów, przy czym głównym produktem jest alkohol pierwszorzędowy, powstały w wyniku otwarcia epoksydu od strony bardziej zatłoczonej sterycznie.



Problem regioselektywności w tej transformacji częściowo rozwiązała Doyle wraz ze współpracownikami.⁷⁹ Wykazali oni, że możliwe jest regioselektywne uzyskanie alkoholi niezależnie od typu podstawnika R (alifatyczny, aromatyczny, cykliczny). W fotokatalizacyjnej metodzie, kluczowe było zastosowanie kompleksu tytanu. Powodował on otwieranie epoksydów z podstawnikiem aromatycznym tylko od strony bardziej zatłoczonej sterycznie, tym samym generując trwalsze rodniki benzyłowe, finalnie prowadząc do alkoholi pierwszorzędowych. Natomiast epoksydy zawierające podstawnik alkilowy bądź cykliczny dawały alkohole drugorzędowe, analogicznie jak u Weixa. Warto podkreślić, iż wykorzystanie światła widzialnego zamiast wysokich temperatur bądź silnych zasad znacząco poprawiły efektywność reakcji (m.in. poprzez zwiększenie tolerancji grup funkcyjnych), a tym samym zwiększyły ich atrakcyjność. *Niestety, opracowane metody wciąż uniemożliwiały tworzenie alkoholi drugorzędowych z epoksydów z podstawnikiem aryłowym.*

W związku z tym postanowiłam opracować metodę, która pozwoliłaby na regioselektywne otwieranie epoksydów od strony mniej zatłoczonej sterycznie. W oparciu o prace naszego zespołu, dotyczące zmiany reaktywności naprężonych cząsteczek dzięki zastosowaniu katalizy witaminą B₁₂, założyłam że możliwe będzie analogiczne otwarcie pierścienia epoksydu i wytworzenie wiązania Co-C (Schemat 50). Co więcej, ze względu na budowę witaminy B₁₂, przypuszczałam, że atak kompleksu kobaltu na epoksyd będzie możliwy jedynie od strony mniej zatłoczonej sterycznie. Następnie homolityczne rozerwanie wiązania Co-C powinno doprowadzić do wytworzenia

pierwszorzędowego rodnika alkilowego, który będzie wstępował w reakcje m.in.: Giese'go, czy krzyżowego sprzężenia z halogenkami aryłowymi wobec katalizatora niklowego.



Schemat 50 Proponowany mechanizm regioselektywnego otwarcia pierścienia epoksydu witaminą B₁₂

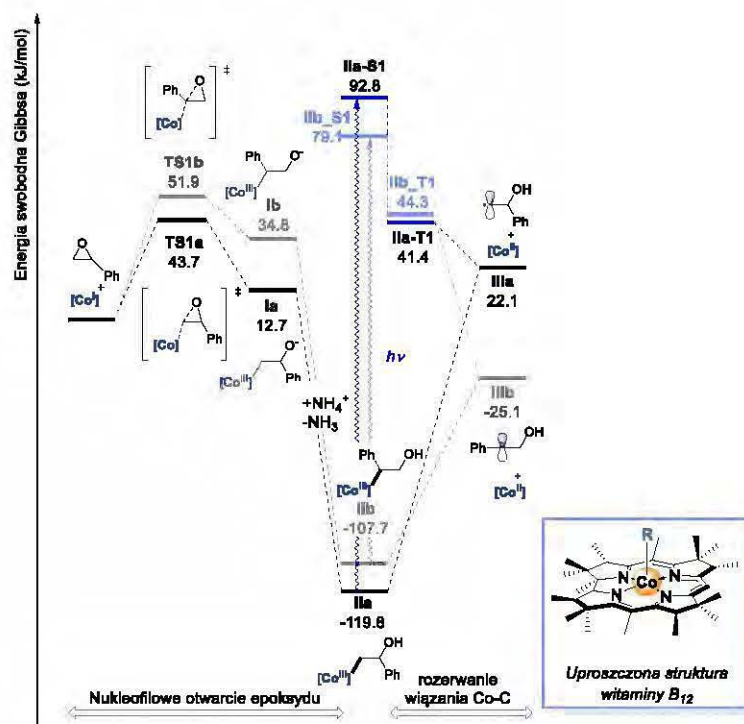
W pierwszym etapie badań przeprowadziłam eksperymenty kontrolne, mające na celu wykazanie roli katalizatora kobaltowego (Schemat 51).



Schemat 51 Eksperymenty kontrolne

Reakcja, w obecności katalizatora niklowego prowadziła do powstania dwóch regioizomerycznych produktów **129** i **130**. Wprowadzenie do mieszaniny reakcyjnej witaminy B₁₂ skutkowało otrzymaniem tylko jednego regioizomeru (**129**). Zatem eksperyment ten jednoznacznie potwierdził wpływ witaminy B₁₂ na powyższą przemianę i wykazał, że to właśnie ten katalizator determinuje jej regioselektywność.

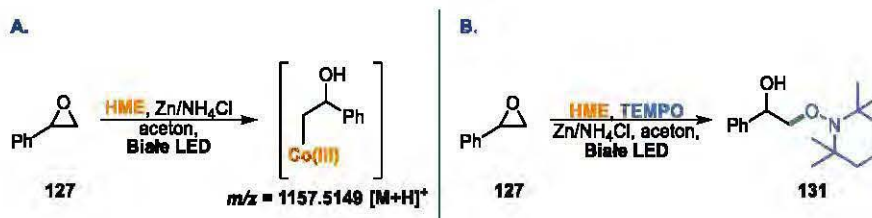
Następnie skupiłam się na przeprowadzeniu badań mechanistycznych opierając się na modelowej reakcji tlenku styrenu (**127**) z 4-jodotoluenem (**128**). Na początku, we współpracy z dr. Chaładajem zostały wykonane obliczenia DFT (*Density Functional Theory*), na poziomie teorii BP86/6-31G(d) uwzględniające współczynnik dyspersji według modelu Grimme i solwatacji opartego na modelu SMD (Rysunek 7). W obliczeniach tym modelem katalizatora była koryna posiadająca 15 grup metylowych na zewnątrz pierścienia.



Rysunek 7 Obliczone energie swobodne Gibbsa w reakcji witaminy B₁₂ i epoksydu

Uzyskane wyniki jasno wykazały, iż podejście witaminy B₁₂ do cząsteczki epoksydu jest bardziej preferowane od strony mniej zatłoczonej sterycznie. Różnica energetyczna stanów przejściowych prowadzących do regioizomerycznych produktów wynosi ~8 kJ/mol.

Tworzenie wiązania Co-C potwierdziłam metodą spektrometrii mas (MS), w widmie obserwowałam pik odpowiadający alkilokobalaminie (Schemat 52A), a generowanie rodnika alkilowego poparałam eksperymentem z pułapką rodnikową (2,2,6,6-tetrametylopiperdyno-1-oksyl, TEMPO) (Schemat 52B). W eksperymentach tych wykorzystałam HME.



Schemat 52 A) Eksperyment potwierdzający tworzenie kompleksu Co-alkil B) Eksperyment z pułapką rodnikową TEMPO

W dalszej części swojej pracy zoptymalizowałam warunki reakcji, w tym strukturę katalizatora zarówno korynowego jak i niklowego, ligandy, czas trwania reakcji, a także rodzaj i natężenie światła (Schemat 53).

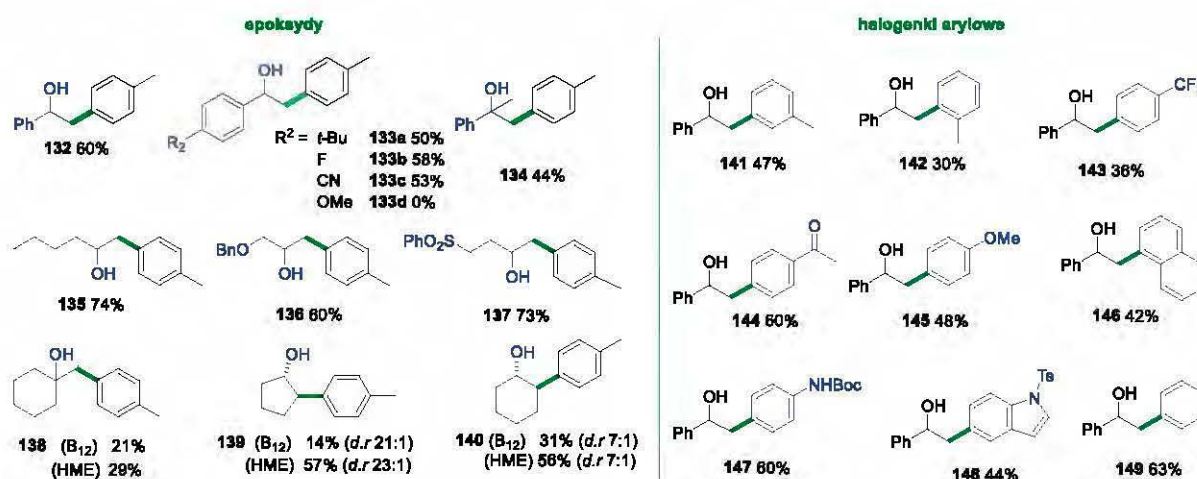


Optymalne warunki: epoksyd (0.2 mmol), halogenek arylu (1.5 ekw.), B₁₂ (1, 5 mol %), NiCl₂(DME) (20 mol %), Zn (1.5 ekw.), NH₄Cl (3 ekw.), dtbbpy (40 mol %), H₂O (1.1 ekw.), NMP_{siachy} (c = 0.1 M), czas: 30 min, niebieskie LED (pojedyncza dioda, 10 W)

Schemat 53 Modelowa reakcja epoksydu aryłowego 127 z 4-jodotoluenu (128)

Badania wykazały, że najbardziej efektywnym kompleksem kobaltowym jest witamina B₁₂, w obecności tego katalizatora produkt 129 tworzył się z wydajnością 60%. Podobne rezultaty obserwowalam dla jej hydrofobowej pochodnej 4 (HME, 57%). W przypadku pozostałych, przetestowanych przez mnie katalizatorów, do których m.in. należały CoCl₂, Co(dmgh)₂Cl(py) (dmgh - dimetyloglioksym; py - pirydyna) i Co(dmgh)₂^tPr(py) (^tPr - *izo*-propyl), obserwowalam tworzenie się jedynie śladowych ilości pożądanego produktu, bądź całkowity jego brak (brak konwersji obu substratów). Natomiast jeśli chodzi o katalizator nikłowy, najbardziej efektywny okazał się NiCl₂(DME) (DME - 1,2-dimetoksyetan) w obecności ligandu dtbbpy (4,4'-di-*tert*-butylo-2,2'-bipirydyna).

Mając zoptymalizowane warunki reakcji przystąpiłam do sprawdzenia zakresu stosowności i ograniczeń opracowanej metody (Rysunek 8); (część oksiranów potrzebnych do tych eksperymentów została zsyntetyzowana w oparciu o dane literaturowe przez dr. Musiejuka). Reakcje epoksydów z podstawnikami aromatycznymi, alkilowymi zarówno cyklicznymi jak i liniowymi prowadziły regioselektywnie do tworzenia się drugorzędowych alkoholi z dobrymi wydajnościami 132-140 (Rysunek 8). Mimo, że reakcja wykazuje wysoką tolerancję grup funkcyjnych, 2-(4-metoksyfenyl)oksiran nie prowadził do powstania produktu, gdyż w warunkach reakcji ulegał rozkładowi.



Rysunek 8 Zakres stosowności i ograniczenia fotokatalitycznej reakcji otwierania epoksydów

Wykazałam, że tylko jednocześnie zastosowanie katalizatora witaminowego i nikłowego zapewnia wysoką regioselektywność w reakcji krzyżowego sprzęgania epoksydów z jodkami arylowymi. Opracowana metodologia uzupełnia istniejące podejścia i pozwala na syntezę alkoholi drugorzędowych.

Powyższe wyniki zostały opublikowane w czasopiśmie *Journal of The American Chemical Society*.

[1] A. Potrzasa, M. Musiejuk, W. Chaładaj, M. Giedyk, D. Gryko, *J. Am. Chem. Soc.*, **2021**, 143, 25, 9368–9376

4.2 Regioselektywna metoda otwierania oksetanów w obecności pochodnej witaminy B₁₂

W toku dalszych badań nad układami naprężonymi postanowiłam sprawdzić aktywność chemiczną ich homologów, czyli oksetanów. Założyłam, że skoro możliwe było wytworzenie rodników alkilowych z naprężonych epoksydów, a także przeprowadzenie transformacji w sposób regioselektywny, analogiczna reakcja otwierania oksetanów powinna również być możliwa.

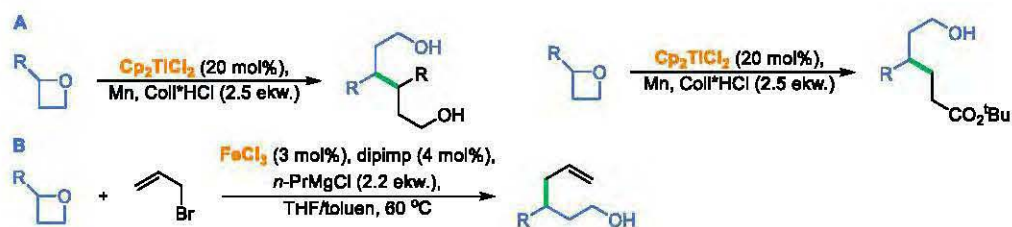
Oksetany **150** należą do prostych czteroczłonowych związków heterocyklicznych zawierających w swojej budowie atom tlenu (*Rysunek 9*).⁸⁰ Ze względu na ich strukturę, mogą być wykorzystywane zarówno jako bloki budulcowe w syntezie naturalnych związków organicznych jak i cząsteczek leków. Ponadto, na przestrzeni ostatnich lat coraz częściej wykorzystywane są jako odpowiedniki grup *gem*-dimetylowych i karbonylowych.



Rysunek 9 Czteroczłonowe związki heterocykliczne

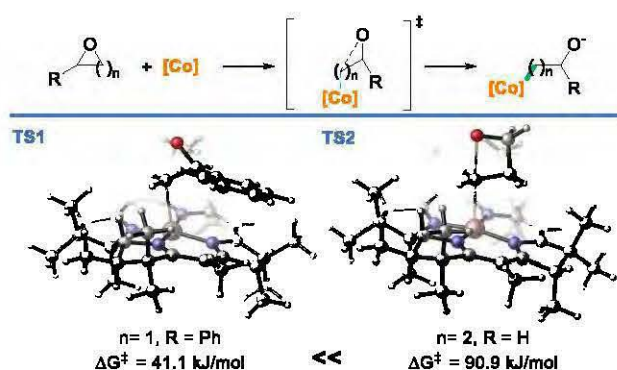
Ze względu na naprężenie pierścienia (106 kJ/mol) związki te łatwo wstępują w reakcje, głównie z jednoczesnym zerwaniem wiązania C-O. W istocie, najbardziej przebadane są reakcje otwierania pierścienia różnymi heteronukleofilami (aminy, odczynniki metaloorganiczne), ale istnieją również nieliczne doniesienia opisujące wykorzystanie do tego celu nukleofili węglowych.⁸¹⁻⁸³ Przykładowo, desymetryzacja 3-podstawionych oksetanów z wykorzystaniem łagodnych kwasów Lewisa okazała się skuteczną metodą w tworzeniu chiralnych alkoholi, ważnych bloków budulcowych w syntezie leków. Niestety, dotychczas opracowane metody, głównie opierają się na wykorzystaniu silnych zasad lub wysokich temperatur, co często skutkuje ograniczonym zastosowaniem ich w syntezie bardziej złożonych związków.

Próby rozwiązania powyższych problemów podjęto już na początku XXI wieku, kiedy to Grimme i Gansäuer, po raz pierwszy zaproponowali otwieranie pierścienia oksetanowego w reakcji katalizowanej kompleksami tytanu od strony bardziej zatłoczonej sterycznie prowadzącej do utworzenia rodników alkilowych (*Schemat 54A*). Produktami reakcji były dimery, a jedyny przykład dalszej funkcjonalizacji polegał na reakcji wygenerowanych rodników z akrylanem tert-butyli. Pożądany produkt tworzył się z dobrą wydajnością jedynie w przypadku zastosowania dużego nadmiaru akceptora Michaela. Co więcej, autorzy stwierdzili, że nie jest to dogodna metoda funkcjonalizacji oksetanów. Podobne rezultaty uzyskała grupa Okamoto, w reakcji katalizowanej kompleksem żelaza, która wymaga zastosowania podwyższonej temperatury oraz odczynników Grignarda, które znacznie ograniczały tolerancje grup funkcyjnych (*Schemat 54b*).



Schemat 54 Rodnikowe metody otwierania oksetanów

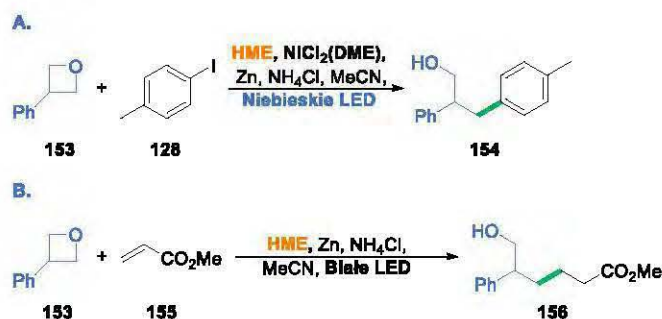
Wychodząc naprzeciw postawionym wyzwaniom naukowym, postanowiłam opracować metodologię regioselektywnego otwierania oksetanów, tym razem od strony mniej zatłoczonej sterycznie wykorzystując katalizę witaminą B₁₂. Z dr. Ociepą stwierdziłam, że proces ten powinien zachodzić analogicznie do tego, opracowanego dla epoksydów. Niestety, obliczenia DFT przeprowadzone przez dr. Chaładaję jasno wykazały, że energia swobodna Gibbsa w procesie otwierania pierścienia oksetanu jest ponad dwukrotnie wyższa, od tej obliczonej dla epoksydów (Schemat 55).



Schemat 55 Porównanie energii swobodnej Gibbsa w procesie otwierania epoksydu i oksetanu

Na podstawie dotychczasowych doniesień literaturowych, założono że aktywacja oksetanu powinna spowodować obniżenie energii procesu otwierania pierścienia. W reakcji modelowej 3-fenylooksetanu (153) z 4-jodotoluenem (128) przetestowano różne kwasy Lewisa (Schemat 56A). Otrzymane rezultaty wykazały, że najefektywniejszym kwasem Lewisa jest bromek trimetylosililu (TMSBr) prowadzący do otrzymania pożądanego produktu 154 z wydajnością 54%. W następnym etapie badań warunki reakcji poddano optymalizacji, w tym katalizatory kobaltowe i niklowe, ligandy oraz czas trwania reakcji. W zoptymalizowanych warunkach zbadano zakres stosowalności i ograniczenia krzyżowej reakcji sprzęgania oksetanów z jodkami aryłowymi, wykazując bardzo wysoką tolerancję grup funkcyjnych, i efektywność metody.

W oparciu o wyżej opisane wyniki, postanowiłam sprawdzić czy możliwe jest przeprowadzenie regioselektywnego otwierania oksetanów wraz z ich następczą addycją do alkenów ubogich w elektrony (Schemat 56B).



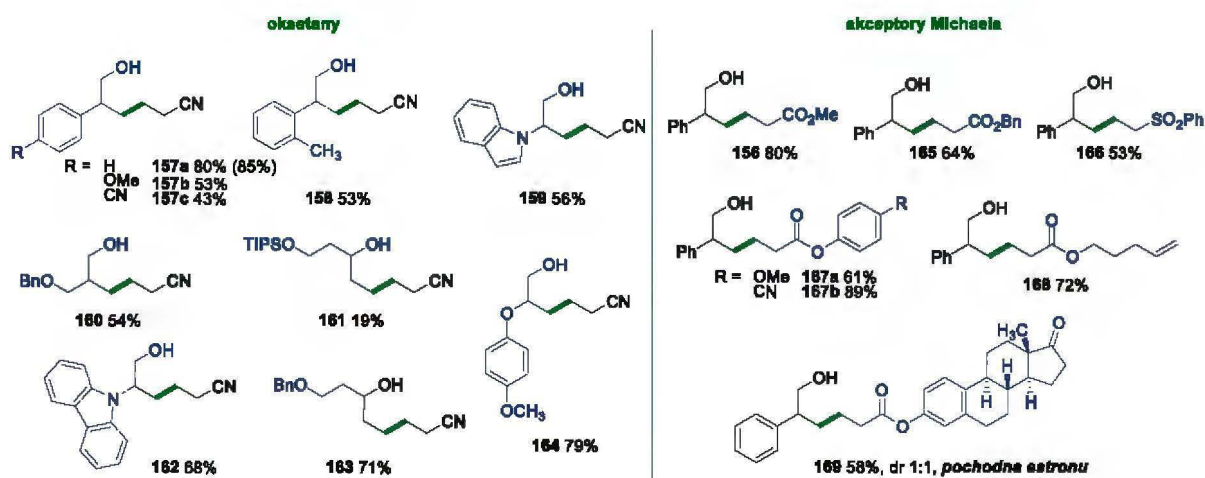
Schemat 56 A) Reakcja sprzęgania krzyżowego oksetanu **153** z 4-jodotoluenem (**128**); B) Reakcja modelowa typu Giese oksetanu **153** z akrylanem metylu (**155**)

Wykorzystując zoptymalizowane warunki reakcji otwierania epoksydów przeprowadziłam reakcję 3-fenylooksetanu (**153**) z akrylanem metylu (**155**). Analiza mieszaniny reakcyjnej (spektrometria mas – MS, magnetyczny rezonans jądrowy – NMR) wykazała obecność oczekiwanego produktu **156**. W następnym etapie przeprowadziłam optymalizację warunków powyższego procesu. Oczywiście, nieodzownym elementem optymalizacji było sprawdzenie różnych kwasów Lewisa, które okazały się kluczowe również i w tej transformacji (Tabela 6). W zasadzie reakcja zachodziła tylko w obecności TMSBr (wiersz 1). W reakcji tej przetestowałam również szereg katalizatorów kobaltowych, czas trwania reakcji, a także stosunek stechiometryczny substratów i stężenie reakcji.

Tabela 6 Porównanie aktywności kwasów Lewisa w reakcji Giesego

L.p.	Kwas Lewisa	Wydajność 156 [%]
1	TMSBr	57
2	TMSI	0
3	TMSCl	0
4	AlCl ₃	0
5	ZnOTf	0
6	MgCl ₂	0
7	(EtO) ₃ SiCl	6

Prace nad optymalizacją przyczyniły się do wzrostu wydajności, finalnie w modelowej reakcji uzyskałam produkt z wydajnością 80%. Ponadto przeprowadzone przeze mnie eksperymenty kontrolne potwierdziły, że reakcja jest ściśle zależna od zastosowanego katalizatora, kwasu Lewisa i użytego światła (brak któregośkolwiek z komponentów skutkowało niepowstaniem pożądanego produktu). W kolejnym etapie pracy zbadałam zakres stosowalności i ograniczenia metody (Rysunek 10).



Rysunek 10 Zakres stosowalności i ograniczenia regioselektywnego otwierania oksetanów katalizowanej witaminą B₁₂

Oksetany, niezależnie od podstawników w pierścieniu, prowadziły do oczekiwanych produktów (157-164) z dobrymi i bardzo dobrymi wydajnościami. W dalszej części badań poddałam reakcji ubogie w elektrony (EWG – estry, nityle, sulfony) olefiny. Badania wykazały, że są one odpowiednimi substratami w tej reakcji. Co ciekawe, w opracowanych warunkach, związki z terminalnym wiązaniem podwójnym i potrójnym, dawały produkty z wysokimi wydajnościami. Pomimo obecności Zn/NH₄Cl nie obserwowałam niepożądaną ich redukcji. Użyteczność opracowanej metody do funkcjonalizacji złożonych cząsteczek wykazałam na przykładzie związków naturalnych (-)-mentolu i estronu.

Finalnym aspektem pracy były badania mechanistyczne, na podstawie których zaproponowałam mechanizm reakcji (Schemat 57).

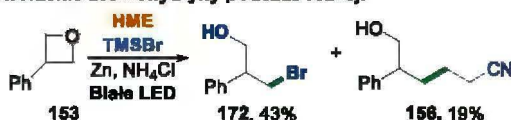
A. Eksperyment z pułapką rodnikową



B. Reakcja z bromohydryną



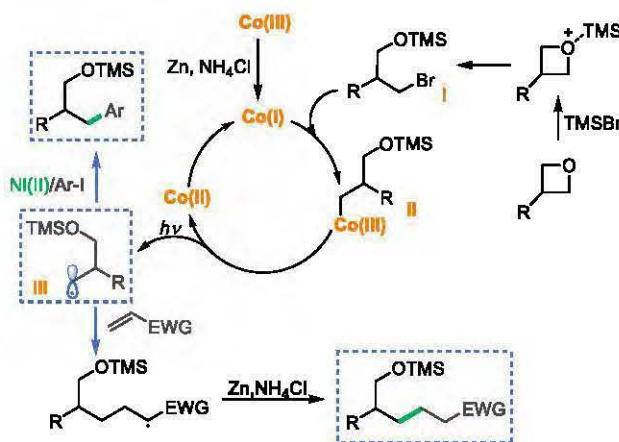
C. Tworzenie bromohydryny podczas reakcji



Schemat 57 Badania mechanistyczne regioselektywnego otwierania oksetanów katalizowanego HME

Tworzenie alkilokobalaminy II potwierdziłam metodą spektrometrii mas (MS), a obecność rodników wykonując reakcję z dodatkiem pułapki rodnikowej TEMPO (Schemat 57A). Ponadto wykonany przeze mnie profil kinetyczny i reakcja bromohydryny (172) z akrylonitrylem (170) udowodniły, że aktywacja oksetanu kwasem Lewisa jest niezbędna w zaproponowanym przeze mnie cyklu

katalitycznym (Schemat 58). Utworzona halohydryna reaguje ze zredukowaną formą katalizatora prowadząc tym samym do odpowiedniej alkilokobalaminy II. Powstałe wiązanie Co-C pod wpływem światła ulega homolitycznemu rozerwaniu, co w konsekwencji prowadzi do rodnika alkilowego III. Tak otrzymane indywiduum wstępuje w reakcje z alkenami lub wprowadzone do cyklu niklowego może tworzyć produkty z jodkami aryłowymi.



Schemat 58 Proponowany mechanizm otwarcia oksetanów katalizowany HME w obecności kwasu Lewisa

Wykazałam, że zastosowanie katalizy witaminą B₁₂ oraz dodatku odpowiedniego kwasu Lewisa, pozwala na otwarcie oksetanu w sposób regioselektywny. Ponadto, utworzony rodnik powstały w wyniku homolitycznego rozpadu alkilokobalaminy może ulegać dalszym przemianom: reagować z akceptorami Michaela lub wstępować w drugi cykl katalizacyjny z niklem i prowadzić do utworzenia wiązania C_{sp3}-C_{sp2}.

Powyższe wyniki zostały opublikowane w czasopiśmie *Organic Letters*.

[2] A. Potrzasał, M. Ociepa, W. Chaładaj, D. Gryko, *Org. Lett.*; DOI: 10.1021/acs.orglett.2c00355

4.3 Generowanie rodnika acylowego i alkilowego z jednego reagenta

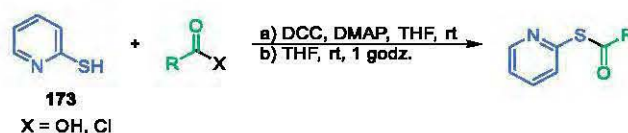
Z punktu widzenia chemika organika, rodniki acylowe należą do bardzo użytecznych indywiduów chemicznych. Mimo, iż generowane są z elektrofili, same przyjmując charakter nukleofilowy, zdolne są do reakcji m.in. z ubogimi w elektrony olefinami (reakcja Giesego) czy ze związkami heterocyklicznymi (reakcja Miniscięgo). Do najczęstszych metod ich generowania zaliczamy: a) rozerwanie homolityczne wiązania RCO-X, b) karbonylowanie rodników za pomocą CO czy c) dekarboksylowanie związków α -oksokarbonylowych.

W przypadku katalizy witaminą B₁₂ istnieją tylko dwa doniesienia literaturowe (Rozdział 3.2.3). W 2017 roku nasz zespół po raz pierwszy opracował katalizowaną estrem metylowym kwasu kobyrinowego metodę generowania rodników acylowych z tioestrów (Schemat 59).



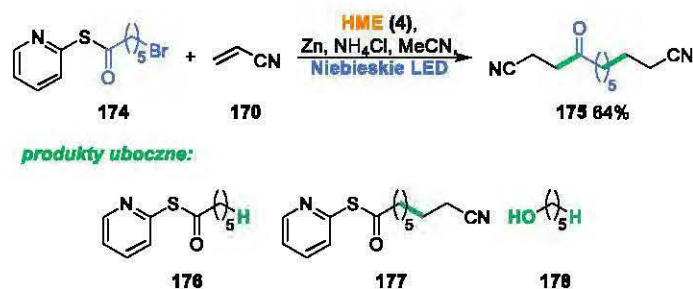
Schemat 59 Fotokatalityczna metoda tworzenia rodników acylowych katalizowana pochodną witaminy B₁₂

Wykazano, że utworzona acylokobalamina pod wpływem światła rozpada się generując rodnik acylowy, a ten z kolei reaguje z akceptorami Michaela. Zainteresowana tymi wynikami postanowiłam sprawdzić, czy możliwe jest zaprojektowanie takiego substratu, który pozwoli na jednoczesne generowanie rodników alkilowych i acylowych w warunkach katalizy witaminą B₁₂. Wraz z dr. Ociepą zaplanowaliśmy strukturę takiego substratu (*Schemat 60*), którego synteza opierała się na reakcji 2-merkaptopirydyny z kwasem karboksylowym w obecności odczynnika sprzęgającego DCC (*N,N'*-dicykloheksylokarbodiimid) lub z chlorkiem kwasowym.



Schemat 60 Strategia syntezy substratów

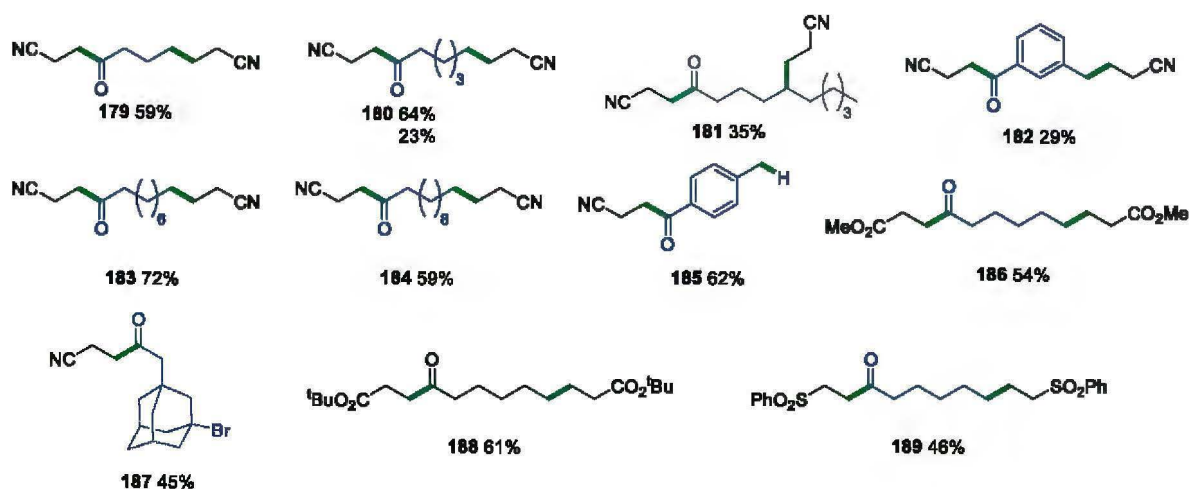
W pierwszym etapie badań sprawdziliśmy czy otrzymany 6-bromoheksanotioanian *S*-pirydyn-2-ylu reaguje z akrylonitrylem (*Schemat 61*).



Schemat 61 Reakcja modelowa tioestru **174** z akrylonitrylem (**170**)

Reakcja modelowa tioestru **174** z akrylonitrylem (**170**) w obecności światła prowadziła do powstania pożądanego produktu **175** z wydajnością 46%, któremu towarzyszyły produkty uboczne: zdehalogenowany tioester **176**, produkt powstały w wyniku addycji akrylonitrylu tylko od strony halogenku **177** oraz alkohol - produkt hydrolizy **178**. W celu wyeliminowania tworzenia się niepożądanych produktów ubocznych, warunki reakcji poddano optymalizacji. Przetestowałam m.in. różne katalizatory, stosunki stechiometryczne w jakich zostały użyte Zn/NH₄Cl oraz substraty, długość fali światła a także czas trwania reakcji. Finalnie oczekiwany produkt otrzymano z wydajnością 64%.

W następnym etapie sprawdziłam zakres stosowalności i ograniczenia opracowanej metody (*Rysunek 11*). Tioestry zawierające w swej strukturze pierwszorzędowy lub drugorzędowy halogenek, dają oczekiwane produkty (**179-189**) z dobrymi wydajnościami.

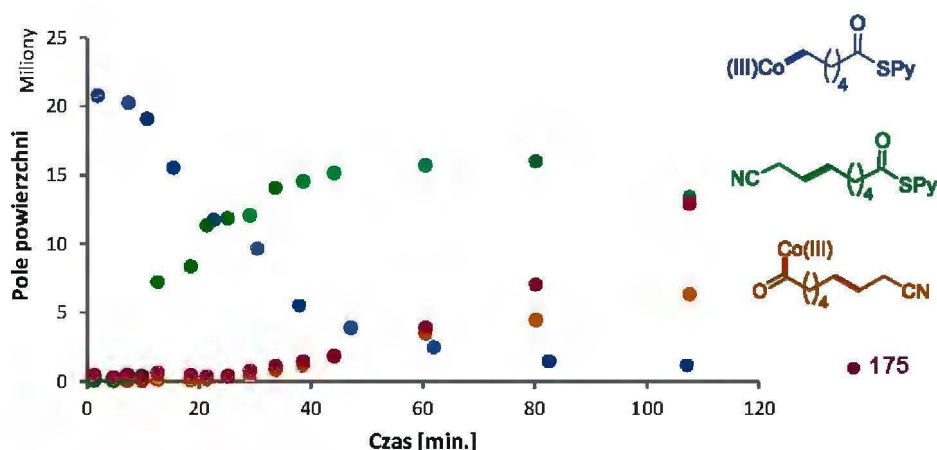


Rysunek 11 Zakres stosowności i ograniczenia metody generowania rodników acylowych i alkiowych z jednego reagenta

W przypadku reakcji tioestru posiadającego w swej strukturze ugrupowanie chlorku lub bromku benzyłowego, pożądany produkt **182** tworzy się z wydajnością 29%. W reakcji tej generuje się bardzo reaktywny rodnik benzyłowy, który łatwo ulega dimeryzacji i redukcji. Jeśli chodzi o akceptory Michaela, to w opisaney reakcji można wykorzystać sulfony, estry i nityle. Wyjątkami są te, które posiadają grupy wrażliwe na warunki redukujące.

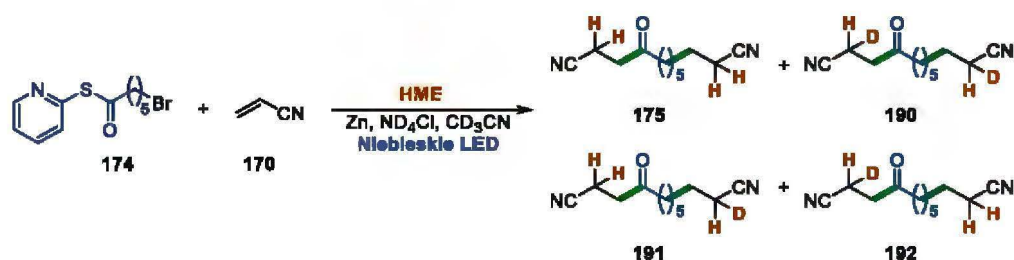
Nieodłącznym aspektem moich badań było wyjaśnienie mechanizmu tej reakcji. W tym celu przeprowadziłam niezbędne eksperymenty, które potwierdziły powstanie zarówno rodnika alkiłowego jak i acylowego, a także pozwoliły na zdefiniowanie etapu limitującego szybkość powyższego procesu.

W pierwszej kolejności wykonałam eksperymenty z dodatkiem pułapki rodnikowej (TEMPO), które potwierdziły tworzenie się zarówno rodników alkiłowych i acylowych. Następnie w celu określenia kolejności ich generowania wykonałam profil kinetyczny reakcji wykorzystując technikę spektrometrii mas (MS) (Schemat 62). Pomiary zostały wykonane we współpracy z mgr. Spólnikiem. W toku badań okazało się, że w pierwszej kolejności tworzy się kompleks Co-alkil, powstały w wyniku ataku Co(I) na bromek alkilu, a dopiero po 20 minutach generuje się kompleks Co-acył.



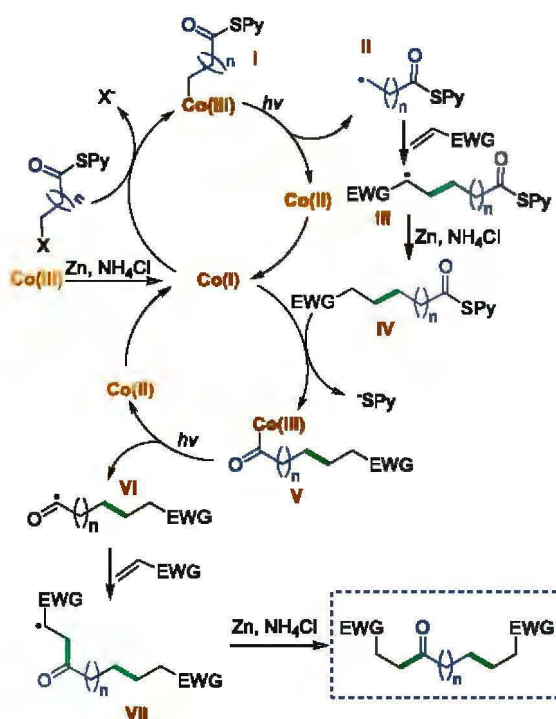
Schemat 62 Profil kinetyczny reakcji tioestru z akceptorem Michaela

Aby potwierdzić mechanizm wykonałam również reakcje w obecności deuterowanego chlorku amonu. W reakcji utworzyła się mieszanina czterech związków 175, 190, 191 i 192 (Schemat 63), które zawierały w swojej strukturze deuter.



Schemat 63 Reakcja z deuterowanym ND_4Cl

Na podstawie przeprowadzonych eksperymentów zaproponowałam mechanizm reakcji (Schemat 64).



Schemat 64 Mechanizm reakcji tioestrów z akceptorami Michaela

Analogicznie jak w pozostałych opracowanych przeze mnie badaniach, pierwszy etap zakłada redukcję katalizatora kobaltowego do formy Co(I) , który działając jako supernukleofil ulegał reakcji $\text{S}_{\text{N}}2$ z tioestrem tworząc alkilokobalaminę I. Na drodze homolizy wiązania Co-C utworzony rodnik reagował z akceptorem Michaela tworząc produkt IV, który w reakcji z Co(I) acylokobalaminę V. Ponowna homoliza wiązania i reakcja z ubogą w elektrony olefiną prowadziła do produktu końcowego.

Zaprezentowane wyniki jasno wskazują, że możliwe jest jednoczesne generowanie rodników alkilowych i acylowych z wykorzystaniem kobalaminy jako katalizatora. Badania mechanistyczne dowodzą, że generowanie rodników alkilowych jest znacznie szybsze od rodników acylowych.

Powyższe wyniki zostały opublikowane w czasopiśmie *European Journal of Organic Chemistry*.

[3] **A. Potraszaj**, M. Ociepa, O. Baka, G. Spólnik, D. Gryko, *Eur. J. Org. Chem.*, **2020**, 1567 – 1571.

4.4 Podsumowanie

Kobalamina i jej pochodne to efektywne katalizatory wielu reakcji organicznych. Większość z nich przebiega poprzez etap tworzenia rodnika, których źródłem są najczęściej halogenki, pseudohalogenki i olefiny. **Celem mojej pracy było rozszerzenie grupy prekursorów rodników użytecznych w katalizie witaminą B₁₂, które stanowiłyby dopełnienie aktualnie istniejącej grupy substratów.**

Przeprowadzone przeze mnie badania znacząco wpłynęły na aktualny stan wiedzy dotyczącej metod generowania rodników alkilowych i acylowych oraz wykorzystanie ich w reakcjach fotochemicznych.

Do moich największych osiągnięć niewątpliwie mogę zaliczyć:

1. Przedstawienie, po raz pierwszy, fotokatalitycznej metody regioselektywnego otwierania pierścienia epoksydowego od strony mniej zatłoczonej sterycznie. Opracowana przeze mnie metodologia doskonale sprawdza się zarówno dla epoksydów zawierających podstawnik aromatyczny, cykliczny jak i alifatyczny dając pożądane produkty z dobrymi wydajnościami. Praca ta z pewnością stanowi dopełnienie aktualnych doniesień dotyczących metod otwierania trójczłonowych związków heterocyklicznych.

2. Opracowanie fotokatalitycznej metody, która w sposób wydajny i regioselektywny pozwala na funkcjonalizację oksetanów, przebiegającą z otwarciem pierścienia. Metodologia ta, w ogromnym stopniu poszerza aktualne doniesienia literaturowe dotyczące naprężonych, cyklicznych eterów. Jest to pierwszy przykład, w którym Co(I) jako supernukleofil otwiera pierścień od strony mniej zatłoczonej sterycznie i prowadzi do selektywnego tworzenia tylko jednego regioizomeru.

3. Opracowanie metody, która pozwala na generowanie rodnika alkilowego i acylowego z tioestru. W oparciu o profil kinetyczny, udowodniłam że tworzenie rodników alkilowych jest procesem determinującym szybkość reakcji.

Badania zaprezentowane w niniejszej rozprawie stanowią zwartą całość i jasno demonstrują użyteczność witaminy B₁₂ i jej pochodnych jako efektywnych katalizatorów w generowaniu rodników alkilowych z naprężonych cząsteczek. Wykazują, że alkilokobalaminy tworzą się znacznie szybciej, niż acylokobalaminy. Ponadto, przedstawione rozważania opisują znaczący wpływ witaminy B₁₂ na reakcje chemiczne, w których występował problem regioselektywności.

Warto jednak podkreślić, że powyższe badania są jedynie początkiem i mogą być wskazówką dla innych do dalszych odkryć.

4.5 Bibliografia

- (1) Folkers, K.; Wolf, D. E. Chemistry of Vitamin B₁₂. *Vitam. Horm.* **1954**, *12*, 1–51.
- (2) Toraya, T. Radical Catalysis in Coenzyme B₁₂-Dependent Isomerization (Eliminating) Reactions. *Chem. Rev.* **2003**, *103*, 2095–2127.
- (3) Jeschke, G.; Jansen, M. NMR Spectroscopy Methyl Transfer from Methanol to Co ± Cobyrinate : A Model for the Coenzyme B₁₂. *Angew. Chemie - Int. Ed.* **1998**, No. 9, 1282–1283.
- (4) Wedemeyer-Exl, C.; Darbre, T.; Keese, R. Model Studies for the Thiol-Mediated Methyl Transfer to Corrinoids. *Org. Biomol. Chem.* **2007**, *5*, 2119–2128.
- (5) Sun, F.; Darbre, T. The Co(I) Induced Methylmalonyl-Succinyl Rearrangement in a Model for the Coenzyme B₁₂ Dependent Methylmalonyl-CoA Mutase. *Org. Biomol. Chem.* **2003**, *1*, 3154–3159.
- (6) Pan, L.; Shimakoshi, H.; Masuko, T.; Hisaeda, Y. Vitamin B₁₂ Model Complex Catalyzed Methyl Transfer Reaction to Alkylthiol under Electrochemical Conditions with Sacrificial Electrode. *Dalt. Trans.* **2009**, No. 44, 9898–9905.
- (7) Kräutler, B.; Hughes, M.; Caderas, C. Thermal Methyl-Group Transfer between Methylcobalt(III) Corrinates and Cobalt(II) Corrinates. Equilibration Experiments with Heptamethyl Cobyrinates and Cobalamins. *Helv. Chim. Acta* **1986**, *69*, 1571–1575.
- (8) Brown, K. L. Chemistry and Enzymology of Vitamin B₁₂. *Chem. Rev.* **2005**, *105*, 2075–2149.
- (9) Banerjee, R. *Chemistry and Biochemistry of B₁₂*; Wiley, 1999.
- (10) Wierzba, A. J.; Hassan, S.; Gryko, D. Synthetic Approaches toward Vitamin B₁₂ Conjugates. *Asian J. Org. Chem.* **2019**, *8*, 6–24.
- (11) Tahara, K.; Pan, L.; Ono, T.; Hisaeda, Y. Learning from B₁₂ Enzymes: Biomimetic and Bioinspired Catalysts for Eco-Friendly Organic Synthesis. *Beilstein J. Org. Chem.* **2018**, *14*, 2553–2567.
- (12) Pattenden, G. Cobalt-Mediated Radical Reactions in Organic Synthesis. *Chem. Soc. Rev.* **1988**, *17*, 361–182.
- (13) Giedyk, M.; Goliszewska, K.; Gryko, D. Vitamin B₁₂ Catalysed Reactions. *Chem. Soc. Rev.* **2015**, *44*, 3391–3404.
- (14) Karczewski, M.; Ociepa, M.; Pluta, K.; ó Proinsias, K.; Gryko, D. Vitamin B₁₂ Catalysis: Probing the Structure/Efficacy Relationship. *Chem. - A Eur. J.* **2017**, *23*, 7024–7030.
- (15) Prina Cerai, G.; Morandi, B. Atom-Economical Cobalt-Catalysed Regioselective Coupling of Epoxides and Aziridines with Alkenes. *Chem. Commun.* **2016**, *52*, 9769–9772.
- (16) Giedyk, M.; Goliszewska, K.; Gryko, D. Vitamin B₁₂ Catalysed Reactions. *Chem. Soc. Rev.* **2015**, *44*, 3391–3404.
- (17) Turkowska, J.; Durka, J.; Ociepa, M.; Gryko, D. Reversal of Regioselectivity in Reactions of Donor–Acceptor Cyclopropanes with Electrophilic Olefins. *Chem. Commun.* **2022**.
- (18) Motwani, H. V.; Fred, C.; Haglund, J.; Golding, B. T.; Törnqvist, M. Cob(I)Alamin for Trapping Butadiene Epoxides in Metabolism with Rat S9 and for Determining Associated Kinetic Parameters. *Chem. Res. Toxicol.* **2009**, *22*, 1509–1516.

- (19) Patel, V. F.; Pattenden, G. Free Radical Reactions in Synthesis. Homolysis of Alkylcobalt Complexes in the Presence of Radical-Trapping Agents. *J. Chem. Soc. Perkin Trans. 1* **1990**, No. 10, 2703.
- (20) Moyeux, A. Cobalt-Catalyzed Cross-Coupling Reactions. **2010**, No. Scheme 1, 1435–1462.
- (21) Crossley, S. W. M.; Obradors, C.; Martinez, R. M.; Shenvi, R. A. Mn-, Fe-, and Co-Catalyzed Radical Hydrofunctionalizations of Olefins. *Chem. Rev.* **2016**, *116*, 8912–9000.
- (22) Bhandal, H.; Patel, V. F.; Pattenden, G.; Russell, J. J. Cobalt-Mediated Radical Reactions in Organic Synthesis. Oxidative Cyclisations of Aryl and Alkyl Halides Leading to Functionalised Reduced Heterocycles and Butyrolactones. *J. Chem. Soc. Perkin Trans. 1* **2004**, No. 10, 2691.
- (23) Nuthakki, B.; Bobbitt, J. M.; Rusling, J. F. Influence of Microemulsions on Enantioselective Synthesis of (R)-Cyclopent-2-Enol Catalyzed by Vitamin B₁₂. *Langmuir* **2006**, *22*, 5289–5293.
- (24) Su, H.; Walder, L.; Zhang, Z.; Scheffold, R. Asymmetric Catalysis by Vitamin B₁₂. The Isomerization of Achiral Epoxides to Optically Active Allylic Alcohols. *Helv. Chim. Acta* **1988**, *71*, 1073–1078.
- (25) Hill, H. A. O.; Pratt, J. M.; O’Riordan, M. P.; Williams, F. R.; Williams, R. J. P. The Chemistry of Vitamin B₁₂. Part XV. Catalysis of Alkyl Halide Reduction by Vitamin B_{12a}: Studies Using Controlled Potential Reduction. *J. Chem. Soc. A Inorganic, Phys. Theor.* **1971**, 1859–1962.
- (26) Komeyama, K.; Ohata, R.; Kiguchi, S.; Osaka, I. Highly Nucleophilic Vitamin B₁₂ -Assisted Nickel-Catalysed Reductive Coupling of Aryl Halides and Non-Activated Alkyl Tosylates. *Chem. Commun.* **2017**, *53*, 6401–6404.
- (27) Bonhôte, P.; Scheffold, R. Asymmetric Catalysis by Vitamin B₁₂. The Mechanism of the Cob(I)Alamin-Catalyzed Isomerization of 1,2-Epoxy-cyclopentane to (R)-Cyclopent-2-Enol. *Helv. Chim. Acta* **1991**, *74*, 1425–1444.
- (28) Giedyk, M.; Shimakoshi, H.; Goliszewska, K.; Gryko, D.; Hisaeda, Y. Electrochemistry and Catalytic Properties of Amphiphilic Vitamin B₁₂ Derivatives in Nonaqueous Media. *Dalt. Trans.* **2016**, *45*, 8340–8346.
- (29) Troxler, T.; Scheffold, R. Asymmetric Catalysis by Vitamin B₁₂: The Isomerization of Achiral Cyclopropanes to Optically Active Olefins. *Helv. Chim. Acta* **1994**, *77*, 1193–1202.
- (30) Shimakoshi, H.; Tokunaga, M.; Hisaeda, Y. Hydrophobic Vitamin B₁₂. Part 19: For Part 18 See Ref. 22. Electroorganic Reaction of DDT Mediated by Hydrophobic Vitamin B₁₂. *Dalt. Trans.* **2004**, *7*, 878.
- (31) Hisaeda, Y.; Tahara, K.; Shimakoshi, H.; Masuko, T. Bioinspired Catalytic Reactions with Vitamin B₁₂ Derivative and Photosensitizers. *Pure Appl. Chem.* **2013**, *85*, 1415–1426.
- (32) Scheffold, R.; Abrecht, S.; Orlinski, R.; Ruf, H.-R.; Stamouli, P.; Tinembart, O.; Walder, L.; Weymuth, C. Vitamin B₁₂-Mediated Electrochemical Reactions in the Synthesis of Natural Products. *Pure Appl. Chem.* **1987**, *59*, 363–372.
- (33) Shimakoshi, H.; Luo, Z.; Inaba, T.; Hisaeda, Y. Electrolysis of Trichloromethylated Organic Compounds under Aerobic Conditions Catalyzed by the B₁₂ Model Complex for Ester and Amide Formation. *Dalt. Trans.* **2016**, *45*, 10173–10180.
- (34) Komeyama, K.; Tsunemitsu, R.; Michiyuki, T.; Yoshida, H.; Osaka, I. Ni/Co-Catalyzed Homocoupling of Alkyl Tosylates. *Molecules* **2019**, *24*, 1458.

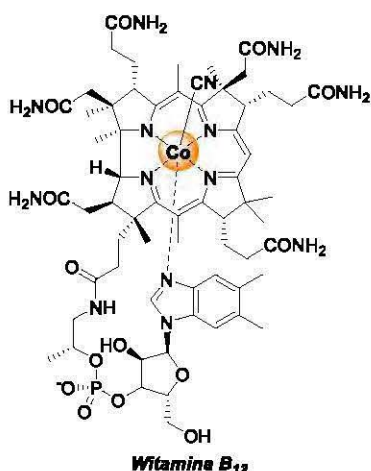
- (35) Liu, H.; Kornobis, K.; Lodowski, P.; Jaworska, M.; Kozłowski, P. M. TD-DFT Insight into Photodissociation of the Co-C Bond in Coenzyme B₁₂. *Front. Chem.* **2014**, *1*, 1–12.
- (36) Garabato, B. D.; Lodowski, P.; Jaworska, M.; Kozłowski, P. M. Mechanism of Co-C Photodissociation in Adenosylcobalamin. *Phys. Chem. Chem. Phys.* **2016**, *18*, 19070–19082.
- (37) Kuta, J.; Patchkovskii, S.; Zgierski, M. Z.; Kozłowski, P. M. Performance of DFT in Modeling Electronic and Structural Properties of Cobalamins. *J. Comput. Chem.* **2006**, *27*, 1429–1437.
- (38) Li, G.; Zhang, F. F.; Chen, H.; Yin, H. F.; Chen, H. L.; Zhang, S. Y. Determination of Co–C Bond Dissociation Energies for Organocobalt Complexes Related to Coenzyme B₁₂ Using Photoacoustic Calorimetry. *J. Chem. Soc. Dalton Trans.* **2002**, No. 1, 105–110.
- (39) Lexa, D.; Savéant, J. M.; Soufflet, J. P. Chemical Catalysis of the Electrochemical Reduction of Alkyl Halides. Comparison between Cobalt-Tetraphenyl Porphin and Vitamin B₁₂ Derivatives. *J. Electroanal. Chem.* **1979**, *100*, 159–172.
- (40) Scheffold, R.; Dike, M.; Dike, S.; Herold, T.; Walder, L. Synthesis and Reactions of Porphine-Type Metal Complexes. 8. Carbon-Carbon Bond Formation Catalyzed by Vitamin B₁₂ and a Vitamin B₁₂ Model Compound. Electrosynthesis of Bicyclic Ketones by 1,4 Addition. *J. Am. Chem. Soc.* **1980**, *102*, 3642–3644.
- (41) Shimakoshi, H.; Tokunaga, M.; Baba, T.; Hisaeda, Y. Photochemical Dechlorination of DDT Catalyzed by a Hydrophobic Vitamin B₁₂ and a Photosensitizer under Irradiation with Visible Light. *Chem. Commun.* **2004**, No. 16, 1806.
- (42) Shey, J.; Donk, W. A. Van Der; V, S. M. A. Mechanistic Studies on the Vitamin B₁₂ - Catalyzed Dechlorination of Chlorinated Alkenes. University of Illinois at Urbana - Champaign Perchloroethylene (PCE) Is an Abundant Pollutant That Ranks High on the Priority List of the US Environmental Protect. **2000**, No. c, 12403–12404.
- (43) Scheffold, R.; Amble, E. Vitamin B₁₂ and a Vitamin B₁₂ Model Compound as Catalysts of Reductive Removal of B-Haloethyl Protecting Groups from Acids. *Angew. Chemie Int. Ed. English* **1980**, *19*, 629–630.
- (44) Forbes, C. L.; Franck, R. W. Improved Version of the Fischer-Zach Synthesis of Glycols: Vitamin B₁₂ Catalyzed Reductive Elimination of Glycosyl Bromides. *J. Org. Chem.* **1999**, *64*, 1424–1425.
- (45) Bam, R.; Pollatos, A. S.; Moser, A. J.; West, J. G. Mild Olefin Formation via bioinspired Vitamin B₁₂ photocatalysis. *Chem. Sci.* **2021**, *12*, 1736–1744.
- (46) Giedyk, M.; Fedosov, S. N.; Gryko, D. An Amphiphilic, Catalytically Active, Vitamin B₁₂ Derivative. *Chem. Commun.* **2014**, *50*, 4674–4676.
- (47) Shey, J.; McGinley, C. M.; McCauley, K. M.; Dearth, A. S.; Young, B. T.; Van der Donk, W. A. Mechanistic Investigation of a Novel Vitamin B₁₂-Catalyzed Carbon-Carbon Bond Forming Reaction, the Reductive Dimerization of Arylalkenes. *J. Org. Chem.* **2002**, *67*, 837–846.
- (48) Erdmann, P.; Schäfer, J.; Springer, R.; Zeitz, H. -G; Giese, B. 1,2-Stereoinduction in Radicals and Anions: A Comparison between Hydrogen Abstraction and Protonation. *Helv. Chim. Acta* **1992**, *75*, 638–644.
- (49) Komeyama, K.; Michiyuki, T.; Teshima, Y.; Osaka, I. Visible Light-Driven Giese Reaction with Alkyl Tosylates Catalysed by Nucleophilic Cobalt. *RSC Adv.* **2021**, *11*, 3539–3546.
- (50) Smoleń, S.; Wincenciuk, A.; Drapała, O.; Gryko, D. Vitamin B₁₂-Catalyzed Dicarbofunctionalization of Bromoalkenes under Visible Light Irradiation. *Synth.* **2021**, *53*,

1645–1653.

- (51) Proinsias, K. O.; Jackowska, A.; Radzewicz, K.; Giedyk, M.; Gryko, D. Vitamin B₁₂ Catalyzed Atom Transfer Radical Addition. *Org. Lett.* **2018**, *20*, 296–299.
- (52) Chen, L.; Hisaeda, Y.; Shimakoshi, H. Visible Light-Driven, Room Temperature Heck-Type Reaction of Alkyl Halides with Styrene Derivatives Catalyzed by B₁₂ Complex. *Adv. Synth. Catal.* **2019**, *361*, 2877–2884.
- (53) Chen, L.; Kametani, Y.; Imamura, K.; Abe, T.; Shiota, Y.; Yoshizawa, K.; Hisaeda, Y.; Shimakoshi, H. Visible Light-Driven Cross-Coupling Reactions of Alkyl Halides with Phenylacetylene Derivatives for C(Sp³)-C(Sp) Bond Formation Catalyzed by a B₁₂ Complex. *Chem. Commun.* **2019**, *55*, 13070–13073.
- (54) Giedyk, M.; Goliszewska, K.; Ó Proinsias, K.; Gryko, D. Cobalt(I)-Catalysed CH-Alkylation of Terminal Olefins, and Beyond. *Chem. Commun.* **2016**, *52*, 1389–1392.
- (55) Chen, Y.; Zhang, X. P. Vitamin B₁₂ Derivatives as Natural Asymmetric Catalysts: Enantioselective Cyclopropanation of Alkenes. *J. Org. Chem.* **2004**, *69*, 2431–2435.
- (56) Takai, K.; Toratsu, C. B₁₂-Catalyzed Generation of Allylic Chromium Reagents from 1,3-Dienes, CrCl₂, and Water. *J. Org. Chem.* **1998**, *63*, 6450–6451.
- (57) Shimakoshi, H.; Hisaeda, Y. Oxygen-Controlled Catalysis by Vitamin B₁₂-TiO₂: Formation of Esters and Amides from Trichlorinated Organic Compounds by Photoirradiation. *Angew. Chemie - Int. Ed.* **2015**, *54*, 15439–15443.
- (58) O'Brien, A. G.; Maruyama, A.; Inokuma, Y.; Fujita, M.; Baran, P. S.; Blackmond, D. G. Radical C-H Functionalization of Heteroarenes under Electrochemical Control. *Angew. Chemie - Int. Ed.* **2014**, *53*, 11868–11871.
- (59) Hossain, M. J.; Ono, T.; Wakiya, K.; Hisaeda, Y. A Vitamin B₁₂ Derivative Catalyzed Electrochemical Trifluoromethylation and Perfluoroalkylation of Arenes and Heteroarenes in Organic Media. *Chem. Commun.* **2017**, *53*, 10878–10881.
- (60) Sladojevich, F.; McNeill, E.; Börgel, J.; Zheng, S. L.; Ritter, T. Condensed-Phase, Halogen-Bonded CF₃I and C₂F₅I Adducts for Perfluoroalkylation Reactions. *Angew. Chemie - Int. Ed.* **2015**, *54*, 3712–3716.
- (61) Ji, Y.; Brueckl, T.; Baxter, R. D.; Fujiwara, Y.; Seiple, I. B.; Su, S.; Blackmond, D. G.; Baran, P. S. Innate C-H Trifluoromethylation of Heterocycles. *Proc. Natl. Acad. Sci. U. S. A.* **2011**, *108*, 14411–14415.
- (62) Banerjee, A.; Lei, Z.; Ngai, M. Y. *Acyl Radical Chemistry via Visible-Light Photoredox Catalysis*; 2019; Vol. 51.
- (63) Enders, D.; Niemeier, O.; Henseler, A. Organocatalysis by N-Heterocyclic Carbenes. *Chem. Rev.* **2007**, *107*, 5606–5655.
- (64) Bugaut, X.; Glorius, F. Organocatalytic Umpolung: N-Heterocyclic Carbenes and Beyond. *Chem. Soc. Rev.* **2012**, *41*, 3511–3522.
- (65) Stetter, H.; Kuhlmann, H. The Catalyzed Nucleophilic Addition of Aldehydes to Electrophilic Double Bonds. *Organic Reactions*. 1991, pp 407–496.
- (66) Duncton, M. A. J. Minisci Reactions: Versatile CH-Functionalizations for Medicinal Chemists. *Medchemcomm* **2011**, *2*, 1135–1161.

- (67) Chatgililoglu, C.; Crich, D.; Komatsu, M.; Ryu, I. Chemistry of Acyl Radicals. *Chem. Rev.* **1999**, *99*, 1991–2070.
- (68) Boger, D. L.; Mathvink, R. J. Radicals: Intermolecular. **1992**, No. 17, 1429–1443.
- (69) Liu, W.; Li, Y.; Liu, K.; Li, Z. Iron-Catalyzed Carbonylation-Peroxidation of Alkenes With. **2011**, *5*, 10756–10759.
- (70) Scheffold, R.; Orlinski, R. Synthesis and Reactions of Porphine-Type Metal Complexes. 15. Carbon-Carbon Bond Formation by Light Assisted B₁₂-Catalysis. Nucleophilic Acylation of Michael Olefins. *J. Am. Chem. Soc.* **1983**, *105*, 7200–7202.
- (71) Norman, A. R.; Yousif, M. N.; McErlean, C. S. P. Photoredox-Catalyzed Indirect Acyl Radical Generation from Thioesters. *Org. Chem. Front.* **2018**, *5*, 3267–3298.
- (72) Ociepa, M.; Baka, O.; Narodowiec, J.; Gryko, D. Light-Driven Vitamin B₁₂-Catalysed Generation of Acyl Radicals from 2-S-Pyridyl Thioesters. *Adv. Synth. Catal.* **2017**, *359*, 3560–3565.
- (73) Ociepa, M.; Wierzba, A. J.; Turkowska, J.; Gryko, D. Polarity-Reversal Strategy for the Functionalization of Electrophilic Strained Molecules via Light-Driven Cobalt Catalysis. *J. Am. Chem. Soc.* **2020**, *142*, 5355–5361.
- (74) Wang, C. Electrophilic Ring Opening of Small Heterocycles. *Synthesis (Stuttg.)*. **2017**, *49*, 5307–5319.
- (75) Huang, C.-Y. (Dennis); Doyle, A. G. The Chemistry of Transition Metals with Three-Membered Ring Heterocycles. *Chem. Rev.* **2014**, *114*, 8153–8198.
- (76) Pineschi, M. Asymmetric Ring-Opening of Epoxides and Aziridines with Carbon Nucleophiles. *European J. Org. Chem.* **2006**, *2006*, 4979–4988.
- (77) Bartmann, E. Organometallic Derivatives of Epoxides. *Angew. Chemie Int. Ed. English* **1986**, *25*, 653–654.
- (78) Zhao, Y.; Weix, D. J. Nickel-Catalyzed Regiodivergent Opening of Epoxides with Aryl Halides: Co-Catalysis Controls Regioselectivity. *J. Am. Chem. Soc.* **2014**, *136*, 48–51.
- (79) Parasram, M.; Shields, B. J.; Ahmad, O.; Knauber, T.; Doyle, A. G. Regioselective Cross-Electrophile Coupling of Epoxides and (Hetero)Aryl Iodides via Ni/Ti/Photoredox Catalysis. *ACS Catal.* **2020**, *10*, 5821–5827.
- (80) Bull, J. A.; Croft, R. A.; Davis, O. A.; Doran, R.; Morgan, K. F. Oxetanes: Recent Advances in Synthesis, Reactivity, and Medicinal Chemistry. *Chem. Rev.* **2016**, *116*, 12150–12233.
- (81) Yang, W.; Wang, Z.; Sun, J. Enantioselective Oxetane Ring Opening with Chloride: Unusual Use of Wet Molecular Sieves for the Controlled Release of HCl. *Angew. Chemie - Int. Ed.* **2016**, *55*, 6954–6958.
- (82) Sandvoß, A.; Wiest, J. M. Recent Advances in Enantioselective Desymmetrizations of Prochiral Oxetanes. *Chem. - A Eur. J.* **2021**, *27*, 5871–5879.
- (83) Strassfeld, D. A.; Wickens, Z. K.; Picazo, E.; Jacobsen, E. N. Highly Enantioselective, Hydrogen-Bond-Donor Catalyzed Additions to Oxetanes. *J. Am. Chem. Soc.* **2020**, *142*, 9175–9180.

5. STRESZCZENIE W JĘZYKU POLSKIM



Witamina B₁₂ należy do grupy składników odżywczych istotnych dla organizmów żywych. W komórkach eukariotycznych pełni rolę kofaktora, który uczestniczy w wielu procesach biochemicznych (transfer grupy metylowej, izomeryzacja czy dehalogenowanie). Jej wysoka zdolność katalityczna uwarunkowana jest występowaniem słabego wiązania kowalencyjnego Co-C, które może, pod wpływem działania czynników redukujących, światła bądź temperatury ulec homolitycznemu rozerwaniu stając się tym samym źródłem rodników. Cecha ta, w połączeniu z jej nietoksycznością, stanowi idealną alternatywę dla drogich i toksycznych katalizatorów zawierających

metale ciężkie takie jak ołów, ruten czy iryd. Opracowano wiele reakcji katalizowanych tym związkiem, jednakże w większości z nich źródłem rodników są halogenki alkilowe.

Celem mojej pracy było rozszerzenie grupy prekursorów rodników użytecznych w katalizie witaminą B₁₂, które stanowiłyby dopełnienie aktualnie istniejącej grupy substratów.

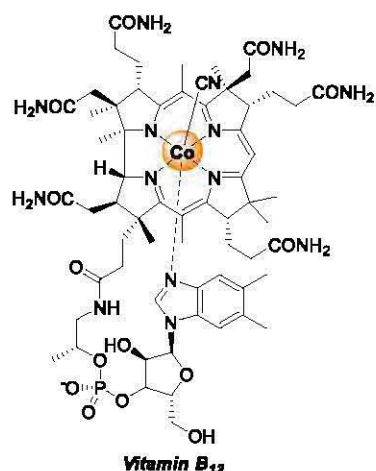
W pierwszej części swoich badań skupiłam się na sprawdzeniu możliwości generowania rodników alkilowych z epoksydów. W przypadku fotokatalitycznych reakcji z udziałem epoksydów arylowych, atak reagentów następuje od strony bardziej zatłoczonej sterycznie, prowadząc do reaktywnych rodników benzytowych. Wykazałam, że duże zatłoczenie steryczne witaminy B₁₂ powoduje generowanie rodników pierwszorzędowych, które w reakcji z elektrofilami dają alkohole drugorzędowe. Zakres stosowalności opracowanej przeze mnie metody obejmuje również epoksydy alifatyczne i cykliczne.

W kolejnym etapie swojej pracy postanowiłam sprawdzić, czy oksetany mogą być prekursorami rodników w katalizie witaminą B₁₂. Ze względu na prawie dwukrotnie większą energię swobodną Gibbsa otwierania pierścienia, w porównaniu do epoksydów, kluczowym etapem badań było wybranie odpowiedniego kwasu Lewisa. Najlepszy okazał się bromek trimetylosililu. Optymalizacja warunków reakcji pozwoliła na uzyskanie finalnych produktów z bardzo dobrymi wydajnościami. Metoda ta jest użyteczna zarówno w reakcji typu Giese jak również w reakcji sprzęgania krzyżowego.

W ostatniej fazie prac zaprojektowałam reagent, który pozwolił na generowanie zarówno rodników alkilowych jak i acylowych. W oparciu o profil kinetyczny, udowodniłam że tworzenie rodników alkilowych jest procesem determinującym szybkość reakcji.

Przeprowadzone przeze mnie badania, wykazały, że w reakcjach katalizowanych witaminą B₁₂ substratami, oprócz powszechnie stosowanych halogenków alkilowych, mogą być również epoksydy i oksetany.

6. STRESZCZENIE W JĘZYKU ANGIELSKIM / ABSTRACT IN ENGLISH



Vitamin B₁₂ is a complex biomolecule of great importance for the normal functioning of all living organisms. In eukaryotic cells, it acts as a cofactor that is involved in many biochemical processes (methyl transfer, isomerization, or dehalogenation). Its high catalytic capacity is conditioned by the presence of a weak covalent Co-C bond that can be selectively cleaved under reducing conditions, light or temperature becoming a source of radicals. This characteristic feature together with its non-toxicity is an ideal alternative to expensive and toxic catalysts containing heavy metals such as lead, ruthenium, or iridium. Many reactions catalyzed by vitamin B₁₂ have been developed, of which, the majority utilise alkyl halides as a source of radicals.

The aim of this work was to expand the library of radical precursors useful in the catalysis of vitamin B₁₂, which would enhance the applicability of its utilization in organic synthesis.

In the first part of this work, I have focused on exploring the possibility of generating alkyl radicals from epoxides. In the case of photocatalytic reactions involving aryl epoxides, the attack of the reagents occurs from the more sterically hindered side, leading to highly reactive benzyl radicals. I revealed that in contrast to known methods, the bulky vitamin B₁₂ catalyst can generate primary radicals, which react with electrophiles, to produce secondary alcohols. The range of applicability of the developed method includes aliphatic and cyclic epoxides.

In the next part of my work, I decided to check whether oxetanes can be a radical precursors in vitamin B₁₂ catalysis. Due to oxetanes having nearly double the Gibbs free energy compared to the ring opening of epoxides, the key step in this transformation was to select the appropriate Lewis acid. It was revealed that bromotrimethylsilane was the optimum Lewis acid. The optimization of the reaction conditions allowed the formation of the desired products in excellent yields. This method is useful for both Giese-type and cross-coupling reactions.

Finally, I have designed a reagent, that can generate, both, acyl and alkyl radicals. The kinetic profile revealed that the generation of alkyl radicals is a rate-determining process.

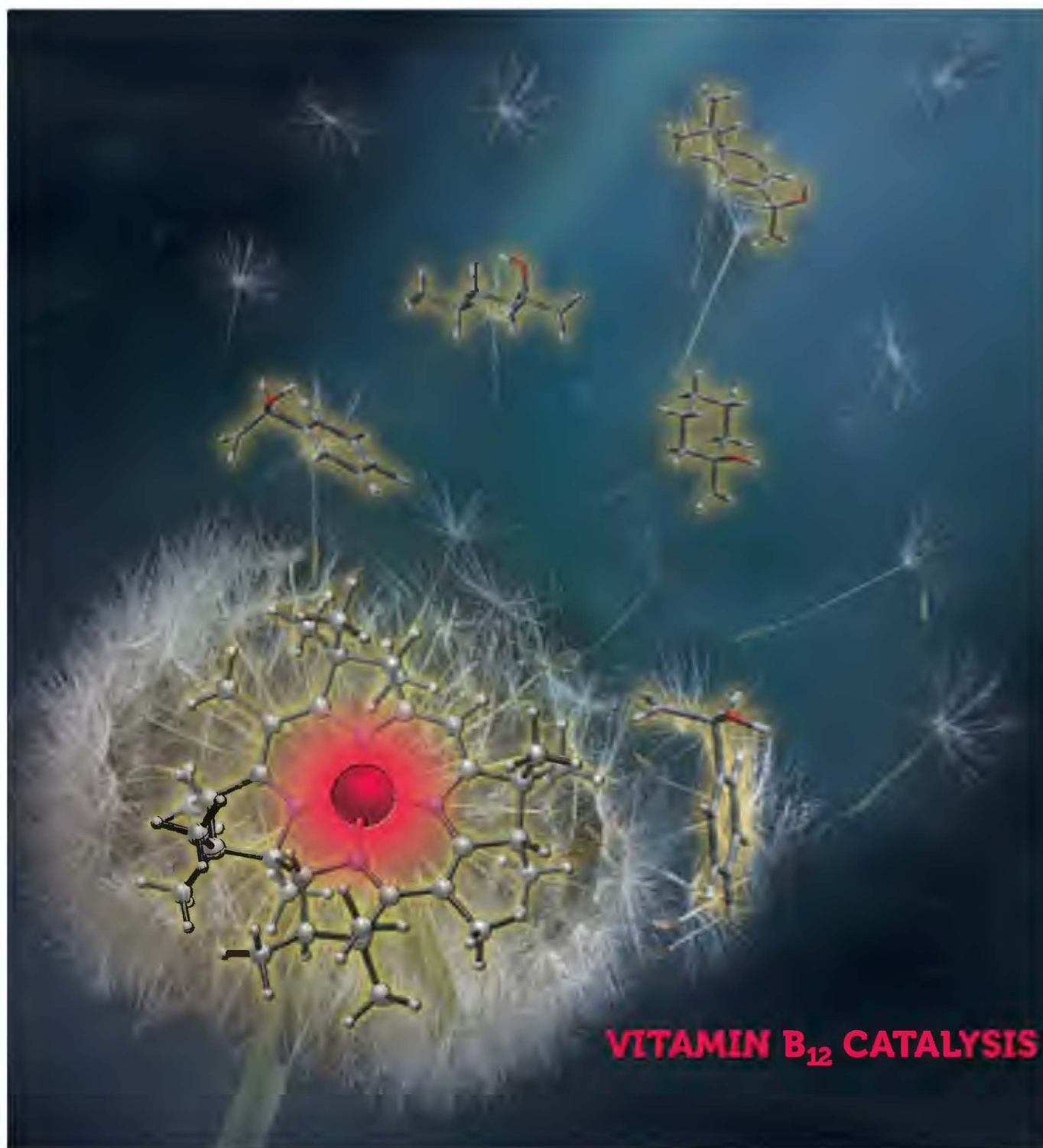
In summary, my studies showed that epoxides and oxetanes can be used, in addition to commonly used alkyl halides, in vitamin B₁₂-catalyzed reactions.

7. PUBLIKACJE ORYGINALNE

June 30, 2021
Volume 143
Number 25
pubs.acs.org/JACS

J | A | C | S

JOURNAL OF THE AMERICAN CHEMICAL SOCIETY



ACS Publications
Most Trusted. Most Cited. Most Read.

www.acs.org

<https://rcin.org.pl>

Cobalt Catalyst Determines Regioselectivity in Ring Opening of Epoxides with Aryl Halides

Aleksandra Potrzęsaj, Mateusz Musiejuk, Wojciech Chaładaj, Maciej Giedyk,* and Dorota Gryko*

Cite This: *J. Am. Chem. Soc.* 2021, 143, 9368–9376

Read Online

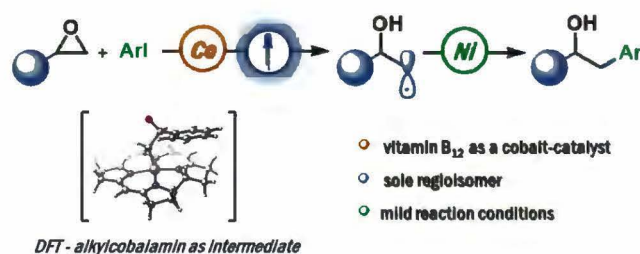
ACCESS |

Metrics & More

Article Recommendations

Supporting Information

ABSTRACT: Ring-opening of epoxides furnishing either linear or branched products belongs to the group of classic transformations in organic synthesis. However, the regioselective cross-electrophile coupling of aryl epoxides with aryl halides still represents a key challenge. Herein, we report that the vitamin B₁₂/Ni dual-catalytic system allows for the selective synthesis of linear products under blue-light irradiation, thus complementing methodologies that give access to branched alcohols. Experimental and theoretical studies corroborate the proposed mechanism involving alkylcobalamin as an intermediate in this reaction.



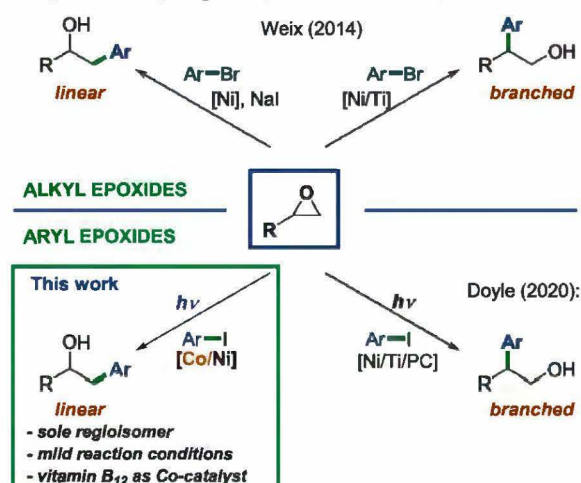
INTRODUCTION

Driven by high demand for sustainable and efficient reactions, the discovery of selective reactivity patterns remains a key challenge. As epoxides are crucial building blocks in the synthesis of nonsymmetrical alcohols, their regioselective reactions have been intensively studied.^{1–3} In particular, considerable attention has been recently devoted to the utilization of epoxides in cross-electrophile couplings leading, in general, to regioisomeric (linear and branched) products (Scheme 1).^{4–7} It has been shown that the innately electrophilic epoxides can be transformed into radicals and, as such, be involved in a transition-metal-catalytic cycle.^{7,8} Depending on reaction conditions, the initial nucleophilic

attack occurs predominantly at either the terminal or internal carbon atom.

In 2014, Weix and co-workers developed a nickel-catalyzed, regiodivergent cross-electrophile coupling of epoxides with various halides and triflates.⁶ For aliphatic epoxides (Scheme 1, upper part), the regioselectivity of the ring-opening step depends on the cocatalyst used. Sodium iodide promotes the formation of a linear product. The nucleophilic attack of the iodide anion at the less substituted carbon atom affords iodohydrin, which in turn undergoes reduction and Ni-catalyzed coupling with an electrophile. On the other hand, in the presence of a titanocene cocatalyst secondary alkyl radicals are generated, facilitating the formation of branched products.^{9,10} Aryl epoxides, however, react predominantly at the benzylic position, regardless of the conditions employed. A similar reactivity pattern has been recently reported by the Doyle group, who used organic iodides and the Ti/Ni/photoredox catalytic system in ring-opening reactions of three major classes of epoxides, namely, aryl, aliphatic, and bicyclic (Scheme 1, lower part).¹¹ By changing a nickel complex, the authors were able to transform aliphatic epoxides into linear products, while aryl epoxides selectively formed branched ones. Despite the enormous importance of these contributions, the synthesis of linear products from aryl epoxides via cross-electrophile coupling still represents an unsolved challenge.

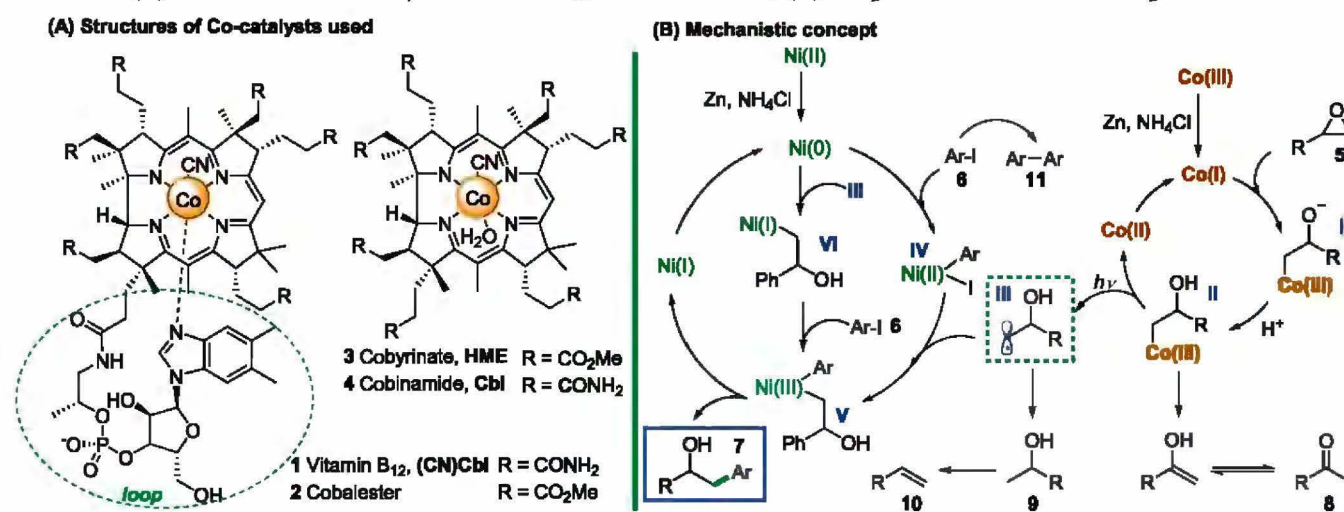
Scheme 1. Regioselective Nickel-Catalyzed Cross-Electrophile Coupling of Epoxides with Aryl Halides



Received: January 19, 2021

Published: June 3, 2021



Scheme 2. (A) Structures of Cocatalysts: Vitamin B₁₂ and Derivatives; (B) Proposed Mechanistic Concept

Our recent work on the alkylation of strained molecules showed that cobalt catalysis opens the path to a polarity-reversal strategy for radical couplings.¹² We questioned whether it would be possible to adapt this methodology to achieve selective reactions of epoxides. Herein, we disclose that the nucleophilicity of Co(I) species along with sterically restricted side chains allows generating C-radicals from epoxides in a selective manner and engage them in Ni-catalyzed cross-coupling.

RESULTS AND DISCUSSION

Design of the Catalytic System. Vitamin B₁₂ (1, cobalamin) is a natural cobalt complex of remarkable stability and high biological importance.^{13–15} Due to the unique ability to form light-sensitive cobalt–carbon bonds, vitamin B₁₂ (1) and its hydrophobic and amphiphilic derivatives 2 and 3 (Scheme 2A)^{16–21} have also been adopted for synthetic chemistry and used as redox mediators for the generation of various radicals.^{22,23} We assumed that a nucleophilic Co(I) complex that forms upon the reduction of cobalamin should open electrophilic epoxides, generating alkyl cobalamins (Scheme 2B). Such intermediates, upon light irradiation, undergo the homolytic Co–C bond cleavage to give alkyl radicals, which can be engaged in a number of both radical reactions and transition-metal-catalyzed cross-couplings. *Importantly, from the viewpoint of regioselective design, a bulky vitamin B₁₂ catalyst should attack an epoxide from the less sterically hindered side.* This kinetic factor may prevail over the high thermodynamic preference for stabilized benzyl radicals and thus allow the selective formation of primary radicals of type III.

To examine our hypothesis, in the first instance, we theoretically investigated the possible formation of alkyl radicals via a sequence of the epoxide ring opening with reduced vitamin B₁₂ (Co(I) complex) followed by homolytic cleavage of the Co–C bond in alkyl cobalamin II. DFT calculations were performed with Gaussian 16.²⁴ Geometry optimizations were computed at the BP86/6-31G(d) level of theory with the D3 version of Grimme's empirical dispersion correction and solvation (acetone) with the SMD model. Frequency analysis was performed at the same level to provide correction to thermodynamic functions and confirm the nature of optimized structures (minima and transition states featured

zero or one imaginary frequency, respectively). Single-point energies were computed at the BP86/6-311++G(2df,p) level of theory with the D3 version of Grimme's empirical dispersion correction and solvation (acetone) with the SMD model. Several hybrid and long-range corrected functionals were tested for the model reaction (see Supporting Information (SI) for details). BP86 was, however, selected for further studies due to good performance reported for both ground and excited state calculations of cobalamin systems.^{25–30} We performed calculations approximating the structure of vitamin B₁₂ (1) with a Co-corrin complex bearing 15 methyl groups, reflecting the substitution pattern at the periphery of the macrocyclic ring (Figure 1).

The calculated Gibbs free energy profile for the benchmark reaction of styrene oxide (5a) with the Co-corrin complex is depicted in Figure 1. Two paths, involving the nucleophilic attack on either side of the epoxide, were considered. In line with our assumptions, the ring opening of the epoxide with the nucleophilic Co(I) complex should proceed at the less hindered terminus with a 43.7 kJ/mol barrier, accessible even under mild conditions (black path). The barrier for the analogous reaction at the more hindered side is ~8 kJ/mol higher (gray path). Sterically driven differences in the reactivity might be even more pronounced for native vitamin B₁₂ or its derivatives compared to the selected model, due to presence of more sizable substituents at the corrin ring. Then, the resulting Co(III) complex (I) is protonated, providing intermediate II. As expected for alkyl cobalamins, the Co–C(sp³) bond in IIa and IIb is relatively weak and quite vulnerable to homolytic cleavage toward alkyl radical IIIa or IIIb and a Co(II) complex ($\Delta G = 141.9$ and 82.6 kJ/mol, respectively). In particular, IIa could undergo Co–C photodissociation, presumably through the mechanism proposed by Kozłowski, involving generation of the singlet radical pair from the first electronically excited state (S1).^{31–33}

The lowest singlet (IIa-S1) vertically excited states of intermediate IIa were found at 2.20 eV (212.5 kJ/mol, TD BP86-D3/6-311++G(2df,p)), while the relaxed S1 state lies 28.2 kJ/mol lower and features elongation of the Co–C bond by 0.22 Å. Noticeably, due to the preference for the nucleophilic attack at the less hindered side of the epoxide, the above-described path (black) should provide access to a 2-hydroxy-2-phenyl ethyl radical (IIIa), even though isomeric

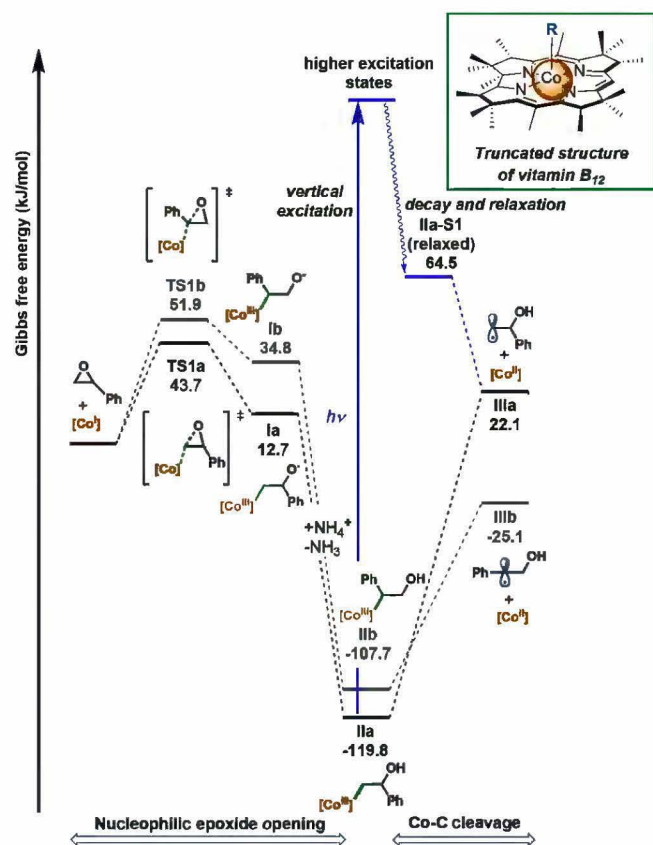
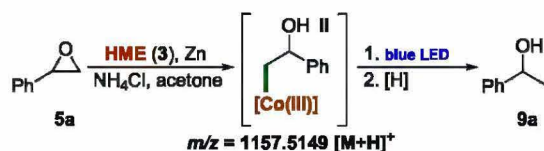


Figure 1. Calculated Gibbs free energy profile for the reaction of styrene oxide with the Co(I)-corrin complex.

benzyl radical **IIIb** is thermodynamically more stable by 47.2 kJ/mol.

To support theoretical studies, the reductive photochemical ring opening of styrene oxide (**5a**) in the presence of a hydrophobic vitamin B₁₂ derivative, HME (**3**), was performed (Scheme 3). The selected Co complex **3** allows convenient monitoring of reactive intermediates by ESI mass spectrometry due to its tendency to undergo facile ionization.

Scheme 3. Vitamin B₁₂-Catalyzed Ring Opening of Epoxide **5**



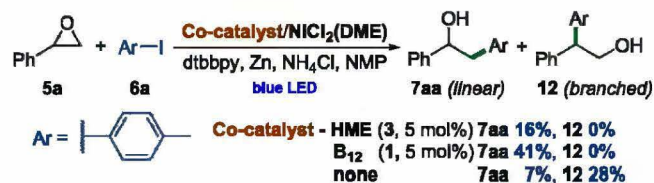
Indeed, the formation of intermediate alkyl-cobalt(III) complex **II** was observed by HR-MS ($m/z = 1157.5149 [M + H]^+$, see the SI, Section 6.2), which is in good agreement with previous reports by Scheffold^{34–38} and Rusling,³⁹ who used vitamin B₁₂ (**1**) for isomerization of symmetrical epoxides to allyl alcohols. Satisfyingly, alcohol **9a** with a –OH group at the benzylic position formed just after 30 min. These results corroborate the proposed mechanistic concept in which vitamin B₁₂ opens the aromatic epoxide from the less hindered side at the thermodynamic expense of forming the less stable radical **III** in the subsequent light-induced cleavage step.

Knowing that B₁₂ catalysis can be merged with metal-catalyzed reactions,¹² we next evaluated the feasibility of

incorporating the generated alkyl radicals in the Ni catalytic cycle. Adding electrophilic aryl halides should enable cross-electrophile coupling and thus provide a convenient method for the carbon–carbon bond formation.⁴⁰ The plausible mechanism for the reaction of epoxides with aryl halides in the presence of the B₁₂/Ni catalytic system based on literature reports is outlined in Scheme 2B.^{7,41–43} The coupling requires the cooperation of both transition metal complexes (Co and Ni) that are activated by Zn/NH₄Cl.^{44,45} The oxidative addition of aryl halide to Ni(0) produces aryl nickel(II) species **IV**, which undergoes subsequent alkylation with radical **III** and generates intermediate **V**. Alternatively, the same Ni(III) species can originate from the interception of alkyl radical **III** by Ni(0), preceding the oxidative addition, as has been recently proposed by Molander and Kozlowski.⁴⁶ Both these possible pathways are followed by irreversible reductive elimination, leading to the regioselective formation of a linear product. Cobalt(II) and nickel(I) complexes are regenerated to Co(I) and Ni(0) with Zn, thereby closing the cycles.

Styrene oxide (**5a**), when subjected to the reaction with *p*-iodotoluene (**6a**) in the presence of HME (**3**) and NiCl₂(DME), generated desired linear product **7aa** as a single regioisomer in 16% yield (Scheme 4). The replacement of

Scheme 4. Proof-of-Concept Experiments



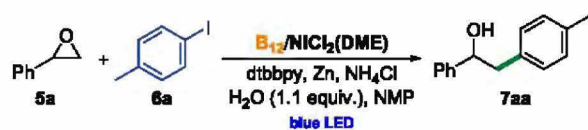
^aConditions: epoxide (**5a**, 0.2 mmol), aryl halide (**6a**, 1.5 equiv), NiCl₂(DME) (20 mol %), Zn (3 equiv), NH₄Cl (3 equiv), dtbbpy (40 mol %), dry NMP ($c = 0.1$ M), blue LED (single diode, 10 W), 30 min.

HME (**3**) with native vitamin B₁₂ increased the yield up to 41%. Noteworthy, the reaction without any cobalt complex added not only was lower-yielding but also led to a mixture of two regioisomers with a predominance of the branched product. This result clearly shows the decisive influence of the cobalt cocatalysis on the selectivity of this transformation. Control experiments confirmed the dual-catalytic and light-induced nature of the process, while the addition of a radical trap (TEMPO) supported its radical character (see SI).

Noteworthy, the reaction without any cobalt complex added not only was lower-yielding but also led to a mixture of two regioisomers with a predominance of the branched product. This result clearly shows the decisive influence of the cobalt cocatalysis on the selectivity of this transformation. Control experiments confirmed the dual-catalytic and light-induced nature of the process, while the addition of a radical trap (TEMPO) supported its radical character (see SI).

Optimization. Next, we turned our attention toward the synthetic utility of the developed method. The reaction was optimized with respect to cobalt and nickel catalysts, solvent, ligand, and reducing system, providing the desired product **7aa** in 60% yield (Table 1, entry 1).

We found that the addition of water (1.1 equiv) improved the yield of the reaction, while kinetic studies allowed us to determine the optimal reaction time (30 min, for details, see SI). The use of hydrophobic HME (**3**) instead of the parent

Table 1. Optimization Studies of the Cross-Electrophile Ring Opening of Epoxides^a

entry	deviation from the standard conditions	yield (%) 7aa ^a
1	none	60
2	HME instead of B ₁₂	57
3	Co(acac) ₃ instead of B ₁₂	5
4	CoCl ₂ instead of B ₁₂	7
5	Co(dmgh) ₂ Cl(py) instead of B ₁₂	8
6	Co(dmgh) ₂ Pr(py) instead of B ₁₂	11
7 ^b	Mn instead of Zn	30
8	NiCl ₂ instead of NiCl ₂ (DME)	36
9	Ni(acac) ₂ instead of NiCl ₂ (DME)	33
10	Ni(OTf) ₂ instead of NiCl ₂ (DME)	39
11	1,10-phenanthroline instead of dtbbpy	24
12	terpyridine instead of dtbbpy	13
13	no water added	53

^aConditions: epoxide (**5**, 0.2 mmol), aryl halide (**7**, 1.5 equiv), B₁₂ (5 mol %), NiCl₂(DME) (20 mol %), Zn (1.5 equiv), NH₄Cl (3 equiv), dtbbpy (40 mol %), H₂O (1.1 equiv), dry NMP (*c* = 0.1 M), time 30 min, blue LED (single diode, 10 W) (for more details see SI). ^bMn (1.5 equiv), TMSCl (0.2 equiv), dmgh = dimethylglyoxime, dtbbpy = 4,4'-di-*tert*-butylbipyridine.

vitamin B₁₂ had little impact on the optimized model reaction (entry 2), while other commonly utilized cobalt complexes (Co(acac)₃, CoCl₂) led to a decrease in the yield of alcohol **7aa** (entries 3, 4). We have also examined cobalt dimethylglyoximate (dmg) complexes, which have been used by Pattenden⁴⁷ and Morandi⁴⁸ in regioselective cobalt-catalyzed coupling of aliphatic epoxides with alkenes. In our system, however, both catalysts afforded the desired product **7aa** only in low yields (entries 5, 6). Evaluation of reducing agents ruled out manganese or tetrakis(dimethylamino)-ethylene (TDAE) as an efficient alternative to the Zn/NH₄Cl system (entry 7). It also allowed establishing the optimal ratio of the two components at the 1.5 equiv: 3 equiv level. The reaction outcome did not improve in the presence of NiCl₂, Ni(acac)₂, or Ni(OTf)₂ as well as other ligands (entries 8–12). Finally, various solvents were tested (for more details, see SI), but NMP with the addition of water (1.1 equiv) assured the highest yield (entry 13).

Detailed analysis of the reaction mixture revealed the formation of byproducts aside from desired product **7aa** under the optimized conditions (Scheme 2B). Acetophenone (**8a**, a side-product originating from epoxide **5a**) formed in 5% yield presumably via β-hydride elimination, while styrene (**10a**) is obtained in 30% yield from intermediate alcohol **9**.⁴⁹ Finally, the reductive elimination in the nickel cycle may account for the observed small amount of biphenyl **11**.^{50–52} In order to gain more insight into the reaction mechanism, we carried out the reaction with enantioenriched styrene oxide (**5a**) under the optimized conditions. The expected coupling product **7aa** was obtained without any erosion of the stereocenter, which further supports the premise of the formation of the radical at the terminal position.

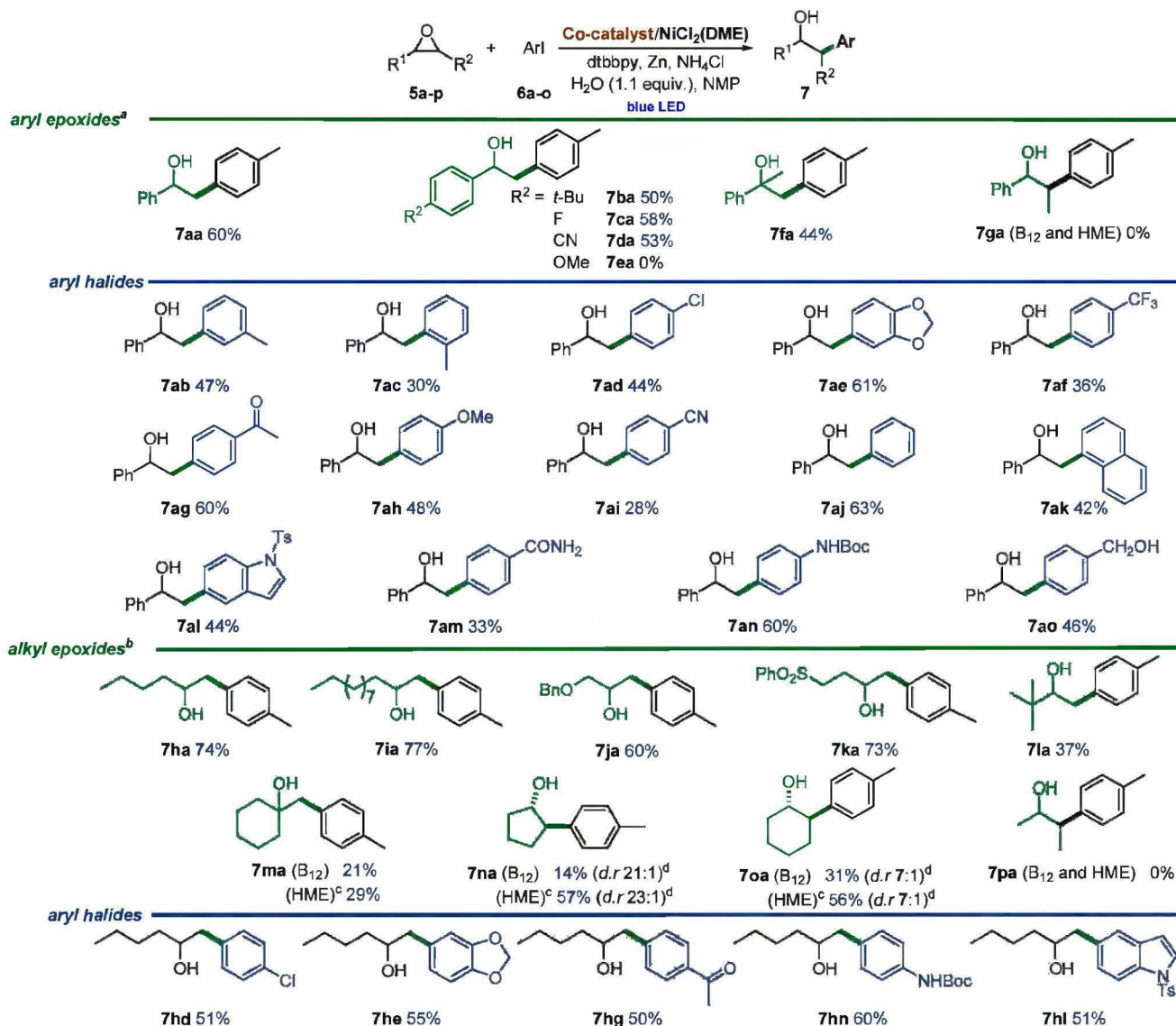
Substrate Scope. With the optimized conditions in hand, we explored the scope and limitations of the developed method (Scheme 5).

Monosubstituted aryl epoxides **5a–f**, bearing both electron-withdrawing and electron-donating substituents, are, in general, well-tolerated and give corresponding products **7aa–fa** in 50–58% yields. However, 2-(4-methoxyphenyl)oxirane (**5e**) does not afford the desired product, as it decomposes rapidly under the present conditions. For disubstituted epoxides, the substitution pattern determines their reactivity. 1,1-Disubstituted epoxide **5f** leads to product **7fa** in 44% yield, while 1,2-disubstituted epoxide **5g** remains unreactive. As far as aryl halides are concerned, under standard conditions, both electron-donating and electron-withdrawing substituents are well tolerated, giving desired products **7ab–ao** in good to moderate yield (28–63%). Substitution at the 3- or 4-position of an aryl halide does not affect the reaction. In contrast, the more hindered halide, 2-iodotoluene (**6c**), undergoes coupling with styrene oxide (**5a**) in reduced reaction yield (compare **7aa**, **7ab**, and **7ac**). Although vitamin B₁₂ exhibits exquisite reactivity in dehalogenation reactions,¹¹ which often precludes the use of halogenated substrates, in our conditions product **7ad** forms in 44% yield. Importantly from the standpoint of possible further functionalizations, other functional groups (hydroxyl, carbonyl, protected amine) remain unaffected. Moreover, the representative heteroaryl halide, 5-iodo-(4-methylphenylsulfonyl)indole (**6l**), proves to be a viable substrate in the studied reaction without any further optimization needed. The developed method is also suitable for epoxides with aliphatic substituents (Scheme 5). The chain length does not impact the transformation's outcome; the reaction with 1,2-epoxyhexane (**5h**) and 1,2-epoxydodecane (**5i**) gives products in 74% and 77% yield, respectively. We also found that aliphatic epoxide **5j**, possessing a protected primary hydroxyl group, could be converted into secondary alcohol **7ja** in 60% yield. The reaction with 4-(phenylsulfonyl)-1,2-epoxybutane (**5k**) gives corresponding product **7ka** in 73% yield. The potential use of aziridines as substrates was also investigated under the developed conditions, but only low yields of the respective products were obtained (see SI). Further studies on extending our methodology to other classes of heterocycles are currently ongoing in our laboratory.

Subsequently, the scope of aryl halides for the reaction with 1,2-epoxyhexane (**5h**) was explored. Substrates with both types of substituents—electron-rich and electron-deficient—on the aromatic ring afford the corresponding products **7hd–ol** in satisfactory yields. The *N*-Boc-protected amine, alkoxy, and carbonyl functionalities are well tolerated. The reaction with 1-chloro-4-iodobenzene (**6d**) leads to anticipated alcohol **7hd** in 51% yield. Similar to the reaction with aryl epoxides, indole-derived halide **6l** proved also a competent substrate, affording 1-(1-tosyl-1*H*-indol-5-yl)hexan-2-ol (**7hl**).

Compared to monosubstituted substrates, bicyclic epoxide **5o** was converted to the desired coupling product **7oa** with a significantly lower yield.⁵ Therefore, to gain a better understanding of how the reaction conditions affect the cross-electrophile coupling of disubstituted epoxides with aryl halides, additional experimental and theoretical studies were performed.

The use of hydrophobic analogue **3** instead of vitamin B₁₂ (**1**) does not bring any substantial improvement (Table 2, entries 1, 2). However, with the simultaneous replacement of NMP with acetone, a 2-fold increase in the yield of **7oa** was observed (entry 3). A similar trend was also present for bicyclic epoxide **5n** and 1-oxaspiro[2.5]octane (**5m**), which provide considerably higher yields of desired alcohols **7na** and **7oa** in

Scheme 5. Vitamin B₁₂-Catalyzed Ring-Opening Cross-Electrophile Coupling of (a) Aryl Epoxides^a and (b) Alkyl Epoxides^{b,c}

^aConditions: epoxide (0.2 mmol), aryl halide (1.5 equiv), B₁₂ (5 mol %), NiCl₂(DME) (20 mol %), Zn (1.5 equiv), NH₄Cl (3 equiv), dtbbpy (40 mol %), H₂O (1.1 equiv), dry NMP ($c = 0.1$ M), blue LED (single diode, 10 W), 30 min (for more details see SI). ^bBlue LED (single diode, 3 W), 16 h. ^cHME (5 mol %), acetone ($c = 0.1$ M), blue LED (single diode, 3 W), 16 h. ^dDetermined by GC.

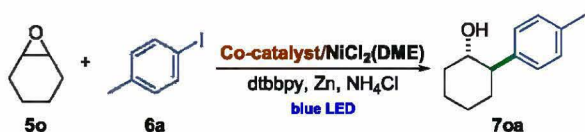
the presence of the HME/acetone system compared to vitamin B₁₂/NMP. The main feature by which the studied Co catalysts differ is the presence/absence of the so-called “nucleotide loop” (the axial ligand located at the α face of the corrin ring with a 5',6'-dimethylbenzimidazol (DMB) moiety) in addition to the replacement of amide into ester groups. Halpern et al. reported that in methyl malonyl-coenzyme A rearrangement switching between base-on and base-off forms of (CN)Cbl (1) changes the strength of the Co–C bond and hence the rate of its homolytic cleavage.⁵³ To assess if the presence of this structural element impacts opening of bicyclic epoxides, we used cobalester **2** as a Co complex. This catalyst bears a nucleotide loop in its structure, but unlike parent vitamin B₁₂, it dissolves well in both NMP and acetone, allowing for a direct comparison. A decisive solvent's dependence was observed, with acetone assuring a higher yield than NMP (entries 4, 5), which corroborates the sole influence of the reaction medium. Likewise, the reaction catalyzed by cobinamide **4** (amide

groups, no nucleotide loop) in NMP gives similar results to reactions catalyzed by other B₁₂ derivatives in this solvent (entry 6).

Performed kinetic studies contributed to a better understanding of the observed differences. The rate of the bicyclic epoxide (**5o**) ring opening was found to vary significantly depending on the conditions applied (Chart 1). It takes 6 h to fully convert epoxide **5o** in both vitamin B₁₂- and HME-catalyzed reactions as long as NMP is used as a solvent (compare fields A and C). On the other hand, the reaction in acetone provides full conversion in less than 3 h, which, presumably, translates to greater availability of alkyl radicals at a particular time (compare fields C and D).

The reactivity of aryl iodide toward a Ni catalyst is assumed to be at a similar level, regardless of the conditions applied. Therefore, in NMP an insufficient concentration of alkyl radicals derived from bicyclic epoxides may promote Ni-catalyzed homocoupling of aryl iodide **6a**, an unproductive

Table 2. Influence of the Co Complex Structure on the Opening of Bicyclic Epoxides^a



entry	solvent	catalyst	yield (%) 7oa
1	NMP	B ₁₂ CONH ₂ loop	31
2	NMP	HME CO ₂ Me no loop	26
3	acetone	HME ¹² CO ₂ Me no loop	56
4	acetone	cobalester ¹⁷ CO ₂ Me loop	55
5	NMP	cobalester CO ₂ Me loop	32
6	NMP	cobinamide ⁵⁺⁴ CONH ₂ no loop	35

^aConditions: epoxide (**5o**, 0.2 mmol), aryl halide (**6a**, 1.5 equiv), Co catalyst (5 mol %), NiCl₂(DME) (20 mol %), Zn (1.5 equiv), NH₄Cl (3.0 equiv), dtbbpy (40 mol %), solvent (*c* = 0.1 M), blue LED (single diode, 3 W), 16 h.

pathway, leading to biphenyl (**11a**) (fields A and C).^{50,52} This side-product is observed only in the presence of the Ni complex. The higher reactivity of monosubstituted aliphatic epoxide **5h** is reflected by its faster conversion as compared to bicyclic epoxide **5o** (compare fields A and B). In their case, the catalyst and the solvent do not affect the reaction; yields are almost identical (74%) in both cases.

The observed reactivity pattern corresponds well with the calculated barriers for the nucleophilic opening of the epoxides

with the Co(I)-corrin complex (Figure 2). In general, the Gibbs free energy of activation for the reaction of aryl- and

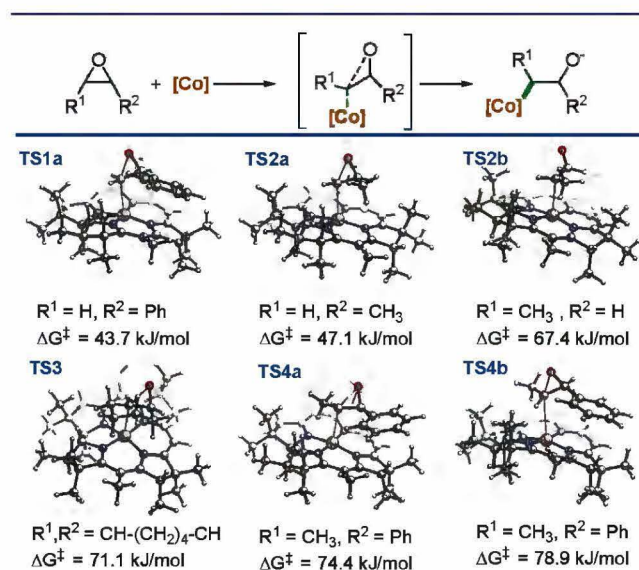
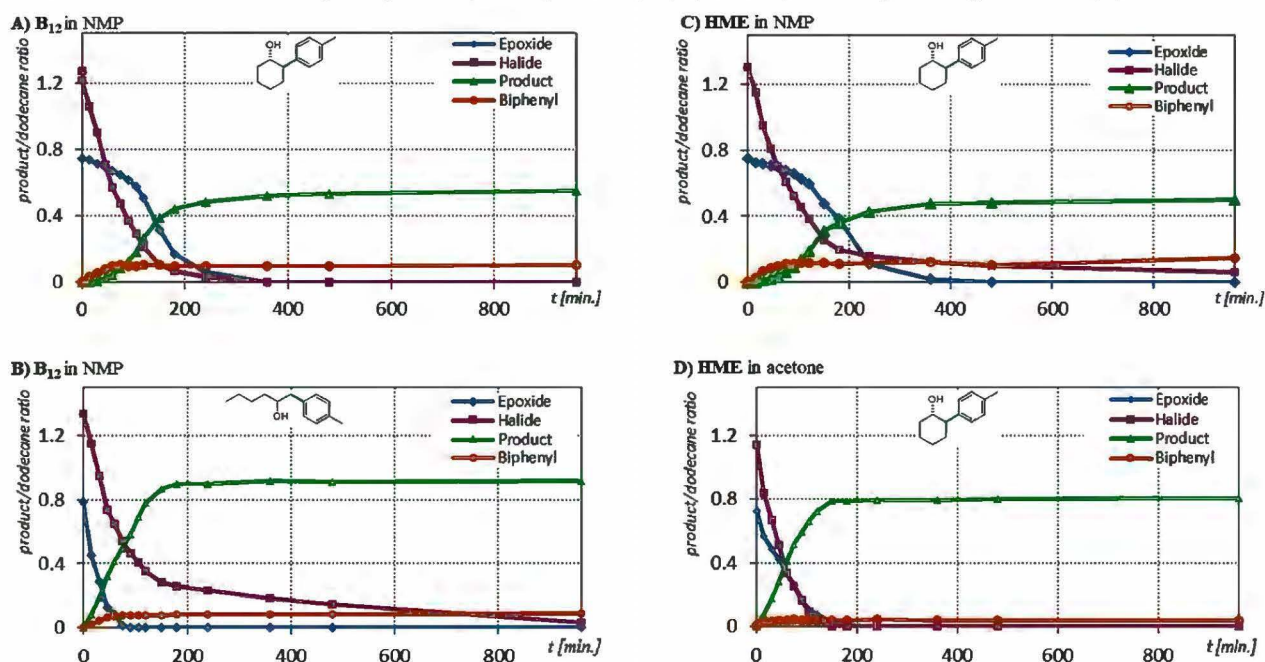


Figure 2. Gibbs free energy barriers for the opening of epoxides with the Co(I)-corrin complex calculated at the BP86-D3/6-311++G-(2df,p)/SMD(acetone)//BP86-D3/6-31G(d)/SMD(acetone) level of theory.

alkyl-monosubstituted epoxides (TS1a and TS2a, 43.7 and 47.1 kJ/mol for Ph- and Me-substituted, respectively) is smaller than for more sterically demanding 1,2-disubstituted epoxides (TS3 and TS4, >70 kJ/mol). Nevertheless, bicyclic substrates **5n,o** provide desired products **7na** and **7oa** in good yields, while epoxide **5g**, for which the activation barrier is ~3 kJ/mol higher, remains unreactive (TS3 versus TS4a)

Chart 1. Kinetic Profile of the Opening of Bicyclic Epoxides (6o**) (A, C, D) and Aliphatic Epoxide **6h** (B)^{a,b}**



^aConditions: epoxide (**5**, 0.2 mmol), aryl halide (**6a**, 1.5 equiv), Co catalyst (5 mol %), NiCl₂(DME) (20 mol %), Zn (1.5 equiv), NH₄Cl (3.0 equiv), dtbbpy (40 mol %), solvent (*c* = 0.1 M), blue LED (single diode, 3 W), 16 h, dodecane as an internal standard. ^bMeasurements at *t* = 0 min refer to concentrations of compounds before mixing two solutions; see SI.

regardless of the *Z/E* configuration of the epoxide (TS4a vs TS4b, $\Delta G^\ddagger = 74.4$ vs 78.9 kJ/mol). Additionally, the observed regioselectivity is well reflected by the energetically favored attack of the Co(I)-corrin on the less hindered side on propylene oxide (a model used for an alkyl epoxide, TS2a vs TS2b, $\Delta G^\ddagger = 47.1$ vs 67.4 kJ/mol).

CONCLUSIONS

We have developed a highly regioselective, Co/Ni-catalyzed ring-opening reaction of epoxides with aryl halides. The scope of our method has been demonstrated in a broad range of aliphatic and aromatic epoxides. Gratifyingly, these include cyclic and disubstituted epoxides even though the Gibbs free energy of activation for their reactions are higher than for alkyl- and aryl-monosubstituted substrates. Due to the mild reaction conditions, a wide range of functional groups is well tolerated.

Only the cooperation of vitamin B₁₂ as a Co catalyst with Ni catalysis assures high regioselectivity of the cross-electrophile coupling. The crucial ring opening by the Co(I) complex occurs from the less hindered side, leading to linear products.

This new methodology complements the existing approaches providing access to a diverse array of substituted alcohols, which are valuable feedstock chemicals in synthetic and medicinal chemistry. Consequently, it closes the gap in the synthesis of linear and branched alcohols via cross-electrophile coupling; they are now accessible from both alkyl and aryl epoxides.

ASSOCIATED CONTENT

Supporting Information

The Supporting Information is available free of charge at <https://pubs.acs.org/doi/10.1021/jacs.1c00659>.

Experimental details and procedures, optimization studies, mechanistic experiments, DFT, and spectral data for all new compounds (PDF)

AUTHOR INFORMATION

Corresponding Authors

Maciej Giedyk – Institute of Organic Chemistry, Polish Academy of Sciences, 01-224 Warsaw, Poland; Email: maciej.giedyk@icho.edu.pl

Dorota Gryko – Institute of Organic Chemistry, Polish Academy of Sciences, 01-224 Warsaw, Poland; orcid.org/0000-0002-5197-4222; Email: dorota.gryko@icho.edu.pl

Authors

Aleksandra Potrzęsaj – Institute of Organic Chemistry, Polish Academy of Sciences, 01-224 Warsaw, Poland; orcid.org/0000-0003-0549-7792

Mateusz Musiejuk – Institute of Organic Chemistry, Polish Academy of Sciences, 01-224 Warsaw, Poland

Wojciech Chaladaj – Institute of Organic Chemistry, Polish Academy of Sciences, 01-224 Warsaw, Poland; orcid.org/0000-0001-8143-3788

Complete contact information is available at: <https://pubs.acs.org/doi/10.1021/jacs.1c00659>

Notes

The authors declare no competing financial interest.

ACKNOWLEDGMENTS

The authors thank Prof. Paweł M. Kozłowski for helpful discussions. Financial support for this work was provided by the Foundation for Polish Sciences (FNP TEAM POIR.04.04.00-00-4232/17-00). M.G. gratefully acknowledges funding from the National Science Centre (SONATA 2018/31/D/ST5/00306). Calculations have been carried out using resources provided by Wrocław Centre for Networking and Supercomputing (<http://wccs.pl>), grant no. 518.

REFERENCES

- (1) Pineschi, M. Asymmetric Ring-Opening of Epoxides and Aziridines with Carbon Nucleophiles. *Eur. J. Org. Chem.* **2006**, *2006* (22), 4979–4988.
- (2) Huang, C.-Y.; Doyle, A. G. The Chemistry of Transition Metals with Three-Membered Ring Heterocycles. *Chem. Rev.* **2014**, *114* (16), 8153–8198.
- (3) Nielsen, L. P. C.; Jacobsen, E. N. *Aziridines and Epoxides in Organic Synthesis*; Yudin, A. K., Ed.; Wiley, 2006; DOI: 10.1002/3527607862.
- (4) Nielsen, D. K.; Doyle, A. G. Nickel-Catalyzed Cross-Coupling of Styrenyl Epoxides with Boronic Acids. *Angew. Chem., Int. Ed.* **2011**, *50* (27), 6056–6059.
- (5) Zhao, Y.; Weix, D. J. Enantioselective Cross-Coupling of Meso-Epoxides with Aryl Halides. *J. Am. Chem. Soc.* **2015**, *137* (9), 3237–3240.
- (6) Zhao, Y.; Weix, D. J. Nickel-Catalyzed Regiodivergent Opening of Epoxides with Aryl Halides: Co-Catalysis Controls Regioselectivity. *J. Am. Chem. Soc.* **2014**, *136* (1), 48–51.
- (7) Wang, X.; Dai, Y.; Gong, H. Nickel-Catalyzed Reductive Couplings. *Top. Curr. Chem.* **2016**, *374* (4), 43.
- (8) Wang, C. Electrophilic Ring Opening of Small Heterocycles. *Synthesis* **2017**, *49* (24), 5307–5319.
- (9) Gansäuer, A.; Barchuk, A.; Keller, F.; Schmitt, M.; Grimme, S.; Gerenkamp, M.; Mück-Lichtenfeld, C.; Daasbjerg, K.; Svith, H. Mechanism of Titanocene-Mediated Epoxide Opening through Homolytic Substitution. *J. Am. Chem. Soc.* **2007**, *129* (5), 1359–1371.
- (10) Gansäuer, A.; Narayan, S. Titanocene-Catalysed Electron Transfer-Mediated Opening of Epoxides. *Adv. Synth. Catal.* **2002**, *344*, 465–475.
- (11) Parasram, M.; Shields, B. J.; Ahmad, O.; Knauber, T.; Doyle, A. G. Regioselective Cross-Electrophile Coupling of Epoxides and (Hetero)Aryl Iodides via Ni/Ti/Photoredox Catalysis. *ACS Catal.* **2020**, *10* (10), 5821–5827.
- (12) Ociepa, M.; Wierzba, A. J.; Turkowska, J.; Gryko, D. Polarity-Reversal Strategy for the Functionalization of Electrophilic Strained Molecules via Light-Driven Cobalt Catalysis. *J. Am. Chem. Soc.* **2020**, *142* (11), 5355–5361.
- (13) Wierzba, A. J.; Hassan, S.; Gryko, D. Synthetic Approaches toward Vitamin B₁₂ Conjugates. *Asian J. Org. Chem.* **2018**, *8* (1), 6–24.
- (14) Brown, K. L. Chemistry and Enzymology of Vitamin B₁₂. *Chem. Rev.* **2005**, *105* (6), 2075–2150.
- (15) Banerjee, R. *Chemistry and Biochemistry of B₁₂*; Wiley, 1999.
- (16) Giedyk, M.; Shimakoshi, H.; Goliszewska, K.; Gryko, D.; Hisaeda, Y. Electrochemistry and Catalytic Properties of Amphiphilic Vitamin B₁₂ Derivatives in Nonaqueous Media. *Dalt. Trans.* **2016**, *45* (20), 8340–8346.
- (17) Giedyk, M.; Fedosov, S. N.; Gryko, D. An Amphiphilic, Catalytically Active, Vitamin B₁₂ Derivative. *Chem. Commun.* **2014**, *50* (36), 4674–4676.
- (18) Giedyk, M.; Goliszewska, K.; Gryko, D. Vitamin B₁₂ Catalysed Reactions. *Chem. Soc. Rev.* **2015**, *44* (11), 3391–3404.
- (19) Pan, L.; Shimakoshi, H.; Masuko, T.; Hisaeda, Y. Vitamin B₁₂ Model Complex Catalyzed Methyl Transfer Reaction to Alkylthiol under Electrochemical Conditions with Sacrificial Electrode. *Dalt. Trans.* **2009**, No. 44, 9898–9905.

- (20) Shimakoshi, H.; Li, L.; Nishi, M.; Hisaeda, Y. Photosensitizing Catalysis of the B₁₂ Complex without an Additional Photosensitizer. *Chem. Commun.* **2011**, 47 (39), 10921–10923.
- (21) Chen, L.; Hisaeda, Y.; Shimakoshi, H. Visible Light-Driven, Room Temperature Heck-Type Reaction of Alkyl Halides with Styrene Derivatives Catalyzed by B₁₂ Complex. *Adv. Synth. Catal.* **2019**, 361 (12), 2877–2884.
- (22) Pattenden, G. Cobalt-Mediated Radical Reactions in Organic Synthesis. *Chem. Soc. Rev.* **1988**, 17, 361–182.
- (23) Toraya, T. Radical Catalysis in Coenzyme B₁₂-Dependent Isomerization (Eliminating) Reactions. *Chem. Rev.* **2003**, 103 (6), 2095–2128.
- (24) Frisch, M. J.; Trucks, G. W.; Schlegel, H. B.; Scuseria, G. E.; Robb, M. A.; Cheeseman, J. R.; Scalmani, G.; Barone, V.; Petersson, G. A.; Nakatsuji, H.; Li, X.; Caricato, M.; Marenich, A. V.; Bloino, J.; Janesko, B. G.; Gomperts, R.; Mennucci, B.; Hratchian, H. P.; Ortiz, J. V.; Izmaylov, A. F.; Sonnenberg, J. L.; Williams-Young, D.; Ding, F.; Lipparini, F.; Egidi, F.; Goings, J.; Peng, B.; Petrone, A.; Henderson, T.; Ranasinghe, D.; Zakrzewski, V. G.; Gao, J.; Rega, N.; Zheng, G.; Liang, W.; Hada, M.; Ehara, M.; Toyota, K.; Fukuda, R.; Hasegawa, J.; Ishida, M.; Nakajima, T.; Honda, Y.; Kitao, O.; Nakai, H.; Vreven, T.; Throssell, K.; Montgomery, J. A., Jr.; Peralta, J. E.; Ogliaro, F.; Bearpark, M. J.; Heyd, J. J.; Brothers, E. N.; Kudin, K. N.; Staroverov, V. N.; Keith, T. A.; Kobayashi, R.; Normand, J.; Raghavachari, K.; Rendell, A. P.; Burant, J. C.; Iyengar, S. S.; Tomasi, J.; Cossi, M.; Millam, J. M.; Klene, M.; Adamo, C.; Cammi, R.; Ochterski, J. W.; Martin, R. L.; Morokuma, K.; Farkas, O.; Foresman, J. B.; Fox, D. J. *Gaussian 16*, Revision B.01; Gaussian, Inc.: Wallingford, CT, 2016.
- (25) Kozłowski, P. M.; Kumar, M.; Piecuch, P.; Li, W.; Bauman, N. P.; Hansen, J. A.; Lodowski, P.; Jaworska, M. The Cobalt-Methyl Bond Dissociation in Methylcobalamin: New Benchmark Analysis Based on Density Functional Theory and Completely Renormalized Coupled-Cluster Calculations. *J. Chem. Theory Comput.* **2012**, 8 (6), 1870–1894.
- (26) Kornobis, K.; Kumar, N.; Lodowski, P.; Jaworska, M.; Piecuch, P.; Lutz, J. J.; Wong, B. M.; Kozłowski, P. M. Electronic Structure of the S 1 State in Methylcobalamin: Insight from CASSCF/MC-XQDPT2, EOM-CCSD, and TD-DFT Calculations. *J. Comput. Chem.* **2013**, 34 (12), 987–1004.
- (27) Govender, P. P.; Navizet, L.; Perry, C. B.; Marques, H. M. DFT Studies of Trans and Cis Influences in the Homolysis of the Co-C Bond in Models of the Alkylcobalamins. *J. Phys. Chem. A* **2013**, 117 (14), 3057–3068.
- (28) Kobylanski, L. J.; Widner, F. J.; Kräutler, B.; Chen, P. Co-C Bond Energies in Adenosylcobinamide and Methylcobinamide in the Gas Phase and in Silico. *J. Am. Chem. Soc.* **2013**, 135 (37), 13648–13651.
- (29) Kepp, K. P. Co-C Dissociation of Adenosylcobalamin (Coenzyme B₁₂): Role of Dispersion, Induction Effects, Solvent Polarity, and Relativistic and Thermal Corrections. *J. Phys. Chem. A* **2014**, 118 (34), 7104–7117.
- (30) Morita, Y.; Oohora, K.; Sawada, A.; Kamachi, T.; Yoshizawa, K.; Hayashi, T. Redox Potentials of Cobalt Corrinoids with Axial Ligands Correlate with Heterolytic Co-C Bond Dissociation Energies. *Inorg. Chem.* **2017**, 56 (4), 1950–1955.
- (31) Kozłowski, P. M.; Garabato, B. D.; Lodowski, P.; Jaworska, M. Photolytic Properties of Cobalamins: A Theoretical Perspective. *Dalt. Trans.* **2016**, 45 (11), 4457–4470.
- (32) Garabato, B. D.; Lodowski, P.; Jaworska, M.; Kozłowski, P. M. Mechanism of Co-C Photodissociation in Adenosylcobalamin. *Phys. Chem. Chem. Phys.* **2016**, 18 (28), 19070–19082.
- (33) Lodowski, P.; Jaworska, M.; Garabato, B. D.; Kozłowski, P. M. Mechanism of Co-C Bond Photolysis in Methylcobalamin: Influence of Axial Base. *J. Phys. Chem. A* **2015**, 119 (17), 3913–3928.
- (34) Scheffold, R.; Abrecht, S.; Orłinski, R.; Ruf, H.-R.; Stamouli, P.; Tinembart, O.; Walder, L.; Weymuth, C. Vitamin B₁₂-Mediated Electrochemical Reactions in the Synthesis of Natural Products. *Pure Appl. Chem.* **1987**, 59, 363–372.
- (35) Troxler, T.; Scheffold, R. Asymmetric Catalysis by Vitamin B₁₂: The Isomerization of Achiral Cyclopropanes to Optically Active Olefins. *Helv. Chim. Acta* **1994**, 77 (5), 1193–1202.
- (36) Su, H.; Walder, L.; Zhang, Z.; Scheffold, R. Asymmetric Catalysis by Vitamin B₁₂. The Isomerization of Achiral Epoxides to Optically Active Allylic Alcohols. *Helv. Chim. Acta* **1988**, 71 (5), 1073–1078.
- (37) Bonhôte, P.; Scheffold, R. Asymmetric Catalysis by Vitamin B₁₂. The Mechanism of the Cob(I)Alamin-Catalyzed Isomerization of 1,2-Epoxy-cyclopentane to (R)-Cyclopent-2-Enol. *Helv. Chim. Acta* **1991**, 74 (7), 1425–1444.
- (38) Zhang, Z.; Da Scheffold, R. Asymmetric Catalysis by Vitamin B₁₂: The Isomerization of Achiral Aziridines to Optically Active Allylic Amines. *Helv. Chim. Acta* **1993**, 76 (7), 2602–2615.
- (39) Nuthakki, B.; Bobbitt, J. M.; Rusling, J. F. Influence of Microemulsions on Enantioselective Synthesis of (R)-Cyclopent-2-Enol Catalyzed by Vitamin B₁₂. *Langmuir* **2006**, 22 (12), 5289–5293.
- (40) Shevick, S. L.; Obrador, C.; Shenvi, R. A. Mechanistic Interrogation of Co/Ni-Dual Catalyzed Hydroarylation. *J. Am. Chem. Soc.* **2018**, 140 (38), 12056–12068.
- (41) Tasker, S. Z.; Standley, E. A.; Jamison, T. F. Recent Advances in Homogeneous Nickel Catalysis. *Nature* **2014**, 509 (7500), 299–309.
- (42) Ackerman, L. K. G.; Anka-Lufford, L. L.; Naodovic, M.; Weix, D. J. Cobalt Co-Catalysis for Cross-Electrophile Coupling: Diaryl-methanes from Benzyl Mesylates and Aryl Halides. *Chem. Sci.* **2015**, 6 (2), 1115–1119.
- (43) Milligan, J. A.; Phelan, J. P.; Badir, S. O.; Molander, G. A. Alkyl Carbon-Carbon Bond Formation by Nickel/Photoredox Cross-Coupling. *Angew. Chem., Int. Ed.* **2019**, 58 (19), 6152–6163.
- (44) Komeyama, K.; Michiyuki, T.; Osaka, I. Nickel/Cobalt-Catalyzed C(Sp³)-C(Sp³) Cross-Coupling of Alkyl Halides with Alkyl Tosylates. *ACS Catal.* **2019**, 9 (10), 9285–9291.
- (45) Komeyama, K.; Ohata, R.; Kiguchi, S.; Osaka, I. Highly Nucleophilic Vitamin B₁₂-Assisted Nickel-Catalyzed Reductive Coupling of Aryl Halides and Non-Activated Alkyl Tosylates. *Chem. Commun.* **2017**, 53 (48), 6401–6404.
- (46) Gutierrez, O.; Tellis, J. C.; Primer, D. N.; Molander, G. A.; Kozłowski, M. C. Nickel-Catalyzed Cross-Coupling of Photoredox-Generated Radicals: Uncovering a General Manifold for Stereoconvergence in Nickel-Catalyzed Cross-Couplings. *J. Am. Chem. Soc.* **2015**, 137 (15), 4896–4899.
- (47) Harrowven, D. C.; Pattenden, G. Cobalt Mediated Cyclisations of Epoxy Olefins. *Tetrahedron Lett.* **1991**, 32 (2), 243–246.
- (48) Prina Cerai, G.; Morandi, B. Atom-Economical Cobalt-Catalyzed Regioselective Coupling of Epoxides and Aziridines with Alkenes. *Chem. Commun.* **2016**, 52 (63), 9769–9772.
- (49) Huang, J.-M.; Lin, Z.-Q.; Chen, D.-S. Electrochemically Supported Deoxygenation of Epoxides into Alkenes in Aqueous Solution. *Org. Lett.* **2012**, 14 (1), 22–25.
- (50) Manzoor, A.; Wienefeld, P.; Baird, M. C.; Budzelaar, P. H. M. Catalysis of Cross-Coupling and Homocoupling Reactions of Aryl Halides Utilizing Ni(0), Ni(I), and Ni(II) Precursors; Ni(0) Compounds as the Probable Catalytic Species but Ni(I) Compounds as Intermediates and Products. *Organometallics* **2017**, 36 (18), 3508–3519.
- (51) Rahil, R.; Sengmany, S.; Le Gall, E.; Léonel, E. Nickel-Catalyzed Electrochemical Reductive Homocouplings of Aryl and Heteroaryl Halides: A Useful Route to Symmetrical Biaryls. *Synthesis* **2018**, 50 (01), 146–154.
- (52) Iyoda, M.; Otsuka, H.; Sato, K.; Nisato, N.; Oda, M. Homocoupling of Aryl Halides Using Nickel(II) Complex and Zinc in the Presence of Et₄NL. An Efficient Method for the Synthesis of Biaryls and Bipyridines. *Bull. Chem. Soc. Jpn.* **1990**, 63 (1), 80–87.
- (53) Halpern, J. Mechanisms of Coenzyme B₁₂-Dependent Rearrangements. *Science (Washington, DC, U. S.)* **1985**, 227 (4689), 869–875.

(54) ó Proinsias, K.; Karczewski, M.; Zieleniewska, A.; Gryko, D. Microwave-Assisted Cobinamide Synthesis. *J. Org. Chem.* **2014**, *79* (16), 7752–7757.

Supporting Information

Cobalt Catalyst Determines Regioselectivity in Ring-opening of Epoxides with Aryl Halides

Aleksandra Potrząsaj, Mateusz Musiejuk, Wojciech Chaładaj,
Maciej Giedyk*, Dorota Gryko*

*Institute of Organic Chemistry Polish Academy of Science
Kasprzaka 44/52, 01-224 Warsaw, Poland*

e-mail: dorota.gryko@icho.edu.pl

Table of Contents

1. General Information	4
2. Setup for photoreactions	5
3. Full Optimization of the Reaction Parameters	6
3.1 Background experiments.....	6
3.2 The influence of light on the model reaction.....	6
3.3 Optimization of a solvent for HME (3) – catalyzed reaction.....	6
3.4 Screening of cobalt catalysts.....	7
3.5 Optimization of a solvent for B ₁₂ (1)– catalyzed reaction.....	8
3.6 B ₁₂ – catalyst loading.....	8
3.7 The influence of Zn and NH ₄ Cl amounts.....	8
3.8 Screening of Ni – catalysts.....	9
3.9 Screening of ligands.....	9
3.10 Optimization of the substrates ratio.....	10
3.11 Concentration of styrene oxide (5a).....	10
3.12 The influence of water on the model reaction.....	10
4. General Procedures	11
4A General Procedure for opening aryl epoxides.....	11
4B General Procedure for opening aliphatic epoxides.....	11
4C General Procedure for opening cyclic epoxides catalyzed by B ₁₂	11
4D General Procedure for opening cyclic epoxides catalyzed by HME.....	12
4.1 General procedure - notes.....	12
5. Scope and characterization of new compounds – epoxides and aziridines	13
6. Mechanistic consideration	30
6.1 Proposed mechanism.....	30
6.2 Mass Spectrometry studies.....	30
6.3 Studies of regioselectivity.....	31
6.4 Stereoselectivity studies.....	34
6.5 DFT Calculations.....	35
6.6 Kinetic studies for model reaction.....	82
6.7 Reactions in deuterated solvents.....	82
7. References	85
8. NMR Spectra	88
1-phenyl-2-(4-tolyl)ethan-1-ol (7aa).....	88
1-(4-(<i>tert</i> -butyl)phenyl)-2-(4-tolyl)ethan-1-ol (7ba).....	89
1-(4-fluorophenyl)-2-(4-tolyl)ethan-1-ol (7ca).....	90
4-(1-hydroxy-2-(4-tolyl)ethyl)benzotrile (7da).....	92
2-phenyl-1-(4-tolyl)propan-2-ol (7fa).....	93
1-phenyl-2-(3-tolyl)ethan-1-ol (7ab).....	94
1-phenyl-2-(2-tolyl)ethan-1-ol (7ac).....	95
2-(4-chlorophenyl)-1-phenylethan-1-ol (7ad).....	96
2-(benzo[<i>d</i>][1,3]dioxol-5-yl)-1-phenylethan-1-ol (7ae).....	97
1-phenyl-2-(4-(trifluoromethyl)phenyl)ethan-1-ol (7af).....	98
1-(4-(2-hydroxy-2-phenylethyl)phenyl)ethan-1-one (7ag).....	100
2-(4-methoxyphenyl)-1-phenylethan-1-ol (7ah).....	101
4-(2-hydroxy-2-phenylethyl)benzotrile (7ai).....	102
1,2-diphenylethan-1-ol (7aj).....	103
2-(naphthalen-1-yl)-1-phenylethan-1-ol (7ak).....	104
1-phenyl-2-(1-tosyl-1 <i>H</i> -indol-5-yl)ethan-1-ol (7al).....	105
4-(2-hydroxy-2-phenylethyl)benzamide (7am).....	106
<i>tert</i> -butyl 4-(2-hydroxy-2-phenylethyl)phenyl)carbamate (7an).....	107

2-(4-(hydroxymethyl)phenyl)-1-phenylethan-1-ol (7ao)	108
1-(4-tolyl)hexan-2-ol (7ha)	109
1-(4-tolyl)dodecan-2-ol (7ia)	110
1-(benzyloxy)-3-(4-tolyl)propan-2-ol (7ja)	111
4-(phenylsulfonyl)-1-(4-tolyl)butan-2-ol (7ka)	112
3,3-dimethyl-1-(4-tolyl)butan-2-ol (7la)	113
1-(4-methylbenzyl)cyclohexan-1-ol (7ma)	114
(1 <i>S</i> ,2 <i>R</i>)-2-(4-tolyl)cyclopentan-1-ol (7na)	115
(1 <i>S</i> ,2 <i>R</i>)-2-(4-tolyl)cyclohexan-1-ol (7oa)	116
1-(4-chlorophenyl)hexan-2-ol (7hd)	117
1-(benzo[<i>d</i>][1,3]dioxol-5-yl)hexan-2-ol (7he)	118
1-(4-(2-hydroxyhexyl)phenyl)ethan-1-one (7hg)	119
<i>tert</i> -butyl (4-(2-hydroxyhexyl)phenyl)carbamate (7hn)	120
1-(1-tosyl-1 <i>H</i> -indol-5-yl)hexan-2-ol (7hl)	121
4-methyl- <i>N</i> -(2-phenyl-(<i>p</i> -tolyl)ethyl)benzenosulphonamide (S23) and 4-methyl- <i>N</i> -(1-phenyl-2-(<i>p</i> -tolyl)ethyl)benzenosulfonamide (S24)	122
4-methyl- <i>N</i> -(2-(<i>p</i> -tolyl)cyclopentyl)benzenosulfonamide (S25)	123
4-methyl- <i>N</i> -(1-(<i>p</i> -tolyl)hexan-2-yl)benzenosulfonamide (S26)	124

1. General Information

General Procedures. Unless otherwise noted, reactions were performed without the exclusion of air or moisture. All the photochemical reactions were performed in 10 mL glassy vials sealed with aluminum caps containing a rubber septa. Reactions were monitored by gas chromatography (GC, specification below) or thin-layer chromatography (TLC) on Merck silica gel (GF254, 0.20 mm thickness), visualizing with UV-light, potassium permanganate (KMnO₄), or ceric ammonium molybdate (CAM)/Hanessian's stain. Column chromatography was performed using Merck silica gel 60 (230-400 mesh). GC yields were calibrated using dodecane as an internal standard.

Materials. Commercial reagents and solvents were purchased from Sigma-Aldrich, Acros Organics, Alfa Aesar, Fluorochem, and TCI, and used as received unless otherwise noted. Dry solvents: dimethyl sulfoxide (DMSO), dichloromethane (CH₂Cl₂), tetrahydrofuran (THF), acetonitrile (CH₃CN) were taken from *Solvent Purification System* (SPS). Deuterated solvents (CDCl₃, (CD₃)₂CO and MeOD) were purchased from Eurisotop. Amidine ligands (**S18**)¹, 5-iodo-1-(4-methylphenylsulfonyl)indole (**6I**)², 4-*tert*-butylphenylethylene oxide (**5b**)³, 4-cyano-butylphenylethylene oxide (**5d**)⁴, 4-(phenylsulfonyl)-1,2-epoxybutane (**5k**)⁵, 1-oxaspiro(2.5)octane (**5m**)⁶, *N*-(*p*-tolylsulfonyl)-2-phenylaziridine (**S20**)⁷, *N*-tosyl-6-azabicyclo[3.1.0]hexane (**S21**)⁷, 2-butyl-*N*-tosylaziridine (**S22**)⁷ and catalysts: NiCl₂(dtbbpy)⁸, (CN)(H₂O)Cby(OMe)₇ (**3**)⁹, Co(dmgh)₂pyⁱPr (**S6**)¹⁰ were synthesized according to literature procedures.

Before the reaction, zinc was activated by the following method: a) washing with 10% HCl, b) grinding, c) washing with H₂O, EtOH, and Et₂O, d) drying in a vacuum.

Instrumentation.

- **NMR Spectroscopy:** ¹H and ¹³C NMR spectra were recorded at 25 °C on a Bruker 400 MHz, 500 MHz or Varian 600 MHz instrument with TMS as an internal standard. NMR chemical shifts are reported in ppm and referenced to the residual solvent peak of CDCl₃ (7.26 ppm - ¹H NMR and 77.16 ppm - ¹³C NMR). Multiplicities are indicated by singlet (s), doublet (d), triplet (t), quartet (q), multiplet (m) and broad (br). Coupling constants (*J*) are reported in Hertz. All data analysis was performed using MestReNova software package.
- **GC/MS Chromatography:** GC-MS analyses were performed using Shimadzu GCMS-QP2010 SE gas chromatograph with FID detector and Zebron ZB 5MSi column.
- **Elemental Analysis:** Elemental analysis (N, H, C, S) were performed on PERKIN-ELMER 240 Elemental Analyzer.
- **High Resolution Mass Spectrometry:** High-resolution mass spectra (HRMS) were recorded on a Waters AutoSpec Premier instrument using electron ionization (EI) or a Waters SYNAPT G2-S HDMS instrument using electrospray ionization (ESI) with time of flight detector (TOF).
- **Low Resolution Mass Spectrometry:** Low-resolution mass spectra (LRMS) were recorded on an Applied Biosystems API 365 mass spectrometer using electrospray ionization (ESI) technique.
- **Melting points:** Melting points were recorded on a Marienfeld MPM-H2 melting point apparatus and are uncorrected.
- **High-performance liquid chromatography (HPLC):** High-performance liquid chromatography (HPLC) was performed on Daicel Chiralpak ID-H column (250 mm x 4.6 mm inside diameter) using a mixture of AcOEt in hexane (10%) as a mobile phase.

2. Setup for photoreactions

Reactions were performed in three different types of photoreactors (Figure 2.1)

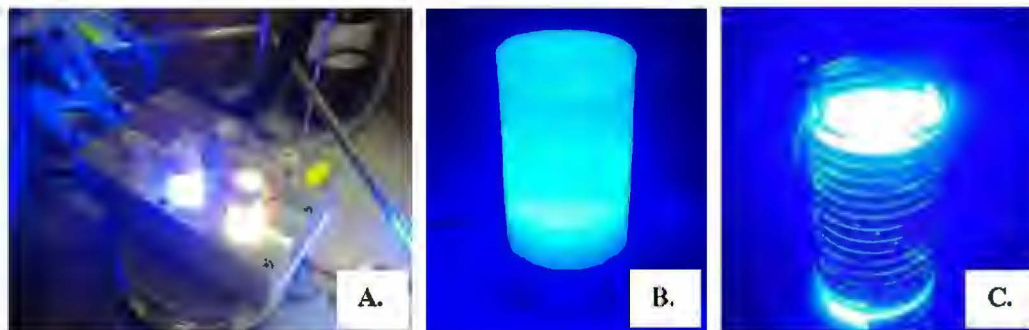


Figure 2.1 Photograph of a photoreactors

Characteristic of photoreactors:

- A. Blue LED; single diode 3 W, controlled by mini chiller set up at 33 °C, reactions in 10 mL vials;
- B. Blue LED; single diode 10 W, fan cooling, reactions in 10 mL vials;
- C. Blue LED; LED tape 9 W, fan cooling, reactions in a test tubes.

3. Full Optimization of the Reaction Parameters

Model reaction:



Reaction conditions: styrene oxide (**5a**) (0.2 mmol, 1 equiv.), 4-iodotoluene (**6a**) (1.5 equiv.), Zn (3 equiv.), NH₄Cl (3 equiv.), B₁₂ (**1**) (5 mol%), NiCl₂(DME) (20 mol%), dtbbpy (40 mol%), water (1.1 equiv.), dry NMP (c = 0.1 M), blue LED, 30 min.

3.1 Background experiments

Entry	Deviation from the Standard Conditions	Yield of 7aa [%]
1	none	60
2	No Co-cat., No NH ₄ Cl	7 and 28 ^a
3	No Co-cat., No Ni-cat., No ligand	0
4	No Ni-cat., No ligand	0
5	No light	<10%
6 ^b	No light, 50 °C	26
7 ^b	No light, 80 °C	28
8	Air atmosphere	product not observed

Reaction conditions: styrene oxide (**5a**) (0.2 mmol, 1 equiv.), 4-iodotoluene (**6a**) (1.5 equiv.), Zn (3 equiv.), NH₄Cl (3 equiv.), B₁₂ (**1**) (5 mol%), NiCl₂(DME) (20 mol%), dtbbpy (40 mol%), water (1.1 equiv.), dry NMP (c = 0.1 M), blue LED, 30 min. ^a - product branched formed - **12**, ^b - reaction time (16 h)

3.2 The influence of light on the model reaction

Entry	Light	Yield of 7aa [%]
1	Violet LEDs (tape)	23
2	White LEDs (tape)	16
3	Green LEDs (tape)	24
4	Blue LED (single diode, 3 W)	30
5	Blue LED (single diode, 10 W)	38

Reaction conditions: styrene oxide (**5a**) (0.2 mmol, 1 equiv.), 4-iodotoluene (**6a**) (1.5 equiv.), Zn (3 equiv.), NH₄Cl (3 equiv.), HME (**3**) (5 mol%), NiCl₂(DME) (20 mol%), dtbbpy (40 mol%), acetone (2 mL), 16 h

3.3 Optimization of a solvent for HME (**3**) – catalyzed reaction

Entry	Solvent	Yield of 7aa [%]
1	CH ₃ CN	32
2	DMSO	7
3	Methanol	19
4	Acetone	38
5	DMF	21
6	THF	27

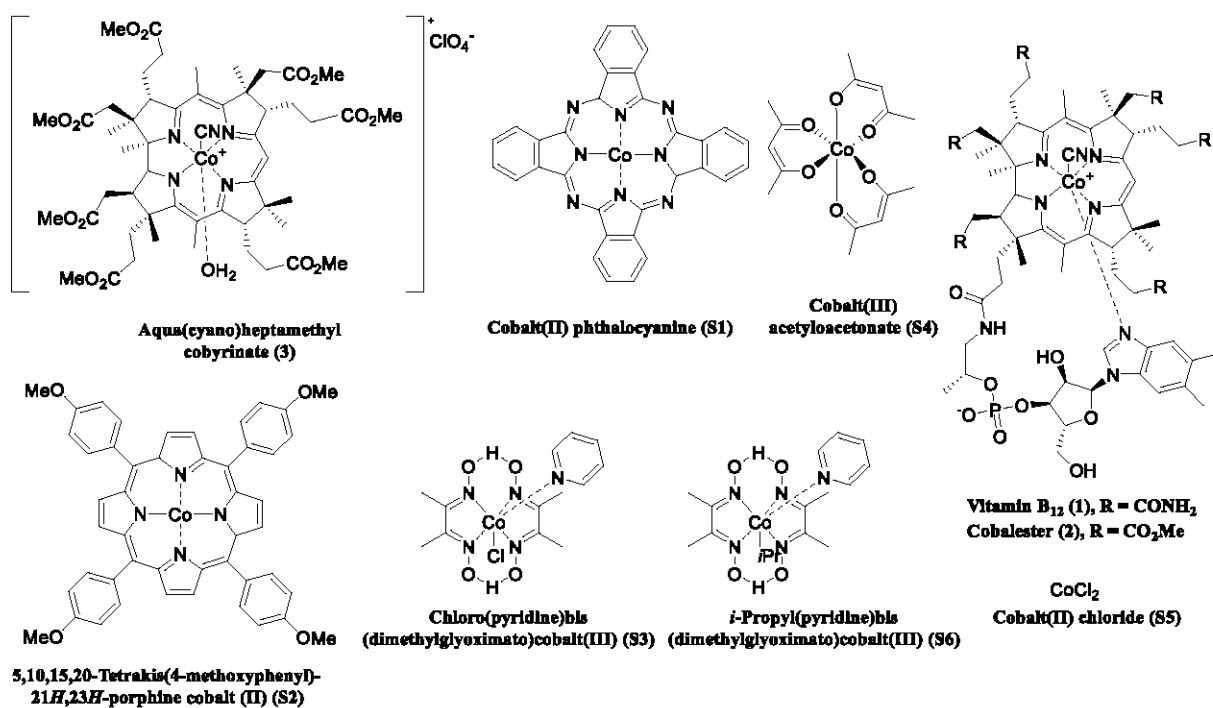
Reaction conditions: styrene oxide (**5a**) (0.2 mmol, 1 equiv.), 4-iodotoluene (**6a**) (1.5 equiv.), Zn (3 equiv.), NH₄Cl (3 equiv.), HME (**3**) (5 mol%), NiCl₂(DME) (20 mol%), dtbbpy (40 mol%), solvent (2 mL), Blue LED, 16 h

3.4 Screening of the cobalt catalysts

Entry	Catalyst	Yield of 7aa [%]
1	3	38
2	S1	10
3^c	1	42
4	2	31
5	S5	5
6	S2	7
7	S3	8
8	S4	7
9	S6	11

Reaction conditions: styrene oxide (**5a**) (0.2 mmol), 4-iodotoluene (**6a**) (1.5 equiv.), Zn (3 eq.), NH₄Cl (3 equiv.), Co-catalyst (5 mol%), NiCl₂(DME) (20 mol%), dtbbpy (40 mol%), Acetone (2 mL), Blue LEDs, 16 h

^cConditions: styrene oxide (**5a**) (0.2 mmol, 1 equiv.), 4-iodotoluene (**6a**) (1.5 equiv.), Zn (3 equiv.), NH₄Cl (3 equiv.), NiCl₂(DME) (20 mol%), dtbbpy (40 mol%), dry NMP (2 mL), Blue LED, 30 min.



3.5 Optimization of a solvent for B₁₂ (1) – catalyzed reaction

Entry	Solvent	Yield of 7aa [%]
1	NMP	42
2	Methanol	28
3	DMA	6
4	DMF	20
5	Acetone:Methanol 1:1	27
6	THF:H ₂ O (1:1)	4

Reaction conditions: styrene oxide (**5a**) (0.2 mmol), 4-iodotoluene (**6a**) (1.5 equiv.), Zn (3 equiv.), NH₄Cl (3 equiv.), B₁₂ (**1**) (5 mol%), NiCl₂(DME) (20 mol%), dtbbpy (40 mol%), solvent (2mL), Blue LED, 30 min.

3.6 B₁₂ – catalyst loading

Entry	Catalyst loading [%]	Yield of 7aa [%]
1	2.5	33
2	5	42
3	7.5	40
4	10	38

Reaction conditions: styrene oxide (**5a**) (0.2 mmol), 4-iodotoluene (**6a**) (1.5 equiv.), Zn (3 equiv.), NH₄Cl (3 equiv.), B₁₂ (**1**), NiCl₂(DME) (20 mol%), dtbbpy (40 mol%), dry NMP (2 mL), Blue LED, 30 min.

3.7 The influence of Zn and NH₄Cl amounts

Entry	Zn (equiv.)	NH ₄ Cl (equiv.)	Yield of 7aa [%]
1	3	3	42
2	3	1	34
3	6	3	22
4	3	5	20
5	3	4	31
6	3	1.5	42
7	3	2	46
8	1.5	3	53
9	1	3	32
10	1	2	30

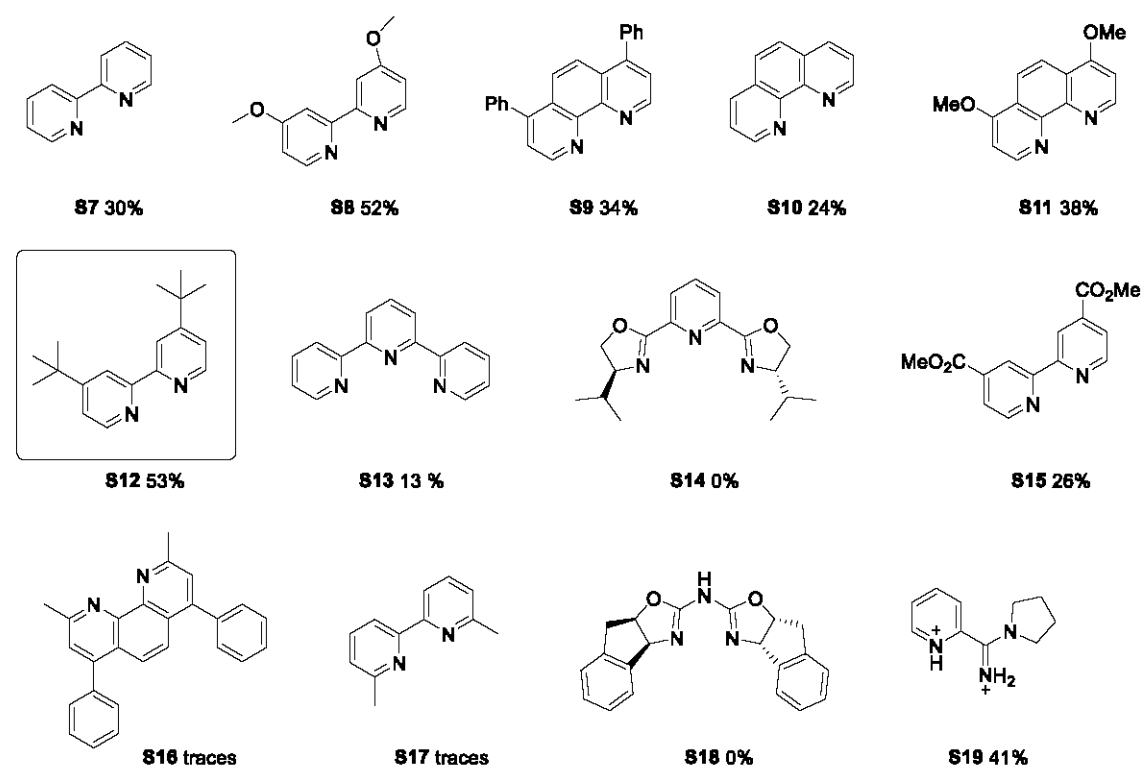
Reaction conditions: styrene oxide (**5a**) (0.2 mmol), 4-iodotoluene (**6a**) (1.5 equiv.), B₁₂ (**1**) (5mol%), NiCl₂(DME) (20 mol%), dtbbpy (40 mol%), dry NMP (2 mL), Blue LED, 30 min.

3.8 Screening of Ni – catalysts

Entry	Catalyst	Catalyst loading [mol%]	Yield of 7aa [%]
1	NiCl₂(DME)	20	53
2	NiBr ₂ (DME)	20	43
3	NiCl ₂	20	36
4	NiBr ₂	20	43
5	NiI ₂	20	40
6	Ni(TMHD) ₂	20	20
7	Ni(acac) ₂	20	33
8	Ni(OAc) ₂ ·4H ₂ O	20	31
9	Ni(OTf) ₂	20	39
10 ^d	NiCl ₂ (dtbbpy)	20	45
11 ^d	NiCl ₂ (dtbbpy)	10	46
12	NiCl ₂ (DME)	10	37
13	NiCl ₂ (DME)	40	50

Reaction conditions: styrene oxide (**5a**) (0.2 mmol, 1 equiv.), 4-iodotoluene (**6a**) (1.5 equiv.), B₁₂ (**1**) (5mol%), Zn (1.5 equiv.), NH₄Cl (3 equiv.), dtbbpy (40 mol%), dry NMP (2 mL), Blue LED, 30 min.; ^c – without ligand

3.9 Screening of ligands



The amount of the ligand added:

Entry	Ligand [mol%]	Yield of 7aa [%]
1	10	39
2	15	41
3	20	36
4	30	37
5	40	53
6	50	39

Reaction conditions: styrene oxide (**5a**) (0.2 mmol, 1eq.), 4-iodotoluene (**6a**) (1.5 eq.), B₁₂ (**1**) (5mol%), Zn (1.5 equiv.), NH₄Cl (3 equiv.) NiCl₂(DME) (20 mol%), dry NMP (2 mL), Blue LED, 30 min

3.10 Optimization of the substrates ratio

Entry	5a (equiv.)	6a (equiv.)	Yield of 7aa [%]
1	1	1.5	53
2	1.5	1	43
3	1	1	40
4	1	2	36
5	2	1	45
6	1	3	42

Reaction conditions: styrene oxide (**5a**) (0.2 mmol), 4-iodotoluene (**6a**), B₁₂ (**1**) (5mol%), Zn (1.5 equiv.), NH₄Cl (3 equiv.) NiCl₂(DME) (20 mol%), dtbbpy (40 mol%), dry NMP (2 mL), Blue LED, 30 min.

3.11 Concentration of styrene oxide (**5a**)

Entry	[mol/dm ³]	Yield of 7aa [%]
1	0.05	18
2	0.1	53
3	0.2	36

Reaction conditions: styrene oxide (**5a**) (0.2 mmol, 1 equiv.), 4-iodotoluene (**6a**) (1.5 equiv.), B₁₂ (**1**) (5 mol%), Zn (1.5 equiv.), NH₄Cl (3 equiv.), NiCl₂(DME) (20 mol%), dtbbpy (40 mol%), dry NMP (2 mL), Blue LED, 30 min.

3.12 The influence of water on the model reaction

Entry	H ₂ O (equiv.)	Yield of 7aa [%]
1	0.3	50
2	0.6	42
3	1.1	60
4	2.2	60
5	4.4	59

Reaction conditions: styrene oxide (**5a**) (0.2 mmol), 4-iodotoluene (**6a**), B₁₂ (**1**) (5 mol%), Zn (1.5 equiv.), NH₄Cl (3 equiv.), NiCl₂(DME) (20 mol%), dtbbpy (40 mol%), dry NMP (2 mL), Blue LED, 30 min.

4. General Procedures

A. General procedure for aryl epoxide:

Each reaction was prepared in two glass vials (10 mL) sealed with aluminum caps with a rubber septa. The first one, equipped with a magnetic stirring bar, was charged with activated Zn⁰ dust (20 mg, 0.3 mmol, 1.5 equiv.), NH₄Cl (32 mg, 0.6 mmol, 3 equiv.), and catalyst **1** (5 mol%, 13.5 mg). To the second vial were consecutively added dtbpy (40 mol%, 21 mg), aryl iodide (65 mg, 0.3 mmol, 1.5 equiv.), and NiCl₂(DME) (20 mol%, 9 mg). Then dry NMP (1 mL containing water – 0.55 equiv.) was added to each vial. The resulting mixture was degassed by purging with argon with simultaneous sonication in an ultrasonic bath for 15 min. An epoxide (0.2 mmol, 1.0 equiv.) was added dropwise *via* a syringe to the first vial and then the solution from the second was transferred to the first vial. The resulting mixture was irradiated with blue LED light (single diode, 10 W; λ = 460 nm) for 30 min. at room temperature. The resulting mixture was diluted with AcOEt, washed with water (10 mL) and brine (15 mL). The organic phase was dried over Na₂SO₄, then filtered through the cotton wool and concentrated *in vacuo*. A crude product was purified by means of column chromatography.

B. General procedure for aliphatic epoxide:

Each reaction was prepared in two glass vials (10 mL) sealed with aluminum caps with a rubber septa. The first one, equipped with a magnetic stirring bar, was charged with activated Zn⁰ dust (20 mg, 0.3 mmol, 1.5 equiv.), NH₄Cl (32 mg, 0.6 mmol, 3 equiv.), and catalyst **1** (5 mol%, 13.5 mg). To the second vial was consecutively added dtbpy (40 mol%, 21 mg), aryl iodide (65 mg, 0.3 mmol, 1.5 equiv.), and NiCl₂(DME) (20 mol%, 9 mg). Then dry NMP (1 mL containing water – 0.55 equiv.) was added to each vial. The resulting mixture was degassed by purging with argon with simultaneous sonication in an ultrasonic bath for 15 min. An epoxide (0.2 mmol, 1.0 equiv.) was added dropwise *via* a syringe to the first vial and then the solution from the second was transferred to the first vial. The resulting mixture was irradiated with blue LED light (single diode, 3 W; λ = 460 nm) for 16 h at room temperature. The resulting mixture was diluted with AcOEt, washed with water (10 mL) and brine (15 mL). The organic phase was dried over Na₂SO₄, then filtered through the cotton wool and concentrated *in vacuo*. A crude product was purified by means of column chromatography.

C. General procedure for cyclic epoxide with B₁₂:

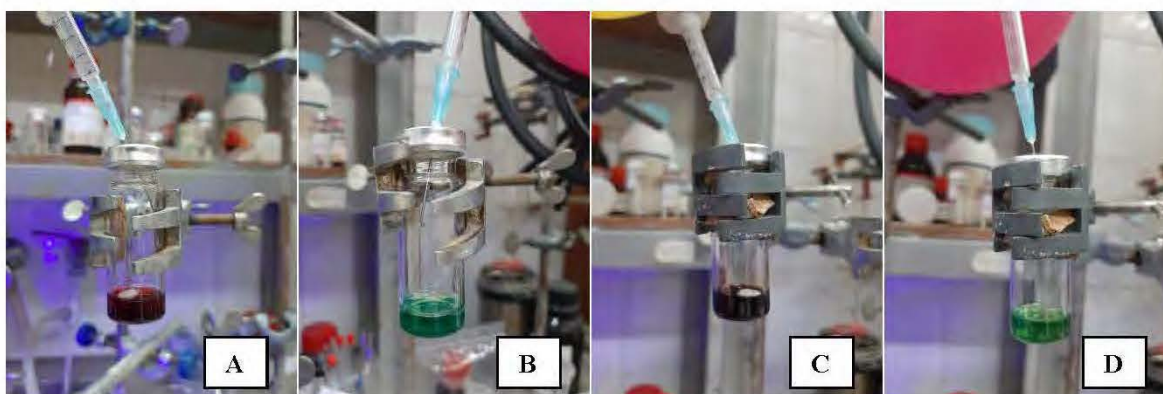
Each reaction was prepared in two glass vials (10 mL) sealed with aluminum caps with a rubber septa. The first one, equipped with a magnetic stirring bar, was charged with activated Zn⁰ dust (20 mg, 0.3 mmol, 1.5 equiv.), NH₄Cl (32 mg, 0.6 mmol, 3 equiv.), and catalyst **1** (5 mol%, 13.5 mg). To the second vial was consecutively added dtbpy (40 mol%, 21 mg), aryl iodide (65 mg, 0.3 mmol, 1.5 equiv.), and NiCl₂(DME) (20 mol%, 9 mg). Then dry NMP (1 mL containing water – 0.55 equiv.) was added to each vial. The resulting mixture was degassed by purging with argon with simultaneous sonication in an ultrasonic bath for 15 min. An epoxide (0.2 mmol, 1.0 equiv.) was added dropwise *via* a syringe to the first vial and then the solution from the second was transferred to the first vial. The resulting mixture was irradiated with blue LED light (single diode, 3 W; λ = 460 nm) for 16 h at room temperature. The resulting mixture was diluted with AcOEt, washed with water (10 mL) and brine (15 mL). The organic phase was dried over Na₂SO₄, then filtered through the cotton wool and concentrated *in vacuo*. A crude product was purified by means of column chromatography.

D. General procedure for cyclic epoxide with HME:

Each reaction was prepared in two glass vials (10 mL) sealed with aluminum caps with a rubber septa. The first one, equipped with a magnetic stirring bar, was charged with activated Zn⁰ dust (20 mg, 0.3 mmol, 1.5 equiv.), NH₄Cl (32 mg, 0.6 mmol, 3 equiv.), and catalyst **3** (5 mol%, 11 mg). To the second vial was consecutively added dtbbpy (40 mol%, 21 mg), aryl iodide (65 mg, 0.3 mmol, 1.5 equiv.), and NiCl₂(DME) (20 mol%, 9 mg). Then acetone (1 mL) was added to each vial. The resulting mixture was degassed by purging with argon with simultaneous sonication in an ultrasonic bath for 5 min. An epoxide (0.2 mmol, 1.0 equiv.) was added dropwise via a syringe to the first vial and then the solution from the second was transferred to the first vial. The resulting mixture was irradiated with blue LED light (single diode, 3 W; λ = 460 nm) for 16 h at room temperature. The resulting mixture was diluted with AcOEt, filtered through the cotton wool and concentrated *in vacuo*. A crude product was purified by means of column chromatography.

4.1 Note:

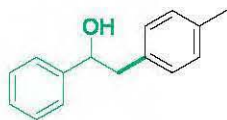
- The reaction can be easily monitored by TLC chromatography (AcOEt/Hexane) using UV visualization, KMnO₄ or the Hanessian's stain;
- Reactions require using activated zinc (unactivated zinc gives a low yield);
- The mixture containing Zn, NH₄Cl, Cobalt-catalyst (B₁₂ or HME) and a solvent should turned from red to dark green and finally brown. The color indicates the reduction of the cobalt from Co(III) to Co(I) oxidation state (see pictures below);
- If the color of the reaction does not change (from red to dark brown/green), we highly recommend to repeat zinc activation step;
- We highly advise to use two vials for two reasons: a) you can check by the color if the cobalt has been reduced, b) the reaction prepared in one vial gives product in slightly decreased yield.



4.1 A) The vial containing B₁₂ (5 mol%), NH₄Cl (3 equiv.), Zn (1.5 equiv.) – before degassing (**color: red**); B) The vial containing NiCl₂(DME) (20 mol%), dtbbpy (40 mol%), aryl halide (1.5 equiv.) – before degassing (**color: bluish green**); C) The vial containing B₁₂ (5 mol%), NH₄Cl (3 equiv.), Zn (1.5 equiv.) – after degassing (**color: dark brown**); D) The vial containing NiCl₂(DME) (20 mol%), dtbbpy (40 mol%), aryl halide (1.5 equiv.) – after degassing (**color: light green**).

5. Scope and characterization of new compounds

1-phenyl-2-(*p*-tolyl)ethan-1-ol (**7aa**)



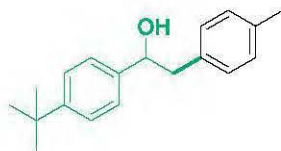
Following the general procedure **A** compound **7aa** was obtained from styrene oxide (**5a**) (24 mg, 0.20 mmol) and 4-iodotoluene (**6a**) (65 mg, 0.30 mmol). The crude product was purified by column chromatography (5:95 AcOEt/Hexane) to afford 25 mg of 1-phenyl-2-(*p*-tolyl)ethan-1-ol (**7aa**) as white solid, (yield = **60%**).

NMR data matched those reported in the literature.¹¹

¹H NMR (400 MHz, CDCl₃): δ 7.39 – 7.26 (m, 5H), 7.13 – 7.07 (m, 4H), 4.88 (dd, *J* = 8.6, 4.7 Hz, 1H), 3.02 (dd, *J* = 13.7, 4.7 Hz, 1H), 2.94 (dd, *J* = 13.7, 8.6 Hz, 1H), 2.33 (s, 3H), 1.93 (s, 1H).

¹³C NMR (100 MHz, CDCl₃): δ 143.9, 136.2, 134.9, 129.4, 129.2, 128.4, 127.6, 125.9, 75.4, 45.7, 21.0.

1-(4-(*tert*-butyl)phenyl)-2-(*p*-tolyl)ethan-1-ol (**7ba**)



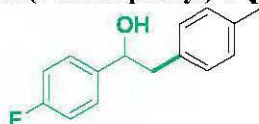
Following the general procedure **A** compound **7ba** was obtained from 4-*tert*-butylphenylethylene oxide (**5b**) (35 mg, 0.20 mmol) and 4-iodotoluene (**6a**) (65 mg, 0.30 mmol). The crude product was purified by column chromatography (5:95 AcOEt/Hexane) to afford 27 mg of 1-(4-(*tert*-butyl)phenyl)-2-(*p*-tolyl)ethan-1-ol (**7ba**) as white solid, (yield = **50%**).

NMR data matched those reported in the literature.¹¹

¹H NMR (400 MHz, CDCl₃): δ 7.41 – 7.37 (m, 2H), 7.34 – 7.30 (m, 2H), 7.13 (s, 4H), 4.85 (dd, *J* = 9.0, 4.3 Hz, 1H), 3.02 (dd, *J* = 13.8, 4.3 Hz, 1H), 2.93 (dd, *J* = 13.8, 9.0 Hz, 1H), 2.34 (s, 3H), 1.90 (s, 1H), 1.33 (s, 9H).

¹³C NMR (125 MHz, CDCl₃): δ 150.5, 141.0, 136.1, 135.2, 129.3, 129.2, 125.6, 125.3, 75.1, 45.5, 34.5, 31.4, 30.0, 21.0.

1-(4-fluorophenyl)-2-(*p*-tolyl)ethan-1-ol (**7ca**)



Following the general procedure **A** compound **7ca** was obtained from 4-fluorostyrene oxide (**5c**) (28 mg, 0.20 mmol) and 4-iodotoluene (**6a**) (65 mg, 0.30 mmol). The crude product was purified by column chromatography (5:95 AcOEt/Hexane) to afford 27 mg of 1-(4-fluorophenyl)-2-(*p*-tolyl)ethan-1-ol (**7ca**) as white solid, (yield = **59%**).

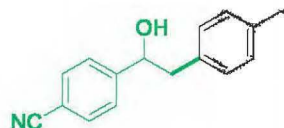
NMR data matched those reported in the literature.¹¹

¹H NMR (400 MHz, CDCl₃): δ 7.33 – 7.30 (m, 2H), 7.13 – 6.98 (m, 6H), 4.87 (dd, *J* = 7.8, 5.4 Hz, 1H), 3.01 (dd, *J* = 12.0, 4.0 Hz, 1H), 2.94 (dd, *J* = 13.7, 8.1 Hz, 1H), 2.33 (s, 3H), 1.91 (s, 1H).

¹³C NMR (150 MHz, CDCl₃): δ 162.2 (d, *J* = 247.0 Hz), 139.5 (d, *J* = 3.4 Hz), 136.3, 134.5, 129.4, 129.3, 127.5 (d, *J* = 8.8 Hz), 115.5 (d, *J* = 21.4 Hz), 74.7, 45.8, 21.1.

¹⁹F NMR (376 MHz, CDCl₃): δ -115.1.

4-(1-hydroxy-2-(*p*-tolyl)ethyl)benzonitrile (**7da**)



Following the general procedure A compound **7da** was obtained from 4-oxiran-2-ylbenzonitrile (**5d**) (29 mg, 0.20 mmol) and 4-iodotoluene (**6a**) (65 mg, 0.30 mmol). The crude product was purified by column chromatography (10:90 AcOEt/Hexane) to afford 25 mg of 4-(1-hydroxy-2-(*p*-tolyl)ethyl)benzonitrile (**7da**) as white solid, (yield = **53%**).

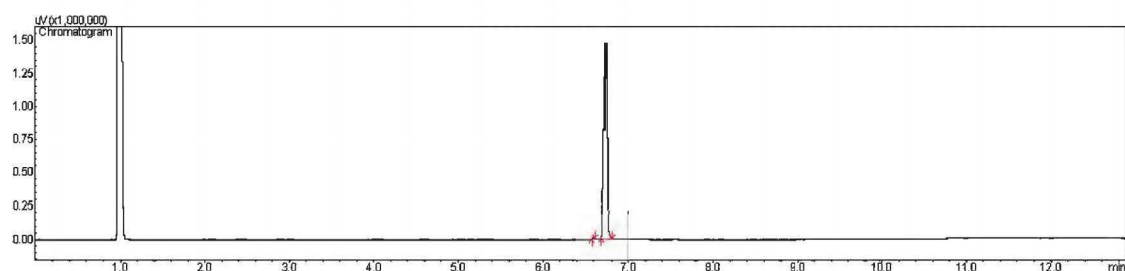
m.p. 79.5-80 °C

¹H NMR (400 MHz, CDCl₃): δ 7.63 (d, *J* = 8.1 Hz, 2H), 7.45 (d, *J* = 8.0 Hz, 2H), 7.13 (d, *J* = 7.8 Hz, 2H), 7.05 (d, *J* = 7.9 Hz, 2H), 4.96 – 4.92 (m, 1H), 3.01 (dd, *J* = 13.5, 4.8 Hz, 1H), 2.89 (dd, *J* = 13.6, 8.5 Hz, 1H), 2.34 (s, 3H), 2.03 (d, *J* = 3.6 Hz, 1H).

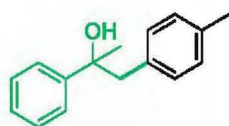
¹³C NMR (125 MHz, CDCl₃): δ 149.0, 136.7, 133.6, 132.2, 129.4, 129.3, 126.6, 118.9, 111.2, 74.5, 45.7, 21.0.

HRMS (ED) [M]⁺ calculated for C₁₆H₁₅NO: 237.1154, found: 237.1154.

GC Chromatogram: (99% purity)



2-phenyl-1-(*p*-tolyl)propan-2-ol (**7fa**)



Following the general procedure A compound **7fa** was obtained from 2-methyl-2-phenyloxirane (**5f**) (27 mg, 0.20 mmol) and 4-iodotoluene (**6a**) (65 mg, 0.30 mmol). The crude product was purified by column chromatography (5:95 AcOEt/Hexane) to afford 20 mg of 2-phenyl-1-(*p*-tolyl)propan-2-ol (**7fa**) as white solid, (yield = **44%**).

NMR data matched those reported in the literature.¹²

¹H NMR (400 MHz, CDCl₃): δ 7.42 – 7.39 (m, 2H), 7.35 – 7.31 (m, 2H), 7.26 – 7.22 (m, 1H), 7.03 (d, *J* = 7.8 Hz, 2H), 6.88 (d, *J* = 8.0 Hz, 2H), 3.11 (d, *J* = 13.4 Hz, 1H), 2.99 (d, *J* = 13.4 Hz, 1H), 2.30 (s, 3H), 1.85 (s, 1H), 1.56 (s, 3H).

¹³C NMR (125 MHz, CDCl₃): δ 147.0, 136.4, 133.7, 130.6, 129.0, 128.2, 126.7, 125.1, 74.5, 50.2, 29.6, 21.2.

1-phenyl-2-(*m*-tolyl)ethan-1-ol (**7ab**)



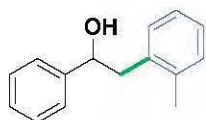
Following the general procedure **A** compound **7ab** was obtained from styrene oxide (**5a**) (24 mg, 0.20 mmol) and 3-iodotoluene (**6b**) (65 mg, 0.30 mmol). The crude product was purified by column chromatography (5:95 AcOEt/Hexane) to afford 20 mg of 1-phenyl-2-(*m*-tolyl)ethan-1-ol (**7ab**) as white solid, (yield = **47%**).

NMR data matched those reported in the literature.¹¹

¹H NMR (400 MHz, CDCl₃): δ 7.40 – 7.26 (m, 5H), 7.22 – 7.18 (m, 1H), 7.08 – 6.99 (m, 3H), 4.90 (dd, *J* = 8.8, 4.5 Hz, 1H), 3.02 (dd, *J* = 13.7, 4.5 Hz, 1H), 2.93 (dd, *J* = 13.7, 8.9 Hz, 1H), 2.34 (s, 3H), 1.96 (s, 1H).

¹³C NMR (125 MHz, CDCl₃): δ 143.9, 138.2, 138.0, 130.3, 128.44, 128.40, 127.6, 127.4, 126.5, 125.9, 75.3, 46.1, 21.4.

1-phenyl-2-(*o*-tolyl)ethan-1-ol (**7ac**)



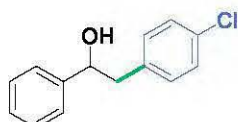
Following the general procedure **A** compound **7ac** was obtained from styrene oxide (**5a**) (24 mg, 0.20 mmol) and 2-iodotoluene (**6c**) (65 mg, 0.30 mmol). The crude product was purified by column chromatography (5:95 AcOEt/Hexane) to afford 14 mg of 1-phenyl-2-(*o*-tolyl)ethan-1-ol (**7ac**) as white solid, (yield = **33%**).

NMR data matched those reported in the literature.¹¹

¹H NMR (400 MHz, CDCl₃): δ 7.39 – 7.27 (m, 5H), 7.18 – 7.14 (m, 4H), 4.91 (dd, *J* = 8.1, 5.2 Hz, 1H), 3.06 (dd, *J* = 12.0, 4.0 Hz, 1H), 3.01 (dd, *J* = 12.0, 8.0 Hz, 1H), 2.31 (s, 3H), 1.94 (s, 1H).

¹³C NMR (125 MHz, CDCl₃): δ 144.1, 136.8, 136.3, 130.5, 130.3, 128.4, 127.6, 126.8, 126.0, 125.8, 74.4, 43.4, 19.6.

2-(4-chlorophenyl)-1-phenylethan-1-ol (**7ad**)



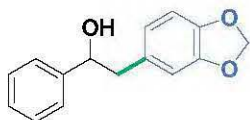
Following the general procedure **A** compound **7ad** was obtained from styrene oxide (**5a**) (24 mg, 0.20 mmol) and 1-chloro-4-iodobenzene (**6d**) (72 mg, 0.30 mmol). The crude product was purified by column chromatography (5:95 AcOEt/Hexane) to afford 21 mg of 2-(4-chlorophenyl)-1-phenylethan-1-ol (**7ad**) as white solid. (Yield = **44%**).

NMR data matched those reported in the literature.¹³

¹H NMR (400 MHz, CDCl₃): δ 7.37 – 7.28 (m, 5H), 7.27 – 7.22 (m, 2H), 7.11 – 7.07 (m, 2H), 4.87 (t, *J* = 6.6 Hz, 1H), 2.99 (d, *J* = 6.6 Hz, 2H), 1.92 (s, 1H).

¹³C NMR (125 MHz, CDCl₃): δ 143.6, 136.5, 132.4, 130.9, 128.5, 128.5, 127.8, 125.9, 75.3, 45.2.

2-(benzo[d][1,3]dioxol-5-yl)-1-phenylethan-1-ol (**7ae**)



Following the general procedure A compound **7ae** was obtained from styrene oxide (**5a**) (24 mg, 0.20 mmol) and 5-iodo-1,3-benzodioxole (**6e**) (74 mg, 0.30 mmol). The crude product was purified by column chromatography (5:95 AcOEt/Hexane) to afford 30 mg of 2-(benzo[d][1,3]dioxol-5-yl)-1-phenylethan-1-ol (**7ae**) as white solid, (yield = 61%).

m.p. 96.5-97.5 °C

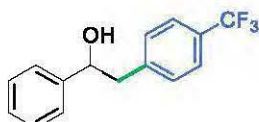
¹H NMR (400 MHz, CDCl₃): δ 7.37 – 7.26 (m, 5H), 6.77 – 6.61 (m, 3H), 5.93 (s, 2H), 4.84 (dd, *J* = 8.3, 4.9 Hz, 1H), 2.96 (dd, *J* = 13.8, 4.9 Hz, 1H), 2.90 (dd, *J* = 13.8, 8.4 Hz, 1H), 2.01 (s, 1H).

¹³C NMR (125 MHz, CDCl₃): δ 147.7, 146.3, 143.8, 131.7, 128.4, 127.6, 125.9, 122.5, 109.8, 108.3, 100.9, 75.4, 45.8.

HRMS (EI) [M]⁺ calculated for C₁₅H₁₄O₃: 242.0943, found: 242.0938.

Elemental Analysis (%) calculated for C₁₅H₁₄O₃: C 74.36, H 5.82, found: C 74.33, H 5.86.

1-phenyl-2-(4-(trifluoromethyl)phenyl)ethan-1-ol (**7af**)



Following the general procedure A compound **7af** was obtained from styrene oxide (**5a**) (24 mg, 0.20 mmol) and 4-iodobenzotrifluoride (**6f**) (82 mg, 0.30 mmol). The crude product was purified by column chromatography (5:95 AcOEt/Hexane) to afford 19 mg of 1-phenyl-2-(4-(trifluoromethyl)phenyl)ethan-1-ol (**7af**) as white solid, (yield = 36%).

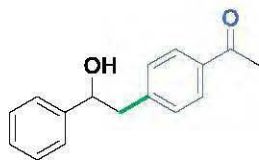
NMR data matched those reported in the literature.¹¹

¹H NMR (400 MHz, CDCl₃): δ 7.54 (d, *J* = 8.0 Hz, 2H), 7.38 – 7.27 (m, 7H), 4.92 (t, *J* = 5.0 Hz, 1H), 3.12 – 3.04 (m, 2H), 1.91 (s, 1H).

¹³C NMR (125 MHz, CDCl₃): δ 143.6, 142.4, 130.0, 129.0 (q, *J* = 32.8 Hz), 128.7, 128.1, 126.0, 124.43 (q, *J* = 273.4 Hz), 125.41 (q, *J* = 2.8 Hz), 75.31, 45.73.

¹⁹F NMR (376 MHz, CDCl₃): δ -62.4.

1-(4-(2-hydroxy-2-phenylethyl)phenyl)ethan-1-one (**7ag**)



Following the general procedure **A** compound **7ag** was obtained from styrene oxide (**5a**) (24 mg, 0.20 mmol) and 4'-iodoacetophenone (**6g**) (74 mg, 0.30 mmol). The crude product was purified by column chromatography (10:90 AcOEt/Hexane) to afford 29 mg of 1-(4-(2-hydroxy-2-phenylethyl)phenyl)ethan-1-one (**7ag**) as white solid, (yield = **60%**).

NMR data matched those reported in the literature.¹⁴

¹H NMR (400 MHz, CDCl₃): δ 7.89 – 7.85 (m, 2H), 7.36 – 7.25 (m, 7H), 4.93 (dd, *J* = 7.4, 5.8 Hz, 1H), 3.11 (dd, *J* = 12.0, 8.0 Hz, 1H), 3.07 (dd, *J* = 16.0, 8.0 Hz, 1H), 2.57 (s, 3H), 1.99 (s, 1H).

¹³C NMR (125 MHz, CDCl₃): δ 197.8, 143.8, 143.5, 135.6, 129.8, 128.5, 128.5, 127.9, 125.9, 75.1, 45.8, 26.5.

2-(4-methoxyphenyl)-1-phenylethan-1-ol (**7ah**)



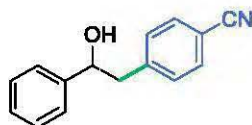
Following the general procedure **A** compound **7ah** was obtained from styrene oxide (**5a**) (24 mg, 0.20 mmol) and 4-iodoanisole (**6h**) (70 mg, 0.30 mmol). The crude product was purified by column chromatography (5:95 AcOEt/Hexane) to afford 22 mg of 2-(4-methoxyphenyl)-1-phenylethan-1-ol (**7ah**) as white solid, (yield = **48%**).

NMR data matched those reported in the literature.¹⁴

¹H NMR (400 MHz, CDCl₃): δ 7.35 (d, *J* = 4.4 Hz, 4H), 7.30 – 7.26 (m, 1H), 7.13 – 7.08 (m, 2H), 6.86 – 6.81 (m, 2H), 4.85 (dd, *J* = 8.3, 5.0 Hz, 1H), 3.79 (s, 3H), 3.00 (dd, *J* = 13.8, 4.9 Hz, 1H), 2.93 (dd, *J* = 13.8, 8.3 Hz, 1H), 1.99 (s, 1H).

¹³C NMR (100 MHz, CDCl₃): δ 158.6, 144.0, 130.6, 130.1, 128.5, 127.7, 126.0, 114.1, 75.6, 55.4, 45.3.

4-(2-hydroxy-2-phenylethyl)benzotrile (**7ai**)



Following the general procedure **A** compound **7ai** was obtained from styrene oxide (**5a**) (24 mg, 0.20 mmol) and 4-iodobenzotrile (**6i**) (69 mg, 0.30 mmol). The crude product was purified by column chromatography (5:95 AcOEt/Hexane) to afford 12 mg of 4-(2-hydroxy-2-phenylethyl)benzotrile (**7ai**) as white solid, (yield = **28%**).

NMR data matched those reported in the literature.¹⁴

¹H NMR (400 MHz, CDCl₃): δ 7.57 – 7.52 (m, 2H), 7.37 – 7.24 (m, 7H), 4.91 (dd, *J* = 7.7, 5.4 Hz, 1H), 3.11 (dd, *J* = 13.6, 7.7 Hz, 1H), 3.05 (dd, *J* = 13.7, 5.4 Hz, 1H), 2.01 (s, 1H).

¹³C NMR (125 MHz, CDCl₃): δ 143.8, 143.3, 132.0, 130.4, 128.6, 128.0, 125.8, 118.9, 110.4, 75.0, 45.7.

1,2-diphenylethan-1-ol (**7aj**)



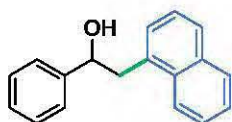
Following the general procedure **A** compound **7aj** was obtained from styrene oxide (**5a**) (24 mg, 0.20 mmol) and iodobenzene (**6j**) (61 mg, 0.30 mmol). The crude product was purified by column chromatography (5:95 AcOEt/Hexane) to afford 25 mg of 1,2-diphenylethan-1-ol (**7aj**) as white solid, (yield = **63%**).

NMR data matched those reported in the literature.¹⁵

¹H NMR (400 MHz, CDCl₃): δ 7.37 – 7.26 (m, 7H), 7.25 – 7.18 (m, 3H), 4.91 (dd, *J* = 8.4, 5.0 Hz, 1H), 3.05 (dd, *J* = 13.7, 4.9 Hz, 1H), 2.99 (dd, *J* = 13.7, 8.4 Hz, 1H), 1.93 (s, 1H).

¹³C NMR (125 MHz, CDCl₃): δ 143.8, 138.0, 129.5, 128.5, 128.4, 127.6, 126.6, 125.9, 75.3, 46.1.

2-(18aphthalene-1-yl)-1-phenylethan-1-ol (**7ak**)



Following the general procedure **A** compound **7ak** was obtained from styrene oxide (**5a**) (24 mg, 0.20 mmol) and 1-iodonaphthalene (**6k**) (76 mg, 0.30 mmol). The crude product was purified by column chromatography (5:95 AcOEt/Hexane) to afford 21 mg of 2-(18aphthalene-1-yl)-1-phenylethan-1-ol (**7ak**) as white solid, (yield = **42%**).

m.p. 66.0-66.5 °C

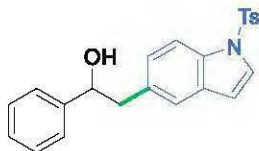
¹H NMR (400 MHz, CDCl₃): δ 8.13 (dd, *J* = 12.0, 4.0 Hz, 1H), 7.89 (dd, *J* = 8.3, 1.1 Hz, 1H), 7.78 (d, *J* = 8.2 Hz, 1H), 7.58 – 7.48 (m, 2H), 7.46 – 7.28 (m, 7H), 5.08 (dd, *J* = 8.9, 4.3 Hz, 1H), 3.56 (dd, *J* = 14.0, 4.3 Hz, 1H), 3.41 (dd, *J* = 14.0, 8.9 Hz, 1H), 1.95 (s, 1H).

¹³C NMR (125 MHz, CDCl₃): δ 144.1, 134.1, 134.0, 132.1, 128.9, 128.5, 127.9, 127.7, 127.6, 126.1, 125.8, 125.7, 125.5, 123.7, 74.4, 43.3.

HRMS (ESI) [M+Na]⁺ calculated for C₁₈H₁₆ONa: 271.1099, found: 271.1096.

Elemental Analysis (%) calculated for C₁₈H₁₆O: C 87.06, H 6.49, found: C 86.92, H 6.59.

1-phenyl-2-(1-tosyl-1*H*-indol-5-yl)ethan-1-ol (**7al**)



Following the general procedure A compound **7al** was obtained from styrene oxide (**5a**) (24 mg, 0.20 mmol) and 5-iodo-1-(4-methylphenylsulfonyl)indole (**6l**) (119 mg, 0.30 mmol). The crude product was purified by column chromatography (10:90 AcOEt/Hexane) to afford 34 mg of 1-phenyl-2-(1-tosyl-1*H*-indol-5-yl)ethan-1-ol (**7al**) as white solid, (yield = 44%).

m.p. 47.6-47.9 °C

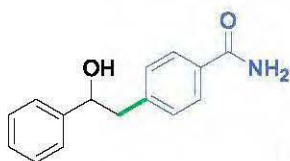
¹H NMR (400 MHz, CDCl₃): δ 7.91 (d, *J* = 8.5 Hz, 1H), 7.78 – 7.73 (m, 2H), 7.54 (d, *J* = 3.7 Hz, 1H), 7.37 – 7.27 (m, 6H), 7.21 (d, *J* = 8.2 Hz, 2H), 7.14 (dd, *J* = 8.5, 1.7 Hz, 1H), 6.60 (dd, *J* = 3.7, 0.8 Hz, 1H), 4.89 (dd, *J* = 8.7, 4.5 Hz, 1H), 3.10 (dd, *J* = 13.8, 4.6 Hz, 1H), 3.02 (dd, *J* = 13.8, 8.7 Hz, 1H), 2.34 (s, 3H), 1.96 (s, 1H).

¹³C NMR (125 MHz, CDCl₃): δ 144.9, 143.8, 135.3, 133.8, 133.1, 131.1, 129.8, 128.4, 127.6, 126.8, 126.62, 126.1, 125.8, 122.0, 113.5, 108.9, 75.4, 45.9, 21.5.

HRMS (ESI) [M+Na]⁺ calculated for C₂₃H₂₁NO₃SNa: 414.1140, found: 414.1134.

Elemental Analysis (%) calculated for C₂₃H₂₁NO₃S: C 70.57, H 5.41, N 3.58, S 8.19, found: C 70.31, H 5.44, N 3.52, S 7.99.

4-(2-hydroxy-2-phenylethyl)benzamide (**7am**)



Hygroscopic compound

Following the general procedure A compound **7am** was obtained from styrene oxide (**5a**) (24 mg, 0.20 mmol) and 4-iodobenzamide (**6m**) (74 mg, 0.30 mmol). The crude product was purified by column chromatography (gradually from AcOEt/Hexane 50:50 to 80:20) to afford 16 mg of 4-(2-hydroxy-2-phenylethyl)benzamide (**7am**) as white solid, (yield = 33%).

m.p. 175.7-176.2 °C

¹H NMR (400 MHz, MeOD): δ 7.74 – 7.70 (m, 2H), 7.27 (d, *J* = 4.3 Hz, 4H), 7.24 – 7.18 (m, 3H), 4.86 (dd, *J* = 7.3, 6.3 Hz, 1H), 3.10 (dd, *J* = 13.4, 7.4 Hz, 1H), 3.01 (dd, *J* = 13.4, 6.2 Hz, 1H).

¹³C NMR (125 MHz, MeOD): δ 172.4, 145.5, 144.3, 132.7, 130.8, 129.2, 128.4, 128.4, 127.2, 76.1, 46.6.

HRMS (ESI) [M+Na]⁺ calculated for C₁₅H₁₅NO₂Na: 264.1000, found: 264.0994.

Elemental Analysis (%) calculated for C₁₅H₁₅NO₂: C 74.67, H 6.27, N 5.81, found: C 74.31, H 6.55, N 5.56.

***tert*-butyl (4-(2-hydroxy-2-phenylethyl)phenyl)carbamate (7an)**



Following the general procedure **A** compound **7an** was obtained from styrene oxide (**5a**) (24 mg, 0.20 mmol) and *N*-Boc-4-iodoaniline (**6n**) (96 mg, 0.30 mmol). The crude product was purified by column chromatography (10:90 AcOEt/Hexane) to afford 38 mg of *tert*-butyl (4-(2-hydroxy-2-phenylethyl)phenyl)carbamate (**7an**) as yellow pale solid, (yield = 60%).

m.p. 119.2-119.6 °C

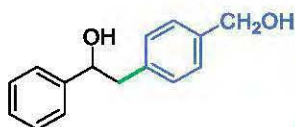
¹H NMR (400 MHz, CDCl₃): δ 7.27 (d, *J* = 4.3 Hz, 4H), 7.24 – 7.18 (m, 3H), 7.02 (d, *J* = 8.5 Hz, 2H), 6.40 (s, 1H), 4.78 (dd, *J* = 8.3, 5.0 Hz, 1H), 2.92 (dd, *J* = 13.7, 5.0 Hz, 1H), 2.87 (dd, *J* = 13.7, 8.3 Hz, 1H), 1.93 (s, 1H), 1.45 (s, 9H).

¹³C NMR (125 MHz, CDCl₃): δ 152.8, 143.8, 136.9, 132.5, 130.0, 128.4, 127.5, 125.9, 118.7, 80.5, 75.30, 45.4, 28.3.

HRMS (ESI) [M+Na]⁺ calculated for C₁₉H₂₃NO₃Na: 336.1576, found: 336.1571.

Elemental Analysis (%) calculated for C₁₉H₂₃NO₃: C 72.82, H 7.40, N 4.47, found: C 72.75, H 7.45, N 4.42.

2-(4-(hydroxymethyl)phenyl)-1-phenylethan-1-ol (7ao)



Hygroscopic compound

Following the general procedure **A** compound **7ao** was obtained from styrene oxide (**5a**) (24 mg, 0.20 mmol) and 4-iodobenzyl alcohol (**6o**) (70 mg, 0.30 mmol). The crude product was purified by column chromatography (25:75 AcOEt/Hexane) to afford 21 mg of 2-(4-(hydroxymethyl)phenyl)-1-phenylethan-1-ol (**7ao**) as white solid, (yield = 46%).

m.p. 71.5-72.0 °C

¹H NMR (400 MHz, CDCl₃): δ 7.35 (d, *J* = 4.1 Hz, 4H), 7.31 – 7.26 (m, 3H), 7.19 (d, *J* = 7.9 Hz, 2H), 4.89 (dd, *J* = 8.3, 5.1 Hz, 1H), 4.65 (s, 2H), 3.05 (dd, *J* = 12.0, 4.0 Hz, 1H), 2.98 (dd, *J* = 16.0, 8.0 Hz, 1H), 1.99 (s, 1H), 1.69 (s, 1H).

¹³C NMR (125 MHz, CDCl₃): δ 143.7, 139.2, 137.5, 129.7, 128.5, 127.7, 127.3, 125.9, 75.4, 65.2, 45.7.

HRMS (ESI) [M+Na]⁺ calculated for C₁₅H₁₆O₂Na: 251.1048, found: 251.1047.

Elemental Analysis (%) calculated for C₁₅H₁₆O₂ + 0.2·H₂O: C 77.69, H 7.13, found C 77.66, H 7.33.

1-(4-tolyl)hexan-2-ol (**7ha**)



Following the general procedure **B** compound **7ha** was obtained from 1,2-epoxyhexane (**5h**) (20 mg, 0.20 mmol) and 4-iodotoluene (**6a**) (65 mg, 0.30 mmol). The crude product was purified by column chromatography (5:95 AcOEt/Hexane) to afford 28 mg of 1-(4-tolyl)hexan-2-ol (**7ha**) as white solid, (yield = **74%**).

m.p. 37.2-36.5 °C

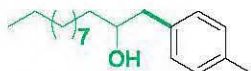
¹H NMR (400 MHz, CDCl₃): δ 7.14 – 7.09 (m, 4H), 3.82 – 3.76 (m, 1H), 2.80 (dd, *J* = 13.6, 4.2 Hz, 1H), 2.60 (dd, *J* = 13.6, 8.4 Hz, 1H), 2.33 (s, 3H), 1.55 – 1.45 (m, 4H), 1.40 – 1.31 (m, 3H), 0.92 (t, *J* = 7.2 Hz, 3H).

¹³C NMR (125 MHz, CDCl₃): δ 136.1, 135.6, 129.44, 129.38, 72.7, 43.7, 36.7, 28.1, 22.9, 21.1, 14.2.

HRMS (EI) [M]⁺ calculated for C₁₃H₂₀O: 192.1514, found: 192.1515.

Elemental Analysis (%) calculated for C₁₃H₂₀O: C 81.20, H 10.48, found: C 80.83, H 10.52.

1-(4-tolyl)dodecan-2-ol (**7ia**)



Following the general procedure **B** compound **7ia** was obtained from 1,2-epoxydodecane (**5i**) (37 mg, 0.20 mmol) and 4-iodotoluene (**6a**) (65 mg, 0.30 mmol). The crude product was purified by column chromatography (2:98 AcOEt/Hexane) to afford 43 mg of 1-(*p*-tolyl)dodecan-2-ol (**7ia**) as white solid, (yield = **77%**).

m.p. 53.9-54.8 °C

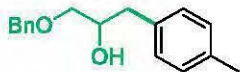
¹H NMR (400 MHz, CDCl₃): δ 7.14 – 7.07 (m, 4H), 3.82 – 3.76 (m, 1H), 2.79 (dd, *J* = 13.6, 4.2 Hz, 1H), 2.60 (dd, *J* = 13.6, 8.4 Hz, 1H), 2.33 (s, 3H), 1.55 – 1.42 (m, 5H), 1.26 (m, 14H), 0.88 (t, *J* = 8.0 Hz, 3H).

¹³C NMR (125 MHz, CDCl₃): δ 135.9, 135.5, 129.29, 129.25, 72.7, 43.6, 36.8, 31.9, 29.7, 29.62, 29.61, 29.3, 25.8, 22.7, 21.0, 14.1.

HRMS (EI) [M]⁺ calculated for C₁₉H₃₂O: 276.2453, found: 276.2454.

Elemental Analysis (%) calculated for C₁₉H₃₂O: C 82.55, H 11.67, found: C 82.67, H 11.48.

1-(benzyloxy)-3-(4-tolyl)propan-2-ol (**7ja**)



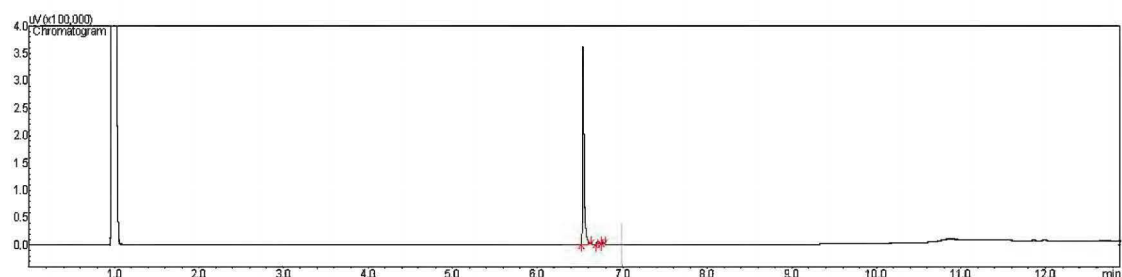
Following the general procedure **B** compound **7ja** was obtained from benzyl glycidyl ether (**5j**) (33 mg, 0.20 mmol) and 4-iodotoluene (**6a**) (65 mg, 0.30 mmol). The crude product was purified by column chromatography (10:90 AcOEt/Hexane) to afford 31 mg of 1-(benzyloxy)-3-(*p*-tolyl)propan-2-ol (**7ja**) as yellow pale oil, (yield = **61%**).

¹H NMR (400 MHz, CDCl₃): δ 7.40 – 7.28 (m, 5H), 7.11 (s, 4H), 4.55 (s, 2H), 4.04 (dd, *J* = 6.8, 3.5 Hz, 1H), 3.52 (dd, *J* = 9.5, 3.5 Hz, 1H), 3.41 (dd, *J* = 9.5, 6.9 Hz, 1H), 2.78 (d, *J* = 6.7 Hz, 2H), 2.33 (s, 3H), 1.62 (s, 1H).

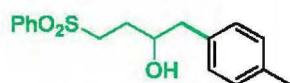
¹³C NMR (125 MHz, CDCl₃): δ 138.0, 135.9, 134.8, 129.19, 129.16, 128.4, 127.7, 73.6, 73.4, 71.5, 39.4, 21.0.

HRMS (EI) [M]⁺ calculated for C₁₇H₂₀O₂: 256.1463, found: 256.1474.

GC Chromatogram: (98% purity)



4-(phenylsulfonyl)-1-(*p*-tolyl)butan-2-ol (7ka)



Following the general procedure **B** compound **7ka** was obtained from 4-(phenylsulfonyl)-1,2-epoxubutane (**5k**) (42 mg, 0.20 mmol) and 4-iodotoluene (**6a**) (65 mg, 0.30 mmol). The crude product was purified by column chromatography (25:75 AcOEt/Hexane) to afford 45 mg of 4-(phenylsulfonyl)-1-(4-tolyl)butan-2-ol (**7ka**) as white solid, (yield = 73%).

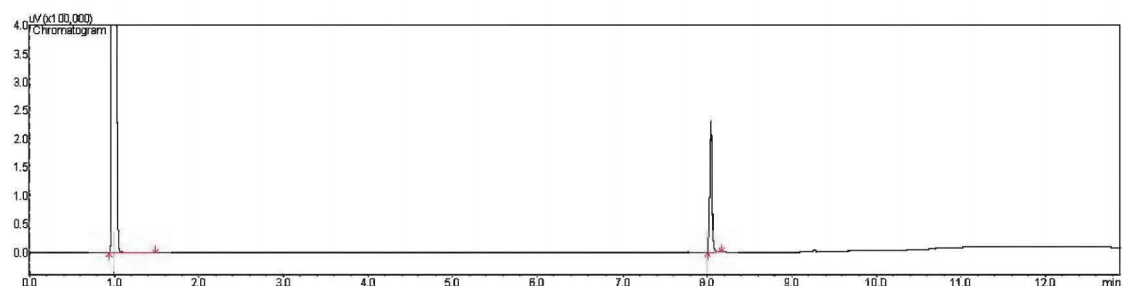
m.p. 94.8-95.2 °C

¹H NMR (400 MHz, CDCl₃): δ 7.90 (d, *J* = 7.3 Hz, 2H), 7.67 – 7.64 (m, 1H), 7.58 – 7.54 (m, 2H), 7.11 (d, *J* = 7.8 Hz, 2H), 7.04 (d, *J* = 7.9 Hz, 2H), 3.92 – 3.84 (m, 1H), 3.34 (ddd, *J* = 15.2, 10.1, 5.3 Hz, 1H), 3.21 (ddd, *J* = 16.0, 12.0, 8.0 Hz, 1H), 2.76 (dd, *J* = 13.6, 4.4 Hz, 1H), 2.62 (dd, *J* = 13.6, 8.3 Hz, 1H), 2.32 (s, 3H), 2.08 – 1.99 (m, 1H), 1.87 – 1.77 (m, 1H), 1.67 (d, *J* = 4.0 Hz, 1H).

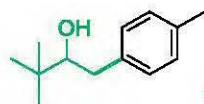
¹³C NMR (125 MHz, CDCl₃): δ 139.2, 136.5, 134.1, 133.7, 129.5, 129.3, 129.2, 128.0, 70.8, 53.2, 43.6, 29.4, 21.0.

HRMS (ESI) [M+Na]⁺ calculated for C₁₇H₂₀O₃Sna: 327.1031, found: 327.1015.

GC Chromatogram: (>99% purity)



3,3-dimethyl-1-(4-tolyl)butan-2-ol (**7la**)



Unstable compound

Following the general procedure **B** compound **7la** was obtained from 3,3-dimethyl-1,2-epoxybutane (**5l**) (20 mg, 0.20 mmol) and 4-iodotoluene (**6a**) (65 mg, 0.30 mmol). The crude product was purified by column chromatography (5:95 AcOEt/Hexane) to afford 19 mg of 3,3-dimethyl-1-(4-tolyl)butan-2-ol (**7la**) as white solid, (yield = 37%).

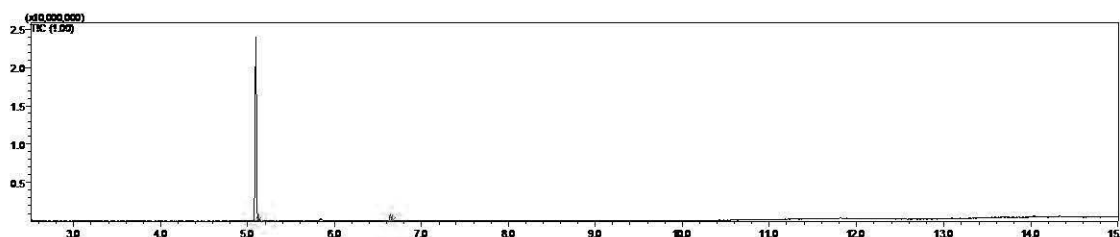
m.p. 65.3-66.0 °C

¹H NMR (400 MHz, CDCl₃): δ 7.13 (s, 4H), 3.41 (dd, *J* = 10.7, 2.1 Hz, 1H), 2.88 (dd, *J* = 13.6, 2.0 Hz, 1H), 2.43 (dd, *J* = 13.6, 10.7 Hz, 1H), 2.33 (s, 3H), 1.57 (s, 1H), 1.00 (s, 9H).

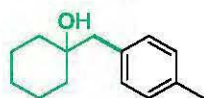
¹³C NMR (125 MHz, CDCl₃): δ 136.7, 135.8, 129.3, 129.2, 80.6, 37.9, 34.8, 25.9, 21.0.

HRMS (EI) [M]⁺ calculated for C₁₃H₂₀O: 192.1514, found: 192.1521.

GC Chromatogram: (97% purity)



1-(4-methylbenzyl)cyclohexan-1-ol (**7ma**)



Following the general procedure **C** compound **7ma** was obtained from 1-oxaspiro(2.5)octane (**5m**) (22 mg, 0.20 mmol) and 4-iodotoluene (**6a**) (65 mg, 0.30 mmol). The crude product was purified by column chromatography (5:95 AcOEt/Hexane) to afford 9 mg of 1-(4-methylbenzyl)cyclohexan-1-ol (**7ma**) as white solid, (yield = 21%).

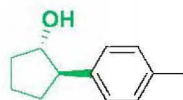
Following the general procedure **D** compound **7ma** was obtained from 1-oxaspiro(2.5)octane (**5m**) (22 mg, 0.20 mmol) and 4-iodotoluene (**6a**) (65 mg, 0.30 mmol). The crude product was purified by column chromatography (5:95 AcOEt/Hexane) to afford 12 mg of 1-(4-methylbenzyl)cyclohexan-1-ol (**7ma**) as white solid, (yield = 29%).

NMR data matched those reported in the literature.¹⁶

¹H NMR (400 MHz, CDCl₃): δ 7.10 (m, 4H), 2.71 (s, 2H), 2.33 (s, 3H), 1.61 – 1.38 (m, 11H).

¹³C NMR (150 MHz, CDCl₃): δ 135.9, 134.0, 130.5, 128.9, 71.1, 48.2, 37.3, 25.8, 22.2, 21.0.

(1*S*,2*R*)-2-(4-tolyl)cyclopentan-1-ol (**7na**)



Following the general procedure **C** compound **7na** was obtained from 1,2-epoxycyclopentane (**5n**) (17 mg, 0.20 mmol) and 4-iodotoluene (**6a**) (65 mg, 0.30 mmol). The crude product was purified by column chromatography (10:90 AcOEt/Hexane) to afford 5 mg of (1*S*,2*R*)-2-(*p*-tolyl)cyclopentan-1-ol (**7na**) as yellow pale oil, (yield = **14%**).

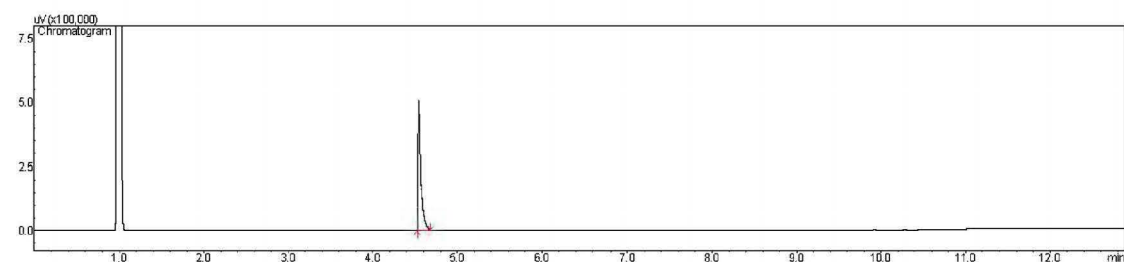
Following the general procedure **D** compound **7na** was obtained from 1,2-epoxycyclopentane (**5n**) (17 mg, 0.20 mmol) and 4-iodotoluene (**6a**) (65 mg, 0.30 mmol). The crude product was purified by column chromatography (10:90 AcOEt/Hexane) to afford 20 mg of (1*S*,2*R*)-2-(4-tolyl)cyclopentan-1-ol (**7na**) as yellow pale oil, (yield = **57%**).

¹H NMR (400 MHz, CDCl₃): δ 7.18 – 7.09 (m, 4H), 4.14 (dd, *J* = 12.0, 8.0 Hz, 1H), (dd, *J* = 16.0, 8.0 Hz 1H), 2.33 (s, 3H), 2.16 – 2.06 (m, 2H), 1.90 – 1.65 (m, 4H), 1.63 (s, 1H).

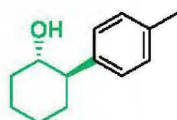
¹³C NMR (150 MHz, CDCl₃): δ 140.1, 136.0, 129.3, 127.3, 80.5, 54.1, 33.9, 31.8, 21.7, 21.0.

HRMS (EI) [M]⁺ calculated for C₁₂H₁₆O: 176.1201, found: 176.1202.

GC Chromatogram: (>99% purity)



(1*S*,2*R*)-2-(4-tolyl)cyclohexan-1-ol (**7oa**)



Following the general procedure **C** compound **7oa** was obtained from 1,2-epoxycyclohexane (**5o**) (20 mg, 0.20 mmol) and 4-iodotoluene (**6a**) (65 mg, 0.30 mmol). The crude product was purified by column chromatography (5:95 AcOEt/Hexane) to afford 12 mg of (1*S*,2*R*)-2-(*p*-tolyl)cyclohexan-1-ol (**7oa**) as white solid, (yield = **31%**).

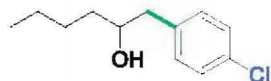
Following the general procedure **D** compound **7oa** was obtained from 1,2-epoxycyclohexane (**5o**) (20 mg, 0.20 mmol) and *p*-iodotoluene (**6a**) (65 mg, 0.30 mmol). The crude product was purified by column chromatography (5:95 AcOEt/Hexane) to afford 21 mg of (1*S*,2*R*)-2-(4-tolyl)cyclohexan-1-ol (**7oa**) as white solid, (yield = **56%**).

NMR data matched those reported in the literature.¹⁷

¹H NMR (400 MHz, CDCl₃): δ 7.15 (s, 4H), 3.63 (td, *J* = 10.1, 4.3 Hz, 1H), 2.39 (ddd, *J* = 13.2, 10.0, 3.6 Hz, 1H), 2.33 (s, 3H), 2.14 – 2.08 (m, 1H), 1.89 – 1.72 (m, 3H), 1.59 – 1.31 (m, 5H).

¹³C NMR (150 MHz, CDCl₃): δ 140.2, 136.4, 129.5, 127.8, 74.5, 52.8, 34.4, 33.4, 26.1, 25.1, 21.0.

1-(4-chlorophenyl)hexan-2-ol (**7hd**)



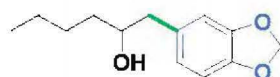
Following the general procedure **B** compound **7hd** was obtained from 1,2-epoxyhexane (**5h**) (20 mg, 0.20 mmol) and 1-chloro-4-iodobenzene (**6d**) (72 mg, 0.30 mmol). The crude product was purified by column chromatography (10:90 AcOEt/Hexane) to afford 23 mg of 1-(4-chlorophenyl)hexan-2-ol (**7hd**) as white solid, (yield = **54%**).

NMR data matched those reported in the literature.¹⁸

¹H NMR (400 MHz, CDCl₃): δ 7.29 – 7.26 (m, 2H), 7.16 – 7.14 (m, 2H), 3.82 – 3.76 (m, 1H), 2.79 (dd, $J = 13.7$, 4.3 Hz, 1H), 2.63 (dd, $J = 13.7$, 8.2 Hz, 1H), 1.56 – 1.30 (m, 7H), 0.91 (t, $J = 7.1$ Hz, 3H).

¹³C NMR (125 MHz, CDCl₃): δ 137.34, 132.4, 130.9, 128.8, 72.7, 43.5, 36.7, 28.0, 22.8, 14.2.

1-(benzo[*d*][1,3]dioxol-5-yl)hexan-2-ol (**7he**)



Following the general procedure **B** compound **7he** was obtained from 1,2-epoxyhexane (**5h**) (20 mg, 0.20 mmol) and 5-iodo-1,3-benzodioxole (**6e**) (74 mg, 0.30 mmol). The crude product was purified by column chromatography (10:90 AcOEt/Hexane) to afford 24 mg of 1-(benzo[*d*][1,3]dioxol-5-yl)hexan-2-ol (**7he**) as white solid, (yield = **55%**).

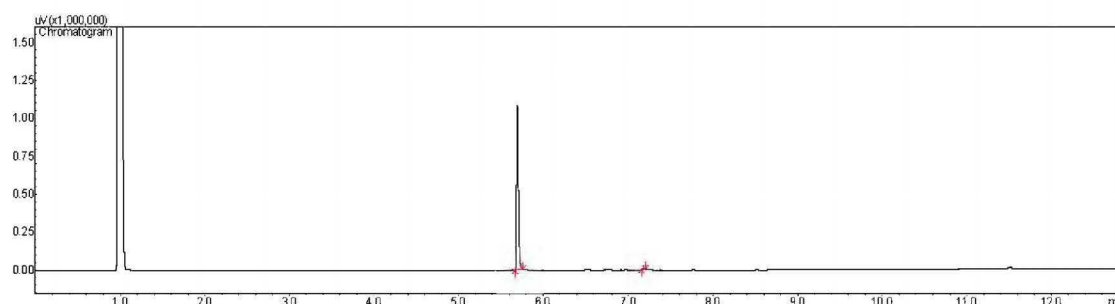
m.p. 65.3-66.0 °C

¹H NMR (400 MHz, CDCl₃): δ 6.78 – 6.63 (m, 3H), 5.93 (s, 2H), 3.758 – 3.72 (m, 1H), 2.75 (dd, $J = 13.7$, 4.2 Hz, 1H), 2.55 (dd, $J = 13.7$, 8.4 Hz, 1H), 1.53 – 1.30 (m, 7H), 0.91 (t, $J = 7.1$ Hz, 3H).

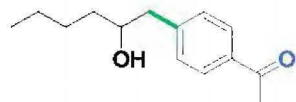
¹³C NMR (125 MHz, CDCl₃): δ 147.8, 146.2, 132.3, 122.3, 109.7, 108.3, 100.9, 72.7, 43.7, 36.5, 27.9, 22.7, 14.0.

HRMS (EI) [M]⁺ calculated for C₁₃H₁₈O₃: 222.1256, found: 222.1260.

GC Chromatogram: (>99% purity)



1-(4-(2-hydroxyhexyl)phenyl)ethan-1-one (**7hg**)



Following the general procedure **B** compound **7hg** was obtained from 1,2-epoxyhexane (**5h**) (20 mg, 0.20 mmol) and 4'-iodoacetophenone (**6g**) (74 mg, 0.30 mmol). The crude product was purified by column chromatography (20:80 AcOEt/Hexane) to afford 22 mg of 1-(4-(2-hydroxyhexyl)phenyl)ethan-1-one (**7hg**) as white solid, (yield = 50%).

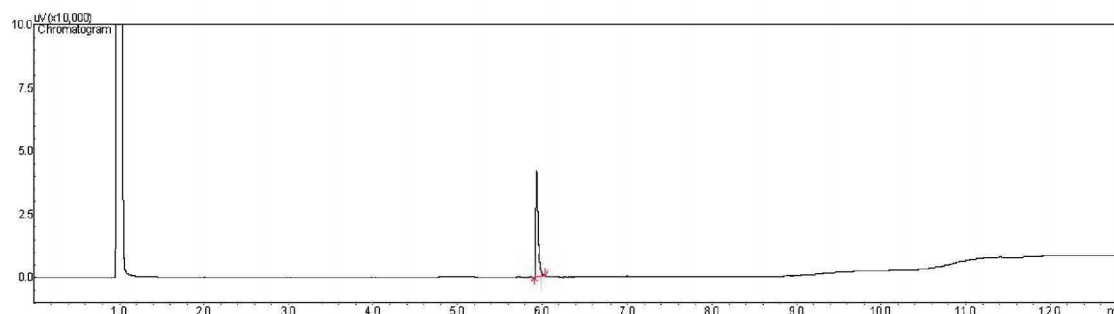
m.p. 65.9-66.4 °C

¹H NMR (400 MHz, CDCl₃): δ 7.92 – 7.87 (m, 2H), 7.33 – 7.29 (m, 2H), 3.88 – 3.82 (m, 1H), 2.87 (dd, *J* = 13.6, 4.3 Hz, 1H), 2.73 (dd, *J* = 13.6, 8.2 Hz, 1H), 2.58 (s, 3H), 1.56 – 1.29 (m, 7H), 0.91 (t, *J* = 7.2 Hz, 3H).

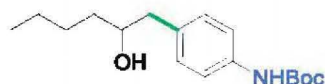
¹³C NMR (125 MHz, CDCl₃): δ 197.8, 144.6, 135.5, 129.6, 128.6, 72.5, 44.0, 36.7, 27.9, 26.5, 22.6, 14.0.

HRMS (ESI) [M+Na]⁺ calculated for C₁₄H₂₀O₂Na: 243.1361, found: 243.1350.

GC Chromatogram: (>99% purity)



tert-butyl (4-(2-hydroxyhexyl)phenyl)carbamate (**7hn**)



Following the general procedure **B** compound **7hn** was obtained from 1,2-epoxyhexane (**5h**) (20 mg, 0.20 mmol) and *N*-Boc-4-iodoaniline (**6n**) (96 mg, 0.30 mmol). The crude product was purified by column chromatography (10:90 AcOEt/Hexane) to afford 35 mg of *tert*-butyl (4-(2-hydroxyhexyl)phenyl)carbamate (**7hn**) as white solid, (yield = 60%).

m.p. 96.6-97.1 °C

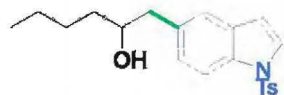
¹H NMR (400 MHz, CDCl₃): δ 7.30 – 7.28 (m, 2H), 7.14 – 7.11 (m, 2H), 6.50 (s, 1H), 3.79 – 3.73 (m, 1H), 2.77 (dd, *J* = 13.7, 4.3 Hz, 1H), 2.58 (dd, *J* = 13.7, 8.3 Hz, 1H), 1.51 (m, 13H), 1.38 – 1.29 (m, 3H), 0.90 (t, *J* = 7.2 Hz, 3H).

¹³C NMR (125 MHz, CDCl₃): δ 152.9, 136.8, 133.2, 129.9, 118.9, 80.4, 72.7, 43.3, 36.4, 28.3, 27.9, 22.7, 14.0.

HRMS (ESI) [M+Na]⁺ calculated for C₁₇H₂₇NO₃Na: 316.1889, found: 316.1879.

Elemental Analysis (%) calculated for C₁₇H₂₇NO₃: C 69.59, H 9.28, N 4.77, found: C 69.40, H 9.37, N 4.84.

1-(1-tosyl-1*H*-indol-5-yl)hexan-2-ol (**7hl**)



Following the general procedure **B** compound **7hl** was obtained from 1,2-epoxyhexane (**5h**) (20 mg, 0.20 mmol) and 5-iodo-1-(4-methylphenylsulfonyl)indole (**6l**) (119 mg, 0.30 mmol). The crude product was purified by column chromatography (10:90 AcOEt/Hexane) to afford 43 mg of 1-(1-tosyl-1*H*-indol-5-yl)hexan-2-ol (**7hl**) as white solid, (yield = **58%**).

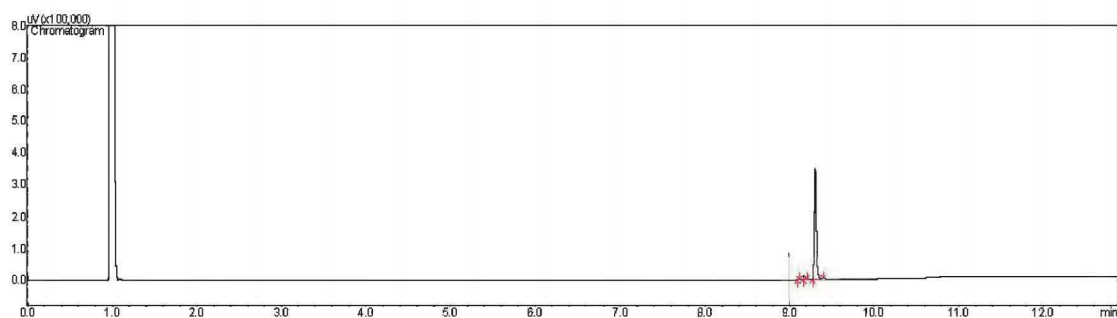
m.p. 65.3-66.0 °C

¹H NMR (500 MHz, CDCl₃): δ 7.94 (d, *J* = 8.5 Hz, 1H), 7.79 (d, *J* = 8.4 Hz, 2H), 7.57 (d, *J* = 3.7 Hz, 1H), 7.39 (d, *J* = 1.7 Hz, 1H), 7.24 (d, *J* = 8.1 Hz, 2H), 7.18 (dd, *J* = 8.5, 1.7 Hz, 1H), 6.63 (dd, *J* = 3.6, 0.8 Hz, 1H), 3.84–3.81 (m, 1H), 2.91 (dd, *J* = 13.7, 4.0 Hz, 1H), 2.70 (dd, *J* = 13.7, 8.6 Hz, 1H), 2.36 (s, 3H), 1.57–1.28 (m, 7H), 0.93 (t, *J* = 7.1 Hz, 3H).

¹³C NMR (125 MHz, CDCl₃): δ 145.0, 135.5, 133.83, 133.79, 131.2, 130.0, 127.0, 126.7, 126.2, 122.0, 113.6, 109.0, 73.0, 44.0, 36.7, 28.1, 22.8, 21.7, 14.2.

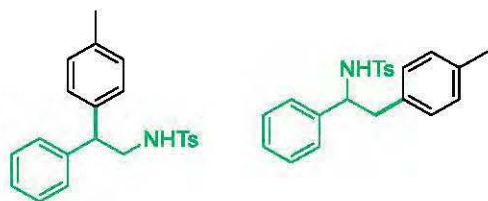
HRMS (EI) [M]⁺ calculated for C₂₁H₂₅NO₃S: 371.1555, found: 371.1549.

GC Chromatogram: (97% purity)



Aziridines – preliminary data

A mixture of 4-methyl-*N*-(2-phenyl-(*p*-tolyl)ethyl)benzenosulphonamide (**S23**) and 4-methyl-*N*-(1-phenyl-2-(*p*-tolyl)ethyl)benzenosulfonamide (**S24**)



Following the general procedure **A** compounds **S23** and **S24** were obtained from *N*-(*p*-tolylsulfonyl)-2-phenylaziridine (**S20**) (55 mg, 0.20 mmol) and 4-iodotoluene (**6a**) (65 mg, 0.30 mmol). The crude product was purified by column chromatography (10:90 AcOEt/Hexane) to afford an inseparable by column chromatography mixture of 4-methyl-*N*-(2-phenyl-(*p*-tolyl)ethyl)benzenosulphonamide (**S23**) and *N*-(1-phenyl-2-(*p*-tolyl)ethyl)benzenosulfonamide (**S24**) as white solid, (17 mg, branched:linear = 1:2, yield = **23%**).

NMR data matched those reported in the literature.^{19,20}

¹H NMR (400 MHz, CDCl₃): δ 7.68 (d, J = 8.0 Hz, 2H_{branched}), 7.42 (d, J = 8.0 Hz, 2H_{linear}), 7.28 (d, J = 10.8 Hz, 2H_{branched}), 7.27 – 7.24 (m, 2H_{branched}), 7.21 – 7.15 (m, 3H_{linear}+1H_{branched}), 7.09 – 7.06 (m, 4H_{branched}+4H_{linear}), 6.98 – 6.96 (m, 2H_{linear}+2H_{branched}), 6.79 (d, J = 7.7 Hz, 2H_{linear}), 4.70 (d, J = 5.9 Hz, 1H_{linear}), 4.50 – 4.46 (m, 1H_{linear}), 4.27 (t, J = 6.3 Hz, 1H_{branched}), 4.07 – 3.98 (m, 1H_{branched}), 3.54 – 3.51 (m, 2H_{branched}), 2.93 (dd, J = 12.0, 4.0 Hz, 2H_{linear}), 2.45 (s, 3H_{branched}), 2.36 (s, 3H_{linear}), 2.30 (s, 3H_{branched}), 2.29 (s, 3H_{linear}).

4-methyl-*N*-(2-(*p*-tolyl)cyclopentyl)benzenosulfonamide (**S25**)



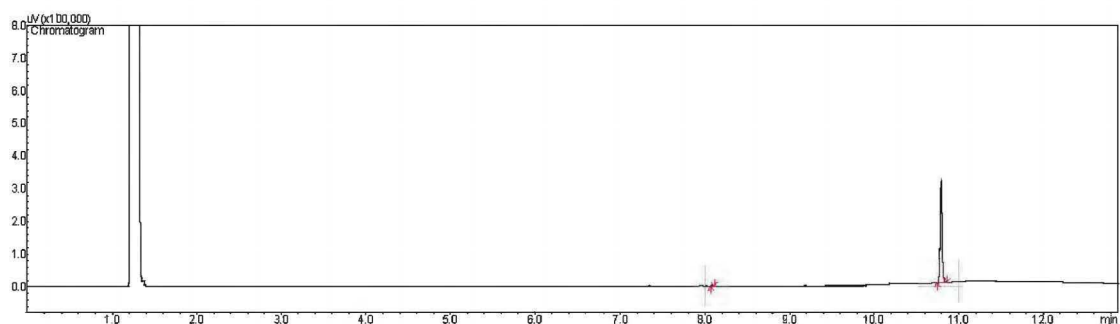
Following the general procedure **D** compound **S25** was obtained from *N*-tosyl-6-azabicyclo[3.1.0]hexane (**S21**) (47 mg, 0.20 mmol) and 4-iodotoluene (**6a**) (65 mg, 0.30 mmol). The crude product was purified by column chromatography (10:90 AcOEt/Hexane) to afford 4-methyl-*N*-(2-(*p*-tolyl)cyclopentyl) benzenosulfonamide (**S25**) as colorless oil, (14 mg, yield = **22%**).

¹H NMR (500 MHz, CDCl₃): δ 7.47 (d, J = 8.0 Hz, 2H), 7.11 (d, J = 7.9 Hz, 2H), 6.96 (d, J = 7.7 Hz, 2H), 6.86 (d, J = 7.7 Hz, 2H), 4.54 (d, J = 6.1 Hz, 1H), 3.47 – 3.37 (m, 1H), 2.69 (q, J = 9.4 Hz, 1H), 2.39 (s, 3H), 2.30 (s, 3H), 2.18 – 2.11 (m, 1H), 2.05 – 2.0 (m, 1H), 1.77 – 1.71 (m, 2H), 1.63 – 1.51 (m, 2H).

¹³C NMR (125 MHz, CDCl₃): δ 143.0, 138.4, 137.3, 136.3, 129.5, 129.4, 127.2, 127.2, 61.5, 52.3, 33.3, 32.3, 22.1, 21.6, 21.2.

HRMS (ESI) [M+Na]⁺ calculated for C₁₉H₂₃NO₂SNa: 352.1347, found: 352.1351.

GC Chromatogram: (99% purity)



4-methyl-*N*-(1-(*p*-tolyl)hexan-2-yl)benzenesulfonamide (**S26**)



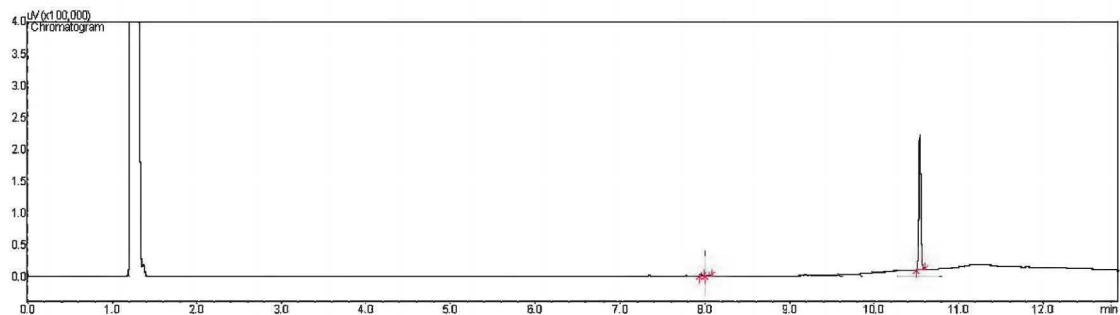
Following the general procedure **D** compound **S26** was obtained from 2-butyl-*N*-tosylaziridine (**S22**) (51 mg, 0.20 mmol) and 4-iodotoluene (**6a**) (65 mg, 0.30 mmol). The crude product was purified by column chromatography (10:90 AcOEt/Hexane) to afford 4-methyl-*N*-(1-(*p*-tolyl)hexan-2-yl)benzenesulfonamide (**S26**) as colorless oil, (19 mg, yield = 28%).

$^1\text{H NMR}$ (500 MHz, CDCl_3): δ 7.63 (d, $J = 8.0$ Hz, 2H), 7.22 (d, $J = 8.0$ Hz, 2H), 7.00 (d, $J = 7.6$ Hz, 2H), 6.88 (d, $J = 7.7$ Hz, 2H), 4.22 (d, $J = 8.1$ Hz, 1H), 3.42 – 3.36 (m, 1H), 2.61 (dd, $J = 12.0, 4.0$ Hz, 2H), 2.40 (s, 3H), 2.30 (s, 3H), 1.46 – 1.42 (m, 1H), 1.33 – 1.26 (m, 2H), 1.18 – 1.13 (m, 3H), 0.78 (t, $J = 6.9$ Hz, 3H).

$^{13}\text{C NMR}$ (125 MHz, CDCl_3): δ 143.1, 138.1, 136.2, 134.1, 129.6, 129.5, 129.3, 127.2, 55.1, 40.9, 34.3, 27.7, 22.5, 21.6, 21.2, 14.0.

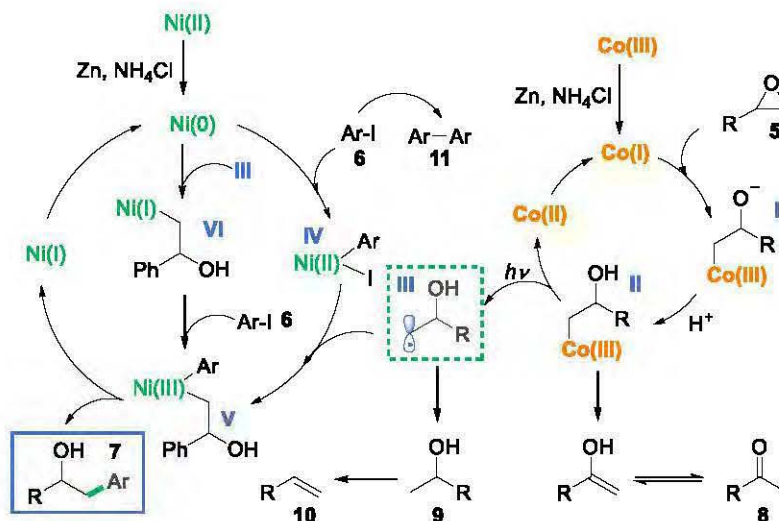
HRMS (ESI) $[M+\text{Na}]^+$ calculated for $\text{C}_{20}\text{H}_{27}\text{NO}_2\text{SNa}$: 368.1660, found: 368.1659.

GC Chromatogram: (98% purity)

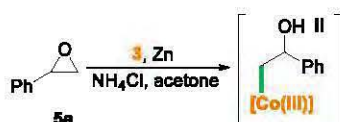


6. Mechanistic consideration

6.1. Proposed mechanism

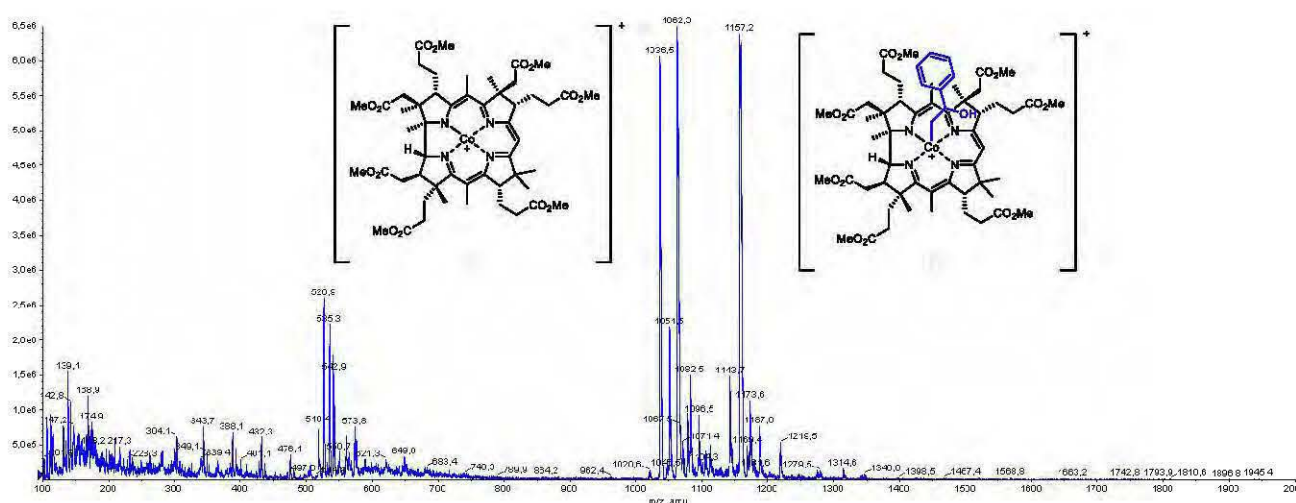


6.2 Mass spectrometry studies

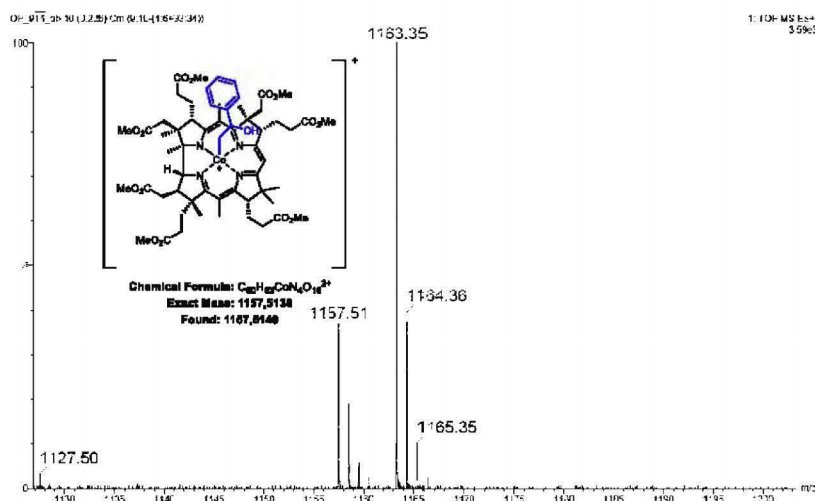


Reaction conditions: styrene oxide (**5a**) (0.2 mmol), Zn (1.5 equiv.), NH_4Cl (3 equiv.), HME (5 mol%), acetone ($c = 0.1 \text{ M}$), Blue LEDs, 30 min.

The reaction was setup according to the procedure **D** (without the addition of aryl halide, dtbpy and $\text{NiCl}_2(\text{DME})$). After 10 minutes of light irradiation a small portion was taken from the reaction mixture and was examined by LRMS.

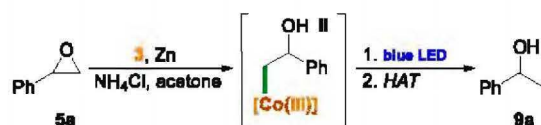


The LRMS spectrum of the reaction mixture recorded after 10 minutes under light irradiation indicates the presence of two forms of the catalyst: **A** and **B**. The first signal (**A**) corresponds to a catalyst lacking both axial ligands: H₂O and CN⁻. The second signal (**B**) corresponds to the mass of the Co-alkyl complex.



Conclusion: Alkylcobalamin is an intermediate in this reaction generated via the nucleophilic attack of the Co(I) form of the catalyst on the epoxide.

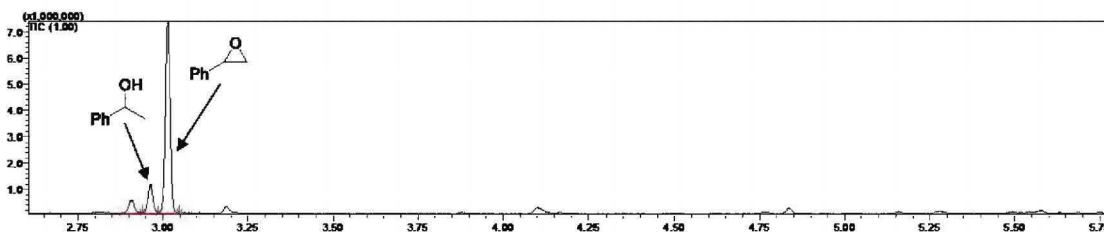
6.3 Studies of regioselectivity



Reaction conditions: styrene oxide (**5a**) (0.2 mmol), Zn (1.5 equiv.), NH₄Cl (3 equiv.), HME (5 mol%), acetone (c = 0.1 M), Blue LEDs, 16h.

Several experiments were performed to confirm the formation of the desired linear regioisomer. The reaction was setup according to procedure **D** (without addition of aryl halide, dtbpy and NiCl₂DME). After that time, the resulting mixture was diluted with AcOEt, filtered through the cotton wool. An aliquot was taken from the reaction mixture and was examined by GC-MS.

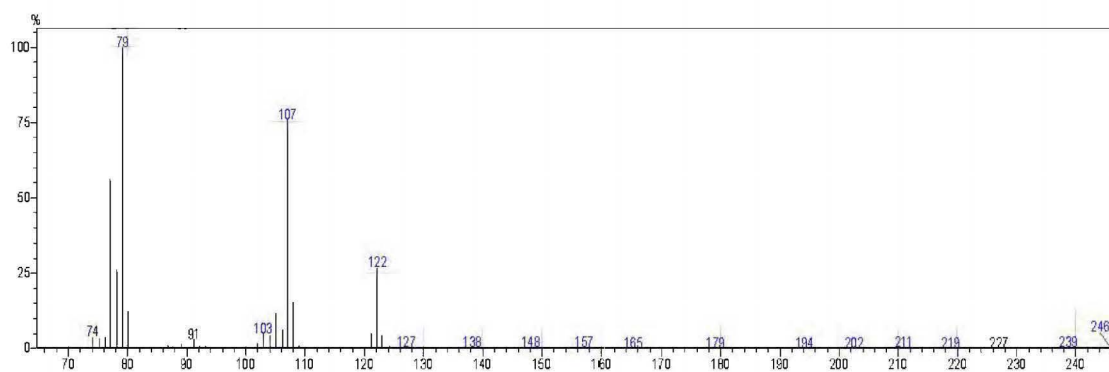
GC-MS from the reaction mixture:



Retention time of compound **9a**: 2.965 min.

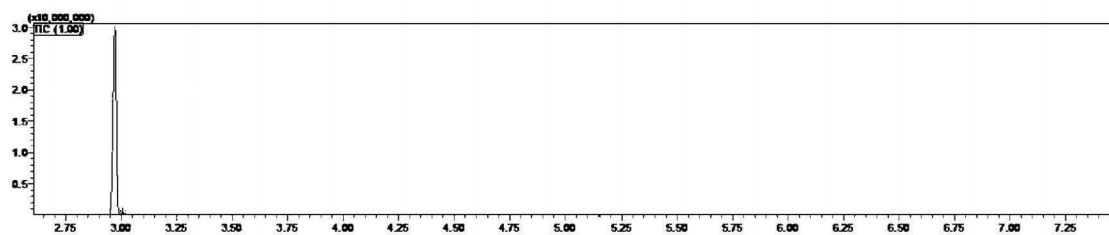
Retention time of compound **5a**: 3.015 min.

Fragmentation peaks detected for compound 9a:



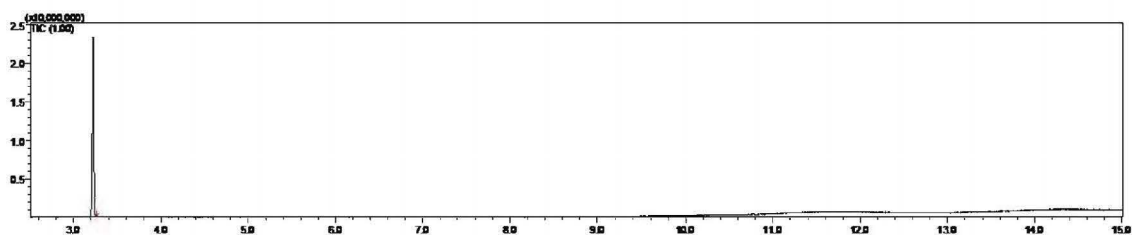
The obtained results were compared with commercially available *1-phenylethanol* and *2-phenylethanol*.

GC-MS of 1-phenylethanol:



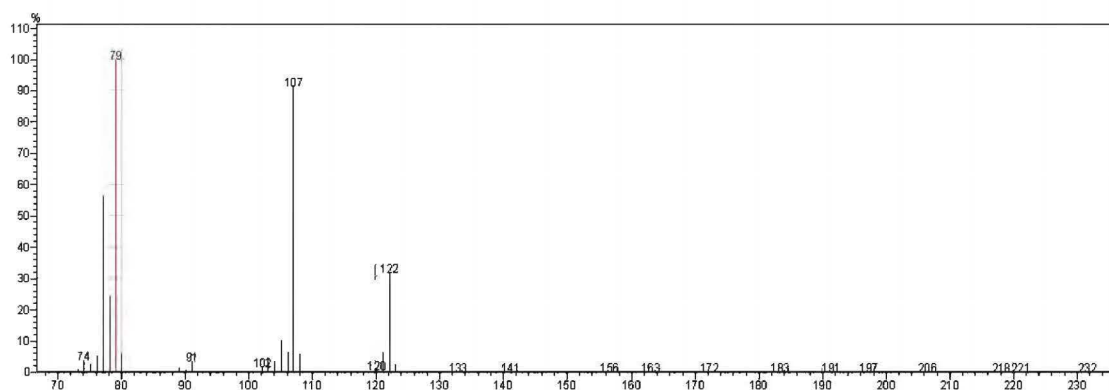
Retention time of 1-phenylethanol: 2.972 min.

GC-MS of 2-phenylethanol:

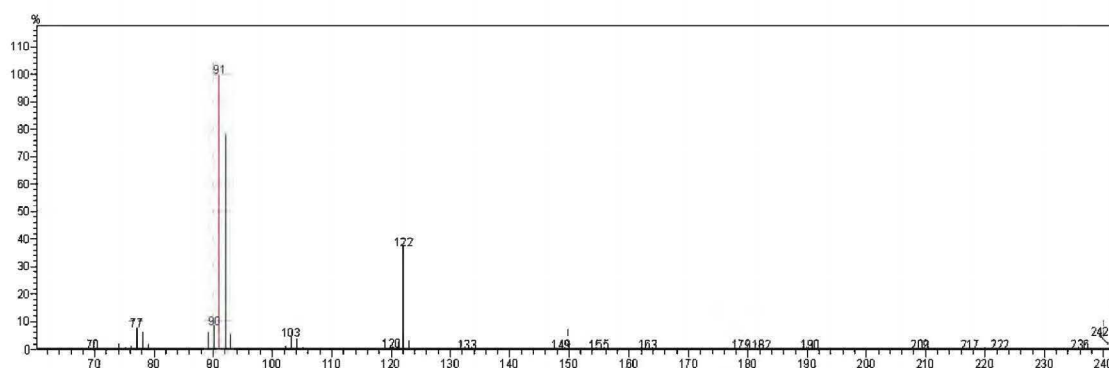


Retention time of 2-phenylethanol: 3.222 min.

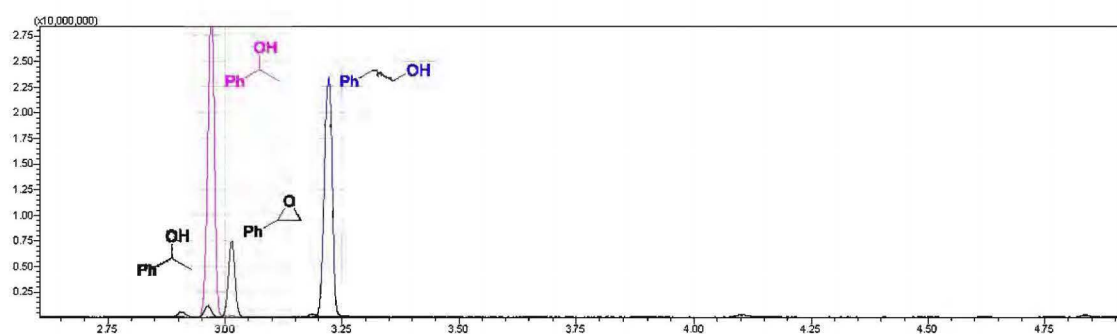
Fragmentation of 1-phenylethanol:



Fragmentation of 2-phenylethanol:



Comparison of the reaction mixture with 1-phenylethanol and 2-phenylethanol:



Conclusion: The signal at 2.965 min. measured for compound **9a** overlaps with the signal corresponding to 1-phenylethanol (Sigma Aldrich) (2.972 min.). In addition, fragmentation peaks (MS) detected for compound **9a** are the same as for 1-phenylethanol. These experiments prove the formation of the linear isomer **9a** as a sole product.

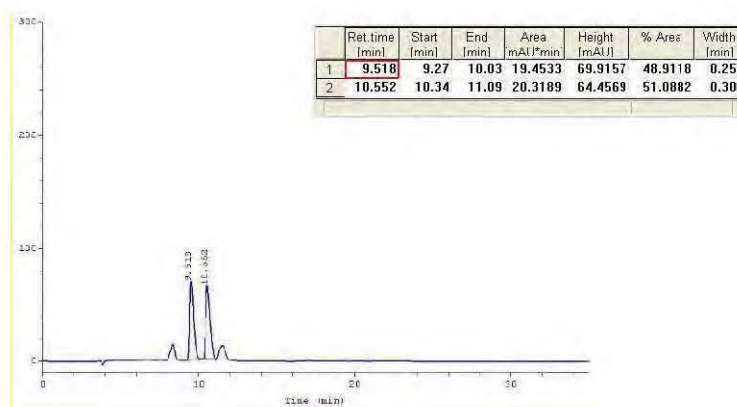
6.4 Stereoselectivity studies

Reaction with racemic styrene oxide: The model reaction with the racemic starting material was stopped after 15 minutes and the enantiomeric purity of both the substrate and the product was evaluated by HPLC. Both compounds were racemic corroborating that the kinetic resolution is not taking place in this reaction.



Reaction conditions: styrene oxide (**5a**) (0.2 mmol, 1 equiv.), 4-iodotoluene (**6a**) (1.5 equiv.), Zn (1.5 equiv.), NH_4Cl (3 equiv.), B_{12} (**1**) (5 mol%), $NiCl_2(DME)$ (20 mol%), dtbbpy (40 mol%), water (1.1 equiv.), dry NMP (c = 0.1 M), blue LED, 30 min.

Racemic product **7aa**: Chiralpak ID-H, 10% AcOEt in hexanes, 40 min run, 1 mL/min

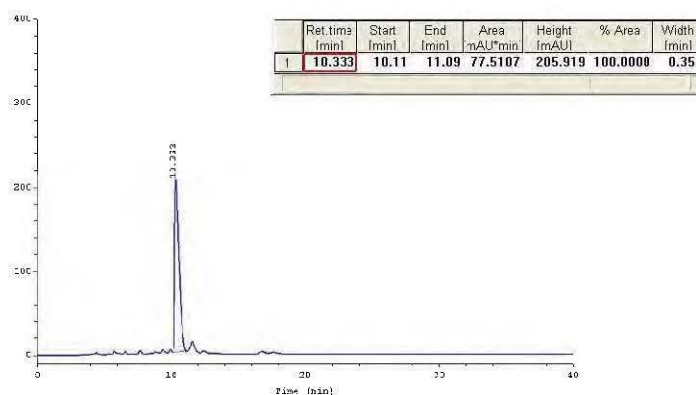


Reaction with enantiomerically pure (R)-styrene oxide: The model reaction with (R)-styrene oxide gave expectedly enantiomerically pure product as the reaction does not involve the stereogenic center.



Reaction conditions: styrene oxide (**S27**) (0.2 mmol, 1 equiv.), 4-iodotoluene (**6a**) (1.5 equiv.), Zn (1.5 equiv.), NH_4Cl (3 equiv.), B_{12} (**1**) (5 mol%), $NiCl_2(DME)$ (20 mol%), dtbbpy (40 mol%), water (1.1 equiv.), dry NMP (c = 0.1 M), blue LED, 30 min.

Reaction product (**S28**): Chiralpak ID-H, 10% AcOEt in hexanes, 40 min run, 1 mL/min



Conclusion: Our observation indicates that the formation of a radical at the internal position of the aryl epoxide does not occur.

6.5 DFT calculations

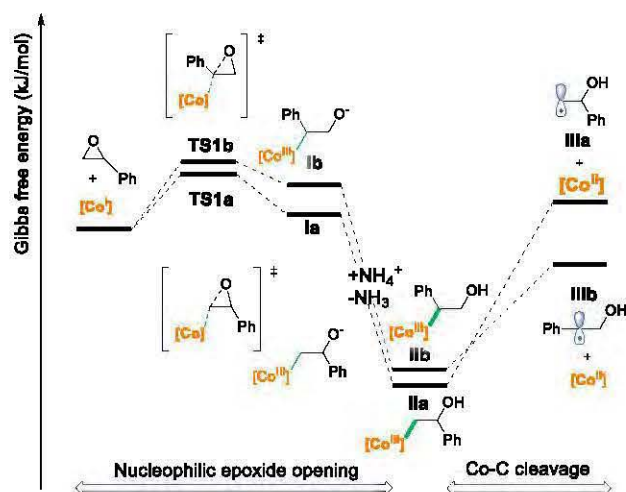
Computational methods

DFT calculations were performed with Gaussian 16. Geometry optimizations were computed at BP86/6-31G(d) level of theory with the D3 version of Grimme's empirical dispersion correction²¹ and solvation (acetone) with SMD model.²² Frequency analysis was performed at the same level to provide correction to thermodynamic functions and confirm the nature of optimized structures (minima and transition states featured zero or one imaginary frequency, respectively). Single point energies were computed at BP86/6-311++G(2df,p) level of theory with the D3 version of Grimme's empirical dispersion correction and solvation (acetone) with SMD model. Molecular structures were visualized in CYLview.²³

Performance of selected DFT methods

Performance of several commonly used functional (BP86, B3LYP, M06, PBE0 and wB97XD) was investigated and summarized in Tables 6.5.1 and 6.5.2. Geometry optimizations and frequency calculations were performed at BP86/6-31G(d) level of theory with the D3 version of Grimme's empirical dispersion correction²¹ and solvation (acetone) with SMD model. Then, single point energies were computed using given functional (with or without dispersion correction) and 6-311++G(2df,p) bases set including solvation (acetone) with PCM model. Performance of BP86-D3 and xB97XD was compared in Scheme 6.5.1.

Table 6.5.1. Calculated Gibbs free energies (in kJ/mol, relative to substrates – styrene oxide and Co(I)-corin complex).



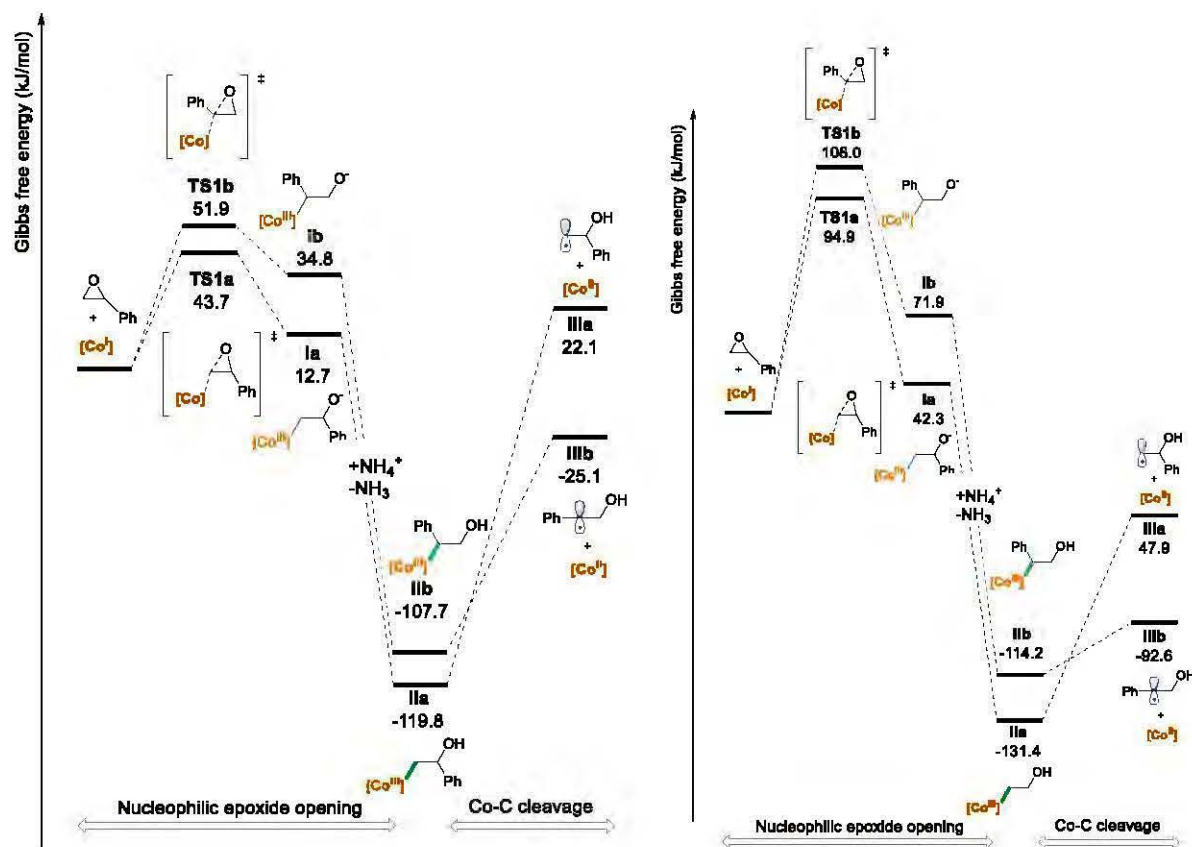
Entry	Functional	TS1a	TS1b	Ia	Ib	IIa	IIb	IIIa + [Co ^{II}]	IIIb + [Co ^{II}]
1	BP86-D3	43.7	51.9	12.7	34.8	-119.8	-107.7	22.1	-25.1
2	wB97XD	94.9	108.0	42.3	71.9	-131.4	-114.2	47.9	-92.6
3	M06-D3	81.6	88.9	45.0	69.5	-112.5	-96.5	-33.9	-82.0
4	M06	112.3	120.3	75.5	100.9	-80.9	-64.0	-33.0	-81.6
5	PBE0-D3	98.6	112.1	56.1	84.0	-108.4	-92.7	-70.5	-115.1
6	B3LYP-D3	84.4	92.2	40.6	65.1	-127.2	-112.8	-75.0	-122.5

Table 6.5.2. Comparison of the calculated barriers for epoxide ring opening and Gibbs free energies of homolysis of intermediate Ia and IIa (in kJ/mol).

Entry	Functional	Barrier height (ΔG^\ddagger) of styrene oxide opening with $[\text{Co}^{\text{I}}]$		ΔG of Co-C cleavage	
		TS1a	TS1b	in IIa	in IIb
1	BP86-D3	43.7	51.9	142.6	82.6
2	wB97XD	94.9	108.0	83.4	21.6
3	M06-D3	81.6	88.9	78.7	14.5
4	M06	112.3	120.3	47.9	-17.6
5	PBE0-D3	98.6	112.1	38.0	-22.4
6	B3LYP-D3	84.4	92.2	52.3	-9.7

BP86-D3

wB97XD

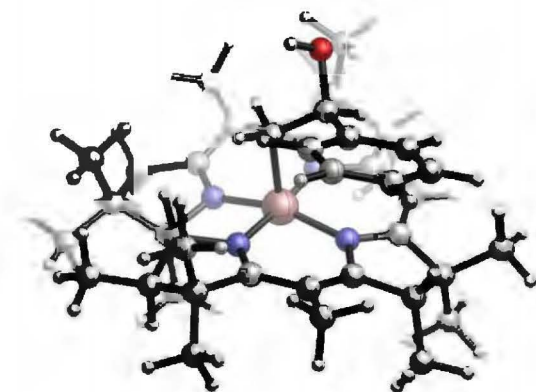


Scheme 6.5.1. Comparison of the reaction profiles calculated with BP86-D3 and xB97XD.

TD DFT calculations

Three lowest singlet and triplet excited states for intermediate **IIa** and **IIb** were calculated at TD-BP86-D3/6-311++G(2df,p) level of theory including solvation (acetone) with SMD model.

(CH₃)₁₅(corrin)Co(III)-CH₂-CH(OH)Ph – IIa (vertical excitation)



Excitation energies and oscillator strengths:

Excited State 1: Singlet-A 2.2027 eV 562.88 nm f=0.0086 <S**2>=0.000
185 -> 188 0.14945
187 -> 188 -0.14429
187 -> 189 0.66047

Total Energy, E(TD-HF/TD-DFT) = -3314.49012657

Excited State 2: Singlet-A 2.2693 eV 546.36 nm f=0.0408 <S**2>=0.000
185 -> 189 -0.21367
186 -> 190 0.10502
187 -> 188 0.63447
187 -> 189 0.13240

Excited State 3: Singlet-A 2.3455 eV 528.60 nm f=0.0118 <S**2>=0.000
186 -> 188 0.67630
187 -> 190 0.13075

Excitation energies and oscillator strengths:

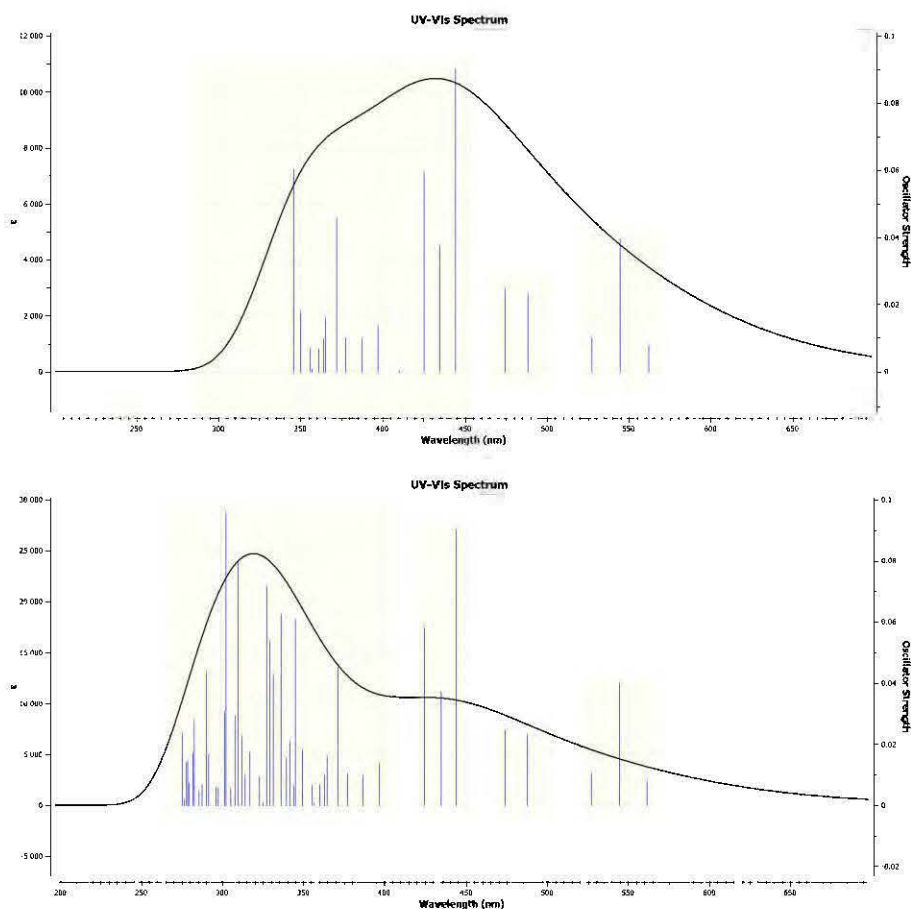
Excited State 1: Triplet-A 1.6701 eV 742.39 nm f=0.0000 <S**2>=2.000
187 -> 188 0.70619

Total Energy, E(TD-HF/TD-DFT) = -3314.50969999

Excited State 2: Triplet-A 1.8431 eV 672.68 nm f=0.0000 <S**2>=2.000
187 -> 189 0.69916

Excited State 3: Triplet-A 2.0703 eV 598.87 nm f=0.0000 <S**2>=2.000
186 -> 188 -0.24033
186 -> 189 0.65698

Simulated UV spectrum of IIa calculated for 20 and 50 excited states at TD-BP86/TZVP level of theory



Performance of selected DFT methods

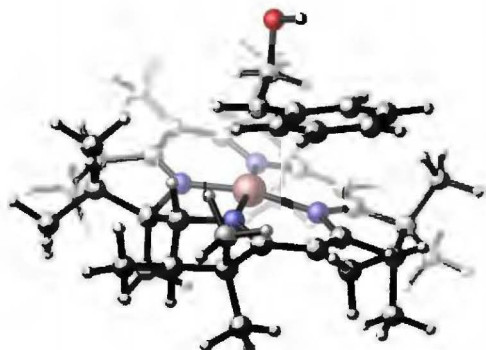
Performance of several commonly used functional, including hybrid and long-range corrected functionals (BP86, wB97XD, B3LYP, CAM-B3LYP M06, PBE0), in calculation of excited states for intermediate **IIa** was investigated. Calculated vertical excitation energies (in eV) for three lowest singlet excited states are summarized in Tables 6.5.3.

Table 6.5.3. Comparison of the calculated three lowest excitation states for intermediate **IIa**

Entry	Level of theory	S1	S2	S3
1	BP86/6-311++G(2df,p)	2.2027	2.2693	2.3455
2	BP86/TZPV	2.2076	2.2777	2.3518
3	wB97XD/6-311++G(2df,p)	2.2063	2.5045	3.0270
4	wB97XD/TZVP	2.2079	2.5142	3.0252
5	CAM-B3LYP/6-311++G(2df,p)	2.2285	2.5266	3.0574
6	CAM-B3LYP/TZVP	2.2304	2.5365	3.0569
7	B3LYP/6-311++G(2df,p)	2.2397	2.5336	2.8627
8	B3LYP/TZVP	2.2428	2.5431	2.8713
9	M06/6-311++G(2df,p)	1.8827	2.1827	2.5712
10	M06/TZVP	1.8968	2.2082	2.5955
11	PBE0/6-311++G(2df,p)	2.1888	2.4840	2.9338
12	PBE0/TZVP	2.1879	2.4904	2.9363

(CH₃)₁₅(corrin)Co(III)-CH₂-CH(OH)Ph – **IIa-S1 (Relaxed)**

Geometry of the **IIa-S1** was optimized at TD-BP86-D3/6-31G(d) (root=1) including solvation (acetone) with SMD model.



E (BP86-D3/6-31G(d) + SMD (acetone)) = -3313.808499

E (TD-BP86-D3/6-311++G(2df,p)//TD-BP86-D3/6-31G(d) + SMD (acetone)) = -3314.500880

Cartesian coordinates of the optimized geometry:

Charge = 1 Multiplicity = 1 Root=1

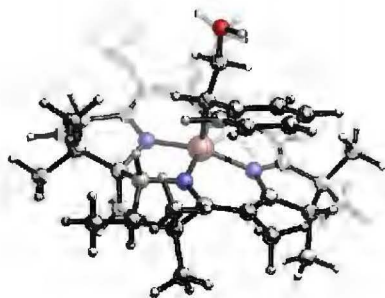
C	2.64652800	-1.90628700	0.22208100
C	2.88288400	-3.39037900	0.55391800
C	1.76460900	-4.06213000	-0.30393500
C	0.76337500	-2.94796600	-0.44260200
N	1.31973200	-1.72537900	-0.18954700
H	1.32061300	-4.92442900	0.22592800
C	-0.53845100	-3.15676300	-0.89210700
H	-0.82100200	-4.18682800	-1.12481600
C	3.56379300	-0.86277100	0.34886000
C	-1.47626500	-2.15775800	-1.14281200
C	-2.78431900	-2.43013900	-1.86085400
N	-1.30174700	-0.83193700	-0.83998200
C	-3.55940700	-1.09168000	-1.63851200
C	-2.50070700	-0.15682500	-1.06147600
C	3.20541900	0.46510200	-0.05725300
C	4.17737700	1.62109800	-0.21330700
N	1.95900700	0.82809400	-0.34733800
C	3.22784500	2.87510500	-0.18709700
C	1.86819000	2.27489400	-0.71940100
C	-2.73383700	1.17373300	-0.71587900
C	-1.63948300	2.04088400	-0.38833300
C	-1.70211400	3.56421800	-0.15743600
N	-0.39601300	1.59029100	-0.24613600
C	-0.20621900	3.95890000	-0.42763900
C	0.55866300	2.70010400	0.00131000
Co	0.35883100	-0.07840000	-0.22524000
H	-4.30470800	-1.26480700	-0.83601200
H	-0.11285200	4.06522400	-1.52493100
H	4.84615700	1.67551500	0.66497100
H	0.74848300	2.71752500	1.08908500
C	0.35925000	-0.14118700	1.94973300
C	-0.59131800	-1.19494200	2.44460000
H	-0.44372100	-2.12832500	1.87095500
O	-0.27224600	-1.61107700	3.82322600

C	-2.06402200	-0.81351500	2.35850200
C	-3.00735200	-1.75880700	1.91128500
C	-2.52924000	0.44965700	2.78023000
C	-4.37769600	-1.45379400	1.87120200
H	-2.65432800	-2.74227900	1.57814400
C	-3.89830000	0.75967800	2.74803500
H	-1.81687600	1.20227900	3.13672500
C	-4.82863900	-0.19009100	2.28992000
H	-5.09276200	-2.20196000	1.50964700
H	-4.23953400	1.74849100	3.07542100
H	-5.89634700	0.05448900	2.25720100
H	0.14767500	0.87401200	2.32466100
H	1.40610000	-0.42025000	2.16128100
C	-4.15528800	1.69881400	-0.68184600
H	-4.28306700	2.41357700	0.14553300
H	-4.45482900	2.21402400	-1.61223000
H	-4.87049300	0.88213100	-0.49823100
C	-2.10427200	3.82276000	1.31667400
H	-3.09653400	3.39539000	1.53702200
H	-1.38187600	3.37415800	2.02120500
H	-2.15272000	4.90854400	1.51282300
C	-2.61691200	4.35187900	-1.11602700
H	-3.67910500	4.30677000	-0.83026700
H	-2.32237800	5.41710700	-1.09788400
H	-2.51644400	3.99025200	-2.15484800
C	0.25432400	5.25985900	0.23230900
H	1.26651700	5.53431400	-0.10860300
H	-0.41890300	6.09573800	-0.03054700
H	0.28026200	5.17580200	1.33258200
C	1.69384400	2.36102000	-2.24893600
H	1.64141700	3.40708100	-2.59052300
H	2.53164800	1.86877900	-2.76671600
H	0.76279100	1.84481000	-2.54218400
C	3.75759200	4.05550100	-1.01507500
H	3.05218800	4.90432800	-0.98503900
H	4.71820300	4.40695300	-0.59658300
H	3.92774100	3.79600200	-2.07231200
C	3.12137300	3.31133300	1.29342100
H	4.12058800	3.61327400	1.65631900
H	2.44622200	4.17234000	1.42639700
H	2.76672100	2.48736200	1.94064900
C	5.08157900	1.42422200	-1.45058000
H	5.78503700	2.26826800	-1.55071500
H	5.67709900	0.50112400	-1.34147200
H	4.50089800	1.34115400	-2.38420700
C	4.96164900	-1.09158900	0.89105700
H	4.94682800	-1.75711000	1.76814000
H	5.64068700	-1.53909500	0.14336900
H	5.41691800	-0.14472400	1.21841700
C	4.26851400	-3.99357700	0.25716000
H	5.01360400	-3.71915000	1.01814000
H	4.18340700	-5.09504100	0.27482000
H	4.65405400	-3.69581800	-0.73197900
C	2.54933800	-3.57519900	2.06204400
H	1.53043000	-3.22538600	2.30420600
H	2.62478800	-4.64545200	2.32794900
H	3.25970700	-3.01196200	2.69188200
C	2.20166800	-4.51864500	-1.71747700
H	2.92665400	-5.34737800	-1.66025000
H	1.32439200	-4.87164200	-2.28672200

H	2.66160400	-3.68433700	-2.27667900
C	-4.30833300	-0.57741900	-2.88175400
H	-4.94316400	-1.38294300	-3.29133200
H	-4.97071800	0.26728900	-2.64328300
H	-3.61148700	-0.24991400	-3.67162300
C	-3.57002400	-3.64045400	-1.32254400
H	-4.53886000	-3.70737800	-1.85020600
H	-3.02968100	-4.58818200	-1.49390700
H	-3.77165600	-3.54249300	-0.24286000
C	-2.40322200	-2.69041800	-3.34698000
H	-1.76855500	-3.59099800	-3.41532100
H	-3.30845100	-2.86346800	-3.95386000
H	-1.84461000	-1.84255100	-3.78043300
H	-0.23545900	-0.77081600	4.33491500

Considerable elongation of Co-C bond was noticed upon relaxation of the S1-excited state (from 1.96 to 2.18 Å).

(CH₃)₁₅ (corrin)Co(III)-CHPh-CH₂OH – IIIb (vertical excitation)



Excitation energies and oscillator strengths:

Excited State 1: Singlet-A 1.9362 eV 640.36 nm f=0.0140 <S**2>=0.000
 187 -> 188 0.66537
 187 -> 189 0.19611
 Total Energy, E(TD-HF/TD-DFT) = -3314.49920187

Excited State 2: Singlet-A 2.2025 eV 562.92 nm f=0.0121 <S**2>=0.000
 185 -> 188 -0.12292
 186 -> 188 0.56061
 187 -> 188 -0.14307
 187 -> 189 0.35481

Excited State 3: Singlet-A 2.2371 eV 554.22 nm f=0.0305 <S**2>=0.000
 185 -> 188 -0.27576
 186 -> 188 -0.40825
 187 -> 188 -0.10239
 187 -> 189 0.47369

Excitation energies and oscillator strengths:

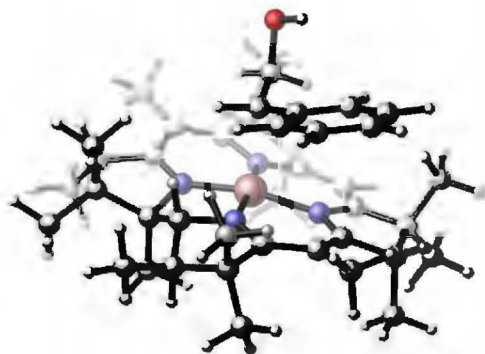
Excited State 1: Triplet-A 1.5754 eV 787.02 nm f=0.0000 <S**2>=2.000
 187 -> 188 0.70532
 Total Energy, E(TD-HF/TD-DFT) = -3314.51246127

Excited State 2: Triplet-A 1.6767 eV 739.46 nm f=0.0000 <S**2>=2.000
 187 -> 189 0.69909

Excited State 3: Triplet-A 1.7828 eV 695.45 nm f=0.0000 <S**2>=2.000
 186 -> 188 0.68287
 186 -> 189 0.16261

(CH₃)₁₅ (corrin)Co(III)-CHPh-CH₂OH – IIb_S1 (Relaxed)

Geometry of the IIb-S1 was optimized at TD-BP86-D3/6-31G(d) (root=1) including solvation (acetone) with SMD model.



E (BP86-D3/6-31G(d) + SMD (acetone)) = -3313.818385

E (TD-BP86-D3/6-311++G(2df,p)//TD-BP86-D3/6-31G(d) + SMD (acetone)) = -3314.293878

Cartesian coordinates of the optimized geometry:

Charge = 1 Multiplicity = 1 Root=1

C	2.64652800	-1.90628700	0.22208100
C	2.88288400	-3.39037900	0.55391800
C	1.76460900	-4.06213000	-0.30393500
C	0.76337500	-2.94796600	-0.44260200
N	1.31973200	-1.72537900	-0.18954700
H	1.32061300	-4.92442900	0.22592800
C	-0.53845100	-3.15676300	-0.89210700
H	-0.82100200	-4.18682800	-1.12481600
C	3.56379300	-0.86277100	0.34886000
C	-1.47626500	-2.15775800	-1.14281200
C	-2.78431900	-2.43013900	-1.86085400
N	-1.30174700	-0.83193700	-0.83998200
C	-3.55940700	-1.09168000	-1.63851200
C	-2.50070700	-0.15682500	-1.06147600
C	3.20541900	0.46510200	-0.05725300
C	4.17737700	1.62109800	-0.21330700
N	1.95900700	0.82809400	-0.34733800
C	3.22784500	2.87510500	-0.18709700
C	1.86819000	2.27489400	-0.71940100
C	-2.73383700	1.17373300	-0.71587900
C	-1.63948300	2.04088400	-0.38833300
C	-1.70211400	3.56421800	-0.15743600
N	-0.39601300	1.59029100	-0.24613600
C	-0.20621900	3.95890000	-0.42763900
C	0.55866300	2.70010400	0.00131000
Co	0.35883100	-0.07840000	-0.22524000
H	-4.30470800	-1.26480700	-0.83601200
H	-0.11285200	4.06522400	-1.52493100

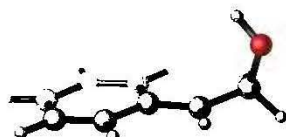
H	4.84615700	1.67551500	0.66497100
H	0.74848300	2.71752500	1.08908500
C	0.35925000	-0.14118700	1.94973300
C	-0.59131800	-1.19494200	2.44460000
H	-0.44372100	-2.12832500	1.87095500
O	-0.27224600	-1.61107700	3.82322600
C	-2.06402200	-0.81351500	2.35850200
C	-3.00735200	-1.75880700	1.91128500
C	-2.52924000	0.44965700	2.78023000
C	-4.37769600	-1.45379400	1.87120200
H	-2.65432800	-2.74227900	1.57814400
C	-3.89830000	0.75967800	2.74803500
H	-1.81687600	1.20227900	3.13672500
C	-4.82863900	-0.19009100	2.28992000
H	-5.09276200	-2.20196000	1.50964700
H	-4.23953400	1.74849100	3.07542100
H	-5.89634700	0.05448900	2.25720100
H	0.14767500	0.87401200	2.32466100
H	1.40610000	-0.42025000	2.16128100
C	-4.15528800	1.69881400	-0.68184600
H	-4.28306700	2.41357700	0.14553300
H	-4.45482900	2.21402400	-1.61223000
H	-4.87049300	0.88213100	-0.49823100
C	-2.10427200	3.82276000	1.31667400
H	-3.09653400	3.39539000	1.53702200
H	-1.38187600	3.37415800	2.02120500
H	-2.15272000	4.90854400	1.51282300
C	-2.61691200	4.35187900	-1.11602700
H	-3.67910500	4.30677000	-0.83026700
H	-2.32237800	5.41710700	-1.09788400
H	-2.51644400	3.99025200	-2.15484800
C	0.25432400	5.25985900	0.23230900
H	1.26651700	5.53431400	-0.10860300
H	-0.41890300	6.09573800	-0.03054700
H	0.28026200	5.17580200	1.33258200
C	1.69384400	2.36102000	-2.24893600
H	1.64141700	3.40708100	-2.59052300
H	2.53164800	1.86877900	-2.76671600
H	0.76279100	1.84481000	-2.54218400
C	3.75759200	4.05550100	-1.01507500
H	3.05218800	4.90432800	-0.98503900
H	4.71820300	4.40695300	-0.59658300
H	3.92774100	3.79600200	-2.07231200
C	3.12137300	3.31133300	1.29342100
H	4.12058800	3.61327400	1.65631900
H	2.44622200	4.17234000	1.42639700
H	2.76672100	2.48736200	1.94064900
C	5.08157900	1.42422200	-1.45058000
H	5.78503700	2.26826800	-1.55071500
H	5.67709900	0.50112400	-1.34147200
H	4.50089800	1.34115400	-2.38420700
C	4.96164900	-1.09158900	0.89105700
H	4.94682800	-1.75711000	1.76814000
H	5.64068700	-1.53909500	0.14336900
H	5.41691800	-0.14472400	1.21841700
C	4.26851400	-3.99357700	0.25716000
H	5.01360400	-3.71915000	1.01814000
H	4.18340700	-5.09504100	0.27482000
H	4.65405400	-3.69581800	-0.73197900
C	2.54933800	-3.57519900	2.06204400

H	1.53043000	-3.22538600	2.30420600
H	2.62478800	-4.64545200	2.32794900
H	3.25970700	-3.01196200	2.69188200
C	2.20166800	-4.51864500	-1.71747700
H	2.92665400	-5.34737800	-1.66025000
H	1.32439200	-4.87164200	-2.28672200
H	2.66160400	-3.68433700	-2.27667900
C	-4.30833300	-0.57741900	-2.88175400
H	-4.94316400	-1.38294300	-3.29133200
H	-4.97071800	0.26728900	-2.64328300
H	-3.61148700	-0.24991400	-3.67162300
C	-3.57002400	-3.64045400	-1.32254400
H	-4.53886000	-3.70737800	-1.85020600
H	-3.02968100	-4.58818200	-1.49390700
H	-3.77165600	-3.54249300	-0.24286000
C	-2.40322200	-2.69041800	-3.34698000
H	-1.76855500	-3.59099800	-3.41532100
H	-3.30845100	-2.86346800	-3.95386000
H	-1.84461000	-1.84255100	-3.78043300
H	-0.23545900	-0.77081600	4.33491500

Exclusion of the ring opening of epoxide via protonation

The pathway involving protonation of the epoxide was not considered as accessible under developed conditions. The pKa of protonated epoxide is estimated to be ~ -3 , while the pKa of NH_4^+ is 10.5 and 9.2 in DMSO and water, respectively. We calculated ΔG for protonation of styrene oxide, which was found to be 86.2 kJ/mol. The calculated geometry of the protonated styrene oxide resembles a benzyl carbocation stabilized by neighboring OH group (opened epoxide ring). It is consistent with the textbook fact that acid mediated ring opening of epoxides proceeds according to Markovnikov's rule, i.e. at side delivering more stabilized carbocation (usually more substituted).

Calculated geometry of protonated styrene oxide:



E (BP86-D3/6-31G(d) + SMD (acetone)) = -385.285837

E (BP86-D3/6-311++G(2df,p) // BP86-D3/6-31G(d) + SMD (acetone)) = -385.409967

Zero-point correction=	0.146957
Thermal correction to Energy=	0.155201
Thermal correction to Enthalpy=	0.156145
Thermal correction to Gibbs Free Energy=	0.113745

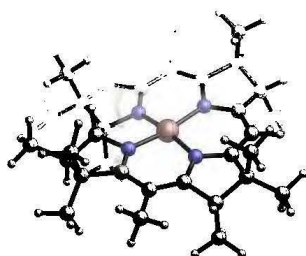
Charge = 0 Multiplicity = 1

C	2.52508100	-0.32356700	0.48023600
C	1.34736500	0.58964600	0.41982600
H	1.60472200	1.65632600	0.45594700
O	3.18431400	0.04159200	-0.75873000
C	0.00844400	0.25230700	0.18870500
C	-0.94453700	1.32364900	0.04286300
C	-0.45038400	-1.11210500	0.13629900
C	-2.29251200	1.03990500	-0.13004300

H	-0.58653800	2.35775500	0.08003100
C	-1.80146700	-1.37683100	-0.03800200
H	0.26369200	-1.93492600	0.23109500
C	-2.71785500	-0.30686500	-0.17148200
H	-3.02156100	1.84837300	-0.23661000
H	-2.16113200	-2.40905600	-0.07748900
H	-3.78111000	-0.52890200	-0.31358100
H	2.29071700	-1.39895300	0.53681200
H	3.20098100	-0.05361700	1.30746800
H	2.67090600	-0.38656700	-1.48424900

Optimized geometries, energies and corrections to thermodynamic functions

(CH₃)₁₅(corrin)Co(I)



E (BP86-D3/6-31G(d) + SMD (acetone)) = -2928.477102
E (BP86-D3/6-311++G(2df,p)// BP86-D3/6-31G(d) + SMD (acetone)) = -2929.055777
E (wB97XD/6-311++G(2df,p)// BP86-D3/6-31G(d) + SMD (acetone)) = -2928.240361
E (M06-D3/6-311++G(2df,p)// BP86-D3/6-31G(d) + SMD (acetone)) = -2927.454493
E (M06/6-311++G(2df,p)// BP86-D3/6-31G(d) + SMD (acetone)) = -2927.427618
E (PBE0-D3/6-311++G(2df,p)// BP86-D3/6-31G(d) + SMD (acetone)) = -2926.656664
E (B3LYP-D3/6-311++G(2df,p)// BP86-D3/6-31G(d) + SMD (acetone)) = -2928.828969

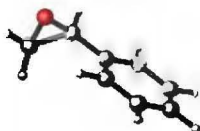
Zero-point correction=	0.777157
Thermal correction to Energy=	0.816751
Thermal correction to Enthalpy=	0.817695
Thermal correction to Gibbs Free Energy=	0.712569

Charge = 0 Multiplicity = 1

C	2.89796800	-0.88780100	-0.29370100
C	4.32173700	-0.37091400	-0.60043500
C	4.26146600	1.04280500	0.05023900
C	2.78668000	1.34831300	-0.03665400
N	2.02435100	0.20638400	-0.10672600
H	4.86199000	1.76519300	-0.53452600
C	2.28150400	2.64274500	0.00507500
H	3.00938400	3.45996900	0.03233000
C	2.49581400	-2.21796200	-0.27565700
C	0.93192300	2.97282400	0.00182100
C	0.41558000	4.40299700	-0.09568000
N	-0.08484000	2.04349700	-0.00739900
C	-1.04433100	4.20901300	0.39642400
C	-1.30331300	2.74106100	0.06831100
C	1.14056600	-2.55441400	0.03138200
C	0.63340400	-3.96386300	0.29524200
N	0.17817600	-1.63445000	0.13849800
C	-0.91955900	-3.80045100	0.12579600
C	-1.12962700	-2.28283300	0.49382800
C	-2.57194400	2.18758600	-0.05012400
C	-2.73328400	0.77184300	-0.18724400
C	-4.05142100	0.00672400	-0.41839000
N	-1.67220300	-0.04597000	-0.18285700
C	-3.61678200	-1.44904000	-0.03270900
C	-2.11827700	-1.45953100	-0.35841900
Co	0.13336500	0.17296300	-0.04823000
H	-1.71663700	4.88538300	-0.15999200
H	-3.73246600	-1.51982700	1.06567300
H	0.99062700	-4.65251800	-0.49373500
H	-1.96420400	-1.71536400	-1.42233300
C	-3.79101700	3.09284600	0.00182300

H	-4.51492300	2.84461300	-0.79279100
H	-4.32978600	3.01926400	0.96461900
H	-3.52131000	4.15041400	-0.13712200
C	-4.43590500	0.12490000	-1.91464900
H	-4.59654400	1.18169800	-2.19153400
H	-3.64312200	-0.27819800	-2.57058100
H	-5.37222600	-0.42294900	-2.12703600
C	-5.24695500	0.41387400	0.46969700
H	-5.76248400	1.31941700	0.11370500
H	-5.99292000	-0.40305300	0.46704900
H	-4.93237000	0.57916600	1.51585900
C	-4.44128700	-2.56548000	-0.67890500
H	-4.18115300	-3.54867900	-0.25168700
H	-5.52220300	-2.41011000	-0.50606100
H	-4.27712700	-2.61879900	-1.76960100
C	-1.38260500	-2.04245800	1.99732700
H	-2.32559900	-2.50050400	2.33898000
H	-0.55990700	-2.45384000	2.60306800
H	-1.42483200	-0.95560100	2.18485700
C	-1.73376000	-4.77629800	0.99049100
H	-2.81733400	-4.60407000	0.86501600
H	-1.52598400	-5.81828700	0.68426800
H	-1.50399400	-4.69289500	2.06506400
C	-1.23281300	-4.08467200	-1.36264900
H	-0.96136700	-5.12968600	-1.60087500
H	-2.30269900	-3.95969600	-1.59728700
H	-0.65197000	-3.42751500	-2.03584800
C	1.15661600	-4.52716500	1.63469100
H	0.78126300	-5.55148500	1.80715600
H	2.25983700	-4.57480700	1.61793900
H	0.86580600	-3.90210000	2.49546100
C	3.45703000	-3.35090500	-0.60068500
H	4.08496000	-3.11231000	-1.47469100
H	4.13653100	-3.59842100	0.23523700
H	2.90916500	-4.27248500	-0.85291600
C	5.52089100	-1.18313700	-0.07330000
H	5.73864700	-2.06495700	-0.69449100
H	6.42336700	-0.54449700	-0.09799200
H	5.37320300	-1.52206400	0.96613700
C	4.44591300	-0.20672200	-2.13932100
H	3.66116000	0.46599000	-2.53154300
H	5.43087900	0.22471300	-2.40027400
H	4.35032400	-1.18040000	-2.65180700
C	4.70988000	1.11033600	1.52840100
H	5.78860400	0.90417200	1.64316000
H	4.51277900	2.11982500	1.93153100
H	4.14863300	0.38401800	2.14467200
C	-1.25862600	4.43909100	1.90851700
H	-1.06322600	5.48925700	2.18950700
H	-2.30000800	4.20052500	2.18753500
H	-0.59135600	3.78990500	2.50458000
C	0.39917500	4.81064500	-1.59374900
H	-0.01522400	5.82979400	-1.71325500
H	1.42166100	4.80005900	-2.01263800
H	-0.22277700	4.11500600	-2.18698900
C	1.23856100	5.43001300	0.69864200
H	2.23817100	5.56491700	0.24732400
H	0.73849600	6.41588500	0.68622800
H	1.38182400	5.12587900	1.74962900

Styrene oxide (5a)



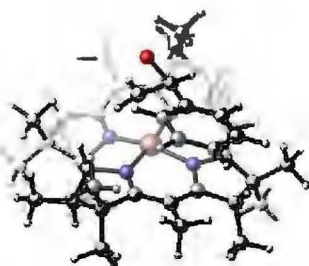
E (BP86-D3/6-31G(d) + SMD (acetone)) = -384.864773
E (BP86-D3/6-311++G(2df,p)// BP86-D3/6-31G(d) + SMD (acetone)) = -384.988857
E (wB97XD/6-311++G(2df,p)// BP86-D3/6-31G(d) + SMD (acetone)) = -384.843489
E (M06-D3/6-311++G(2df,p)// BP86-D3/6-31G(d) + SMD (acetone)) = -384.694325
E (M06/6-311++G(2df,p)// BP86-D3/6-31G(d) + SMD (acetone)) = -384.692796
E (PBE0-D3/6-311++G(2df,p)// BP86-D3/6-31G(d) + SMD (acetone)) = -384.530381
E (B3LYP-D3/6-311++G(2df,p)// BP86-D3/6-31G(d) + SMD (acetone)) = -384.99321

Zero-point correction= 0.134965
Thermal correction to Energy= 0.142345
Thermal correction to Enthalpy= 0.143289
Thermal correction to Gibbs Free Energy= 0.102785

Charge = 0 Multiplicity = 1

C	2.59437100	-0.04897300	0.73917500
C	1.60686700	0.60965100	-0.15344600
H	1.84497600	1.62556100	-0.50545200
O	2.50403700	-0.42054900	-0.65567200
C	0.15006000	0.27919200	-0.09355000
C	-0.80201500	1.31717800	-0.04163800
C	-0.28956500	-1.06077600	-0.06972200
C	-2.17191700	1.02083600	0.05138800
H	-0.46623700	2.36109000	-0.07257900
C	-1.65808000	-1.35582500	0.01841700
H	0.45175900	-1.86484600	-0.13803000
C	-2.60395800	-0.31618800	0.08296500
H	-2.90277300	1.83667500	0.09291900
H	-1.98905300	-2.40072700	0.03241600
H	-3.67296900	-0.54792500	0.15065200
H	2.23834300	-0.80622300	1.45422700
H	3.50907200	0.49023100	1.02968200

(CH₃)₁₅(corrin)Co(I) - styrene oxide – TS1a



E (BP86-D3/6-31G(d) + SMD (acetone)) = -3313.352516
E (BP86-D3/6-311++G(2df,p)// BP86-D3/6-31G(d) + SMD (acetone)) = -3314.051616
E (wB97XD/6-311++G(2df,p)// BP86-D3/6-31G(d) + SMD (acetone)) = -3313.071329
E (M06-D3/6-311++G(2df,p)// BP86-D3/6-31G(d) + SMD (acetone)) = -3312.141359

E (M06/6-311++G(2df,p)// BP86-D3/6-31G(d) + SMD (acetone)) = -3312.134298
 E (PBE0-D3/6-311++G(2df,p)// BP86-D3/6-31G(d) + SMD (acetone)) = -3311.203294
 E (B3LYP-D3/6-311++G(2df,p)// BP86-D3/6-31G(d) + SMD (acetone)) = -3313.83971

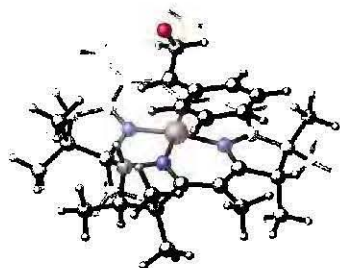
Zero-point correction= 0.912471
 Thermal correction to Energy= 0.960448
 Thermal correction to Enthalpy= 0.961392
 Thermal correction to Gibbs Free Energy= 0.838993

Charge = 0 Multiplicity = 1

C	2.66075000	-1.88004100	0.21567600
C	2.92143400	-3.34429900	0.63074000
C	1.81071700	-4.08364700	-0.17857200
C	0.78609600	-2.98954300	-0.36804900
N	1.32655100	-1.74131100	-0.21360400
H	1.39890300	-4.92420400	0.41129000
C	-0.51742000	-3.23896300	-0.78725700
H	-0.78922900	-4.28450300	-0.96538500
C	3.55661100	-0.82082900	0.31870300
C	-1.47963000	-2.26908300	-1.05293600
C	-2.80783600	-2.59163900	-1.72285500
N	-1.30735400	-0.93050300	-0.80936800
C	-3.59344800	-1.25249800	-1.52741900
C	-2.53062800	-0.27940000	-1.01543300
C	3.17070900	0.49808900	-0.09331300
C	4.12082300	1.67224100	-0.26639700
N	1.91228400	0.81991000	-0.38165700
C	3.14183500	2.90207200	-0.25880600
C	1.80200700	2.26124300	-0.79036400
C	-2.78218500	1.05663600	-0.71939900
C	-1.70303200	1.95544100	-0.44015000
C	-1.79489800	3.48216400	-0.23612100
N	-0.44316700	1.52362600	-0.34376900
C	-0.31604400	3.89939100	-0.55694200
C	0.47877400	2.66945400	-0.10504300
Co	0.35013200	-0.12038700	-0.36851000
H	-4.32713500	-1.40760900	-0.71051100
H	-0.25028100	3.96915300	-1.65996500
H	4.78390100	1.76094300	0.61448000
H	0.65415700	2.72562600	0.98471600
C	0.50260600	-0.03356300	2.05436400
C	-0.46569100	-1.00662300	2.61104900
H	-0.26219200	-2.06126800	2.31886900
O	0.18293000	-0.53909400	3.75944400
C	-1.94541400	-0.70921400	2.50708500
C	-2.84722400	-1.68258000	2.04259100
C	-2.44797200	0.53818300	2.92784300
C	-4.22569900	-1.41491100	1.98349600
H	-2.45948400	-2.65474800	1.71448000
C	-3.82114700	0.81539900	2.86141600
H	-1.75032800	1.28265100	3.32739000
C	-4.71652500	-0.16213000	2.38764400
H	-4.91630900	-2.18595900	1.62222500
H	-4.19745500	1.79297500	3.18473100
H	-5.79046500	0.05154100	2.33939700
H	0.25426200	1.02696800	2.11383300
H	1.55300300	-0.31920300	1.99010000
C	-4.21546700	1.55760200	-0.66855900
H	-4.33920600	2.29449500	0.14069300
H	-4.55249300	2.04040700	-1.60427000

H	-4.91273000	0.73520100	-0.44239600
C	-2.16815500	3.78276700	1.23659700
H	-3.15024400	3.34857900	1.48824100
H	-1.42837800	3.35946400	1.93910200
H	-2.22706000	4.87276300	1.40972700
C	-2.74642900	4.23112500	-1.19183400
H	-3.80231700	4.16839000	-0.88514100
H	-2.47798100	5.30403300	-1.20512900
H	-2.65999600	3.84820400	-2.22466500
C	0.13067700	5.23267400	0.04651400
H	1.12658000	5.52195300	-0.32899100
H	-0.56952500	6.04460700	-0.22299200
H	0.18789900	5.18638000	1.14815600
C	1.65425700	2.31715200	-2.32437900
H	1.58402800	3.35461100	-2.69122600
H	2.51005500	1.83180000	-2.81957300
H	0.74061500	1.77330300	-2.62155200
C	3.65318000	4.08607900	-1.09456000
H	2.93215500	4.92215300	-1.08034600
H	4.60396000	4.46232300	-0.67383000
H	3.83723800	3.82024600	-2.14807000
C	3.01603300	3.35511600	1.21509300
H	4.00437400	3.68801600	1.58195800
H	2.31695500	4.19943900	1.33431100
H	2.67759000	2.52999200	1.86914000
C	5.04095600	1.48911300	-1.49275900
H	5.72825000	2.34628600	-1.60315100
H	5.65696200	0.58085700	-1.36825900
H	4.47164100	1.37786100	-2.43085300
C	4.96099000	-1.00951300	0.87006200
H	4.95894000	-1.63238900	1.77924700
H	5.64973000	-1.48249900	0.14668800
H	5.40635300	-0.04345100	1.15416400
C	4.31561500	-3.94096500	0.35375300
H	5.06550300	-3.61261000	1.08880000
H	4.25480000	-5.04217500	0.43034900
H	4.68744200	-3.69007800	-0.65409600
C	2.60734100	-3.46219600	2.14661000
H	1.57577400	-3.13730500	2.36971500
H	2.71717700	-4.51219000	2.47748500
H	3.29556900	-2.83876200	2.74430800
C	2.24415600	-4.61973000	-1.56262300
H	2.98621200	-5.43241000	-1.47600600
H	1.36636100	-5.01982700	-2.10051900
H	2.68005600	-3.81278800	-2.17974700
C	-4.37268300	-0.79145300	-2.77397500
H	-5.01727700	-1.61102000	-3.14000600
H	-5.02992900	0.06381200	-2.55780500
H	-3.69453300	-0.49508800	-3.59265700
C	-3.55963500	-3.77791300	-1.08918800
H	-4.55030700	-3.89145900	-1.56837700
H	-3.01386700	-4.72917900	-1.22573500
H	-3.71794900	-3.62328100	-0.00800900
C	-2.49812300	-2.92691200	-3.20633300
H	-1.85206500	-3.82178900	-3.25415600
H	-3.41956200	-3.14441400	-3.77550800
H	-1.96504300	-2.09942700	-3.70747400

(CH₃)₁₅(corrin)Co(I) - styrene oxide – TS1b



E (BP86-D3/6-31G(d) + SMD (acetone)) = -3313.346153
E (BP86-D3/6-311++G(2df,p)// BP86-D3/6-31G(d) + SMD (acetone)) = -3314.048305
E (wB97XD/6-311++G(2df,p)// BP86-D3/6-31G(d) + SMD (acetone)) = -3313.066167
E (M06-D3/6-311++G(2df,p)// BP86-D3/6-31G(d) + SMD (acetone)) = -3312.138419
E (M06/6-311++G(2df,p)// BP86-D3/6-31G(d) + SMD (acetone)) = -3312.098033
E (PBE0-D3/6-311++G(2df,p)// BP86-D3/6-31G(d) + SMD (acetone)) = -3311.167819
E (B3LYP-D3/6-311++G(2df,p)// BP86-D3/6-31G(d) + SMD (acetone)) = -3313.810532

Zero-point correction=	0.912828
Thermal correction to Energy=	0.960938
Thermal correction to Enthalpy=	0.961883
Thermal correction to Gibbs Free Energy=	0.838808

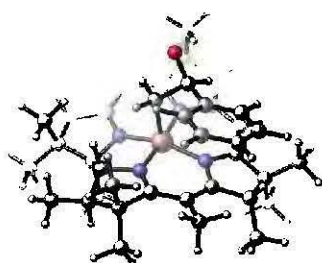
Charge = 0 Multiplicity = 1

C	3.09586900	-0.98180400	0.12629100
C	3.93977200	-2.27050700	0.24968300
C	3.11217500	-3.23764300	-0.65189400
C	1.73075400	-2.63836800	-0.54651800
N	1.77270500	-1.30186000	-0.24025100
H	3.14092200	-4.26700000	-0.24818100
C	0.57154800	-3.35977300	-0.80465800
H	0.68949100	-4.43038300	-0.99897300
C	3.54136100	0.31136700	0.36745300
C	-0.71310800	-2.82777600	-0.86092000
C	-1.94862400	-3.69381800	-1.08881100
N	-1.00130000	-1.49667200	-0.67986900
C	-3.03305000	-2.60569400	-1.35719400
C	-2.37957700	-1.32047700	-0.85049400
C	2.70319500	1.42379100	0.03423700
C	3.19274900	2.85772300	-0.10266400
N	1.41616000	1.28868300	-0.27554800
C	1.85143700	3.66995400	-0.24096000
C	0.86677500	2.57854300	-0.81219200
C	-3.07121800	-0.12095600	-0.72529300
C	-2.36382800	1.11915100	-0.60463900
C	-2.96899400	2.53443100	-0.75616100
N	-1.04028100	1.14735100	-0.42637600
C	-1.66977300	3.37345500	-1.01900300
C	-0.58539900	2.56222000	-0.29850100
Co	0.26894300	-0.13394200	-0.30426200
H	-3.94908400	-2.84340400	-0.78611900
H	-1.47801900	3.30335800	-2.10601300
H	3.69196500	3.17173300	0.83455600
H	-0.59221000	2.79933400	0.78166600
C	0.10154200	0.05691800	2.30075300
C	1.16178200	-0.83327100	2.82331000
H	2.17812000	-0.61944300	2.43874400
O	0.79944400	-0.20528600	4.01033600

H	0.37865600	1.10241600	2.15168200
C	-4.58973300	-0.13955000	-0.76858300
H	-5.01584600	0.63671700	-0.11446900
H	-5.00534100	0.02435700	-1.78001200
H	-4.98219700	-1.10420700	-0.40734900
C	-3.70049500	3.01686100	0.51797800
H	-4.50631500	2.32474800	0.80846800
H	-3.01545400	3.11330100	1.37504200
H	-4.15954200	4.00555900	0.33580700
C	-3.91330400	2.67714400	-1.97088500
H	-4.92600400	2.29177500	-1.77115300
H	-4.01742600	3.74906300	-2.22475400
H	-3.51003500	2.15497800	-2.85740700
C	-1.75621400	4.85330500	-0.63985100
H	-0.86868600	5.40185500	-0.99568500
H	-2.64106900	5.32820200	-1.10228200
H	-1.82377300	4.99868600	0.45245400
C	0.89528500	2.47472300	-2.35275900
H	0.53525200	3.39677900	-2.83815500
H	1.91700300	2.27181800	-2.71034800
H	0.25628800	1.63140400	-2.66937500
C	2.00275800	4.91999300	-1.12330400
H	1.04749900	5.46568700	-1.20534600
H	2.73800200	5.61196900	-0.67274200
H	2.34586200	4.68807000	-2.14425100
C	1.43994400	4.12150300	1.17917000
H	2.21841900	4.78806200	1.59381300
H	0.48965200	4.68313900	1.17636800
H	1.33361500	3.26322400	1.86856700
C	4.23671100	3.01895700	-1.23024200
H	4.57230400	4.06778800	-1.30850900
H	5.12700200	2.40305500	-1.01826900
H	3.84489900	2.70729900	-2.21290100
C	4.90308700	0.59552700	0.97950400
H	5.14947900	-0.13531200	1.76656500
H	5.73047800	0.58165800	0.24681900
H	4.91217000	1.58880900	1.45801900
C	5.41074900	-2.17938000	-0.20133100
H	6.05138500	-1.70869100	0.55978900
H	5.80260300	-3.20055200	-0.36244300
H	5.52506400	-1.61670700	-1.14356000
C	3.88332300	-2.79865700	1.70737800
H	2.84558600	-3.01993200	2.01185100
H	4.47033000	-3.73288000	1.78769800
H	4.30269400	-2.06801900	2.42072700
C	3.53119900	-3.27874000	-2.13954300
H	4.53730100	-3.71397000	-2.27088600
H	2.81609800	-3.89677400	-2.71128900
H	3.52993200	-2.26429200	-2.57888600
C	-3.42018000	-2.43349800	-2.84385400
H	-3.86167600	-3.35910500	-3.25282700
H	-4.16261900	-1.62762300	-2.96441700
H	-2.53695200	-2.17097000	-3.45348800
C	-2.28022300	-4.46651400	0.21182500
H	-3.17983900	-5.09384500	0.06499800
H	-1.44195500	-5.12435600	0.50500600
H	-2.48005900	-3.77117900	1.04173600
C	-1.75759900	-4.71790300	-2.22618200
H	-1.00831800	-5.47735900	-1.93976200
H	-2.70288800	-5.25374700	-2.42693500

H	-1.41734000	-4.24664700	-3.16373200
H	0.96302900	-1.92699700	2.74296200
C	-1.32786400	-0.24255700	2.49084100
C	-2.23687300	0.81912200	2.69662800
C	-1.83264200	-1.56350900	2.51347200
C	-3.59982400	0.57759300	2.91986000
H	-1.85236300	1.84517400	2.69532600
C	-3.19345900	-1.80798200	2.74168200
H	-1.15037300	-2.40128800	2.33472100
C	-4.08774400	-0.73978600	2.94196800
H	-4.28126100	1.41985300	3.08178500
H	-3.56440900	-2.83925700	2.76129500
H	-5.15178800	-0.93442700	3.11716900

(CH₃)₁₅(corrin)Co(III)-CH₂-CH(O)Ph - **Ia**



E (BP86-D3/6-31G(d) + SMD (acetone)) = -3313.362102
 E (BP86-D3/6-311++G(2df,p)// BP86-D3/6-31G(d) + SMD (acetone)) = -3314.063958
 E (wB97XD/6-311++G(2df,p)// BP86-D3/6-31G(d) + SMD (acetone)) = -3313.091918
 E (M06-D3/6-311++G(2df,p)// BP86-D3/6-31G(d) + SMD (acetone)) = -3312.155852
 E (M06/6-311++G(2df,p)// BP86-D3/6-31G(d) + SMD (acetone)) = -3312.115847
 E (PBE0-D3/6-311++G(2df,p)// BP86-D3/6-31G(d) + SMD (acetone)) = -3311.189843
 E (B3LYP-D3/6-311++G(2df,p)// BP86-D3/6-31G(d) + SMD (acetone)) = -3313.830875

Zero-point correction= 0.912884
 Thermal correction to Energy= 0.960990
 Thermal correction to Enthalpy= 0.961935
 Thermal correction to Gibbs Free Energy= 0.839526

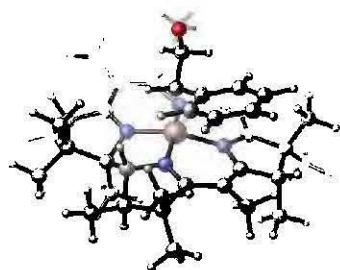
Charge = 0 Multiplicity = 1

C	2.60941200	-1.95715700	0.21475400
C	2.79440100	-3.43267300	0.62295300
C	1.67352500	-4.11797000	-0.22221600
C	0.70749000	-2.97859500	-0.43925300
N	1.29523100	-1.76358400	-0.24850800
H	1.19934900	-4.93441500	0.35322700
C	-0.59430300	-3.16625300	-0.90077300
H	-0.89780600	-4.19378500	-1.12295700
C	3.53704300	-0.93330300	0.35412200
C	-1.52044800	-2.15547800	-1.13330100
C	-2.84335500	-2.39731700	-1.84380400
N	-1.32316700	-0.83911100	-0.80949100
C	-3.61014000	-1.06843000	-1.54185800
C	-2.51995000	-0.14117700	-1.00433400
C	3.20329300	0.40812000	-0.04324700
C	4.20009600	1.54499600	-0.20360900
N	1.96706200	0.78694200	-0.33186900
C	3.27123200	2.81469600	-0.18957800

C	1.90797300	2.23389200	-0.72983100
C	-2.72316100	1.19517100	-0.67844700
C	-1.60919800	2.05314200	-0.39351700
C	-1.64582600	3.57927800	-0.16969700
N	-0.36869500	1.58501200	-0.30507200
C	-0.15105100	3.94876200	-0.48158400
C	0.59805900	2.68518300	-0.04314500
Co	0.36116900	-0.09956400	-0.29833000
H	-4.30769500	-1.26820000	-0.70314200
H	-0.07934600	4.03011400	-1.58339100
H	4.86011400	1.59610900	0.68197300
H	0.76708300	2.70899400	1.04851800
C	0.36770900	-0.13613500	1.73333700
C	-0.55557000	-1.15531600	2.42521700
H	-0.45385500	-2.14537700	1.88842300
O	-0.06388300	-1.12097000	3.69335100
C	-2.04434000	-0.78164100	2.36798700
C	-3.01608900	-1.71259400	1.95707800
C	-2.48750100	0.47313700	2.83920200
C	-4.38838200	-1.40243000	1.98990500
H	-2.68473900	-2.69311500	1.59045600
C	-3.85133300	0.80019800	2.85973600
H	-1.74676100	1.19659700	3.19922300
C	-4.81234200	-0.13882400	2.43418600
H	-5.12547800	-2.14706600	1.66393500
H	-4.17123400	1.78910800	3.21082800
H	-5.87919500	0.11323000	2.45424400
H	0.16038700	0.88663600	2.09925600
H	1.41207900	-0.39817000	1.97636800
C	-4.13750500	1.74162800	-0.60230300
H	-4.22411900	2.47718500	0.21228100
H	-4.47321600	2.23851500	-1.53076500
H	-4.85388500	0.93898300	-0.36644800
C	-2.00650200	3.85934500	1.31083500
H	-3.00117600	3.45237200	1.55854000
H	-1.27805900	3.39977400	2.00219500
H	-2.02976900	4.94716400	1.50309400
C	-2.57274600	4.37316000	-1.11169700
H	-3.62967100	4.33851800	-0.80460600
H	-2.26966900	5.43657700	-1.10647100
H	-2.49845300	4.00540400	-2.15089100
C	0.34177700	5.25616800	0.14125600
H	1.34941900	5.51127400	-0.22781800
H	-0.32638800	6.09666700	-0.12119000
H	0.39267900	5.19337900	1.24220400
C	1.76482600	2.30365200	-2.26364500
H	1.73397200	3.34608100	-2.62093800
H	2.60335200	1.79153400	-2.76095900
H	0.83141500	1.79919700	-2.56937900
C	3.83146300	3.98267100	-1.01578500
H	3.14428800	4.84673100	-0.99451400
H	4.79577400	4.31619500	-0.59031800
H	4.00617600	3.71773700	-2.07110900
C	3.15747700	3.26096800	1.28711700
H	4.15708900	3.55065100	1.65966100
H	2.49289700	4.13226000	1.40865900
H	2.78280000	2.44609600	1.93407400
C	5.11687600	1.33034700	-1.42704700
H	5.83706700	2.16086700	-1.52755300
H	5.69631300	0.39816700	-1.30475300

H	4.54800600	1.24801600	-2.36828900
C	4.92324800	-1.17967000	0.92544000
H	4.88068600	-1.80991500	1.82815400
H	5.60226600	-1.67306400	0.20687200
H	5.40062200	-0.23422700	1.22540100
C	4.16623200	-4.09062900	0.37748200
H	4.91469900	-3.78920500	1.12506900
H	4.05533000	-5.18736400	0.46030300
H	4.56783100	-3.86390600	-0.62456000
C	2.44112300	-3.52923700	2.13430000
H	1.46712400	-3.06504500	2.37200900
H	2.41321300	-4.59029800	2.44614700
H	3.20647200	-3.01526600	2.74275000
C	2.11971200	-4.67488400	-1.59405300
H	2.81710200	-5.52280400	-1.48337500
H	1.23979600	-5.03283100	-2.15740600
H	2.61339500	-3.89158600	-2.19765400
C	-4.43435200	-0.54065600	-2.73045200
H	-5.06250000	-1.35377800	-3.13675600
H	-5.11275900	0.27397600	-2.43826900
H	-3.78746500	-0.16689500	-3.54271100
C	-3.62250400	-3.62262100	-1.33291600
H	-4.61117500	-3.66453400	-1.82687400
H	-3.09724300	-4.56762200	-1.56059700
H	-3.78511500	-3.56957800	-0.24249900
C	-2.50942700	-2.59395600	-3.34728000
H	-1.86450900	-3.48253100	-3.46827700
H	-3.42366400	-2.75428300	-3.94556200
H	-1.96902300	-1.72348100	-3.76034900

(CH₃)₁₅(corrin)Co(III)-CHPh-CH₂(O) - **Ib**



E (BP86-D3/6-31G(d) + SMD (acetone)) = -3313.353368
 E (BP86-D3/6-311++G(2df,p)// BP86-D3/6-31G(d) + SMD (acetone)) = -3314.056514
 E (wB97XD/6-311++G(2df,p)// BP86-D3/6-31G(d) + SMD (acetone)) = -3313.081588
 E (M06-D3/6-311++G(2df,p)// BP86-D3/6-31G(d) + SMD (acetone)) = -3312.147473
 E (M06/6-311++G(2df,p)// BP86-D3/6-31G(d) + SMD (acetone)) = -3312.107111
 E (PBE0-D3/6-311++G(2df,p)// BP86-D3/6-31G(d) + SMD (acetone)) = -3311.180201
 E (B3LYP-D3/6-311++G(2df,p)// BP86-D3/6-31G(d) + SMD (acetone)) = -3313.822528

Zero-point correction= 0.913456
 Thermal correction to Energy= 0.961535
 Thermal correction to Enthalpy= 0.962479
 Thermal correction to Gibbs Free Energy= 0.840491

Charge = 0 Multiplicity = 1

C 3.10634600 -0.96790400 0.15658900

C	3.95554200	-2.25702800	0.21719900
C	3.11331200	-3.19480900	-0.70379000
C	1.73392000	-2.59941700	-0.56111200
N	1.78261500	-1.27911900	-0.21035000
H	3.14232500	-4.23579600	-0.33292800
C	0.57198100	-3.31505200	-0.82731300
H	0.69093900	-4.37815000	-1.05595000
C	3.55477500	0.31817700	0.42457500
C	-0.71344800	-2.78282700	-0.87091200
C	-1.94310300	-3.63755100	-1.16490500
N	-1.00694600	-1.46311300	-0.64849700
C	-3.02133800	-2.53853100	-1.41515500
C	-2.37713500	-1.27336600	-0.85101100
C	2.71624300	1.43705200	0.10936600
C	3.21448200	2.86786400	-0.03301200
N	1.42875200	1.31709000	-0.18200300
C	1.87688500	3.68848400	-0.17168500
C	0.88539900	2.60039600	-0.73614900
C	-3.06498200	-0.07460700	-0.71094600
C	-2.35267500	1.16351200	-0.56711400
C	-2.94897000	2.58237900	-0.72227200
N	-1.03895100	1.19144900	-0.36194400
C	-1.64220600	3.42021700	-0.95564800
C	-0.56950900	2.59865300	-0.22849200
Co	0.26020000	-0.11331000	-0.16987900
H	-3.94744000	-2.79250100	-0.86863700
H	-1.43468600	3.36328100	-2.04034200
H	3.71387200	3.17418800	0.90636800
H	-0.57706300	2.83032000	0.85252000
C	0.05067800	-0.11725400	1.93924900
C	1.02339000	-1.06165900	2.67244300
H	2.07103900	-0.82250400	2.35195900
O	0.72430000	-0.79251500	3.96234400
H	0.33151900	0.92829600	2.15931000
C	-4.58194700	-0.08596500	-0.77551300
H	-5.01190300	0.67889900	-0.11098900
H	-4.98270400	0.09967300	-1.78874500
H	-4.98099400	-1.05609700	-0.43773000
C	-3.69877000	3.05251100	0.54633400
H	-4.50924100	2.35901100	0.81909100
H	-3.02726800	3.14245600	1.41484900
H	-4.15371500	4.04250100	0.36274300
C	-3.87286100	2.73588500	-1.95059400
H	-4.89047800	2.35547900	-1.76809300
H	-3.96610500	3.80987000	-2.19886000
H	-3.45843200	2.21706800	-2.83385900
C	-1.72962000	4.89521000	-0.55846300
H	-0.83348400	5.44414000	-0.89132700
H	-2.60409600	5.37888400	-1.03104200
H	-1.81608600	5.02606300	0.53415600
C	0.92091400	2.47687500	-2.27550400
H	0.57270600	3.39740600	-2.77177500
H	1.94265200	2.26119700	-2.62493600
H	0.27414900	1.63867300	-2.59054300
C	2.03195500	4.93256200	-1.06077400
H	1.07702300	5.47800400	-1.14708800
H	2.76711700	5.62580300	-0.61242400
H	2.37646900	4.69400100	-2.07970200
C	1.46729400	4.14485000	1.24730300
H	2.25193300	4.80316800	1.66306200

H	0.52325600	4.71684900	1.24076400
H	1.34906400	3.28760900	1.93608700
C	4.26114000	3.02133800	-1.15846400
H	4.59814900	4.06935700	-1.23678200
H	5.14974600	2.40471000	-0.94286000
H	3.87080700	2.70935700	-2.14147500
C	4.91486400	0.58813900	1.04355000
H	5.16071700	-0.16598100	1.80829700
H	5.74223400	0.59859700	0.31121200
H	4.91908100	1.56666800	1.55164900
C	5.41613000	-2.13770300	-0.25918700
H	6.06699900	-1.69042600	0.50722100
H	5.81111800	-3.14949400	-0.46413900
H	5.50819200	-1.54046100	-1.18231300
C	3.93049200	-2.83916300	1.65510800
H	2.90036100	-3.07464700	1.97365600
H	4.52354000	-3.77240400	1.68409900
H	4.36312500	-2.13370200	2.38515600
C	3.50820000	-3.18984400	-2.19856400
H	4.51158800	-3.62194300	-2.35509800
H	2.78452500	-3.79031500	-2.77792800
H	3.50244600	-2.16254700	-2.60642500
C	-3.37948000	-2.31181900	-2.90185200
H	-3.81378400	-3.22217400	-3.34997200
H	-4.11920200	-1.50174500	-3.00784100
H	-2.48463800	-2.02982100	-3.48503000
C	-2.30906600	-4.46606900	0.09178800
H	-3.18623600	-5.10490600	-0.12284200
H	-1.46981700	-5.11801700	0.39441100
H	-2.56329400	-3.81016300	0.93875400
C	-1.71901600	-4.61083500	-2.34051000
H	-0.98437500	-5.38748900	-2.06350100
H	-2.66062500	-5.12976000	-2.59397900
H	-1.34653800	-4.10039600	-3.24462700
H	0.85580700	-2.12858600	2.31865600
C	-1.37974000	-0.35069500	2.30543700
C	-2.25167900	0.72936200	2.55920000
C	-1.92026700	-1.65500300	2.40043200
C	-3.60430000	0.52855700	2.88162500
H	-1.84727100	1.74696100	2.51241300
C	-3.26765600	-1.86605900	2.71816600
H	-1.26362200	-2.51156000	2.21486500
C	-4.12479100	-0.77320100	2.95649300
H	-4.25016800	1.39225300	3.07709000
H	-3.65632900	-2.88954100	2.78727100
H	-5.17930100	-0.93825400	3.20617800

NH₃



E (BP86-D3/6-31G(d) + SMD (acetone)) = -56.553288
 E (BP86-D3/6-311++G(2df,p)// BP86-D3/6-31G(d) + SMD (acetone)) = -56.58880
 E (wB97XD/6-311++G(2df,p)// BP86-D3/6-31G(d) + SMD (acetone)) = -56.567956
 E (M06-D3/6-311++G(2df,p)// BP86-D3/6-31G(d) + SMD (acetone)) = -56.544989
 E (M06/6-311++G(2df,p)// BP86-D3/6-31G(d) + SMD (acetone)) = -56.544988

E (PBE0-D3/6-311++G(2df,p)// BP86-D3/6-31G(d) + SMD (acetone)) = -56.516998
 E (B3LYP-D3/6-311++G(2df,p)// BP86-D3/6-31G(d) + SMD (acetone)) = -56.58989

Zero-point correction= 0.033453
 Thermal correction to Energy= 0.036310
 Thermal correction to Enthalpy= 0.037255
 Thermal correction to Gibbs Free Energy= 0.015381

Charge = 0 Multiplicity = 1

N	0.00000000	0.00000000	0.12792900
H	0.00000000	0.93828000	-0.29850200
H	-0.81257500	-0.46914000	-0.29850200
H	0.81257500	-0.46914000	-0.29850200

NH₄⁺



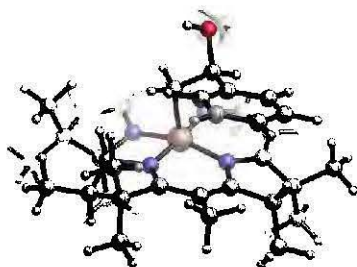
E (BP86-D3/6-31G(d) + SMD (acetone)) = -57.021003
 E (BP86-D3/6-311++G(2df,p)// BP86-D3/6-31G(d) + SMD (acetone)) = -57.047387
 E (wB97XD/6-311++G(2df,p)// BP86-D3/6-31G(d) + SMD (acetone)) = -57.031286
 E (M06-D3/6-311++G(2df,p)// BP86-D3/6-31G(d) + SMD (acetone)) = -57.001833
 E (M06/6-311++G(2df,p)// BP86-D3/6-31G(d) + SMD (acetone)) = -57.001831
 E (PBE0-D3/6-311++G(2df,p)// BP86-D3/6-31G(d) + SMD (acetone)) = -56.978602
 E (B3LYP-D3/6-311++G(2df,p)// BP86-D3/6-31G(d) + SMD (acetone)) = -57.049074

Zero-point correction= 0.048305
 Thermal correction to Energy= 0.051165
 Thermal correction to Enthalpy= 0.052109
 Thermal correction to Gibbs Free Energy= 0.030973

Charge = 1 Multiplicity = 1

N	0.00000000	0.00000000	0.00000000
H	0.59708800	0.59708800	0.59708800
H	-0.59708800	-0.59708800	0.59708800
H	-0.59708800	0.59708800	-0.59708800
H	0.59708800	-0.59708800	-0.59708800

(CH₃)₁₅(corrin)Co(III)-CH₂-CH(OH)Ph - IIa



E (BP86-D3/6-31G(d) + SMD (acetone)) = -3313.879274
 E (BP86-D3/6-311++G(2df,p)// BP86-D3/6-31G(d) + SMD (acetone)) = -3314.571074
 E (wB97XD/6-311++G(2df,p)// BP86-D3/6-31G(d) + SMD (acetone)) = -3313.619455
 E (M06-D3/6-311++G(2df,p)// BP86-D3/6-31G(d) + SMD (acetone)) = -3312.67077

E (M06/6-311++G(2df,p)// BP86-D3/6-31G(d) + SMD (acetone)) = -3312.6303
 E (PBE0-D3/6-311++G(2df,p)// BP86-D3/6-31G(d) + SMD (acetone)) = -3311.712196
 E (B3LYP-D3/6-311++G(2df,p)// BP86-D3/6-31G(d) + SMD (acetone)) = -3314.352068

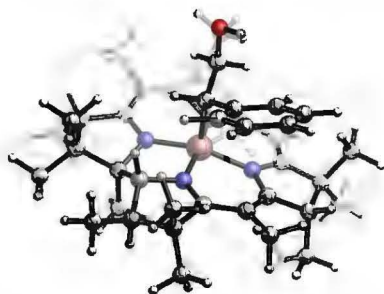
Zero-point correction= 0.927117
 Thermal correction to Energy= 0.975645
 Thermal correction to Enthalpy= 0.976589
 Thermal correction to Gibbs Free Energy= 0.853187

Charge = 1 Multiplicity = 1

C	2.62964900	-1.94135100	0.21759200
C	2.84535500	-3.43469000	0.53143600
C	1.74738500	-4.08554800	-0.36807000
C	0.74818100	-2.96290700	-0.49070200
N	1.31613700	-1.74729400	-0.25039900
H	1.29945300	-4.96181900	0.13465200
C	-0.56737500	-3.15852900	-0.90222100
H	-0.86229400	-4.18519800	-1.13738200
C	3.53595800	-0.91081700	0.41815300
C	-1.51065100	-2.15620000	-1.10635100
C	-2.83832900	-2.41427400	-1.79960300
N	-1.31825200	-0.83634100	-0.79806000
C	-3.60769700	-1.08327100	-1.51757900
C	-2.52100200	-0.14493400	-0.99559300
C	3.19856900	0.43298000	0.02793200
C	4.19365300	1.57182900	-0.11928300
N	1.96983500	0.80758200	-0.28301600
C	3.26173400	2.84018200	-0.13849700
C	1.90966500	2.25097400	-0.69843000
C	-2.72685700	1.19413200	-0.68997600
C	-1.61531200	2.05940300	-0.41397900
C	-1.65885000	3.58904500	-0.21950100
N	-0.37520000	1.59975900	-0.30663100
C	-0.16053500	3.95827000	-0.51514700
C	0.58633800	2.70582600	-0.04217800
Co	0.36036300	-0.09060300	-0.26761100
H	-4.30280200	-1.26981400	-0.67417000
H	-0.07138700	4.01953400	-1.61658900
H	4.83305500	1.62897000	0.78061300
H	0.73305400	2.74596400	1.05255800
C	0.35727900	-0.13023600	1.69730900
C	-0.59948400	-1.15777100	2.28865100
H	-0.48518000	-2.11864000	1.75950800
O	-0.17401800	-1.46133400	3.65076200
C	-2.07123700	-0.77248900	2.28651700
C	-3.04501700	-1.74347400	1.98555300
C	-2.49840200	0.51676600	2.66467900
C	-4.41376500	-1.43702000	2.04490900
H	-2.71912300	-2.74711400	1.68717200
C	-3.86600200	0.82704600	2.73472000
H	-1.76128500	1.29270700	2.89990000
C	-4.82912700	-0.14765500	2.42121100
H	-5.15557900	-2.20408700	1.79424300
H	-4.17969300	1.83621700	3.02481700
H	-5.89629900	0.09723600	2.46623000
H	0.14056800	0.88688700	2.06925900
H	1.38542500	-0.40205500	1.99361500
C	-4.14165600	1.73778500	-0.62381300
H	-4.22912500	2.48963400	0.17491100
H	-4.47466000	2.21355900	-1.56344400

H	-4.85502300	0.93775900	-0.37191400
C	-2.04132800	3.89436800	1.25089700
H	-3.03573100	3.48568400	1.49543400
H	-1.31659200	3.45898400	1.96156500
H	-2.07561000	4.98577300	1.41645900
C	-2.57564900	4.35833500	-1.19098300
H	-3.63580900	4.32900600	-0.89572000
H	-2.27305600	5.42141900	-1.20514600
H	-2.48708800	3.96736200	-2.22028500
C	0.31746200	5.27795700	0.09265600
H	1.32868500	5.53142100	-0.26661400
H	-0.35107200	6.10948100	-0.19488700
H	0.35224400	5.23446400	1.19500500
C	1.79588500	2.29722400	-2.23539800
H	1.77141700	3.33487100	-2.60578200
H	2.64497400	1.77995400	-2.70809400
H	0.86915500	1.78868800	-2.55456500
C	3.83625200	3.99700000	-0.97021400
H	3.14903500	4.86076100	-0.97208600
H	4.79236000	4.33525500	-0.53100200
H	4.02998800	3.71799100	-2.01834400
C	3.11717500	3.30591300	1.32912000
H	4.10844600	3.60320100	1.71672800
H	2.44843100	4.17733800	1.42384800
H	2.73213700	2.49947400	1.98076500
C	5.13725600	1.34608700	-1.32049200
H	5.85524700	2.17908000	-1.41043200
H	5.71752500	0.41810700	-1.17618500
H	4.58969700	1.25404100	-2.27316700
C	4.90426000	-1.15008400	1.03052100
H	4.84791000	-1.85152100	1.87721300
H	5.63203600	-1.55810300	0.30638700
H	5.32697000	-0.21313600	1.42498800
C	4.23696700	-4.03398100	0.25463300
H	4.96559500	-3.77824900	1.03800800
H	4.15250600	-5.13576900	0.24325700
H	4.64543700	-3.71246800	-0.71803700
C	2.46856500	-3.65059800	2.02283900
H	1.44404300	-3.30021900	2.23989900
H	2.52850900	-4.72649300	2.27032300
H	3.15951700	-3.10460200	2.68865600
C	2.20903100	-4.50375600	-1.78328500
H	2.93373800	-5.33425500	-1.74120400
H	1.34059500	-4.84005500	-2.37665600
H	2.67776100	-3.65516300	-2.31361800
C	-4.43349400	-0.57554200	-2.71397300
H	-5.05791000	-1.39806800	-3.10564600
H	-5.11495000	0.24015600	-2.43369400
H	-3.78769300	-0.21277500	-3.53163000
C	-3.60802400	-3.63479100	-1.26355100
H	-4.59504700	-3.69070200	-1.75848600
H	-3.07618100	-4.57983500	-1.47393400
H	-3.77301700	-3.56134400	-0.17522500
C	-2.50897100	-2.63544500	-3.30157000
H	-1.86360300	-3.52469600	-3.41165900
H	-3.42781500	-2.80808600	-3.88820300
H	-1.97423100	-1.77048200	-3.73249100
H	-0.27008600	-0.61977900	4.15279800

(CH₃)₁₅(corrin)Co(III)-CHPh-CH₂OH - IIb



E (BP86-D3/6-31G(d) + SMD (acetone)) = -3313.877792
 E (BP86-D3/6-311++G(2df,p)// BP86-D3/6-31G(d) + SMD (acetone)) = -3314.570354
 E (wB97XD/6-311++G(2df,p)// BP86-D3/6-31G(d) + SMD (acetone)) = -3313.616803
 E (M06-D3/6-311++G(2df,p)// BP86-D3/6-31G(d) + SMD (acetone)) = -3312.668526
 E (M06/6-311++G(2df,p)// BP86-D3/6-31G(d) + SMD (acetone)) = -3312.627742
 E (PBE0-D3/6-311++G(2df,p)// BP86-D3/6-31G(d) + SMD (acetone)) = -3311.710079
 E (B3LYP-D3/6-311++G(2df,p)// BP86-D3/6-31G(d) + SMD (acetone)) = -3314.35043

Zero-point correction=	0.928394
Thermal correction to Energy=	0.975817
Thermal correction to Enthalpy=	0.976761
Thermal correction to Gibbs Free Energy=	0.857064

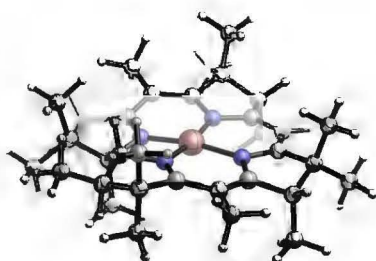
Charge = 1 Multiplicity = 1

C	3.11167700	-0.94832000	0.14500900
C	3.96513100	-2.23129800	0.20900400
C	3.13266800	-3.17303500	-0.71747900
C	1.75060500	-2.58496000	-0.58320400
N	1.79326700	-1.26358400	-0.23895100
H	3.16205200	-4.21357900	-0.34733200
C	0.59161700	-3.30853300	-0.83932900
H	0.71587500	-4.37225800	-1.06044200
C	3.53696600	0.33526000	0.45161000
C	-0.69653300	-2.78402800	-0.88953700
C	-1.91793400	-3.64647700	-1.18928200
N	-0.99930000	-1.46632500	-0.67464600
C	-3.01534600	-2.55827600	-1.40702000
C	-2.37341100	-1.28781900	-0.85678300
C	2.69880700	1.45331900	0.11500200
C	3.19393500	2.88390400	-0.02610600
N	1.42310900	1.32815500	-0.20794800
C	1.85511700	3.70093200	-0.18147000
C	0.87153700	2.61234700	-0.75960400
C	-3.06829400	-0.09459900	-0.69975900
C	-2.36205800	1.15012400	-0.57551900
C	-2.96724000	2.56533800	-0.72454900
N	-1.04829500	1.19226700	-0.39200600
C	-1.66746000	3.40729000	-0.98747900
C	-0.58536600	2.60083800	-0.25745200
Co	0.26145900	-0.11011400	-0.18572400
H	-3.92151700	-2.82239400	-0.83310200
H	-1.47115300	3.33255400	-2.07310200
H	3.68320700	3.19199200	0.91739000
H	-0.60111500	2.83130800	0.82372400
C	0.01752600	-0.07458400	1.81979700
C	0.99177700	-1.01834000	2.52797800
H	2.02769200	-0.72474500	2.31781800

O	0.85460300	-0.90893700	3.95923600
H	0.28739100	0.96679100	2.07012800
C	-4.58495300	-0.11806200	-0.72872900
H	-5.00427400	0.64326600	-0.05388900
H	-5.00705900	0.06597900	-1.73296600
H	-4.96742800	-1.09238700	-0.38466500
C	-3.68686200	3.03261400	0.56319400
H	-4.47512000	2.32752900	0.86898100
H	-2.99011700	3.14647900	1.40866300
H	-4.16406100	4.01201600	0.38136600
C	-3.91919300	2.70653600	-1.93168200
H	-4.93163300	2.32769800	-1.72069700
H	-4.01800900	3.77834800	-2.18530900
H	-3.52540800	2.18113600	-2.82024500
C	-1.75673800	4.88701200	-0.61095200
H	-0.86758600	5.43361200	-0.96535200
H	-2.64000600	5.35799500	-1.07929900
H	-1.82891600	5.03429600	0.48043700
C	0.91500800	2.49246800	-2.29830100
H	0.55985500	3.41314800	-2.78873500
H	1.93998500	2.28898800	-2.64520100
H	0.27608600	1.65121300	-2.62129600
C	2.01730800	4.94445200	-1.06946300
H	1.06308200	5.48990200	-1.16199800
H	2.74919100	5.63635200	-0.61442900
H	2.36982100	4.70541900	-2.08537800
C	1.42811000	4.15505800	1.23283900
H	2.20555400	4.81680900	1.65583600
H	0.48191200	4.72291200	1.21495400
H	1.30675000	3.29799400	1.92169700
C	4.25038600	3.03124800	-1.14336800
H	4.58069900	4.08064300	-1.22488500
H	5.14063200	2.42213600	-0.91493700
H	3.86912100	2.71015300	-2.12676200
C	4.88482200	0.61384100	1.08999400
H	5.13793900	-0.15313800	1.83820800
H	5.71409200	0.65350400	0.36153300
H	4.86694500	1.58144000	1.61767200
C	5.42738200	-2.09780100	-0.25654800
H	6.06764600	-1.64480100	0.51522900
H	5.83203500	-3.10596900	-0.45857800
H	5.51950500	-1.49937500	-1.17863000
C	3.92996600	-2.81136800	1.64855100
H	2.90107400	-3.06477300	1.95660500
H	4.53533000	-3.73562700	1.68379800
H	4.34470800	-2.10038600	2.38341200
C	3.53335200	-3.16378900	-2.21081400
H	4.53960700	-3.59117700	-2.35830700
H	2.81656400	-3.76860400	-2.79379600
H	3.52532800	-2.13637400	-2.61763300
C	-3.42089600	-2.33150800	-2.88153200
H	-3.85310200	-3.24855700	-3.31673400
H	-4.17769400	-1.53476700	-2.96175800
H	-2.54933300	-2.03319000	-3.49069100
C	-2.25979700	-4.51165400	0.04970800
H	-3.12348800	-5.16206800	-0.18133400
H	-1.40677800	-5.15442400	0.33201100
H	-2.52886500	-3.88559800	0.91477000
C	-1.68358600	-4.58711100	-2.38989000
H	-0.92980400	-5.35312800	-2.13713700

H	-2.61684400	-5.11919200	-2.64489000
H	-1.33196400	-4.04703500	-3.28480100
H	0.85510100	-2.06520800	2.18944700
C	-1.39903600	-0.32862500	2.22047500
C	-2.23892900	0.74573300	2.58383100
C	-1.93213700	-1.63682400	2.30448300
C	-3.56659600	0.53421400	2.98334900
H	-1.83213600	1.76200200	2.54900600
C	-3.25745900	-1.85671700	2.70584600
H	-1.30004600	-2.48789800	2.03015400
C	-4.08588600	-0.77034000	3.04015100
H	-4.19562800	1.39009700	3.25180600
H	-3.64763400	-2.87986900	2.75579500
H	-5.12319900	-0.94052800	3.34928300
H	-0.07045700	-1.17644200	4.16026300

(CH₃)₁₅(corrin)Co(II)



E (BP86-D3/6-31G(d) + SMD (acetone)) = -2928.348782
 E (BP86-D3/6-311++G(2df,p)// BP86-D3/6-31G(d) + SMD (acetone)) = -2928.920801
 E (wB97XD/6-311++G(2df,p)// BP86-D3/6-31G(d) + SMD (acetone)) = -2928.135257
 E (M06-D3/6-311++G(2df,p)// BP86-D3/6-31G(d) + SMD (acetone)) = -2927.342949
 E (M06/6-311++G(2df,p)// BP86-D3/6-31G(d) + SMD (acetone)) = -2927.316126
 E (PBE0-D3/6-311++G(2df,p)// BP86-D3/6-31G(d) + SMD (acetone)) = -2926.56083
 E (B3LYP-D3/6-311++G(2df,p)// BP86-D3/6-31G(d) + SMD (acetone)) = -2928.726932

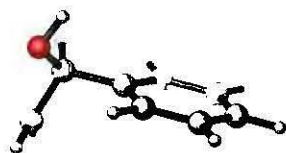
Zero-point correction= 0.365872
 Thermal correction to Energy= 0.385009
 Thermal correction to Enthalpy= 0.385953
 Thermal correction to Gibbs Free Energy= 0.318753

Charge = 0 Multiplicity = 1

C	-1.04576000	2.77500100	-0.08371400
C	-2.31403100	3.58787200	-0.24874800
C	-3.43292300	2.55671800	-0.01268900
C	-2.69138400	1.23811300	-0.01699200
N	-1.33315300	1.40921800	-0.01248900
H	-2.35333100	4.00502300	-1.27222600
H	-4.22628700	2.57687900	-0.77884500
C	-3.33201600	0.00011700	0.00016900
H	-4.42623800	0.00015300	0.00027900
C	0.21724400	3.32453300	-0.03381900
H	0.31604700	4.41141000	-0.10211700
C	-2.69146800	-1.23792900	0.01720600
C	-3.43314800	-2.55645600	0.01310800
N	-1.33325400	-1.40914000	0.01245400

C	-2.31425200	-3.58781700	0.24826600
H	-4.22596700	-2.57663600	0.77983500
C	-1.04594500	-2.77494600	0.08347400
H	-2.35335400	-4.00574600	1.27142600
C	1.39269200	2.54047100	0.10500500
C	2.81064700	3.05983100	0.24160300
N	1.35051800	1.21856300	0.16189900
C	3.65766400	1.79254200	-0.03678300
H	2.96384200	3.43676000	1.27244000
C	2.71229400	0.65575600	0.38739100
H	4.61302700	1.77719600	0.51064900
C	0.21703400	-3.32454300	0.03358700
H	0.31576200	-4.41143600	0.10176400
C	1.39254100	-2.54054900	-0.10508000
C	2.81048200	-3.05999400	-0.24151900
N	1.35045600	-1.21863600	-0.16195200
C	3.65754000	-1.79276400	0.03700700
H	2.96378300	-3.43690300	-1.27234800
C	2.71229700	-0.65591500	-0.38727500
H	4.61297900	-1.77746600	-0.51029400
Co	-0.03616400	0.00000100	-0.00004600
H	-2.34146400	-4.43918400	-0.45187000
H	-3.92719900	-2.69661200	-0.96700900
H	-3.92622700	2.69712100	0.96777600
H	-2.34105000	4.43975400	0.45076000
H	3.01544400	-3.89714400	0.44706000
H	3.87130100	-1.71107200	1.11865400
H	3.87156900	1.71081600	-1.11839900
H	3.01574600	3.89695000	-0.44697300
H	2.80958900	-0.43021000	-1.46913500
H	2.80943900	0.43004700	1.46926300

2-hydroxy-2-phenyl-ethyl radical - IIIa



E (BP86-D3/6-31G(d) + SMD (acetone)) = -385.430636
 E (BP86-D3/6-311++G(2df,p)// BP86-D3/6-31G(d) + SMD (acetone)) = -385.564351
 E (wB97XD/6-311++G(2df,p)// BP86-D3/6-31G(d) + SMD (acetone)) = -385.420779
 E (M06-D3/6-311++G(2df,p)// BP86-D3/6-31G(d) + SMD (acetone)) = -385.266213
 E (M06/6-311++G(2df,p)// BP86-D3/6-31G(d) + SMD (acetone)) = -385.264301
 E (PBE0-D3/6-311++G(2df,p)// BP86-D3/6-31G(d) + SMD (acetone)) = -385.105271
 E (B3LYP-D3/6-311++G(2df,p)// BP86-D3/6-31G(d) + SMD (acetone)) = -385.573588

Zero-point correction= 0.142268
 Thermal correction to Energy= 0.151030
 Thermal correction to Enthalpy= 0.151974
 Thermal correction to Gibbs Free Energy= 0.108138

Charge = 0 Multiplicity = 2

C	-2.23005100	-0.60482000	1.16092700
C	-1.72567800	-0.36823400	-0.22392600

H	-1.91888800	-1.26567700	-0.85363600
O	-2.40456200	0.78681900	-0.75075400
C	-0.20369900	-0.16363700	-0.14353100
C	0.67707700	-1.24905800	-0.32525600
C	0.32461900	1.10746900	0.16587300
C	2.06402500	-1.06747800	-0.20081900
H	0.27086200	-2.23876000	-0.56959100
C	1.71093500	1.28960300	0.28487400
H	-0.36329100	1.95021600	0.29728100
C	2.58550600	0.20239300	0.10467600
H	2.74010200	-1.91733000	-0.35093800
H	2.11121700	2.28329500	0.51816200
H	3.66814300	0.34526500	0.19759200
H	-2.39645400	0.25840800	1.81462800
H	-2.14508400	-1.60008300	1.60701500
H	-1.94651400	1.01268800	-1.59138600

2-hydroxy-1-phenyl-ethyl radical - IIIb



E (BP86-D3/6-31G(d) + SMD (acetone)) = -385.450209
 E (BP86-D3/6-311++G(2df,p)// BP86-D3/6-31G(d) + SMD (acetone)) = -385.584219
 E (wB97XD/6-311++G(2df,p)// BP86-D3/6-31G(d) + SMD (acetone)) = -385.439457
 E (M06-D3/6-311++G(2df,p)// BP86-D3/6-31G(d) + SMD (acetone)) = -385.286187
 E (M06/6-311++G(2df,p)// BP86-D3/6-31G(d) + SMD (acetone)) = -385.284479
 E (PBE0-D3/6-311++G(2df,p)// BP86-D3/6-31G(d) + SMD (acetone)) = -385.1239
 E (B3LYP-D3/6-311++G(2df,p)// BP86-D3/6-31G(d) + SMD (acetone)) = -385.593337

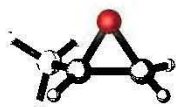
Zero-point correction= 0.143843
 Thermal correction to Energy= 0.152401
 Thermal correction to Enthalpy= 0.153345
 Thermal correction to Gibbs Free Energy= 0.109788

Charge = 0 Multiplicity = 2

C	-1.32076300	1.04368600	0.13564300
C	-2.57326800	0.26091200	0.38926200
O	-2.76024300	-0.73707800	-0.64816600
H	-1.40877900	2.13286700	0.04157300
H	-2.50585700	-0.23731400	1.38451000
C	-0.01828600	0.47738900	0.06493500
C	1.12451500	1.32510200	-0.12133200
C	0.22126100	-0.93234600	0.19225000
C	2.41640500	0.79966500	-0.16615800
H	0.96736700	2.40594500	-0.22429900
C	1.51903300	-1.44502400	0.14891400
H	-0.63525600	-1.60510200	0.29730000
C	2.62697900	-0.58908600	-0.02857100
H	3.27153600	1.47116600	-0.30689600
H	1.67697000	-2.52551100	0.24886000
H	3.64209900	-0.99975800	-0.06397900
H	-3.44048000	0.95230400	0.43295300

H -3.46092300 -1.33976500 -0.31434900

Propylene oxide



E (BP86-D3/6-31G(d) + SMD (acetone)) = -193.116591

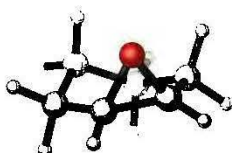
E (BP86-D3/6-311++G(2df,p)// BP86-D3/6-31G(d) + SMD (acetone)) = -193.186628

Zero-point correction= 0.083131
Thermal correction to Energy= 0.087595
Thermal correction to Enthalpy= 0.088539
Thermal correction to Gibbs Free Energy= 0.056727

Charge = 0 Multiplicity = 1

C	-1.04194000	0.62571000	-0.06391300
C	0.15610700	-0.03405300	0.49377000
C	1.51540900	0.09572200	-0.15239600
H	0.16153700	-0.24285800	1.57660700
O	-0.84014200	-0.80137600	-0.23956200
H	2.09476300	0.90418400	0.33121200
H	2.09058600	-0.84271300	-0.04722800
H	-1.87544500	0.90924500	0.59769200
H	-0.94595700	1.23152200	-0.97878000
H	1.41819500	0.32735800	-1.22777400

Cyclohexene oxide (5o)



E (BP86-D3/6-31G(d) + SMD (acetone)) = -309.867094

E (BP86-D3/6-311++G(2df,p)// BP86-D3/6-31G(d) + SMD (acetone)) = -309.968367

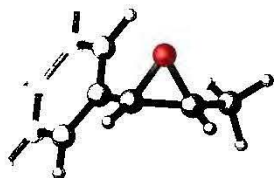
Zero-point correction= 0.147541
Thermal correction to Energy= 0.153648
Thermal correction to Enthalpy= 0.154592
Thermal correction to Gibbs Free Energy= 0.117916

Charge = 0 Multiplicity = 1

C	0.98720600	0.84213000	-0.30180800
C	1.09675000	-0.63335600	-0.42211500
C	-0.35046800	1.52228900	-0.02911000
C	-0.13082900	-1.51657600	-0.29172400
H	1.92233100	-1.04800600	-1.02479000
O	1.53195800	0.03967700	0.79048300
C	-1.55708600	0.57047200	-0.17687400
H	-0.46002900	2.38496800	-0.71272100
H	-0.31378400	1.93646200	0.99770400
C	-1.28127000	-0.80788200	0.44934800

H	-0.45628400	-1.79308800	-1.31519300
H	0.14931300	-2.45882300	0.21863200
H	-1.78004300	0.43006200	-1.25403100
H	-2.45393500	1.03393100	0.27491100
H	-2.18839500	-1.43902200	0.41403600
H	-1.01084100	-0.68485000	1.51563800
H	1.75019000	1.45848900	-0.80435500

cis-1-phenylpropylene oxide

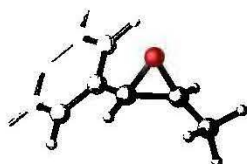


E (BP86-D3/6-31G(d) + SMD (acetone)) = -424.187226
E (BP86-D3/6-311++G(2df,p)// BP86-D3/6-31G(d) + SMD (acetone)) = -424.322652
Zero-point correction= 0.162298
Thermal correction to Energy= 0.171145
Thermal correction to Enthalpy= 0.172089
Thermal correction to Gibbs Free Energy= 0.128320

Charge = 0 Multiplicity = 1

C	2.40649000	0.29792400	0.23858800
C	1.23298000	0.83124600	-0.51606500
H	1.32445000	1.86349400	-0.89299200
O	2.15040700	-0.10866300	-1.13430800
C	-0.17545500	0.38453500	-0.28213900
C	-1.12375500	1.31641000	0.19037400
C	-0.58054400	-0.94390300	-0.52419300
C	-2.44764200	0.92110700	0.43681800
H	-0.81933900	2.35560900	0.36671200
C	-1.90654300	-1.33758000	-0.28139200
H	0.15308000	-1.65613500	-0.91581200
C	-2.84325300	-0.40832200	0.20316100
H	-3.17363300	1.65376000	0.80780600
H	-2.20971300	-2.37282800	-0.47632700
H	-3.87821800	-0.71566300	0.39147000
C	2.31128700	-0.75660100	1.31314900
H	1.38642900	-1.35052200	1.22872400
H	3.17540600	-1.44309700	1.25234900
H	2.33042700	-0.27608300	2.30869800
H	3.26647200	0.98187700	0.33402700

trans-1-phenylpropylene oxide

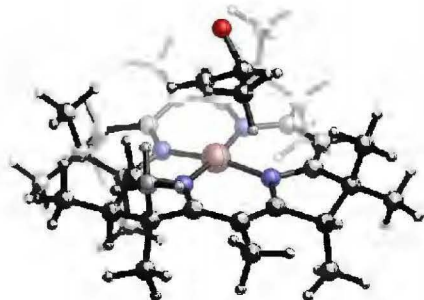


E (BP86-D3/6-31G(d) + SMD (acetone)) = -424.188449
E (BP86-D3/6-311++G(2df,p)// BP86-D3/6-31G(d) + SMD (acetone)) = -424.324107
Zero-point correction= 0.162156
Thermal correction to Energy= 0.171092
Thermal correction to Enthalpy= 0.172036
Thermal correction to Gibbs Free Energy= 0.127970

Charge = 0 Multiplicity = 1

C	2.18947200	-0.23741400	0.40991800
C	1.15634400	0.39687200	-0.45341800
H	1.42933500	1.35009700	-0.93414100
O	1.92408800	-0.74852400	-0.92402400
C	-0.30620700	0.19571500	-0.22276500
C	-1.16838700	1.31026500	-0.17300500
C	-0.84011900	-1.09587500	-0.03151500
C	-2.53893500	1.13826900	0.08110200
H	-0.76122000	2.31645000	-0.33262900
C	-2.20999600	-1.26715600	0.21815700
H	-0.17151900	-1.96140900	-0.09827200
C	-3.06389800	-0.15070700	0.27861200
H	-3.19875000	2.01278100	0.11830500
H	-2.61439800	-2.27596400	0.36136700
H	-4.13413900	-0.28567900	0.47222300
C	3.54280100	0.39023700	0.63967000
H	3.81605500	1.05576400	-0.19761400
H	3.53660700	0.98067700	1.57425100
H	4.32054500	-0.38965300	0.73558100
H	1.81834400	-0.89611300	1.21257900

(CH₃)₁₅(corrin)Co(I) - Propylene oxide – TS2a



E (BP86-D3/6-31G(d) + SMD (acetone)) = -3121.599058

E (BP86-D3/6-311++G(2df,p)//BP86-D3/6-31G(d) + SMD (acetone)) = -3122.245755

Zero-point correction=	0.860764
Thermal correction to Energy=	0.905782
Thermal correction to Enthalpy=	0.906727
Thermal correction to Gibbs Free Energy=	0.790568

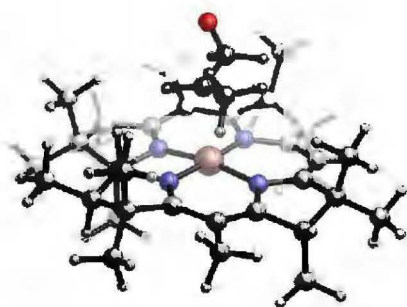
Charge = 0 Multiplicity = 1

C	-3.01576600	-0.48713100	-0.03235100
C	-4.33582400	0.25550100	0.26985500
C	-4.05912600	1.62640400	-0.41519500
C	-2.55448600	1.69600700	-0.33624400
N	-1.98649500	0.45259600	-0.24791300
H	-4.53224600	2.44837700	0.15395600
C	-1.85096300	2.89511300	-0.38755700
H	-2.44208500	3.81496400	-0.43050700
C	-2.81888800	-1.86220700	0.02063500
C	-0.46623600	3.01030300	-0.39212200
C	0.26505200	4.34617800	-0.35667600
N	0.39541200	1.93969200	-0.35411600
C	1.66905600	3.91102100	-0.85986100

C	1.70296100	2.43164300	-0.48677800
C	-1.52781500	-2.42058200	-0.25425300
C	-1.24511500	-3.90137500	-0.45734700
N	-0.43364300	-1.67233000	-0.37485800
C	0.31565700	-3.97259200	-0.28457600
C	0.75809600	-2.52186300	-0.71024900
C	2.87146100	1.68928700	-0.36717800
C	2.81419500	0.27114900	-0.16407100
C	4.00309700	-0.67516200	0.09680200
N	1.64626500	-0.37540500	-0.10975000
C	3.35010300	-2.06281700	-0.22612800
C	1.87158600	-1.83183300	0.10734600
Co	-0.11439400	0.11779700	-0.21318100
H	2.44752200	4.48895200	-0.33231300
H	3.44401400	-2.19657800	-1.32052600
H	-1.70377400	-4.48907500	0.36012200
H	1.69692200	-2.02878600	1.18009000
C	-0.43240700	-0.20621700	2.18216800
C	-0.14746300	1.07338800	2.86830200
H	-0.77263000	1.92907200	2.51638500
O	-0.66628200	0.32157600	3.92150600
H	0.29523800	-1.01297400	2.30262700
H	-1.46485800	-0.49074300	1.98249000
C	4.21591800	2.38838600	-0.47338000
H	4.89627700	2.08017200	0.33844100
H	4.72942500	2.17065200	-1.42767900
H	4.11559000	3.48152100	-0.40242000
C	4.39541000	-0.55081400	1.59101600
H	4.68974700	0.48565800	1.83188200
H	3.55425600	-0.82265000	2.25343400
H	5.25105100	-1.20849200	1.82974100
C	5.24687100	-0.49404300	-0.79847300
H	5.89716600	0.33337900	-0.47476900
H	5.85578200	-1.41660000	-0.75729900
H	4.96285300	-0.32499700	-1.85265700
C	3.99950400	-3.26222700	0.46917000
H	3.58741900	-4.21214300	0.08926400
H	5.08971800	-3.28252300	0.28719700
H	3.83828300	-3.23975200	1.56137300
C	1.03187900	-2.37810400	-2.22225300
H	1.88149200	-3.00005900	-2.54887800
H	0.14606100	-2.66788900	-2.80878500
H	1.25623200	-1.32226300	-2.45304300
C	0.96757900	-5.09710200	-1.10448700
H	2.06488200	-5.09080500	-0.98126000
H	0.60056300	-6.08034000	-0.75670100
H	0.75121700	-5.02285900	-2.18246200
C	0.58184700	-4.23598600	1.21651200
H	0.15057100	-5.21389600	1.49918800
H	1.65865800	-4.26907700	1.45133600
H	0.11124700	-3.46632100	1.85604200
C	-1.85101700	-4.43645000	-1.77305300
H	-1.64105000	-5.51384700	-1.89375600
H	-2.94797500	-4.30990800	-1.76205100
H	-1.46546700	-3.90739500	-2.66047600
C	-3.94694900	-2.81605700	0.38030200
H	-4.52904000	-2.44798200	1.24068400
H	-4.65576500	-2.98071400	-0.45146900
H	-3.55372100	-3.80308200	0.66916300
C	-5.65569000	-0.36721000	-0.22427600

H	-6.00188000	-1.18860600	0.42071900
H	-6.44442600	0.40761000	-0.20702600
H	-5.57729400	-0.74902400	-1.25638700
C	-4.40076400	0.46958000	1.80712500
H	-3.50178700	0.99629300	2.17671800
H	-5.28910100	1.07376400	2.07128900
H	-4.47051400	-0.49559700	2.33916500
C	-4.49960500	1.72882900	-1.89346200
H	-5.59794400	1.69193400	-1.99876600
H	-4.14944600	2.68511000	-2.32149400
H	-4.06389400	0.90871100	-2.49323300
C	1.89014300	4.05788000	-2.38125500
H	1.85550800	5.11648500	-2.69360300
H	2.87654500	3.65145200	-2.66560900
H	1.11933900	3.50276500	-2.94660100
C	0.36795900	4.79971300	1.12455900
H	0.92882500	5.75078800	1.19697300
H	-0.63754100	4.95492700	1.55553600
H	0.89085700	4.04377600	1.73715900
C	-0.40432000	5.45834100	-1.18005800
H	-1.36064600	5.76495700	-0.71932400
H	0.24389600	6.35304700	-1.21345500
H	-0.61432900	5.14187200	-2.21598900
C	1.31628300	1.48312100	3.00757100
H	1.91436400	0.61181300	3.33277600
H	1.72751700	1.85349200	2.05312700
H	1.42316200	2.27600000	3.77148500

(CH₃)₁₅(corrin)Co(I) - Propylene oxide – TS2b



E (BP86-D3/6-31G(d) + SMD (acetone)) = -3121.590068

E (BP86-D3/6-311++G(2df,p)// BP86-D3/6-31G(d) + SMD (acetone)) = -3122.237732

Zero-point correction=	0.860720
Thermal correction to Energy=	0.905896
Thermal correction to Enthalpy=	0.906841
Thermal correction to Gibbs Free Energy=	0.790292

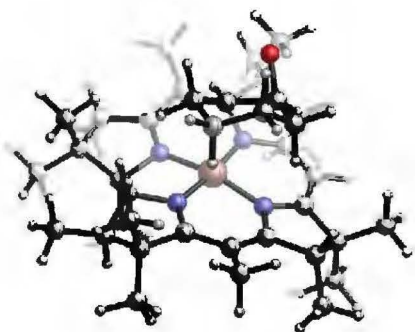
Charge = 0 Multiplicity = 1

C	-3.00724000	-0.39843900	-0.08430200
C	-4.35624600	0.34798900	0.03397600
C	-3.97374400	1.73401000	-0.56695200
C	-2.49071500	1.78123500	-0.29491700
N	-1.94752100	0.52743400	-0.17967400
H	-4.50882500	2.54782000	-0.04281800

C	-1.77288900	2.97170700	-0.24063600
H	-2.35010400	3.90045200	-0.28081000
C	-2.83490400	-1.77609200	-0.02787200
C	-0.38762900	3.06724900	-0.19373300
C	0.36763800	4.38669800	-0.10048700
N	0.45808600	1.98267900	-0.21955000
C	1.74267500	3.95728300	-0.68227300
C	1.76765700	2.46164000	-0.37783300
C	-1.53848300	-2.34879100	-0.23411100
C	-1.27439800	-3.83483300	-0.43736300
N	-0.42889200	-1.61651400	-0.31058400
C	0.28793100	-3.92576700	-0.28035800
C	0.73839000	-2.47859500	-0.70169400
C	2.92849500	1.69794100	-0.34750300
C	2.85850000	0.27273500	-0.19989900
C	4.04176600	-0.69500700	-0.00243600
N	1.68458900	-0.35800700	-0.11648200
C	3.35725000	-2.06829300	-0.32277200
C	1.89686200	-1.82028000	0.07092800
Co	-0.07294500	0.16995100	-0.12241100
H	2.55154700	4.49984000	-0.16304400
H	3.40970200	-2.18819700	-1.42148500
H	-1.73512600	-4.40773700	0.39036600
H	1.76909000	-2.03004200	1.14799900
C	0.09606000	-0.03485900	2.37141800
C	-1.31729500	0.05189800	2.81468600
H	-2.01355800	-0.65599400	2.31218500
O	-0.80199500	-0.33410500	4.03702500
H	0.48191400	-1.05017900	2.25229500
C	4.27827100	2.37842300	-0.49644600
H	4.98868200	2.04110600	0.27726300
H	4.74442500	2.17216400	-1.47715400
H	4.20104100	3.47109300	-0.39845600
C	4.48562700	-0.59895500	1.47982400
H	4.82005000	0.42538700	1.72017200
H	3.65792900	-0.85167400	2.16689200
H	5.32829700	-1.28417800	1.68405200
C	5.25499900	-0.51540300	-0.93848500
H	5.92757900	0.29809800	-0.62527900
H	5.85247200	-1.44628500	-0.93424900
H	4.93552900	-0.32533900	-1.97884600
C	4.01229700	-3.28590200	0.33508900
H	3.57443700	-4.22531900	-0.04179300
H	5.09551100	-3.31900500	0.11699600
H	3.88700600	-3.27521900	1.43215600
C	0.95182600	-2.31703200	-2.22253000
H	1.77783200	-2.94669400	-2.59214100
H	0.03907200	-2.58395800	-2.77725400
H	1.18333900	-1.26150300	-2.44782700
C	0.91845300	-5.05107300	-1.11581900
H	2.01713000	-5.05309700	-1.00877400
H	0.54976700	-6.03363400	-0.76799600
H	0.68768200	-4.96933500	-2.19015800
C	0.57429100	-4.19874200	1.21493400
H	0.13152700	-5.17007400	1.50238600
H	1.65476200	-4.25073200	1.43066600
H	0.12828200	-3.42300200	1.86480000
C	-1.89232100	-4.38296000	-1.74257000
H	-1.68805600	-5.46300600	-1.84754200
H	-2.98797100	-4.25326100	-1.73144500

H	-1.50791800	-3.87102100	-2.64018900
C	-3.99232500	-2.71725200	0.26522000
H	-4.66248400	-2.30742100	1.03722200
H	-4.61083800	-2.93991800	-0.62344200
H	-3.62427100	-3.68120600	0.65183000
C	-5.56697100	-0.27556500	-0.68879900
H	-6.00514900	-1.11342000	-0.12607700
H	-6.35860100	0.48951100	-0.79003600
H	-5.31004200	-0.63661300	-1.69933500
C	-4.69644300	0.54752800	1.53508700
H	-3.90511700	1.12097300	2.04879400
H	-5.64532900	1.10794000	1.63213200
H	-4.81366400	-0.41738800	2.05800400
C	-4.20895900	1.88857200	-2.08752400
H	-5.28300400	1.86461000	-2.34170100
H	-3.79976000	2.85530500	-2.43128300
H	-3.69919700	1.08498800	-2.65009600
C	1.89739100	4.17107900	-2.20384700
H	1.86944800	5.24382300	-2.46447500
H	2.86107200	3.76103000	-2.55317900
H	1.09015200	3.65730000	-2.75727800
C	0.54094700	4.74817900	1.39901300
H	1.10459400	5.69467200	1.50190700
H	-0.44190600	4.87332700	1.88803700
H	1.09563400	3.95833500	1.93623500
C	-0.30821400	5.55936900	-0.82810600
H	-1.23624400	5.85933300	-0.30874700
H	0.36044100	6.43937100	-0.83800400
H	-0.56980300	5.30924100	-1.87044300
H	-1.74317300	1.08522600	2.74038500
C	1.07848200	1.03991900	2.76679900
H	1.64960000	0.75102900	3.66743900
H	1.80691300	1.23642800	1.96539300
H	0.54713500	1.98338700	2.98244300

(CH₃)₁₅(corrin)Co(I) – cyclohexane oxide – TS3



E (BP86-D3/6-31G(d) + SMD (acetone)) = -3238.344929

E (BP86-D3/6-311++G(2df,p)// BP86-D3/6-31G(d) + SMD (acetone)) = -3239.020761

Zero-point correction=	0.925281
Thermal correction to Energy=	0.971894
Thermal correction to Enthalpy=	0.972838
Thermal correction to Gibbs Free Energy=	0.854170

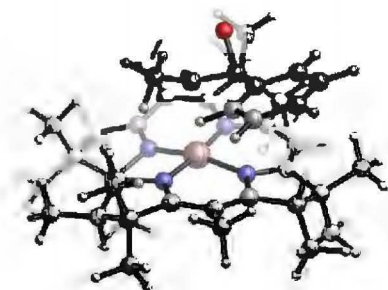
Charge = 0 Multiplicity = 1

C	3.03053400	-0.60714300	-0.01642000
---	------------	-------------	-------------

C	3.97700300	-1.80752700	0.19110300
C	3.24906300	-2.90340700	-0.65266500
C	1.82494400	-2.40421600	-0.64291700
N	1.74705500	-1.06730300	-0.36987600
H	3.33070900	-3.88902200	-0.15732800
C	0.73249200	-3.21436700	-0.93733100
H	0.94287500	-4.25801700	-1.19139100
C	3.34612700	0.73302300	0.17133400
C	-0.59945300	-2.81114000	-0.91855400
C	-1.73668200	-3.72949300	-1.33293000
N	-1.02740800	-1.54845100	-0.59464600
C	-2.97226900	-2.96507600	-0.75930500
C	-2.43085100	-1.54731100	-0.54808400
C	2.38313200	1.74302700	-0.16088100
C	2.70947400	3.20962300	-0.39192100
N	1.10002400	1.46620300	-0.36758100
C	1.28576300	3.88046300	-0.41195900
C	0.36162600	2.67986200	-0.85580800
C	-3.21546400	-0.43257400	-0.26900200
C	-2.63577800	0.87764600	-0.22517100
C	-3.39441800	2.22134700	-0.17931600
N	-1.31214100	1.05681700	-0.22592100
C	-2.27238500	3.18575900	-0.70241600
C	-1.00386700	2.51645200	-0.16306200
Co	0.12072200	-0.07123600	-0.28987000
H	-3.17489900	-3.38522600	0.25059500
H	-2.27277300	3.08966200	-1.80553700
H	3.26872200	3.61244500	0.47407300
H	-0.88620300	2.77511600	0.90415800
C	0.46458400	-0.34400800	2.19043000
C	0.22957400	-1.79640000	2.45676400
H	0.64756100	-2.47724100	1.68216800
O	1.04359500	-1.57141700	3.56225000
H	1.48213100	-0.05193000	1.92406700
C	-4.68929600	-0.61247300	0.05587900
H	-5.04190900	0.17998800	0.73218600
H	-5.34893000	-0.60110200	-0.83084700
H	-4.85576300	-1.56545700	0.58533300
C	-3.79635200	2.57702100	1.27483400
H	-4.45844800	1.81005600	1.70958300
H	-2.91475100	2.66593800	1.93314800
H	-4.34126400	3.53819000	1.29734600
C	-4.62106700	2.30230000	-1.11016300
H	-5.50939200	1.80158800	-0.69310000
H	-4.89212100	3.36275500	-1.26935000
H	-4.40272500	1.85566000	-2.09706400
C	-2.44999500	4.66044100	-0.33657400
H	-1.70544400	5.28557500	-0.85707200
H	-3.45008700	5.02507800	-0.63467100
H	-2.33447500	4.83377600	0.74751400
C	0.20738300	2.55177000	-2.38540700
H	-0.31633600	3.42054300	-2.81773100
H	1.19054800	2.45901900	-2.87332800
H	-0.36932400	1.63869500	-2.61642300
C	1.21705400	5.11008300	-1.33206800
H	0.20552200	5.55141200	-1.32725400
H	1.91708700	5.88751800	-0.97438100
H	1.47914700	4.88094900	-2.37747900
C	0.98195600	4.33459600	1.03476400
H	1.72680500	5.08970600	1.34640800

H	-0.01590200	4.79698900	1.12450900
H	1.03974900	3.49323700	1.75006400
C	3.61167500	3.41233200	-1.62933700
H	3.84059600	4.48192500	-1.77929800
H	4.57075700	2.88388400	-1.49026800
H	3.14952400	3.02453800	-2.55271500
C	4.70033700	1.18458900	0.69282700
H	5.05045700	0.54114200	1.51596200
H	5.48883500	1.18877300	-0.08190600
H	4.63903900	2.20796500	1.09754800
C	5.44449600	-1.63816400	-0.25026400
H	6.03134800	-1.04569900	0.46738800
H	5.92060600	-2.63442900	-0.30686300
H	5.53226500	-1.16230200	-1.24184500
C	3.93593800	-2.19468300	1.69474900
H	2.90635300	-2.29048100	2.08399000
H	4.46996700	-3.15107000	1.85286200
H	4.43805800	-1.42277700	2.30536800
C	3.72769000	-3.04772800	-2.11572600
H	4.76375600	-3.42396200	-2.17571200
H	3.07689600	-3.76193500	-2.65129400
H	3.67599800	-2.07942400	-2.64641200
C	-4.24237600	-3.14785300	-1.61018700
H	-4.34451700	-4.21161900	-1.89216700
H	-5.15907300	-2.87429600	-1.06879000
H	-4.20270600	-2.55081000	-2.53767600
C	-1.63793300	-5.15048100	-0.75109400
H	-2.56575400	-5.71195300	-0.96959400
H	-0.79782900	-5.71746900	-1.19118200
H	-1.50012400	-5.12294800	0.34491000
C	-1.73002700	-3.79739100	-2.88336000
H	-0.76470600	-4.20776100	-3.23001500
H	-2.53297800	-4.45160700	-3.26720100
H	-1.85353100	-2.79448500	-3.33064400
C	-0.37659900	0.68256200	2.91790700
H	-0.37046800	1.62201400	2.33808700
H	0.11250400	0.91973500	3.88337700
C	-1.21592300	-2.20171900	2.79284000
H	-1.80453500	-2.25452000	1.85740900
H	-1.19519100	-3.22036700	3.22873500
C	-1.86822700	-1.20390600	3.76407300
H	-1.31433100	-1.22523900	4.72221200
H	-2.91390600	-1.49838000	3.97687000
C	-1.82204900	0.21370300	3.16842200
H	-2.36653800	0.20579400	2.20654600
H	-2.34085500	0.93847000	3.82474500

(CH₃)₁₅(corrin)Co(I) - *cis*-1-phenylpropylene oxide – TS4a



E (BP86-D3/6-31G(d) + SMD (acetone)) = -3352.66206

E (BP86-D3/6-311++G(2df,p)// BP86-D3/6-31G(d) + SMD (acetone)) = -3353.373699

Zero-point correction=	0.940140
Thermal correction to Energy=	0.989665
Thermal correction to Enthalpy=	0.990609
Thermal correction to Gibbs Free Energy=	0.864500

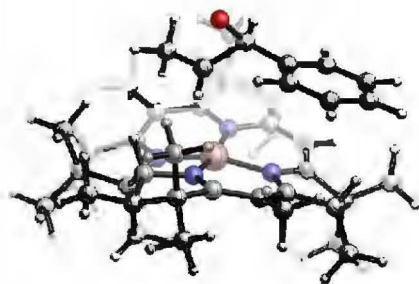
Charge = 0 Multiplicity = 1

C	2.01640900	-2.52315600	0.04273900
C	1.80227400	-4.04121900	0.21771700
C	0.63198400	-4.28794000	-0.78623600
C	-0.01669200	-2.92702600	-0.83841400
N	0.83705300	-1.93103700	-0.45179800
H	-0.06521200	-5.04865700	-0.38799300
C	-1.31846700	-2.72342100	-1.28303100
H	-1.87571900	-3.60751400	-1.60836600
C	3.15647900	-1.80661400	0.38554400
C	-1.96962300	-1.49504700	-1.34117100
C	-3.35802000	-1.34298700	-1.93788400
N	-1.42048800	-0.30035300	-0.94952700
C	-3.74884300	0.08523800	-1.44499900
C	-2.40126200	0.69889600	-1.05378100
C	3.22571400	-0.40117800	0.10870800
C	4.50681900	0.41664200	0.08338600
N	2.15491400	0.31763500	-0.21456600
C	3.97000900	1.89511400	0.08015800
C	2.54178800	1.72536700	-0.56906000
C	-2.20850700	2.03854400	-0.73284600
C	-0.90321500	2.54128800	-0.42491400
C	-0.51503600	4.01810600	-0.20271000
N	0.14774700	1.72861300	-0.28389500
C	1.03192200	3.94141700	-0.45212300
C	1.37000600	2.52688800	0.03022100
Co	0.38354700	-0.07811600	-0.39371100
H	-4.31688500	-0.03691100	-0.49636100
H	1.16748000	3.97491500	-1.55039700
H	5.07541300	0.26028500	1.01968300
H	1.48083300	2.53083900	1.12840800
C	0.13378500	-0.54160100	2.07898000
C	-1.11465800	-1.35257400	2.10620300
H	-1.12295700	-2.12299000	1.30441500
O	-0.61019400	-1.80216400	3.33014900
C	-2.50668800	-0.73909900	2.16614100
C	-3.58585800	-1.64199600	2.29505000
C	-2.79526500	0.63867700	2.13150400

C	-4.90984600	-1.18875700	2.40025300
H	-3.37577000	-2.71927200	2.30983700
C	-4.11921000	1.10063500	2.24563700
H	-1.99040800	1.36211200	1.98537400
C	-5.18189000	0.19194200	2.38010400
H	-5.72972600	-1.91090400	2.49348900
H	-4.31790200	2.17814800	2.21903600
H	-6.21307500	0.55432000	2.46357500
H	1.03249000	-1.12680400	1.88162700
C	-3.41057700	2.96078200	-0.62490300
H	-3.22930300	3.76407000	0.10329800
H	-3.68816700	3.44322000	-1.57998500
H	-4.29002100	2.40959100	-0.25647600
C	-0.83241600	4.43155200	1.25710600
H	-1.90887200	4.33023400	1.47663500
H	-0.28446300	3.80927000	1.98691900
H	-0.55572700	5.48725000	1.43114800
C	-1.13812000	5.02058400	-1.19627300
H	-2.17667800	5.28905700	-0.94631100
H	-0.55084500	5.95778800	-1.18569600
H	-1.12172700	4.62226600	-2.22683200
C	1.85182900	5.06895000	0.17806800
H	2.90152000	5.02649600	-0.15734100
H	1.45438400	6.05836100	-0.11397400
H	1.84883700	5.01427900	1.28076100
C	2.54582900	1.84254300	-2.10726400
H	2.84006500	2.85196900	-2.43966500
H	3.23906600	1.11307900	-2.55513000
H	1.53382900	1.62421500	-2.49123200
C	4.89609800	2.86836500	-0.66678500
H	4.48400000	3.89238500	-0.65806500
H	5.88256500	2.90610100	-0.16889300
H	5.06410200	2.58247300	-1.71756900
C	3.88017000	2.34103500	1.55814600
H	4.89059300	2.33121000	2.00658000
H	3.48183800	3.36451300	1.66064200
H	3.24358000	1.66030000	2.15275600
C	5.43812500	-0.01017300	-1.07246600
H	6.36467500	0.59032700	-1.07463200
H	5.72805500	-1.06872500	-0.95334000
H	4.95586400	0.09328100	-2.05902900
C	4.36203100	-2.46602300	1.03493800
H	4.05800800	-3.18374700	1.81353800
H	5.00143700	-3.00982700	0.31567300
H	4.99862800	-1.71580500	1.53080100
C	2.99659500	-4.97229800	-0.07062200
H	3.72600400	-4.98557600	0.75294200
H	2.62483300	-6.00725900	-0.18493900
H	3.52875400	-4.69766200	-0.99724300
C	1.30121400	-4.28277900	1.66829100
H	0.45143900	-3.63068600	1.94070500
H	0.99241100	-5.33848500	1.79022900
H	2.10863500	-4.08031600	2.39489300
C	1.05505900	-4.70543300	-2.21345600
H	1.52286000	-5.70515000	-2.22913700
H	0.16752800	-4.73656400	-2.87052300
H	1.76875600	-3.97868200	-2.64291000
C	-4.64661000	0.83658500	-2.44597500
H	-5.42889800	0.15151800	-2.82050000
H	-5.16709900	1.69257000	-1.99416000

H	-4.07300500	1.20586800	-3.31370700
C	-4.36609800	-2.39797700	-1.44937200
H	-5.38034700	-2.14446400	-1.81154500
H	-4.12215800	-3.40699200	-1.82823000
H	-4.39287200	-2.43632100	-0.34573900
C	-3.20596900	-1.43867300	-3.47957400
H	-2.78370800	-2.42360400	-3.74787100
H	-4.17825200	-1.33706900	-3.99360000
H	-2.52396100	-0.65986900	-3.86633600
C	0.31421900	0.71200500	2.90325000
H	1.34076300	0.77606100	3.30458700
H	0.13362800	1.62596600	2.31347000
H	-0.39084800	0.71684800	3.75048400

(CH₃)₁₅(corrin)Co(I) - *trans*-1-phenylpropylene oxide – TS4b



E (BP86-D3/6-31G(d) + SMD (acetone)) = -3352.662226

E (BP86-D3/6-311++G(2df,p)// BP86-D3/6-31G(d) + SMD (acetone)) = -3353.373598

Zero-point correction=	0.938001
Thermal correction to Energy=	0.988071
Thermal correction to Enthalpy=	0.989015
Thermal correction to Gibbs Free Energy=	0.861067

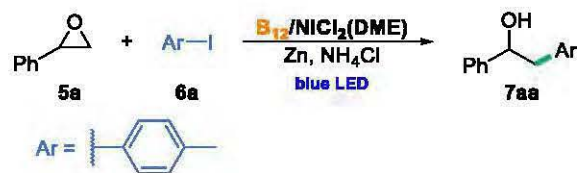
Charge = 0 Multiplicity = 1

C	1.94354400	-2.53425200	0.05994100
C	1.69349000	-3.98988400	0.50951300
C	0.40659000	-4.33425400	-0.30526100
C	-0.19606700	-2.96529300	-0.52531600
N	0.71924400	-1.96085800	-0.33475700
H	-0.26379900	-4.98015400	0.29328900
C	-1.47496100	-2.76668400	-1.04244400
H	-2.05613000	-3.65911500	-1.29616100
C	3.15089500	-1.83987400	0.08740500
C	-2.04188400	-1.52554100	-1.31304400
C	-3.30270100	-1.31701700	-2.13319700
N	-1.47939400	-0.33246800	-0.92677300
C	-3.73176900	0.11043600	-1.66287000
C	-2.43649400	0.68024600	-1.07679400
C	3.19926200	-0.45710100	-0.29130100
C	4.46324000	0.36479900	-0.48944900
N	2.09417200	0.26433300	-0.47811100
C	3.93272800	1.84092400	-0.36010900
C	2.42729900	1.69185500	-0.80457600
C	-2.26507700	1.99700200	-0.65702700
C	-0.96532400	2.48238200	-0.30399100
C	-0.56919700	3.92564100	0.06372900
N	0.09298300	1.66626400	-0.26839700
C	0.96292000	3.89191900	-0.28206200
C	1.33987100	2.43409900	0.01008200
Co	0.32191200	-0.12671800	-0.45059300
H	-4.44605400	-0.02108400	-0.82343200
H	1.03044900	4.05440700	-1.37524200
H	5.17123700	0.18763700	0.34173300
H	1.57145900	2.31261400	1.08424300
C	0.17307500	0.09673200	2.57527400
C	-0.97297900	-0.64535300	3.19166400
H	-0.73445800	-1.71217100	3.40638500
O	-0.69992800	0.25075300	4.25076800
C	-2.36220500	-0.53184600	2.60010300
C	-3.06396400	-1.67377200	2.17037300

C	-3.00710900	0.72084100	2.57067800
C	-4.39713100	-1.57061200	1.73951800
H	-2.56880900	-2.65251200	2.19642600
C	-4.33374000	0.82911300	2.12800100
H	-2.46178800	1.59925200	2.93308000
C	-5.03654100	-0.31902200	1.71833000
H	-4.94528300	-2.47013100	1.43742900
H	-4.82645300	1.80775200	2.11445800
H	-6.07935600	-0.23956900	1.39022100
H	-0.06130900	1.04615800	2.09090100
C	-3.47659600	2.90401500	-0.52945500
H	-3.37321700	3.57112200	0.34108400
H	-3.65038900	3.54524100	-1.41334800
H	-4.39005000	2.31356200	-0.35688300
C	-0.81560100	4.14201700	1.57859400
H	-1.88546300	4.02045600	1.82216200
H	-0.24975500	3.41715700	2.19184100
H	-0.51659000	5.16120400	1.88494600
C	-1.24452900	5.04345500	-0.75624400
H	-2.26689900	5.27069700	-0.41554900
H	-0.65731900	5.97542600	-0.65629900
H	-1.28536900	4.78292600	-1.82922200
C	1.81542800	4.94933500	0.42270200
H	2.84384600	4.95819500	0.02262600
H	1.39671200	5.96128300	0.27171900
H	1.87849100	4.76771800	1.51019500
C	2.21069600	1.90836800	-2.31665100
H	2.43973200	2.94326900	-2.62074900
H	2.84602900	1.22644100	-2.90391400
H	1.15904900	1.68823400	-2.56866800
C	4.73404700	2.85477500	-1.19292400
H	4.30676000	3.86865400	-1.09282100
H	5.77882300	2.89815500	-0.83367300
H	4.76080200	2.60593900	-2.26605400
C	4.06451000	2.22615600	1.13167100
H	5.13235300	2.22092200	1.41822000
H	3.67052600	3.23396400	1.34118800
H	3.54133700	1.50751600	1.78634600
C	5.20136000	-0.02735800	-1.78718600
H	6.11915200	0.57257500	-1.91979800
H	5.49947200	-1.09030800	-1.74055400
H	4.56981600	0.10129800	-2.68242300
C	4.43517200	-2.49404100	0.57174700
H	4.28206600	-3.01470500	1.53245800
H	4.84226700	-3.23115100	-0.14299200
H	5.22245300	-1.74434200	0.74333100
C	2.79980100	-5.03822500	0.28662100
H	3.61033100	-4.95469700	1.02621100
H	2.36232000	-6.04693900	0.40409900
H	3.24337100	-4.97649100	-0.72134300
C	1.33871300	-3.93909100	2.02037200
H	0.48414100	-3.26325900	2.20557700
H	1.06855200	-4.94834900	2.38476300
H	2.19743100	-3.57588100	2.61269700
C	0.65564900	-5.01496400	-1.67079900
H	1.08507600	-6.02550000	-1.55554700
H	-0.29686100	-5.11475500	-2.22073700
H	1.34289500	-4.41178200	-2.29214700
C	-4.42683700	0.93499900	-2.76165400
H	-5.19587700	0.31645700	-3.25993000

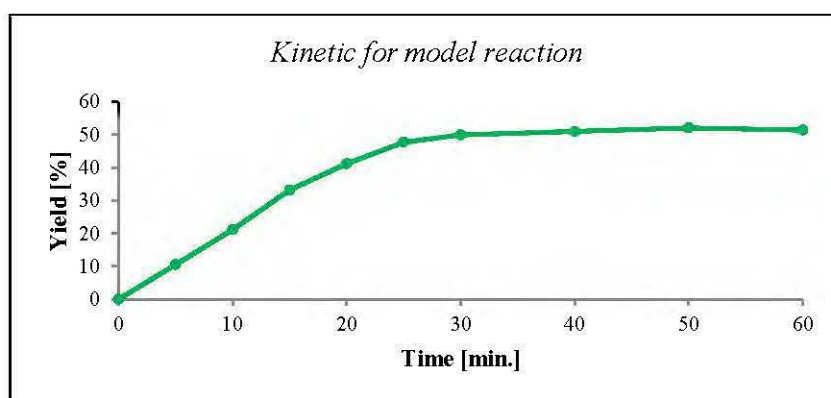
H	-4.93977700	1.82234600	-2.36181500
H	-3.71177400	1.27675200	-3.53000900
C	-4.40723100	-2.36061100	-1.90739200
H	-5.33304900	-2.04954700	-2.42624200
H	-4.11999600	-3.34920600	-2.31000200
H	-4.63249700	-2.47815200	-0.83418800
C	-2.86704500	-1.34706400	-3.62488900
H	-2.42901900	-2.33366600	-3.86028400
H	-3.72439000	-1.18483800	-4.30278300
H	-2.10399700	-0.57640100	-3.83745200
C	1.58184500	-0.29747700	2.86948100
H	1.61275600	-1.09702600	3.62801700
H	2.06713200	-0.67885900	1.95506700
H	2.17675600	0.56109200	3.22869200

6.6 Kinetic studies for model reaction



Reaction conditions: styrene oxide (**5a**) (0.2 mmol), 4-iodotoluene (**6a**) (1.5 equiv.), Zn (1.5 equiv.), NH_4Cl (3 equiv.), B_{12} (**1**) (5mol%), $NiCl_2(DME)$ (20mol%), dtbbpy (40mol%), H_2O (1.1 equiv.), dry NMP (c = 0.1 M), Blue LED (single diode 3 W).

The reaction was setup according to the procedure **A** on 0.4 mmol scale with the addition of dodecane as an internal standard (58 mg). The reaction was monitored by GC/FID for 16 h.



Conclusion: This experiment suggests that optimal time for this reaction is only 30 minutes.

6.7 Reactions with deuterated solvents

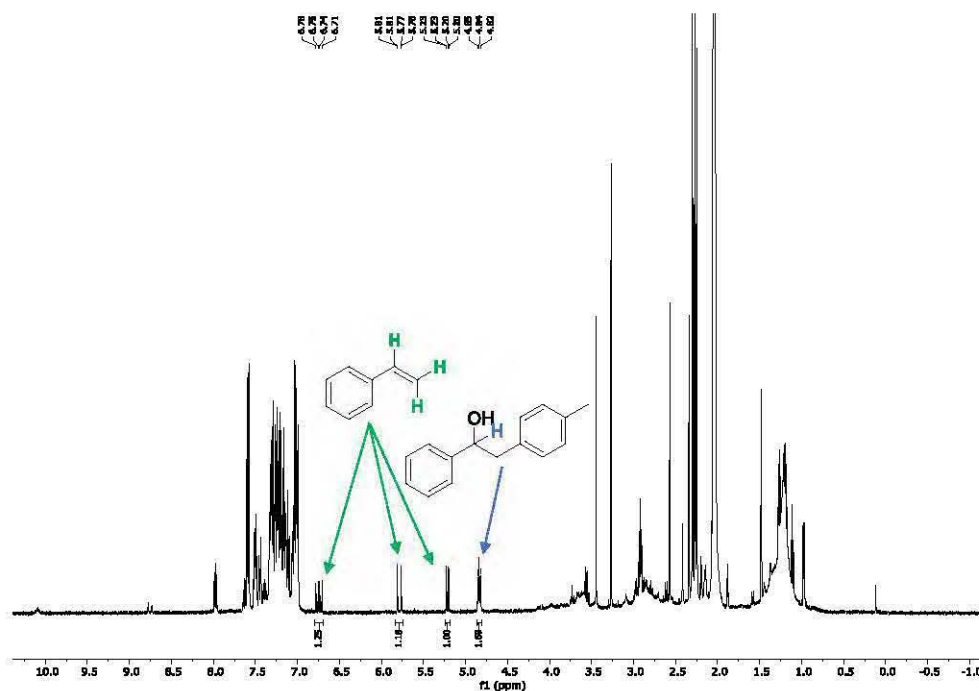
Side-products by reaction with aryl epoxide



Reaction conditions: styrene oxide (**5a**) (0.2 mmol), 4-iodotoluene (**6a**) (1.5 equiv.), Zn (1.5 equiv.), NH_4Cl (3 equiv.), HME (**3**) (5mol%), $NiCl_2(DME)$ (20mol%), dtbbpy (40 mol%), acetone- d_6 , Blue LED (single diode, 3 W), 16 h.

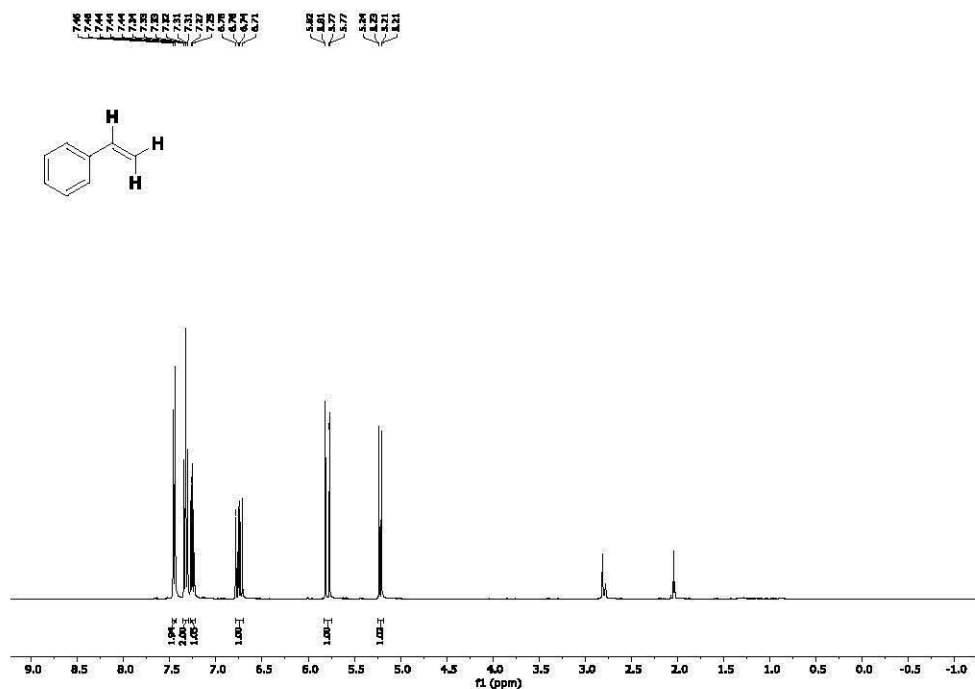
The reaction was setup according to the procedure **D** (acetone was replacement on acetone- d_6). After 16 h a small portion was taken from the reaction mixture and 1H NMR spectrum was recorded. This experiment enabled identification of side-products formed.

^1H NMR of the crude reaction mixture:

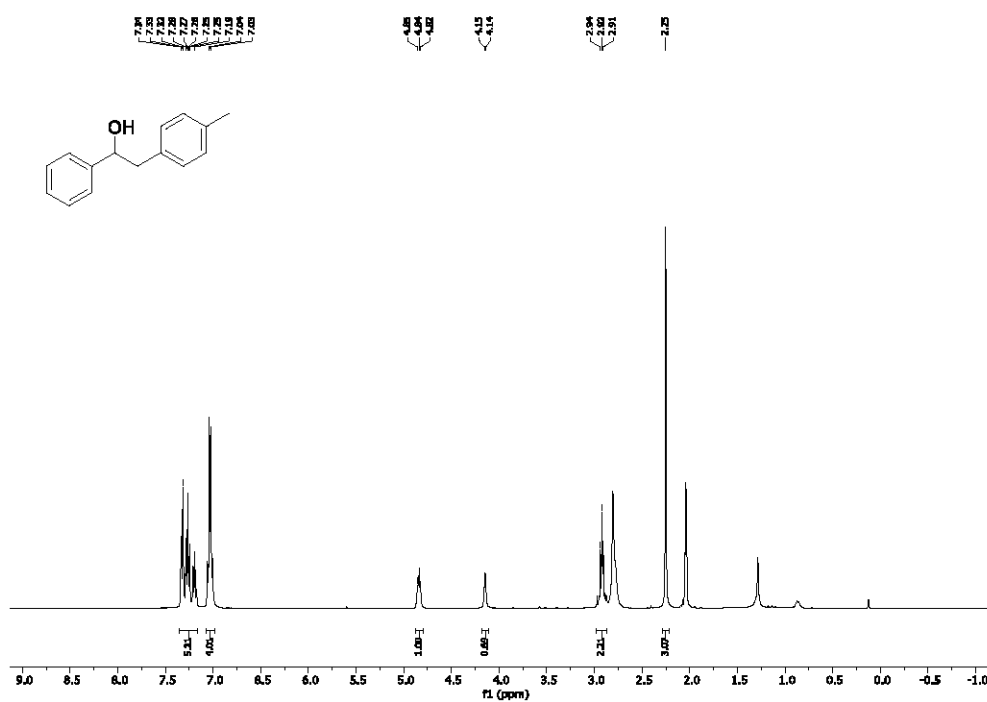


We compared the obtained ^1H NMR spectrum with spectra measured for the samples of the original styrene and product in the same deuterated solvent.

^1H NMR spectrum of styrene (solvent: acetone- d_6):



^1H NMR spectrum of product (7aa) (solvent: acetone- d_6):



Conclusion: Based on ^1H NMR spectrum, the major side-product is styrene. The ratio between product and styrene is 1:0.6.

7. References

- (1) HISANO, T.; TASAKI, M.; TSUMOTO, K.; MATSUOKA, T.; ICHIKAWA, M. Synthesis and Antiinflammatory Activity of N1-(Substituted Phenyl)Pyridinecarboxamidines. *Chem. Pharm. Bull. (Tokyo)*. **1983**, *31* (7), 2484–2490. <https://doi.org/10.1248/cpb.31.2484>.
- (2) Chen, G.; Shigenari, T.; Jain, P.; Zhang, Z.; Jin, Z.; He, J.; Li, S.; Mapelli, C.; Miller, M. M.; Poss, M. A.; Scola, P. M.; Yeung, K.-S.; Yu, J.-Q. Ligand-Enabled β -C–H Arylation of α -Amino Acids Using a Simple and Practical Auxiliary. *J. Am. Chem. Soc.* **2015**, *137* (9), 3338–3351. <https://doi.org/10.1021/ja512690x>.
- (3) Ma, X.; Pan, S.; Wang, H.; Chen, W. Rhodium-Catalyzed Transannulation of N-Sulfonyl-1,2,3-Triazoles and Epoxides: Regioselective Synthesis of Substituted 3,4-Dihydro-2 H-1,4-Oxazines. *Org. Lett.* **2014**, *16* (17), 4554–4557. <https://doi.org/10.1021/ol5021042>.
- (4) Li, S.; Shi, Y.; Li, P.; Xu, J. Nucleophilic Organic Base DABCO-Mediated Chemospecific Meinwald Rearrangement of Terminal Epoxides into Methyl Ketones. *J. Org. Chem.* **2019**, *84* (7), 4443–4450. <https://doi.org/10.1021/acs.joc.8b03171>.
- (5) Lopchuk, J. M.; Fjelbye, K.; Kawamata, Y.; Malins, L. R.; Pan, C.-M.; Gianatassio, R.; Wang, J.; Prieto, L.; Bradow, J.; Brandt, T. A.; Collins, M. R.; Elleraas, J.; Ewanicki, J.; Farrell, W.; Fadeyi, O. O.; Gallego, G. M.; Mousseau, J. J.; Oliver, R.; Sach, N. W.; Smith, J. K.; Spangler, J. E.; Zhu, H.; Zhu, J.; Baran, P. S. Strain-Release Heteroatom Functionalization: Development, Scope, and Stereospecificity. *J. Am. Chem. Soc.* **2017**, *139* (8), 3209–3226. <https://doi.org/10.1021/jacs.6b13229>.
- (6) Weijers, C. A. G. M.; Könst, P. M.; Franssen, M. C. R.; Sudhölter, E. J. R. Stereochemical Preference of Yeast Epoxide Hydrolase for the O-Axial C3 Epimers of 1-Oxaspiro[2.5]Octanes, 2007, Vol. 5. <https://doi.org/10.1039/b709742e>.
- (7) Steiman, T. J.; Liu, J.; Mengiste, A.; Doyle, A. G. Synthesis of β -Phenethylamines via Ni/Photoredox Cross-Electrophile Coupling of Aliphatic Aziridines and Aryl Iodides. *J. Am. Chem. Soc.* **2020**, *142* (16), 7598–7605. <https://doi.org/10.1021/jacs.0c01724>.
- (8) Singh, A.; Anandhi, U.; Cinellu, M. A.; Sharp, P. R. Diimine Supported Group 10 Hydroxo, Oxo, Amido, and Imido Complexes. *Dalt. Trans.* **2008**, No. 17, 2314–2327. <https://doi.org/10.1039/b715663d>.
- (9) Ociepa, M.; Wierzba, A. J.; Turkowska, J.; Gryko, D. Polarity-Reversal Strategy for the Functionalization of Electrophilic Strained Molecules via Light-Driven Cobalt Catalysis. *J. Am. Chem. Soc.* **2020**, *142* (11), 5355–5361. <https://doi.org/10.1021/jacs.0c00245>.
- (10) Weiss, M. E.; Kreis, L. M.; Lauber, A.; Carreira, E. M. Cobalt-Catalyzed Coupling of Alkyl Iodides with Alkenes: Deprotonation of Hydridocobalt Enables Turnover. *Angew. Chemie Int. Ed.* **2011**, *50* (47), 11125–11128. <https://doi.org/10.1002/anie.201105235>.
- (11) Nielsen, D. K.; Doyle, A. G. Nickel-Catalyzed Cross-Coupling of Styrenyl Epoxides with

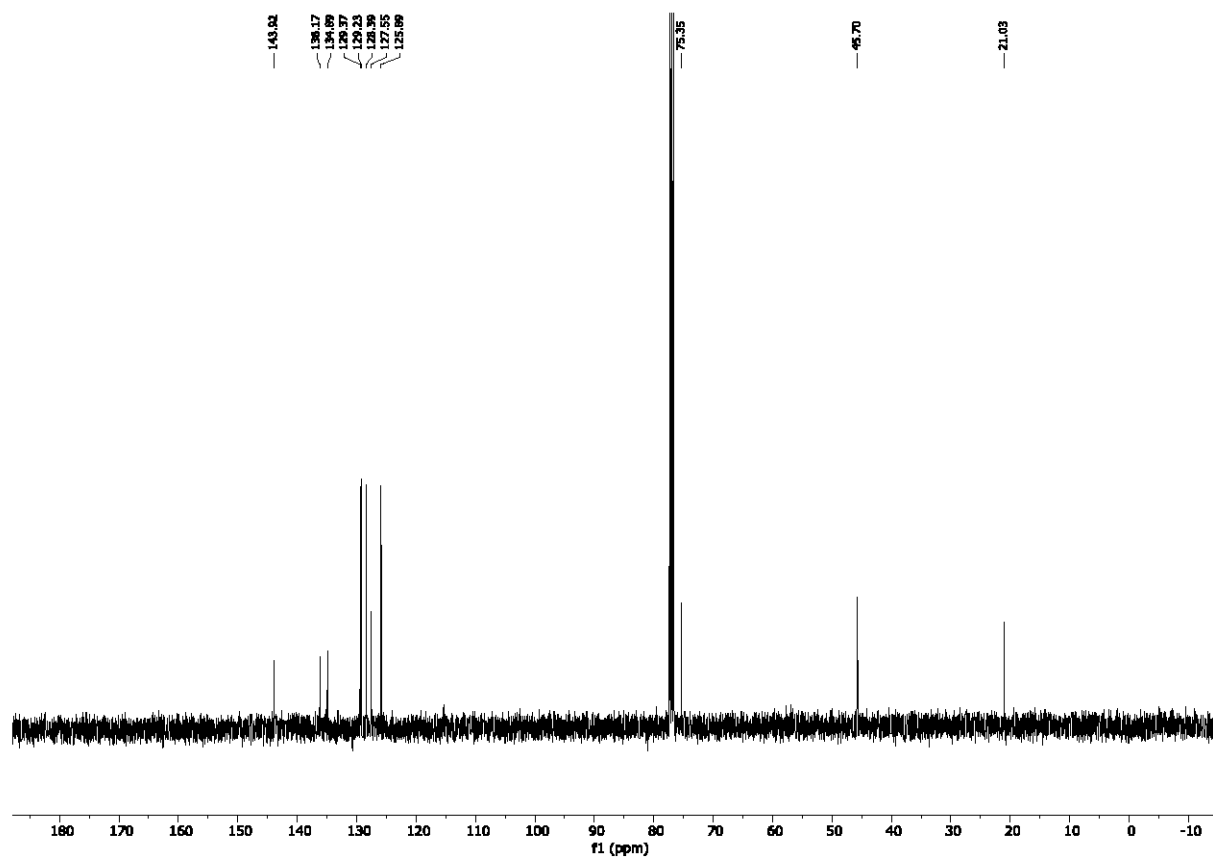
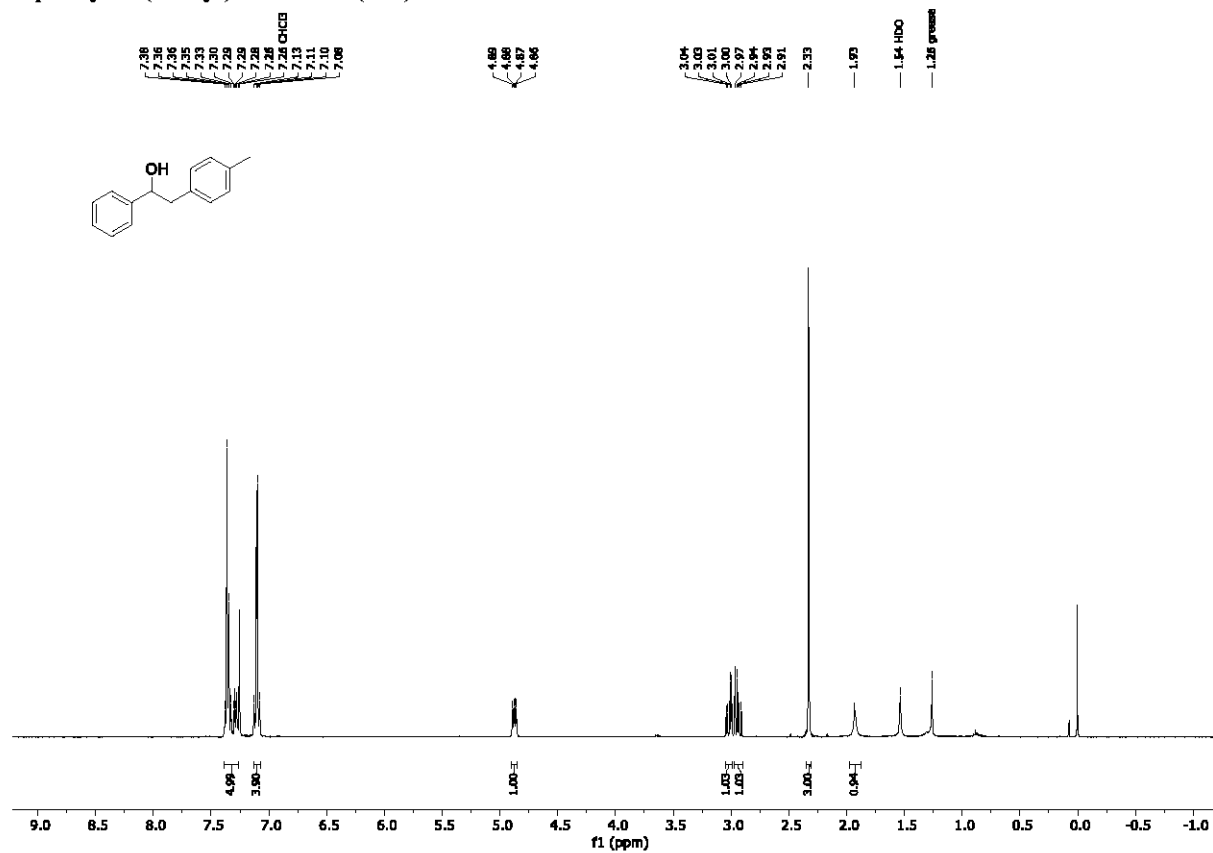
- Boronic Acids. *Angew. Chemie Int. Ed.* **2011**, *50* (27), 6056–6059.
<https://doi.org/10.1002/anie.201101191>.
- (12) Taniguchi, T.; Zaimoku, H.; Ishibashi, H. A Mild Oxidative Aryl Radical Addition into Alkenes by Aerobic Oxidation of Arylhydrazines. *Chem. - A Eur. J.* **2011**, *17* (15), 4307–4312.
<https://doi.org/10.1002/chem.201003060>.
- (13) Suh, Y.; Lee, J.; Kim, S.-H.; Rieke, R. D. Direct Preparation of Benzylic Manganese Reagents from Benzyl Halides, Sulfonates, and Phosphates and Their Reactions: Applications in Organic Synthesis. *J. Organomet. Chem.* **2003**, *684* (1–2), 20–36. [https://doi.org/10.1016/S0022-328X\(03\)00500-X](https://doi.org/10.1016/S0022-328X(03)00500-X).
- (14) Wang, J.; Xue, L.; Hong, M.; Ni, B.; Niu, T. Heterogeneous Visible-Light-Induced Meerwein Hydration Reaction of Alkenes in Water Using Mpg-C₃N₄ as a Recyclable Photocatalyst. *Green Chem.* **2020**, *22* (2), 411–416. <https://doi.org/10.1039/C9GC03679B>.
- (15) Zhao, Y.; Weix, D. J. Nickel-Catalyzed Regiodivergent Opening of Epoxides with Aryl Halides: Co-Catalysis Controls Regioselectivity. *J. Am. Chem. Soc.* **2014**, *136* (1), 48–51.
<https://doi.org/10.1021/ja410704d>.
- (16) Harada, T.; Kaneko, T.; Fujiwara, T.; Oku, A. A Novel 1,2-Migration of Arylzincates Bearing a Leaving Group at Benzylic Position: Application to a Three-Component Coupling of p-Iodobenzyl Derivatives, Trialkylzincates, and Electrophiles Leading to Functionalized p-Substituted Benzenes. *Tetrahedron* **1998**, *54* (32), 9317–9332. [https://doi.org/10.1016/S0040-4020\(98\)00569-9](https://doi.org/10.1016/S0040-4020(98)00569-9).
- (17) Parasram, M.; Shields, B. J.; Ahmad, O.; Knauber, T.; Doyle, A. G. Regioselective Cross-Electrophile Coupling of Epoxides and (Hetero)Aryl Iodides via Ni/Ti/Photoredox Catalysis. *ACS Catal.* **2020**, *10* (10), 5821–5827. <https://doi.org/10.1021/acscatal.0c01199>.
- (18) Li, C.; Kan, J.; Qiu, Z.; Li, J.; Lv, L.; Li, C. Synergistic Relay Reactions To Achieve Redox-Neutral α -Alkylations of Olefinic Alcohols with Ruthenium(II) Catalysis. *Angew. Chemie Int. Ed.* **2020**, *59* (11), 4544–4549. <https://doi.org/10.1002/anie.201915218>.
- (19) Woods, B. P.; Orlandi, M.; Huang, C.-Y.; Sigman, M. S.; Doyle, A. G. Nickel-Catalyzed Enantioselective Reductive Cross-Coupling of Styrenyl Aziridines. *J. Am. Chem. Soc.* **2017**, *139* (16), 5688–5691. <https://doi.org/10.1021/jacs.7b03448>.
- (20) Guo, J.; Wu, Q. L.; Xie, Y.; Weng, J.; Lu, G. Visible-Light-Mediated Decarboxylative Benzoylation of Imines with Arylacetic Acids. *J. Org. Chem.* **2018**, *83* (20), 12559–12567.
<https://doi.org/10.1021/acs.joc.8b01849>.
- (21) Grimme, S.; Antony, J.; Ehrlich, S.; Krieg, H. A Consistent and Accurate Ab Initio Parametrization of Density Functional Dispersion Correction (DFT-D) for the 94 Elements H–Pu. *J. Chem. Phys.* **2010**, *132* (15). <https://doi.org/10.1063/1.3382344>.
- (22) Marenich, A. V.; Cramer, C. J.; Truhlar, D. G. Universal Solvation Model Based on Solute Electron Density and on a Continuum Model of the Solvent Defined by the Bulk Dielectric

Constant and Atomic Surface Tensions. *J. Phys. Chem. B* **2009**, *113* (18), 6378–6396.
<https://doi.org/10.1021/jp810292n>.

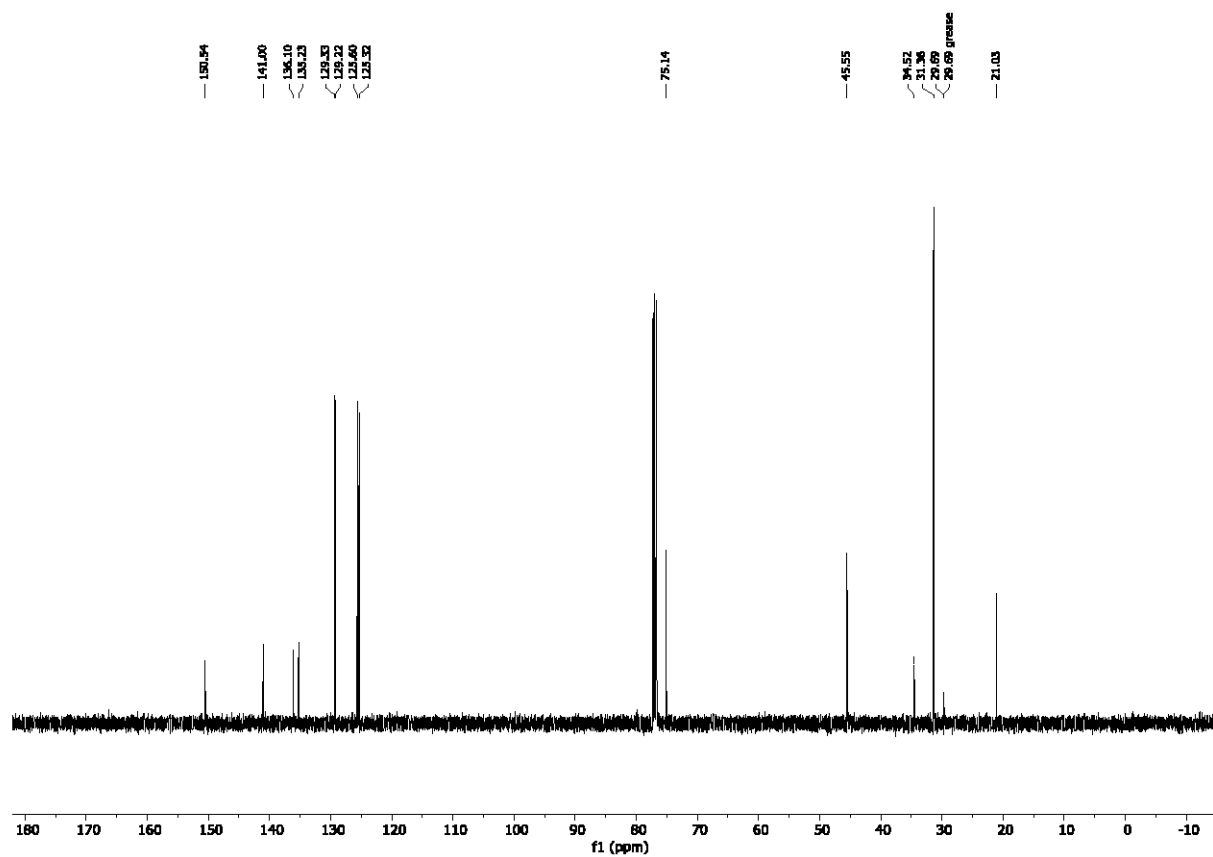
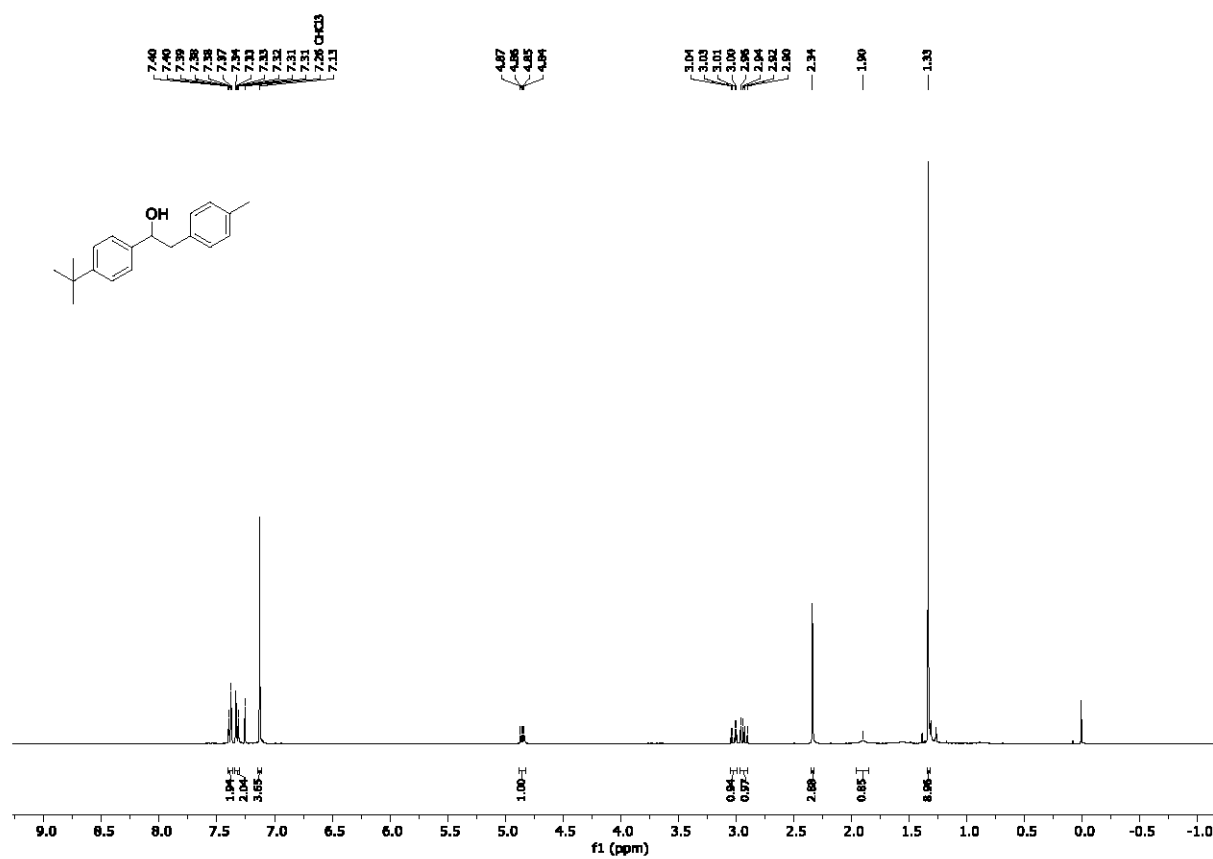
(23) Legault, C. Y., CYLview, 1.0b; Université de Sherbrooke, 2009, <http://www.cylview.org>.

6. NMR Spectra

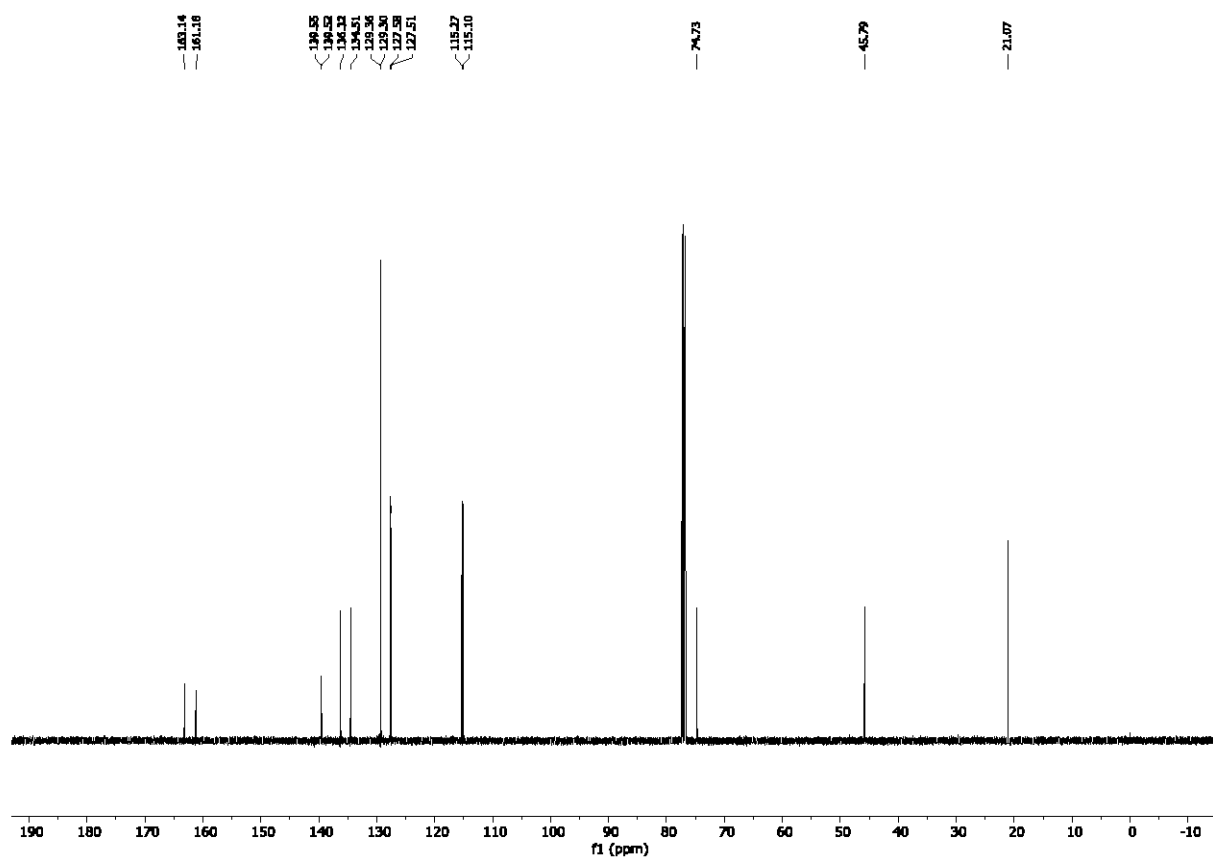
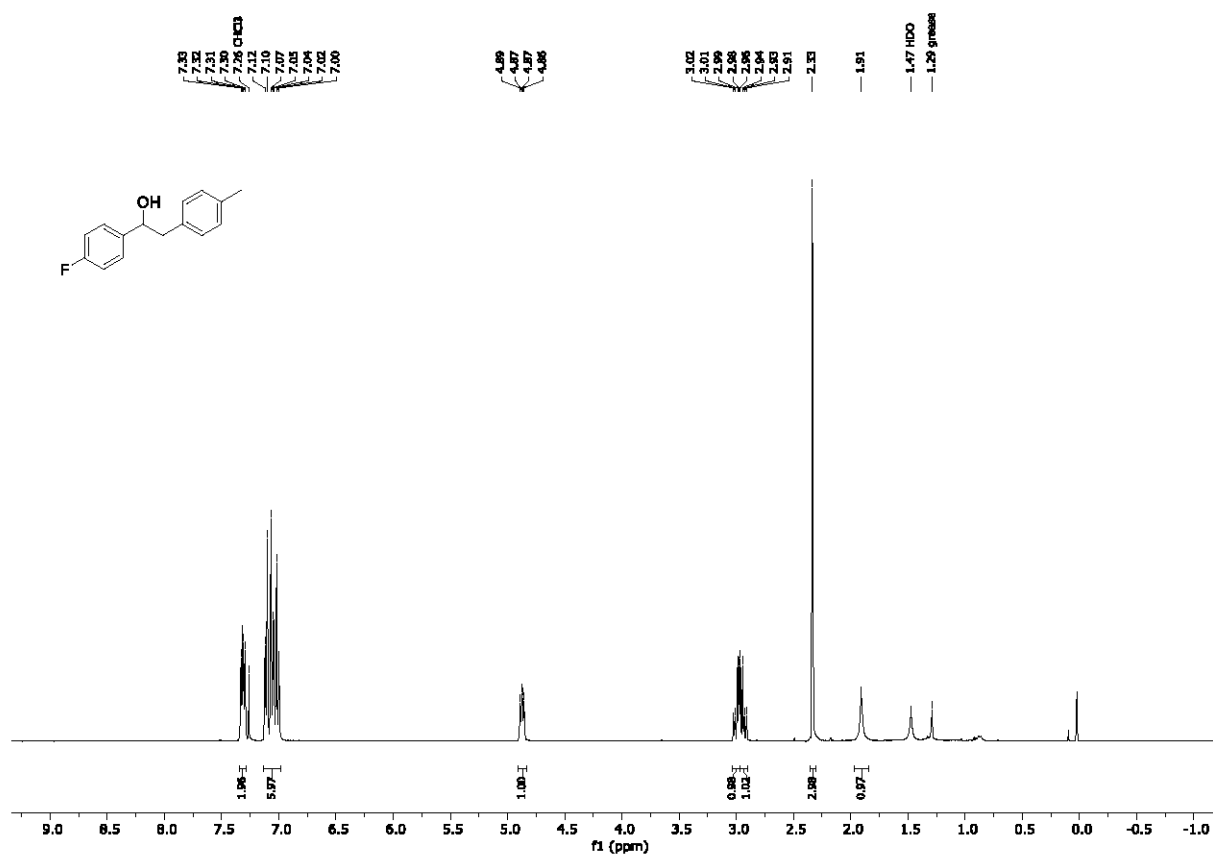
1-phenyl-2-(4-tolyl)ethan-1-ol (7aa)

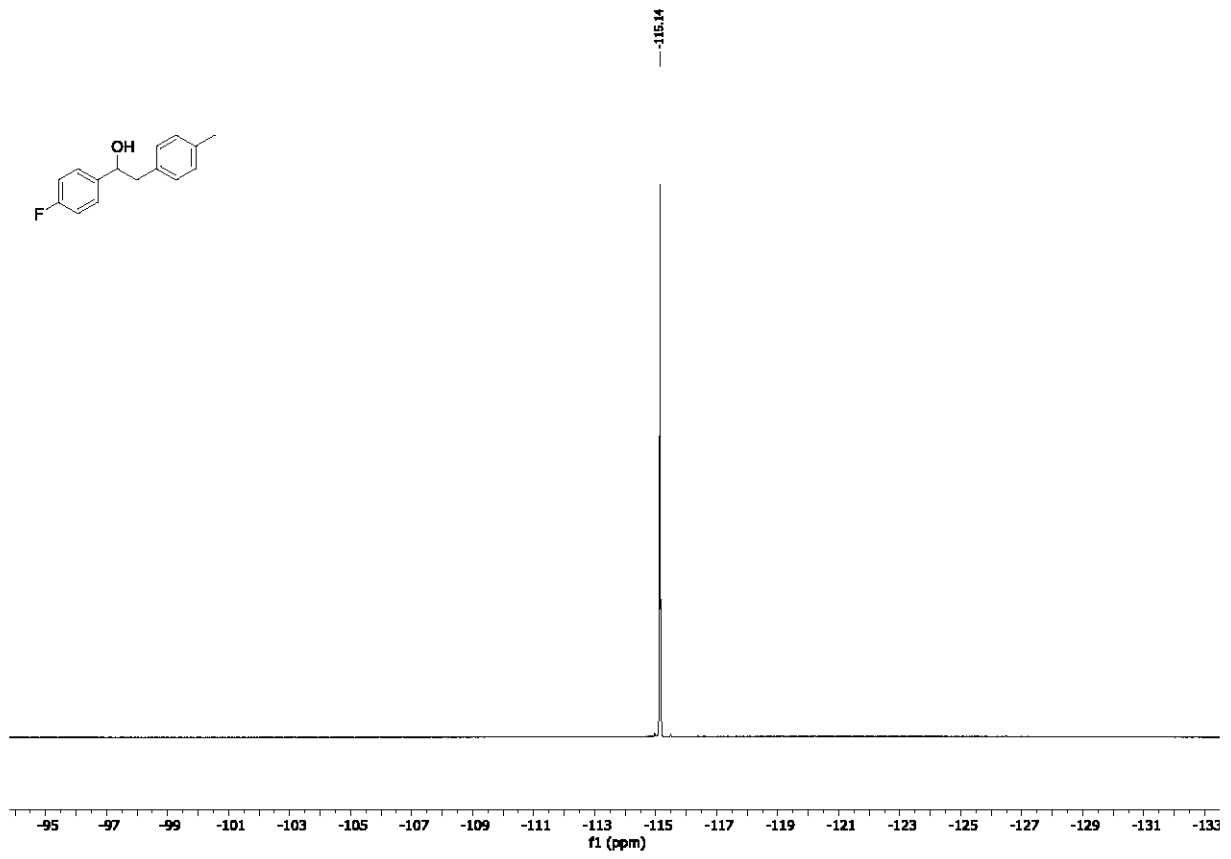


1-(4-(*tert*-butyl)phenyl)-2-(4-tolyl)ethan-1-ol (7ba)

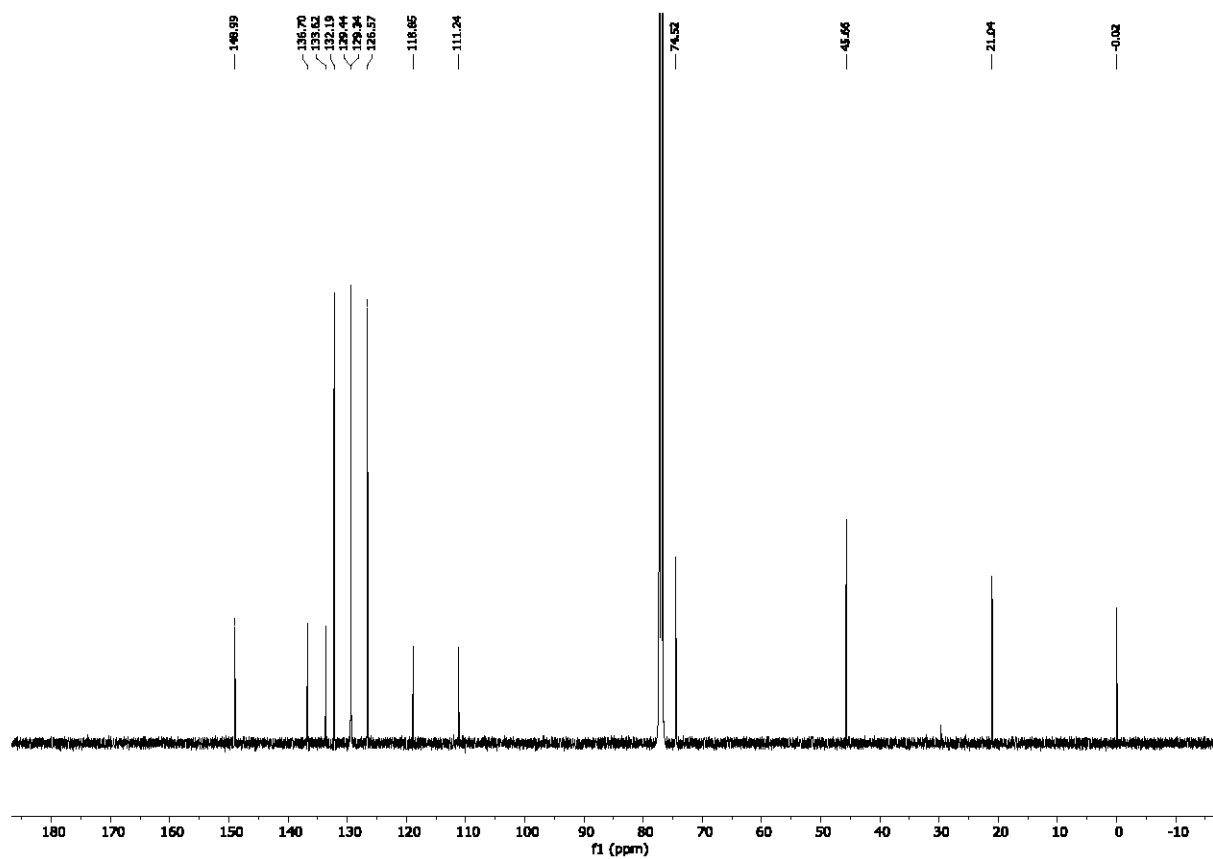
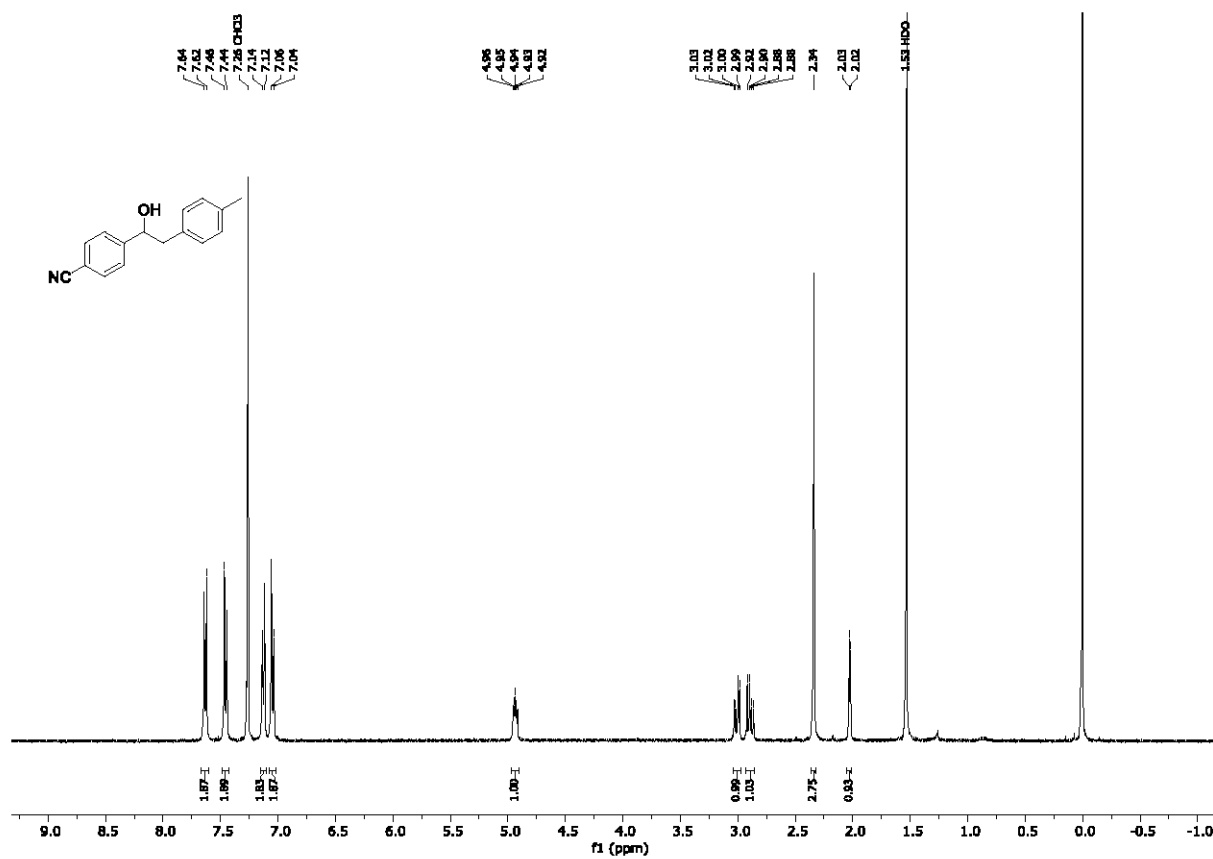


1-(4-fluorophenyl)-2-(4-tolyl)ethan-1-ol (7ca)

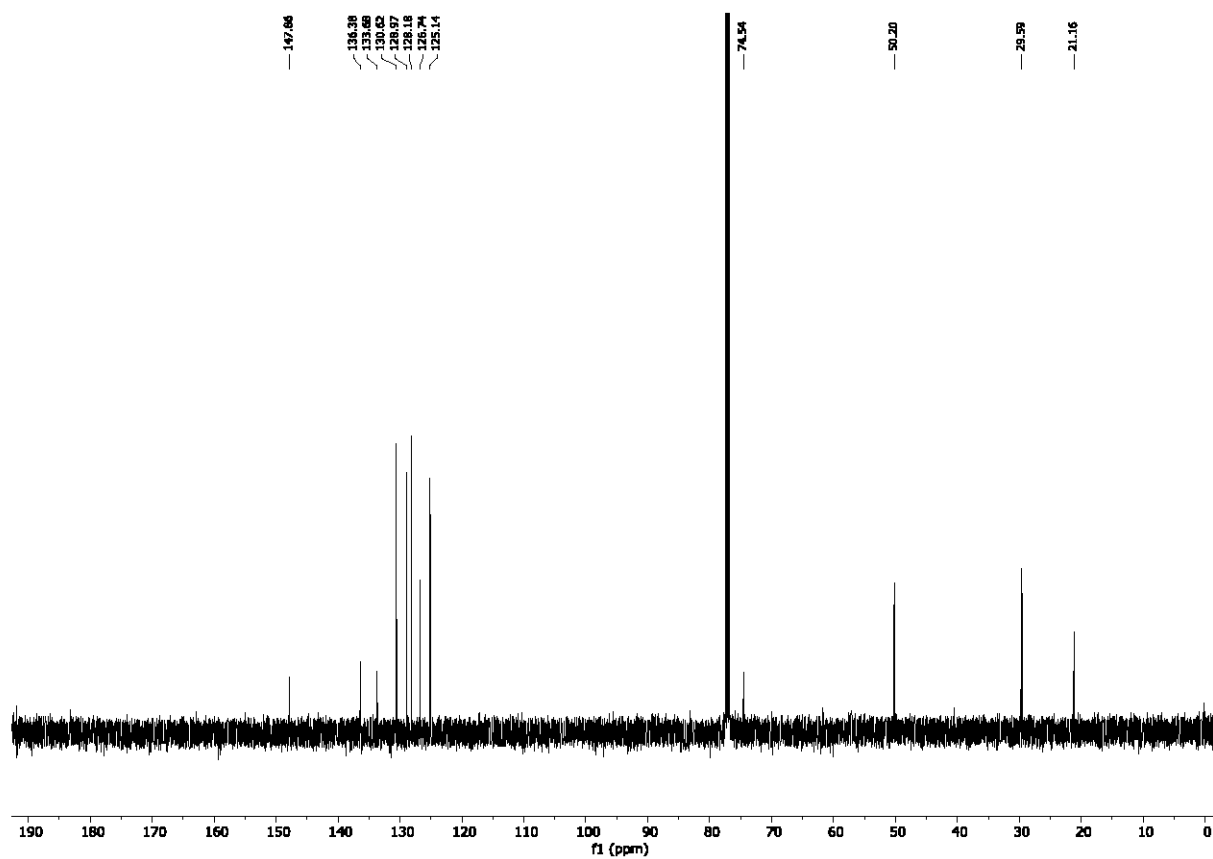
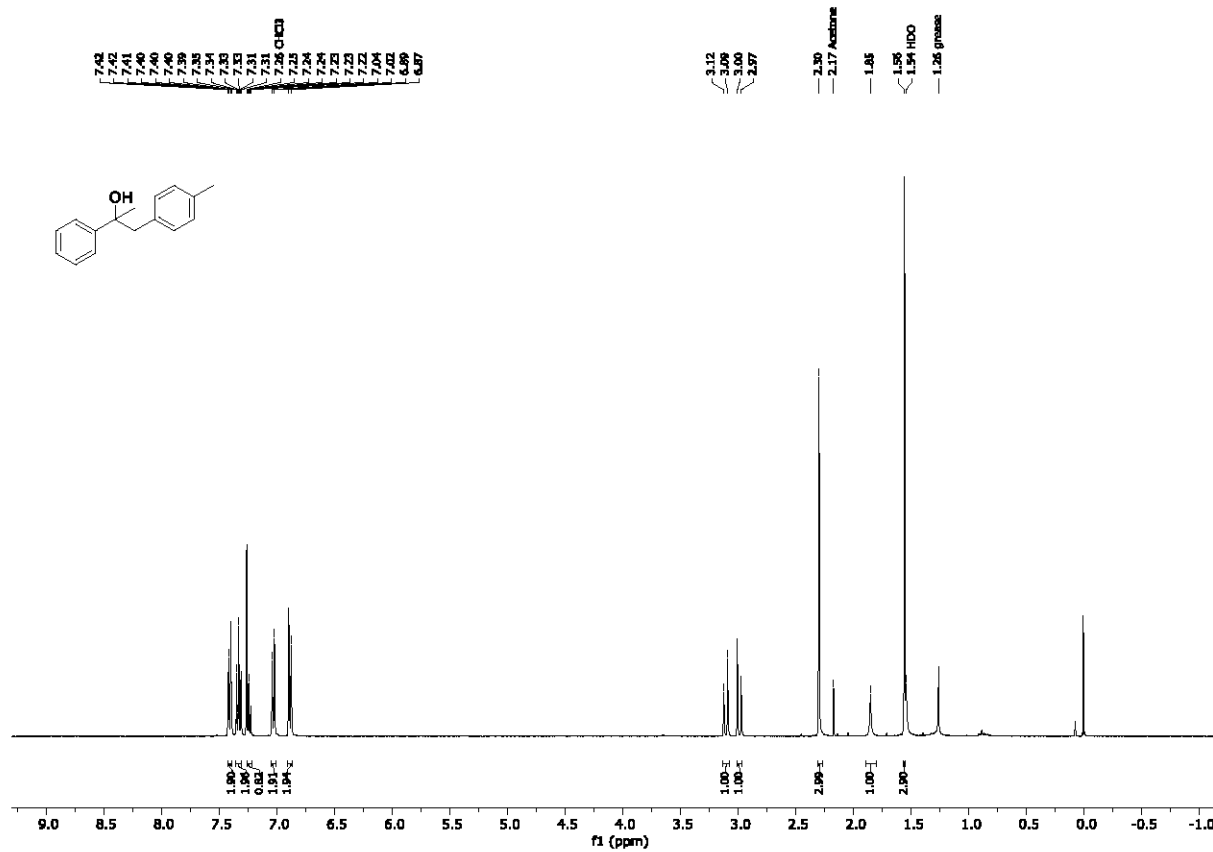




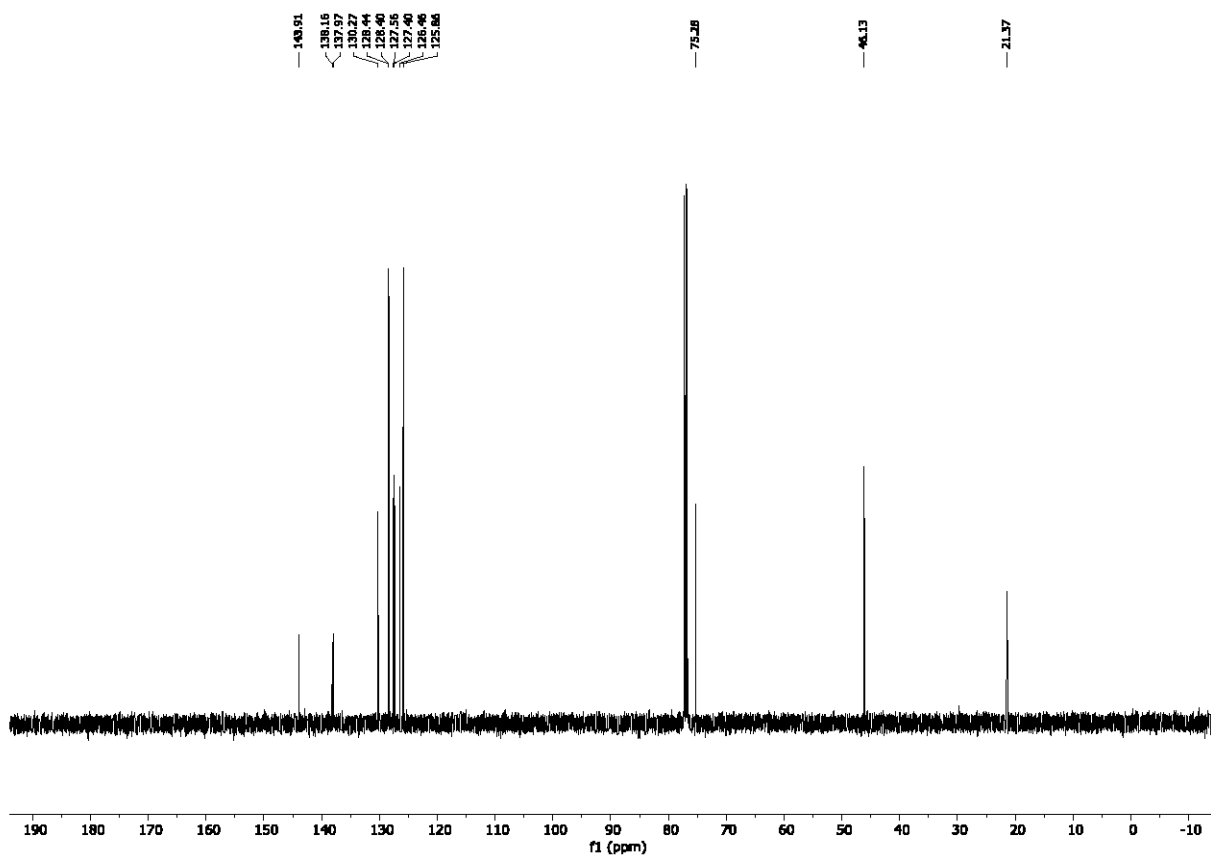
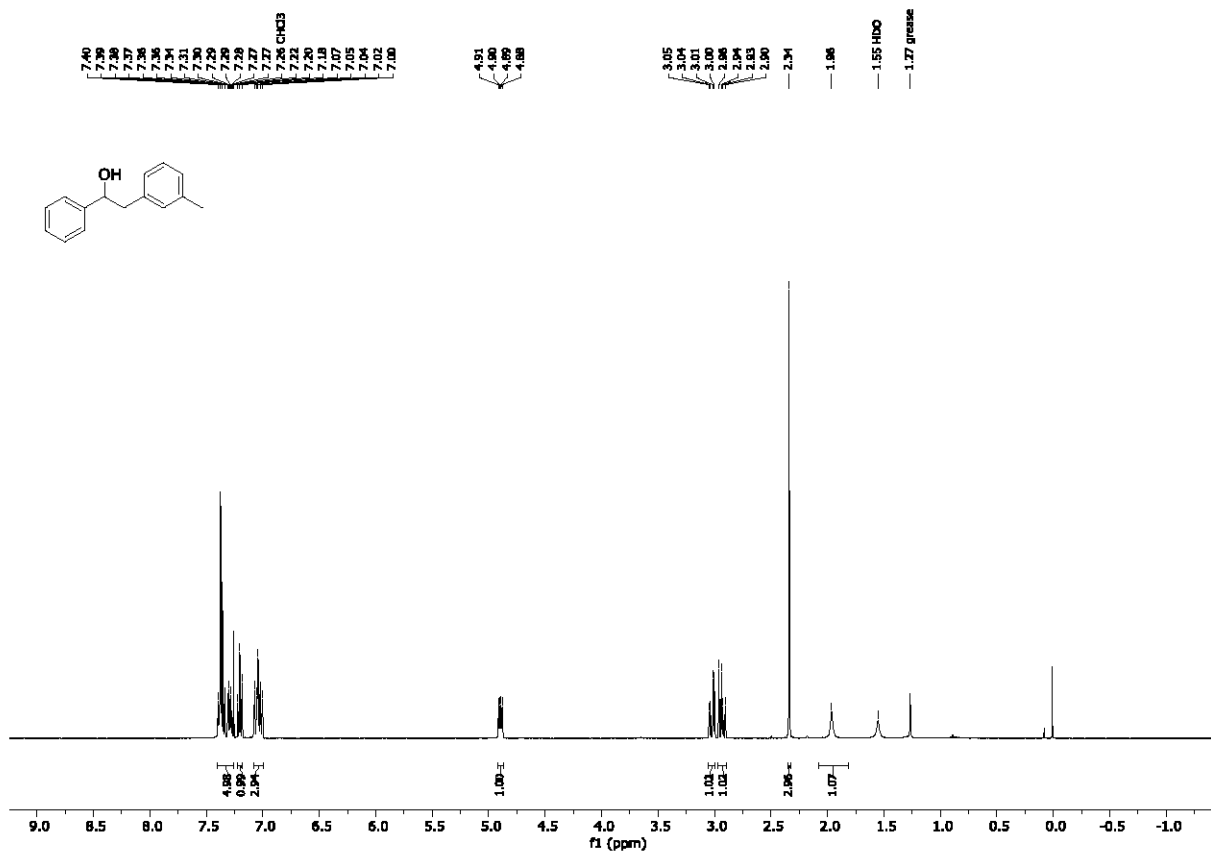
4-(1-hydroxy-2-(4-tolyl)ethyl)benzotrile (7da)



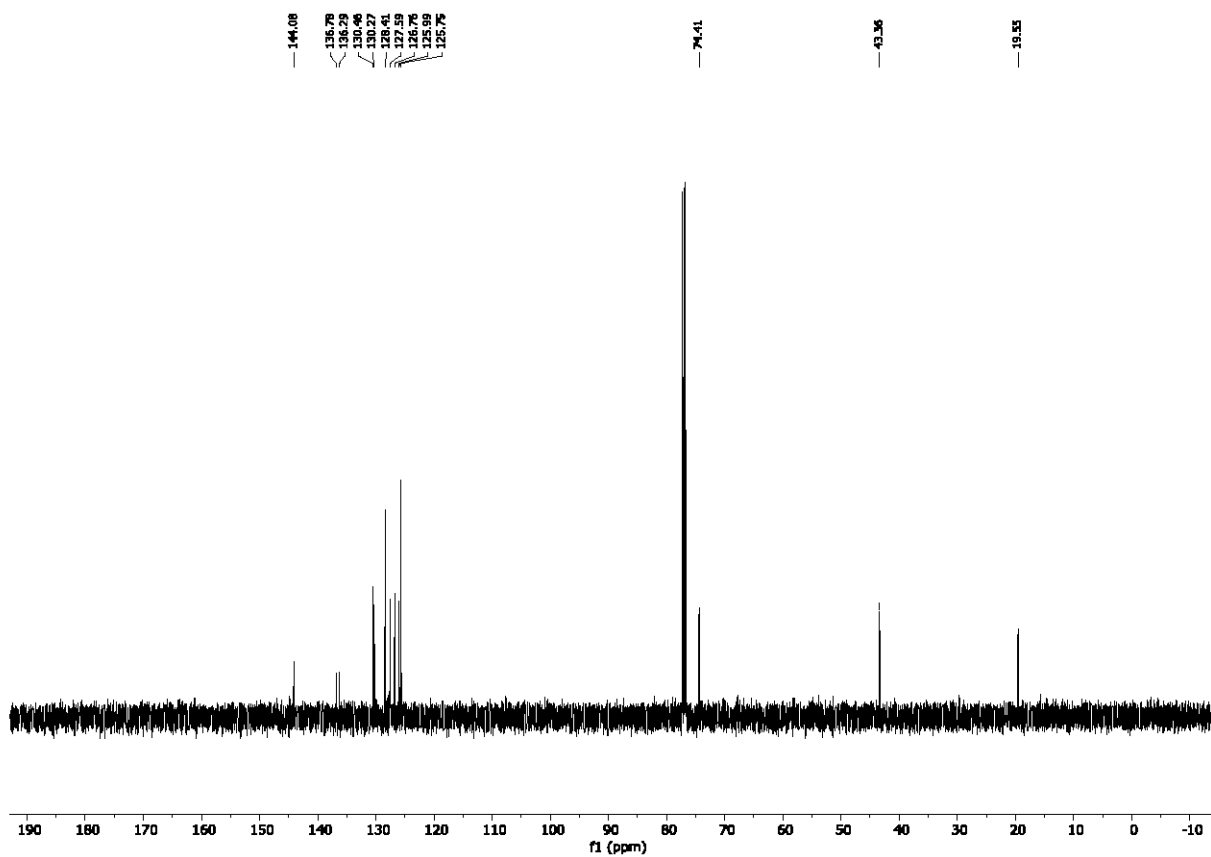
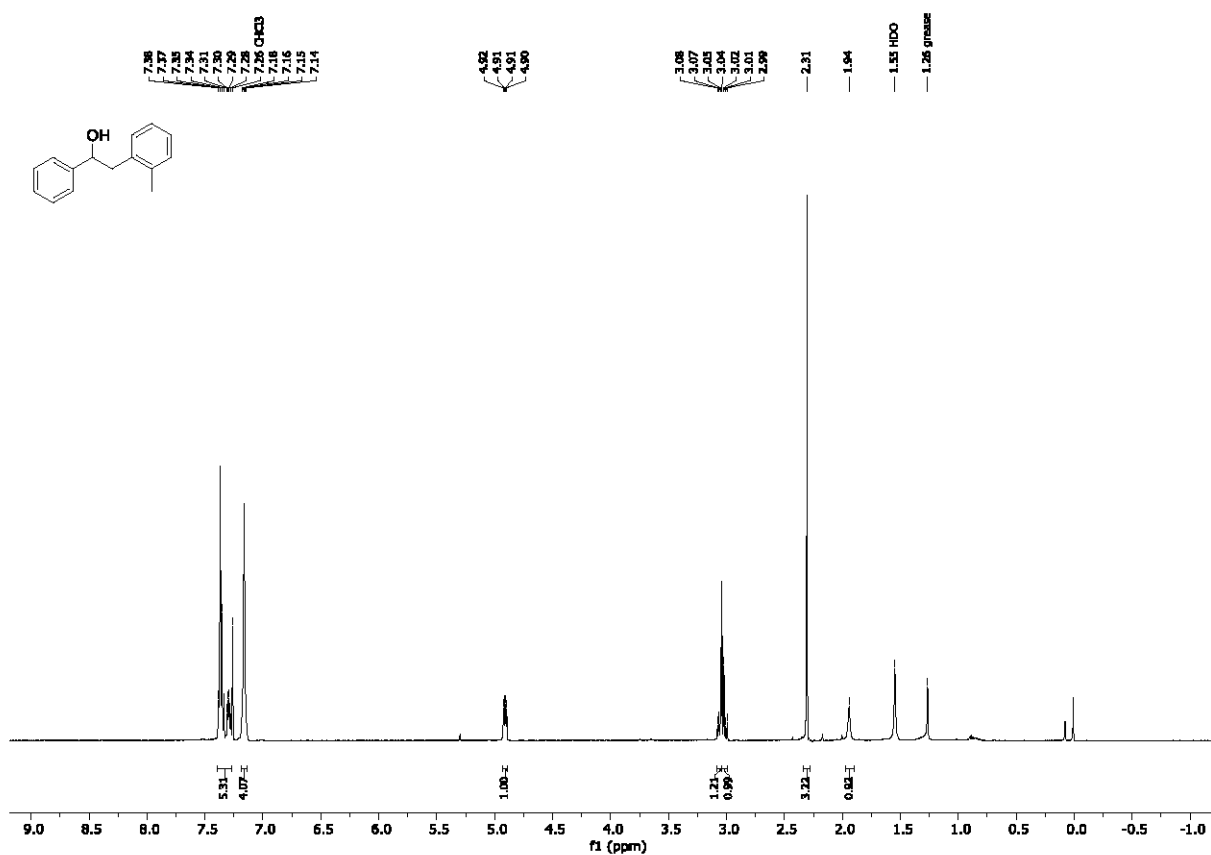
2-phenyl-1-(4-tolyl)propan-2-ol (7fa)



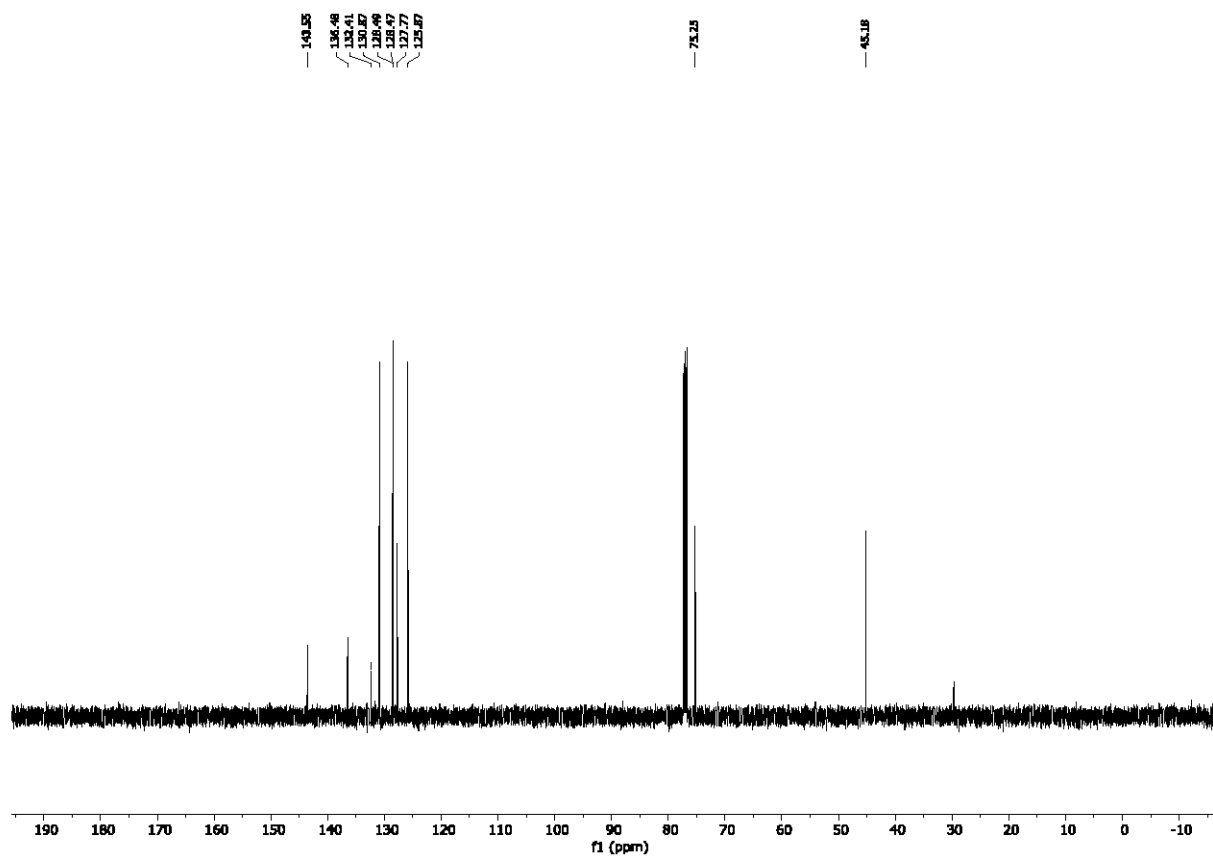
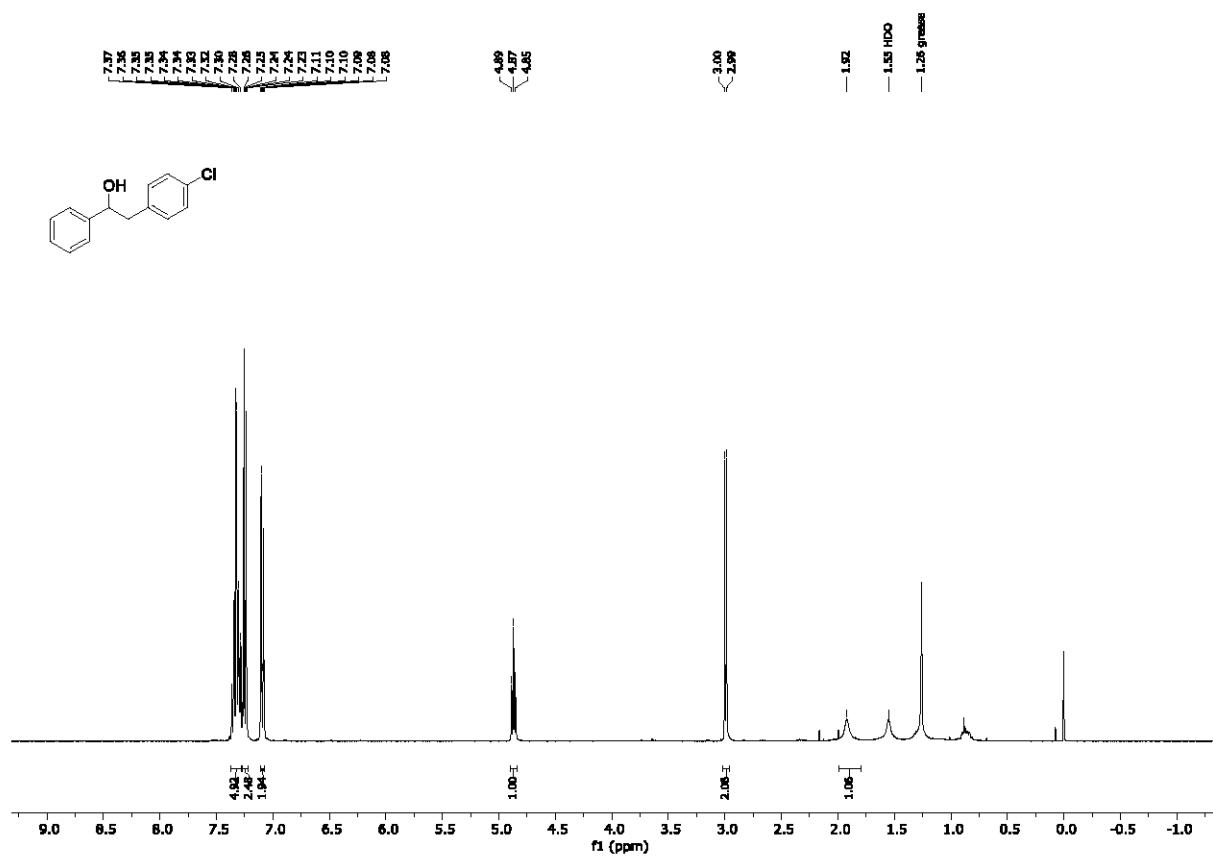
1-phenyl-2-(3-tolyl)ethan-1-ol (7ab)



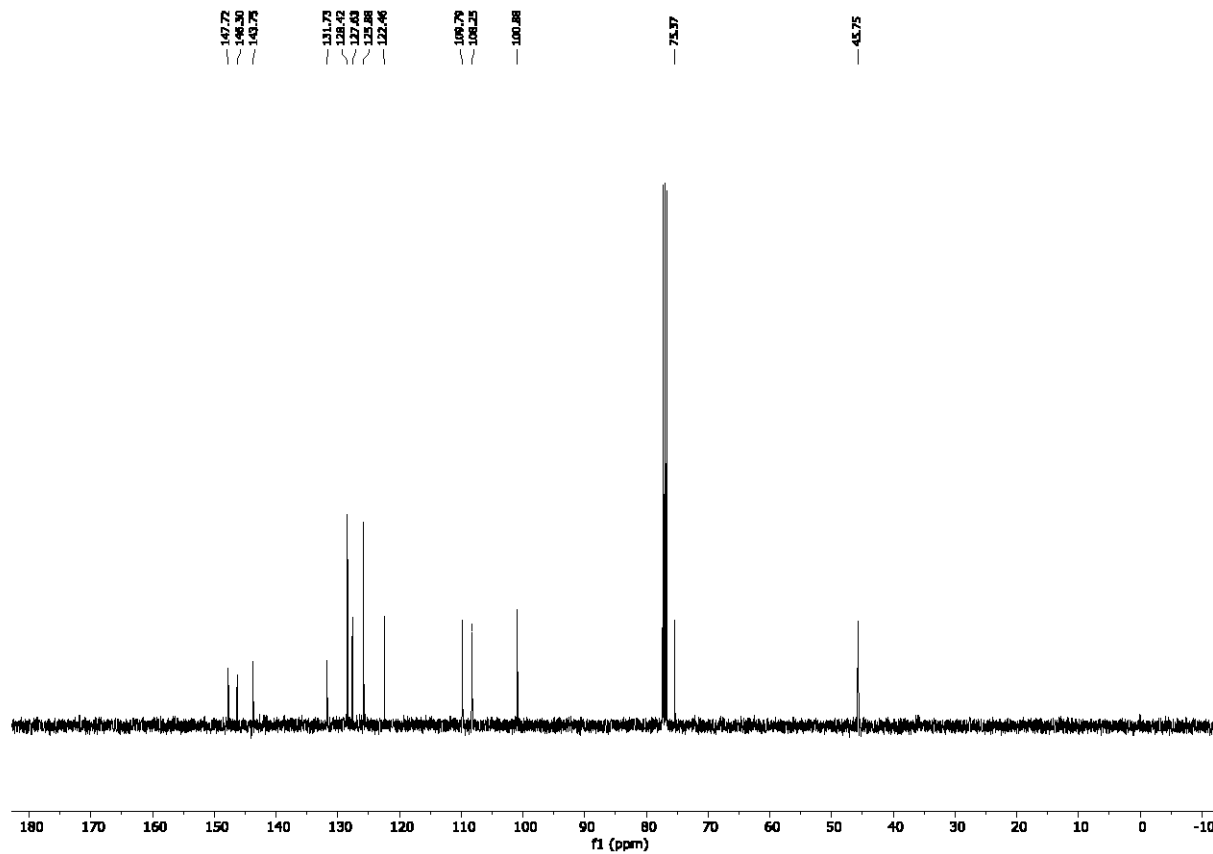
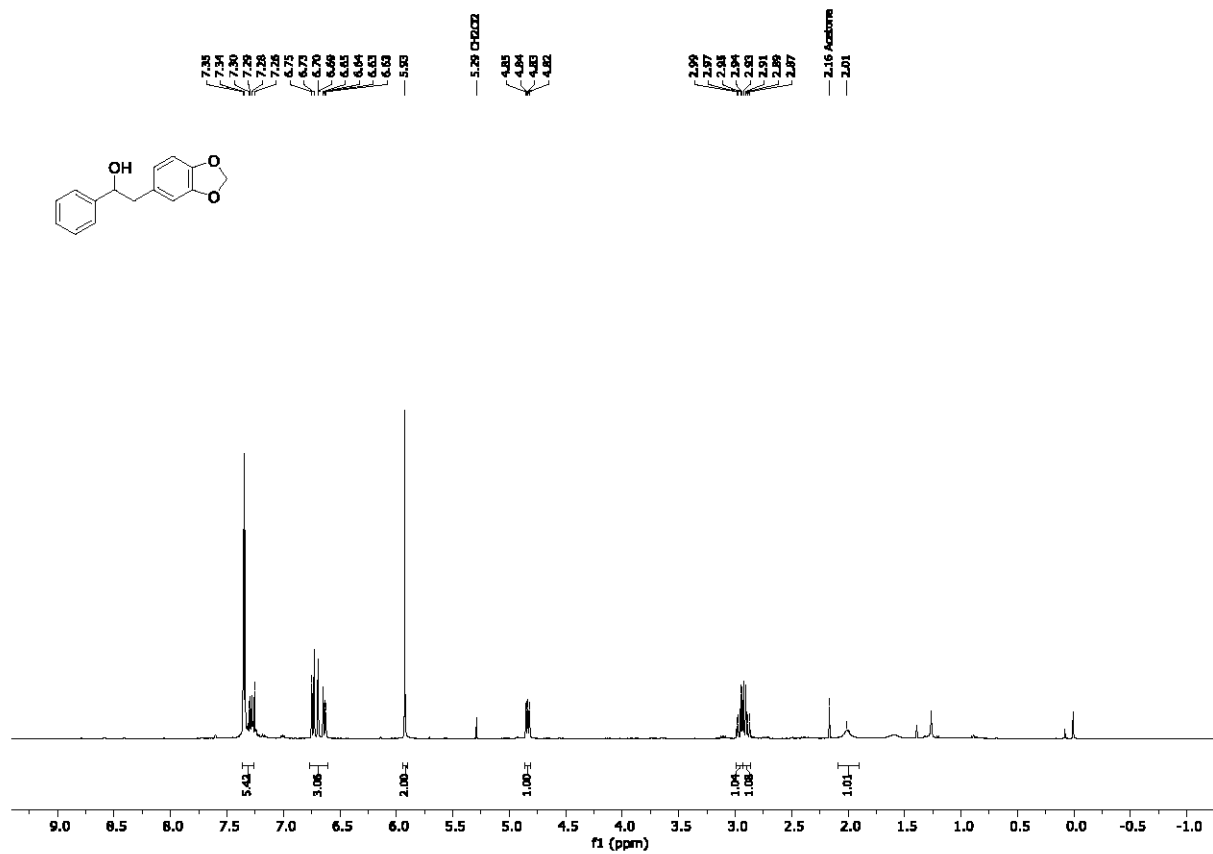
1-phenyl-2-(2-tolyl)ethan-1-ol (7ac)



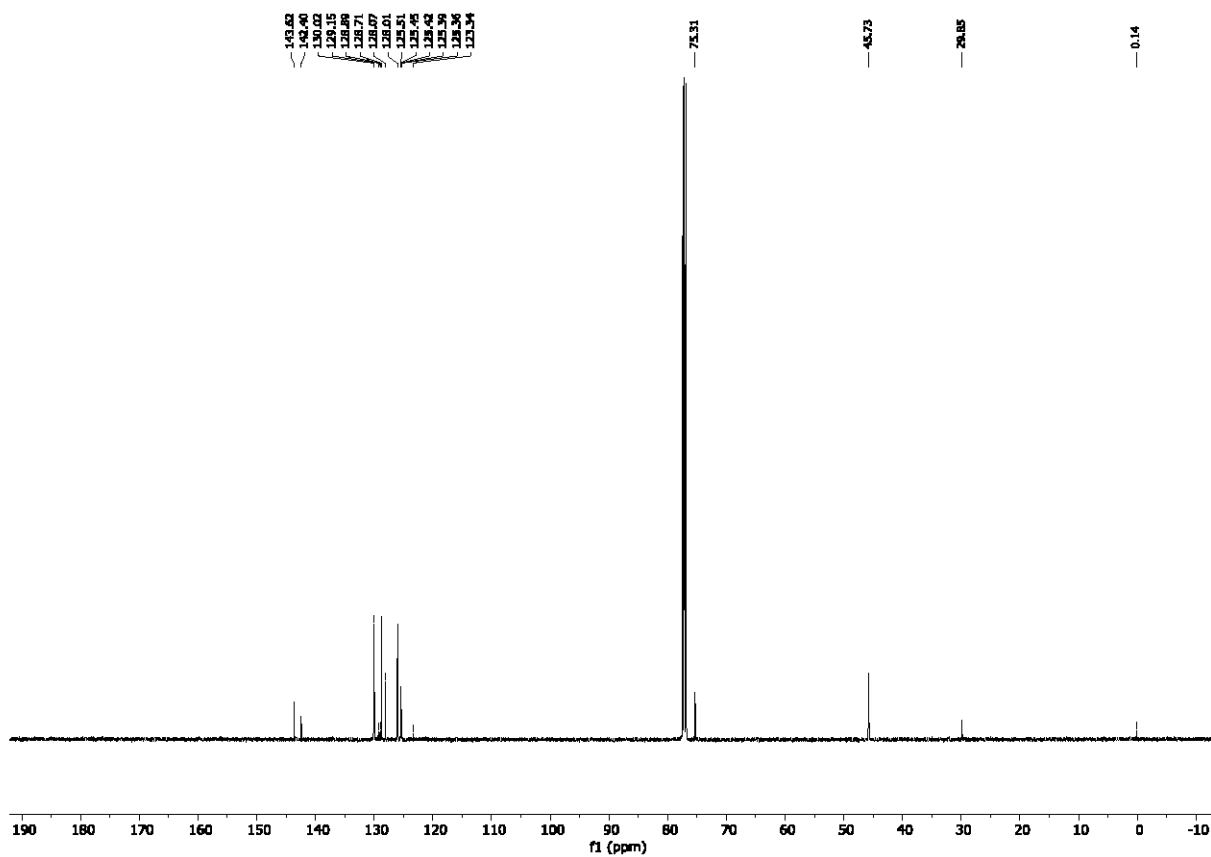
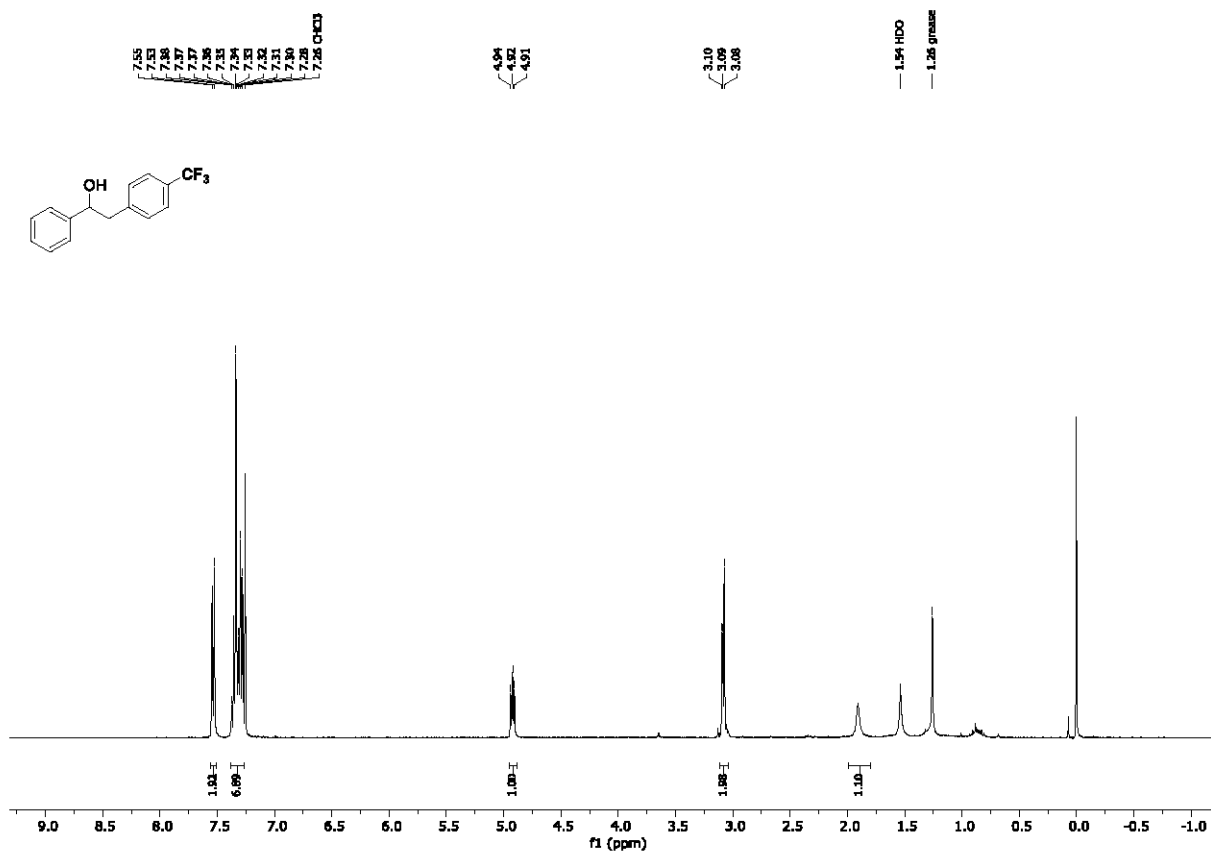
2-(4-chlorophenyl)-1-phenylethan-1-ol (7ad)

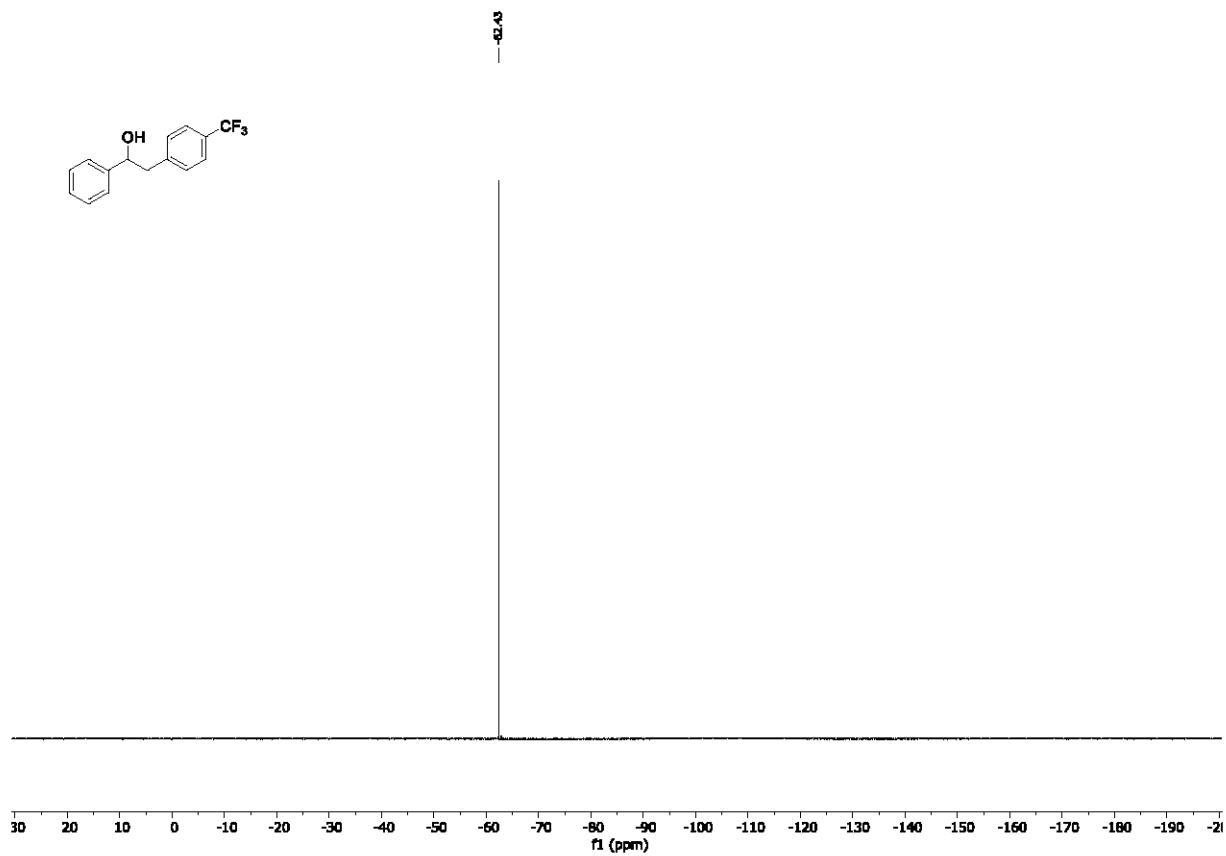


2-(benzo[d][1,3]dioxol-5-yl)-1-phenylethan-1-ol (7ae)

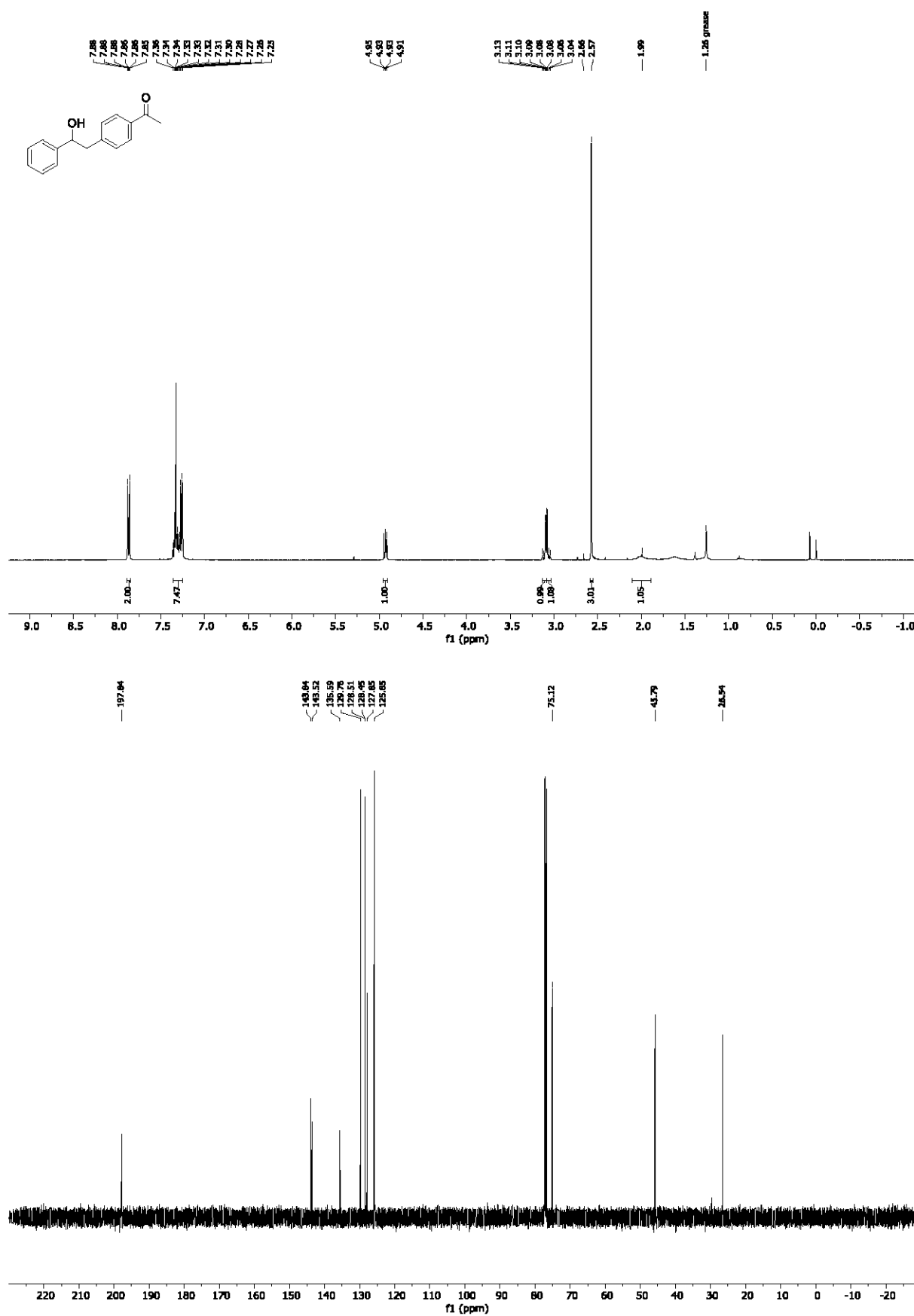


1-phenyl-2-(4-(trifluoromethyl)phenyl)ethan-1-ol (7af)

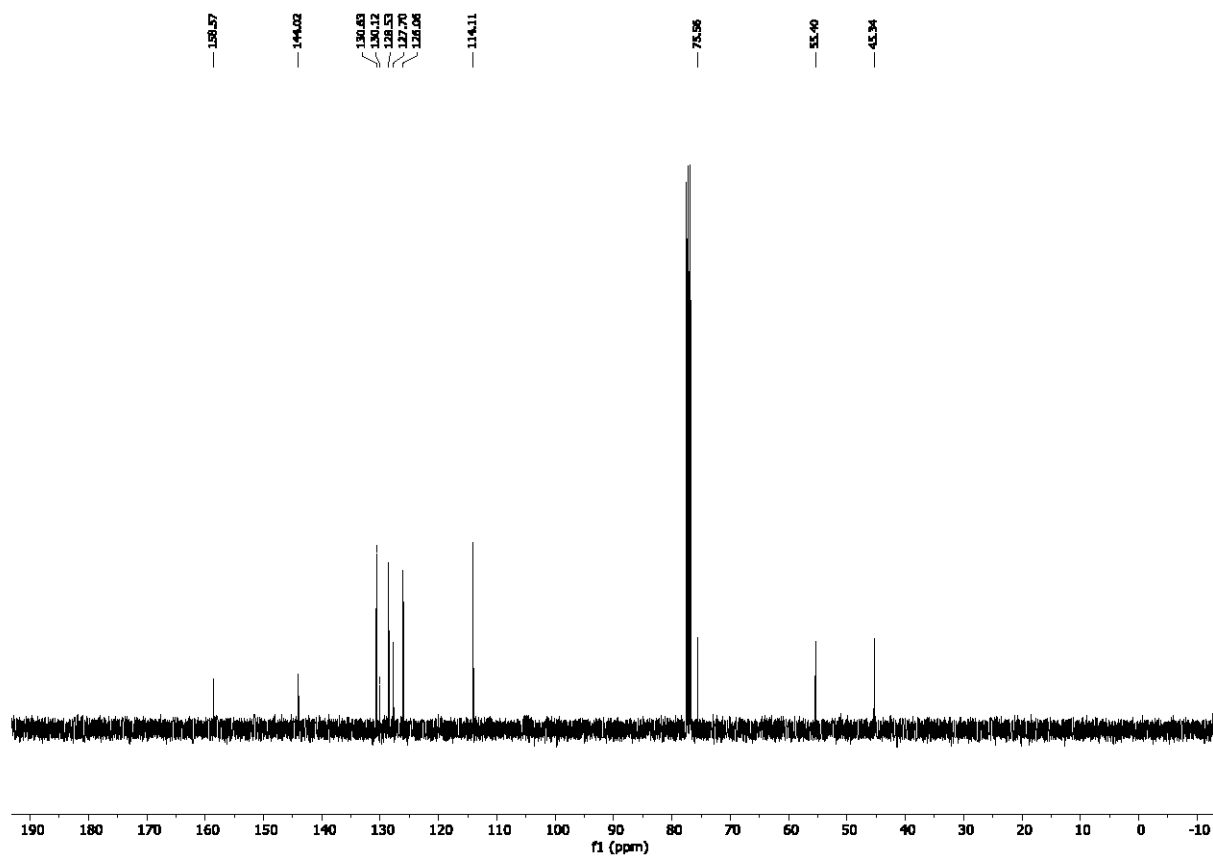
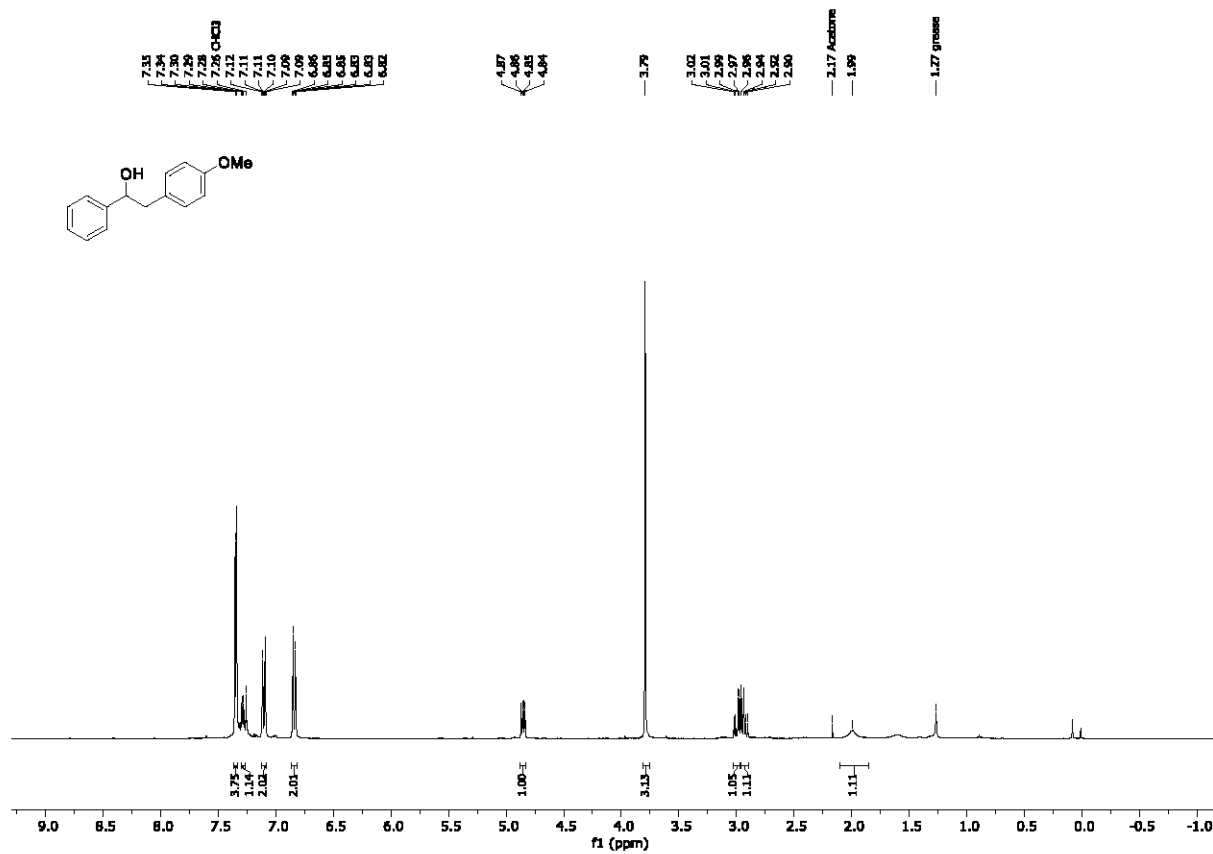




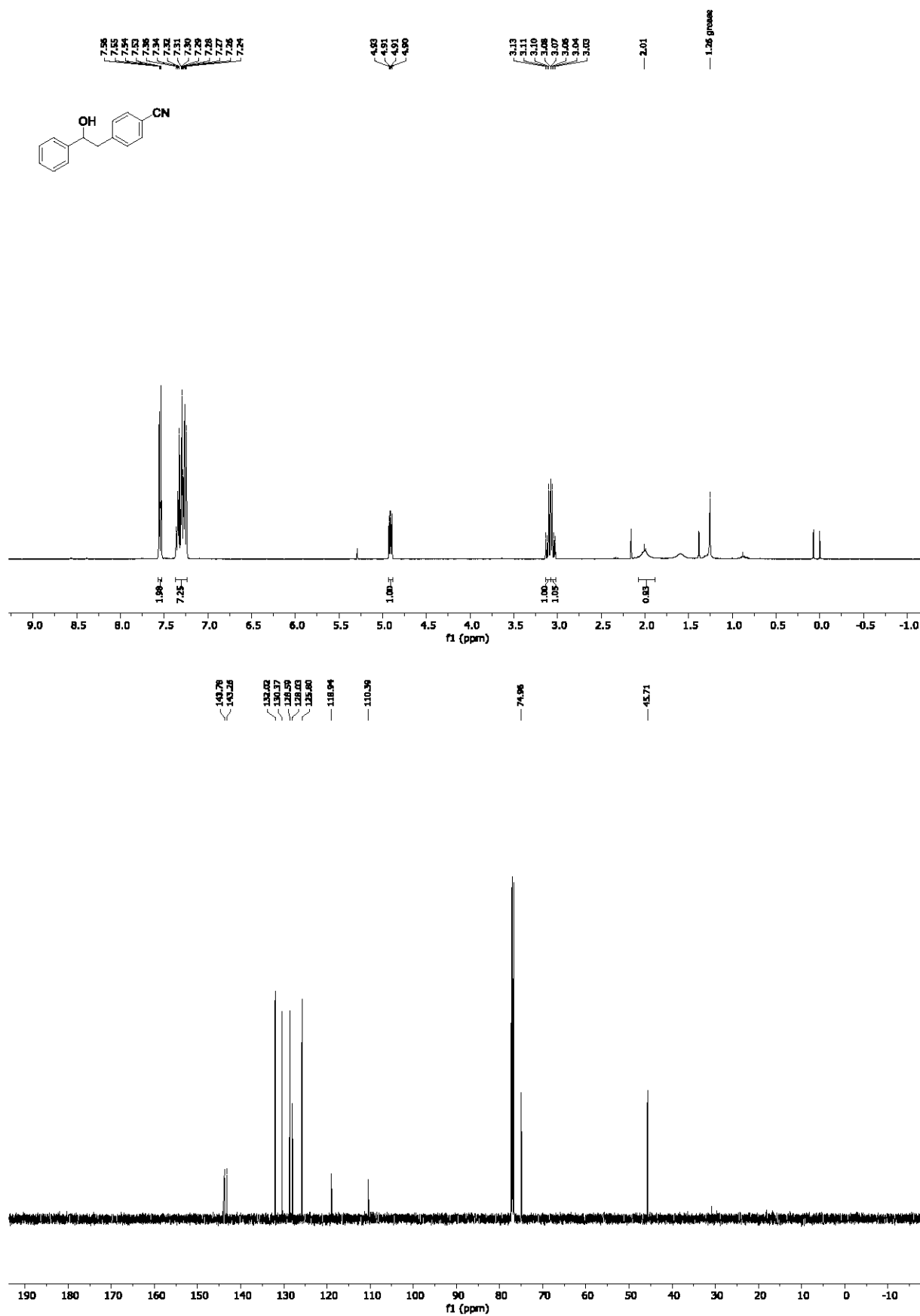
1-(4-(2-hydroxy-2-phenylethyl)phenyl)ethan-1-one (7ag)



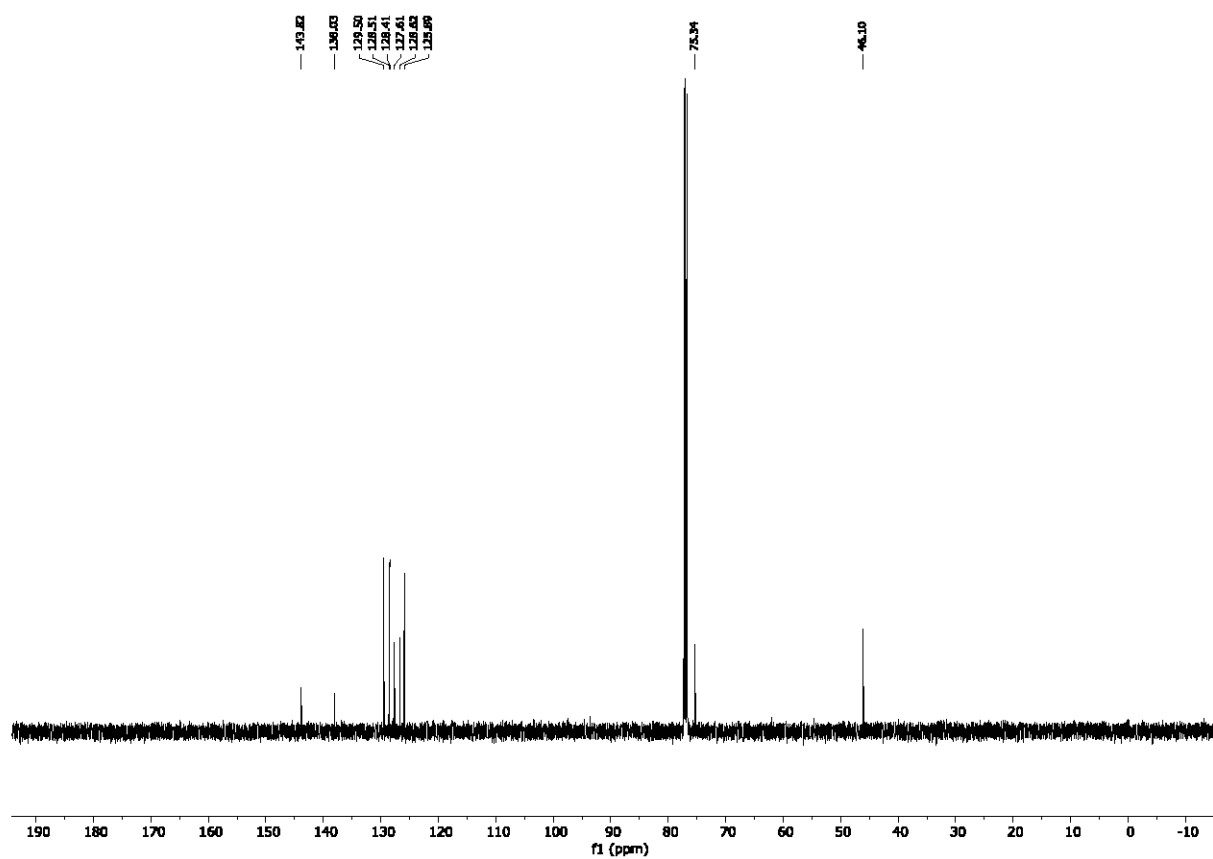
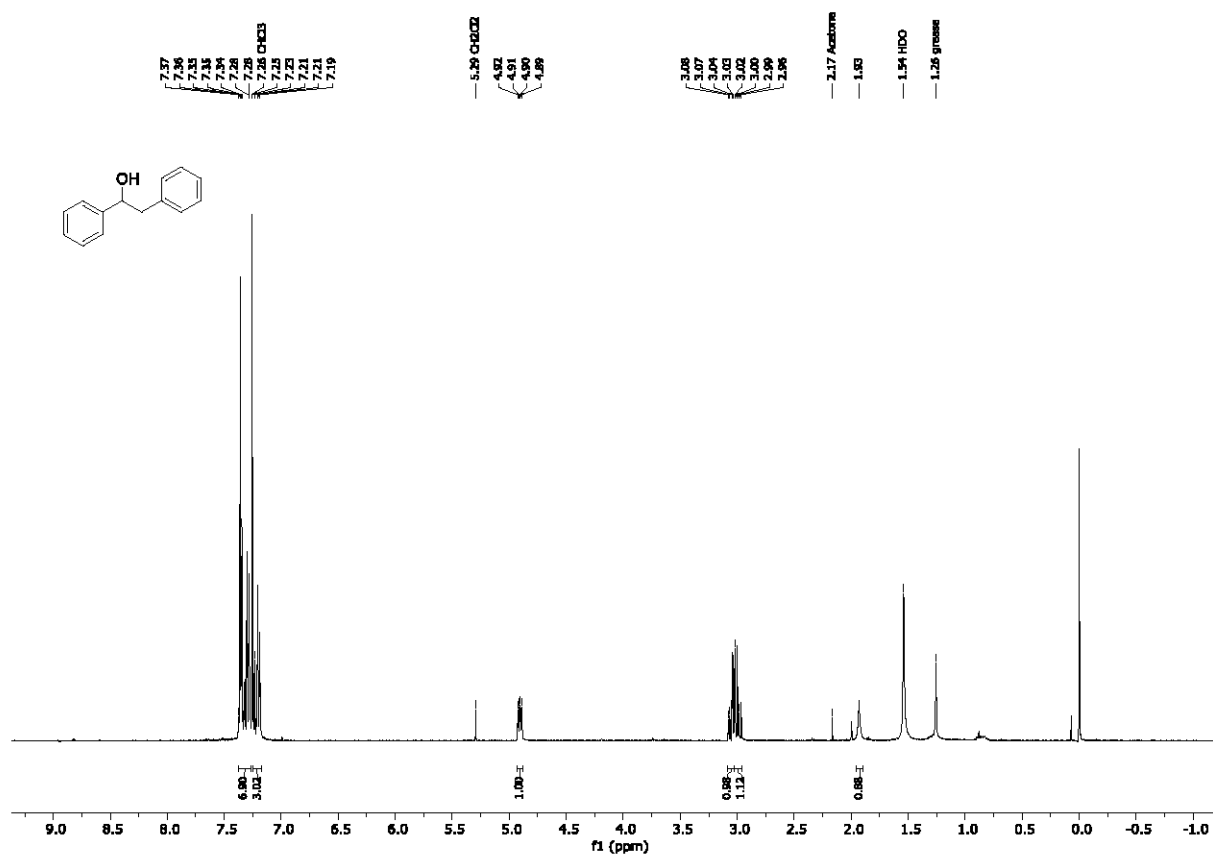
2-(4-methoxyphenyl)-1-phenylethan-1-ol (7ah)



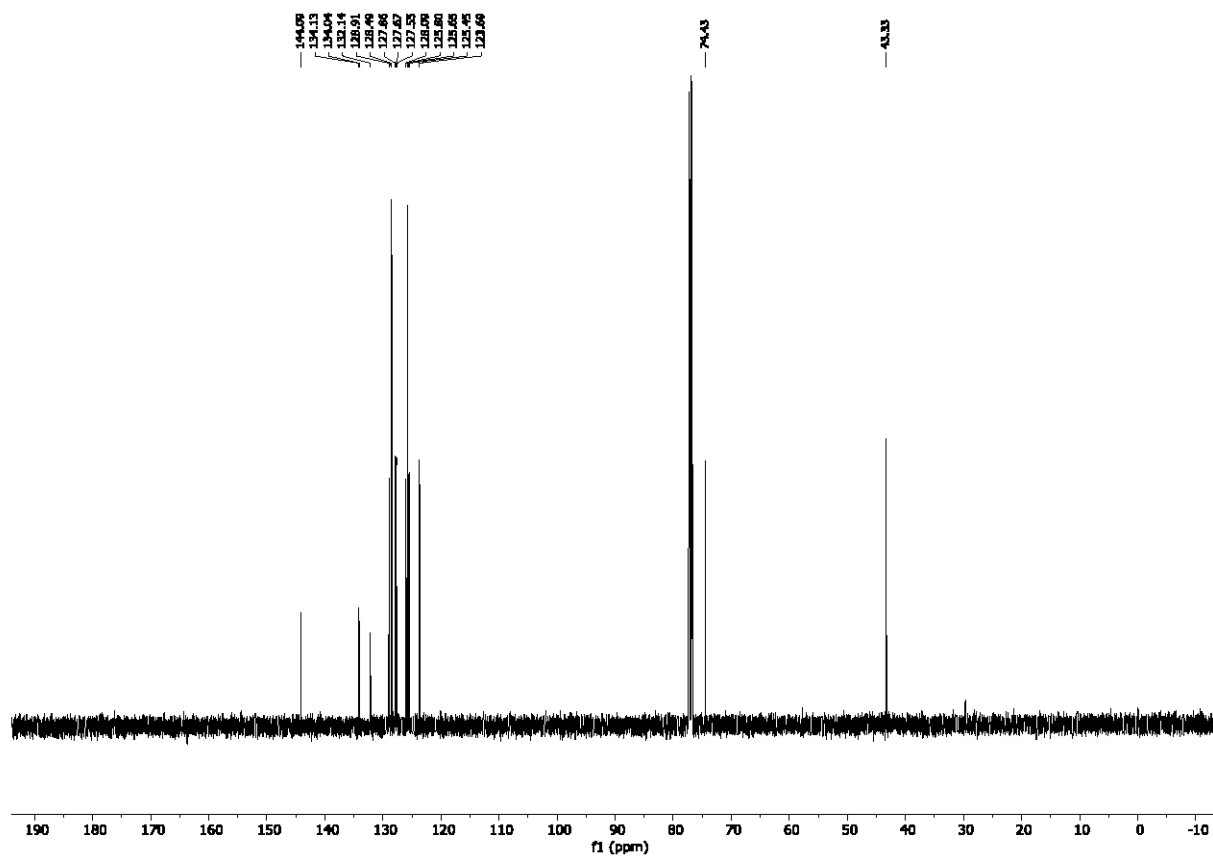
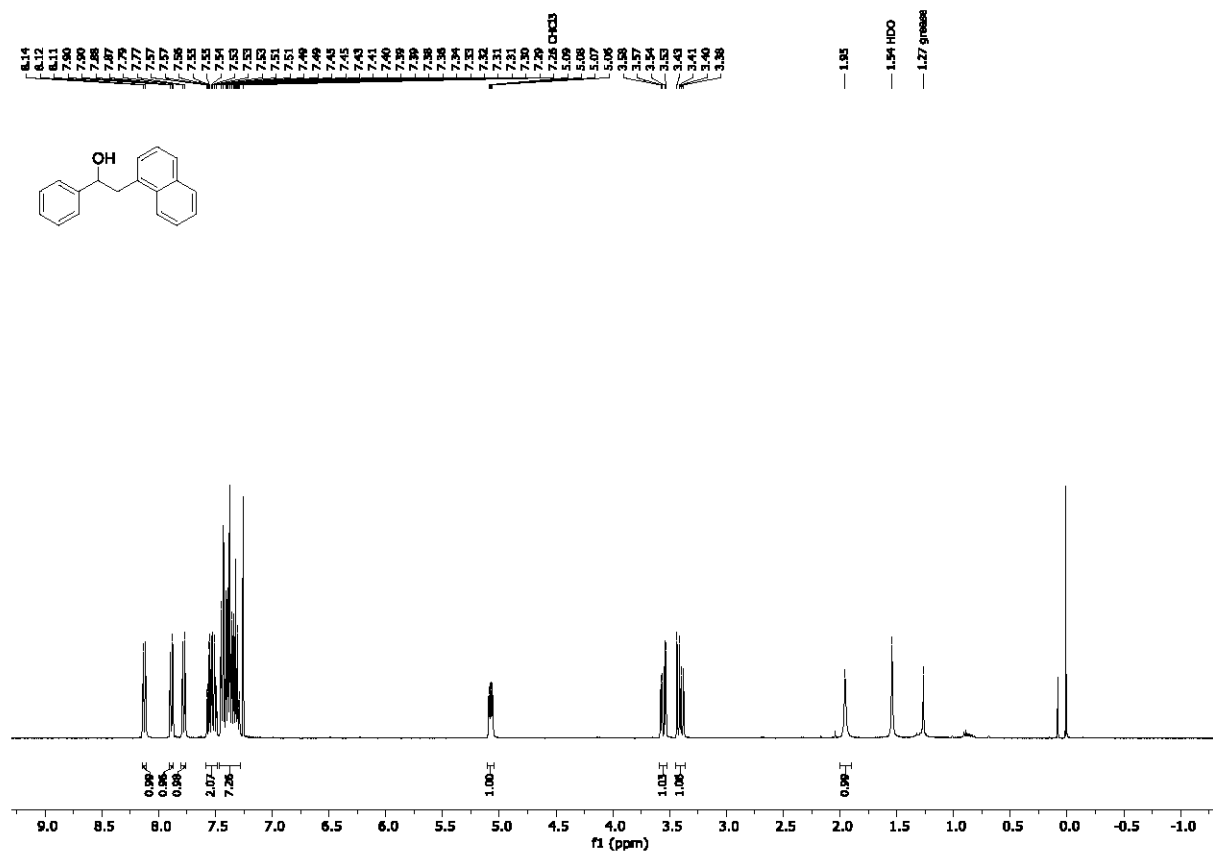
4-(2-hydroxy-2-phenylethyl)benzonitrile (7ai)



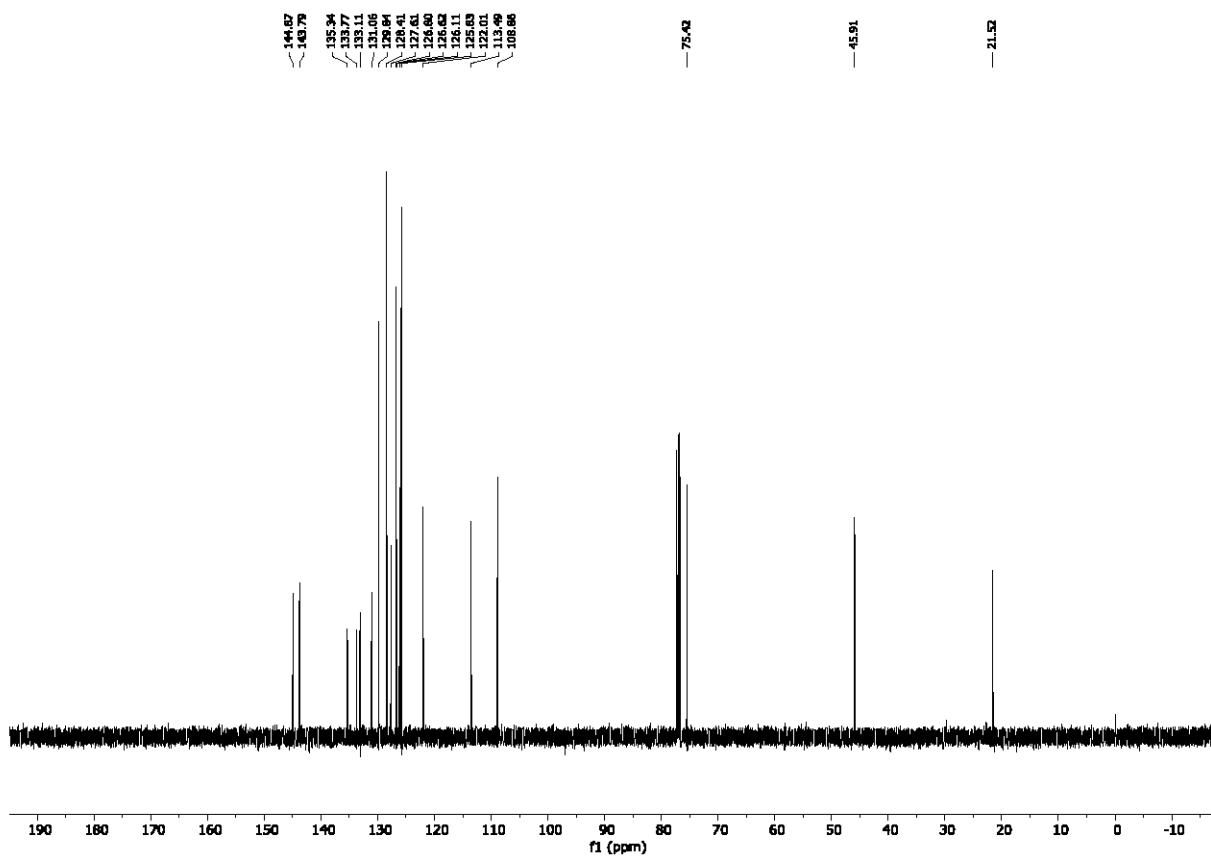
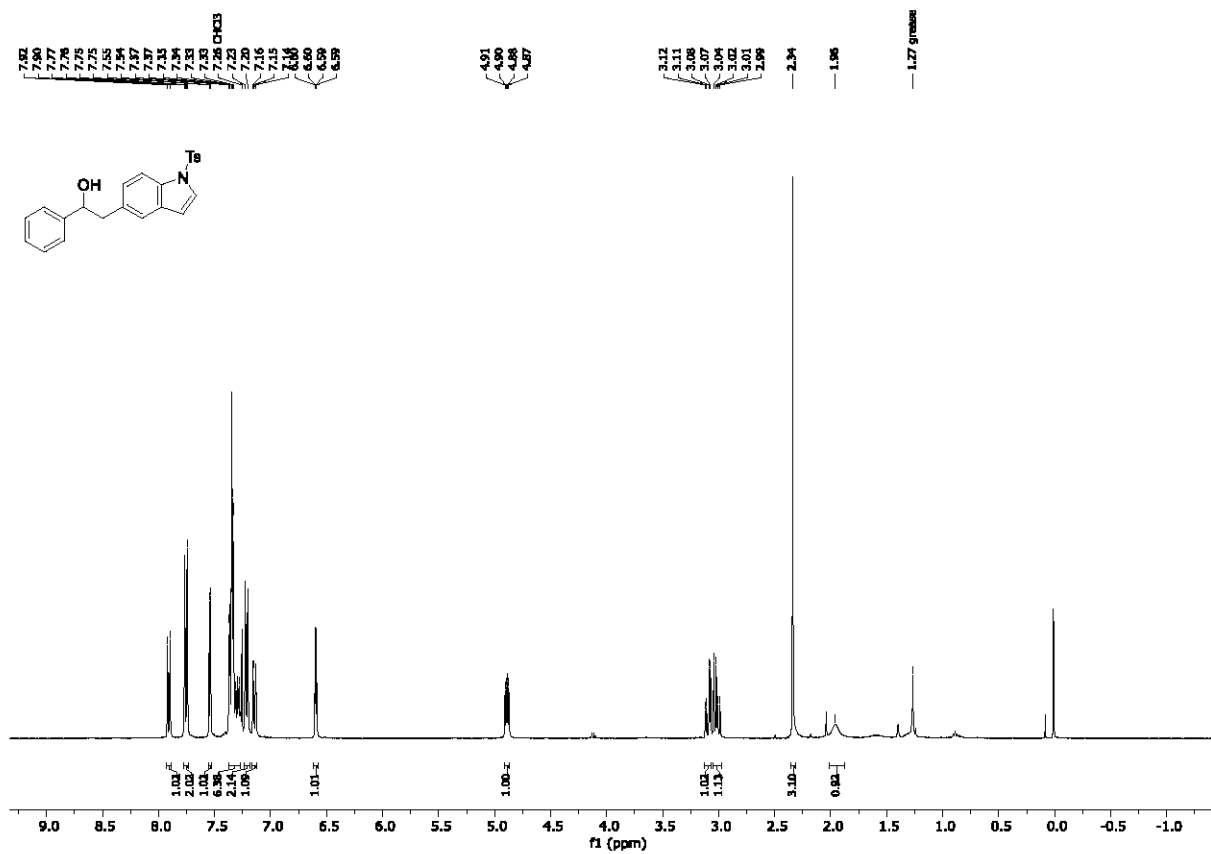
1,2-diphenylethan-1-ol (7aj)



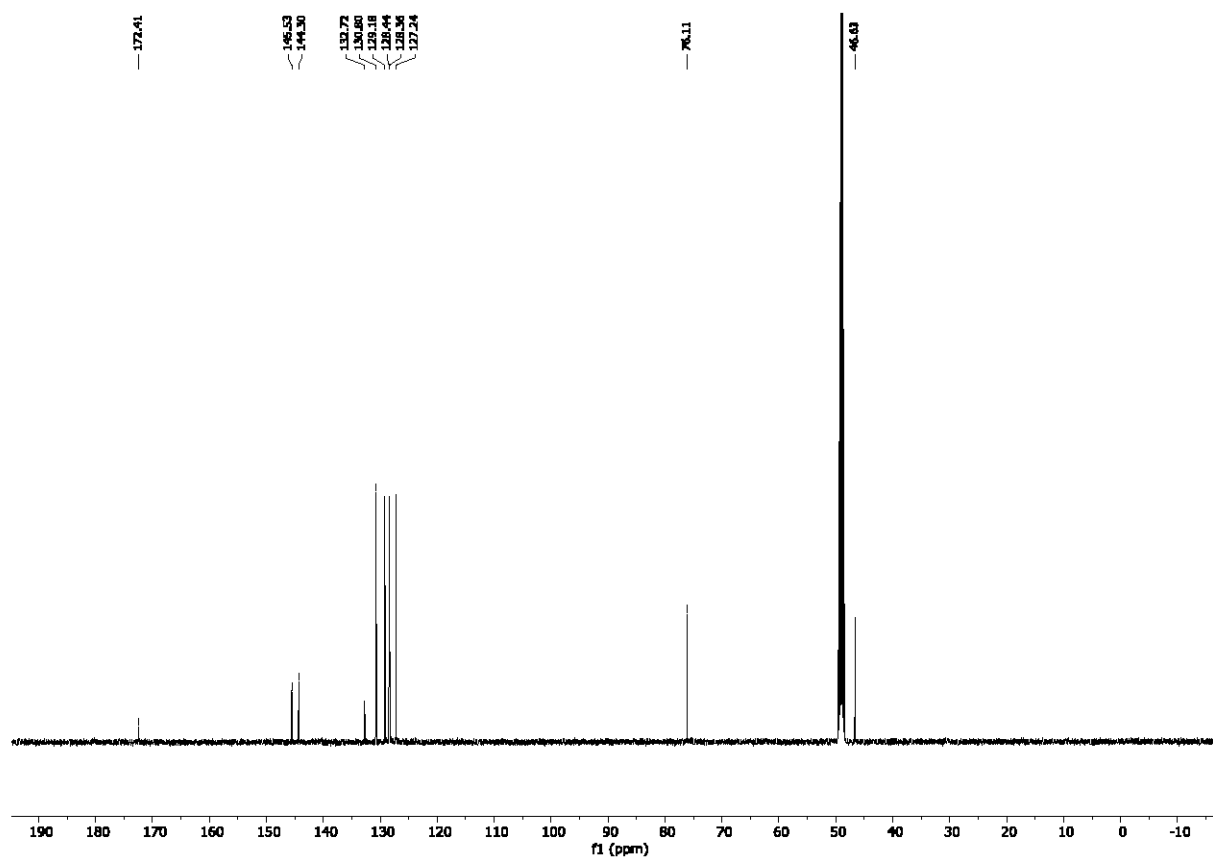
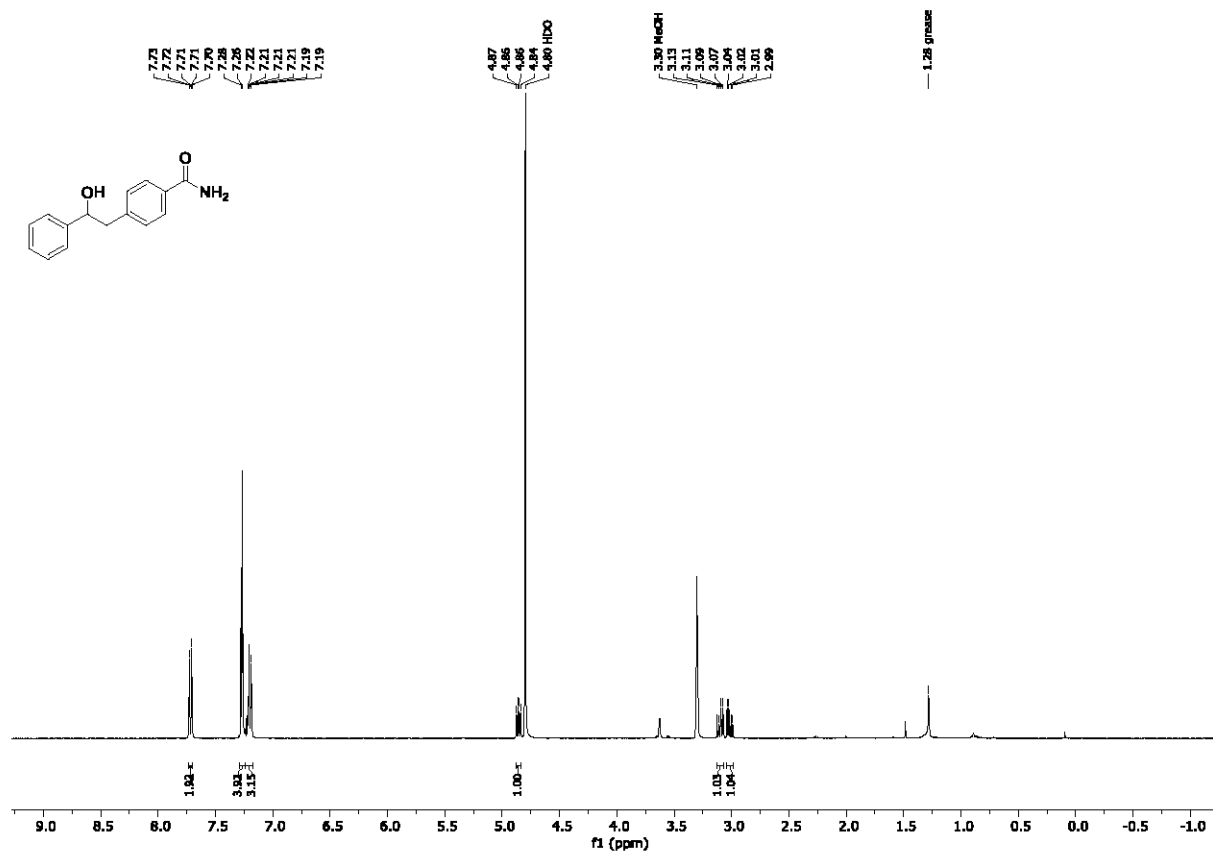
2-(naphthalen-1-yl)-1-phenylethan-1-ol (7ak)



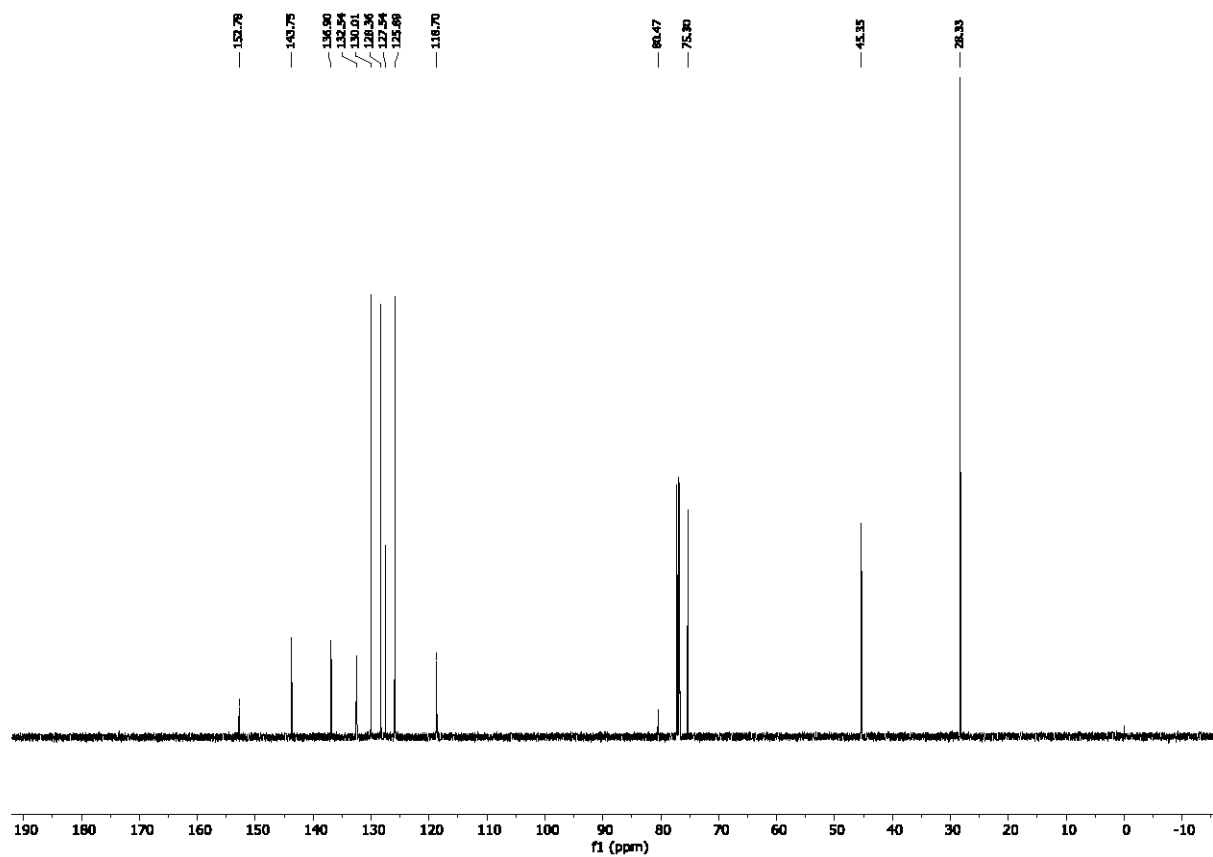
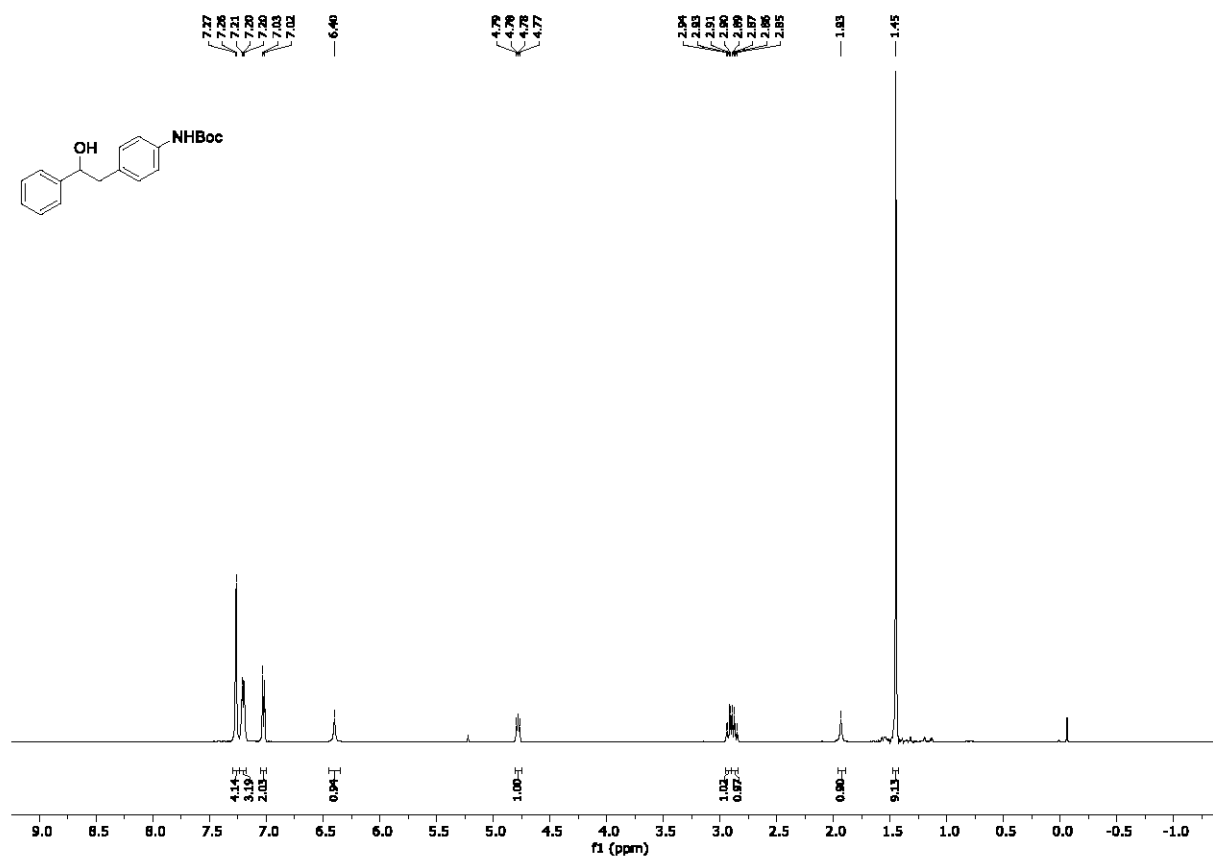
1-phenyl-2-(1-tosyl-1*H*-indol-5-yl)ethan-1-ol (7a)



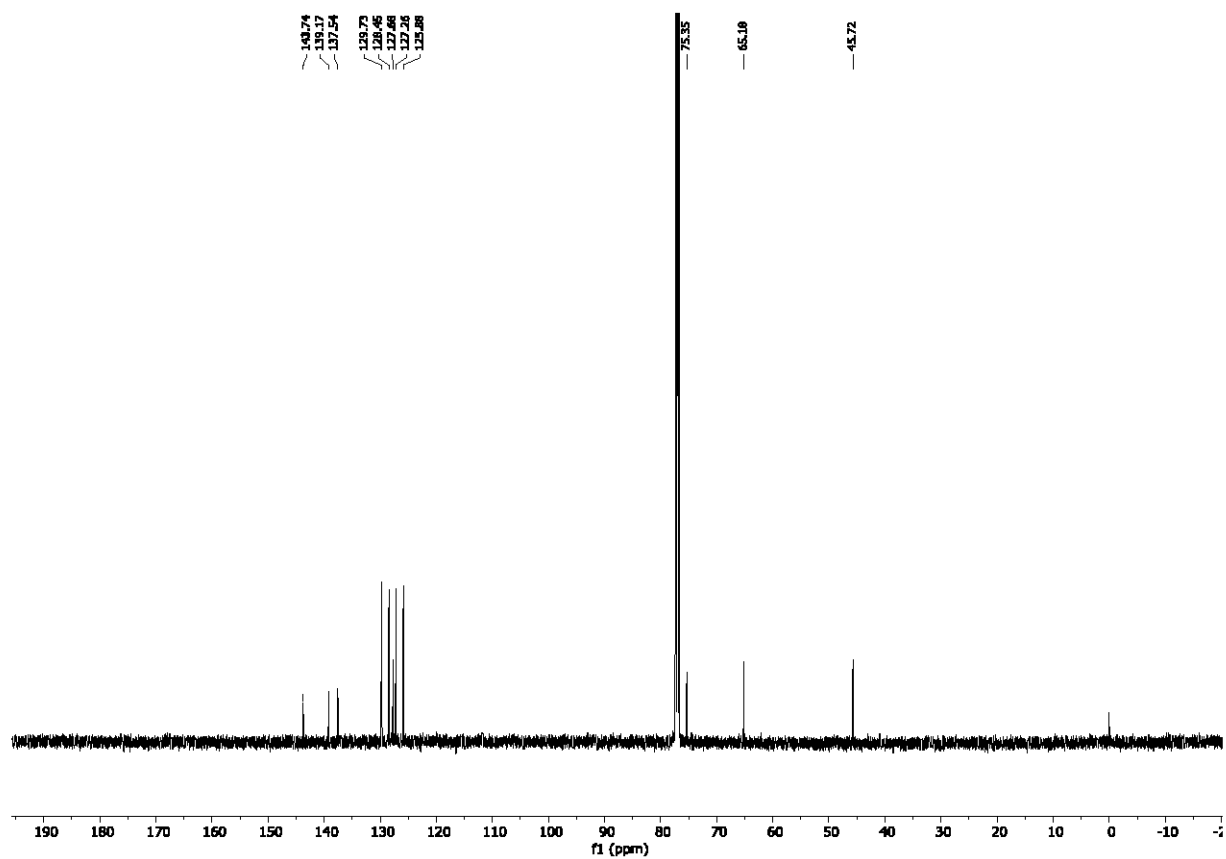
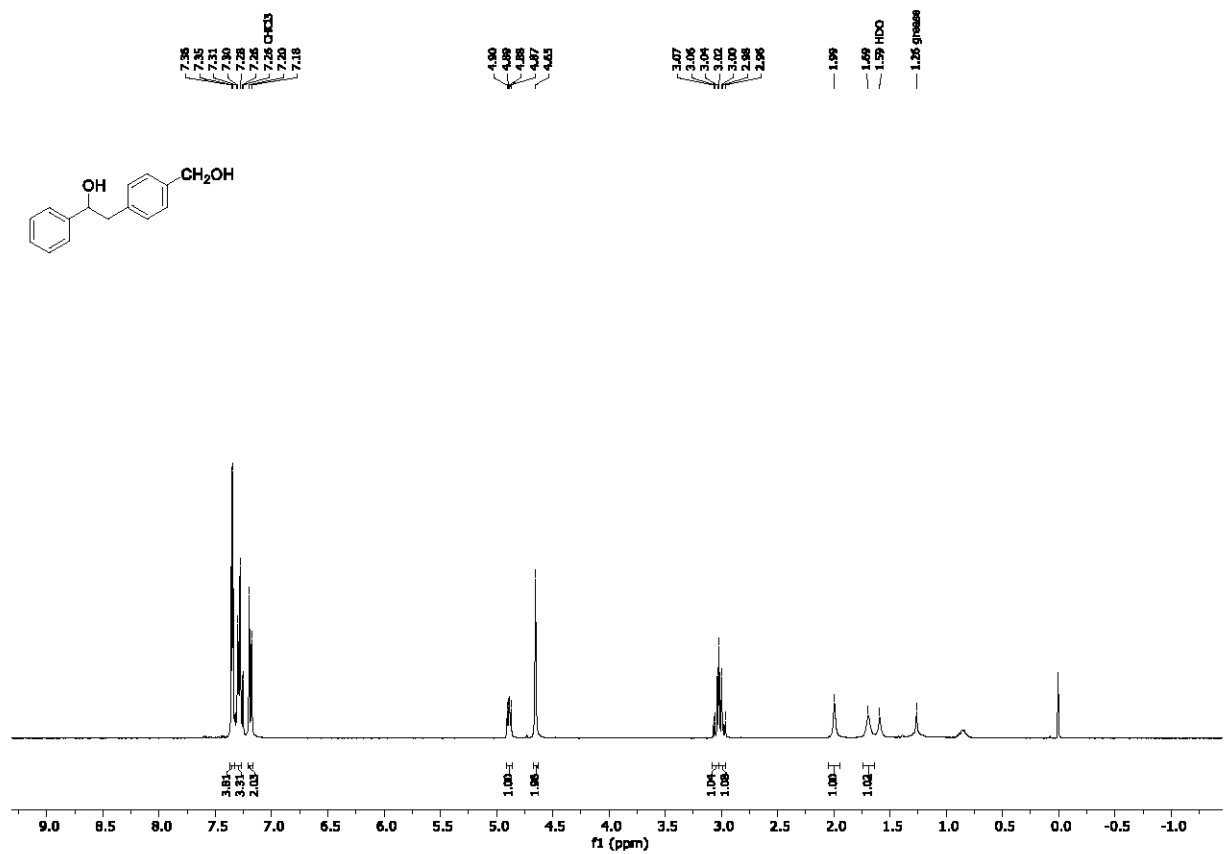
4-(2-hydroxy-2-phenylethyl)benzamide (7am)



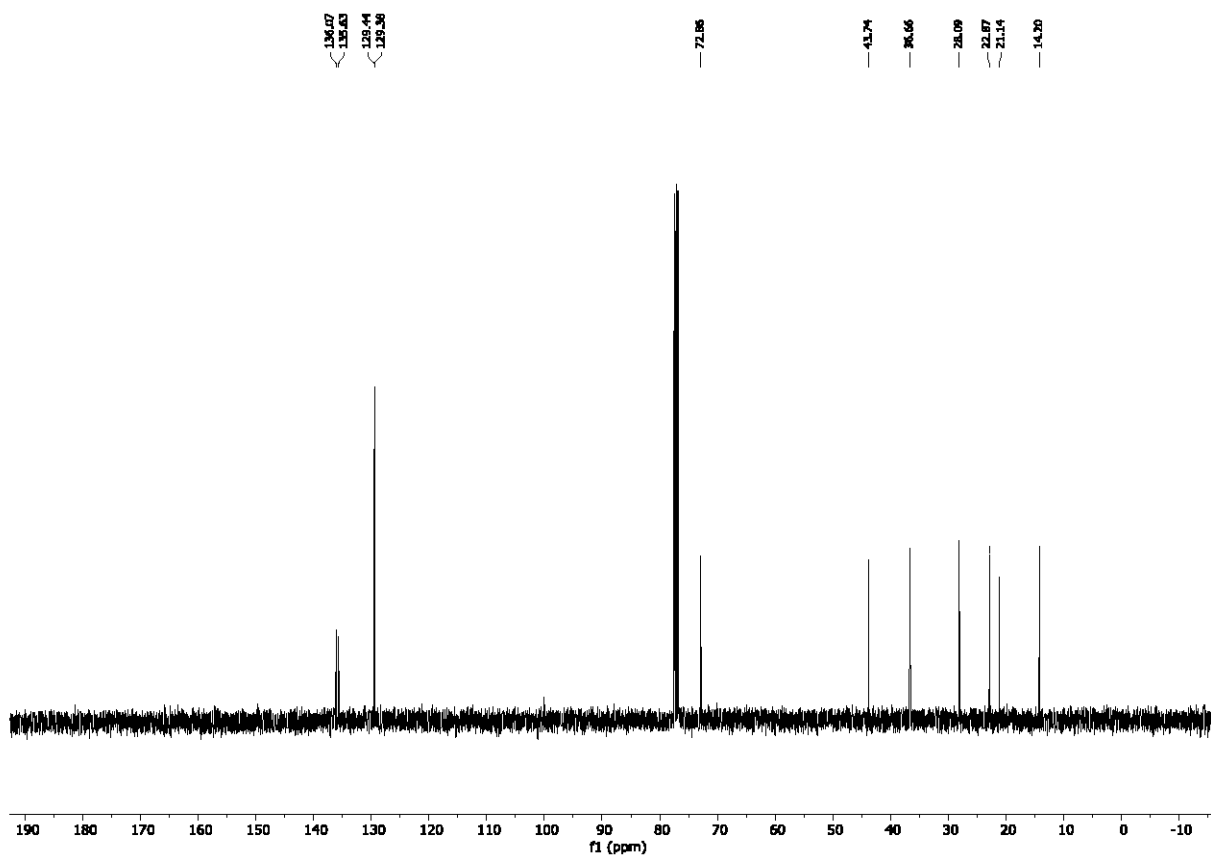
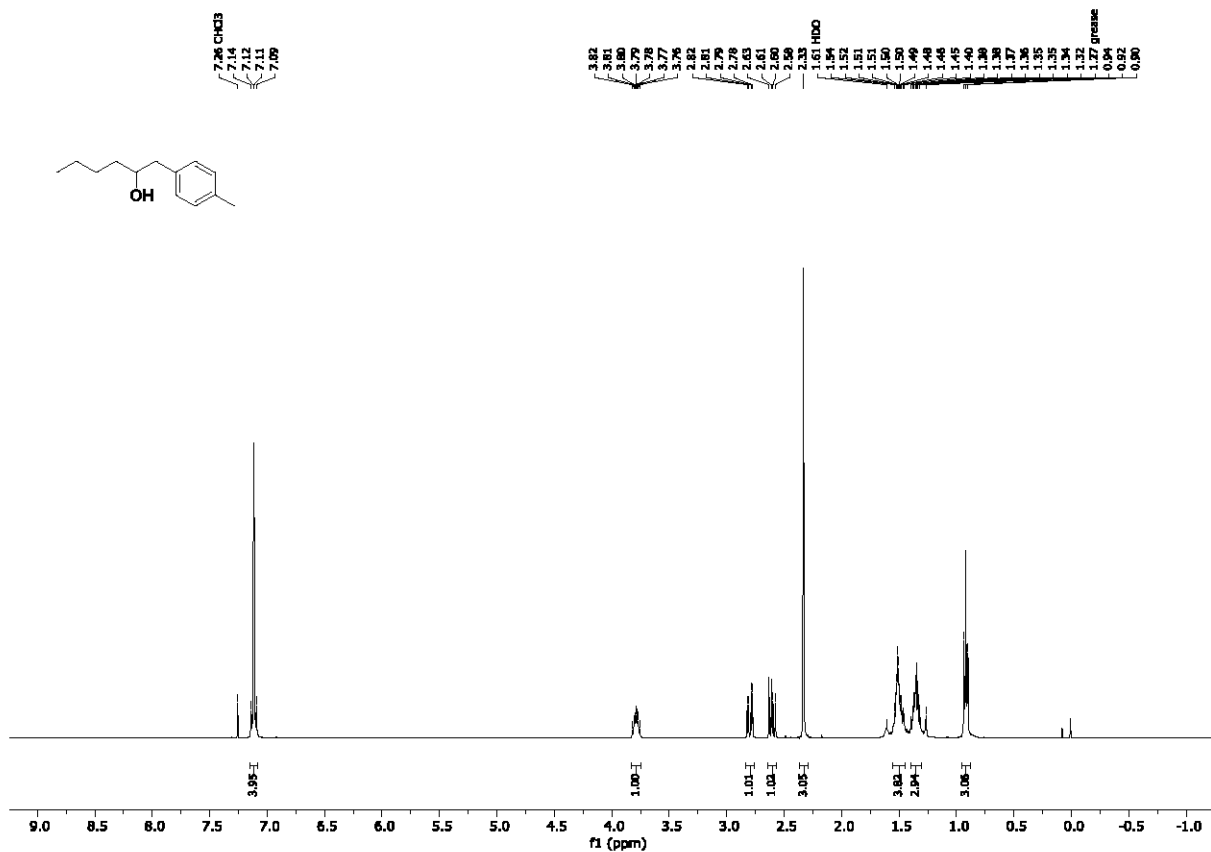
tert-butyl (4-(2-hydroxy-2-phenylethyl)phenyl)carbamate (7an)



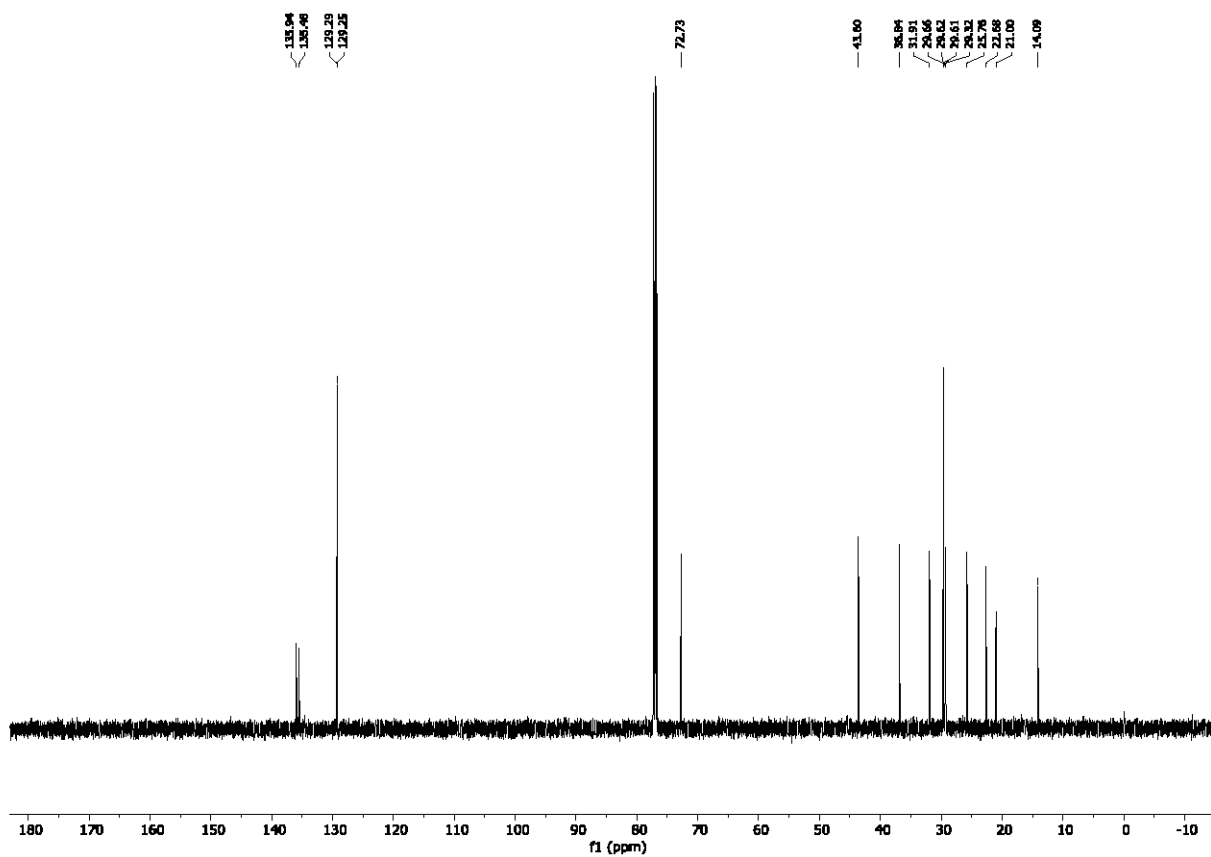
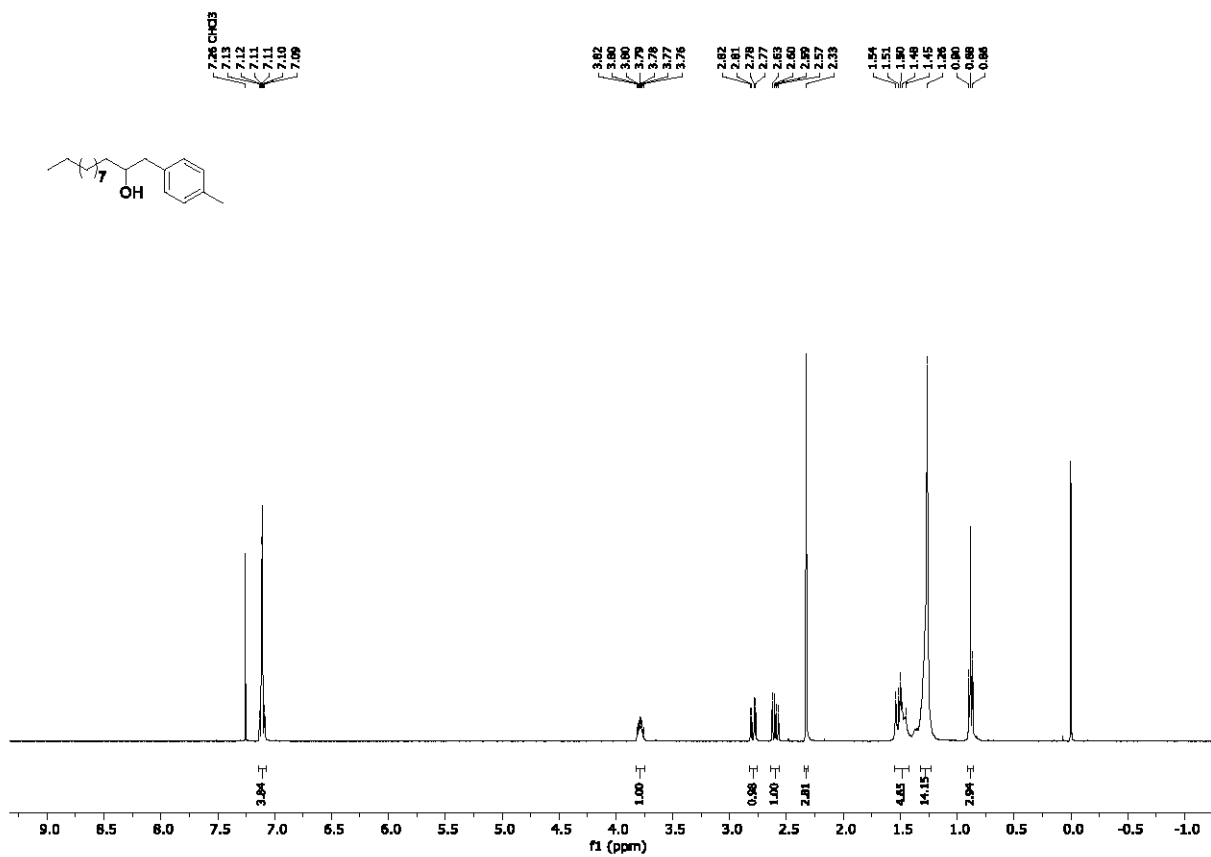
2-(4-(hydroxymethyl)phenyl)-1-phenylethan-1-ol (7ao)



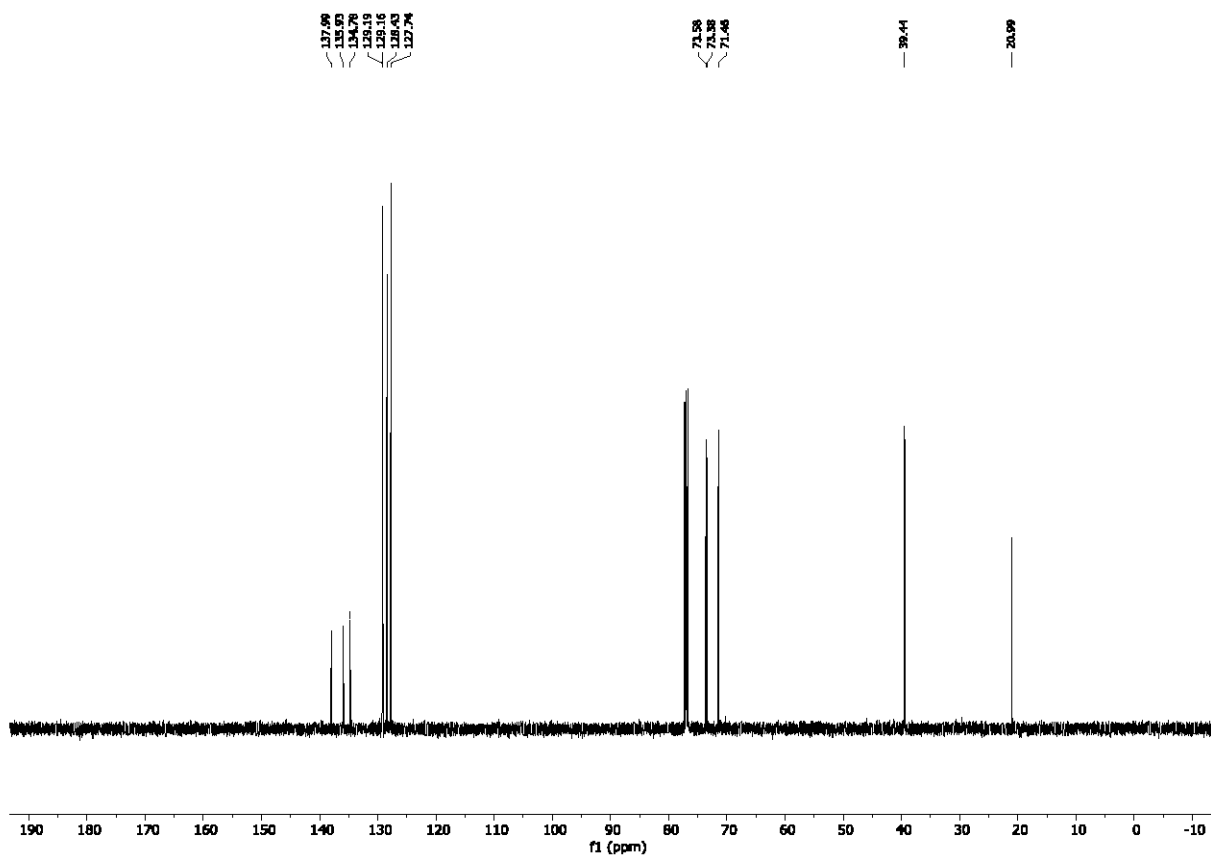
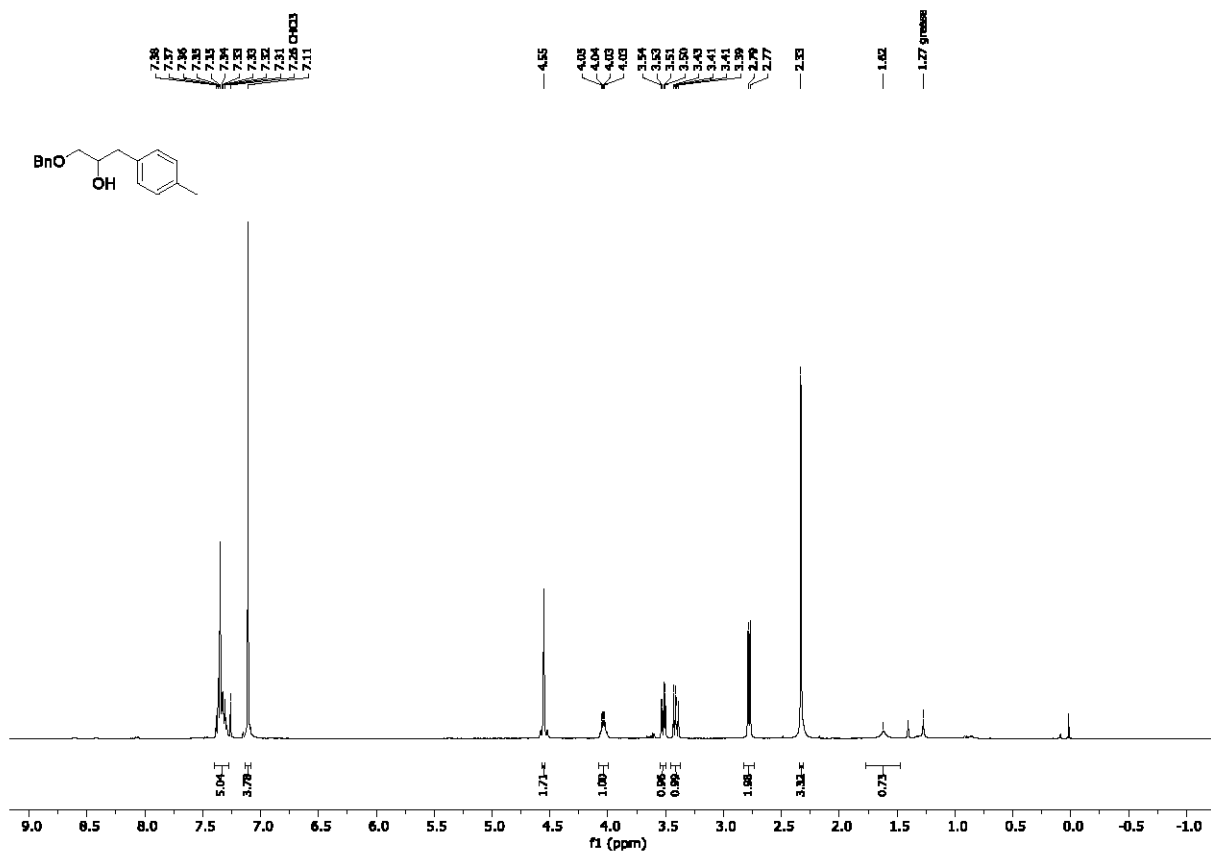
1-(*p*-tolyl)hexan-2-ol (7ha)



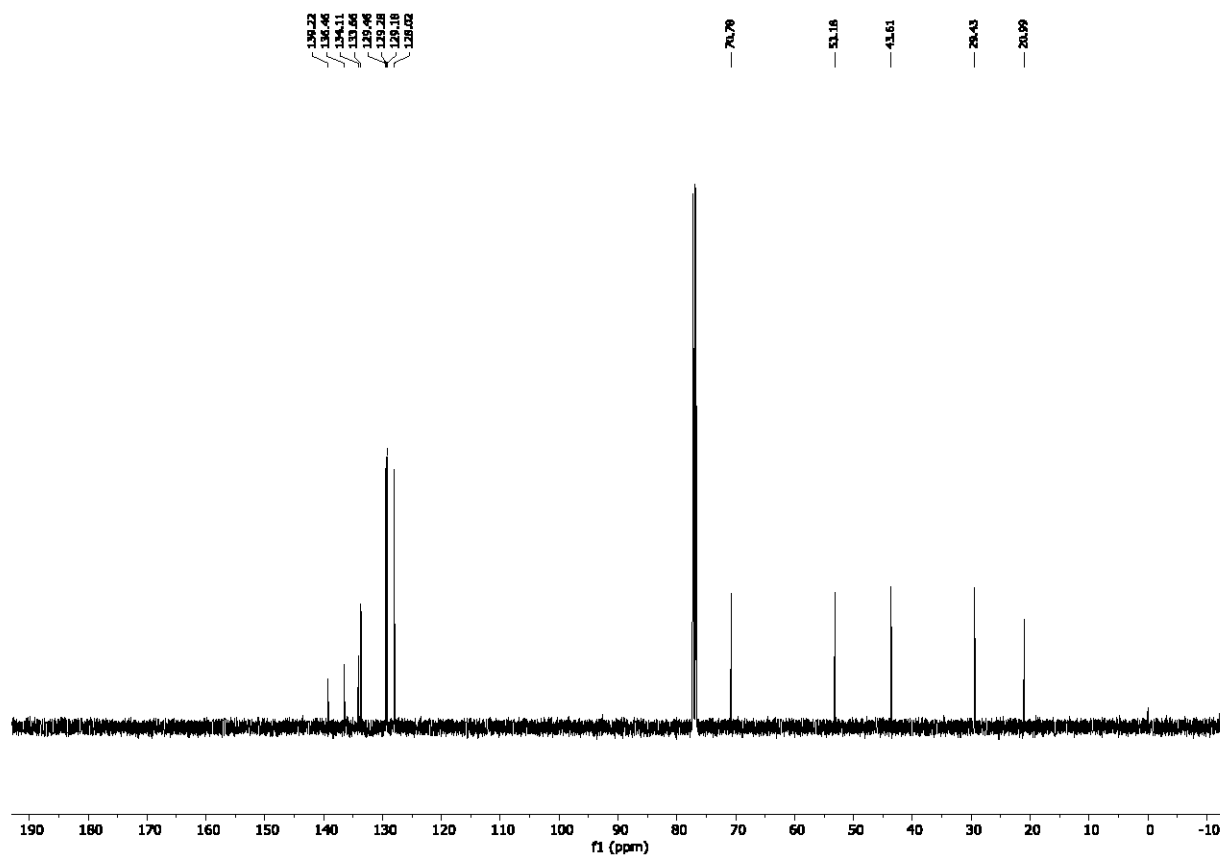
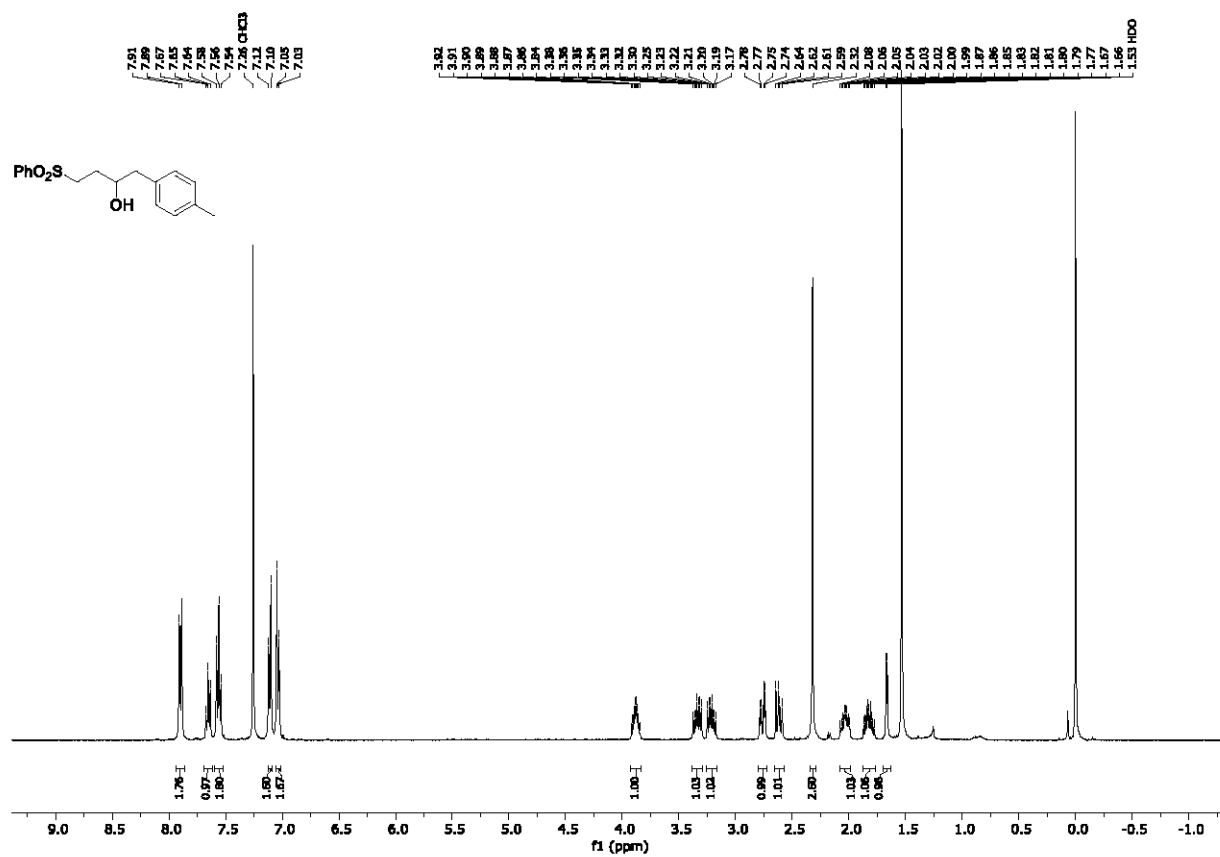
1-(*p*-tolyl)dodecan-2-ol (7ia)



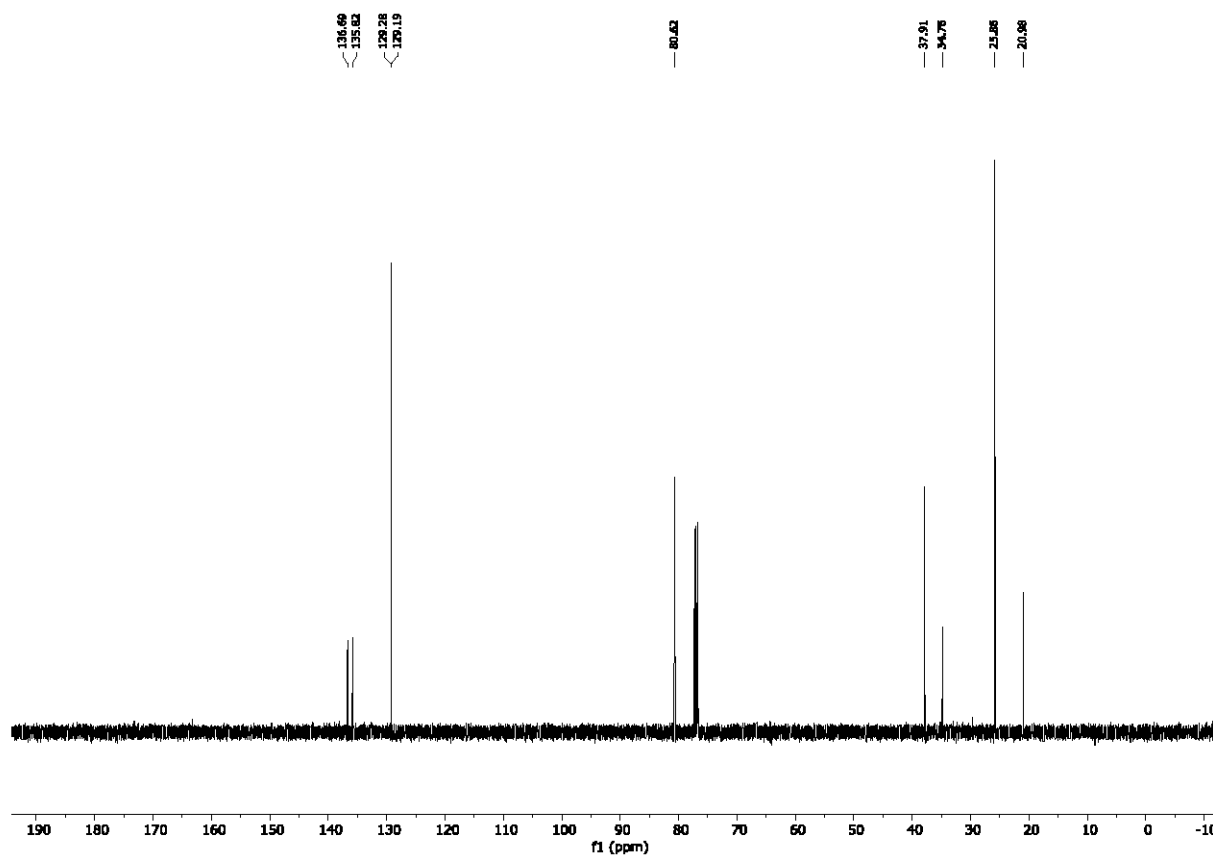
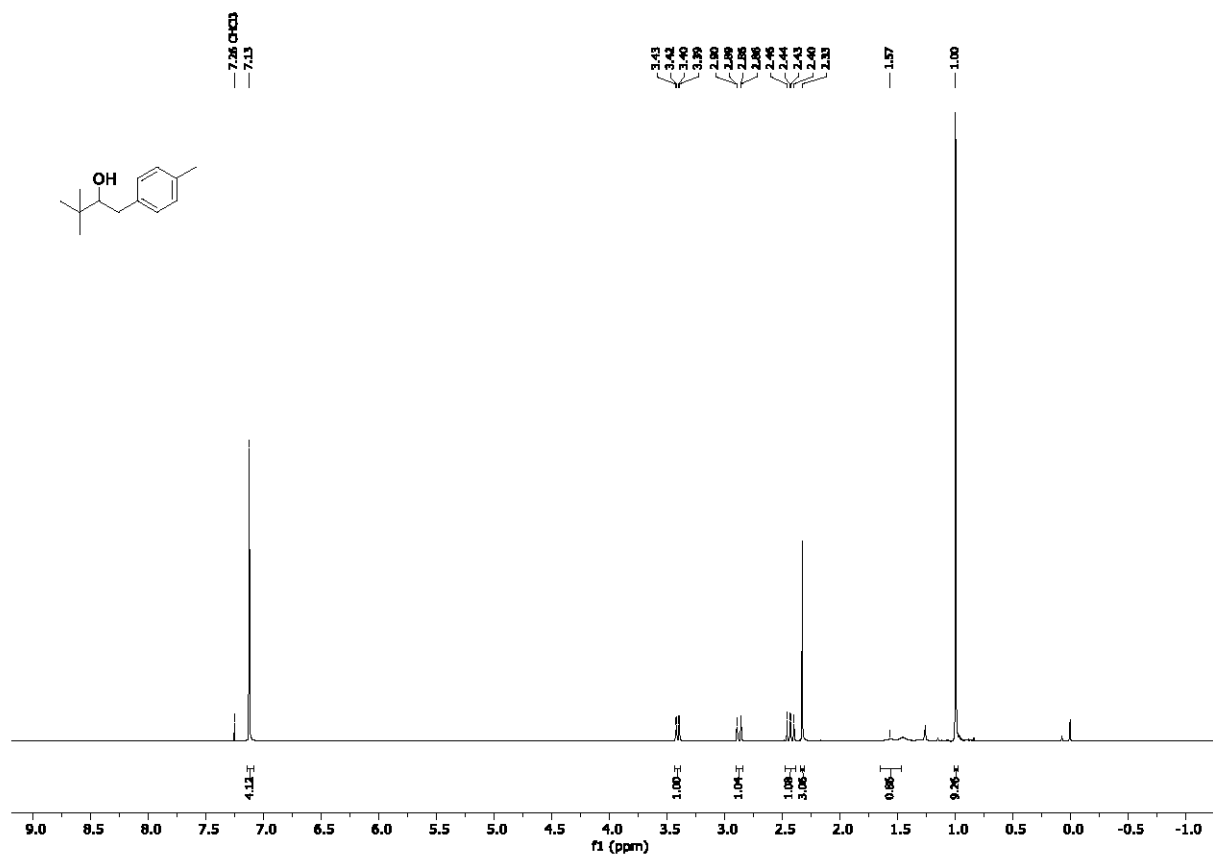
1-(benzyloxy)-3-(4-tolyl)propan-2-ol (7ja)



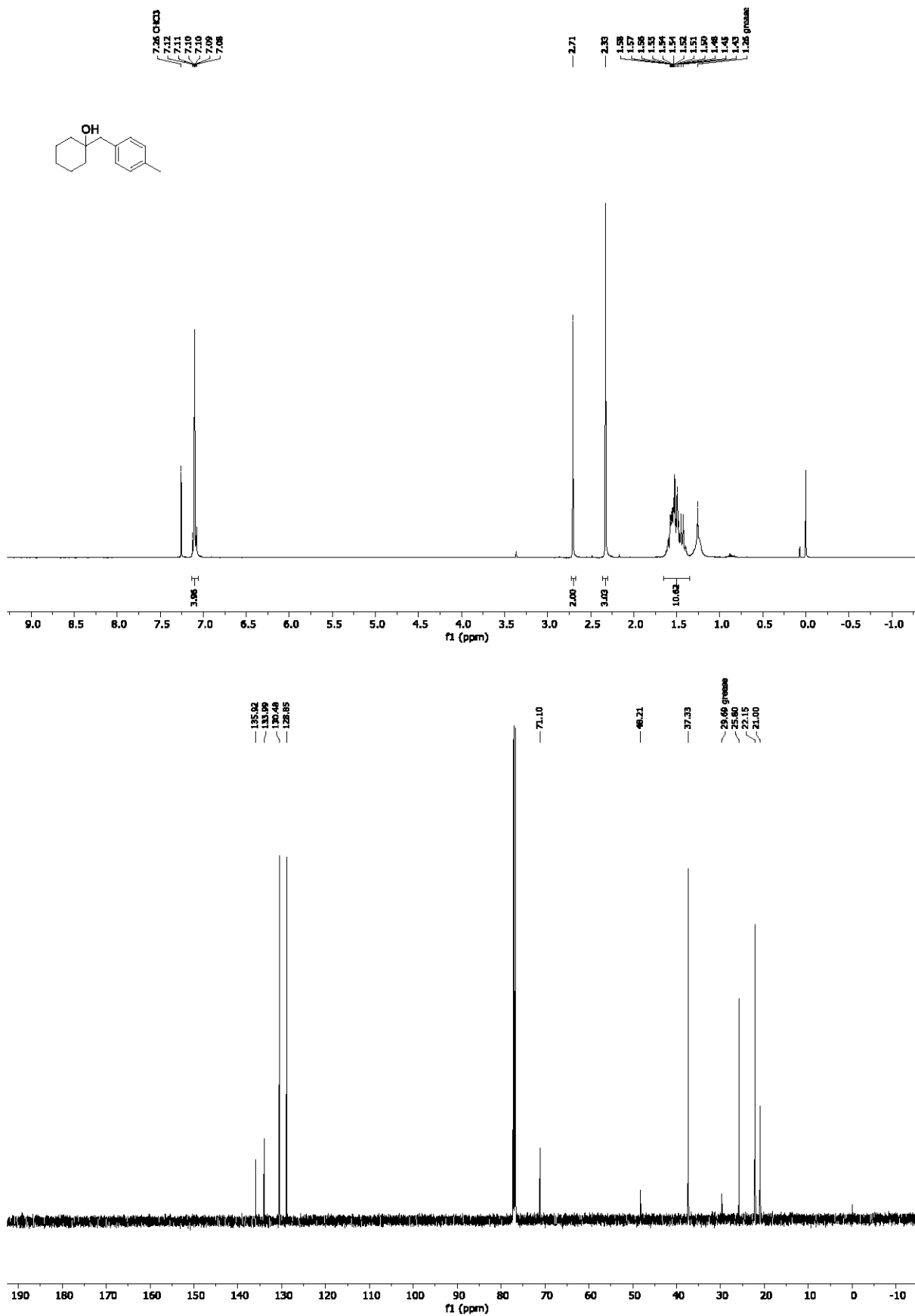
4-(phenylsulfonyl)-1-(4-tolyl)butan-2-ol (7ka)



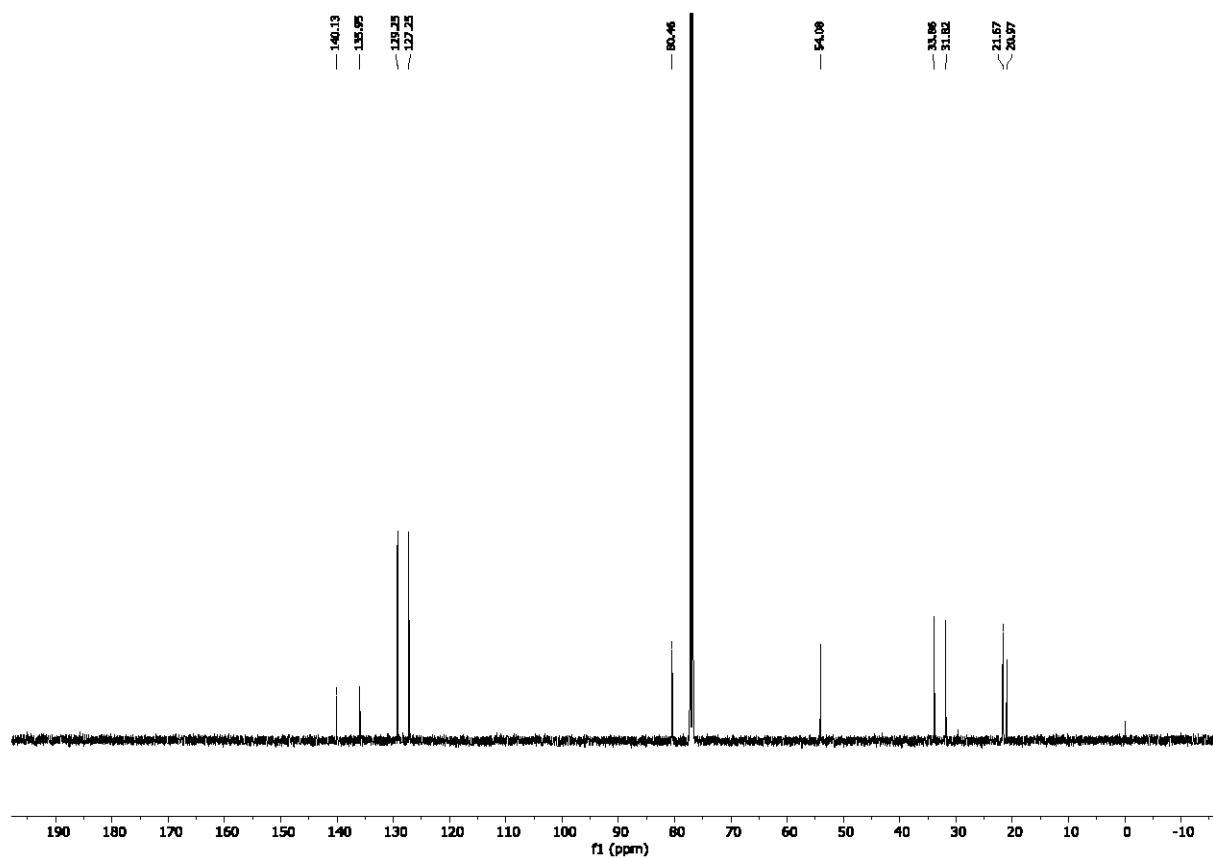
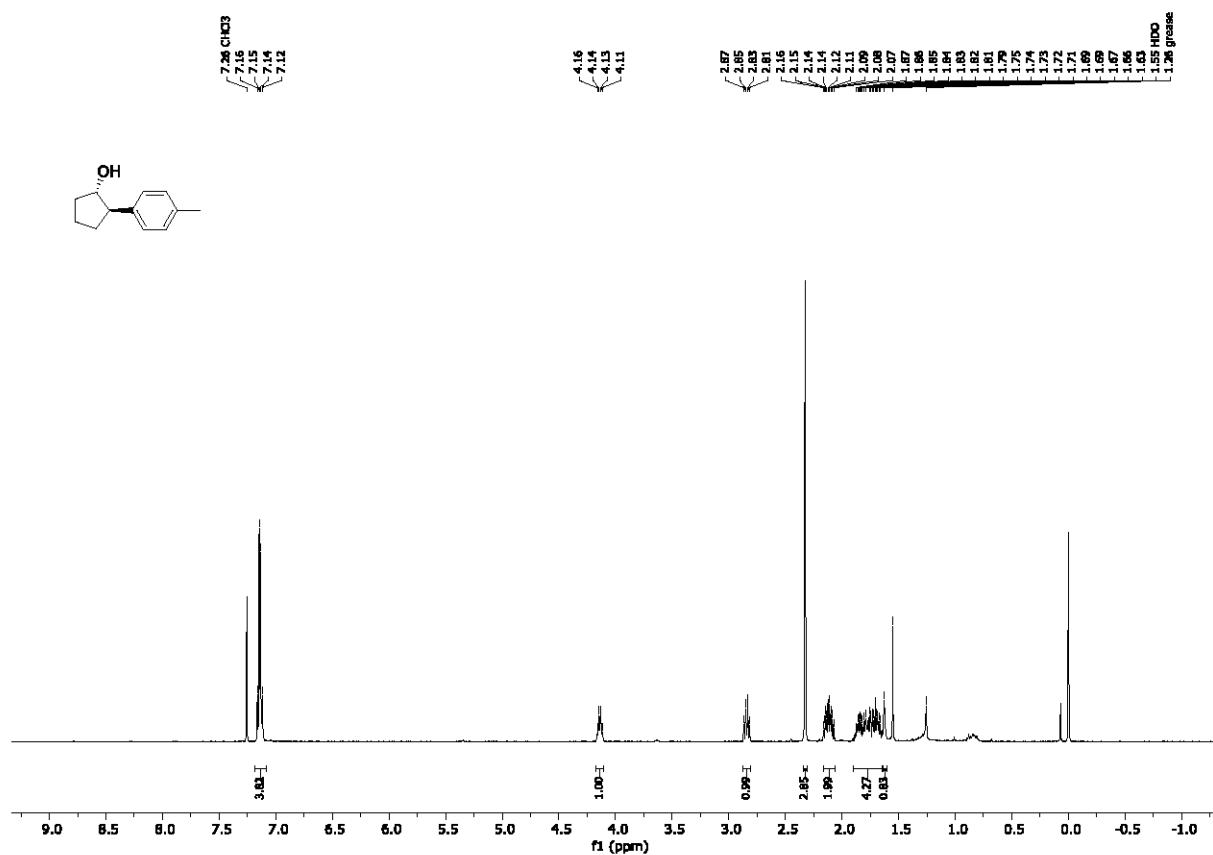
3,3-dimethyl-1-(4-tolyl)butan-2-ol (71a)



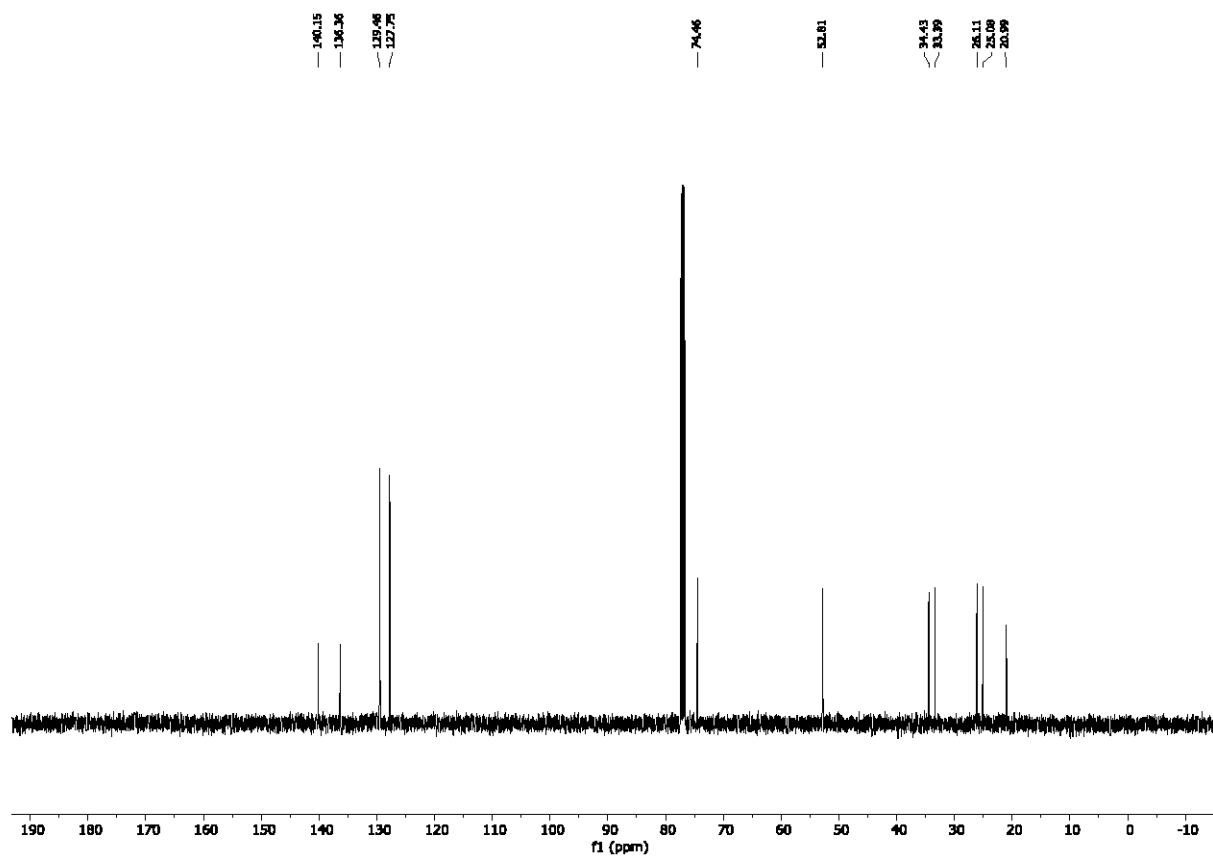
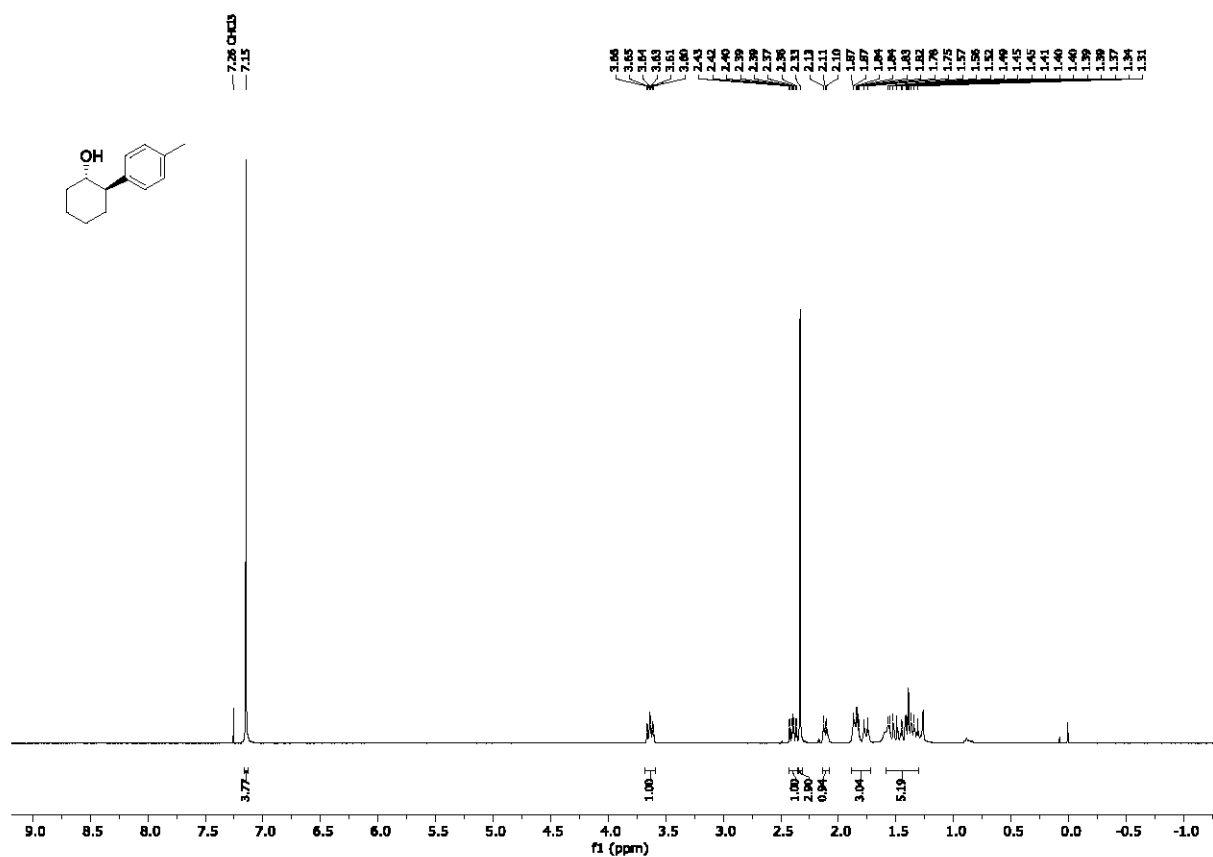
1-(4-methylbenzyl)cyclohexan-1-ol (7ma)



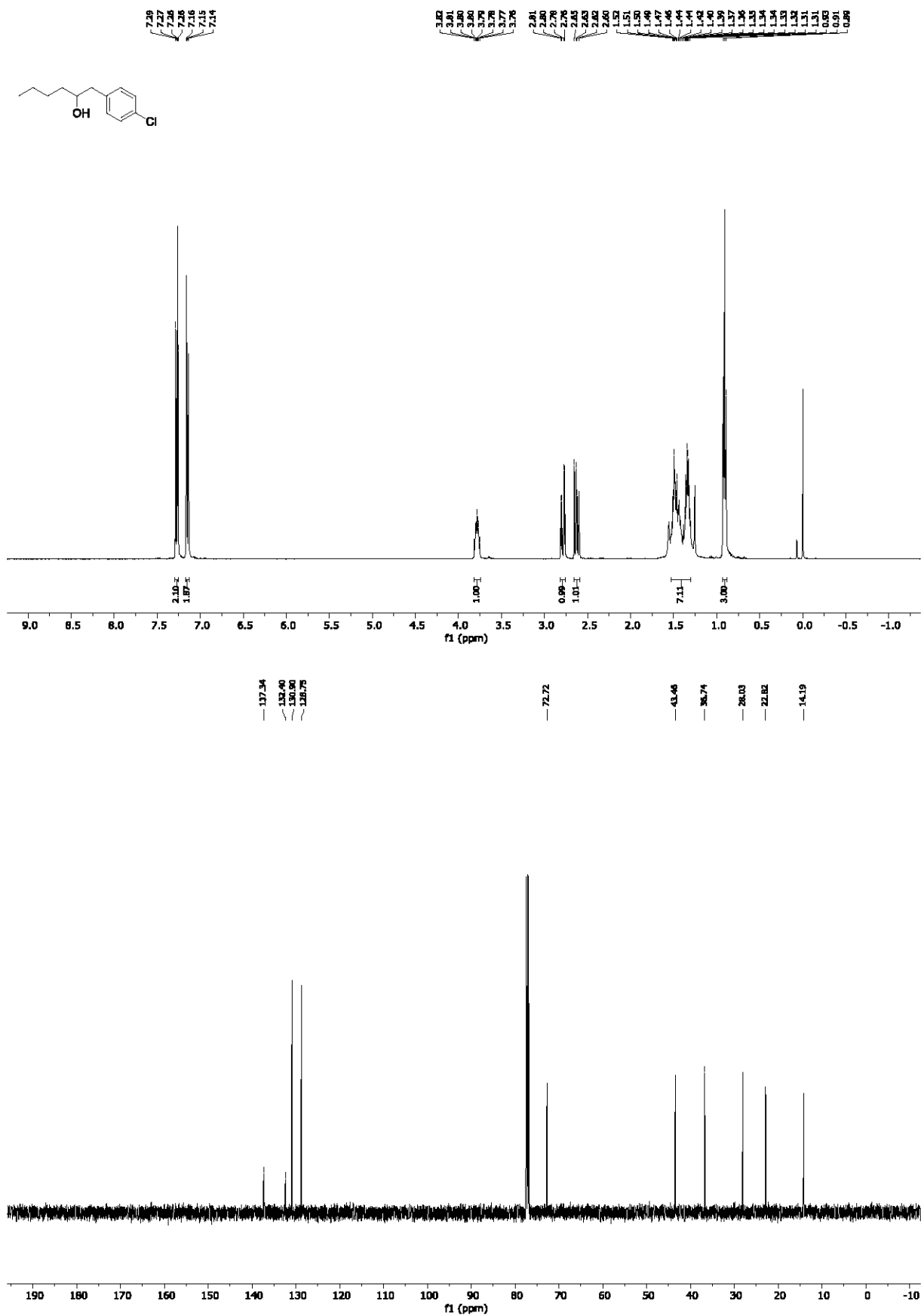
(1*S*,2*R*)-2-(4-tolyl)cyclopentan-1-ol (7na)



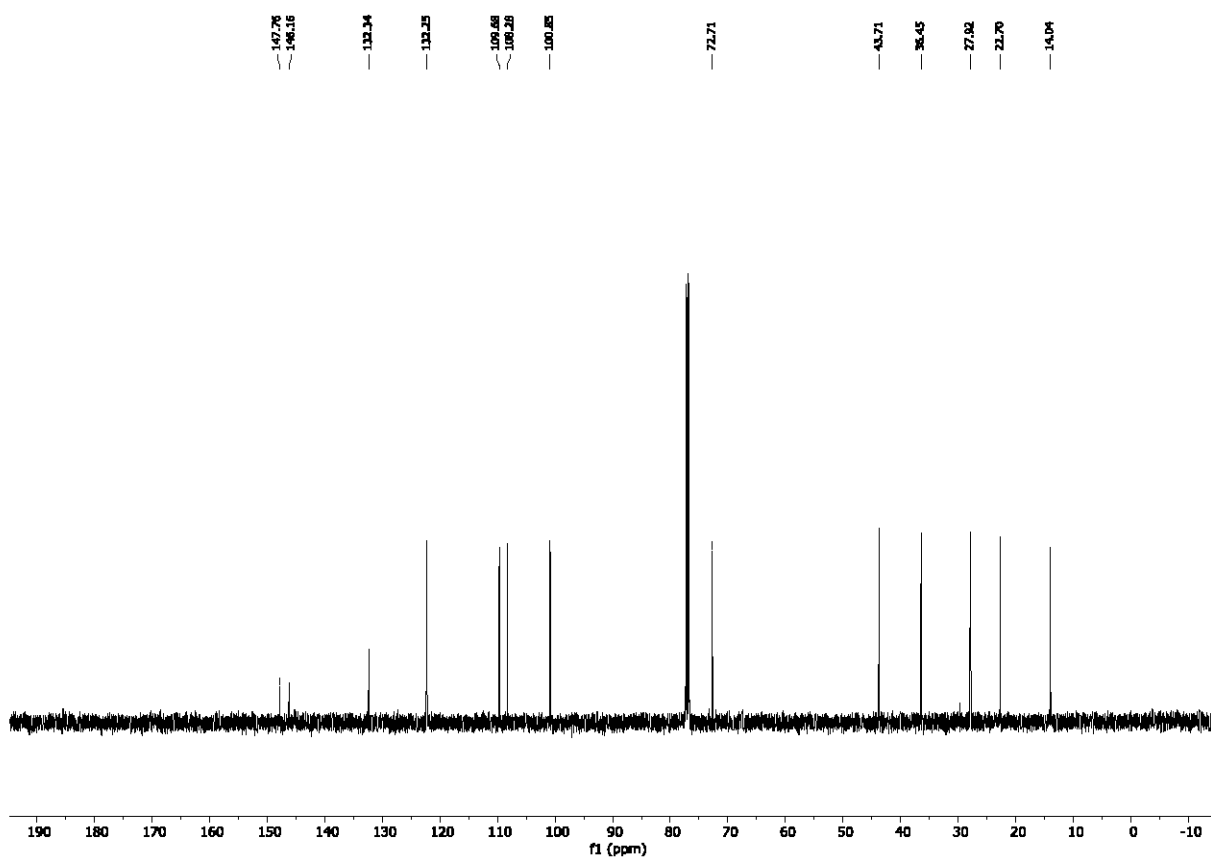
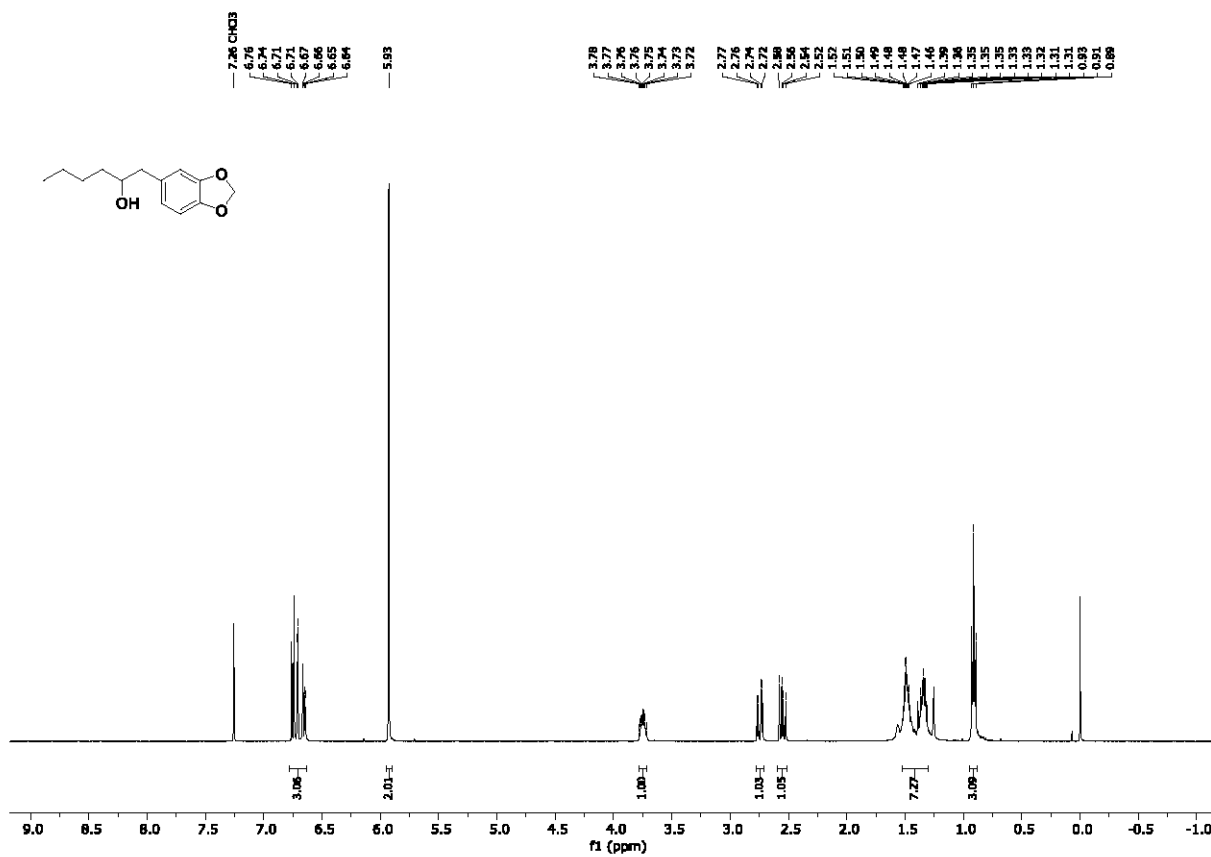
(1*S*,2*R*)-2-(4-tolyl)cyclohexan-1-ol (70a)



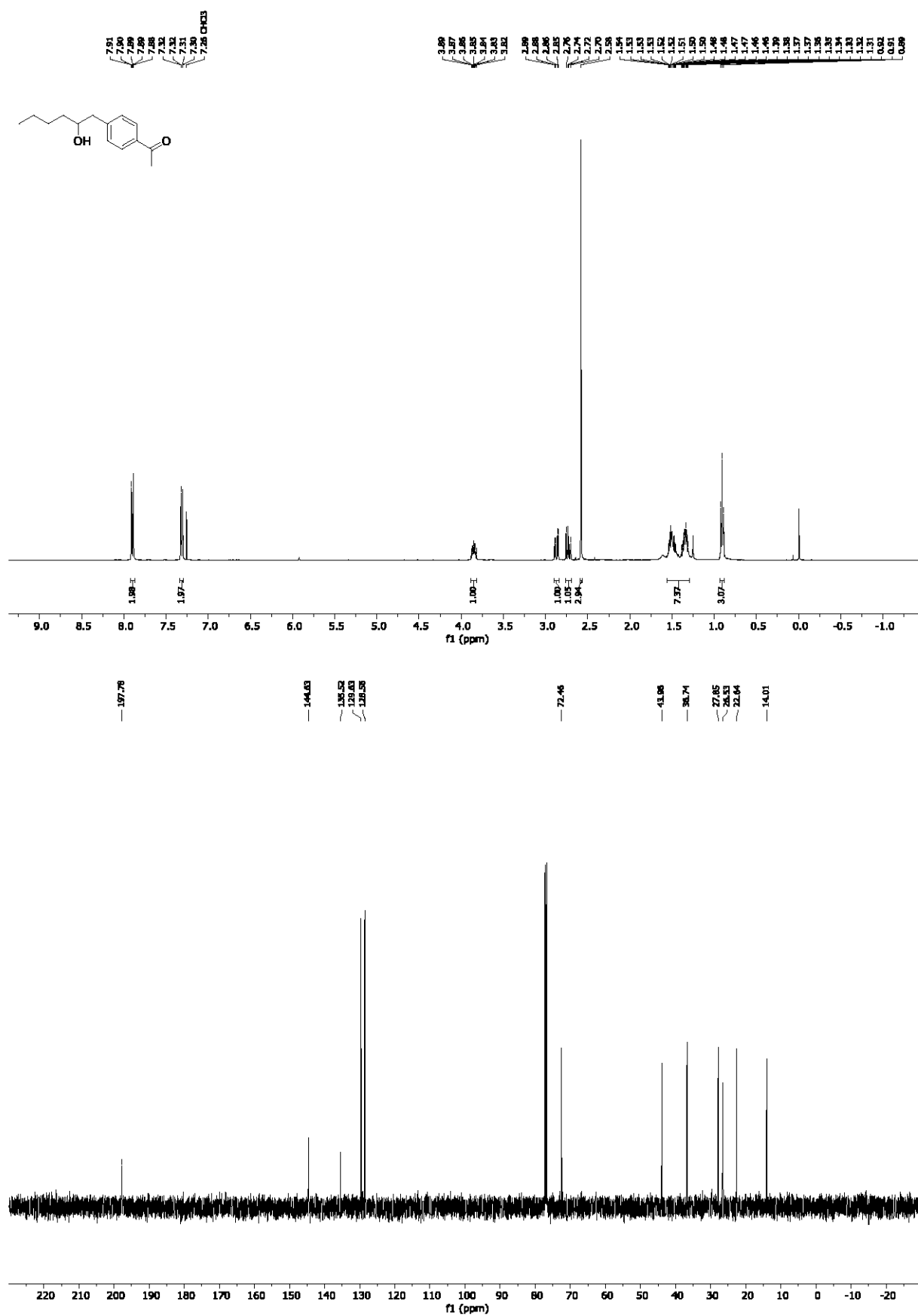
1-(4-chlorophenyl)hexan-2-ol (7hd)



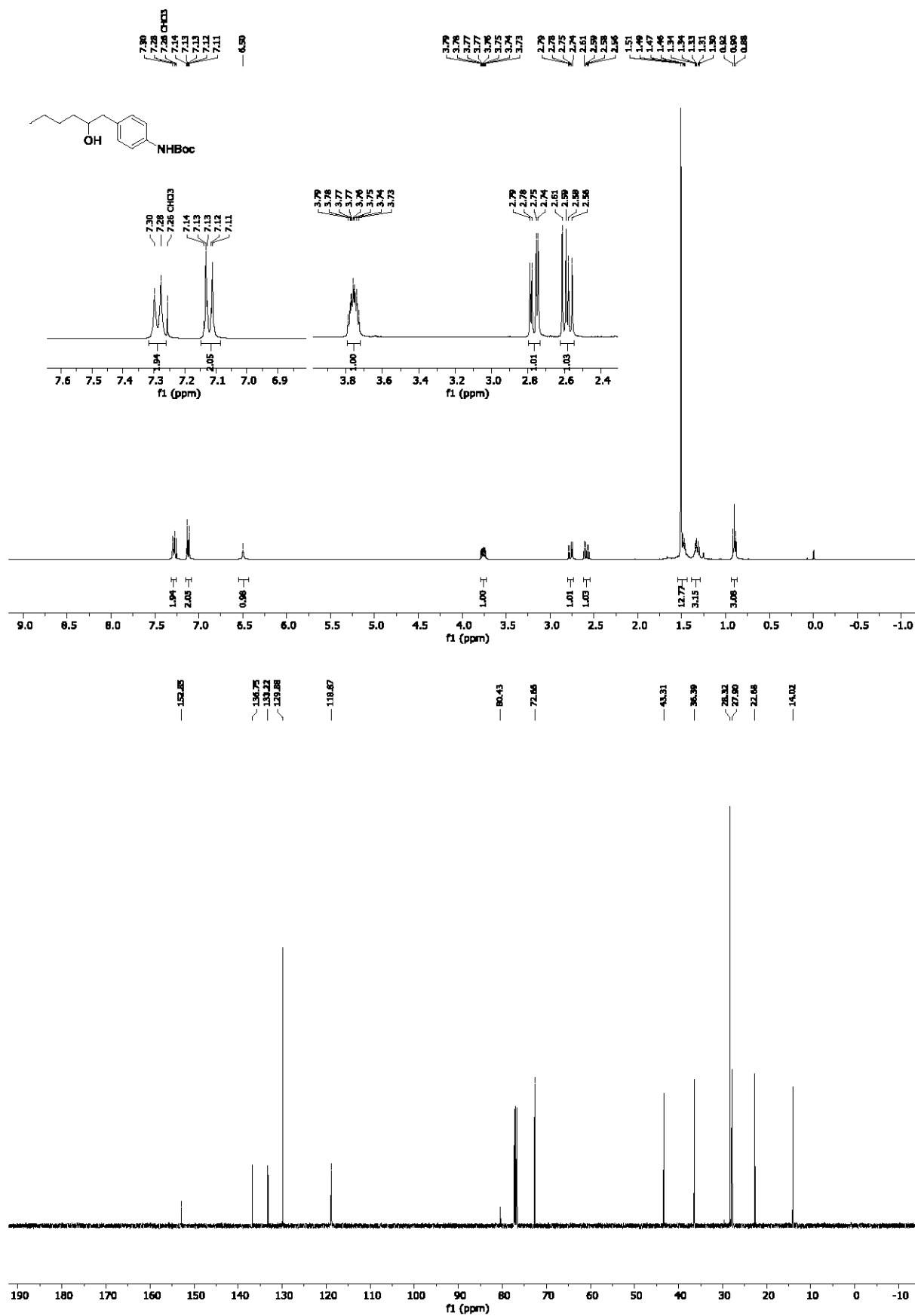
1-(benzo[d][1,3]dioxol-5-yl)hexan-2-ol (7he)



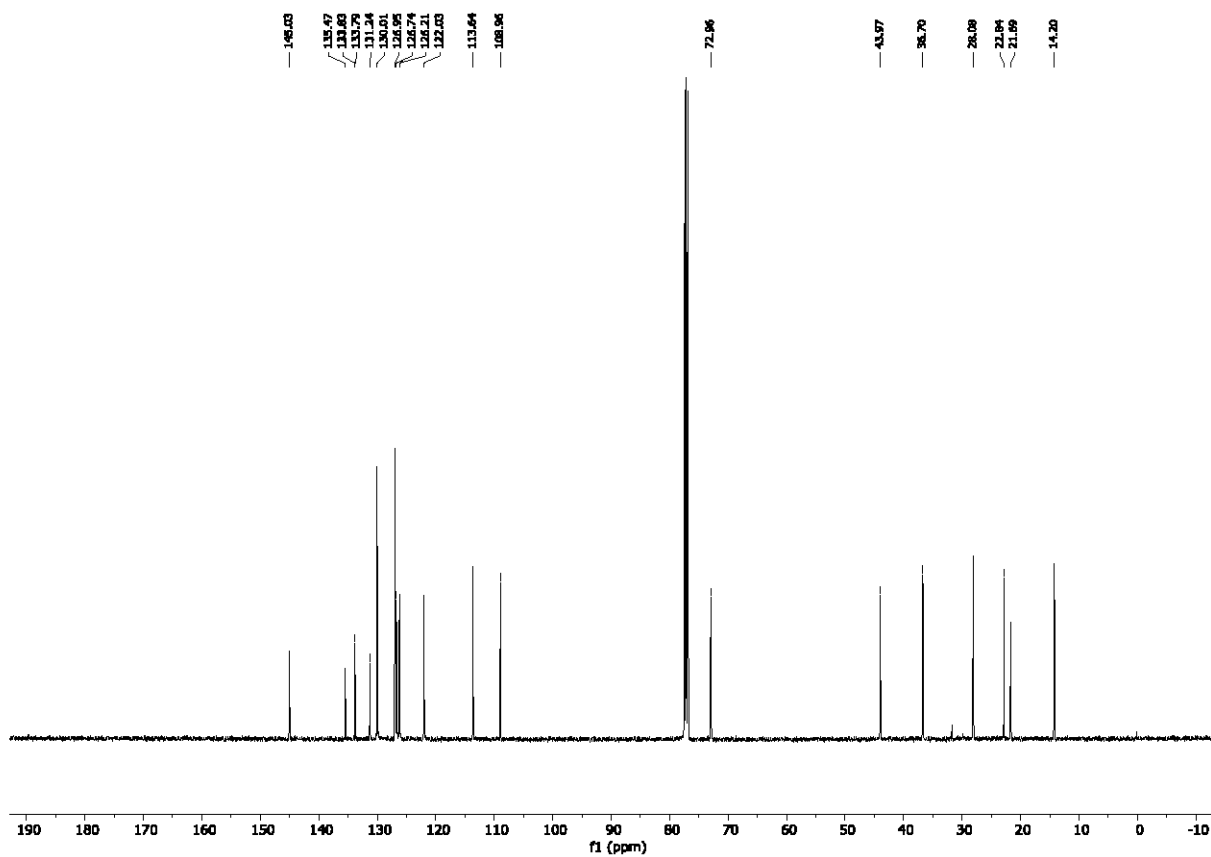
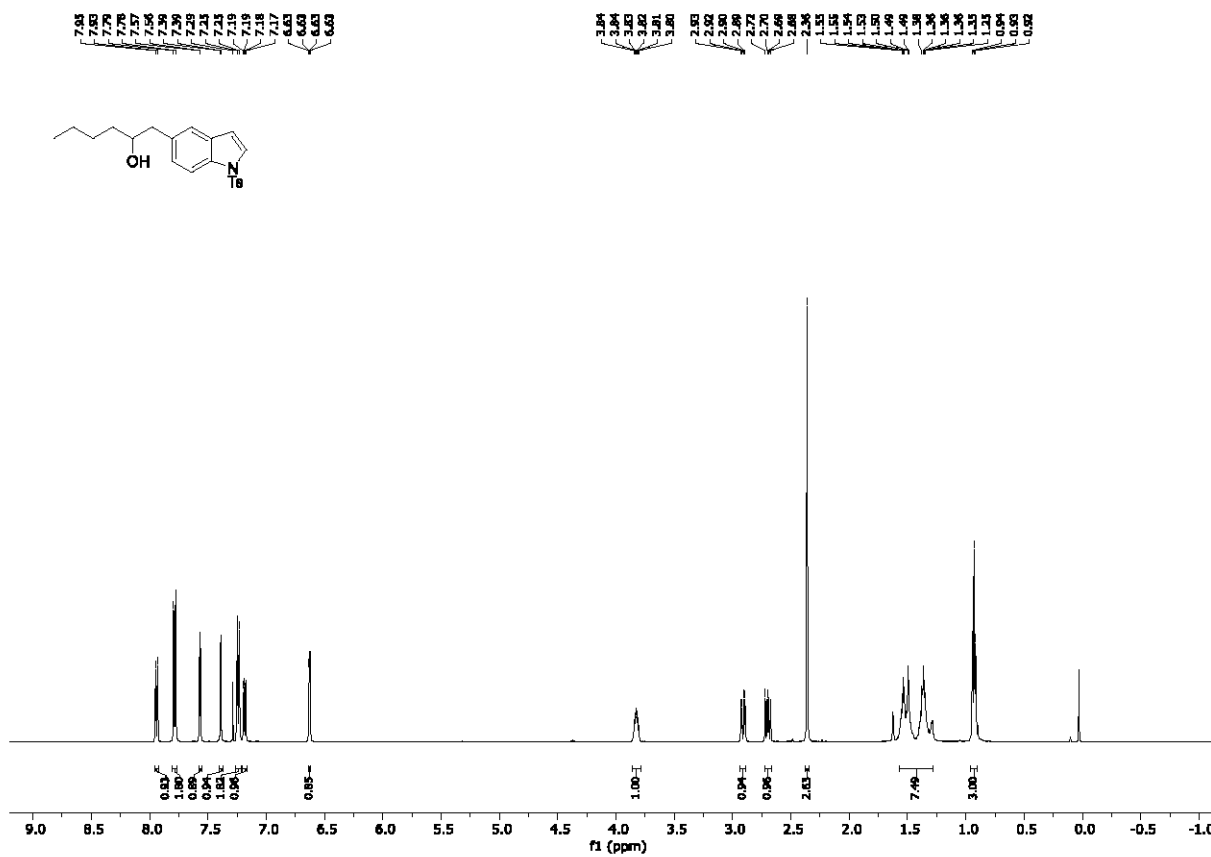
1-(4-(2-hydroxyhexyl)phenyl)ethan-1-one (7hg)



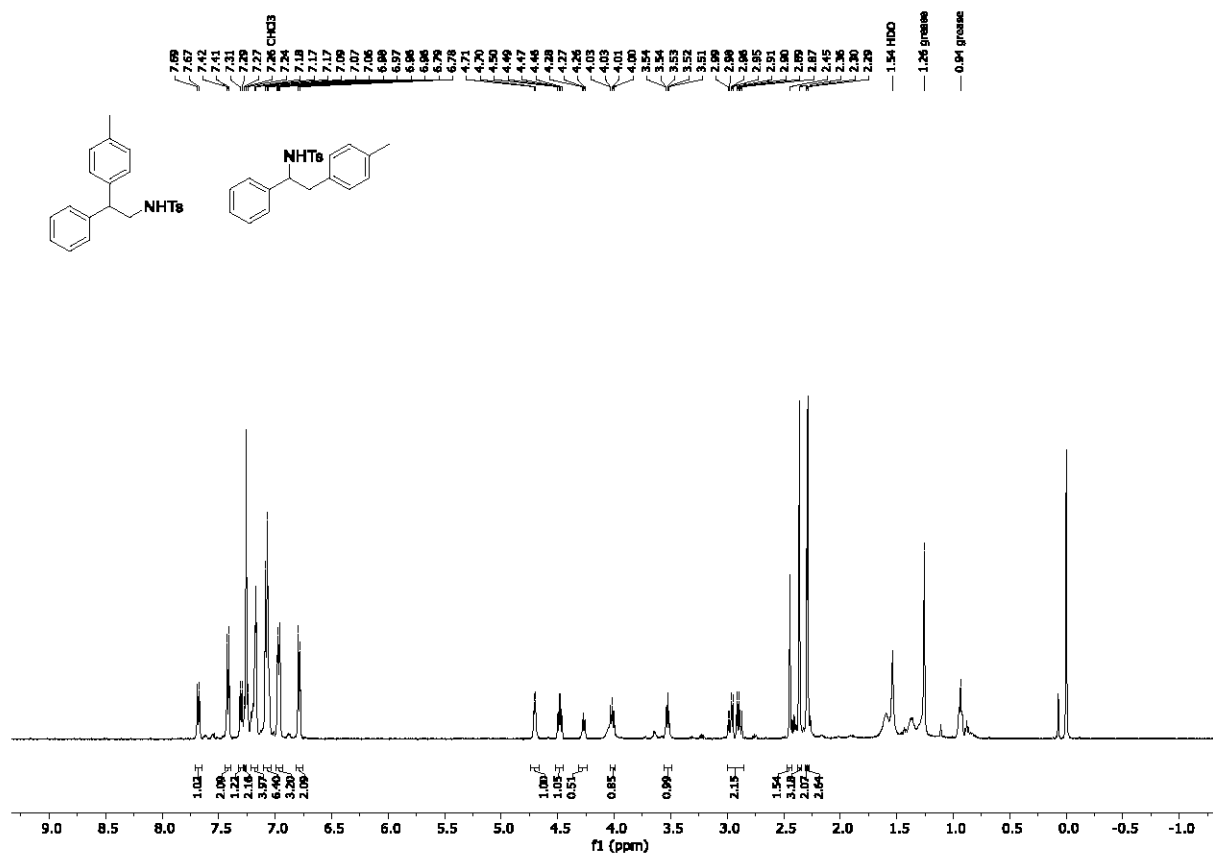
tert-butyl (4-(2-hydroxyhexyl)phenyl)carbamate (7hn)



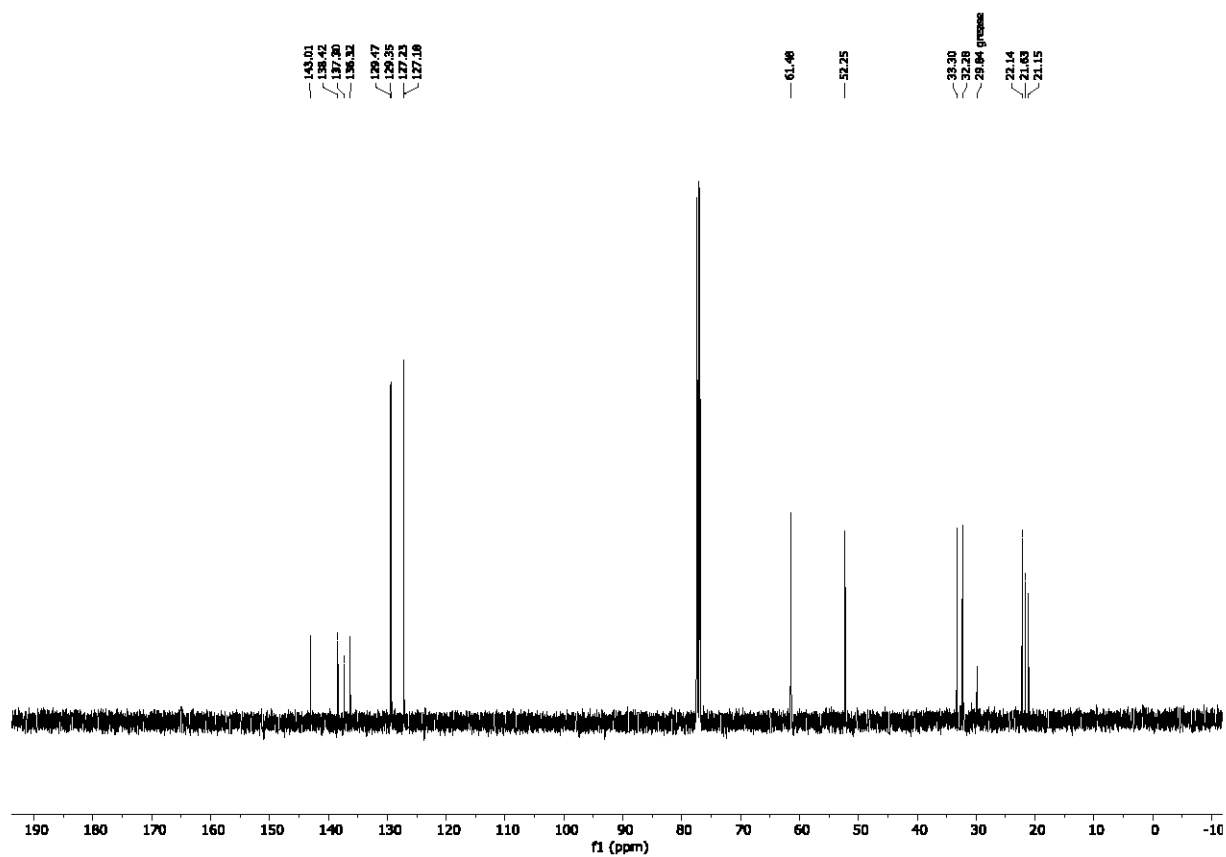
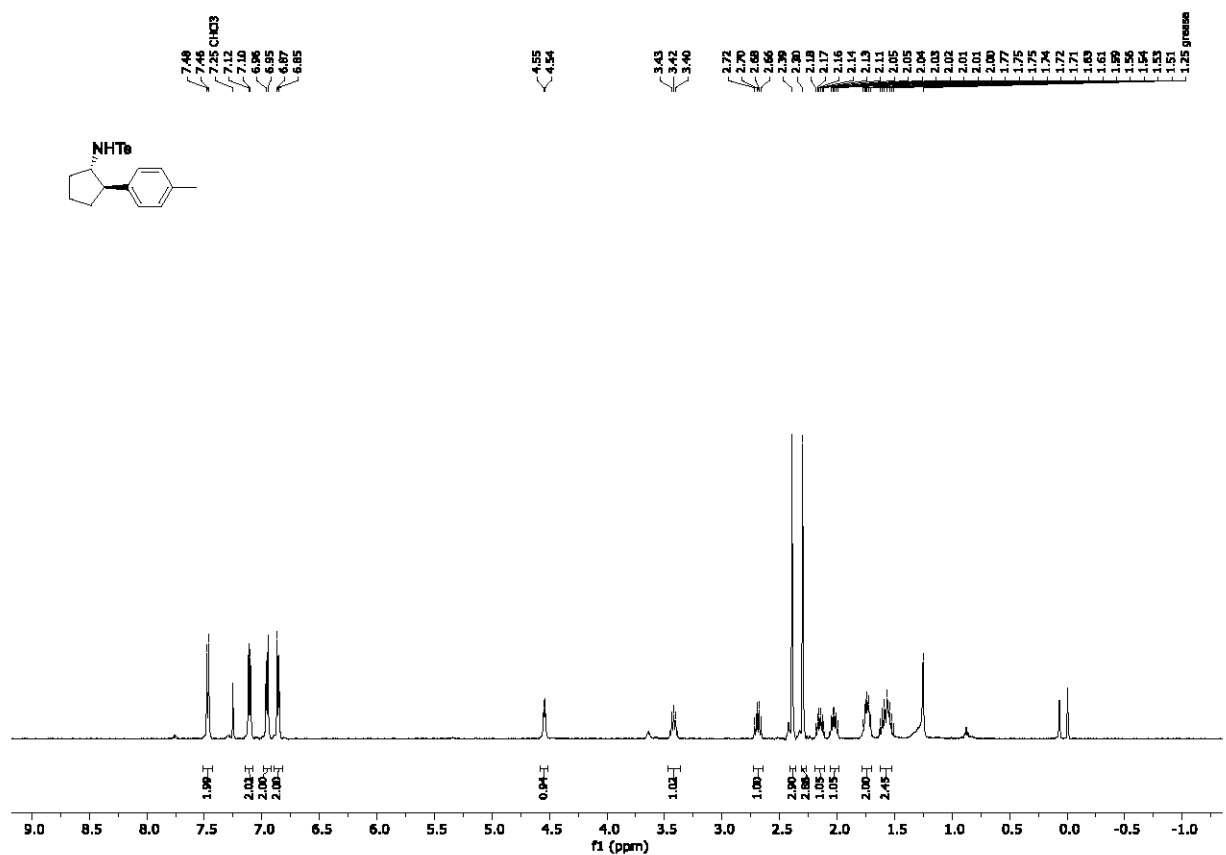
1-(1-tosyl-1*H*-indol-5-yl)hexan-2-ol (7hl)



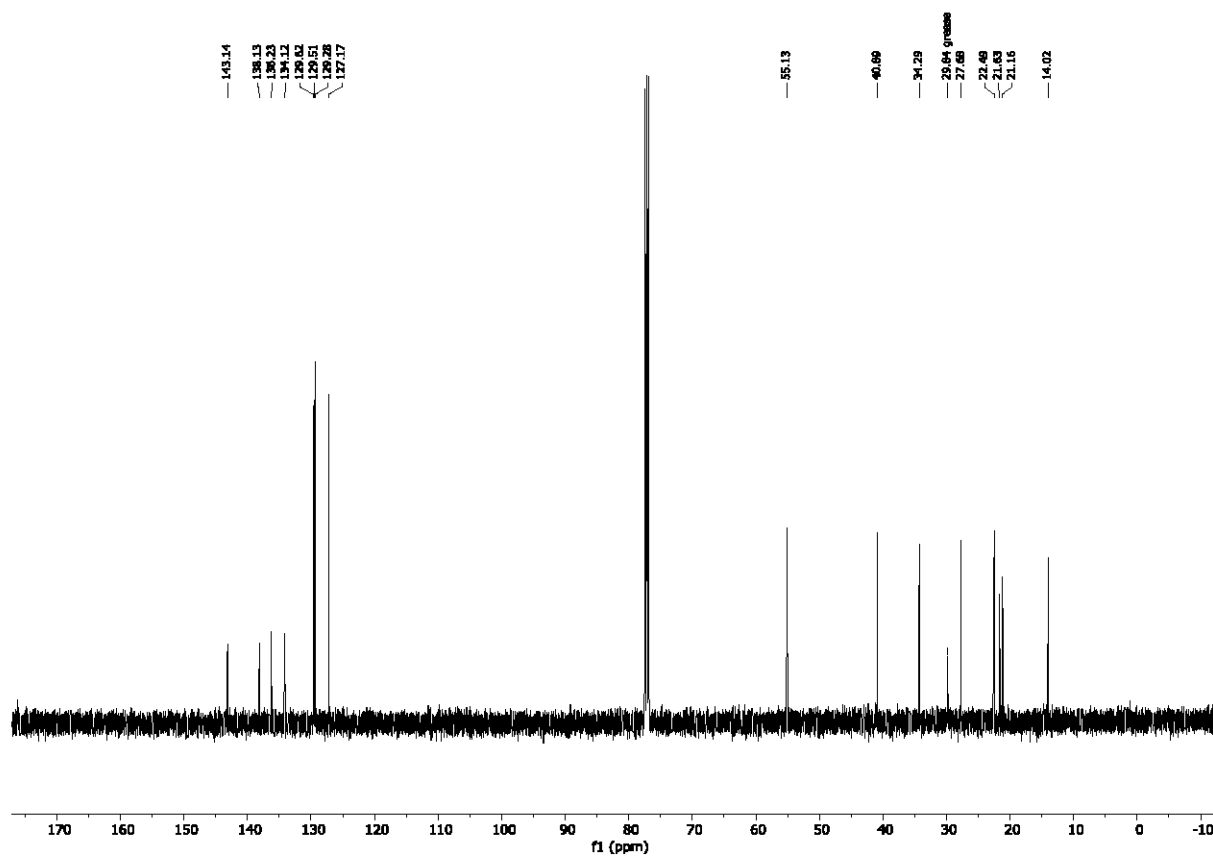
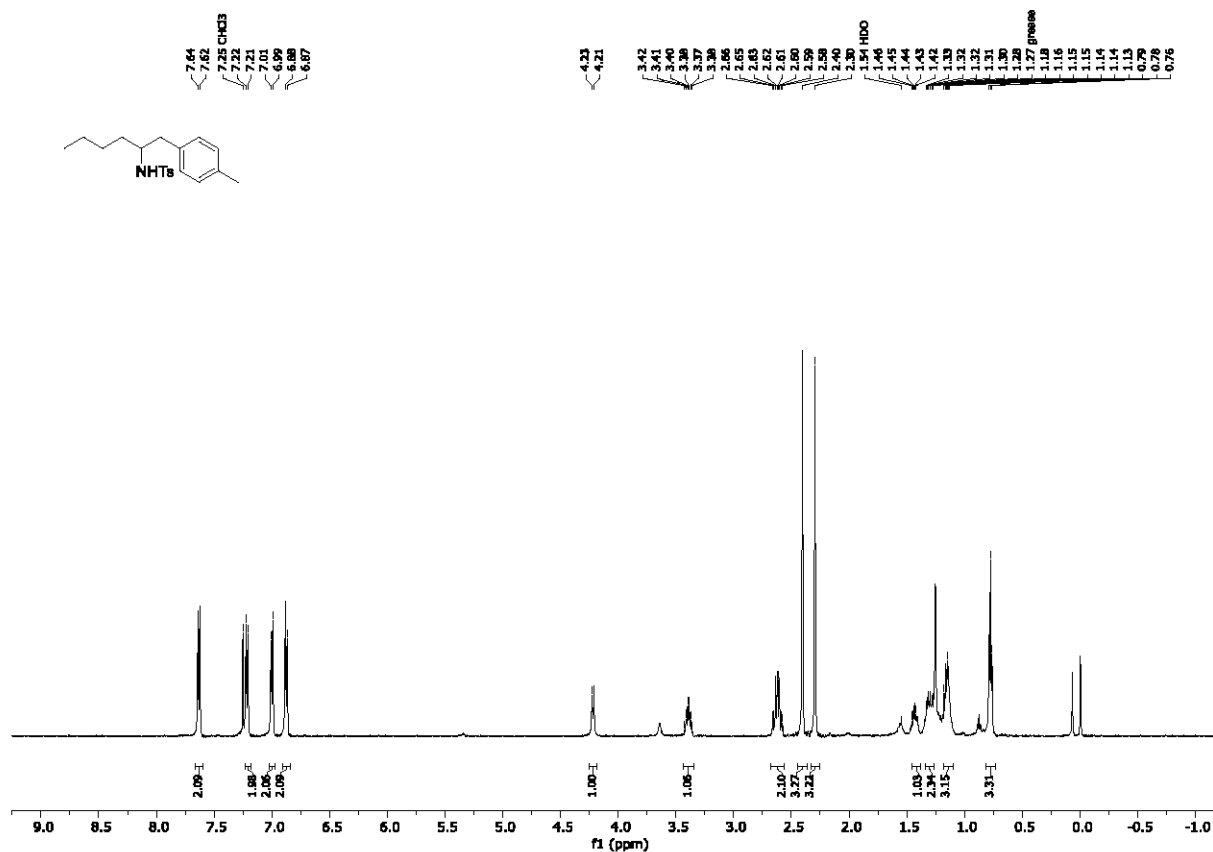
4-methyl-N-(2-phenyl-(*p*-tolyl)ethyl)benzenesulphonamide (S23) and 4-methyl-N-(1-phenyl-2-(*p*-tolyl)ethyl)benzenesulfonamide (S24)



4-methyl-N-(2-(*p*-tolyl)cyclopentyl)benzenesulfonamide (S25)



4-methyl-N-(1-(*p*-tolyl)hexan-2-yl)benzenesulfonamide (S26)



Bioinspired Cobalt-Catalysis Enables Generation of Nucleophilic Radicals from Oxetanes

Aleksandra Potrzęsaj,[‡] Michał Ociepa,[‡] Wojciech Chaładaj,^{*,‡} and Dorota Gryko^{*}



Cite This: <https://doi.org/10.1021/acs.orglett.2c00355>



Read Online

ACCESS |



Metrics & More

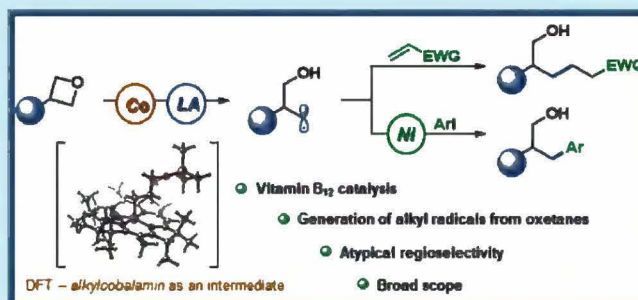


Article Recommendations



Supporting Information

ABSTRACT: Oxetanes are valuable building blocks due to their well-explored propensity to undergo ring-opening reactions with nucleophiles. However, their application as precursors of radical species is still elusive. Herein, we present a bioinspired cobalt-catalysis-based strategy to access unprecedented modes of radical reactivity via oxetane ring-opening. This powerful approach gives access to nucleophilic radicals that engage in reactions with SOMOphiles and low-valent transition metals. Importantly, the regioselectivity of these processes complements known methodologies.



The oxetane moiety is present in many natural compounds and drug molecules. Due to their position as both carbonyl and *gem*-dimethyl group surrogates, oxetanes are important scaffolds in drug discovery (bioisosteres). They are also valuable as C-3 building blocks for the synthesis of highly functionalized organic frameworks.¹

The high ring-strain governs the reactivity of oxetanes facilitating a plethora of transformations; among these, strategies based on breaking the C–O or C–C bonds predominate.^{2a,b} Indeed, the most explored reaction is nucleophilic ring-opening with heteroatom nucleophiles, but there are also a few reports describing their reactions with C-nucleophiles.^{1–6} In addition, oxetanes are a convenient source of α -oxy radicals. The MacMillan group developed an efficient methodology for the deoxygenative arylation of alcohols⁷ and for the α -arylation of ethers, including oxetanes,⁸ while Ravelli et al. demonstrated their photochemical reaction with electron-deficient olefins.⁹ These examples represent radical functionalizations, where the 4-membered ring is preserved.

On the other hand, despite the significant strain energy of the oxetanes (c.a. 106 kJ/mol), their application in radical transformations initiated by opening of strained-ring systems is limited to only few examples. Grimme and Gansäuer developed a Cp₂TiCl-catalyzed system for the generation of γ -titanoxy radicals.¹⁰ The authors however concluded that “ γ -titanoxy radicals are not suitable for efficient formation of C–C bonds”. Similar reactivity was achieved by the Okamoto group in the presence of low-valent titanium alkoxides.¹¹ They also used iron-catalysis to access 3-oxidopropylmagnesium compounds from 2-substituted oxetanes.¹² Although the above transformation likely proceeds via an γ -oxidoradical intermediate, it is immediately intercepted by an iron catalyst, which thus precludes free-radical reactivity. *Despite the immense importance of these seminal contributions, the possibility to access*

various modes of radical reactivity via ring-opening of oxetanes remains challenging.

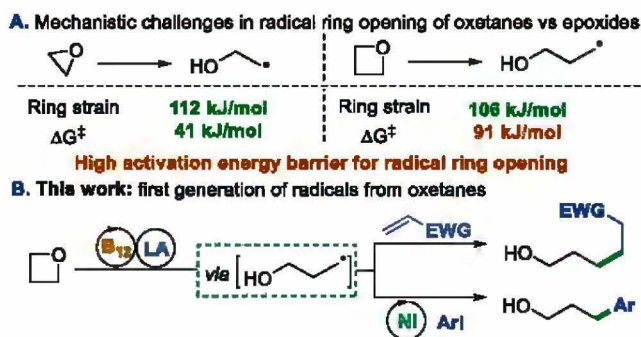
Recently, we have reported a polarity reversal strategy enabling functionalization of strained cycloalkanes¹³ and regioselective ring-opening of epoxides (oxiranes).¹⁴ The crucial step of these processes involves the formation of alkyl cobalamins from vitamin B₁₂ and electrophilic substrates followed by the homolytic cleavage of the Co–C leading to alkyl radicals. Although the strain energies of oxirane (112 kJ/mol) and oxetane (106 kJ/mol) rings are on a similar level, ring-opening of the latter is kinetically unfavorable due to the high activation energy of this process (Scheme 1A).

We envisioned that the merger of cobalt-catalysis with a suitable oxetane’s activation mode should enable the generation of alkyl radicals from oxetanes, by overcoming the challenging kinetics of the ring-opening step (Scheme 1B). Herein, we report a general method that give access to nucleophilic C-centered radicals from oxetanes in the bioinspired vitamin B₁₂-catalyzed ring-opening reaction and its application in both Ni-catalyzed cross-electrophile coupling and the Giese-type addition.

Nucleophilic radicals engage in cross-electrophile coupling with aryl halides via cooperative Co/Ni-catalysis.^{15–17} We hypothesize that radicals generated from oxetanes should react in a similar manner. To this end, our experimental investigations began with the conditions developed for

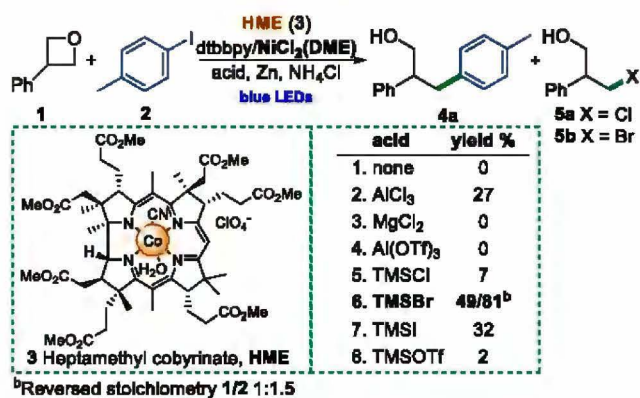
Received: February 1, 2022

Scheme 1. Radical Ring-Opening of Strained Ethers



epoxides.¹⁴ The model reaction of oxetane (1) with aryl iodide (2) did not however lead to desired product 4a (Scheme 2).

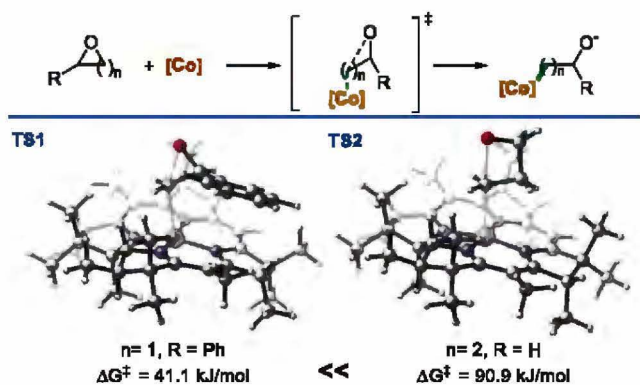
Scheme 2. Influence of Acids on the Co/Ni Cross-Electrophile Coupling of Oxetane 1 with Aryl Iodide 2



DFT calculations revealed that the free Gibbs energy for the ring-opening of oxetanes with the model corrin is substantially higher than the one calculated for the generation of radicals from epoxides (Scheme 3).^{18,19}

Due to the Lewis basicity of the oxygen atom, oxetanes are activated by acids making them susceptible toward nucleophiles.^{1,3} However, the use of these reagents, from the standpoint of our catalytic approach, poses several challenges. Hydrophilic vitamin B₁₂ bearing Lewis basic amide groups may undergo side-reactions with acids, hindering its catalytic

Scheme 3. Gibbs Free Energy Barriers for the Opening of Epoxides and Oxetanes with the Co(I)-Corrin complex



activity. Moreover, the activated oxonium cation may be prone to reductive cleavage of the C–O bond. Thus, hydrophobic heptamethyl cobyrinate (3), a vitamin B₁₂ derivative, in combination with various acid additives, was tested in the model reaction (see Scheme 2 and SI). In the presence of Brønsted acids (TFA, *p*TSA), only the reductive ring-opening occurred. In contrast, some Lewis acids promoted the formation of the desired product 4a, but a notable difference in the reactivity was observed depending on the anion of the salt. DFT calculations suggested that the ring-opening of oxetanes that are activated via coordination of AlCl₃ is practically barrierless (see SI). Indeed, in the experiment with AlCl₃, product 4a formed in 27% yield, and halohydrin 5a was observed as a side product, while the use of Al(OTf)₃ led exclusively to the products resulting from the reductive ring-opening. We hypothesized that halohydrin might act as an intermediate. On the basis of further screening of halide-containing Lewis acids, TMSBr proved the most effective activator in promoting the model reaction.

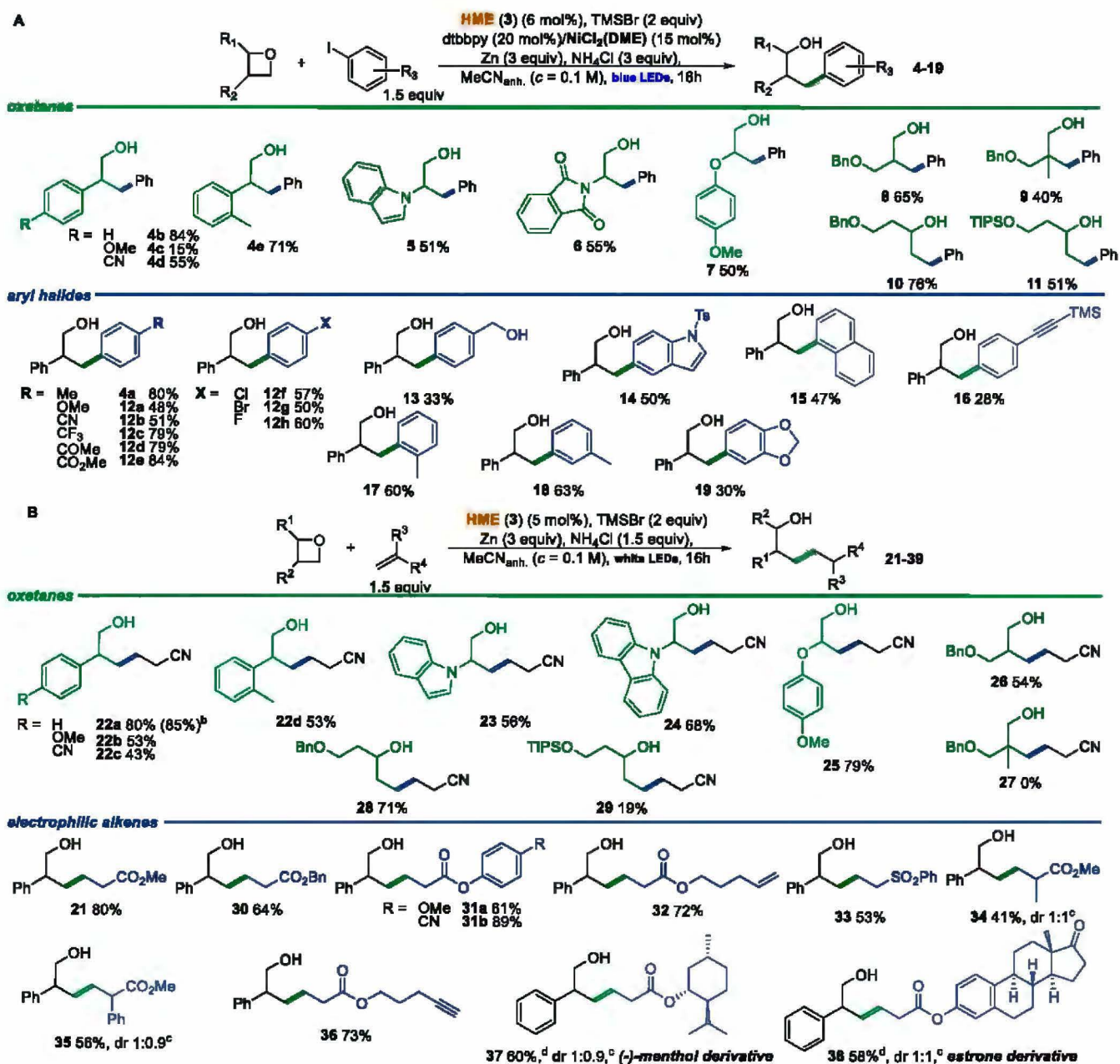
The Zultanski group has recently showed that the use of a Ni/Co dual catalytic system facilitates reaction optimizations as a Ni-catalyst activates aryl halides while Co-catalysis induces the formation of radicals from alkyl halides.²⁰ Consequently, generation of reactive intermediates can be tuned separately. Our in-depth optimization studies revealed that various Ni-complexes catalyze the cross-electrophile ring-opening of oxetane 1 with aryl iodide 2; with NiCl₂(DME) and dtbbpy the yield increased to an appreciable 84% (see SI). To check how the optimization process leveraged the effect of the cobalt catalyst, the model reaction was performed under the optimized conditions but without HME (3). The reaction stopped at the bromohydrin formation step corroborating exclusive generation of alkyl radicals only in the Co-catalytic cycle.

Having identified the optimal reaction conditions, we examined the generality of the developed method (Scheme 4A). Initially, we focused our effort on 3-phenyl-substituted oxetanes of type 1. Oxetanes with an electron-deficient phenyl ring yielded the product while those with an electron-donating substituent did not. In general, various substituents at the C3 position are well-tolerated. Not only aryl and heteroaryl substituents but also protected hydroxy and amino groups can be present at this position. Alkyl groups, on the other hand, can occupy both the C3 and C2 positions giving the corresponding products (8, 10) in 65% and 76% yields, respectively.

Regarding the aryl halide, a wide range of phenyl iodides with both electron-withdrawing and electron-donating substituents at the C-4 position are suitable starting materials (alcohols 12). For more hindered halides, the yield slightly decreased (products 17 and 18). It is worth mentioning that although vitamin B₁₂ is a known catalyst for dehalogenation reactions,^{21,22} for aryl halides bearing Cl and Br this side-reaction was not observed. Electron-rich aryl halides are less reactive in this transformation. It is gratifying that even sensitive 1-iodo-4-(trimethylsilylethynyl)-benzene furnished desired product 16, which can be further used in the sila-Sonogashira–Hagihara coupling.²³

Like the described cross-coupling reaction, alkyl radicals generated from oxetanes should also engage in reactions with SOMOphiles. The model reaction of 3-phenyloxetane (1) with methyl acrylate (20) without any activator did not lead to desired product 21 (Scheme 4B). Not surprisingly, the

Scheme 4. Scope of the Co/Ni-Catalyzed Cross Electrophile of Oxetanes and Aryl Iodides and the Giese Addition of Oxetanes to Electrophilic Alkenes



^aReaction was performed on 0.1 mmol scale. ^bdr determined by ¹³C NMR. ^c(*c* = 0.03 M.) Reactions were quenched with 2 equiv of citric acid, for 11 K₂CO₃ was used.

activation with TMSBr proved also crucial in this case and led to product **21** in 57% yield. Other acids tested were less effective in catalyzing the Giese-type addition (see SI). Further systematic studies on this model reaction identified the optimal conditions under which desired product **21** formed in 80% yield. Irradiation with blue or green light yielded the desired product, though in a diminished 57% and 69% yield, respectively. Other tested cobalt complexes were less effective in catalyzing the model reaction.

The reactivity of oxetanes in the Giese-type addition follows a similar pattern as in the cross-coupling reaction (Scheme 4B). Both EDG and EWG at the 3-phenyl substituent are well-tolerated (for **22b** and **22c**, 53% and 43%, respectively), and

the substitution pattern did not significantly affect the reaction yield. Both *N*-oxetanyl indole and carbazole underwent the reaction effectively giving **23** and **24** in 56% and 68% yields. Furthermore, oxetanes bearing a protected hydroxy group are well-tolerated though the protecting group must be chosen carefully, as silyloxy oxetane furnished product **29** in low yield. C2-alkyl-substituted substrates behaved similarly to oxiranes, and the ring-opening occurred at the less hindered site due to the steric hindrance, a feature characteristic for vitamin B₁₂-catalyzed reactions.¹⁴ These results are however in contrast to reports from Grímme.¹⁰ Both Cp₂TiCl₂-catalyzed reactions predominantly lead to primary alcohols. Thus, our Co-based methodology complements the existing approaches.

A large array of electron-deficient olefins are well-tolerated for the reaction (Scheme 4B). Acrylates provide products in good to excellent yields (**21**, **30–32**, **36**). Esters **32** and **36**, containing a terminal double and triple bond, respectively, are worth mentioning as no reduction was observed at these ends. 1,2-Disubstituted olefins furnish products, though in very low yield. However, the presence of a substituent at the α -position to the ester group does not have a negative impact on the reaction (**34**, **35**). The utility of the developed method was realized when applying it to complex molecules such as an estrone derivative. Due to an issue with solubility, this reaction was performed at a lower concentration, and as a result, the yield of product **38** significantly increased from 28% to 58%.

To gain a better understanding of the developed transformations, mechanistic experiments were performed (see SI). First, control experiments revealed that the cobalt complex, Zn, and light are all crucial for the developed reaction to occur. Second, the radical nature of this process was supported by the complete shutdown of the reaction in the presence of a radical trap (Figure 1A). Third, TMSBr reacts swiftly with oxetanes,

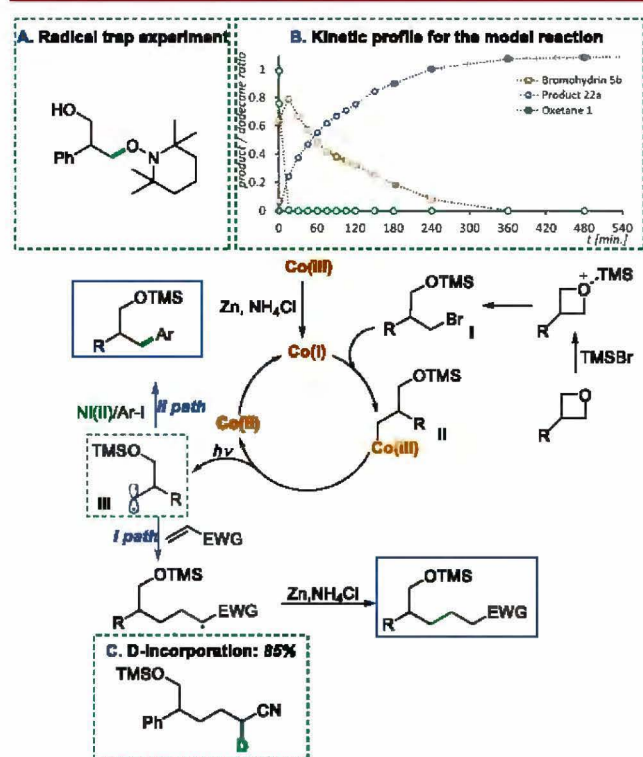


Figure 1. Proposed a mechanism: I path, Giese-type addition; II path, Co/Ni cross coupling.

delivering bromohydrin within 10 min. It has been already reported that the addition of TMSBr to oxetanes gives silylated bromohydrins.²⁴ Thus, although direct reaction of Co(I) with oxetane activated by Lewis acid seems rational and cannot be unambiguously ruled out, the dominant pathway involves TMSBr-mediated formation of bromohydrin, followed by its reaction with low-valent cobalt species. To examine the intermediacy of the bromohydrin, compound **5b** was subjected to the reaction conditions. Product **22a** formed in 77% yield, suggesting that bromohydrin is indeed involved in the catalytic cycle. The kinetic experiments clearly show that the oxetane is fully converted into bromohydrin within the first few minutes, while the product gradually forms over 10 h (Figure 1B). In

addition, the MS analysis also shows the peak corresponding to the alkyl-cobalt complex. Furthermore, the model reaction performed with deuterated reagents (ND₄Cl) showed deuterium-incorporation only at the α -position to the electron-withdrawing group originating from the olefin. This indicates the formation of an anion at this position.

On the basis of our mechanistic considerations and DFT calculations (see SI), we proposed the key steps in the developed transformations (Figure 1). First, oxetane undergoes exergonic ring-opening with TMSBr ($\Delta G = -51.4$ kJ/mol). The resulting silyl ether of γ -bromohydrin enters a facile reaction with the nucleophilic Co(I) complex through a S_N2 manifold^{25,26} ($\Delta G^\ddagger = 29.4$ kJ/mol), giving rise to a Co(III)-alkyl intermediate **II**, featuring a relatively weak Co–C(sp³). This species is photoactive in the visible region, which can trigger a homolytic cleavage of the Co–C bond providing alkyl radical **III** and the Co(II) complex. As proposed by Kozłowski, photodissociation proceeds presumably from the first electronically excited state (S₁) through the generation of a singlet radical pair. The generated radical **III** either is trapped by an electron-deficient olefin or enters the Ni-catalytic cycle.

Herein, we described the vitamin B₁₂ assisted generation of C-centered alkyl radicals from oxetanes via an alkylated cobalt complex. Subsequent, light-induced homolysis of the Co–C bond yields radical species that engage in reactions with SOMOphiles and low-valent transition metal complexes. Thus, this useful C3 synthon can now be employed in various radical reactions such as Giese addition and cross-electrophile coupling. Both reactions tolerate a broad range of starting materials with different functional groups. The unique regioselectivity of the developed reaction complements the existing strategies; here, the less substituted C2 carbon atom is functionalized. These examples suggest that bioinspired Co-catalysis will enable other radical transformations of oxetanes to be developed.

Ultimately, we believe that the reported bioinspired activation mode for the generation of C-centered radicals opens new opportunities in radical chemistry of oxetanes and will enable broader application of this valuable C3 synthon in the construction of complex molecules.

ASSOCIATED CONTENT

Supporting Information

The Supporting Information is available free of charge at <https://pubs.acs.org/doi/10.1021/acs.orglett.2c00355>.

Experimental details and procedures, optimization studies, mechanistic experiments, and spectral data for all new compounds (PDF)

AUTHOR INFORMATION

Corresponding Authors

Dorota Gryko – Institute of Organic Chemistry Polish Academy of Sciences, 01-224 Warsaw, Poland; orcid.org/0000-0002-5197-4222; Email: dorota.gryko@icho.edu.pl
Wojciech Chaladaj – Institute of Organic Chemistry Polish Academy of Sciences, 01-224 Warsaw, Poland; orcid.org/0000-0001-8143-3788; Email: wojciech.chaladaj@icho.edu.pl

Authors

Aleksandra Potrzęsaj – Institute of Organic Chemistry Polish Academy of Sciences, 01-224 Warsaw, Poland; orcid.org/0000-0003-0549-7792

Michał Ociepa – Institute of Organic Chemistry Polish Academy of Sciences, 01-224 Warsaw, Poland

Complete contact information is available at:

<https://pubs.acs.org/10.1021/acs.orglett.2c00355>

Author Contributions

[‡]A.P. and M.O. contributed equally to this work. W.C. performed DFT calculations.

Notes

The authors declare no competing financial interest.

ACKNOWLEDGMENTS

Financial support for this work was provided by the National Science Foundation (D.G. MAESTRO UMO-2020/38/A/ST4/00185) and the Foundation for Polish Sciences (A.P. FNP TEAM POIR.04.04.00–00–4232/17–00, M.O. no. START 64.2020). Calculations have been carried out using resources provided by Wrocław Centre for Networking and Supercomputing (<http://wcss.pl>), grant No. 518.

REFERENCES

- (1) Bull, J. A.; Croft, R. A.; Davis, O. A.; Doran, R.; Morgan, K. F. Oxetanes: Recent Advances in Synthesis, Reactivity, and Medicinal Chemistry. *Chem. Rev.* **2016**, *116*, 12150–12233.
- (2) (a) Sandvoß, A.; Wiest, J. M. Recent Advances in Enantioselective Desymmetrizations of Prochiral Oxetanes. *Chem. - A Eur. J.* **2021**, *27*, 5871–5879. (b) Wang, Z.; Chen, Z.; Sun, J. Catalytic asymmetric nucleophilic openings of 3-substituted oxetanes. *Org. Biomol. Chem.* **2014**, *12*, 6028–6032.
- (3) Huang, H.; Zhang, T.; Sun, J.; Mild, C. C–C Bond Formation via Lewis Acid Catalyzed Oxetane Ring Opening with Soft Carbon Nucleophiles. *Angew. Chem. Int. Ed.* **2021**, *60*, 2668–2673.
- (4) Yang, W.; Wang, Z.; Sun, J. Enantioselective Oxetane Ring Opening with Chloride: Unusual Use of Wet Molecular Sieves for the Controlled Release of HCl. *Angew. Chem. Int. Ed.* **2016**, *55*, 6954–6958.
- (5) Wang, Z.; Chen, Z.; Sun, J. Catalytic Enantioselective Intermolecular Desymmetrization of 3-Substituted Oxetanes. *Angew. Chem. Int. Ed.* **2013**, *52*, 6685–6688.
- (6) Strassfeld, D. A.; Wickens, Z. K.; Picazo, E.; Jacobsen, E. N. Highly Enantioselective, Hydrogen-Bond-Donor Catalyzed Additions to Oxetanes. *J. Am. Chem. Soc.* **2020**, *142*, 9175–9180.
- (7) Dong, Z.; MacMillan, D. W. C. Metallaphotoredox-Enabled Deoxygenative Arylation of Alcohols. *Nature* **2021**, *598*, 451–456.
- (8) Jin, J.; MacMillan, D. W. C. Direct α -Arylation of Ethers through the Combination of Photoredox-Mediated C–H Functionalization and the Minisci Reaction. *Angew. Chem. Int. Ed.* **2015**, *54*, 1565–1569.
- (9) Ravelli, D.; Zoccolillo, M.; Mella, M.; Fagnoni, M. Photocatalytic Synthesis of Oxetane Derivatives by Selective C–H Activation. *Adv. Synth. Catal.* **2014**, *356*, 2781–2786.
- (10) Gansäuer, A.; Ndene, N.; Lauterbach, T.; Justicia, J.; Winkler, I.; Mück-Lichtenfeld, C.; Grimme, S. Titanocene Catalyzed Opening of Oxetanes. *Tetrahedron* **2008**, *64*, 11839–11845.
- (11) Takekoshi, N.; Miyashita, K.; Shoji, N.; Okamoto, S. Generation of a Low-Valent Titanium Species from Titanatranne and Its Catalytic Reactions: Radical Ring Opening of Oxetanes. *Adv. Synth. Catal.* **2013**, *355*, 2151–2157.
- (12) Sugiyama, Y. K.; Heigozono, S.; Okamoto, S. Iron-Catalyzed Reductive Magnesiumation of Oxetanes to Generate (3-Oxidopropyl) Magnesium Reagents. *Org. Lett.* **2014**, *16*, 6278–6281.
- (13) Ociepa, M.; Wierzba, A. J.; Turkowska, J.; Gryko, D. Polarity-Reversal Strategy for the Functionalization of Electrophilic Strained Molecules via Light-Driven Cobalt Catalysis. *J. Am. Chem. Soc.* **2020**, *142*, 5355–5361.
- (14) Potrzęsaj, A.; Musiejuk, M.; Chaladaj, W.; Giedyk, M.; Gryko, D. Cobalt Catalyst Determines Regioselectivity in Ring Opening of Epoxides with Aryl Halides. *J. Am. Chem. Soc.* **2021**, *143*, 9368–9376.
- (15) Komeyama, K.; Michiyuki, T.; Osaka, I. Nickel/Cobalt-Catalyzed C(sp³)–C(sp³) Cross-Coupling of Alkyl Halides with Alkyl Tosylates. *ACS Catal.* **2019**, *9*, 9285–9291 and references cited therein.
- (16) Shevick, S. L.; Obradors, C.; Shenvi, R. A. Mechanistic Interrogation of Co/Ni-Dual Catalyzed Hydroarylation. *J. Am. Chem. Soc.* **2018**, *140*, 12056–12068.
- (17) Ackerman, L. K. G.; Anka-Lufford, L. L.; Naodovic, M.; Weix, D. J. Cobalt Co-Catalysis for Cross-Electrophile Coupling: Diaryl-methanes from Benzyl Mesylates and Aryl Halides. *Chem. Sci.* **2015**, *6*, 1115–1119.
- (18) Grimme, S.; Antony, J.; Ehrlich, S.; Krieg, H. A Consistent and Accurate Ab Initio Parametrization of Density Functional Dispersion Correction (DFT-D) for the 94 Elements H–Pu. *J. Chem. Phys.* **2010**, *132*, 154104.
- (19) Marenich, A. V.; Cramer, C. J.; Truhlar, D. G. Universal Solvation Model Based on Solute Electron Density and on a Continuum Model of the Solvent Defined by the Bulk Dielectric Constant and Atomic Surface Tensions. *J. Phys. Chem. B* **2009**, *113*, 6378–6396.
- (20) Charboneau, D. J.; Barth, E. L.; Hazari, N.; Uehling, M. R.; Zultanski, S. L. A Widely Applicable Dual Catalytic System for Cross-Electrophile Coupling Enabled by Mechanistic Studies. *ACS Catal.* **2020**, *10*, 12642–12656.
- (21) Giedyk, M.; Golszewska, K.; Gryko, D. Vitamin B₁₂ Catalysed Reactions. *Chem. Soc. Rev.* **2015**, *44*, 3391–3404.
- (22) Hisaeda, Y.; Tahara, K.; Shimakoshi, H.; Masuko, T. Bioinspired Catalytic Reactions with Vitamin B₁₂ Derivative and Photosensitizers. *Pure Appl. Chem.* **2013**, *85*, 1415–1426.
- (23) Buendia, J.; Darses, B.; Dauban, P. Tandem Catalytic C(sp³)-H Amination/Sila-Sonogashira-Hagihara Coupling Reactions with Iodine Reagents. *Angew. Chem. Int. Ed.* **2015**, *54*, 5697–5701.
- (24) Kricheldorf, H. R.; Mörber, G.; Regel, W. Syntheses of Alkyl Bromides from Ethers and Bromotrimethylsilane. *Synthesis* **1981**, *1981*, 383–384.
- (25) Zhou, D. -L.; Walder, P.; Scheffold, R.; Walder, L. S_N2 or Electron Transfer? A New Technique Discriminates the Mechanisms of Oxidative Addition of Alkyl Halides to Corrinato- and Porphyrinatocobalt(I). *Helv. Chim. Acta* **1992**, *75*, 995–1011.
- (26) Ghosh, A. P.; Lodowski, P.; Chmielowska, A.; Jaworska, M.; Kozłowski, P. M. Elucidating the Mechanism of Cob(I)Alamin Mediated Methylation Reactions by Alkyl Halides: S_N2 or Radical Mechanism? *J. Catal.* **2019**, *376*, 32–43 and references cited therein.

Supporting Information

Bioinspired Co-Catalysis Enables Generation of Nucleophilic Radicals from Oxetanes

Aleksandra Potrząsaj[‡], Michał Ociepa[‡], Wojciech Chaładaj*, Dorota Gryko*

*Institute of Organic Chemistry Polish Academy of Sciences
Kasprzaka 44/52, 01-224 Warsaw, Poland*

e-mail: dorota.gryko@icho.edu.pl

Table of contents

1. General Information	5
2. Setup for photoreactions.....	6
3. Full Optimization of the Co/Ni – catalyzed cross-electrophile coupling Parameters.....	7
3.1 Background experiments	7
3.2 Optimization of the substrates ratio.....	7
3.3 Optimization of a solvent for HME (3) – catalyzed reaction	8
3.4 Concentration of oxetane (1).....	8
3.5 Screening of Lewis acid	9
3.6 Screening of the cobalt catalysts	10
3.7 HME (3) – catalyst loading	10
3.8 Screening of Ni – catalysts.....	11
3.9 Screening of ligands	11
3.10 The influence of Zn and NH ₄ Cl amounts	12
4. Full Optimization of Giese-type addition Parameters	13
4.1 Background experiments	14
4.2 Screening of Lewis acid	14
4.3 The influence of light on the model reaction.....	14
4.4 Optimization of the substrates ratio.....	15
4.5 Screening of the cobalt catalyst.....	15
4.6 HME (3) – catalyst loading	16
4.7 Optimization of the solvent for HME (3) catalyzed reaction	16
4.8 Concentration of oxetane (1).....	16
4.9 The influence of Zn and NH ₄ Cl amounts	16
4.10 The influence of an amount of Lewis acid.....	17
5. General Procedures.....	18
A. General procedure for the Co/Ni-catalyzed cross-electrophile coupling.....	18
B. General procedure for the Giese-type reaction.....	18
5.1 Note	18
5.2 Graphical procedure for the Co/Ni cross-electrophile coupling.....	19
5.3 Graphical procedure for the Giese-type addition	20
6. Scope and characterization of new compounds.....	21
6.1 Substrates.....	21

6.2 Cross-electrophile coupling: oxetanes.....	22
6.3 Cross-electrophile coupling: aryl halides	26
6.4 Giese-type addition: oxetanes.....	32
6.5 Giese-type addition: Michael acceptors	35
7. Mechanistic consideration	40
7.1 Proposed mechanism	40
7.2 Mass spectrometry studies.....	40
7.3 Kinetic studies for the model reaction.....	41
7.4 Reactions with deuterated reagents	42
7.5 Experiment with a radical trap	43
7.6 DFT calculations	43
8. References	64
9. NMR spectra.....	67
triisopropyl(2-(oxetan-2-yl)ethoxy)silane (S14)	67
3-bromo-2-phenyl-propan-1-ol (5b).....	68
2,3-diphenylpropan-1-ol (4b).....	69
4-(1-hydroxy-3-phenylpropan-2-yl)benzotrile (4d).....	70
3-phenyl-2-(<i>o</i> -tolyl)propan-1-ol (4e).....	71
2-(1 <i>H</i> -indol-1-yl)-3-phenylpropan-1-ol (5).....	72
2-(1-hydroxy-3-phenylpropan-2-yl)isoindoline-1,3-dione (6)	73
2-(4-methoxyphenoxy)-3-phenylpropan-1-ol (7)	74
2-benzyl-3-(benzyloxy)propan-1-ol (8).....	75
2-benzyl-3-(benzyloxy)-2-methylpropan-1-ol (9).....	76
1-(benzyloxy)-5-phenylpentan-3-ol (10).....	77
1-phenyl-5-((triisopropylsilyl)oxy)pentan-3-ol (11)	78
2-phenyl-3-(4-methylphenyl)propan-1-ol (4a).....	79
3-(4-methoxyphenyl)-2-phenylpropan-1-ol (12a).....	80
4-(3-hydroxy-2-phenylpropyl)benzotrile (12b).....	81
2-phenyl-3-(4-(trifluoromethyl)phenyl)propan-1-ol (12c).....	82
1-(4-(3-hydroxy-2-phenylpropyl)phenyl)ethanone (12d)	84
methyl 4-(3-hydroxy-2-phenylpropyl)benzoate (12e).....	85
3-(4-chlorophenyl)-2-phenylpropan-1-ol (12f)	86
3-(4-bromophenyl)-2-phenylpropan-1-ol (12g)	87
3-(4-fluorophenyl)-2-phenylpropan-1-ol (12h).....	88

3-(4-(hydroxymethyl)phenyl)-2-phenylpropan-1-ol (13).....	90
2-phenyl-3-(1-tosyl-1 <i>H</i> -indol-5-yl)propan-1-ol (14)	91
3-(naphthalen-1-yl)-2-phenylpropan-1-ol (15).....	92
2-phenyl-3-(4-((trimethylsilyl)ethynyl)phenyl)propan-1-ol (16)	93
2-phenyl-3-(2-methylphenyl)propan-1-ol (17).....	94
2-phenyl-3-(3-methylphenyl)propan-1-ol (18).....	95
3-(benzo[<i>d</i>][1,3]dioxol-5-yl)-2-phenylpropan-1-ol (19)	96
6-hydroxy-5-phenylhexanenitrile (22a)	97
6-hydroxy-5-(4-methoxyphenyl)hexanenitrile (22b)	98
4-(5-cyano-1-hydroxypentan-2-yl)benzonitrile (22c)	99
6-hydroxy-5-(2-methylphenyl)hexanenitrile (22d).....	100
6-hydroxy-5-(1 <i>H</i> -indol-1-yl)hexanenitrile (23)	101
5-(9 <i>H</i> -carbazol-9-yl)-6-hydroxyhexanenitrile (24)	102
6-hydroxy-5-(4-methoxyphenoxy)hexanenitrile (25).....	103
6-(benzyloxy)-5-(hydroxymethyl)hexanenitrile (26)	104
8-(benzyloxy)-6-hydroxyoctanenitrile (28).....	105
6-hydroxy-8-((triisopropylsilyl)oxy)octanenitrile (29)	106
methyl 6-hydroxy-5-phenylhexanoate (21).....	107
benzyl 6-hydroxy-5-phenylhexanoate (30)	108
4-methoxyphenyl 6-hydroxy-5-phenylhexanoate (31a).....	109
4-cyanophenyl 6-hydroxy-5-phenylhexanoate (31b)	110
pent-4-en-1-yl 6-hydroxy-5-phenylhexanoate (32).....	111
2-phenyl-5-(phenylsulfonyl)pentan-1-ol (33)	112
methyl 6-hydroxy-2-methyl-5-phenylhexanoate (34).....	113
methyl 6-hydroxy-2,5-diphenylhexanoate (35).....	114
pent-4-yn-1-yl 6-hydroxy-5-phenylhexanoate (36).....	115
(1 <i>R</i> ,2 <i>S</i> ,5 <i>R</i>)-2-isopropyl-5-methylcyclohexyl 6-hydroxy-5-phenylhexanoate (37).....	116
(8 <i>R</i> ,9 <i>S</i> ,13 <i>S</i> ,14 <i>S</i>)-13-methyl-17-oxo-7,8,9,11,12,13,14,15,16,17-decahydro-6 <i>H</i> - cyclopenta[<i>a</i>]phenanthren-3-yl 6-hydroxy-5-phenylhexanoate (38).....	117

1. General Information

General Procedures. Unless otherwise noted, reactions were performed without the exclusion of air or moisture. All the photochemical reactions were performed in 10 mL glass vials sealed with a rubber septum. Reactions were monitored by gas chromatography (GC, specification below) or thin-layer chromatography (TLC) on Merck silica gel (GF254, 0.20 mm thickness), visualizing with UV-light, potassium permanganate (KMnO₄), or ceric ammonium molybdate (CAM)/Hanessian's stain. Column chromatography was performed using Merck silica gel 60 (230-400 mesh). GC yields were using dodecane as an internal standard.

Materials. Commercial reagents and solvents were purchased from Sigma-Aldrich, Acros Organics, Alfa Aesar, Fluorochem, and TCI, and used as received unless otherwise noted. Dry solvents: dimethyl sulfoxide (DMSO), dichloromethane (CH₂Cl₂), tetrahydrofuran (THF), acetonitrile (CH₃CN) were taken from the *Solvent Purification System* (SPS). Deuterated solvents (CDCl₃ and CD₃CN) were purchased from Eurisotop. Substrates: 3-phenyloxetane (**1**)¹, 3-(4-methoxyphenyl)oxetane², 4-(oxetan-3-yl)benzotrile¹, 3-(2-methylphenyl)oxetane², 1-(oxetan-3-yl)-1H-indole³, 9-(oxetan-3-yl)-9H-carbazole³, 3-(4-methoxyphenoxy)oxetane³, 3-((benzyloxy)methyl)oxetane¹, 2-(2-(benzyloxy)ethyl)oxetane⁴, 2-(oxetan-3-yl)isoindoline-1,3-dione¹, 3-methyl-3-(3-phenyl-2-oxapropyl)oxetane¹, 3-methyl-3-(3-phenyl-2-oxapropyl)oxetane¹ and catalysts: NiCl₂(dtbbpy)⁵, (CN)(H₂O)Cby(OMe)₇ (**3**)⁶, were synthesized according to literature procedures.

Before the use, zinc was activated by the following method: a) washing with 10% HCl, b) grinding, c) washing with H₂O, EtOH, and Et₂O, d) drying in a vacuum.⁶

Instrumentation.

- **NMR Spectroscopy:** ¹H and ¹³C NMR spectra were recorded at 25 °C on a Bruker 400 MHz, 500 MHz or Varian 600 MHz instrument with TMS as an internal standard. NMR chemical shifts are reported in ppm and referenced to the residual solvent peak of CDCl₃ (7.26 ppm - ¹H NMR and 77.16 ppm - ¹³C NMR). Multiplicities are indicated by singlet (s), doublet (d), triplet (t), quartet (q), multiplet (m) and broad (br). Coupling constants (*J*) are reported in Hertz. All data analysis was performed using MestReNova software package.
- **GC/MS Chromatography:** GC-MS analyses were performed using Shimadzu GCMS-QP2010 SE gas chromatograph with FID detector and Zebron ZB 5MSi column.
- **High Resolution Mass Spectrometry:** High-resolution mass spectra (HRMS) were recorded on a Waters AutoSpec Premier instrument using electron ionization (EI) or a Waters SYNAPT G2-S HDMS instrument using electrospray ionization (ESI) with time-of-flight detector (TOF).
- **Low Resolution Mass Spectrometry:** Low-resolution mass spectra (LRMS) were recorded on an Applied Biosystems API 365 mass spectrometer using electrospray ionization (ESI) technique.
- **Melting points:** Melting points were recorded on a Marienfeld MPM-H2 melting point apparatus and are uncorrected.
- **Preparative HPLC:** Preparative HPLC separations were performed using Knauer HPLC chromatograph with PDA detector and Preparative column chromatography Knauer EII 100-10 Si column (250 x 20 mm).

2. Setup for photoreactions

Reactions were performed in a homemade photoreactor comprised of a 400 mL beaker with the inside covered with LED tape (Figure S1). A cooling fan with adjustable spin rate was used to maintain ambient temperature inside the photoreactor.

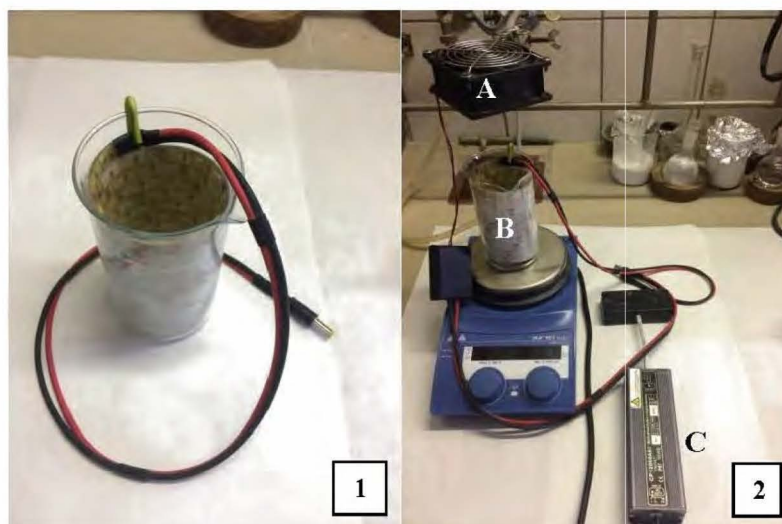


Figure S1 (1) The photoreactor; (2) Assembled photoreaction setup: A – cooling fan, B – photoreactor, C – 12 V power supply module for photoreactor and fan.

LED tapes characteristics:

Blue LED tape: 8 mm SMD3528 LED strip, 60 LED diodes/m

Power consumption: 4.8 W/m

Blue light: $\lambda_{\max} = 460$ nm, 4.5 lm

Green LED tape: 10 mm SMD5050 LED strip, 60 LED diodes/m

Power consumption: 14.4 W/m

Green light: $\lambda_{\max} = 525$ nm, 20 lm

White LED tape: 8 mm SMD3528 LED strip, 120 LED diodes/m

Power consumption: 9.6 W/m

White light: 6500 K, 30 lm

3. Full Optimization of the Co/Ni – catalyzed cross-electrophile coupling Parameters:

Model reaction:



Reaction conditions: oxetane (**1**) (0.2 mmol, 1 equiv), 4-iodotoluene (**2**) (1.5 equiv), Zn (3 equiv), NH₄Cl (3 equiv), HME (**3**) (6 mol%), NiCl₂(DME) (15 mol%), dtbby (20 mol%), TMSBr (2 equiv), MeCN_{anh} (*c* = 0.1 M), blue LEDs, 16 h; each reaction was quenched by treatment with 2 equiv of citric acid.

Table S1 Background experiments^a

Entry	Deviation from the Initial Conditions	Yield of 4a [%]
1	none	29/26^b
2	no Co-catalyst	5
3	no Ni-catalyst	Product not observed
4	no reducing agent	Product not observed
5	no Lewis acid	Product not observed
6	no light	3
7	MeCN („wet”)	Product not observed
8	Air atmosphere	17

^aReaction conditions: oxetane (**1**) (0.1 mmol, 1 equiv), 4-iodotoluene (**2**) (1.5 equiv), Zn (3 equiv), NH₄Cl (3 equiv), HME (**3**) (5 mol%), NiCl₂(DME) (20 mol%), dtbby (40 mol%), TMSBr (2 equiv), MeCN_{anh} (*c* = 0.1 M), blue LEDs, yields determined by GC, 16 h, ^bIsolated yield.

Table S2 Optimization of the substrates ratio^a

Entry	Oxetane 1 (equiv)	Aryl iodide 2 (equiv)	Yield of 4a [%]
1	1	1.5	29/26 ^b
2	1	3	17
3	1.5	1	27
4	3	1	21

^aReaction conditions: oxetane (**1**), 4-iodotoluene (**2**), Zn (3 equiv), NH₄Cl (3 equiv), HME (**3**) (5 mol%), NiCl₂(DME) (20 mol%), dtbby (40 mol%), TMSBr (2 equiv), MeCN_{anh} (*c* = 0.1 M), blue LEDs, 16 h, yields determined by GC, ^bIsolated yield.

Table S3 Optimization of a solvent for HME (3) – catalyzed reaction^a

Entry	Solvent	Yield of 4a [%]
1	MeCN	27
2	MeOH	0
3	DMF	0
4	DMA	3
5	NMP	0
6	THF	7
7	Ethyl acetate	0
8	Acetone	4
9	DME	16

^aReaction conditions: oxetane (**1**) (1.5 equiv), 4-iodotoluene (**2**) (0.1 mmol, 1.0 equiv), Zn (3 equiv), NH₄Cl (3 equiv), HME (**3**) (5 mol%), NiCl₂(DME) (20 mol%), dtbby (40 mol%), TMSBr (2 equiv), solvent (*c* = 0.1 M), blue LEDs, 16 h, yields determined by GC.

Table S4 Concentration of oxetane (1)^a

Entry	[mol/dm ³]	Yield of 4a [%]
1	0.05	8
2	0.1	27
3	0.2	23

^aReaction conditions: oxetane (**1**) (1.5 equiv), 4-iodotoluene (**2**) (0.1 mmol, 1.0 equiv), Zn (3 equiv), NH₄Cl (3 equiv), HME (**3**) (5 mol%), NiCl₂(DME) (20 mol%), dtbby (40 mol%), TMSBr (2 equiv), MeCN_{anh}, blue LEDs, 16 h, yields determined by GC.

Table S5 Screening of Lewis acid^a

Entry	Lewis acid	Yield of 4a [%]
1	AlCl ₃	27
2	LiBF ₄	0
3	MgCl ₂	0
4	In(OTf) ₃	0
5	Al(OTf) ₃	0
6	Fe(OTf) ₂	0
7	Ga(OTf) ₃	0
8	SnCl ₄	0
9	InI ₃	0
10	TMSCl	7
11	(ETO) ₃ SiCl	0
12	TMSBr	49
13	TMSI	32
14	TMSOTf	2
15^b	TMSBr	81/78^c

^aReaction conditions: oxetane (**1**) (1.5 equiv), 4-iodotoluene (**2**) (0.1 mmol, 1 equiv), Zn (3 equiv), NH₄Cl (3 equiv), HME (**3**) (5 mol%), NiCl₂(DME) (20 mol%), dtbby (40 mol%), Lewis acid (2 equiv), MeCN_{anh} (*c* = 0.1 M), blue LEDs, 16 h.; ^bReversed stoichiometry: **1/2** 1:1.5; yields determined by GC, ^cIsolated yield.

Table S6 Screening of the cobalt catalysts^a

Entry	Co-catalyst	Yield of 4a [%]
1	3	81
2	S1	50
3	S2	29
4	S3	0

^aReaction conditions: oxetane (**1**) (0.1 mmol, 1 equiv), 4-iodotoluene (**2**) (1.5 equiv), Zn (3 equiv), NH₄Cl (3 equiv), Co-catalyst (5 mol%), NiCl₂(DME) (20 mol%), dtbby (40 mol%), TMSBr (2 equiv), MeCN_{anh} (c = 0.1 M), blue LEDs, 16 h, yields determined by GC.

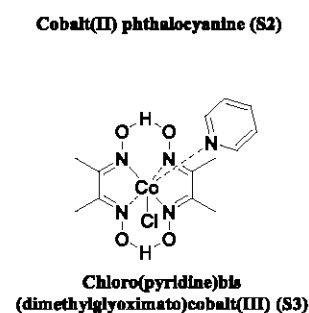
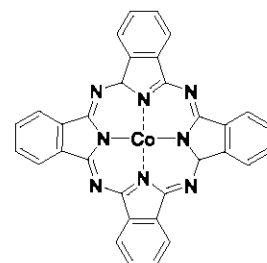
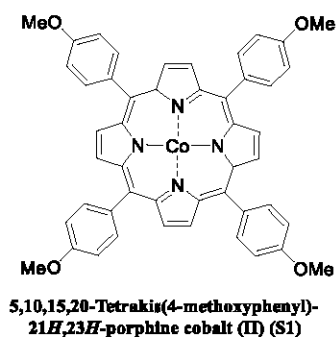
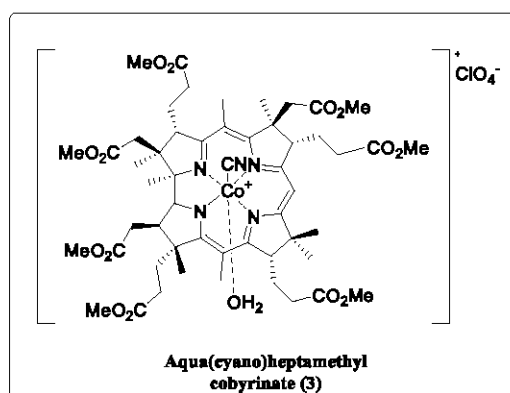


Table S7 HME (**3**) – catalyst loading^a

Entry	Catalyst loading [%]	Yield of 4a [%]
1	2.5	32
2	5	81
3	7.5	25

^aReaction conditions: oxetane (**1**) (0.1 mmol, 1 equiv), 4-iodotoluene (**2**) (1.5 equiv), Zn (3 equiv), HME (**3**), NiCl₂(DME) (20 mol%), dtbby (40 mol%), TMSBr (2 equiv), MeCN_{anh} (c = 0.1 M), blue LEDs, 16 h, yields determined by GC.

Table S8 Screening of Ni – catalysts^a

Entry	Catalyst	Catalyst loading [mol%]	Yield of 4a [%]
1	NiCl ₂ (DME)	20	81/78 ^b
2	NiBr ₂ (DME)	20	66
3	NiBr ₂	20	77
4	NiI ₂	20	56
5	Ni(OTf) ₂	20	76
6	NiCl ₂ (dtbbpy)	20	43
7	NiCl₂(DME)	15	82/80^b
8	NiCl ₂ (DME)	10	78
9	NiCl ₂ (DME)	5	66

^aReaction conditions: oxetane (**1**) (0.1 mmol, 1 equiv), 4-iodotoluene (**2**) (1.5 equiv), Zn (3 equiv), NH₄Cl (3 equiv), HME (**3**) (5 mol%), Ni-catalyst, dtbbpy (40 mol%), TMSBr (2 equiv), MeCN_{anh} (c = 0.1 M), blue LEDs, 16h, yield was determined by GC; ^bIsolated yield.

Screening of ligands^a

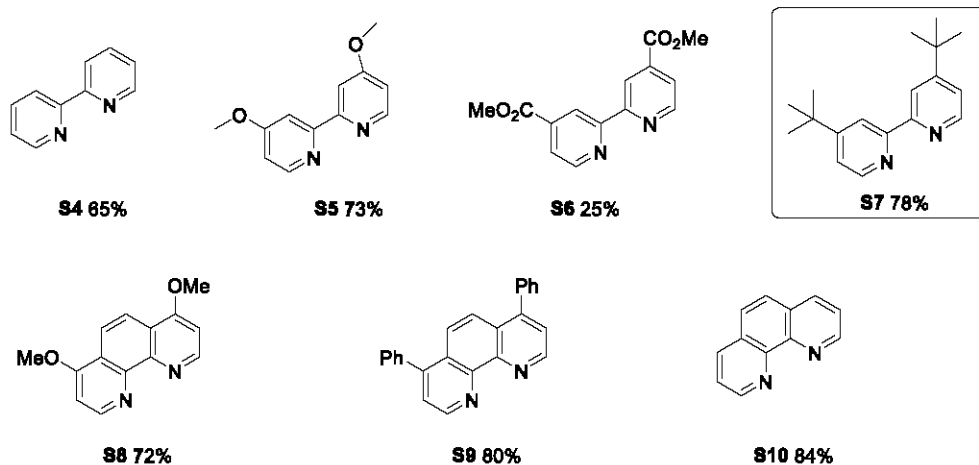


Table S9 The amount of the ligand added:

Entry	Ligand [mol%]	Yield of 4a [%]
1	40	78
2	30	90
3	20	90/87^b
4	15	70

^aReaction conditions: oxetane (**1**) (0.1 mmol, 1 equiv), 4-iodotoluene (**2**) (1.5 equiv), Zn (3 equiv), NH₄Cl (3 equiv), HME (**3**) (5 mol%), NiCl₂(DME) (15 mol%), ligand, TMSBr (2 equiv), MeCN_{anh} (c = 0.1 M), blue LEDs, 16h, yield was determined by GC; ^bIsolated yield.

Table S10 The influence of Zn and NH₄Cl amounts^a

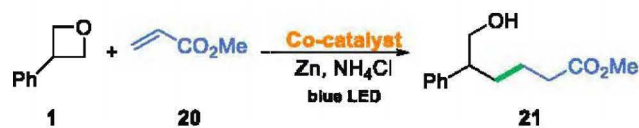
Entry	Zn (equiv)	NH ₄ Cl (equiv)	Yield of 4a [%]
1	3	3	90/87^b
2	4	3	65
3	2	3	33
4	3	1.5	49
5	3	0	23

^aReaction conditions: oxetane (**1**) (0.1 mmol, 1 equiv), 4-iodotoluene (**2**) (1.5 equiv), Zn, NH₄Cl, HME (**3**) (5 mol%), NiCl₂(DME) (15 mol%), dtbbv (20 mol%), TMSBr (2 equiv), MeCN_{anh} (c = 0.1 M), blue LEDs, 16h, yield was determined by GC; ^bIsolated yield.

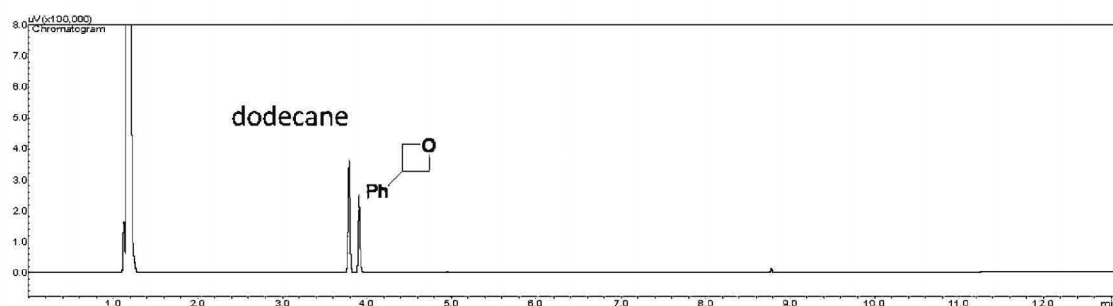
4. Full Optimization of Giese-type addition Parameters

Initial studies:

According to our previous experience with epoxides we decided to conduct the initial experiment with oxetane under the developed conditions.



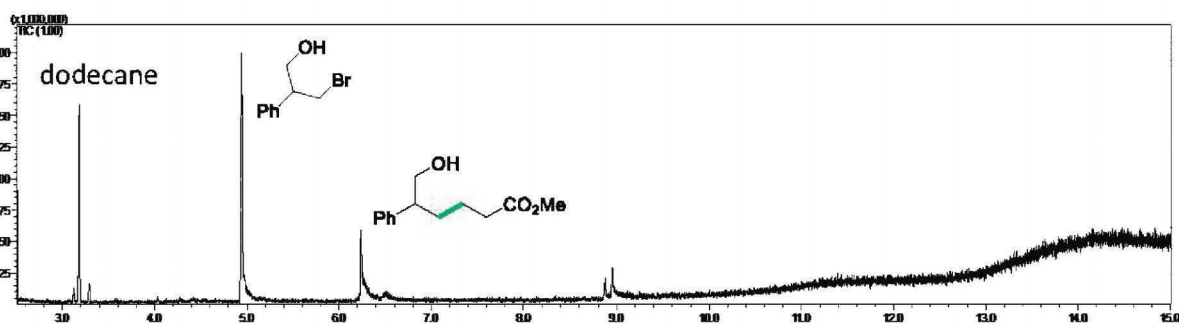
Reaction conditions: oxetane 1 (0.2 mmol, 1 equiv), methyl acrylate (20) (1.5 equiv), Zn (1.5 equiv), NH₄Cl (3 equiv), HME (3) (5 mol%), MeCN_{anh} (c = 0.1 M), blue LEDs (single diode, 10 W), 30 min, dodecane as an internal standard.



The reaction performed utilizing the conditions reported for epoxides conditions does not proceed. The GC chromatogram indicates two peaks which corresponds to dodecane (internal standard) and the unreacted substrate. Thus, the model reaction with the addition of a Lewis acid (TMSBr) was carried out.



Reaction conditions: oxetane (1) (0.2 mmol, 1 equiv), methyl acrylate (20) (1.5 equiv), Zn (1.5 equiv), NH₄Cl (3 equiv), HME (3) (5 mol%), MeCN_{anh} (c = 0.1 M), blue LEDs (single diode, 10 W), 30 min, TMSBr (2 equiv), dodecane as an internal standard.



The reaction with the addition of a Lewis acid affords the desired product. The GC chromatogram shows three peaks which corresponds to dodecane (internal standard), bromohydrin 5b and product 21.

Conclusion: The reaction requires the use of a Lewis acid.

Model reaction:



Reaction conditions: oxetane (**1**) (0.2 mmol, 1 equiv), methyl acrylate (**20**) (1.5 equiv), Zn (3 equiv), NH₄Cl (1.5 equiv), HME (**3**) (5 mol%), MeCN_{anh} (c = 0.1 M), white LEDs, 16 h; each reaction was quenched by treatment with 2 equiv of citric acid.

Table S11 Background experiments^a

Entry	Deviation from the Initial Conditions	Yield of 21 [%]
1	none	59/57^b
2	no Co-catalyst	Product not observed
3	no reducing agent	Product not observed
4	no light	44
5	no light, 30 °C	38
6	MeCN („wet“)	24

^aReaction conditions: oxetane (**1**) (0.1 mmol, 1 equiv), methyl acrylate (**20**) (2 equiv), Zn (3 equiv), NH₄Cl (3 equiv), HME (**3**) (5 mol%), MeCN (c = 0.1 M), blue LEDs, 16 h, yields determined by GC; ^bIsolated yield.

Table S12 Screening of Lewis acid^a

Entry	Lewis acid	Yield of 21 [%]
1	TMSBr	57
2	TMSI	0
3	TMSCl	0
4	AlCl ₃	0
5	ZnOTf	0
6	MgCl ₂	0
7	(EtO) ₃ SiCl	6

^aReaction conditions: oxetane (**1a**) (0.1 mmol, 1 equiv), methyl acrylate (**2a**) (2 equiv), Zn (3 equiv), NH₄Cl (3 equiv), HME (**3**) (5 mol%), Lewis acid (2 equiv), MeCN_{anh} (c = 0.1 M), blue LEDs, 16 h, yields determined by GC; ^bIsolated yield.

Table S13 The influence of light on the model reaction^a

Entry	Light	Yield of 21 [%]
1	Blue LEDs (tape)	57
2	Green LEDs (tape)	65
3	White LEDs (tape)	69

^aReaction conditions: oxetane (**1**) (0.1 mmol, 1 equiv), methyl acrylate (**20**) (2 equiv), Zn (3 equiv), NH₄Cl (3 equiv), HME (**3**) (5 mol%), TMSBr (2 equiv), MeCN_{anh} (c = 0.1 M), 16 h, yields determined by GC.

Table S14 Optimization of the substrates ratio^a

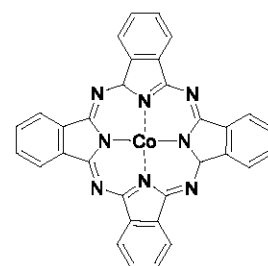
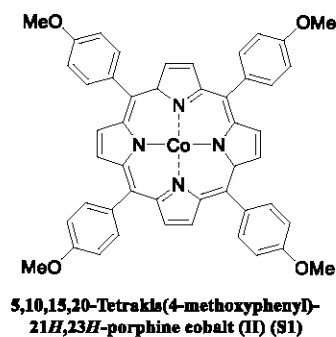
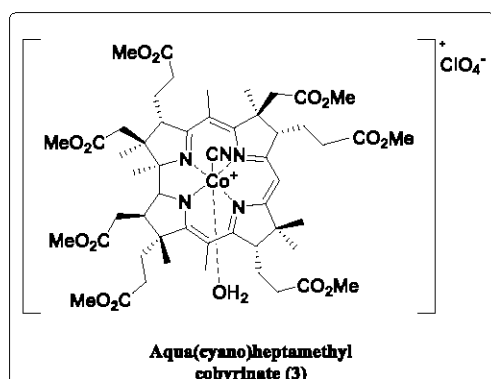
Entry	Oxetane 1 (equiv)	Olefin 20 (equiv)	Yield of 21 [%]
1	1	2	69
2	2	1	24
3	3	1	32
4	1	3	18
5	1	1.5	77

^aReaction conditions: oxetane (**1**), methyl acrylate (**20**) (2 equiv), Zn (3 equiv), NH₄Cl (3 equiv), HME (**3**) (5 mol%), TMSBr (2 equiv), MeCN_{anh} (c = 0.1 M), white LEDs, 16 h, yields determined by GC.

Table S15 Screening of the cobalt catalyst^a

Entry	Co-catalyst	Yield of 21 [%]
1	3	77
2	S1	16
3	S2	31
4	S3	0

^aReaction conditions: oxetane (**1**) (0.1 mmol, 1 equiv), methyl acrylate (**20**) (1.5 equiv), Zn (3 equiv), NH₄Cl (3 equiv), Co-catalyst (5 mol%), TMSBr (2 equiv), MeCN_{anh} (c = 0.1 M), white LEDs, 16 h, yields determined by GC.



Cobalt(II) phthalocyanine (S2)

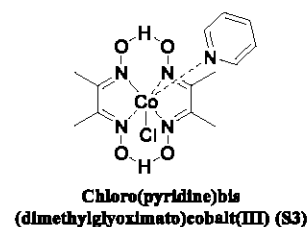


Table S16 HME (3) – catalyst loading^a

Entry	Catalyst loading [%]	Yield of 21 [%]
1	2.5	67
2	5	77
3	7.5	61

^aReaction conditions: oxetane (**1**) (0.1 mmol, 1 equiv), methyl acrylate (**20**) (1.5 equiv), Zn (3 equiv), NH₄Cl (3 equiv), HME (**3**), TMSBr (2 equiv), MeCN_{anh} (c = 0.1 M), white LEDs, 16 h, yields determined by GC.

Table S17 Optimization of the solvent for HME (3) catalyzed reaction^a

Entry	Solvent	Yield of 21 [%]
1	MeCN	77
2	DMA	23
3	DME	53
4	THF	44

^aReaction conditions: oxetane (**1**) (0.1 mmol, 1 equiv), methyl acrylate (**20**) (1.5 equiv), Zn (3 equiv), NH₄Cl (3 equiv), HME (**3**) (5 mol%), TMSBr (2 equiv), solvent (c = 0.1 M), white LEDs, 16 h, yields determined by GC.

Table S18 Concentration of oxetane (1)^a

Entry	[mol/dm ³]	Yield of 21 [%]
1	0.05	54
2	0.1	77
3	0.2	55

^aReaction conditions: oxetane (**1**) (0.1 mmol, 1 equiv), methyl acrylate (**20**) (1.5 equiv), Zn (3 equiv), NH₄Cl (3 equiv), HME (**3**) (5 mol%), TMSBr (2 equiv), MeCN_{anh}, white LEDs, 16 h, yields determined by GC.

Table S19 The influence of Zn and NH₄Cl amounts^a

Entry	Zn (equiv)	NH ₄ Cl (equiv)	Yield of 21 [%]
1	3	3	77
2	1	1	14
3	3	1	74
4	1	3	18
5	3	1.5	82
6	4	3	65

^aReaction conditions: oxetane (**1**) (0.1 mmol, 1 equiv), methyl acrylate (**20**) (1.5 equiv), Zn, NH₄Cl, HME (**3**) (5 mol%), TMSBr (2 equiv), MeCN_{anh} (c = 0.1 M), white LEDs, 16 h, yields determined by GC.

Table S20 The influence of an amount of Lewis acid^a

Entry	TMSBr (equiv)	Yield of 21 [%]
1	1	39
2	2	82/80^b
3	3	60

^aReaction conditions: oxetane (**1**) (0.1 mmol, 1 equiv), methyl acrylate (**20**) (1.5 equiv), Zn (3 equiv), NH₄Cl (1.5 equiv), HME (**3**) (5 mol%), TMSBr, MeCN_{anh} (c = 0.1 M), white LEDs, 16 h, yields determined by GC, ^bIsolated yield.

5. General Procedures

A. General procedure for the Co/Ni-catalyzed cross-electrophile coupling

A glass reaction tube (10 mL) equipped with a magnetic stirring bar was charged with activated Zn⁰ dust (39 mg, 0.6 mmol, 3.0 equiv), NH₄Cl (32 mg, 0.6 mmol, 3.0 equiv), catalyst **3** (6.0 mol%, 14.4 mg), dtbpy (20.0 mol%, 12.3 mg), aryl iodide (0.35 mmol, 1.75 equiv), NiCl₂(DME) (15.0 mol%, 7 mg) and was sealed with a rubber septum. Then dry MeCN (1 mL) was added, and the resulting mixture was degassed by three freeze-thaw cycles and backfilled with argon. An oxetane (0.2 mmol, 1.0 equiv) followed by TMSBr (52 μL, 2.0 equiv) were added dropwise via a syringe. The resulting mixture was irradiated with blue LED light for 16h at room temperature. The resulting mixture was diluted with MeOH (2 mL) and citric acid was added (77 mg, 2.0 equiv). After 30 min, the reaction mixture was filtered through cotton wool and concentrated *in vacuo*. The crude product was purified by column chromatography.

B. General procedure for the Giese-type reaction

A glass reaction tube (10 mL) equipped with a magnetic stirring bar was charged with activated Zn⁰ dust (39 mg, 0.6 mmol, 3.0 equiv), NH₄Cl (16 mg, 0.3 mmol, 1.5 equiv), catalyst **3** (5.0 mol%, 12.4 mg) and was sealed with a rubber septum. Then dry MeCN (2 mL) was added, and the resulting mixture was degassed by three freeze-thaw cycles and backfilled with argon. An oxetane (0.2 mmol, 1.0 equiv) followed by a Michael acceptor (0.3 mmol, 1.5 equiv) and TMSBr (52 μL, 2.0 equiv) were added dropwise via a syringe. The resulting mixture was irradiated with white LEDs light for 16 h at room temperature. The resulting mixture was diluted with MeOH (2 mL) and citric acid was added (77 mg, 2.0 equiv). After 30 min, the reaction mixture was filtered through cotton wool and concentrated *in vacuo*. The crude product was purified by column chromatography.

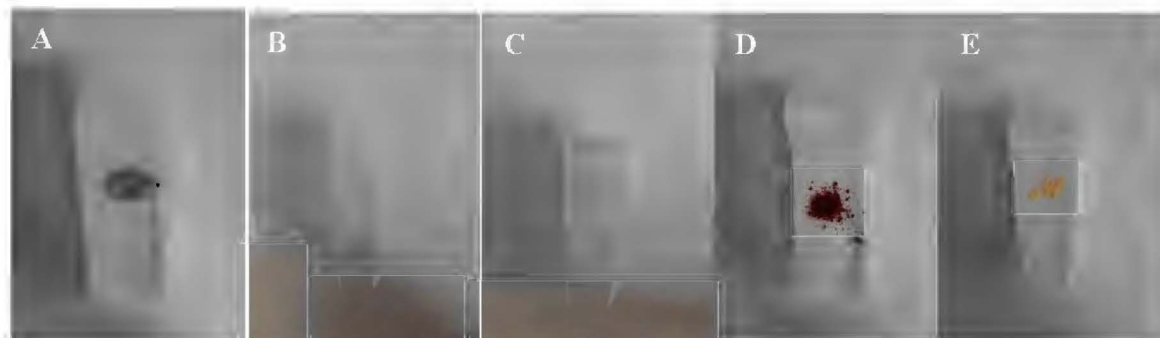
5.1 Note:

- Both reactions can be easily monitored by TLC chromatography (AcOEt/Hexane) using UV visualization, KMnO₄ or the Hanessian's stain;
- Reactions require using activated zinc (unactivated zinc gives low yields);
- A mixture containing Zn, NH₄Cl, HME and MeCN should turn from red to dark green and finally brown. The color indicates the reduction of the cobalt cation from Co(III) to Co(I) oxidation state;
- If the color of the reaction does not change (from red to dark brown/green), we highly recommend repeating the zinc activation step;

5.2 Graphical procedure for the Co/Ni cross-electrophile coupling



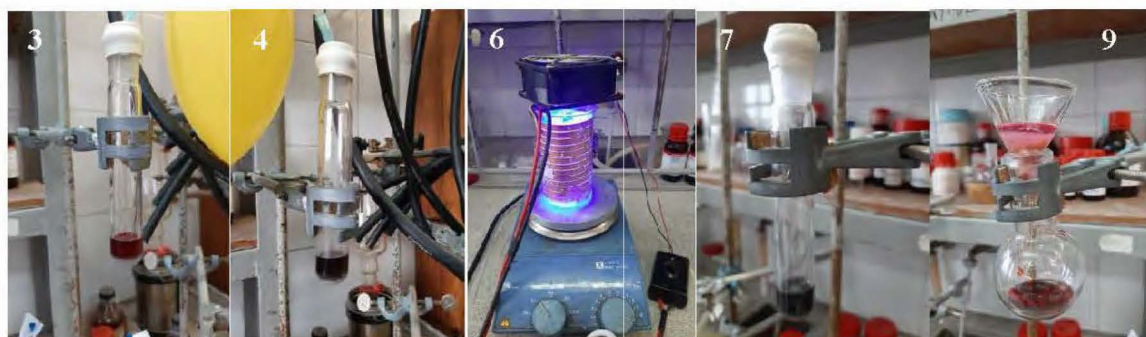
1. Weighted samples of reagents: A – activated zinc, B – NH_4Cl , C – dtbbpy, D – HME (**3**), E – $\text{NiCl}_2(\text{DME})$;



2. Glass reaction tube charged with all reagents;

3. Reagents dissolved in MeCN (*red color of the reaction mixture*);

4. Reaction mixture degassed by three freeze-thaw cycles and backfilled with argon (*note color change to brown*);



5. Oxetane, aryl halide and TMSBr were added (*if the reagents are solids, they are added on the beginning*);

6. The reaction vessel placed in a photoreactor and irradiated with blue LEDs;

7. The reaction mixture after 16 h (*color change to dark green usually indicates completion of the reaction*);

8. The reaction after 16 h is diluted with MeOH and citric acid was then added;

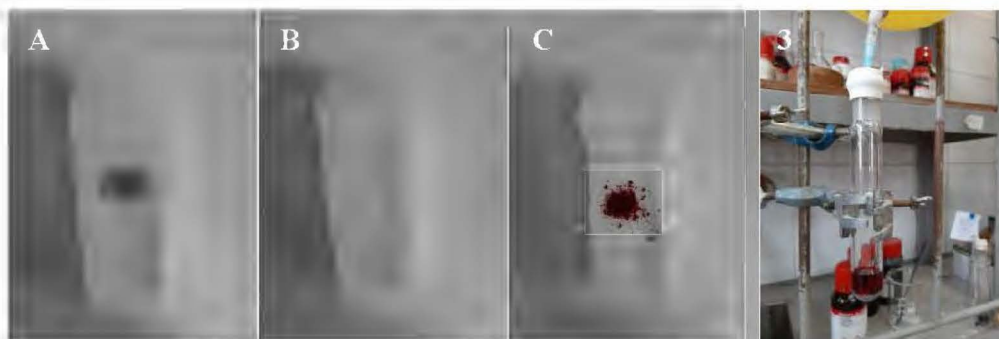
9. After 30 min of stirring, the reaction mixture is filtered via a cotton pad;

10. The filtrate is concentrated *in vacuo* and purified by column chromatography.

5.3 Graphical procedure for the Giese-type addition



1. Weighted samples of reagents: A – activated zinc, B – NH₄Cl, C – HME (**3**);
2. Glass reaction tube charged with reagents;
3. Reagents dissolved in MeCN (*red color of the reaction mixture*);



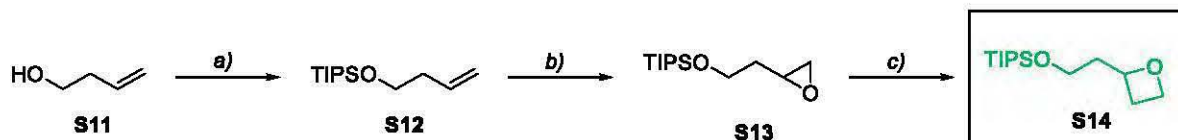
4. Reaction mixture degassed by three freeze-thaw cycles and backfilled with argon (*note color change to brown*);
5. Oxetane, Michael acceptors and TMSBr were added (*if the reagents are solids, they are added on the beginning*);
6. The reaction vessel placed in a photoreactor and irradiated with white LEDs;
7. The reaction mixture after 16 h (*color change to dark green usually indicates completion of the reaction*);
8. The reaction after 16 h is diluted with MeOH and citric acid was then added;
9. After 30 min of stirring, the reaction mixture is filtered via a cotton pad;
10. The filtrate is concentrated *in vacuo* and purified by column chromatography.



6. Scope and characterization of new compounds

6.1 Substrates

triisopropyl(2-(oxetan-2-yl)ethoxy)silane (**S14**)



Products **S12** and **S13** (steps a and b) were synthesized according to literature procedures.^{7,8}

General procedure for step c:

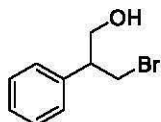
A mixture of KOBu-*t* (1.1 g, 10.0 mmol, 2.0 equiv) and trimethylloxosulfonium iodide (2.2 g, 10 mmol, 2.0 equiv) in dry *t*-BuOH (13 mL) was stirred magnetically at 50 °C for 1 h. A solution of epoxide **S13** (1.2 g, 5 mmol, 1.0 equiv) in dry *t*-BuOH (10 mL) was then added dropwise and stirred for 24 h. The reaction was concentrated under reduced pressure, and water was added to the residual suspension. The resulting mixture was extracted with DCM, dried over Na₂SO₄, and concentrated in *vacuo* to give the crude product **S14**, which was purified by column chromatography (5:95 EtOAc:Hexane) to afford the title compound as colorless oil, (yield = 56%).

¹H NMR (400 MHz, CDCl₃) δ 5.04 – 4.97 (m, 1H), 4.67 (dt, *J* = 8.0, 5.9 Hz, 1H), 4.52 (dt, *J* = 9.1, 5.8 Hz, 1H), 3.81 – 3.71 (m, 2H), 2.73 – 2.65 (m, 1H), 2.45 – 2.37 (m, 1H), 2.08 – 2.00 (m, 1H), 1.96 – 1.88 (m, 1H), 1.12 – 0.99 (m, 3H), 1.04 (d, *J* = 4.3 Hz, 18H).

¹³C NMR (100 MHz, CDCl₃) δ 80.5, 68.6, 59.2, 41.3, 28.0, 18.1, 12.1.

HRMS (ESI) [M+Na]⁺ calculated for C₁₄H₃₀O₂SiNa: 281.1913, found: 281.1911.

3-bromo-2-phenyl-propan-1-ol (**5b**)



Product **5b** was synthesized according to literature procedure.

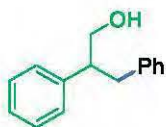
NMR data matched those reported in the literature.⁹

¹H NMR (500 MHz, CDCl₃): δ 7.39 – 7.23 (m, 5H), 3.96 (d, *J* = 6.0 Hz, 2H), 3.75 (dd, *J* = 10.1, 7.6 Hz, 1H), 3.64 (dd, *J* = 10.2, 6.5 Hz, 1H), 3.21 (p, *J* = 6.2 Hz, 1H), 1.51 (s, 1H).

¹³C NMR (125 MHz, CDCl₃): δ 139.7, 128.8, 127.9, 127.6, 64.9, 49.9, 34.1.

6.2 Cross-electrophile coupling: oxetanes

2,3-diphenylpropan-1-ol (**4b**)



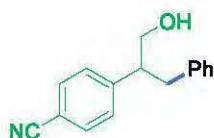
Following the general procedure **5A** compound **4b** was obtained from 3-phenyloxetane (**1**) (27 mg, 0.20 mmol) and iodobenzene (40 μ L, 0.35 mmol). The crude product was purified by column chromatography (10:90 AcOEt/Hexane) to afford 36 mg of compound 2,3-diphenylpropan-1-ol (**4b**) as colorless oil, (yield = **84%**).

NMR data matched those reported in the literature.¹⁰

¹H NMR (400 MHz, CDCl₃): δ 7.34 – 7.30 (m, 2H), 7.26 – 7.20 (m, 5H), 7.19 – 7.14 (m, 1H), 7.12 – 7.08 (m, 2H), 3.80 (d, J = 6.3 Hz, 2H), 3.12 – 3.02 (m, 2H), 2.92 (dd, J = 13.3, 7.3 Hz, 1H), 1.34 (br s, 1H).

¹³C NMR (100 MHz, CDCl₃): δ 142.1, 140.1, 129.2, 128.8, 128.4, 128.2, 127.0, 126.2, 66.5, 50.3, 38.9.

4-(1-hydroxy-3-phenylpropan-2-yl)benzotrile (**4d**)



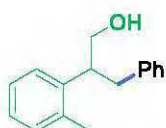
Following the general procedure **5A** compound **4d** was obtained from 4-(oxetan-3-yl)benzotrile (32 mg, 0.20 mmol) and iodobenzene (40 μ L, 0.35 mmol). The crude product was purified by column chromatography (10:40:50 AcOEt/Hexane/DCM) to afford 26 mg of 4-(1-hydroxy-3-phenylpropan-2-yl)benzotrile (**4d**) as pale yellow oil, (yield = **71%**).

¹H NMR (400 MHz, CDCl₃): δ 7.57 (d, J = 8.3 Hz, 2H), 7.30 (d, J = 8.3 Hz, 2H), 7.24 – 7.15 (m, 3H), 7.05 – 7.03 (m, 2H), 3.87 – 3.79 (m, 2H), 3.20 – 3.13 (m, 1H), 3.09 (dd, J = 13.5, 7.0 Hz, 1H), 2.87 (dd, J = 13.5, 7.9 Hz, 1H), 1.46 (br s, 1H).

¹³C NMR (100 MHz, CDCl₃): δ 148.1, 139.1, 132.4, 129.10, 129.08, 128.5, 126.5, 119.0, 110.7, 65.9, 50.5, 38.5.

HRMS (EI) [M]⁺ calculated for C₁₆H₁₅NO: 237.1154, found: 237.1156.

3-phenyl-2-(2-methylphenyl)propan-1-ol (**4e**)



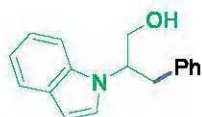
Following the general procedure **5A** compound **4e** was obtained from 3-(2-methylphenyl)oxetane (30 mg, 0.20 mmol) and iodobenzene (40 μ L, 0.35 mmol). The crude product was purified by column chromatography (2:48:50 AcOEt/Hexane/DCM) to afford 32 mg of 3-phenyl-2-(2-methylphenyl)propan-1-ol (**4e**) as colorless oil, (yield = **71%**).

NMR data matched those reported in the literature.¹¹

¹H NMR (400 MHz, CDCl₃): δ 7.32 – 7.28 (m, 1H), 7.25 – 7.19 (m, 3H), 7.18 – 7.11 (m, 3H), 7.09 – 7.06 (m, 2H), 3.82 (t, *J* = 5.8 Hz, 2H), 3.49 – 3.39 (m, 1H), 3.03 (dd, *J* = 13.5, 7.2 Hz, 1H), 2.86 (dd, *J* = 13.5, 7.5 Hz, 1H), 2.18 (s, 3H), 1.30 (t, *J* = 5.8 Hz, 1H).

¹³C NMR (100 MHz, CDCl₃): δ 140.2, 137.2, 130.7, 129.1, 128.4, 126.5, 126.4, 126.2, 126.1, 66.0, 45.0, 39.1, 19.8. (*In the aromatic region signals overlap*).

2-(1*H*-indol-1-yl)-3-phenylpropan-1-ol (**5**)



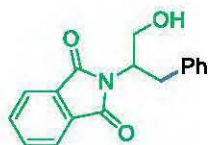
Following the general procedure **5A** compound **5** was obtained from 1-(oxetan-3-yl)-1*H*-indole (35 mg, 0.20 mmol) and iodobenzene (40 μL, 0.35 mmol). The crude product was purified by column chromatography (5:45:50 AcOEt/Hexane/DCM) to afford 26 mg of 2-(1*H*-indol-1-yl)-3-phenylpropan-1-ol (**5**) as colorless oil, (yield = **51%**).

¹H NMR (400 MHz, CDCl₃): δ 7.63 (d, *J* = 7.8 Hz, 1H), 7.33 (d, *J* = 8.2 Hz, 1H), 7.26 – 7.16 (m, 5H), 7.13 – 7.08 (m, 3H), 6.56 (d, *J* = 3.2 Hz, 1H), 4.73 – 4.66 (m, 1H), 4.00 – 3.90 (m, 2H), 3.25 (dd, *J* = 13.8, 7.3 Hz, 1H), 3.19 (dd, *J* = 13.8, 7.3 Hz, 1H), 1.49 (br s, 1H).

¹³C NMR (100 MHz, CDCl₃): δ 137.7, 136.5, 129.1, 128.8, 128.7, 126.9, 125.0, 121.8, 121.2, 119.8, 109.6, 102.4, 64.2, 59.7, 37.7.

HRMS (ESI) [M+Na]⁺ calculated for C₁₇H₁₇NONa: 274.1208, found: 274.1204.

2-(1-hydroxy-3-phenylpropan-2-yl)isoindoline-1,3-dione (**6**)



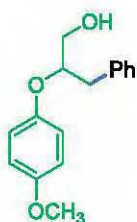
Following the general procedure **5A** compound **6** was obtained from 2-(oxetan-3-yl)isoindoline-1,3-dione (41 mg, 0.20 mmol) and iodobenzene (40 μL, 0.35 mmol). The crude product was purified by column chromatography (15:35:50 AcOEt/Hexane/DCM) to afford 31 mg of 2-(1-hydroxy-3-phenylpropan-2-yl)isoindoline-1,3-dione (**6**) as white solid, (yield = **55%**).

NMR data matched those reported in the literature.¹²

¹H NMR (400 MHz, CDCl₃) δ 7.80 – 7.75 (m, 2H), 7.70 – 7.65 (m, 2H), 7.22 – 7.19 (m, 4H), 7.18 – 7.12 (m, 1H), 4.67 – 4.60 (m, 1H), 4.12 – 4.04 (m, 1H), 3.96 – 3.91 (m, 1H), 3.20 (d, *J* = 8.2 Hz, 2H), 2.82 (dd, *J* = 8.2, 3.2 Hz, 1H).

¹³C NMR (100 MHz, CDCl₃) δ 169.1, 137.6, 134.2, 131.8, 129.2, 128.7, 126.8, 123.4, 63.0, 55.4, 34.9.

2-(4-methoxyphenoxy)-3-phenylpropan-1-ol (7)



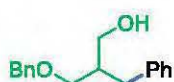
Following the general procedure **5A** compound **7** was obtained from 3-(4-methoxyphenoxy)oxetane (36 mg, 0.20 mmol) and iodobenzene (40 μ L, 0.35 mmol). The crude product was purified by column chromatography (5:45:50 AcOEt/Hexane/DCM) to afford 26 mg of 2-(4-methoxyphenoxy)-3-phenylpropan-1-ol (**7**) as colorless oil, (yield = 50%).

¹H NMR (400 MHz, CDCl₃): δ 7.32 – 7.27 (m, 2H), 7.25 – 7.20 (m, 3H), 6.88 (d, J = 9.3 Hz, 2H), 6.83 (d, J = 9.3 Hz, 2H), 4.43 – 4.37 (m, 1H), 3.80 – 3.76 (m, 1H), 3.77 (s, 3H), 3.67 (dd, J = 11.7, 5.6 Hz, 1H), 3.05 (dd, J = 13.8, 5.6 Hz, 1H), 2.92 (dd, J = 13.8, 7.6 Hz, 1H), 2.03 (br s, 1H).

¹³C NMR (100 MHz, CDCl₃): δ 154.6, 151.9, 137.6, 129.6, 128.6, 126.7, 118.1, 114.9, 81.3, 63.7, 55.8, 37.0.

HRMS (ESI) [M+Na]⁺ calculated for C₁₆H₁₈O₃Na: 281.1154, found: 281.1145.

2-benzyl-3-(benzyloxy)propan-1-ol (8)



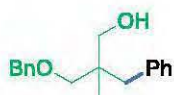
Following the general procedure **5A** compound **8** was obtained from 3-((benzyloxy)methyl)oxetane (36 mg, 0.20 mmol) and iodobenzene (40 μ L, 0.35 mmol). The crude product was purified by column chromatography (5:45:50 AcOEt/Hexane/DCM) to afford 33 mg of 2-benzyl-3-(benzyloxy)propan-1-ol (**8**) as colorless oil, (yield = 65%).

NMR data matched those reported in the literature.¹³

¹H NMR (400 MHz, CDCl₃): δ 7.36 – 7.24 (m, 7H), 7.21 – 7.14 (m, 3H), 4.51 (d, J = 11.9 Hz, 1H), 4.46 (d, J = 11.9 Hz, 1H), 3.76 – 3.70 (m, 1H), 3.66 – 3.60 (m, 1H), 3.58 (dd, J = 9.1, 4.2 Hz, 1H), 3.48 (dd, J = 9.1, 6.7 Hz, 1H), 2.70 – 2.61 (m, 2H), 2.41 (br s, 1H), 2.18 – 2.09 (m, 1H).

¹³C NMR (100 MHz, CDCl₃): δ 140.1, 138.2, 129.2, 128.6, 128.5, 127.9, 127.8, 126.2, 73.6, 72.9, 65.4, 42.8, 34.7.

2-benzyl-3-(benzyloxy)-2-methylpropan-1-ol (9)



Following the general procedure **5A** compound **9** was obtained from 3-methyl-3-(3-phenyl-2-oxapropyl)oxetane (38 mg, 0.20 mmol) and iodobenzene (40 μ L, 0.35 mmol). The crude product was purified by column chromatography (2:48:50 AcOEt/Hexane/DCM) to afford 22 mg of 2-benzyl-3-(benzyloxy)-2-methylpropan-1-ol (**9**) as colorless oil, (yield = 40%).

¹H NMR (400 MHz, CDCl₃): δ 7.39 – 7.28 (m, 5H), 7.27 – 7.22 (m, 2H), 7.21 – 7.14 (m, 3H), 4.52 (s, 2H), 3.55 (d, *J* = 10.8 Hz, 1H), 3.47 (dd, *J* = 10.8, 5.3 Hz, 1H), 3.32 (s, 2H), 2.77 (d, *J* = 13.2 Hz, 1H), 2.72 (d, *J* = 13.2 Hz, 1H), 2.68 (br s, 1H), 0.75 (s, 3H).

¹³C NMR (100 MHz, CDCl₃): δ 138.1, 130.8, 128.7, 128.0, 127.9, 127.8, 126.2, 77.6, 73.7, 70.4, 40.2, 40.1, 19.1.
(In the aromatic region signals overlap).

HRMS (ESI) [M+Na]⁺ calculated for C₁₈H₂₂O₂Na: 293.1517, found: 293.1521.

1-(benzyloxy)-5-phenylpentan-3-ol (**10**)



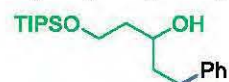
Following the general procedure **5A** compound **10** was obtained from 2-(2-(benzyloxy)ethyl)oxetane (38 mg, 0.20 mmol) and iodobenzene (40 μL, 0.35 mmol). The crude product was purified by column chromatography (5:45:50 AcOEt/Hexane/DCM) to afford 41 mg of 1-(benzyloxy)-5-phenylpentan-3-ol (**10**) as colorless oil, (yield = **76%**).

NMR data matched those reported in the literature.¹⁴

¹H NMR (400 MHz, CDCl₃): δ 7.36 – 7.24 (m, 7H), 7.20 – 7.15 (m, 3H), 4.51 (s, 2H), 3.87 – 3.81 (m, 1H), 3.75 – 3.70 (m, 1H), 3.67 – 3.62 (m, 1H), 2.91 (d, *J* = 3.2 Hz, 1H), 2.80 (ddd, *J* = 13.9, 9.9, 5.7 Hz, 1H), 2.67 (ddd, *J* = 13.9, 9.7, 6.7 Hz, 1H), 1.86 – 1.69 (m, 4H).

¹³C NMR (100 MHz, CDCl₃): δ 142.4, 138.0, 128.60, 128.58, 128.5, 127.9, 127.8, 125.9, 73.5, 70.9, 69.3, 39.3, 36.6, 32.1.

1-phenyl-5-((triisopropylsilyl)oxy)pentan-3-ol (**11**)



Following the general procedure **5A** compound **11** was obtained from triisopropyl(2-(oxetan-2-yl)ethoxy)silane (51 mg, 0.20 mmol) and iodobenzene (40 μL, 0.35 mmol). The crude product was purified by column chromatography (5:95 AcOEt/Hexane) to afford 34 mg of 1-phenyl-5-((triisopropylsilyl)oxy)pentan-3-ol (**11**) as colorless oil, (yield = **51%**).

¹H NMR (400 MHz, CDCl₃) δ 7.29 – 7.25 (m, 2H), 7.23 – 7.15 (m, 3H), 4.03 – 3.98 (m, 1H), 3.94 – 3.86 (m, 2H), 3.62 (d, *J* = 2.1 Hz, 1H), 2.82 (ddd, *J* = 13.9, 10.2, 5.5 Hz, 1H), 2.69 (ddd, *J* = 13.9, 10.0, 6.5 Hz, 1H), 1.85 (dddd, *J* = 13.6, 10.0, 8.0, 5.5 Hz, 1H), 1.76 – 1.63 (m, 3H), 1.16 – 1.05 (m, 3H), 1.08 (d, *J* = 5.2 Hz, 18H).

¹³C NMR (100 MHz, CDCl₃) δ 142.6, 128.6, 128.5, 125.8, 71.9, 63.6, 39.4, 38.5, 32.1, 18.1, 11.9.

HRMS (ESI) [M+Na]⁺ calculated for C₂₀H₃₆O₂SiNa: 359.2382, found: 359.2388.

6.3 Cross-electrophile coupling: aryl halides

2-phenyl-3-(4-methylphenyl)propan-1-ol (**4a**)



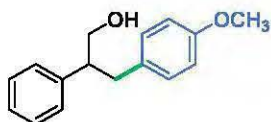
Following the general procedure **5A** compound **4a** was obtained from 3-phenyloxetane (**1**) (27 mg, 0.20 mmol) and 4-iodotoluene (**2**) (76 mg, 0.35 mmol). The crude product was purified by column chromatography (15:85 AcOEt/Hexane) to afford 36 mg of 2-phenyl-3-(4-methylphenyl)propan-1-ol (**4a**) as colorless oil, (yield = **80%**).

NMR data matched those reported in the literature.¹⁵

¹H NMR (400 MHz, CDCl₃): δ 7.35 – 7.30 (m, 2H), 7.26 – 7.20 (m, 3H), 7.04 (d, J = 8.0 Hz, 2H), 6.99 (d, J = 8.0 Hz, 2H), 3.79 (dd, J = 6.1, 2.6 Hz, 2H), 3.11 – 3.05 (m, 1H), 2.99 (dd, J = 13.6, 7.4 Hz, 1H), 2.89 (dd, J = 13.6, 7.5 Hz, 1H), 2.30 (s, 3H), 1.31 (br s, 1H).

¹³C NMR (100 MHz, CDCl₃): δ 142.2, 136.9, 135.2, 129.00, 128.96, 128.7, 128.2, 126.9, 66.5, 50.3, 38.4, 21.0.

3-(4-methoxyphenyl)-2-phenylpropan-1-ol (**12a**)



Following the general procedure **5A** compound **12a** was obtained from 3-phenyloxetane (**1**) (27 mg, 0.20 mmol) and 4-iodoanisole (82 mg, 0.35 mmol). The crude product was purified by column chromatography (5:45:50 AcOEt/Hexane/DCM) to afford 23 mg of 3-(4-methoxyphenyl)-2-phenylpropan-1-ol (**12a**) as colorless oil, (yield = **48%**).

NMR data matched those reported in the literature.¹⁵

¹H NMR (400 MHz, CDCl₃): δ 7.34 – 7.29 (m, 2H), 7.25 – 7.18 (m, 3H), 7.00 (d, J = 8.7 Hz, 2H), 6.77 (d, J = 8.7 Hz, 2H), 3.81 – 3.76 (m, 2H), 3.76 (s, 3H), 3.09 – 3.02 (m, 1H), 2.97 (dd, J = 13.6, 7.3 Hz, 1H), 2.86 (dd, J = 13.6, 7.5 Hz, 1H), 1.29 (br s, 1H).

¹³C NMR (100 MHz, CDCl₃): δ 158.1, 142.2, 132.1, 130.1, 128.8, 128.3, 127.0, 113.8, 66.5, 55.4, 50.5, 38.0.

4-(3-hydroxy-2-phenylpropyl)benzotrile (**12b**)



Following the general procedure **5A** compound **12b** was obtained from 3-phenyloxetane (**1**) (27 mg, 0.20 mmol) and 4-iodobenzotrile (80 mg, 0.35 mmol). The crude product was purified by column chromatography (10:40:50 AcOEt/Hexane/DCM) to afford 24 mg 4-(3-hydroxy-2-phenylpropyl)benzotrile (**12b**) as white solid, (yield = **51%**).

m.p. 62.0 – 62.9 °C

¹H NMR (400 MHz, CDCl₃) δ 7.48 (d, J = 8.4 Hz, 2H), 7.32 – 7.21 (m, 3H), 7.15 – 7.11 (m, 4H), 3.82 – 3.79 (m, 2H), 3.17 (dd, J = 13.1, 6.1 Hz, 1H), 3.10 – 3.04 (m, 1H), 2.94 (dd, J = 13.1, 8.4 Hz, 1H), 1.43 (br s, 1H).

^{13}C NMR (100 MHz, CDCl_3) δ 145.8, 140.9, 132.1, 130.0, 128.9, 128.1, 127.3, 119.1, 110.1, 66.4, 50.1, 38.8.

HRMS (ESI) $[\text{M}+\text{Na}]^+$ calculated for $\text{C}_{16}\text{H}_{15}\text{NONa}$: 260.1051, found: 260.1046.

2-phenyl-3-(4-(trifluoromethyl)phenyl)propan-1-ol (**12c**)



Following the general procedure **5A** compound **12c** was obtained from 3-phenyloxetane (**1**) (27 mg, 0.20 mmol) and 4-iodobenzotrifluoride (51 μL , 0.35 mmol). The crude product was purified by column chromatography (5:45:50 AcOEt/Hexane/DCM) to afford 44 mg of 2-phenyl-3-(4-(trifluoromethyl)phenyl)propan-1-ol (**12c**) as white solid, (yield = 79%).

m.p. 60.6 – 61.6 $^\circ\text{C}$

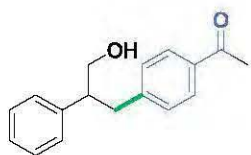
^1H NMR (400 MHz, CDCl_3): δ 7.47 (d, J = 8.0 Hz, 2H), 7.35 – 7.28 (m, 2H), 7.25 – 7.22 (m, 1H), 7.20 – 7.15 (m, 4H), 3.80 (d, J = 6.0 Hz, 2H), 3.17 – 3.07 (m, 2H), 2.96 (dd, J = 12.4, 7.2 Hz, 1H), 1.46 (br s, 1H).

^{13}C NMR (100 MHz, CDCl_3): δ 144.2 (q, J = 1.1 Hz), 141.3, 129.5, 128.9, 128.7, 128.5 (q, J = 32.1 Hz), 128.2, 127.2, 125.3 (q, J = 3.8 Hz), 124.4 (q, J = 270.2 Hz), 66.4, 50.1, 38.5.

^{19}F NMR (376 MHz, CDCl_3): δ -62.36.

HRMS (ESI) $[\text{M}-\text{H}]^-$ calculated for $\text{C}_{16}\text{H}_{14}\text{F}_3\text{O}$: 279.0997, found: 279.0995.

1-(4-(3-hydroxy-2-phenylpropyl)phenyl)ethanone (**12d**)



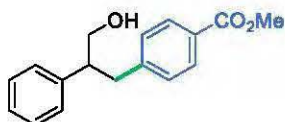
Following the general procedure **5A** compound **12d** was obtained from 3-phenyloxetane (**1**) (27 mg, 0.20 mmol) and 4'-iodoacetophenone (86 mg, 0.35 mmol). The crude product was purified by column chromatography (10:40:50 AcOEt/Hexane/DCM) to afford 40 mg of 1-(4-(3-hydroxy-2-phenylpropyl)phenyl)ethanone (**12d**) as colorless semi-solid, (yield = 79%).

^1H NMR (400 MHz, CDCl_3): δ 7.80 (d, J = 8.4 Hz, 2H), 7.32 – 7.27 (m, 2H), 7.25 – 7.20 (m, 1H), 7.18 – 7.13 (m, 4H), 3.80 (d, J = 5.5 Hz, 2H), 3.17 – 3.08 (m, 2H), 2.99 – 2.91 (m, 1H), 2.54 (s, 3H), 1.45 (br s, 1H).

^{13}C NMR (100 MHz, CDCl_3): δ 198.0, 145.9, 141.4, 135.4, 129.4, 128.8, 128.5, 128.2, 127.2, 66.5, 50.1, 38.7, 26.6.

HRMS (ESI) $[\text{M}+\text{Na}]^+$ calculated for $\text{C}_{17}\text{H}_{18}\text{O}_2\text{Na}$: 277.1204, found: 277.1198.

methyl 4-(3-hydroxy-2-phenylpropyl)benzoate (**12e**)



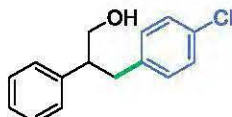
Following the general procedure **5A** compound **12e** was obtained from 3-phenyloxetane (**1**) (27 mg, 0.20 mmol) and methyl 4-iodobenzoate (92 mg, 0.35 mmol). The crude product was purified by column chromatography (gradually from AcOEt/Hexane/DCM 5:45:50 to 8:42:50) to afford 45 mg of methyl 4-(3-hydroxy-2-phenylpropyl)benzoate (**12e**) as colorless oil, (yield = 84%).

¹H NMR (400 MHz, CDCl₃): δ 7.88 (d, *J* = 8.3 Hz, 2H), 7.32 – 7.27 (m, 2H), 7.24 – 7.19 (m, 1H), 7.17 – 7.15 (m, 2H), 7.13 (d, *J* = 8.3 Hz, 2H), 3.88 (s, 3H), 3.80 (d, *J* = 5.2 Hz, 2H), 3.16 – 3.07 (m, 2H), 2.97 – 2.90 (m, 1H), 1.43 (br s, 1H).

¹³C NMR (100 MHz, CDCl₃): δ 167.2, 145.6, 141.4, 129.7, 129.2, 128.8, 128.2, 128.1, 127.1, 66.4, 52.1, 50.1, 38.8.

HRMS (ESI) [M+Na]⁺ calculated for C₁₇H₁₈O₃Na: 293.1154, found: 293.1150.

3-(4-chlorophenyl)-2-phenylpropan-1-ol (**12f**)



Following the general procedure **5A** compound **12f** was obtained from 3-phenyloxetane (**1**) (27 mg, 0.20 mmol) and 4-chloriodobenzene (83 mg, 0.35 mmol). The crude product was purified by column chromatography (2:48:50 AcOEt/Hexane/DCM) to afford 28 mg 3-(4-chlorophenyl)-2-phenylpropan-1-ol (**12f**) as colorless oil, (yield = 57%).

NMR data matched those reported in the literature.¹⁵

¹H NMR (400 MHz, CDCl₃): δ 7.33 – 7.28 (m, 2H), 7.25 – 7.21 (m, 1H), 7.18 – 7.15 (m, 4H), 6.99 (d, *J* = 8.4 Hz, 2H), 3.79 (d, *J* = 5.9 Hz, 2H), 3.09 – 3.01 (m, 2H), 2.90 – 2.82 (m, 1H), 1.36 (br s, 1H).

¹³C NMR (100 MHz, CDCl₃): δ 141.5, 138.5, 131.9, 130.5, 128.8, 128.5, 128.2, 127.1, 66.4, 50.3, 38.1.

3-(4-bromophenyl)-2-phenylpropan-1-ol (**12g**)



Following the general procedure **5A** compound **12g** was obtained from 3-phenyloxetane (**1**) (27 mg, 0.20 mmol) and 4-bromoiodobenzene (99 mg, 0.35 mmol). The crude product was purified by column chromatography (2:48:50 AcOEt/Hexane/DCM) to afford 29 mg of 3-(4-bromophenyl)-2-phenylpropan-1-ol (**12g**) as colorless oil, (yield = 50%).

¹H NMR (400 MHz, CDCl₃): δ 7.34 – 7.28 (m, 4H), 7.26 – 7.21 (m, 1H), 7.18 – 7.16 (m, 2H), 6.93 (d, *J* = 8.3 Hz, 2H), 3.78 (d, *J* = 6.0 Hz, 2H), 3.08 – 2.99 (m, 2H), 2.88 – 2.82 (m, 1H), 1.39 (br s, 1H).

¹³C NMR (100 MHz, CDCl₃): δ 141.5, 139.0, 131.4, 130.9, 128.8, 128.2, 127.1, 120.0, 66.4, 50.2, 38.1.

HRMS (EI) [M]⁺ calculated for C₁₅H₁₅BrO: 290.0306, found: 290.0313.

3-(4-fluorophenyl)-2-phenylpropan-1-ol (**12h**)



Following the general procedure **5A** compound **12h** was obtained from 3-phenyloxetane (**1**) (27 mg, 0.20 mmol) and 4-fluoroiodobenzene (41 μL, 0.35 mmol). The crude product was purified by column chromatography (2:48:50

AcOEt/Hexanes/DCM) to afford 28 mg of 3-(4-fluorophenyl)-2-phenylpropan-1-ol (**12h**) as colorless oil, (yield = 60%).

¹H NMR (400 MHz, CDCl₃): δ 7.34 – 7.28 (m, 2H), 7.26 – 7.21 (m, 1H), 7.20 – 7.15 (m, 2H), 7.03 – 6.99 (m, 2H), 6.92 – 6.86 (m, 2H), 3.79 (d, *J* = 5.9 Hz, 2H), 3.08 – 3.01 (m, 2H), 2.90 – 2.84 (m, 1H), 1.36 (br s, 1H).

¹³C NMR (100 MHz, CDCl₃): δ 161.5 (d, *J* = 243.7 Hz), 141.7, 135.6 (d, *J* = 3.3 Hz), 130.5 (d, *J* = 7.8 Hz), 128.8, 128.2, 127.1, 115.1 (d, *J* = 21.1 Hz), 66.4, 50.5 (d, *J* = 0.6 Hz), 38.0.

¹⁹F NMR (376 MHz, CDCl₃): δ -117.35.

HRMS (EI) [M]⁺ calculated for C₁₅H₁₅FO: 230.1107, found: 230.1106.

3-(4-(hydroxymethyl)phenyl)-2-phenylpropan-1-ol (**13**)



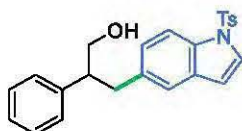
Following modified general procedure **5A** compound **13** was obtained from 3-phenyloxetane (**1**) (27 mg, 0.20 mmol) and 4-iodobenzyl alcohol (82 mg, 0.35 mmol) using 4.0 equiv of TMSBr. The crude product was purified by column chromatography (15:85 AcOEt/DCM) to afford 16 mg of 3-(4-(hydroxymethyl)phenyl)-2-phenylpropan-1-ol (**13**) as colorless oil, (yield = 33%).

¹H NMR (400 MHz, CDCl₃): δ 7.34-7.29 (m, 2H), 7.25-7.18 (m, 5H), 7.08 (d, *J* = 8.0 Hz, 2H), 4.62 (s, 2H), 3.79 (d, *J* = 5.8 Hz, 2H), 3.12-3.01 (m, 2H), 2.91 (dd, *J* = 13.0, 7.2 Hz, 1H), 1.65 (br s, 1H), 1.36 (br s, 1H).

¹³C NMR (100 MHz, CDCl₃): δ 141.9, 139.6, 138.7, 129.4, 128.8, 128.2, 127.2, 127.0, 66.5, 66.3, 50.3, 38.5.

HRMS (ESI) [M+Na]⁺ calculated for C₁₆H₁₈O₂Na: 265.1204, found: 265.1196.

2-phenyl-3-(*N*-tosyl-1*H*-indol-5-yl)propan-1-ol (**14**)



Following the general procedure **5A** compound **14** was obtained from 3-phenyloxetane (**1**) (27 mg, 0.20 mmol) and 5-iodo-1-(4-methylphenylsulfonyl)indole (138 mg, 0.35 mmol). The crude product was purified by column chromatography (gradually from AcOEt/Hexanes/DCM 2:48:50 to 5:45:50) to afford 41 mg of 2-phenyl-3-(*N*-tosyl-1*H*-indol-5-yl)propan-1-ol (**14**) as white solid, (yield = 50%).

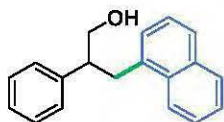
m.p. 121.9 – 122.3 °C

¹H NMR (400 MHz, CDCl₃) δ 7.84 (d, *J* = 8.5 Hz, 1H), 7.74 (d, *J* = 8.4 Hz, 2H), 7.50 (d, *J* = 3.6 Hz, 1H), 7.31 – 7.16 (m, 8H), 7.05 (dd, *J* = 8.5, 1.5 Hz, 1H), 6.55 (d, *J* = 3.6 Hz, 1H), 3.76 (d, *J* = 5.3 Hz, 2H), 3.11 – 3.05 (m, 2H), 3.00 – 2.94 (m, 1H), 2.33 (s, 3H), 1.35 (br s, 1H).

¹³C NMR (100 MHz, CDCl₃) δ 144.9, 142.1, 135.5, 135.2, 133.6, 131.0, 130.0, 128.8, 128.2, 127.0, 126.9, 126.6, 126.0, 121.6, 113.4, 109.0, 66.4, 50.5, 38.6, 21.7.

HRMS (ESI) [M+Na]⁺ calculated for C₂₄H₂₃NO₃SNa: 428.1296, found: 428.1299.

3-(naphthalen-1-yl)-2-phenylpropan-1-ol (**15**)



Following the general procedure **5A** compound **14** was obtained from 3-phenyloxetane (**1**) (27 mg, 0.20 mmol) and 1-iodonaphthalene (51 μ L, 0.35 mmol). The crude product was purified by column chromatography (2:48:50 AcOEt/Hexane/DCM) to afford 25 mg of 3-(naphthalen-1-yl)-2-phenylpropan-1-ol (**15**) as colorless oil, (yield = 47%).

¹H NMR (400 MHz, CDCl₃): δ 8.05 (d, J = 8.2 Hz, 1H), 7.86 – 7.83 (m, 1H), 7.69 (d, J = 8.2 Hz, 1H), 7.52 – 7.45 (m, 2H), 7.33 – 7.20 (m, 6H), 7.15 (d, J = 6.9 Hz, 1H), 3.86 – 3.80 (m, 2H), 3.52 (dd, J = 13.5, 7.5 Hz, 1H), 3.35 – 3.24 (m, 2H), 1.33 (br s, 1H).

¹³C NMR (100 MHz, CDCl₃): δ 142.5, 136.1, 134.1, 132.1, 129.0, 128.8, 128.2, 127.4, 127.10, 127.05, 126.1, 125.6, 125.4, 124.0, 66.6, 49.2, 36.0.

HRMS (ESI) [M+Na]⁺ calculated for C₁₉H₁₈ONa: 285.1255, found: 249.1248.

2-phenyl-3-(4-((trimethylsilyl)ethynyl)phenyl)propan-1-ol (**16**)



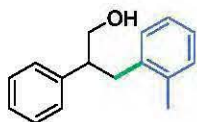
Following the general procedure **5A** compound **16** was obtained from 3-phenyloxetane (**1**) (27 mg, 0.20 mmol) and (4-iodophenylethynyl)trimethylsilane (105 mg, 0.35 mmol). The crude product was purified by column chromatography (2:48:50 AcOEt/Hexane/DCM) to afford 17 mg of 2-phenyl-3-(4-((trimethylsilyl)ethynyl)phenyl)propan-1-ol (**16**) as yellow oil, (yield = 28%).

¹H NMR (400 MHz, CDCl₃) δ 7.31 – 7.25 (m, 4H), 7.23 – 7.18 (m, 1H), 7.15 – 7.13 (m, 2H), 6.98 (d, J = 8.1 Hz, 2H), 3.77 (d, J = 5.7 Hz, 2H), 3.08 – 3.01 (m, 2H), 2.87 – 2.82 (m, 1H), 1.32 (br s, 1H), 0.23 (s, 9H).

¹³C NMR (100 MHz, CDCl₃) δ 141.6, 140.7, 132.0, 129.1, 128.8, 128.2, 127.1, 120.9, 105.3, 93.8, 66.5, 50.3, 38.8, 0.1.

HRMS (ESI) [M+Na]⁺ calculated for C₂₀H₂₄OSiNa: 331.1494, found: 331.1495.

2-phenyl-3-(2-methylphenyl)propan-1-ol (**17**)



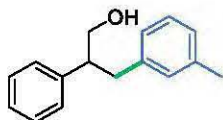
Following the general procedure **5A** compound **17** was obtained from 3-phenyloxetane (**1**) (27 mg, 0.20 mmol) and 2-iodotoluene (45 μ L, 0.35 mmol). The crude product was purified by column chromatography (2:48:50 AcOEt/Hexane/DCM) to afford 27 mg of 2-phenyl-3-(2-methylphenyl)propan-1-ol (**17**) as colorless oil, (yield = 60%).

NMR data matched those reported in the literature.¹⁶

¹H NMR (400 MHz, CDCl₃): δ 7.35 – 7.30 (m, 2H), 7.27 – 7.21 (m, 3H), 7.14 – 7.03 (m, 3H), 7.02 – 6.99 (m, 1H), 3.83 (d, *J* = 5.9 Hz, 2H), 3.11 – 3.03 (m, 2H), 2.92 – 2.84 (m, 1H), 2.28 (s, 3H), 1.34 (br s, 1H).

¹³C NMR (100 MHz, CDCl₃): δ 142.4, 138.3, 136.4, 130.4, 130.0, 128.8, 128.1, 127.0, 126.3, 125.9, 66.4, 49.1, 36.3, 19.6.

2-phenyl-3-(3-methylphenyl)propan-1-ol (**18**)



Following the general procedure **5A** compound **18** was obtained from 3-phenyloxetane (**1**) (27 mg, 0.20 mmol) and 3-iodotoluene (45 μL, 0.35 mmol). The crude product was purified by column chromatography (2:48:50 AcOEt/Hexane/DCM) to afford 28 mg of 2-phenyl-3-(3-methylphenyl)propan-1-ol (**18**) as colorless oil, (yield = 63%).

¹H NMR (400 MHz, CDCl₃): δ 7.33 – 7.27 (m, 2H), 7.25 – 7.18 (m, 3H), 7.12 – 7.08 (m, 1H), 6.99 – 6.94 (m, 1H), 6.93 – 6.88 (m, 2H), 3.76 (d, *J* = 6.9 Hz, 2H), 3.11 – 3.04 (m, 1H), 2.96 (dd, *J* = 13.5, 7.7 Hz, 1H), 2.87 (dd, *J* = 13.5, 7.3 Hz, 1H), 2.28 (s, 3H), 1.32 (br s, 1H).

¹³C NMR (100 MHz, CDCl₃): δ 142.3, 140.0, 137.9, 130.0, 128.7, 128.3, 128.2, 126.93, 126.91, 126.2, 66.5, 50.2, 38.8, 21.5.

HRMS (ESI) [M+Na]⁺ calculated for C₁₆H₁₈ONa: 249.1255, found: 249.1244.

3-(benzo[*d*][1,3]dioxol-5-yl)-2-phenylpropan-1-ol (**19**)



Following the general procedure **5A** compound **19** was obtained from 3-phenyloxetane (**1**) (27 mg, 0.20 mmol) and 5-iodo-1,3-benzodioxole (45 μL, 0.35 mmol). The crude product was purified by column chromatography (gradually from AcOEt/Hexanes/DCM 2:48:50 to 8:42:50) to afford 15 mg of 3-(benzo[*d*][1,3]dioxol-5-yl)-2-phenylpropan-1-ol (**19**) as colorless oil, (yield = 30%).

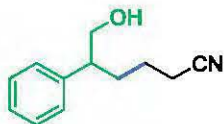
¹H NMR (400 MHz, CDCl₃): δ 7.34 – 7.29 (m, 2H), 7.25 – 7.17 (m, 3H), 6.66 (d, *J* = 7.9 Hz, 1H), 6.59 (d, *J* = 1.6 Hz, 1H), 6.54 (dd, *J* = 7.9, 1.6 Hz, 1H), 5.89 (s, 2H), 3.78 (d, *J* = 6.7 Hz, 2H), 3.08 – 3.00 (m, 1H), 2.96 (dd, *J* = 13.6, 7.3 Hz, 1H), 2.83 (dd, *J* = 13.6, 7.5 Hz, 1H), 1.34 (br s, 1H).

¹³C NMR (100 MHz, CDCl₃): δ 147.6, 145.9, 142.0, 133.8, 128.8, 128.2, 127.0, 122.1, 109.5, 108.2, 100.9, 66.5, 50.5, 38.5.

HRMS (ESI) [M+Na]⁺ calculated for C₁₆H₁₆O₃Na: 279.0997, found: 279.0994.

6.4 Giese-type addition: oxetanes

6-hydroxy-5-phenylhexanenitrile (**22a**)



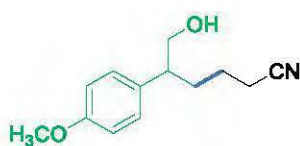
Following the general procedure **5B** compound **22a** was obtained from 3-phenyloxetane (**1**) (27 mg, 0.20 mmol) and acrylonitrile (**39**) (16 mg, 0.30 mmol). The crude product was purified by column chromatography (gradually from AcOEt/Hexane 20:80 to 30:70) to afford 30 mg of 6-hydroxy-5-phenylhexanenitrile (**22a**) as colorless oil, (yield = 80%).

NMR data matched those reported in the literature.¹⁷

¹H NMR (500 MHz, CDCl₃): δ 7.35 – 7.31 (m, 2H), 7.29 – 7.23 (m, 1H), 7.21 – 7.17 (m, 2H), 3.74 (d, J = 6.7 Hz, 2H), 2.80 – 2.77 (m, 1H), 2.28 (t, J = 7.1 Hz, 2H), 1.94 – 1.87 (m, 1H), 1.77 – 1.69 (m, 1H), 1.62 – 1.50 (m, 3H).

¹³C NMR (125 MHz, CDCl₃): δ 141.2, 128.9, 127.9, 127.2, 119.5, 67.3, 48.1, 30.9, 23.3, 17.2.

6-hydroxy-5-(4-methoxyphenyl)hexanenitrile (**22b**)



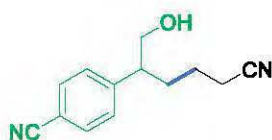
Following the general procedure **5B** compound **22b** was obtained from 3-(4-methoxyphenyl)oxetane (33 mg, 0.20 mmol) and acrylonitrile (**39**) (16 mg, 0.30 mmol). The crude product was purified by column chromatography (20:80 AcOEt/Hexane) to afford 23 mg of 6-hydroxy-5-(4-methoxyphenyl)hexanenitrile (**22b**) as colorless oil, (yield = 53%).

¹H NMR (400 MHz, CDCl₃): δ 7.14 – 7.09 (m, 2H), 6.91 – 6.86 (m, 2H), 3.80 (s, 3H), 3.71 (dd, J = 6.7, 4.2 Hz, 2H), 2.77 – 2.70 (m, 1H), 2.27 (t, J = 7.0 Hz, 2H), 1.93 – 1.83 (m, 1H), 1.74 – 1.65 (m, 1H), 1.61 – 1.51 (m, 2H), 1.38 (br s, 1H).

¹³C NMR (100 MHz, CDCl₃): δ 158.7, 132.9, 128.8, 119.5, 114.4, 67.4, 55.3, 47.2, 31.1, 23.3, 17.2.

HRMS (EI) [M]⁺ calculated for C₁₃H₁₇NO₂: 219.1259, found: 219.1261.

4-(5-cyano-1-hydroxypentan-2-yl)benzonitrile (**22c**)



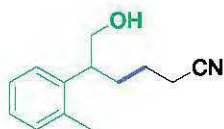
Following the general procedure **5B** compound **22c** was obtained from 4-(oxetan-3-yl)benzonitrile (32 mg, 0.20 mmol) and acrylonitrile (**39**) (16 mg, 0.30 mmol). The crude product was purified by column chromatography (50:50 AcOEt/Hexane) to afford 19 mg of 4-(5-cyano-1-hydroxypentan-2-yl)benzonitrile (**22c**) as colorless oil, (yield = 45%).

¹H NMR (400 MHz, CDCl₃): δ 7.63 (d, *J* = 7.9 Hz, 2H), 7.34 (d, *J* = 7.8 Hz, 2H), 3.78 (d, *J* = 6.3 Hz, 2H), 2.80 – 2.83 (m, 1H), 2.32 (t, *J* = 6.9 Hz, 2H), 2.01 – 1.91 (m, 1H), 1.81 – 1.70 (m, 1H), 1.64 – 1.44 (m, 3H).

¹³C NMR (100 MHz, CDCl₃): δ 147.6, 132.7, 128.9, 119.3, 118.8, 111.0, 66.6, 48.2, 30.8, 23.4, 17.3.

HRMS (EI) [M]⁺ calculated for C₁₃H₁₄N₂O: 214.1106, found: 214.1100.

6-hydroxy-5-(2-methylphenyl)hexanenitrile (**22d**)



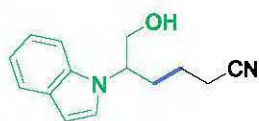
Following the general procedure **5B** compound **22d** was obtained from 3-(2-methylphenyl)oxetane (15 mg, 0.10 mmol) and acrylonitrile (**39**) (8 mg, 0.15 mmol). The crude product was purified by column chromatography (20:80 AcOEt/Hexane) to afford 11 mg of 6-hydroxy-5-(2-methylphenyl)hexanenitrile (**22d**) as colorless oil, (yield = 53%).

¹H NMR (400 MHz, CDCl₃): δ 7.23 – 7.12 (m, 4H), 3.73 (d, *J* = 6.6 Hz, 2H), 3.22 – 3.12 (m, 1H), 2.35 (s, 3H), 2.28 (t, *J* = 7.1 Hz, 2H), 1.99 – 1.89 (m, 1H), 1.81 – 1.70 (m, 1H), 1.66 – 1.49 (m, 2H), 1.39 (br s, 1H).

¹³C NMR (100 MHz, CDCl₃): δ 139.3, 136.9, 130.8, 126.7, 126.6, 125.7, 119.4, 67.0, 42.4, 31.1, 23.3, 20.0, 17.4.

HRMS (ESI) [M+Na]⁺ calculated for C₁₃H₁₇NONa: 226.1208, found: 226.1199.

6-hydroxy-5-(1H-indol-1-yl)hexanenitrile (**23**)



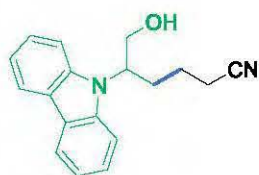
Following the general procedure **5B** compound **23** was obtained from 1-(oxetan-3-yl)-1H-indole (35 mg, 0.20 mmol) and acrylonitrile (**39**) (16 mg, 0.30 mmol). The crude product was purified by column chromatography (30:70 AcOEt/Hexane) to afford 25 mg of 6-hydroxy-5-(1H-indol-1-yl)hexanenitrile (**23**) as colorless oil, (yield = 56%).

¹H NMR (400 MHz, CDCl₃): δ 7.64 (d, *J* = 8.0 Hz, 1H), 7.36 (d, *J* = 8.1 Hz, 1H), 7.25 – 7.10 (m, 3H), 6.59 (d, *J* = 3.8 Hz, 1H), 4.49 – 4.43 (m, 1H), 3.95 – 3.86 (m, 2H), 2.32 – 2.16 (m, 2H), 2.07 – 2.04 (m, 2H), 1.68 – 1.52 (m, 2H), 1.47 – 1.36 (m, 1H).

¹³C NMR (100 MHz, CDCl₃): δ 136.6, 128.6, 124.1, 122.0, 121.3, 119.9, 119.0, 109.2, 103.0, 65.3, 57.4, 30.2, 22.1, 16.9.

HRMS (ESI) [M+H]⁺ calculated for C₁₄H₁₇N₂O: 229.1341, found: 229.1337.

5-(9H-carbazol-9-yl)-6-hydroxyhexanenitrile (**24**)



Following the general procedure **5B** compound **24** was obtained from 9-(oxetan-3-yl)-9H-carbazole (45 mg, 0.20 mmol) and acrylonitrile (**39**) (16 mg, 0.30 mmol). The crude product was purified by column chromatography

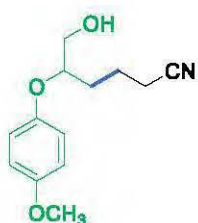
(20:80 AcOEt/Hexane) to afford 38 mg of 5-(9*H*-carbazol-9-yl)-6-hydroxyhexanenitrile (**24**) as colorless oil, (yield = 68%).

¹H NMR (500 MHz, CDCl₃): δ 8.11 (d, *J* = 7.8 Hz, 2H), 7.46 – 7.42 (m, 4H), 7.30 – 7.22 (m, 2H), 4.80 – 4.72 (m, 1H), 4.31 (dd, *J* = 11.4, 8.5 Hz, 1H), 4.02 (dd, *J* = 11.3, 5.0 Hz, 1H), 2.51 – 2.39 (m, 1H), 2.27 – 2.06 (m, 3H), 1.63 (s, 1H), 1.59 – 1.46 (m, 1H), 1.37 – 1.25 (m, 1H).

¹³C NMR (125 MHz, CDCl₃): δ 126.0, 120.5, 119.5, 119.0, 63.5, 57.6, 28.1, 22.2, 16.9.

HRMS (ESI) [M+Na]⁺ calculated for C₁₈H₁₈N₂ONa: 301.1317, found: 301.1330.

6-hydroxy-5-(4-methoxyphenoxy)hexanenitrile (**25**)



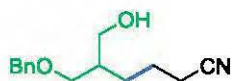
Following the general procedure **5B** compound **25** was obtained from 3-(4-methoxyphenoxy)oxetane (36 mg, 0.20 mmol) and acrylonitrile (**39**) (16 mg, 0.30 mmol). The crude product was purified by column chromatography (10:90 AcOEt/Hexane) to afford 37 mg of 6-hydroxy-5-(4-methoxyphenoxy)hexanenitrile (**25**) as colorless oil, (yield = 79%).

¹H NMR (500 MHz, CDCl₃): δ 6.90 – 6.86 (m, 2H), 6.85 – 6.80 (m, 2H), 4.27 – 4.20 (m, 1H), 3.77 (s, 3H), 3.70 (dd, *J* = 11.7, 5.5 Hz, 1H), 2.36 (t, *J* = 6.6 Hz, 2H), 1.93 – 1.73 (m, 5H), 1.60 (br s, 1H).

¹³C NMR (125 MHz, CDCl₃): δ 154.6, 151.9, 119.3, 117.7, 114.9, 79.1, 64.0, 55.7, 30.1, 21.6, 17.3.

HRMS (ESI) [M+Na]⁺ calculated for C₁₃H₁₇NO₃Na: 258.1106, found: 258.1104.

6-(benzyloxy)-5-(hydroxymethyl)hexanenitrile (**26**)



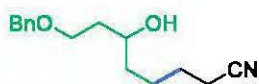
Following the general procedure **5B** compound **26** was obtained from 3-((benzyloxy)methyl)oxetane (36 mg, 0.20 mmol) and acrylonitrile (**39**) (16 mg, 0.30 mmol). The crude product was purified by column chromatography (20:80 AcOEt/Hexane) to afford 26 mg of 6-(benzyloxy)-5-(hydroxymethyl)hexanenitrile (**26**) as colorless oil, (yield = 56%).

¹H NMR (400 MHz, CDCl₃): δ 7.39 – 7.27 (m, 5H), 4.56 – 4.46 (m, 2H), 3.73 – 3.70 (m, 1H), 3.67 – 3.61 (m, 1H), 3.60 – 3.55 (m, 1H), 3.51 – 3.45 (m, 1H), 2.33 (t, *J* = 8.0 Hz, 3H), 1.89 – 1.78 (m, 1H), 1.76 – 1.61 (m, 2H), 1.57 – 1.42 (m, 2H).

¹³C NMR (125 MHz, CDCl₃): δ 137.8, 128.5, 127.9, 127.7, 119.5, 73.5, 73.0, 65.2, 40.2, 27.4, 23.3, 17.4.

HRMS (ESI) [M+Na]⁺ calculated for C₁₄H₁₉NO₂Na: 256.1313, found: 256.1308.

8-(benzyloxy)-6-hydroxyoctanenitrile (**28**)



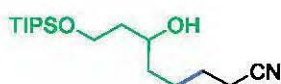
Following the general procedure **5B** compound **28** was obtained from 2-(2-(benzyloxy)ethyl)oxetane (38 mg, 0.20 mmol) and acrylonitrile (**39**) (16 mg, 0.30 mmol). The crude product was purified by column chromatography (20:80 AcOEt/Hexane) to afford 35 mg of 8-(benzyloxy)-6-hydroxyoctanenitrile (**28**) as colorless oil, (yield = 71%).

$^1\text{H NMR}$ (400 MHz, CDCl_3): δ 7.38 – 7.27 (m, 5H), 4.52 (s, 2H), 3.85 – 3.80 (m, 1H), 3.76 – 3.69 (m, 1H), 3.68 – 3.62 (m, 1H), 2.98 (br s, 1H), 2.33 (t, $J = 7.0$ Hz, 2H), 1.82 – 1.41 (m, 8H).

$^{13}\text{C NMR}$ (100 MHz, CDCl_3): δ 137.8, 128.5, 127.8, 127.7, 119.7, 73.4, 71.1, 69.3, 36.4, 36.4, 25.4, 24.8, 17.1.

HRMS (ESI) $[\text{M}+\text{Na}]^+$ calculated for $\text{C}_{15}\text{H}_{21}\text{NO}_2\text{Na}$: 270.1470, found: 270.1465.

6-hydroxy-8-((triisopropylsilyl)oxy)octanenitrile (**29**)



Following the general procedure **5B** compound **29** was obtained from triisopropyl(2-(oxetan-2-yl)ethoxy)silane (52 mg, 0.20 mmol) and acrylonitrile (**39**) (16 mg, 0.30 mmol). The crude product was purified by column chromatography (15:85 AcOEt/Hexane) to afford 12 mg of 6-hydroxy-8-((triisopropylsilyl)oxy)octanenitrile (**29**) as colorless oil, (yield = 19%).

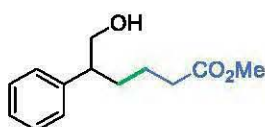
$^1\text{H NMR}$ (500 MHz, CDCl_3): δ 4.03 – 3.98 (m, 1H), 3.94 – 3.83 (m, 2H), 3.70 (br s, 1H), 2.35 (t, $J = 7.1$ Hz, 2H), 1.75 – 1.42 (m, 9H), 1.11 – 1.09 (m, 20H).

$^{13}\text{C NMR}$ (125 MHz, CDCl_3): δ 119.7, 72.1, 63.6, 38.2, 36.6, 25.5, 24.8, 17.9, 17.1, 11.7.

HRMS (ESI) $[\text{M}+\text{Na}]^+$ calculated for $\text{C}_{17}\text{H}_{35}\text{NO}_2\text{SiNa}$: 336.2335, found: 336.2330.

6.5 Giese-type addition: Michael acceptors

methyl 6-hydroxy-5-phenylhexanoate (**21**)



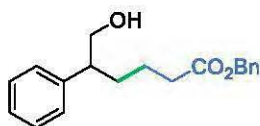
Following the general procedure **5B** compound **21** was obtained from 3-phenyloxetane (**1**) (27 mg, 0.20 mmol) and methyl acrylate (**20**) (26 mg, 0.30 mmol). The crude product was purified by column chromatography (20:80 AcOEt/Hexane) to afford 36 mg of methyl 6-hydroxy-5-phenylhexanoate (**21**) as colorless oil, (yield = 80%).

$^1\text{H NMR}$ (400 MHz, CDCl_3): δ 7.34 – 7.30 (m, 2H), 7.25 – 7.19 (m, 3H), 3.73 (dd, $J = 6.7, 4.2$ Hz, 2H), 3.63 (s, 3H), 2.80 – 2.76 (m, 1H), 2.29 – 2.25 (m, 2H), 1.76 – 1.72 (m, 1H), 1.65 – 1.51 (m, 3H), 1.42 (br s, 1H).

$^{13}\text{C NMR}$ (100 MHz, CDCl_3): δ 173.9, 141.9, 128.7, 128.0, 126.9, 67.4, 51.5, 48.4, 34.0, 31.4, 22.7.

HRMS (ESI) $[\text{M}+\text{Na}]^+$ calculated for $\text{C}_{13}\text{H}_{18}\text{O}_3\text{Na}$: 245.1154, found: 245.1143.

benzyl 6-hydroxy-5-phenylhexanoate (**30**)



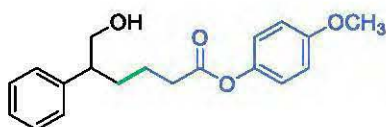
Following the general procedure **5B** compound **30** was obtained from 3-phenyloxetane (**1**) (27 mg, 0.20 mmol) and benzyl acrylate (49 mg, 0.30 mmol). The crude product was purified by column chromatography (10:90 AcOEt/Hexane) to afford 38 mg of benzyl 6-hydroxy-5-phenylhexanoate (**30**) as colorless oil, (yield = **64%**).

$^1\text{H NMR}$ (400 MHz, CDCl_3): δ 7.39 – 7.29 (m, 7H), 7.25 – 7.21 (m, 1H), 7.20 – 7.16 (m, 2H), 5.09 (s, 2H), 3.75 – 3.67 (m, 2H), 2.81 – 2.73 (m, 1H), 2.37 – 2.30 (m, 2H), 1.80 – 1.69 (m, 1H), 1.67 – 1.53 (m, 3H), 1.42 (br s, 1H).

$^{13}\text{C NMR}$ (125 MHz, CDCl_3): δ 173.2, 141.8, 136.0, 128.7, 128.5, 128.17, 128.16, 128.0, 126.8, 67.4, 66.1, 48.4, 34.2, 31.3, 22.7.

HRMS (ESI) $[\text{M}+\text{Na}]^+$ calculated for $\text{C}_{19}\text{H}_{22}\text{O}_3\text{Na}$: 321.1467, found: 321.1445.

4-methoxyphenyl 6-hydroxy-5-phenylhexanoate (**31a**)



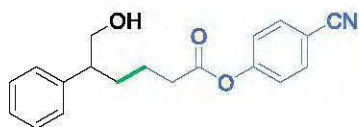
Following the general procedure **5B** compound **31a** was obtained from 3-phenyloxetane (**1**) (27 mg, 0.20 mmol) and 4-methoxyphenyl acrylate (53 mg, 0.30 mmol). The crude product was purified by column chromatography (15:85 AcOEt/Hexane) to afford 38 mg of 4-methoxyphenyl 6-hydroxy-5-phenylhexanoate (**31a**) as colorless oil, (yield = **61%**).

$^1\text{H NMR}$ (500 MHz, CDCl_3): δ 7.36 – 7.33 (m, 2H), 7.27 – 7.21 (m, 3H), 6.97 – 6.95 (m, 2H), 6.88 – 6.86 (m, 2H), 3.79 (s, 3H), 3.75 (dd, $J = 6.7, 4.3$ Hz, 2H), 2.85 – 2.80 (m, 1H), 2.51 (td, $J = 7.2, 2.7$ Hz, 2H), 1.89 – 1.81 (m, 1H), 1.75 – 1.63 (m, 3H), 1.56 (br s, 1H).

$^{13}\text{C NMR}$ (125 MHz, CDCl_3): δ 172.3, 157.2, 144.1, 141.8, 128.7, 128.0, 126.9, 122.2, 114.4, 67.4, 55.5, 48.4, 34.1, 31.3, 22.7.

HRMS (ESI) $[\text{M}+\text{Na}]^+$ calculated for $\text{C}_{19}\text{H}_{22}\text{O}_4\text{Na}$: 337.1416, found: 337.1399.

4-cyanophenyl 6-hydroxy-5-phenylhexanoate (**31b**)



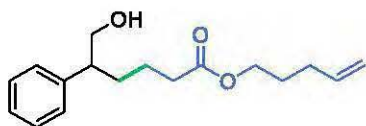
Following the general procedure **5B** compound **31b** was obtained from 3-phenyloxetane (**1**) (27 mg, 0.20 mmol) and 4-cyanophenyl acrylate (52 mg, 0.30 mmol). The crude product was purified by column chromatography (30:70 AcOEt/Hexane) to afford 55 mg of 4-cyanophenyl 6-hydroxy-5-phenylhexanoate (**31b**) as colorless oil, (yield = **89%**).

$^1\text{H NMR}$ (500 MHz, CDCl_3): δ 7.67 (d, $J = 5.0$ Hz, 2H), 7.36 – 7.33 (m, 2H), 7.28 – 7.18 (m, 5H), 3.77 (d, $J = 6.9$ Hz, 2H), 2.84 – 2.80 (m, 1H), 2.61 – 2.50 (m, 2H), 1.90 – 1.83 (m, 1H), 1.77 – 1.61 (m, 3H), 1.31 (br s, 1H).

¹³C NMR (125 MHz, CDCl₃): δ 171.0, 153.9, 141.6, 133.6, 128.8, 128.0, 127.0, 122.7, 118.2, 109.7, 67.4, 48.4, 34.2, 31.2, 22.6.

HRMS (ESI) [M+Na]⁺ calculated for C₁₉H₁₉NO₃Na: 332.1263, found: 332.1271.

pent-4-en-1-yl 6-hydroxy-5-phenylhexanoate (32)



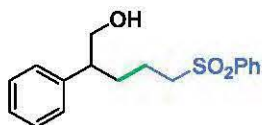
Following the general procedure **5B** compound **32** was obtained from 3-phenyloxetane (**1**) (27 mg, 0.20 mmol) and acrylic ester pent-4-enyl ester (42 mg, 0.30 mmol). The crude product was purified by column chromatography (10:90 AcOEt/Hexane) to afford 40 mg of pent-4-en-1-yl 6-hydroxy-5-phenylhexanoate (**32**) as colorless oil, (yield = 72%).

¹H NMR (400 MHz, CDCl₃): δ 7.34 – 7.30 (m, 2H), 7.25 – 7.17 (m, 3H), 5.78 (ddt, *J* = 16.9, 10.2, 6.6 Hz, 1H), 5.05 – 4.95 (m, 2H), 4.04 (t, *J* = 6.7 Hz, 2H), 3.73 (dd, *J* = 6.6, 3.9 Hz, 2H), 2.81 – 2.74 (m, 1H), 2.31 – 2.21 (m, 2H), 2.13 – 2.05 (m, 2H), 1.76 – 1.51 (m, 7H).

¹³C NMR (125 MHz, CDCl₃): δ 173.5, 141.9, 137.5, 128.7, 128.0, 126.8, 115.3, 67.4, 63.7, 48.4, 34.2, 31.4, 30.0, 27.8, 22.8.

HRMS (ESI) [M+Na]⁺ calculated for C₁₇H₂₄O₃Na: 299.1623, found: 299.1617.

2-phenyl-5-(phenylsulfonyl)pentan-1-ol (33)



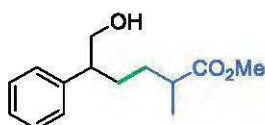
Following the general procedure **5B** compound **33** was obtained from 3-phenyloxetane (**1**) (27 mg, 0.20 mmol) and phenyl vinyl sulfone (51 mg, 0.30 mmol). The crude product was purified by column chromatography (30:70 AcOEt/Hexane) to afford 32 mg of 2-phenyl-5-(phenylsulfonyl)pentan-1-ol (**33**) as colorless oil, (yield = 53%).

¹H NMR (500 MHz, CDCl₃): δ 7.85 – 7.79 (m, 2H), 7.64 – 7.61 (m, 1H), 7.54 – 7.51 (m, 2H), 7.32 – 7.29 (m, 2H), 7.25 – 7.22 (m, 1H), 7.14 – 7.12 (m, 2H), 3.70 (d, *J* = 6.7 Hz, 2H), 3.09 – 2.97 (m, 2H), 2.75 – 2.68 (m, 1H), 1.87 – 1.82 (m, 1H), 1.71 – 1.61 (m, 3H), 1.35 (br s, 1H).

¹³C NMR (125 MHz, CDCl₃): δ 141.1, 139.1, 133.6, 129.2, 128.9, 128.0, 127.9, 127.1, 67.1, 56.1, 48.2, 30.5, 20.7.

HRMS (ESI) [M+Na]⁺ calculated for C₁₇H₂₀O₃SNa: 327.1031, found: 327.1034.

methyl 6-hydroxy-2-methyl-5-phenylhexanoate (34)



Following the general procedure **5B** compound **34** was obtained from 3-phenyloxetane (**1**) (27 mg, 0.20 mmol) and methacrylic acid methyl ester (30 mg, 0.30 mmol). The crude product was purified by column chromatography

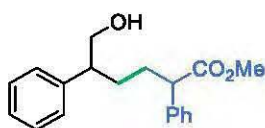
(20:80 AcOEt/Hexane) to afford 19 mg of methyl 6-hydroxy-2-methyl-5-phenylhexanoate (**34**) as colorless oil (a *mixture of diastereoisomers*), (yield = **41%**).

¹H NMR (500 MHz, CDCl₃): δ 7.34 – 7.31 (m, 2H), 7.25 – 7.18 (m, 3H), 3.74 – 3.70 (m, 2H), 3.64 (s, 3H), 2.79 – 2.70 (m, 1H), 2.46 – 2.35 (m, 1H), 1.77 – 1.66 (m, 1H), 1.64 – 1.51 (m, 2H), 1.39 – 1.28 (m, 2H), 1.10 (dd, *J* = 8.0, 4.0 Hz, 3H).

¹³C NMR (125 MHz, CDCl₃): δ 141.8, 128.7, 127.98, 127.98, 126.8, 67.5, 67.4, 51.5, 51.5, 48.7, 48.5, 39.5, 39.4, 31.5, 31.4, 29.6, 29.3, 17.1, 17.0. (*In the aromatic region signals overlap*)

HRMS (ESI) [M+Na]⁺ calculated for C₁₄H₂₀O₃Na: 259.1310, found: 259.1280.

methyl 6-hydroxy-2,5-diphenylhexanoate (**35**)



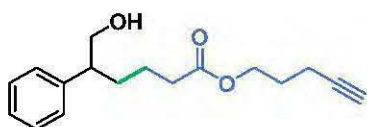
Following the general procedure **5B** compound **35** was obtained from 3-phenyloxetane (**1**) (27 mg, 0.20 mmol) and 2-phenyl-acrylic acid methyl ester (49 mg, 0.30 mmol). The crude product was purified by column chromatography (15:85 AcOEt/Hexane) to afford 33 mg of methyl 6-hydroxy-2,5-diphenylhexanoate (**35**) as colorless oil (a *mixture of diastereoisomers*), (yield = **56%**).

¹H NMR (500 MHz, CDCl₃): δ 7.36 – 7.08 (m, 10H), 3.68 – 3.65 (m, 2H), 3.61 (d, *J* = 1.4 Hz, 3H), 3.52 – 3.46 (m, 1H), 2.80 – 2.71 (m, 1H), 2.03 – 1.91 (m, 1H), 1.74 – 1.55 (m, 3H), 1.41 (br s, 1H).

¹³C NMR (125 MHz, CDCl₃): δ 141.7, 128.70, 128.67, 128.60, 128.57, 128.00, 127.97, 127.89, 127.80, 127.2, 126.85, 126.82, 67.5, 67.4, 51.93, 51.89, 51.61, 51.56, 48.5, 48.4, 31.2, 31.1, 29.74, 29.66. (*In the aromatic region signals overlap*)

HRMS (ESI) [M+Na]⁺ calculated for C₁₉H₂₂O₃Na: 321.1467, found: 321.1465.

pent-4-yn-1-yl 6-hydroxy-5-phenylhexanoate (**36**)



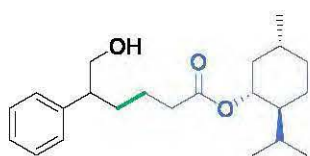
Following the general procedure **5B** compound **36** was obtained from 3-phenyloxetane (**1**) (27 mg, 0.20 mmol) and pent-4-yn-1-yl acrylate (41 mg, 0.30 mmol). The crude product was purified by column chromatography (10:90 AcOEt/Hexane) to afford 40 mg of pent-4-yn-1-yl 6-hydroxy-5-phenylhexanoate (**36**) as colorless oil, (yield = **73%**).

¹H NMR (500 MHz, CDCl₃): δ 7.34 – 7.31 (m, 2H), 7.25 – 7.22 (m, 3H), 4.14 (t, *J* = 5.9 Hz, 2H), 3.77 – 3.69 (m, 2H), 2.81 – 2.75 (m, 1H), 2.29 – 2.24 (m, 4H), 1.96 – 1.95 (m, 1H), 1.85 – 1.80 (m, 2H), 1.76 – 1.73 (m, 1H), 1.66 – 1.49 (m, 4H).

¹³C NMR (125 MHz, CDCl₃): δ 173.4, 141.9, 128.7, 128.0, 126.9, 83.0, 69.0, 67.4, 62.8, 48.4, 34.1, 31.4, 27.5, 22.7, 15.2.

HRMS (ESI) [M+Na]⁺ calculated for C₁₇H₂₂O₃Na: 297.1467, found: 297.1480.

(1*R*,2*S*,5*R*)-2-isopropyl-5-methylcyclohexyl 6-hydroxy-5-phenylhexanoate (37)



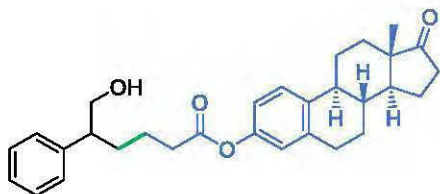
Following the general procedure **5B** compound **37** was obtained from 3-phenyloxetane (**1**) (27 mg, 0.20 mmol) and (-)-methol acrylate (63 mg, 0.30 mmol). The crude product was purified by column chromatography (10:90 AcOEt/Hexane) to afford 18 mg of (1*R*,2*S*,5*R*)-2-isopropyl-5-methylcyclohexyl 6-hydroxy-5-phenylhexanoate (**37**) as colorless oil (a mixture of diastereoisomers), (yield = **26%**).

¹H NMR (500 MHz, CDCl₃): δ 7.34 – 7.31 (m, 2H), 7.26 – 7.20 (m, 3H), 4.65 (td, *J* = 10.9, 4.4 Hz, 1H), 3.76 – 3.73 (m, 2H), 2.80 – 2.77 (m, 1H), 2.25 (t, *J* = 7.2 Hz, 2H), 1.96 – 1.94 (m, 1H), 1.81 (m, 1H), 1.76 – 1.71 (m, 1H), 1.68 – 1.45 (m, 6H), 1.41 – 1.30 (m, 2H), 1.08 – 1.00 (m, 1H), 0.96 – 0.83 (m, 8H), 0.73 (d, *J* = 7.0 Hz, 3H).

¹³C NMR (125 MHz, CDCl₃): δ 128.7, 128.00, 127.99, 126.8, 74.1, 74.04, 67.39, 67.35, 48.5, 48.4, 47.00, 41.0, 34.6, 34.5, 34.3, 31.44, 31.36, 26.3, 23.4, 22.92, 22.90, 22.0, 20.7, 16.3.

HRMS (ESI) [M+Na]⁺ calculated for C₂₂H₃₄O₃Na: 369.2406, found: 369.2392.

(8*R*,9*S*,13*S*,14*S*)-13-methyl-17-oxo-7,8,9,11,12,13,14,15,16,17-decahydro-6*H*-cyclopenta[*a*]phenanthren-3-yl 6-hydroxy-5-phenylhexanoate (38)



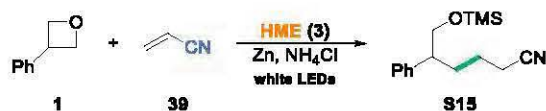
Following the general procedure **5B** compound **38** was obtained from 3-phenyloxetane (**1**) (27 mg, 0.20 mmol) and (8*R*,9*S*,13*S*,14*S*)-13-methyl-17-oxo-7,8,9,11,12,13,14,15,16,17-decahydro-6*H*-cyclopenta[*a*]phenanthren-3-yl acrylate (97 mg, 0.30 mmol). The crude product was purified by column chromatography (25:75 AcOEt/Hexane) to afford 26 mg of (8*R*,9*S*,13*S*,14*S*)-13-methyl-17-oxo-7,8,9,11,12,13,14,15,16,17-decahydro-6*H*-cyclopenta[*a*]phenanthren-3-yl 6-hydroxy-5-phenylhexanoate (**38**) as colorless oil, (yield = **58%**).

¹H NMR (500 MHz, CDCl₃): δ 7.35 – 7.32 (m, 2H), 7.29 – 7.20 (m, 4H), 6.81 (dd, *J* = 8.5, 2.6 Hz, 1H), 6.77 (d, *J* = 2.5 Hz, 1H), 3.76 – 3.74 (m, 2H), 2.94 – 2.86 (m, 2H), 2.86 – 2.80 (m, 1H), 2.55 – 2.44 (m, 3H), 2.41 – 2.38 (m, 1H), 2.29 – 2.27 (m, 1H), 2.19 – 1.93 (m, 4H), 1.91 – 1.82 (m, 1H), 1.77 – 1.42 (m, 10H), 0.91 (s, 3H).

¹³C NMR (125 MHz, CDCl₃): δ 220.7, 172.1, 148.5, 141.8, 137.9, 137.3, 128.7, 128.0, 126.9, 126.3, 121.5, 118.7, 67.4, 50.4, 48.4, 47.9, 44.1, 38.0, 35.8, 34.2, 31.5, 31.3, 29.3, 26.3, 25.7, 22.8, 21.6, 13.8.

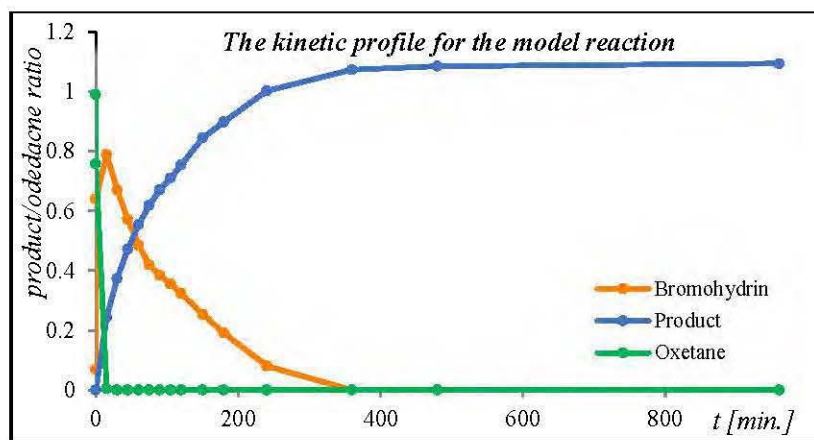
HRMS (ESI) [M+Na]⁺ calculated for C₃₀H₃₆O₄Na: 483.2511, found: 483.2510.

7.3 Kinetic studies for the model reaction

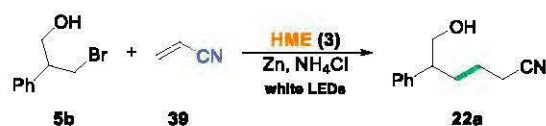


Reaction conditions: oxetane (**1**) (0.4 mmol), acrylonitrile (**39**) (1.5 equiv), Zn (3 equiv), NH₄Cl (1.5 equiv), HME (**3**) (5 mol%), MeCN_{anh} (c = 0.1M), white LEDs, 16h.

The reaction was setup according to general procedure **5B** on a 0.4 mmol scale with the addition of dodecane as an internal standard (65.6 mg). The reaction was monitored by GC/FID for 16h.

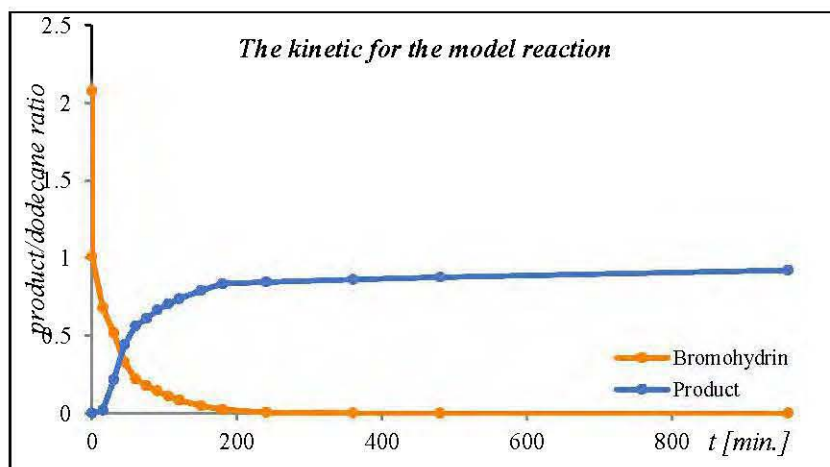


To prove the formation of bromohydrin during the reaction, another kinetics experiment was performed:



Reaction conditions: bromohydrin (**5b**) (0.2 mmol), acrylonitrile (**39**) (1.5 equiv), Zn (3 equiv), NH₄Cl (1.5 equiv), HME (**3**) (5 mol%), MeCN_{anh} (c = 0.1M), white LEDs, 16h.

The reaction was setup according to general procedure **5B** on 0.2 mmol scale with the addition of dodecane as an internal standard (31.0 mg). The reaction was monitored by GC/FID for 16h.



Conclusion: The kinetic experiments show that oxetane **1** is fully converted into bromohydrin within 15 min, while the product gradually forms over 10h.

7.4 Reactions with deuterated reagents



Reaction conditions: oxetane (1) (0.2 mmol), acrylonitrile (39) (1.5 equiv), Zn (3 equiv), ND₄Cl (1.5 equiv), HME (3) (5 mol%), TMSBr (2 equiv), MeCN (c = 0.1M), white LEDs. 16h.

Reaction was setup according to general procedure 5B on a 0.2 mmol scale using ND₄Cl (ND₄Cl contained 98 atom% of deuterium). After 16 h of light irradiation a small portion was taken from reaction mixture and ¹H NMR spectrum was recorded.

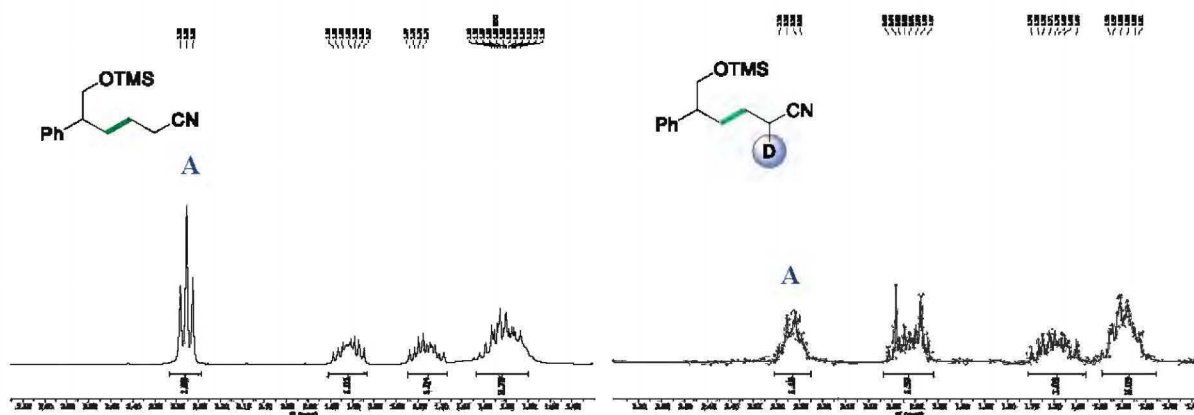
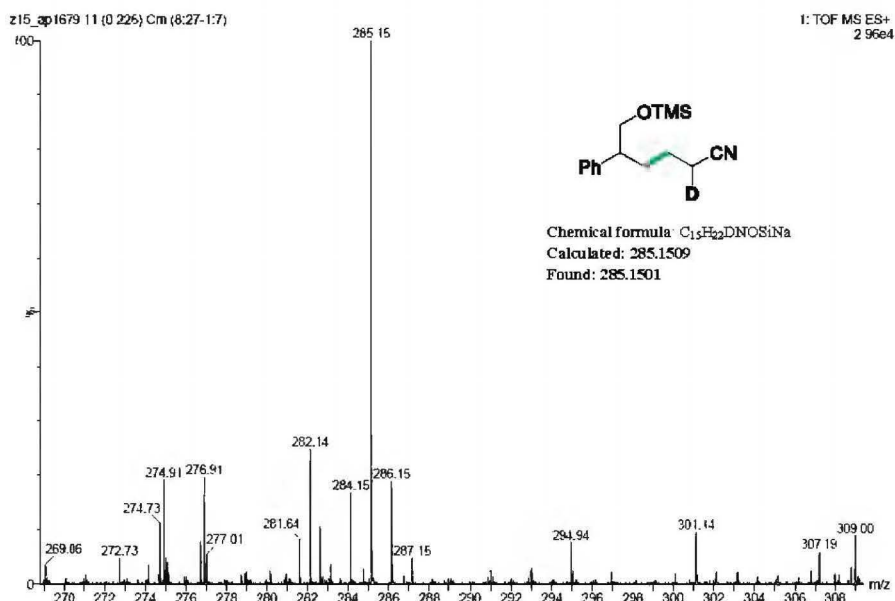
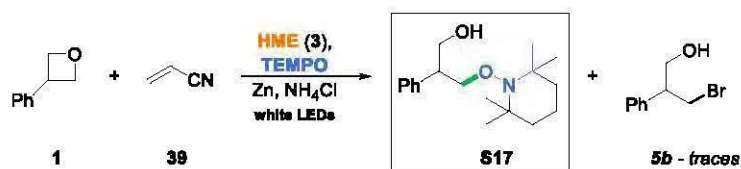


Figure S2 Left) ¹H NMR fragment of the spectra of product 41; **Right)** ¹H NMR spectra of a mixture of products formed in the deuterium incorporation experiment.



Conclusion: The integration 1.15 ppm for signal A (Scheme 7.4.1) in ¹H NMR indicates 85%-D incorporation at the *a* position to the electron-withdrawing group.

7.5 Experiment with a radical trap



Reaction conditions: oxetane (**1**) (0.2 mmol), acrylonitrile (**39**) (1.5 equiv), Zn (3 equiv), NH₄Cl (1.5 equiv), HME (**3**) (5 mol%), TMSBr (2 equiv), TEMPO (3 equiv), MeCN_{anh} (c = 0.1M), white LEDs, 16h, reaction was quenched by treatment with 2 equiv of citric acid.

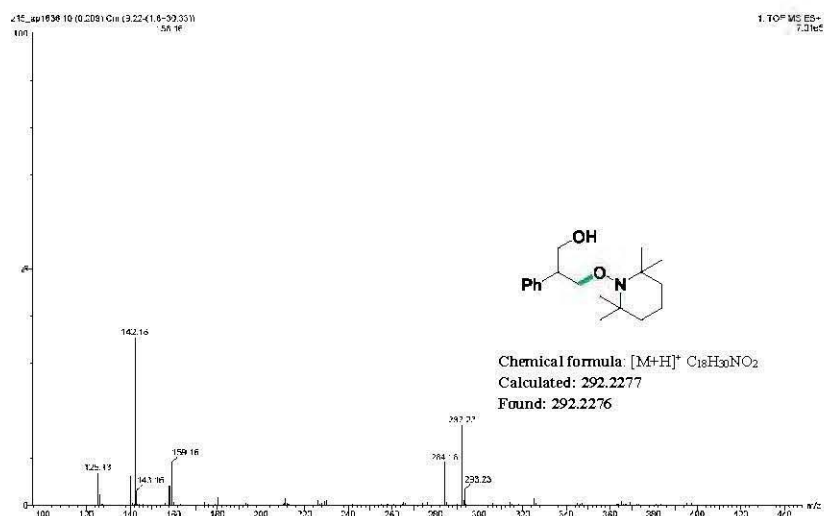


Figure S3 HRMS ESI analysis of the product obtained in the radical trap experiment.

Conclusion: Product **40** formed in the reaction of an alkyl radical with radical trap (TEMPO). This result proves the hypothesis that reaction involves the formation of radicals as intermediates.

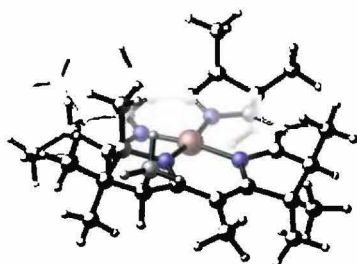
7.6 DFT calculations

Computational methods

All the calculations were performed with Gaussian 16 package.¹⁸ Geometry optimizations were computed at BP86/6-31G(d) level of theory with the D3 version of Grimme's empirical dispersion correction¹⁹ and SMD model of solvation (acetonitrile).²⁰ Frequency analysis was performed at the same level to provide correction to thermodynamic functions and confirm the nature of optimized structures (minima and transition states featured zero or one imaginary frequency, respectively). Single point energies were computed at BP86/6-311++G(2df,p) level of theory with the D3 version of Grimme's empirical dispersion correction and SMD model of solvation (acetonitrile). We performed calculations approximating the structure of vitamin B₁₂ with Co-corrin complex bearing 15 methyl groups, reflecting substitution pattern at a rim. Molecular structures were visualized in CYLview.²¹

Optimized geometries, energies and corrections to thermodynamic functions.

(CH₃)₁₅(corrin)Co(I)



E (BP86-D3/6-31G(d)/SMD (MeCN)) = -2928.476207

E (BP86-D3/6-311++G(2df,p)/SMD (MeCN)// BP86-D3/6-31G(d))/SMD (MeCN)) = -2929.055031

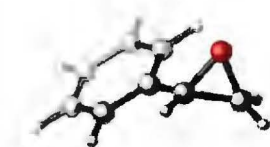
Zero-point correction=	0.777035
Thermal correction to Energy=	0.816636
Thermal correction to Enthalpy=	0.817580
Thermal correction to Gibbs Free Energy=	0.712422

Charge = 0 Multiplicity = 1

C	2.89754400	-0.89013600	-0.29398400
C	4.32154900	-0.37444100	-0.60113500
C	4.26251700	1.03989500	0.04830800
C	2.78793000	1.34632300	-0.03760400
N	2.02450300	0.20488000	-0.10706500
H	4.86289700	1.76141400	-0.53748600
C	2.28356300	2.64114000	0.00498000
H	3.01207600	3.45778500	0.03219800
C	2.49413600	-2.21994600	-0.27583900
C	0.93415800	2.97238200	0.00248900
C	0.41910600	4.40302100	-0.09404600
N	-0.08337700	2.04358600	-0.00741500
C	-1.04165600	4.21004000	0.39588100
C	-1.30149000	2.74240200	0.06751400
C	1.13851500	-2.55535300	0.03153500
C	0.63021800	-3.96442100	0.29474500
N	0.17694600	-1.63450800	0.13908300
C	-0.92264700	-3.79969000	0.12573100
C	-1.13152600	-2.28213300	0.49434700
C	-2.57044200	2.18974200	-0.05150700
C	-2.73277500	0.77390300	-0.18785700
C	-4.05137400	0.00952000	-0.41850700
N	-1.67218200	-0.04465900	-0.18297900
C	-3.61787500	-1.44601100	-0.03094100
C	-2.11969200	-1.45814400	-0.35745400
Co	0.13362200	0.17300800	-0.04798000
H	-1.71270500	4.88677700	-0.16144700
H	-3.73311700	-1.51520500	1.06756000
H	0.98688200	-4.65267600	-0.49472900
H	-1.96696200	-1.71458900	-1.42140600
C	-3.78893700	3.09594100	-0.00058800
H	-4.51260000	2.84733200	-0.79522100
H	-4.32787800	3.02279100	0.96207300
H	-3.51816800	4.15315800	-0.13967700
C	-4.43499000	0.12620800	-1.91517300

H	-4.59473700	1.18281300	-2.19319500
H	-3.64244400	-0.27917700	-2.56997000
H	-5.37165400	-0.42128600	-2.12662800
C	-5.24706200	0.41866900	0.46843200
H	-5.76132200	1.32426400	0.11089700
H	-5.99325200	-0.39795700	0.46585900
H	-4.93279400	0.58478000	1.51453100
C	-4.44330000	-2.56270800	-0.67546700
H	-4.18319200	-3.54524200	-0.24688700
H	-5.52393500	-2.40586200	-0.50259000
H	-4.27887900	-2.61726600	-1.76603600
C	-1.38418300	-2.04237000	1.99797800
H	-2.32782100	-2.49966400	2.33861300
H	-0.56217400	-2.45562900	2.60334000
H	-1.42559700	-0.95557300	2.18614400
C	-1.73741900	-4.77514800	0.99036600
H	-2.82074600	-4.60186000	0.86479600
H	-1.52977000	-5.81697500	0.68372700
H	-1.50718700	-4.69174400	2.06480600
C	-1.23666100	-4.08315800	-1.36272200
H	-0.96593000	-5.12829500	-1.60087600
H	-2.30651700	-3.95686200	-1.59660100
H	-0.65542400	-3.42624000	-2.03584700
C	1.15320000	-4.52890400	1.63383800
H	0.77695500	-5.55303100	1.80500600
H	2.25635100	-4.57717000	1.61692000
H	0.86198700	-3.90447800	2.49493500
C	3.45455500	-3.35380800	-0.60036900
H	4.08338500	-3.11545400	-1.47370800
H	4.13307100	-3.60137200	0.23627300
H	2.90590000	-4.27487000	-0.85245400
C	5.51996100	-1.18744300	-0.07342800
H	5.73634900	-2.06987800	-0.69411300
H	6.42273200	-0.54938400	-0.09866600
H	5.37169800	-1.52537600	0.96623300
C	4.44598200	-0.21164200	-2.14020700
H	3.66182100	0.46143200	-2.53305900
H	5.43122100	0.21921000	-2.40072500
H	4.35025400	-1.18585500	-2.65155200
C	4.71232800	1.10853700	1.52603000
H	5.79099700	0.90176600	1.63937400
H	4.51624400	2.11854500	1.92823500
H	4.15164300	0.38263600	2.14333100
C	-1.25803500	4.44049000	1.90767300
H	-1.06176100	5.49049400	2.18832300
H	-2.30011600	4.20314400	2.18492700
H	-0.59196200	3.79098200	2.50476700
C	0.40517600	4.81255300	-1.59166000
H	-0.00858400	5.83200200	-1.70989500
H	1.42836900	4.80205200	-2.00873400
H	-0.21664700	4.11822900	-2.18660100
C	1.24219600	5.42830300	0.70249600
H	2.24270500	5.56174000	0.25290700
H	0.74306100	6.41455300	0.68979000
H	1.38283500	5.12309600	1.75350600

Styrene oxide



E (BP86-D3/6-31G(d)/SMD (MeCN)) = -384.864461

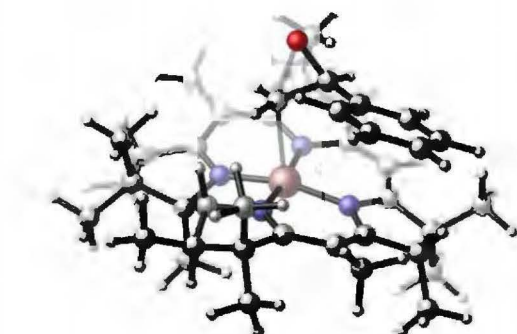
E (BP86-D3/6-311++G(2df,p)/SMD (MeCN)// BP86-D3/6-31G(d))/SMD (MeCN)) = -384.988582

Zero-point correction=	0.134929
Thermal correction to Energy=	0.142323
Thermal correction to Enthalpy=	0.143268
Thermal correction to Gibbs Free Energy=	0.102709

Charge = 0 Multiplicity = 1

C	2.59533100	-0.05141700	0.73801600
C	1.60678600	0.61063100	-0.15115500
H	1.84491700	1.62749300	-0.49995400
O	2.50307600	-0.41835300	-0.65813500
C	0.15006900	0.27965900	-0.09177900
C	-0.80234000	1.31743200	-0.04058400
C	-0.28915200	-1.06059200	-0.06860100
C	-2.17236100	1.02058000	0.05100700
H	-0.46668500	2.36132300	-0.07096800
C	-1.65774100	-1.35614500	0.01805800
H	0.45248500	-1.86447300	-0.13561600
C	-2.60404800	-0.31668400	0.08179000
H	-2.90347300	1.83613700	0.09201200
H	-1.98839300	-2.40108900	0.03171400
H	-3.67300400	-0.54875600	0.14830600
H	2.23992900	-0.81139600	1.45028900
H	3.51035600	0.48680400	1.02878200

TS1



E (BP86-D3/6-31G(d)/SMD (MeCN)) =

E (BP86-D3/6-311++G(2df,p)/SMD (MeCN)// BP86-D3/6-31G(d))/SMD (MeCN)) =

Zero-point correction=	0.912264
------------------------	----------

Thermal correction to Energy=	0.960310
Thermal correction to Enthalpy=	0.961254
Thermal correction to Gibbs Free Energy=	0.838326

Charge = 0 Multiplicity = 1

C	2.66648100	-1.87273800	0.21649600
C	2.93247300	-3.33591400	0.63178100
C	1.82334700	-4.07955900	-0.17568100
C	0.79523700	-2.98895800	-0.36595800
N	1.33159100	-1.73859200	-0.21300800
H	1.41448500	-4.92054200	0.41546700
C	-0.50758900	-3.24335800	-0.78474000
H	-0.77585500	-4.29013600	-0.96091100
C	3.55881000	-0.81049800	0.31899300
C	-1.47303300	-2.27721300	-1.05262800
C	-2.80136200	-2.60621900	-1.71921300
N	-1.30412100	-0.93721000	-0.81335300
C	-3.58924500	-1.26721800	-1.53166400
C	-2.52940000	-0.29009400	-1.02157800
C	3.16863300	0.50699100	-0.09387100
C	4.11489300	1.68416600	-0.26696300
N	1.90932100	0.82428500	-0.38327400
C	3.13179800	2.91062900	-0.26049600
C	1.79469000	2.26524400	-0.79289600
C	-2.78525900	1.04573200	-0.72721100
C	-1.70930300	1.94829600	-0.44694400
C	-1.80639700	3.47471300	-0.24320800
N	-0.44824900	1.52027100	-0.34810400
C	-0.32853900	3.89655000	-0.56238700
C	0.46971400	2.66947900	-0.10900900
Co	0.35016600	-0.12122500	-0.37107000
H	-4.32496700	-1.41977100	-0.71609200
H	-0.26163900	3.96621500	-1.66531200
H	4.77716800	1.77524900	0.61418900
H	0.64370900	2.72699400	0.98084500
C	0.50315200	-0.02962000	2.05863300
C	-0.46255700	-1.00142800	2.62253300
H	-0.25795200	-2.05745800	2.33699600
O	0.19022500	-0.52529700	3.76603000
C	-1.94287100	-0.70624400	2.52123200
C	-2.84265300	-1.67841100	2.04986300
C	-2.44686400	0.54013100	2.94371700
C	-4.22094500	-1.41068200	1.98631500
H	-2.45362000	-2.64912900	1.71905700
C	-3.82009000	0.81719900	2.87305700
H	-1.75015400	1.28445500	3.34529200
C	-4.71348200	-0.15923000	2.39302800
H	-4.90965100	-2.18017100	1.61848000
H	-4.19754700	1.79413500	3.19665900
H	-5.78707000	0.05470300	2.34059600
H	0.25270600	1.03073900	2.11130700
H	1.55327200	-0.31499200	1.98922700
C	-4.22031800	1.54228700	-0.67853600
H	-4.34722600	2.27953400	0.12990200
H	-4.55728400	2.02348400	-1.61500800
H	-4.91554100	0.71782800	-0.45349700
C	-2.18224100	3.77408200	1.22920800
H	-3.16449300	3.33912200	1.47907100
H	-1.44274700	3.35139200	1.93240300
H	-2.24233700	4.86397000	1.40216700

C	-2.75932000	4.22058200	-1.19993400
H	-3.81528600	4.15367000	-0.89452100
H	-2.49431600	5.29429600	-1.21209700
H	-2.66989200	3.83830100	-2.23272600
C	0.11330000	5.23124500	0.04149400
H	1.10854300	5.52338000	-0.33340100
H	-0.58975200	6.04053300	-0.22838000
H	0.16993400	5.18434700	1.14311800
C	1.64829700	2.32022300	-2.32707900
H	1.57413700	3.35749300	-2.69350800
H	2.50684700	1.83873400	-2.82123600
H	0.73694500	1.77296600	-2.62505000
C	3.63955300	4.09610600	-1.09632300
H	2.91502500	4.92908900	-1.08297400
H	4.58860200	4.47560200	-0.67473200
H	3.82538400	3.83004500	-2.14943700
C	3.00319200	3.36364600	1.21316800
H	3.99037100	3.69924200	1.58053700
H	2.30137400	4.20582300	1.33106600
H	2.66626800	2.53758700	1.86684100
C	5.03621800	1.50347000	-1.49283100
H	5.72024400	2.36320900	-1.60293600
H	5.65530500	0.59748000	-1.36735500
H	4.46747600	1.39029200	-2.43102100
C	4.96403200	-0.99408500	0.87006400
H	4.96449400	-1.61762300	1.77873400
H	5.65396500	-1.46412800	0.14598200
H	5.40561600	-0.02630400	1.15403300
C	4.32852000	-3.92753200	0.35317700
H	5.07778100	-3.59624000	1.08746100
H	4.27136900	-5.02887700	0.42960700
H	4.69802300	-3.67493300	-0.65507800
C	2.62071200	-3.45454600	2.14807600
H	1.58791400	-3.13381800	2.37162500
H	2.73490100	-4.50411100	2.47857900
H	3.30759200	-2.82840900	2.74447300
C	2.25724500	-4.61633800	-1.55934700
H	3.00178600	-5.42651400	-1.47160800
H	1.38009700	-5.01986800	-2.09564600
H	2.69069100	-3.80900900	-2.17770600
C	-4.36594800	-0.81182300	-2.78192200
H	-5.01080800	-1.63270100	-3.14427800
H	-5.02204800	0.04562600	-2.57099200
H	-3.68584900	-0.52107200	-3.60097800
C	-3.55029000	-3.78941200	-1.07613400
H	-4.54032100	-3.90885400	-1.55506600
H	-3.00156900	-4.73998600	-1.20502700
H	-3.70963000	-3.62622100	0.00361400
C	-2.49348400	-2.95176600	-3.20065600
H	-1.84711500	-3.84666300	-3.24278200
H	-3.41593500	-3.17381300	-3.76628700
H	-1.96214500	-2.12731500	-3.70859400

Oxetane



E (BP86-D3/6-31G(d)/SMD (MeCN)) = -193.111200

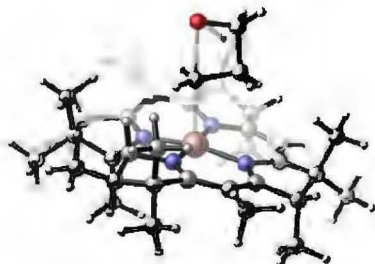
E (BP86-D3/6-311++G(2df,p)/SMD (MeCN)// BP86-D3/6-31G(d))/SMD (MeCN)) = -193.180285

Zero-point correction=	0.084291
Thermal correction to Energy=	0.088597
Thermal correction to Enthalpy=	0.089542
Thermal correction to Gibbs Free Energy=	0.056243

Charge = 0 Multiplicity = 1

C	-0.00008000	1.08145900	-0.00020500
C	-1.04163700	-0.05973800	0.00020000
C	1.04163900	-0.05959400	0.00020600
H	-0.00010100	1.71644700	-0.90022000
H	-0.00013500	1.71731200	0.89919900
H	-1.68501800	-0.12539100	-0.90018700
H	-1.68406300	-0.12530500	0.90129100
H	1.68500800	-0.12514600	-0.90020000
H	1.68407500	-0.12508100	0.90128800
O	0.00008800	-1.08819900	-0.00029700

TS2



E (BP86-D3/6-31G(d)/SMD (MeCN)) = -3121.572096

E (BP86-D3/6-311++G(2df,p)/SMD (MeCN)// BP86-D3/6-31G(d))/SMD (MeCN)) = -3122.22262

Zero-point correction=	0.860382
Thermal correction to Energy=	0.905161
Thermal correction to Enthalpy=	0.906106
Thermal correction to Gibbs Free Energy=	0.790597

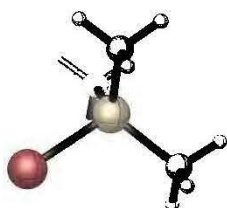
Charge = 0 Multiplicity = 1

C	-2.72425500	-1.21924800	-0.09687800
C	-4.20670400	-0.84451900	0.10768200
C	-4.26477900	0.51660200	-0.65130600
C	-2.83997500	0.99132500	-0.51214000
N	-1.97121500	-0.04824600	-0.31777800
H	-4.97000800	1.20899200	-0.15531700
C	-2.47436100	2.33206100	-0.58911000

H	-3.28206500	3.05969700	-0.71239900
C	-2.17469300	-2.49076200	-0.00625100
C	-1.17428800	2.81452800	-0.48433100
C	-0.83933200	4.29763400	-0.39080300
N	-0.06498000	2.01668100	-0.33927700
C	0.68031900	4.26863700	-0.70950600
C	1.06801500	2.84181000	-0.33074000
C	-0.78168800	-2.69285100	-0.28778400
C	-0.13145500	-4.04600600	-0.52317400
N	0.07852300	-1.68928800	-0.40601000
C	1.39716500	-3.71659200	-0.36011100
C	1.44982000	-2.19035200	-0.75531800
C	2.37819800	2.43001900	-0.12027500
C	2.69490400	1.03536400	-0.01672100
C	4.08991900	0.41755500	0.20828800
N	1.74521400	0.10056000	-0.07351500
C	3.82843900	-1.06200200	-0.24142700
C	2.34395500	-1.25449500	0.08591100
Co	-0.08689500	0.12441600	-0.20017700
H	1.20514800	5.01775500	-0.09182200
H	3.94507300	-1.07124500	-1.34200700
H	-0.41765100	-4.74888600	0.28128500
H	2.23184500	-1.52775500	1.15110500
C	-0.27068900	-0.21480600	2.07799200
C	-0.79869500	1.14681300	2.54276600
H	-1.58585100	1.56415300	1.88980200
C	3.48404700	3.46998300	-0.06243300
H	4.20634700	3.24490200	0.73905900
H	4.05560100	3.53393500	-1.00668300
H	3.08543900	4.47458000	0.14504900
C	4.42972700	0.51274700	1.71719900
H	4.46606200	1.56625000	2.04478200
H	3.67700800	-0.00712900	2.33713300
H	5.41794600	0.06348400	1.92348200
C	5.24068200	0.99878300	-0.63955300
H	5.64358600	1.93983400	-0.23426000
H	6.07461200	0.27273400	-0.65959000
H	4.92166600	1.17476900	-1.68249900
C	4.77742300	-2.10080000	0.36042900
H	4.62968700	-3.08843300	-0.10746300
H	5.83243200	-1.81479800	0.19583100
H	4.62263100	-2.21644300	1.44742100
C	1.67793400	-1.94625500	-2.26122100
H	2.66306800	-2.31553400	-2.59064200
H	0.90277400	-2.44738700	-2.86178500
H	1.61927900	-0.86355600	-2.46960500
C	2.30361600	-4.62161900	-1.20854600
H	3.36543800	-4.34768800	-1.08172400
H	2.19190300	-5.67353700	-0.88735500
H	2.07018100	-4.57439100	-2.28445700
C	1.73649900	-3.93346100	1.13358900
H	1.56892100	-4.99407500	1.39609200
H	2.78924900	-3.69780900	1.36091500
H	1.09385600	-3.32011700	1.79237800
C	-0.59728400	-4.68383100	-1.85007600
H	-0.11415400	-5.66424900	-2.00543600
H	-1.68870000	-4.84958200	-1.82538200
H	-0.37688000	-4.04611700	-2.72245000
C	-3.00779600	-3.70247700	0.37696400
H	-3.69920700	-3.47044600	1.20262400

H	-3.61136000	-4.09683500	-0.46059000
H	-2.36409600	-4.52457400	0.72751200
C	-5.27913400	-1.82510300	-0.40258900
H	-5.42580600	-2.67764100	0.27725700
H	-6.24660100	-1.29368500	-0.46493900
H	-5.04193700	-2.21943600	-1.40517000
C	-4.41572000	-0.57995500	1.62322700
H	-3.72410400	0.20020800	1.99048600
H	-5.45165700	-0.24062900	1.81059500
H	-4.23970000	-1.49625800	2.21365900
C	-4.63026700	0.42296000	-2.15016300
H	-5.67143300	0.08693400	-2.29649400
H	-4.52338000	1.41558800	-2.62281300
H	-3.95918100	-0.27959900	-2.67750800
C	1.03923300	4.51448600	-2.19171700
H	0.75498500	5.53301100	-2.50918500
H	2.12596100	4.40066000	-2.34746600
H	0.52410300	3.78887700	-2.84737300
C	-1.04378300	4.73634400	1.08459600
H	-0.77215600	5.80167300	1.20670600
H	-2.09812300	4.60752500	1.38824300
H	-0.41366600	4.13864100	1.76783000
C	-1.68185800	5.19718000	-1.30925800
H	-2.73403400	5.22264400	-0.97363900
H	-1.30303500	6.23489400	-1.27928400
H	-1.66881400	4.85177800	-2.35702200
H	0.03746000	1.86947100	2.56177900
H	-0.97059100	-1.04396300	1.95139400
H	0.78481300	-0.45911800	2.17221200
C	-1.22978500	0.70004100	3.94191000
H	-1.13186500	1.49431000	4.73427600
H	-2.33622900	0.45017900	3.92365200
O	-0.39644100	-0.41026900	4.12948600

TMSBr



E (BP86-D3/6-31G(d)/SMD (MeCN)) = -2981.298478

E (BP86-D3/6-311++G(2df,p)/SMD (MeCN)// BP86-D3/6-31G(d))/SMD (MeCN)) = -2983.804338

Zero-point correction=	0.109642
Thermal correction to Energy=	0.118528
Thermal correction to Enthalpy=	0.119472
Thermal correction to Gibbs Free Energy=	0.075902

Charge = 0 Multiplicity = 1

Si	0.83574600	-0.00003600	-0.00008600
C	1.39015300	1.03230800	-1.47175900
H	2.49629700	1.05747800	-1.50605100
H	1.02739200	0.60311000	-2.42256300
H	1.02582400	2.07194800	-1.39274900
C	1.39066200	0.75834300	1.62973400
H	1.02780900	0.16953200	2.49085900

H	2.49683700	0.77664000	1.66772500
H	1.02703300	1.79598800	1.73420900
C	1.39013900	-1.79076500	-0.15823300
H	2.49628200	-1.83318100	-0.16151400
H	1.02641900	-2.39995400	0.68816700
H	1.02693400	-2.24185900	-1.09867400
Br	-1.43934300	0.00004300	0.00009500

Br(CH₂)₃OTMS



E (BP86-D3/6-31G(d)/SMD (MeCN)) = -3174.442469

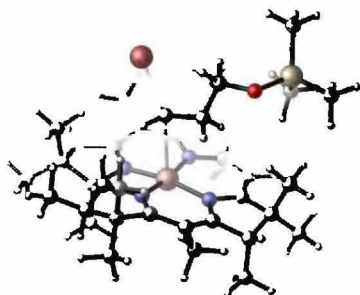
E (BP86-D3/6-311++G(2df,p)/SMD (MeCN)// BP86-D3/6-31G(d))/SMD (MeCN)) = -3177.023972

Zero-point correction=	0.196034
Thermal correction to Energy=	0.210523
Thermal correction to Enthalpy=	0.211467
Thermal correction to Gibbs Free Energy=	0.151908

Charge = 0 Multiplicity = 1

C	0.93136100	-0.24491100	0.00027200
C	-0.42712700	0.47061300	-0.00001700
C	2.07259700	0.76248800	0.00022500
H	0.99508200	-0.89357300	0.89249100
H	0.99530700	-0.89397500	-0.89164200
H	-0.51017400	1.12197300	-0.89586100
H	-0.51008500	1.12297300	0.89511500
H	2.08082600	1.39643100	0.89997700
H	2.08058300	1.39668600	-0.89935700
O	-1.45593200	-0.52961400	0.00058300
Si	-3.09280600	-0.07269700	-0.00007800
C	-3.48576700	0.93849900	1.54725000
H	-2.92745700	1.89255600	1.56812800
H	-4.56417900	1.18369400	1.58395500
H	-3.23556300	0.37674600	2.46625000
C	-4.03905100	-1.70086200	0.00097200
H	-5.12909600	-1.51327100	-0.00001200
H	-3.79993200	-2.30576800	-0.89286400
H	-3.80120500	-2.30376700	0.89650100
C	-3.48572800	0.93650200	-1.54868400
H	-3.23495200	0.37413800	-2.46714400
H	-4.56438100	1.18065100	-1.58569200
H	-2.92832600	1.89106500	-1.57034400
Br	3.84578800	-0.16416800	-0.00009100

Co1b_BrPrOTMS1_ts1a



E (BP86-D3/6-31G(d)/SMD (MeCN)) = -6102.942436

E (BP86-D3/6-311++G(2df,p)/SMD (MeCN)// BP86-D3/6-31G(d))/SMD (MeCN)) = -6106.094499

Zero-point correction=	0.974500
Thermal correction to Energy=	1.029556
Thermal correction to Enthalpy=	1.030500
Thermal correction to Gibbs Free Energy=	0.891014

Charge = 0 Multiplicity = 1

C	-0.03532700	-2.51440400	-1.50012100
C	-1.31606300	-3.34534800	-1.72107500
C	-2.16924600	-2.35258000	-2.56659300
C	-1.60628100	-1.02459500	-2.12463800
N	-0.34921800	-1.14153500	-1.59409200
H	-3.23970200	-2.43751100	-2.29900900
C	-2.30013600	0.17246200	-2.27499800
H	-3.29588000	0.11360400	-2.72495900
C	1.20716900	-3.00617100	-1.12041200
C	-1.84811700	1.42086000	-1.86129800
C	-2.71680700	2.67243700	-1.89949400
N	-0.64181900	1.63159000	-1.24012900
C	-1.65445100	3.77298400	-1.62775400
C	-0.54323600	2.99546200	-0.93051000
C	2.28638500	-2.10822800	-0.83048900
C	3.72222000	-2.53338300	-0.57228500
N	2.12258900	-0.79097800	-0.74138100
C	4.31216400	-1.27993800	0.16587400
C	3.42224400	-0.11282000	-0.40918800
C	0.45659400	3.59096900	-0.17101900
C	1.58719800	2.82909700	0.26893400
C	2.75519700	3.32665600	1.14351700
N	1.70586400	1.53039700	-0.02240500
C	3.82512700	2.21674400	0.85802400
C	2.96023200	0.98533000	0.57056200
Co	0.66186200	0.29985500	-0.88716800
H	-2.08654700	4.55165500	-0.97571100
H	4.33131700	2.51428000	-0.08018100
H	3.74521100	-3.38252100	0.13555900
H	2.68570800	0.50580900	1.52696500
C	-0.01911700	-0.73015300	1.39691600
C	-1.34385900	0.00023100	1.42406600
H	-1.87273200	-0.18408700	0.47347900
H	0.87356600	-0.21827900	1.74183800
H	0.11451700	-1.60907000	0.77747600
C	0.36427700	5.07272100	0.15095200
H	0.62830500	5.27308700	1.20240700

H	1.03827600	5.68494600	-0.47607900
H	-0.65564300	5.45818900	0.00273000
C	2.29061900	3.32224100	2.62203200
H	1.44047300	4.01228200	2.76363800
H	1.96540000	2.31602200	2.94343700
H	3.10600300	3.65259100	3.29078100
C	3.35696000	4.69930700	0.77549700
H	2.77165900	5.54683700	1.16443000
H	4.36860900	4.77749600	1.21552600
H	3.45558900	4.81427600	-0.31880000
C	4.88153500	2.03848300	1.95070300
H	5.67723400	1.34912900	1.62248300
H	5.36339500	3.00274500	2.19547100
H	4.44549600	1.63128800	2.87972600
C	3.97784300	0.51795600	-1.70224400
H	4.94654800	1.01611300	-1.53210400
H	4.11409400	-0.24519900	-2.48438300
H	3.25815400	1.26476900	-2.08108100
C	5.82020400	-1.09986700	-0.06657700
H	6.19668100	-0.20184500	0.45329700
H	6.36998200	-1.97065700	0.33565300
H	6.08005000	-1.00497600	-1.13334100
C	4.06478700	-1.50454100	1.67843400
H	4.62626500	-2.39922800	2.00596200
H	4.41775200	-0.65551800	2.28761000
H	2.99733200	-1.68101300	1.91522400
C	4.42281400	-3.01568500	-1.86101600
H	5.46109900	-3.32761500	-1.65191000
H	3.88783900	-3.88899800	-2.27471200
H	4.44506000	-2.23891100	-2.64339400
C	1.45302300	-4.49719700	-0.95434600
H	0.65852400	-4.97192500	-0.35549900
H	1.50598900	-5.03298700	-1.91872600
H	2.39887600	-4.68918400	-0.42644800
C	-1.20559200	-4.71995100	-2.40722500
H	-0.84404200	-5.50337600	-1.72470000
H	-2.21223900	-5.02885300	-2.74440500
H	-0.54426800	-4.69702900	-3.28980400
C	-1.97030600	-3.50999900	-0.32084800
H	-2.17190000	-2.52598900	0.13716500
H	-2.92823100	-4.05619400	-0.40767900
H	-1.30938100	-4.06590100	0.36703600
C	-2.02525400	-2.49239000	-4.09870300
H	-2.44099000	-3.44719200	-4.46463600
H	-2.56724700	-1.67148200	-4.60119700
H	-0.96378200	-2.43487100	-4.40218300
C	-1.07893500	4.45570400	-2.88836500
H	-1.85932400	5.01355100	-3.43515500
H	-0.28443000	5.16886900	-2.60763500
H	-0.63840600	3.70980000	-3.57480800
C	-3.70515600	2.60027300	-0.70514600
H	-4.28392400	3.54011400	-0.62849300
H	-4.41575100	1.76738000	-0.84418700
H	-3.17531700	2.43723700	0.25092700
C	-3.51263200	2.84431900	-3.20420800
H	-4.27699800	2.05273700	-3.30233200
H	-4.04273900	3.81418500	-3.20541700
H	-2.86505300	2.80048300	-4.09635800
H	-1.15078000	1.08674900	1.47401900
C	-2.32309300	-0.34845000	2.56350300

H	-1.85084400	-0.16245000	3.54469800
H	-2.57230400	-1.42760400	2.52604400
O	-3.48892100	0.48702000	2.45270300
Si	-4.97741200	-0.16157900	1.96779300
C	-4.82911200	-1.05888500	0.30869300
H	-4.21615200	-0.49304600	-0.41464900
H	-4.36798900	-2.05381400	0.43767000
H	-5.83102700	-1.21223300	-0.13601700
C	-6.14000800	1.31813600	1.86639600
H	-7.15118700	0.99203800	1.55828600
H	-6.23257900	1.81507100	2.84982800
H	-5.78968000	2.06906500	1.13641700
C	-5.59577400	-1.38999600	3.26677300
H	-4.87360300	-2.21450000	3.41565500
H	-5.75594400	-0.89775800	4.24388700
H	-6.55590000	-1.84195100	2.95236900
Br	0.18405500	-2.21319500	3.26409200

Br

E (BP86-D3/6-31G(d)/SMD (MeCN)) = -2572.098445

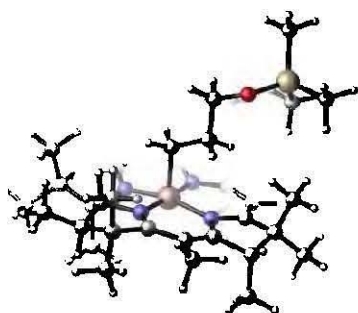
E (BP86-D3/6-311++G(2df,p)/SMD (MeCN)// BP86-D3/6-31G(d))/SMD (MeCN)) = -2574.565447

Zero-point correction=	0.000000
Thermal correction to Energy=	0.001416
Thermal correction to Enthalpy=	0.002360
Thermal correction to Gibbs Free Energy=	-0.016176

Charge = -1 Multiplicity = 1

Br	0.00000000	0.00000000	0.00000000
----	------------	------------	------------

(CH₃)₁₅(corrin)Co(III)-(CH₂)₃-OTMS - II



E (BP86-D3/6-31G(d)/SMD (MeCN)) = -3530.848806

E (BP86-D3/6-311++G(2df,p)/SMD (MeCN)// BP86-D3/6-31G(d))/SMD (MeCN)) = -3531.554037

Zero-point correction=	0.975627
Thermal correction to Energy=	1.028655
Thermal correction to Enthalpy=	1.029599
Thermal correction to Gibbs Free Energy=	0.895520

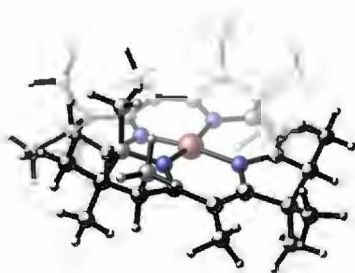
Charge = 1 Multiplicity = 1

C	-0.02249300	2.94578400	0.56731500
C	-1.26055000	3.83448300	0.79396800
C	-1.99019900	3.03923100	1.91991900

C	-1.49916200	1.63849000	1.66095600
N	-0.30972500	1.63282000	0.99226900
H	-3.08635900	3.10245700	1.79515000
C	-2.19102000	0.50613700	2.08333600
H	-3.14596300	0.67352300	2.58902200
C	1.16015500	3.32000300	-0.05197900
C	-1.78157500	-0.80908300	1.89097400
C	-2.65022200	-2.00915400	2.24207300
N	-0.61752400	-1.17019800	1.26632900
C	-1.60458100	-3.15689300	2.16810600
C	-0.52570600	-2.56653700	1.26708200
C	2.23928900	2.37700300	-0.17685400
C	3.67138500	2.73719100	-0.53537800
N	2.09447200	1.08357500	0.05215500
C	4.28951400	1.34095100	-0.91556800
C	3.39537900	0.34483500	-0.08222000
C	0.44897400	-3.32175100	0.62946200
C	1.57553200	-2.68512600	0.00302700
C	2.75241100	-3.38139100	-0.71175100
N	1.69954900	-1.36398600	-0.04169900
C	3.81611500	-2.22674000	-0.71891000
C	2.94333500	-0.96783500	-0.75841200
Co	0.62688600	0.05387000	0.47651300
H	-2.06725900	-4.05247300	1.72018600
H	4.31950800	-2.26888600	0.26558500
H	3.67918000	3.37333700	-1.43944100
H	2.65059700	-0.74583300	-1.80068600
C	-0.10987800	0.23962100	-1.34562800
C	-1.50413400	-0.34953400	-1.42370900
H	-2.14990600	0.07387000	-0.63518200
H	0.57962800	-0.27009800	-2.04186100
H	-0.10151000	1.32261300	-1.56994600
C	0.35299800	-4.83619000	0.66410100
H	0.61322600	-5.27912400	-0.31020700
H	1.02825200	-5.28117600	1.41708200
H	-0.66741600	-5.17123400	0.90179200
C	2.29087300	-3.75064000	-2.14447900
H	1.44390300	-4.45724000	-2.11639300
H	1.96903400	-2.85890200	-2.71181100
H	3.11396200	-4.23586000	-2.69849300
C	3.35453800	-4.61111800	-0.00189600
H	2.77525700	-5.53226600	-0.16733400
H	4.36884000	-4.79105500	-0.40291300
H	3.44659300	-4.44256200	1.08574600
C	4.87529600	-2.32667400	-1.81844900
H	5.66173000	-1.56671700	-1.67771300
H	5.36792300	-3.31570700	-1.80146400
H	4.43976300	-2.17985900	-2.82200200
C	3.92549200	0.06795500	1.33993700
H	4.89914200	-0.44754100	1.31464200
H	4.04352700	1.00644900	1.90367200
H	3.20640600	-0.56735100	1.88619300
C	5.79129600	1.24140300	-0.60847700
H	6.17762200	0.23879600	-0.86033300
H	6.34861000	1.97631700	-1.21732500
H	6.02593300	1.43705600	0.45004000
C	4.07745900	1.16371400	-2.43730600
H	4.62863600	1.95561600	-2.97619800
H	4.45277600	0.19244300	-2.79924300
H	3.01076800	1.25009800	-2.71612800

C	4.35294000	3.54980500	0.58657000
H	5.38644800	3.81039100	0.30114200
H	3.80504000	4.49251900	0.75878200
H	4.38414200	3.00013400	1.54182900
C	1.37067800	4.71947400	-0.60251600
H	0.48537300	5.07070600	-1.15589000
H	1.58628400	5.46063300	0.18744300
H	2.21409800	4.74171300	-1.30932400
C	-1.04015600	5.30632300	1.18693300
H	-0.76652800	5.93339500	0.32570600
H	-1.98634200	5.70959200	1.59131700
H	-0.26219800	5.41988500	1.96038800
C	-2.10641300	3.74911900	-0.50600800
H	-2.32231700	2.69751500	-0.76592200
H	-3.06720500	4.27798100	-0.36787900
H	-1.57465600	4.21043400	-1.35608000
C	-1.62490000	3.44699800	3.36530800
H	-1.98089000	4.46494200	3.59737700
H	-2.09527100	2.74947900	4.08059000
H	-0.53147500	3.41313700	3.52201300
C	-0.97017700	-3.55153100	3.52053000
H	-1.72823100	-3.96567900	4.20717000
H	-0.19174400	-4.31895300	3.37022500
H	-0.49879000	-2.67780700	4.00572800
C	-3.68983900	-2.18515000	1.10078900
H	-4.29968900	-3.08808200	1.28805100
H	-4.36459600	-1.31317600	1.05026600
H	-3.19618800	-2.29685400	0.11931100
C	-3.38624100	-1.87969900	3.58536800
H	-4.15560700	-1.08916100	3.53361000
H	-3.90275700	-2.82599600	3.82612500
H	-2.70119900	-1.63477300	4.41445600
H	-1.46279900	-1.44072000	-1.25570700
C	-2.19901700	-0.11390700	-2.77647000
H	-1.55900700	-0.47391100	-3.60581800
H	-2.36503100	0.97236600	-2.93763600
O	-3.42683200	-0.85897400	-2.82521500
Si	-4.93994400	-0.18764900	-2.45862400
C	-4.84144000	1.05598000	-1.03800700
H	-4.34345100	0.64458000	-0.14216600
H	-4.29781200	1.96785600	-1.34206700
H	-5.86378400	1.36459200	-0.74639100
C	-6.02133900	-1.66086600	-1.99948300
H	-7.05849600	-1.33345500	-1.79777600
H	-6.05617500	-2.40439500	-2.81702900
H	-5.64283900	-2.16752800	-1.09302400
C	-5.62143500	0.69790700	-3.98390700
H	-4.94735600	1.51532700	-4.30234900
H	-5.73857800	0.00303000	-4.83600300
H	-6.61132400	1.14497200	-3.77175800

(CH₃)₁₅(corrin)Co(II)



E (BP86-D3/6-31G(d)/SMD (MeCN)) = -2928.348697

E (BP86-D3/6-311++G(2df,p)/SMD (MeCN)// BP86-D3/6-31G(d))/SMD (MeCN)) = -2928.92078

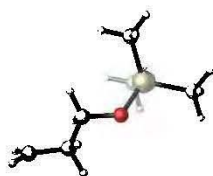
Zero-point correction=	0.778592
Thermal correction to Energy=	0.818236
Thermal correction to Enthalpy=	0.819181
Thermal correction to Gibbs Free Energy=	0.713227

Charge = 1 Multiplicity = 2

C	2.90498200	-0.90195900	-0.30446300
C	4.33074400	-0.38391700	-0.59130600
C	4.26947300	1.02558600	0.07486500
C	2.79671400	1.33400800	-0.00989800
N	2.04706500	0.19558500	-0.09529300
H	4.86572800	1.75674000	-0.50045800
C	2.29062500	2.63069000	0.03041200
H	3.02054400	3.44349700	0.07654000
C	2.48974000	-2.22584700	-0.31325300
C	0.94221900	2.97223700	-0.00210200
C	0.44122000	4.40810400	-0.07837300
N	-0.08344700	2.06585400	-0.04190800
C	-1.03607500	4.22043600	0.36969000
C	-1.30022400	2.75671600	0.03320100
C	1.12923900	-2.56176500	0.01082000
C	0.62396100	-3.96906400	0.28788100
N	0.16984700	-1.65986700	0.13702400
C	-0.93442400	-3.80651400	0.14738100
C	-1.14172000	-2.28414600	0.50344300
C	-2.56676400	2.20189600	-0.08441900
C	-2.73603700	0.77819600	-0.20907000
C	-4.06283500	0.01647400	-0.40895700
N	-1.69976200	-0.05101600	-0.21148100
C	-3.63172100	-1.44177500	-0.01861200
C	-2.13591700	-1.46734800	-0.35957600
Co	0.13802700	0.17678200	-0.07992700
H	-1.68965200	4.89938500	-0.20384900
H	-3.73428700	-1.50390900	1.08110400
H	0.97070400	-4.65652700	-0.50509300
H	-1.98750900	-1.73777600	-1.42051800
C	-3.78371400	3.10797400	-0.03237600
H	-4.51296900	2.84977100	-0.81770300
H	-4.31049500	3.04383200	0.93685100
H	-3.51184000	4.16230400	-0.18678500
C	-4.45785200	0.12971400	-1.90262600
H	-4.61600400	1.18456200	-2.18636600
H	-3.67608400	-0.28674200	-2.56295600

H	-5.39974800	-0.41456800	-2.09363500
C	-5.23870700	0.44258500	0.49456000
H	-5.75774300	1.34316800	0.13279600
H	-5.98363800	-0.37414700	0.51492200
H	-4.90516500	0.62044600	1.53235500
C	-4.46922800	-2.55690100	-0.64863400
H	-4.20807800	-3.53705100	-0.21540900
H	-5.54618100	-2.39245300	-0.46315200
H	-4.31688300	-2.61785200	-1.74030100
C	-1.37903300	-2.01522200	2.00377500
H	-2.32577500	-2.45612900	2.35496000
H	-0.55804400	-2.43019200	2.60880200
H	-1.41152100	-0.92535600	2.18025600
C	-1.73310700	-4.76764100	1.04086800
H	-2.81756100	-4.59258600	0.92956400
H	-1.53149300	-5.81318300	0.74483700
H	-1.48357600	-4.66785900	2.10943700
C	-1.27497500	-4.10670500	-1.33166100
H	-1.00784400	-5.15453200	-1.55983800
H	-2.34909500	-3.98432700	-1.54604700
H	-0.70651700	-3.45963700	-2.02503500
C	1.17610900	-4.51409200	1.62272700
H	0.79969000	-5.53465900	1.80844200
H	2.27818800	-4.56482200	1.58487200
H	0.89894100	-3.87907900	2.48041300
C	3.43684800	-3.36093000	-0.66486100
H	4.07101000	-3.10421000	-1.52812200
H	4.10597000	-3.63557600	0.17016700
H	2.87792000	-4.26728400	-0.94426000
C	5.51724400	-1.21131600	-0.06260000
H	5.73246900	-2.08537600	-0.69475900
H	6.42237400	-0.57718700	-0.07214800
H	5.35620000	-1.56127200	0.97080300
C	4.46260900	-0.20144200	-2.12826400
H	3.68551900	0.48069300	-2.51897700
H	5.45203200	0.22820600	-2.37047600
H	4.36788000	-1.16811600	-2.65270800
C	4.70791000	1.07920500	1.55658200
H	5.78559800	0.86975500	1.66461000
H	4.51320500	2.08541000	1.96772900
H	4.14579800	0.34613100	2.16315000
C	-1.29103600	4.44175700	1.87750100
H	-1.09133000	5.48869500	2.16374600
H	-2.34196700	4.21469800	2.12597000
H	-0.64617800	3.78378700	2.48783700
C	0.47611400	4.84116100	-1.56919500
H	0.07655000	5.86680100	-1.67211200
H	1.51081300	4.82888700	-1.95529400
H	-0.13671500	4.16707600	-2.19528600
C	1.25567500	5.40423800	0.76234300
H	2.26529700	5.54166500	0.33636200
H	0.76088200	6.39192700	0.76169300
H	1.36958800	5.07162000	1.80787100

(CH₂)₃OTMS



E (BP86-D3/6-31G(d)/SMD (MeCN)) = -602.403478

E (BP86-D3/6-311++G(2df,p)/SMD (MeCN)// BP86-D3/6-31G(d))/SMD (MeCN)) = -602.549784

Zero-point correction=	0.189658
Thermal correction to Energy=	0.202598
Thermal correction to Enthalpy=	0.203542
Thermal correction to Gibbs Free Energy=	0.150106

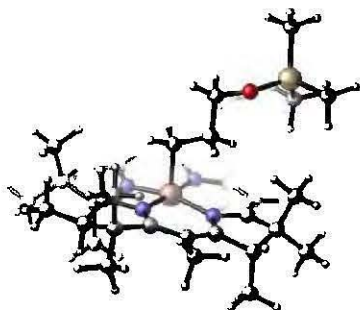
Charge = 0 Multiplicity = 2

C	3.96232800	-0.22748700	0.02902600
C	2.72313500	0.59571600	-0.08527000
H	2.70404100	1.39475100	0.68063500
H	2.67767000	1.11908500	-1.07029400
C	1.44093000	-0.24378400	0.03268000
H	1.45521100	-1.05167700	-0.73025800
H	1.40476900	-0.72994700	1.03046200
O	0.30612600	0.61458500	-0.16174100
Si	-1.26904200	0.00254500	0.00065300
C	-1.55187500	-1.40173300	-1.23244800
H	-0.89272200	-2.26566900	-1.02840300
H	-2.59714700	-1.76049900	-1.17642900
H	-1.36445800	-1.06772400	-2.26982300
C	-1.54961300	-0.62229300	1.76239500
H	-1.36859000	0.17729500	2.50443300
H	-2.59321900	-0.96869600	1.88665400
H	-0.88647900	-1.47203200	2.00854900
C	-2.39330100	1.46597000	-0.37709400
H	-2.21951700	2.29952500	0.32800300
H	-2.23059900	1.84531500	-1.40262700
H	-3.45524900	1.16842600	-0.29203300
H	4.02787700	-1.20459000	-0.46410100
H	4.86636300	0.16580600	0.50429800

TD DFT calculations

Three lowest singlet excited states for intermediate **II** were calculated at TD-BP86-D3/6-311++G(2df,p) level of theory including solvation (acetonitrile) with SMD model.

(CH₃)₁₅(corrin)Co(III)-(CH₂)₃-OTMS – II (*vertical excitation*)



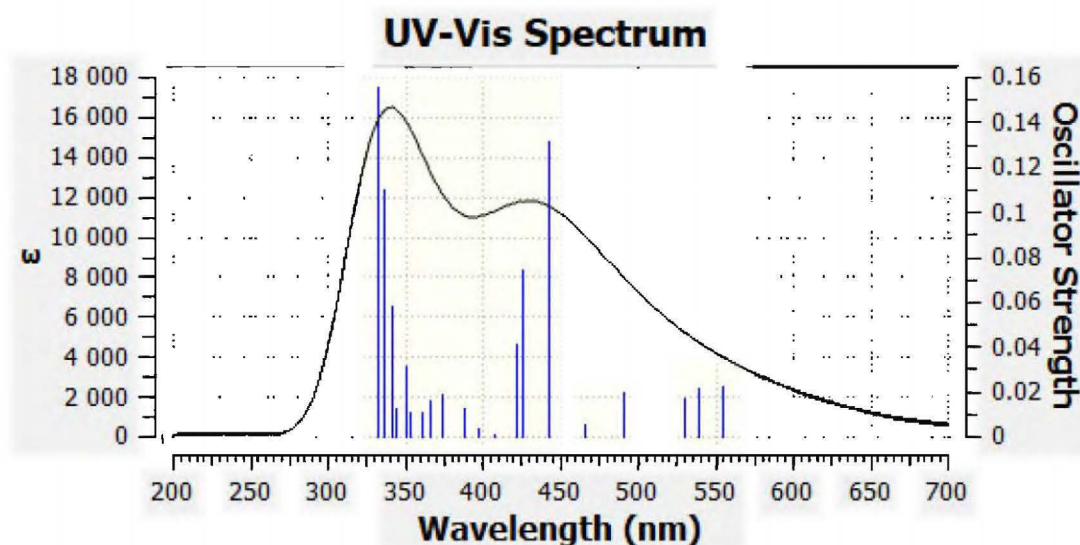
Excitation energies and oscillator strengths:

Excited State 1: Singlet-A 2.2335 eV 555.11 nm f=0.0225 <S**2>=0.000
189 -> 193 -0.13359
190 -> 192 0.31747
191 -> 192 0.50814
191 -> 193 -0.32300
Total Energy, E(TD-HF/TD-DFT) = -3531.47195770

Excited State 2: Singlet-A 2.2995 eV 539.18 nm f=0.0211 <S**2>=0.000
189 -> 193 -0.13850
190 -> 192 -0.21775
191 -> 192 0.40684
191 -> 193 0.49373

Excited State 3: Singlet-A 2.3412 eV 529.57 nm f=0.0161 <S**2>=0.000
189 -> 192 0.18852
190 -> 192 0.56898
191 -> 192 -0.11554
191 -> 193 0.32439
191 -> 194 -0.12033

Simulated UV spectrum of **II** calculated for 20 excited states at TD-BP86/6-311++G(2df,p)level of theory



(CH₃)₁₅(corrin)Co(III)-(CH₂)₃-OTMS – **II (Relaxed)**

Geometry of the **II** was optimized at TD-BP86-D3/6-31G(d) (root=1) including solvation (acetone) with SMD model. Frequency analysis was performed at the same level to provide correction to thermodynamic functions. Then the energy of the lowest singlet excited state was calculated employing TD-BP86-D3/6-311++G(2df,p).

E (TD-BP86-D3/6-31G(d)/SMD (MeCN)) = -3530.776482

E (TD-BP86-D3/6-311++G(2df,p)/SMD (MeCN)// TD-BP86-D3/6-31G(d))/SMD (MeCN)) = -3531.471958

Zero-point correction=	0.972234
Thermal correction to Energy=	1.026142
Thermal correction to Enthalpy=	1.027087
Thermal correction to Gibbs Free Energy=	0.890414

Charge = 0 Multiplicity = 1

C	-0.05597300	2.95315800	0.51546400
C	-1.25993200	3.87600000	0.78692900
C	-1.99762400	3.07513100	1.90783500
C	-1.55005400	1.66692400	1.61765700
N	-0.36947900	1.66558000	0.89620700
H	-3.09307800	3.17258000	1.79710400
C	-2.20301800	0.52747200	2.06337300
H	-3.16008300	0.68409000	2.57039200
C	1.16713300	3.31830700	-0.08187300
C	-1.77739600	-0.79239700	1.90868300
C	-2.64637500	-2.00120800	2.23338800
N	-0.57321200	-1.17858900	1.35501900
C	-1.58050100	-3.13648400	2.23810900
C	-0.48976600	-2.56155600	1.34147900
C	2.22604300	2.37490400	-0.14438300
C	3.65744300	2.72325500	-0.51844500
N	2.11913500	1.07964200	0.18125100
C	4.27985300	1.33021700	-0.88594700
C	3.40347700	0.32734900	-0.03346700
C	0.47318100	-3.33208100	0.67083200
C	1.56450100	-2.70093200	0.01437600
C	2.74212900	-3.38597800	-0.70763400

N	1.68264000	-1.36888500	-0.05812700
C	3.80329900	-2.22863500	-0.71135400
C	2.93261700	-0.96386400	-0.74307600
Co	0.54621400	0.06131100	0.37220200
H	-2.01988600	-4.05485500	1.81377100
H	4.30699200	-2.27769300	0.27211800
H	3.67207100	3.36061400	-1.42055500
H	2.66746800	-0.71885500	-1.78778200
C	-0.06985200	0.26197000	-1.45820900
C	-1.45791300	-0.35823300	-1.45747300
H	-2.09475000	0.08192200	-0.67115100
H	0.61606800	-0.26193400	-2.14333600
H	-0.08474800	1.34616800	-1.67555700
C	0.35610100	-4.84532400	0.70809600
H	0.64473900	-5.29931600	-0.25278400
H	0.99176200	-5.30085200	1.49026600
H	-0.67878000	-5.16375700	0.90717200
C	2.27591500	-3.74673300	-2.14076100
H	1.43119100	-4.45645500	-2.11111000
H	1.94702300	-2.85136800	-2.69863700
H	3.09684600	-4.22456600	-2.70482500
C	3.34981200	-4.61818500	-0.00767800
H	2.76733700	-5.53793400	-0.17047400
H	4.36102300	-4.79983700	-0.41592800
H	3.44894400	-4.45293900	1.07988200
C	4.86374300	-2.32429600	-1.81009200
H	5.64993400	-1.56447600	-1.66623800
H	5.35710900	-3.31304500	-1.79555900
H	4.42969000	-2.17526800	-2.81404300
C	3.97404300	0.01282700	1.36360000
H	4.94238100	-0.50980400	1.30109900
H	4.11635900	0.93691700	1.94574300
H	3.26313700	-0.63106400	1.91143900
C	5.78530900	1.24408100	-0.59157900
H	6.17799700	0.24564200	-0.85000900
H	6.33082600	1.98568200	-1.20302500
H	6.02715000	1.43843900	0.46550800
C	4.05964400	1.15067000	-2.40687100
H	4.60514700	1.94656000	-2.94582500
H	4.43758600	0.18276100	-2.77411100
H	2.99162700	1.23525600	-2.68139400
C	4.32515200	3.53341800	0.61546100
H	5.36495500	3.78363600	0.34451700
H	3.78276400	4.48066500	0.77766300
H	4.33483600	2.98215800	1.57016000
C	1.39001300	4.71238000	-0.63692900
H	0.50315600	5.07268100	-1.18271200
H	1.62251600	5.45678900	0.14631100
H	2.22640900	4.72428100	-1.35283700
C	-0.98382400	5.33087000	1.20464100
H	-0.69911200	5.96274400	0.35047200
H	-1.91045200	5.75884900	1.62803500
H	-0.19281900	5.40323200	1.96966500
C	-2.12434500	3.84701800	-0.50422300
H	-2.37963800	2.80856600	-0.78061300
H	-3.06413100	4.40531900	-0.33987400
H	-1.58913400	4.30847300	-1.35205300
C	-1.60470200	3.45300600	3.35478700
H	-1.92173000	4.47957800	3.60560500
H	-2.09280400	2.76133600	4.06373000

H	-0.51166800	3.37795000	3.50005700
C	-0.97720000	-3.47291500	3.61946700
H	-1.74433500	-3.87950700	4.30122300
H	-0.18060100	-4.22965700	3.51203300
H	-0.53479200	-2.57494100	4.08778600
C	-3.62324900	-2.22046100	1.04607200
H	-4.21534200	-3.13974100	1.21220600
H	-4.31926800	-1.36903700	0.95452700
H	-3.08110800	-2.32771900	0.08981400
C	-3.45006500	-1.86072400	3.53583200
H	-4.22707800	-1.08230300	3.43433800
H	-3.96429000	-2.81107700	3.76605300
H	-2.80960000	-1.59326800	4.39330000
H	-1.38928900	-1.44290900	-1.26413600
C	-2.18853400	-0.16740600	-2.80811600
H	-1.56157400	-0.55501500	-3.63368900
H	-2.35882300	0.91327500	-2.99407600
O	-3.40710500	-0.91616800	-2.79325000
Si	-4.91626500	-0.21888200	-2.43240000
C	-4.79215500	1.02590400	-1.01614500
H	-4.29528800	0.61109800	-0.12148400
H	-4.23730100	1.92864500	-1.32726600
H	-5.80795300	1.35106000	-0.71993400
C	-6.01434800	-1.67927200	-1.97826600
H	-7.04335900	-1.33731800	-1.76017100
H	-6.07056900	-2.41058100	-2.80547900
H	-5.63378900	-2.20397200	-1.08330000
C	-5.56730200	0.67280800	-3.96579300
H	-4.87317900	1.47329600	-4.28386600
H	-5.69536300	-0.02404200	-4.81449900
H	-6.54781500	1.14299800	-3.76057000

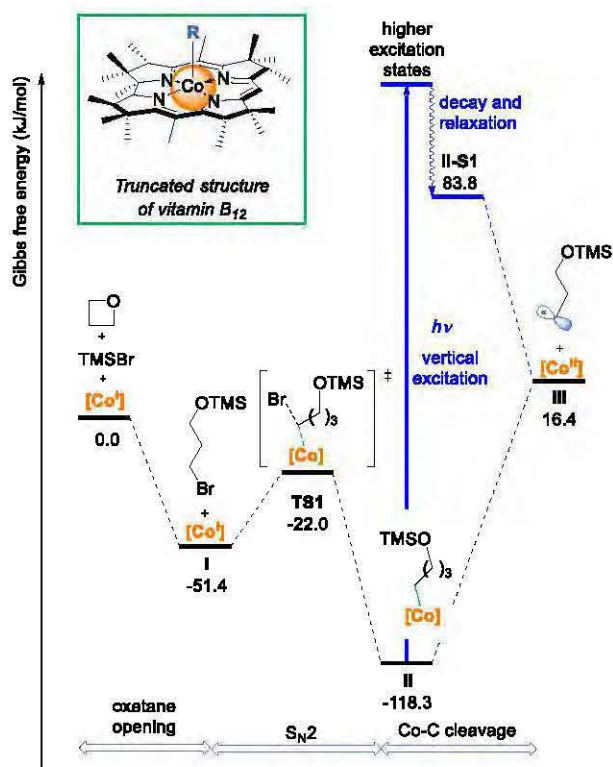


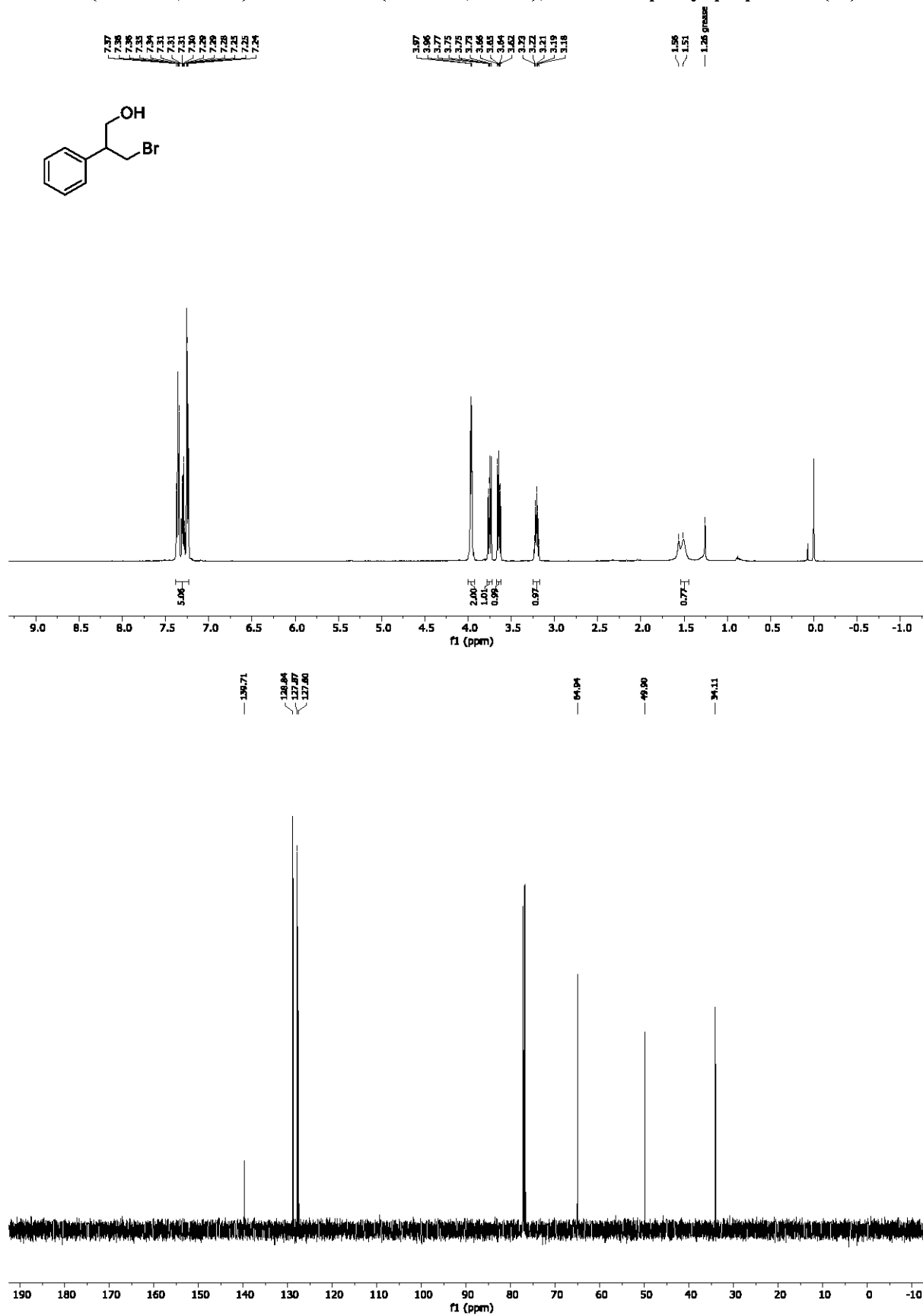
Figure S4 Calculated Gibbs free energy profile for the reaction of oxetanes with the Co(I)-corrin complex in the presence of TMSBr

8. References

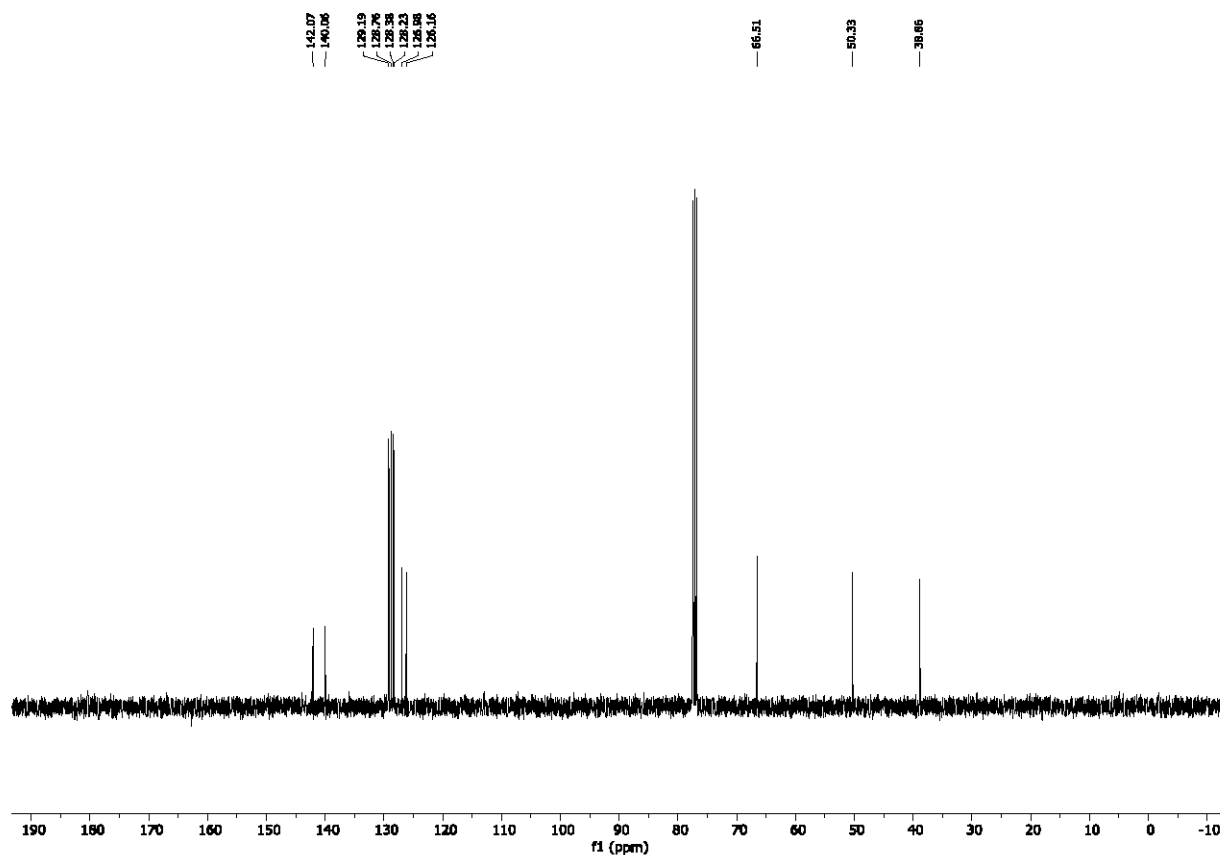
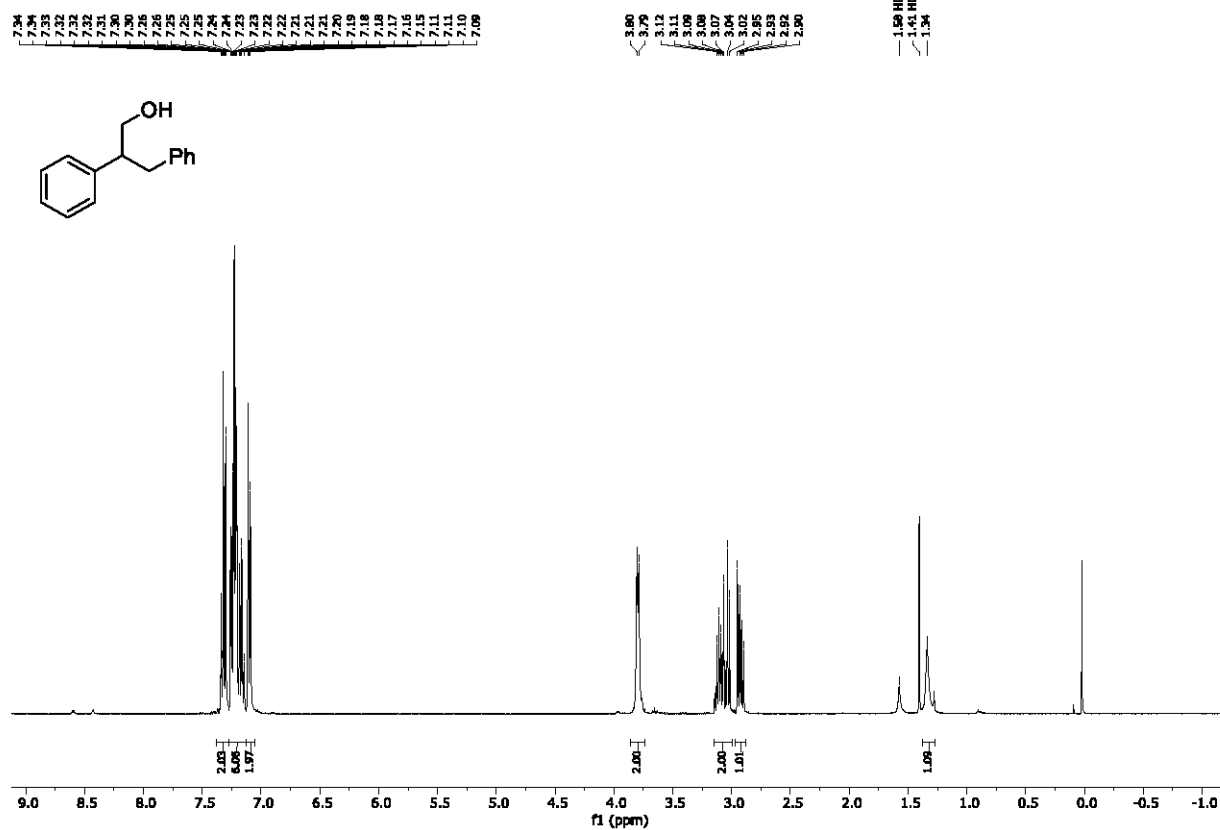
- (1) Strassfeld, D. A.; Wickens, Z. K.; Picazo, E.; Jacobsen, E. N. Highly Enantioselective, Hydrogen-Bond-Donor Catalyzed Additions to Oxetanes. *J. Am. Chem. Soc.* **2020**, *142* (20), 9175–9180. <https://doi.org/10.1021/jacs.0c03991>.
- (2) Altenbach, Robert J.; Bogdan, Andrew; Couty, Sylvain; Desroy, Nicolas; Gfesser, Gregory A.; Housseman, Christopher Gaëtan; Kym, Philip R.; Liu, Bo; Mai, Thi Thu Trang; Malagu, Karine Fabienne; Merayo Merayo, Nuria; Picolet, Olivier Laurent; Pizzonero, Mat, M. C. Modulators of the Cystic Fibrosis Transmembrane Conductance Regulator Protein and Methods of Use. US2019/77784, 2019, A1.
- (3) Wang, Z.; Chen, Z.; Sun, J. Catalytic Enantioselective Intermolecular Desymmetrization of 3-Substituted Oxetanes. *Angew. Chemie Int. Ed.* **2013**, *52* (26), 6685–6688. <https://doi.org/10.1002/anie.201300188>.
- (4) Kwon, D. W.; Kim, Y. H.; Lee, K. Highly Regioselective Cleavages and Iodinations of Cyclic Ethers Utilizing Sml 2. *J. Org. Chem.* **2002**, *67* (26), 9488–9491. <https://doi.org/10.1021/jo020179r>.
- (5) Singh, A.; Anandhi, U.; Cinellu, M. A.; Sharp, P. R. Diimine Supported Group 10 Hydroxo, Oxo, Amido, and Imido Complexes. *Dalt. Trans.* **2008**, No. 17, 2314–2327. <https://doi.org/10.1039/b715663d>.
- (6) Ociepa, M.; Wierzba, A. J.; Turkowska, J.; Gryko, D. Polarity-Reversal Strategy for the Functionalization of Electrophilic Strained Molecules via Light-Driven Cobalt Catalysis. *J. Am. Chem. Soc.* **2020**, *142* (11), 5355–5361. <https://doi.org/10.1021/jacs.0c00245>.
- (7) Cheung, L. L.; Marumoto, S.; Anderson, C. D.; Rychnovsky, S. D. Assignment of Absolute Configuration to SCH 351448 via Total Synthesis. *Org. Lett.* **2008**, *10* (14), 3101–3104. <https://doi.org/10.1021/ol8011474>.
- (8) Shen, R.; Inoue, T.; Forgac, M.; Porco, J. A. Synthesis of Photoactivatable Acyclic Analogues of the Lobatamides. *J. Org. Chem.* **2005**, *70* (9), 3686–3692. <https://doi.org/10.1021/jo0477751>.
- (9) Westerbeek, A.; Van Leeuwen, J. G. E.; Szymański, W.; Feringa, B. L.; Janssen, D. B. Haloalkane Dehalogenase Catalysed Desymmetrisation and Tandem Kinetic Resolution for the Preparation of Chiral Haloalcohols. *Tetrahedron* **2012**, *68* (37), 7645–7650. <https://doi.org/10.1016/j.tet.2012.06.059>.
- (10) Bettoni, L.; Gaillard, S.; Renaud, J.-L. Iron-Catalyzed β -Alkylation of Alcohols. *Org. Lett.* **2019**, *21* (20), 8404–8408. <https://doi.org/10.1021/acs.orglett.9b03171>.
- (11) Manojveer, S.; Salahi, S.; Wendt, O. F.; Johnson, M. T. Ru-Catalyzed Cross-Dehydrogenative Coupling between Primary Alcohols to Guerbet Alcohol Derivatives: With Relevance for Fragrance Synthesis. *J. Org. Chem.* **2018**, *83* (18), 10864–10870. <https://doi.org/10.1021/acs.joc.8b01558>.
- (12) Stach, T.; Dräger, J.; Huy, P. H. Nucleophilic Substitutions of Alcohols in High Levels of Catalytic Efficiency. *Org. Lett.* **2018**, *20* (10), 2980–2983. <https://doi.org/10.1021/acs.orglett.8b01023>.
- (13) Lee, D.; Williamson, C. L.; Chan, L.; Taylor, M. S. Regioselective, Borinic Acid-Catalyzed Monoacylation, Sulfonylation and Alkylation of Diols and Carbohydrates: Expansion of Substrate Scope and Mechanistic Studies. *J. Am. Chem. Soc.* **2012**, *134* (19), 8260–8267. <https://doi.org/10.1021/ja302549c>.
- (14) Fujioka, H.; Ohba, Y.; Hirose, H.; Murai, K.; Kita, Y. Mild and Efficient Removal of Hydroxyethyl Unit from 2-Hydroxyethyl Ether Derivatives Leading to Alcohols. *Org. Lett.* **2005**, *7* (15), 3303–3306. <https://doi.org/10.1021/ol051135i>.
- (15) Cano, R.; Yus, M.; Ramón, D. J. First Practical Cross-Alkylation of Primary Alcohols with a New and Recyclable Impregnated Iridium on Magnetite Catalyst. *Chem. Commun.* **2012**, *48* (61), 7628. <https://doi.org/10.1039/c2cc33101b>.
- (16) James, B. G.; Pattenden, G. Regiospecificity of Methylation of Unsymmetrical Stilbenes by Methylsulphonylmethanide. *J. Chem. Soc. Perkin Trans. 1* **1974**, 1195. <https://doi.org/10.1039/p19740001195>.

- (17) Hayashi, H.; Kaga, A.; Wang, B.; Gagosz, F.; Chiba, S. Use of a Benzyl Ether as a Traceless Hydrogen Donor in the Anti-Markovnikov Hydrofunctionalization of Alkenes with Xanthates. *Chem. Commun.* **2018**, *54* (54), 7535–7538. <https://doi.org/10.1039/c8cc02971g>.
- (18) Frisch, M. J.; Trucks, G. W.; Schlegel, H. B.; Scuseria, G. E.; Robb, M. A.; Cheeseman, J. R.; Scalmani, G.; Barone, V.; Petersson, G. A.; Nakatsuji, H.; Li, X.; Caricato, M.; Marenich, A. V.; Bloino, J.; Janesko, B. G.; Gomperts, R.; Mennucci, B.; Hratchian, H. P.; Ortiz, J. V.; Izmaylov, A. F.; Sonnenberg, J. L.; Williams-Young, D.; Ding, F.; Lipparini, F.; Egidi, F.; Goings, J.; Peng, B.; Petrone, A.; Henderson, T.; Ranasinghe, D.; Zakrzewski, V. G.; Gao, J.; Rega, N.; Zheng, G.; Liang, W.; Hada, M.; Ehara, M.; Toyota, K.; Fukuda, R.; Hasegawa, J.; Ishida, M.; Nakajima, T.; Honda, Y.; Kitao, O.; Nakai, H.; Vreven, T.; Throssell, K.; Montgomery, J. A., Jr.; Peralta, J. E.; Ogliaro, F.; Bearpark, M. J.; Heyd, J. J.; Brothers, E. N.; Kudin, K. N.; Staroverov, V. N.; Keith, T. A.; Kobayashi, R.; Normand, J.; Raghavachari, K.; Rendell, A. P.; Burant, J. C.; Iyengar, S. S.; Tomasi, J.; Cossi, M.; Millam, J. M.; Klene, M.; Adamo, C.; Cammi, R.; Ochterski, J. W.; Martin, R. L.; Morokuma, K.; Farkas, O.; Foresman, J. B.; Fox, D. J. Gaussian 16, Revision B.01; Gaussian, Inc.: Wallingford, CT, 2016
- (19) Grimme, S.; Antony, J.; Ehrlich, S.; Krieg, H. A Consistent and Accurate Ab Initio Parametrization of Density Functional Dispersion Correction (DFT-D) for the 94 Elements H-Pu. *J. Chem. Phys.* **2010**, *132* (15). <https://doi.org/10.1063/1.3382344>.
- (20) Marenich, A. V.; Cramer, C. J.; Truhlar, D. G. Universal Solvation Model Based on Solute Electron Density and on a Continuum Model of the Solvent Defined by the Bulk Dielectric Constant and Atomic Surface Tensions. *J. Phys. Chem. B* **2009**, *113* (18), 6378–6396. <https://doi.org/10.1021/jp810292n>.
- (21) Legault, C. Y., CYLview, 1.0b; Université de Sherbrooke, 2009, <http://www.cylview.org>.

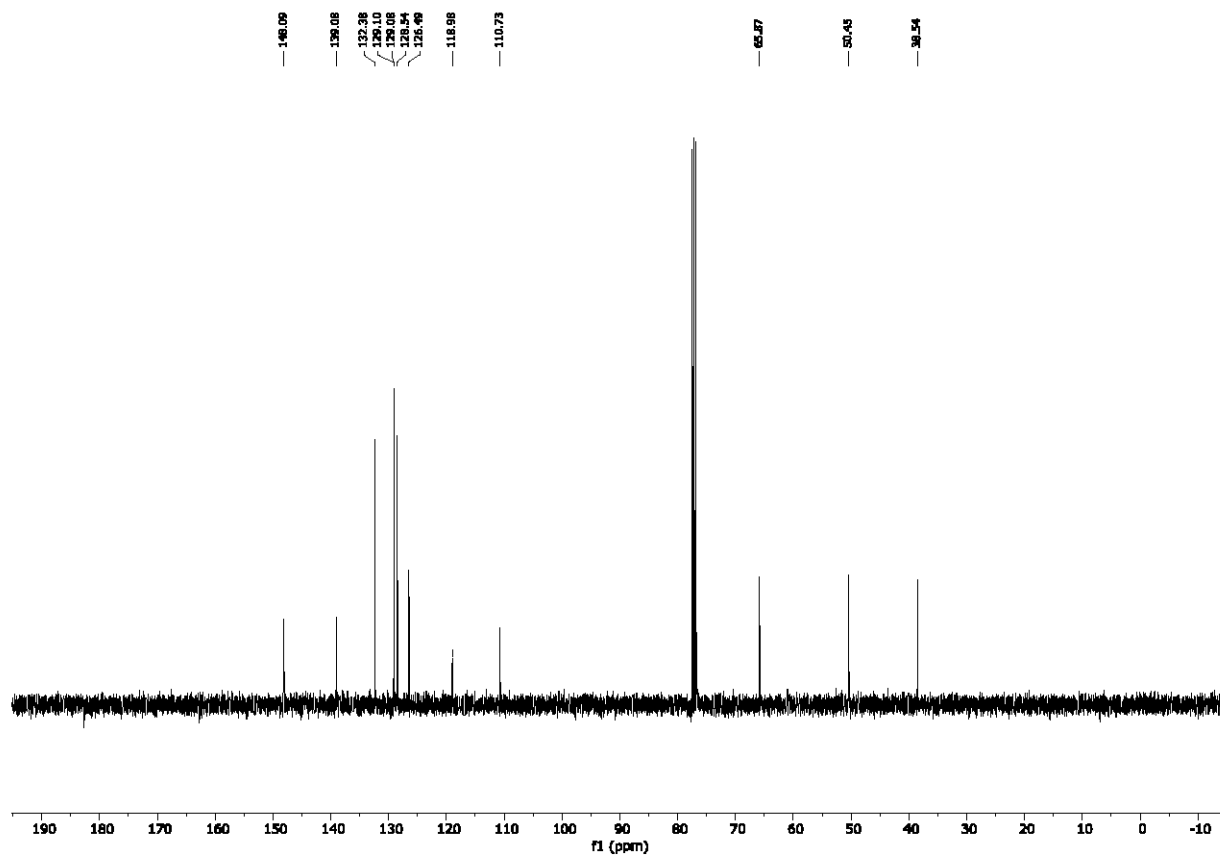
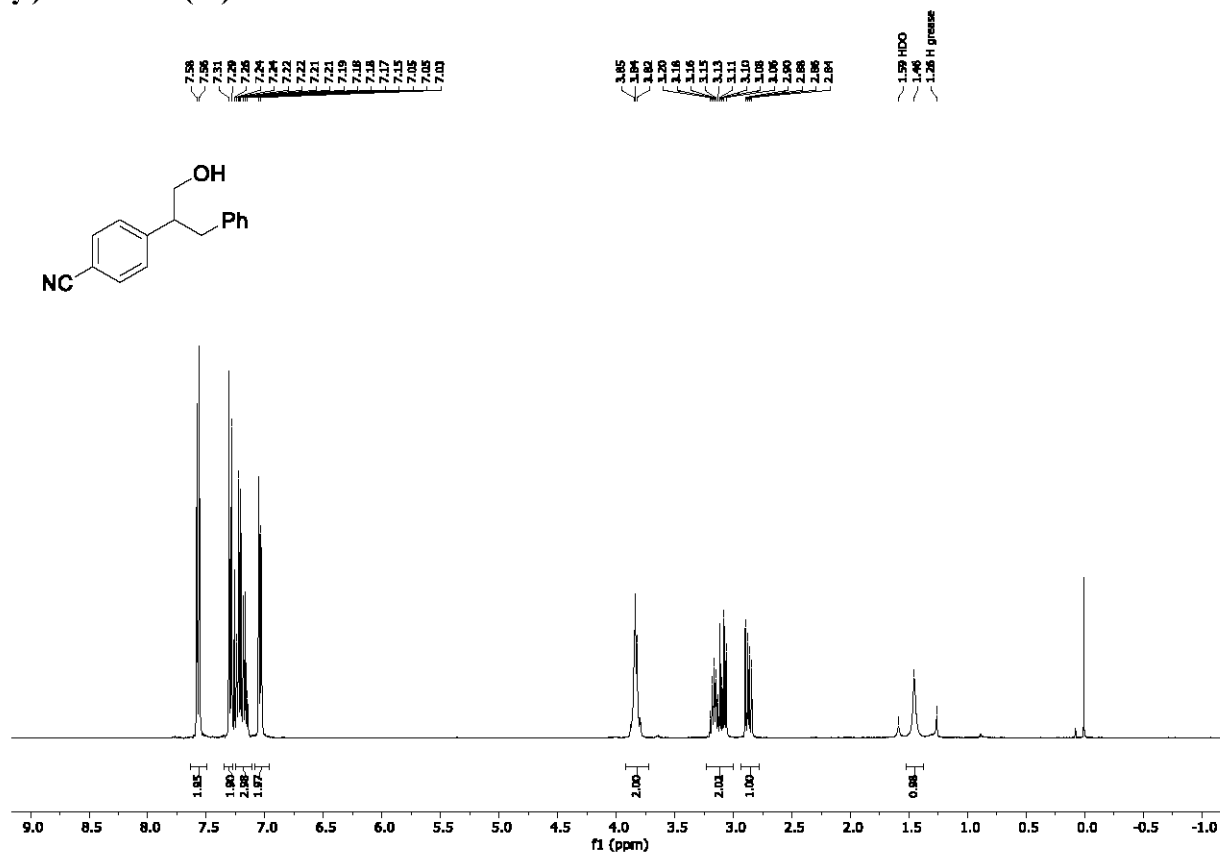
^1H NMR (500 MHz, CDCl_3) and ^{13}C NMR (125 MHz, CDCl_3); 3-bromo-2-phenylpropan-1-ol (5b)



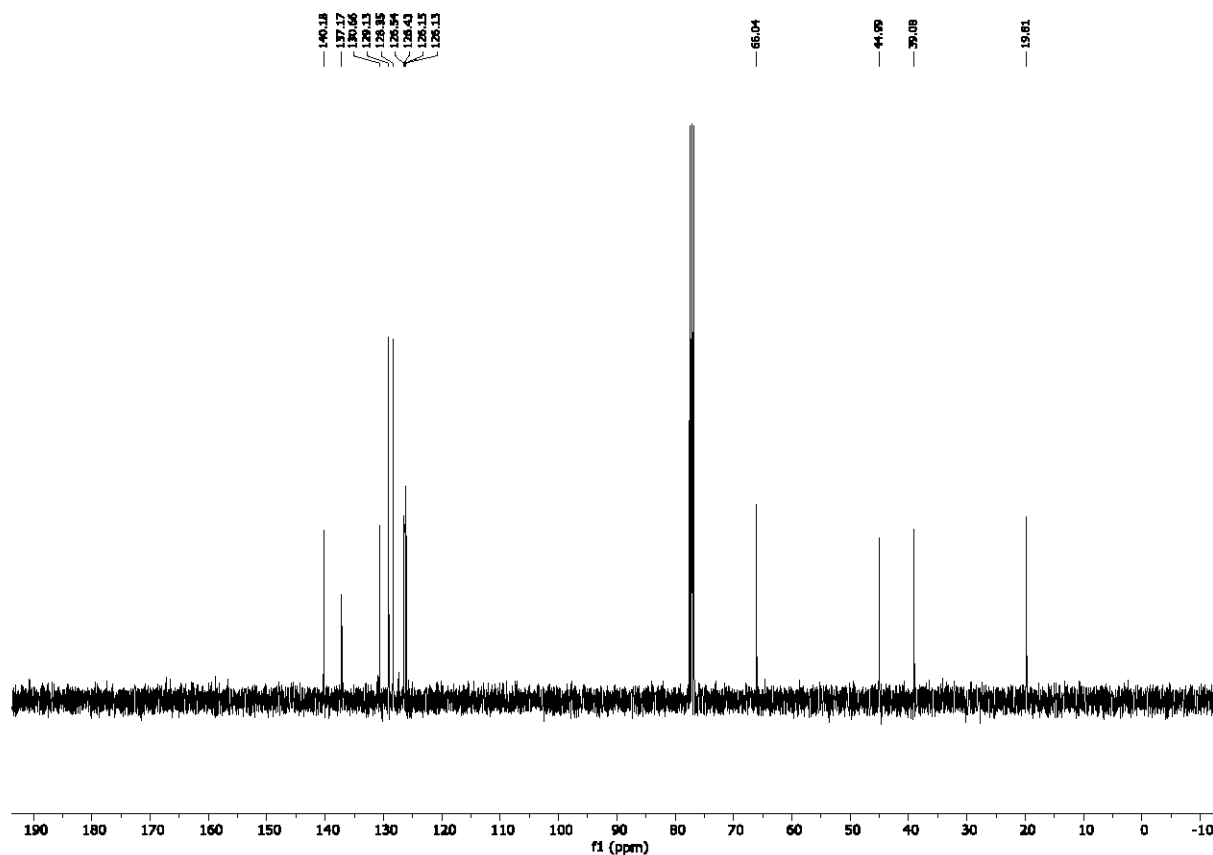
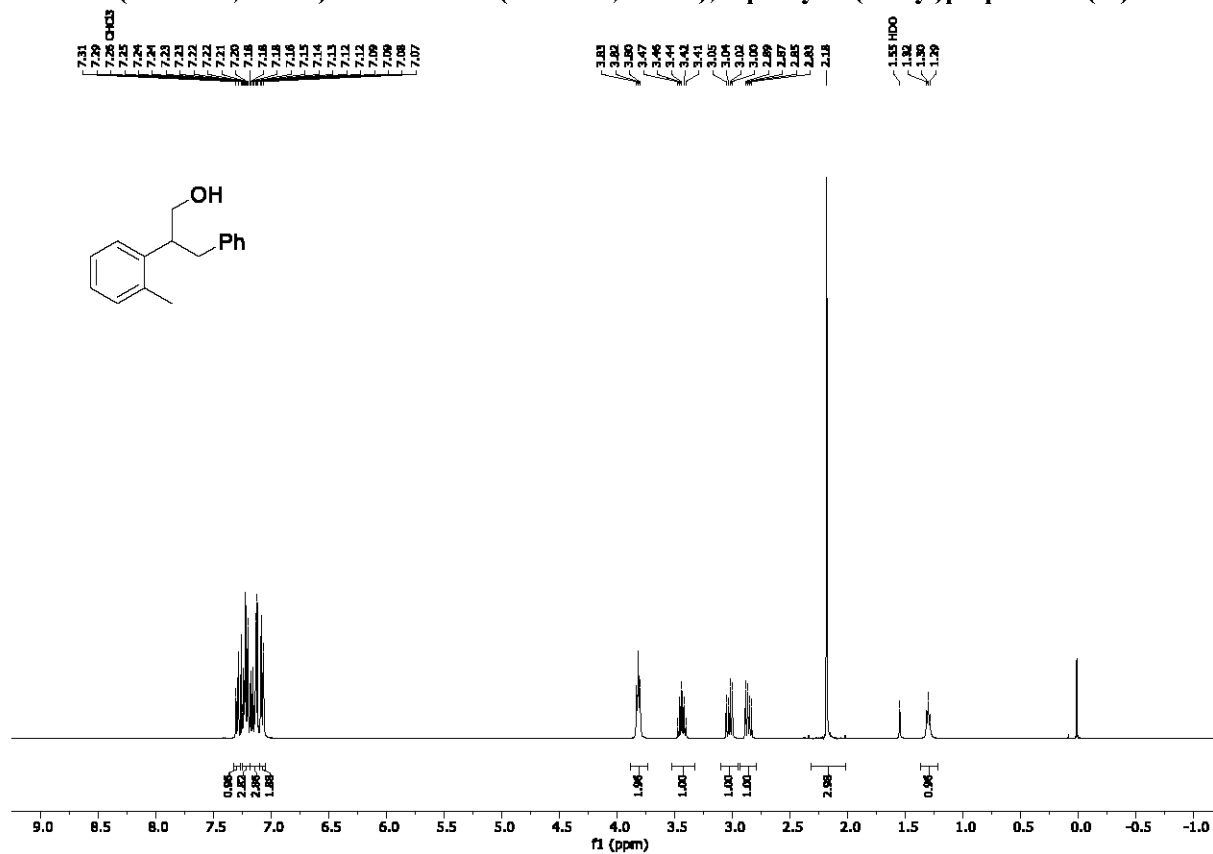
¹H NMR (400 MHz, CDCl₃) and ¹³C NMR (100 MHz, CDCl₃); 2,3-diphenylpropan-1-ol (4b)



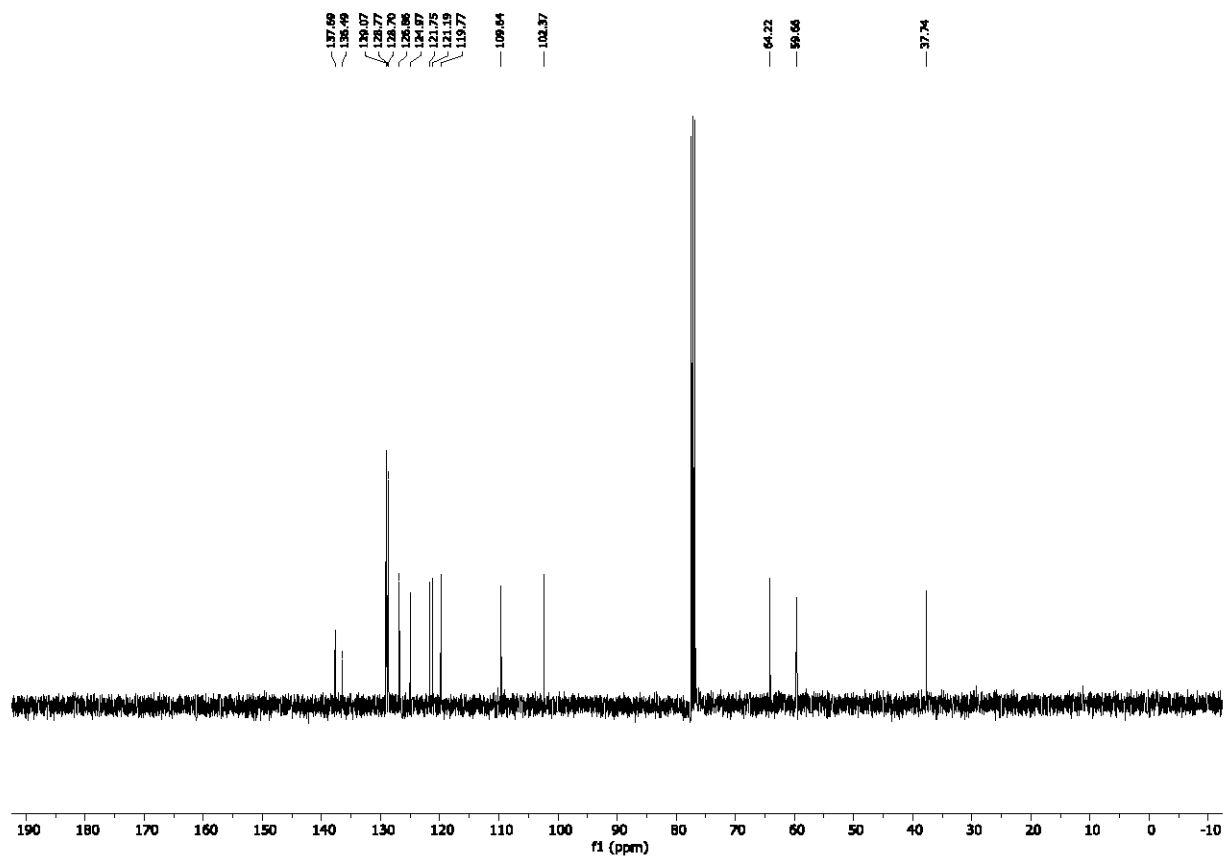
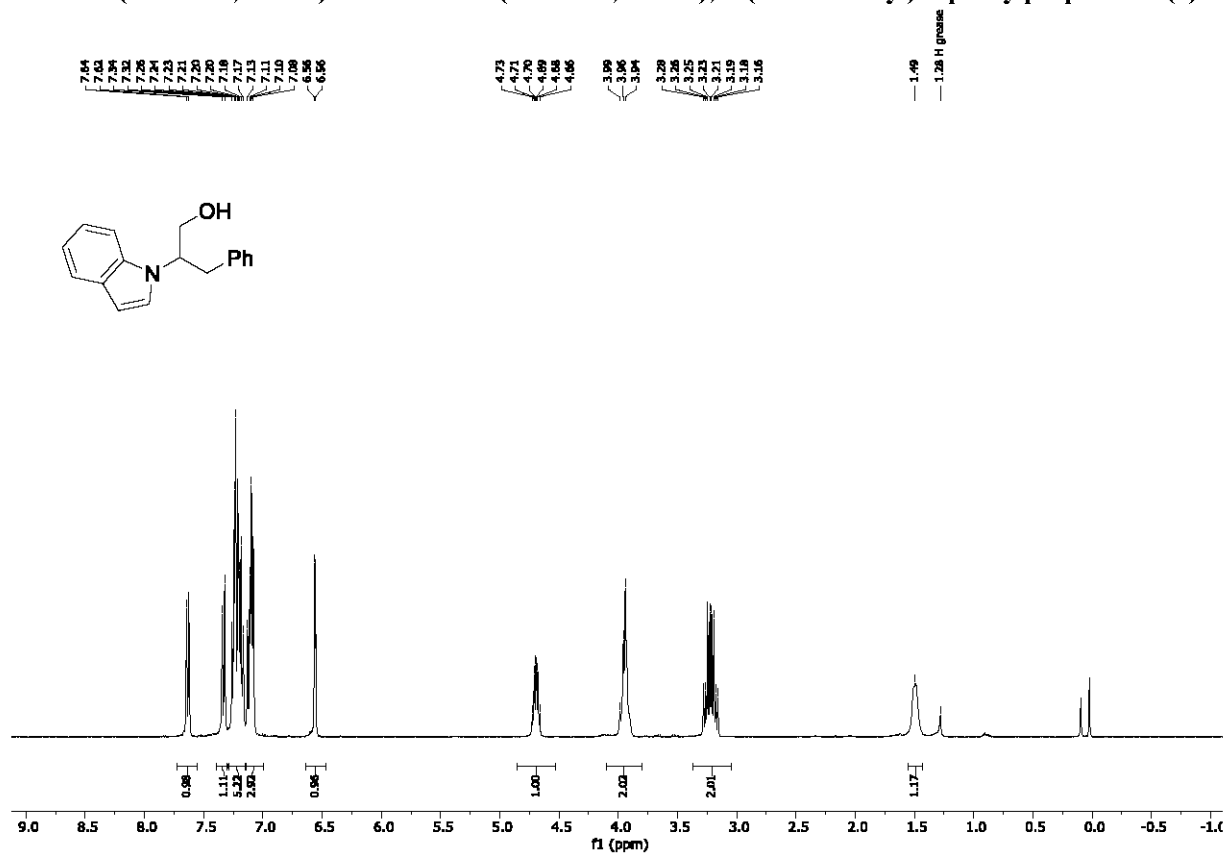
¹H NMR (400 MHz, CDCl₃) and ¹³C NMR (100 MHz, CDCl₃); 4-(1-hydroxy-3-phenylpropan-2-yl)benzonitrile (4d)



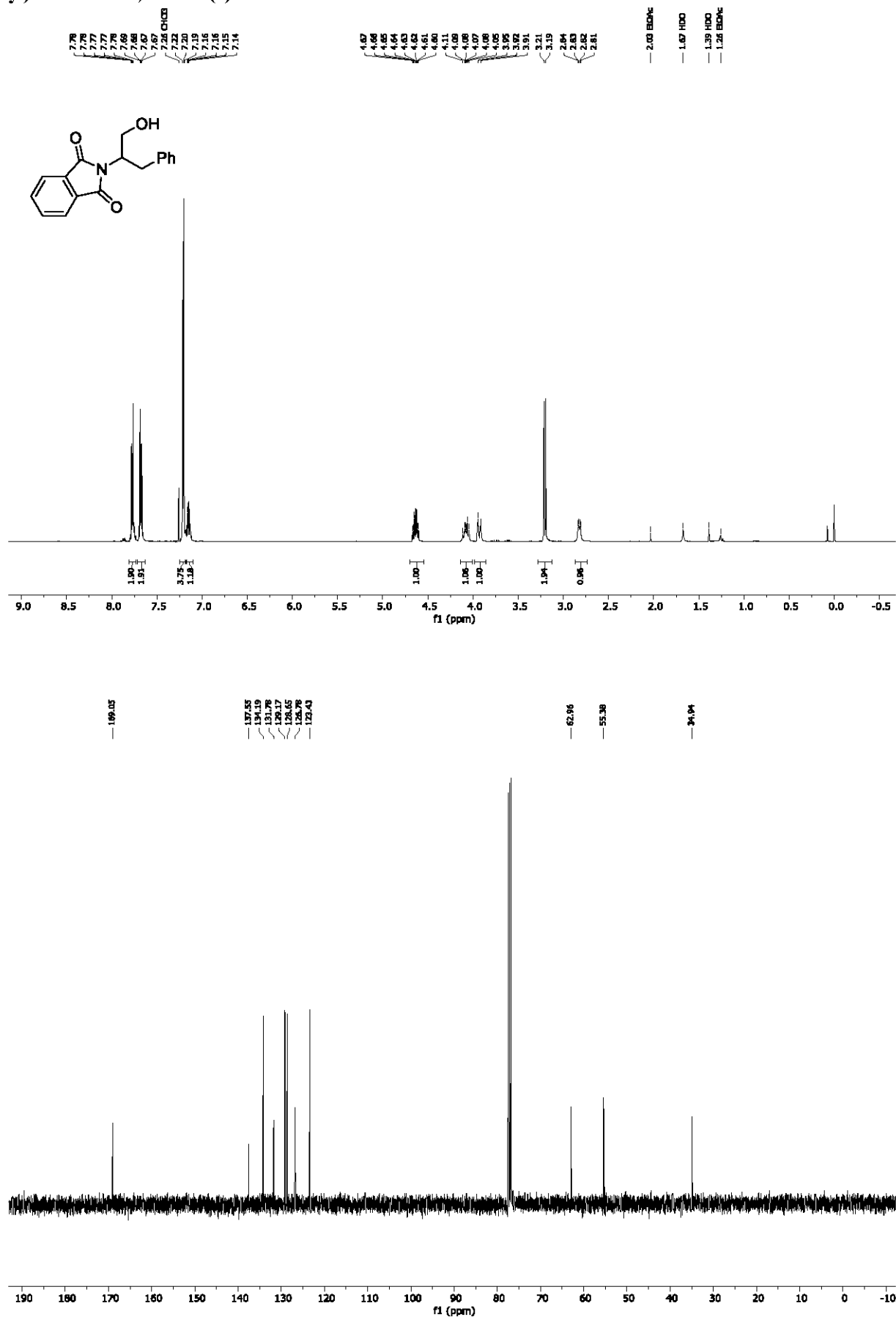
¹H NMR (400 MHz, CDCl₃) and ¹³C NMR (100 MHz, CDCl₃); 3-phenyl-2-(*o*-tolyl)propan-1-ol (4e)



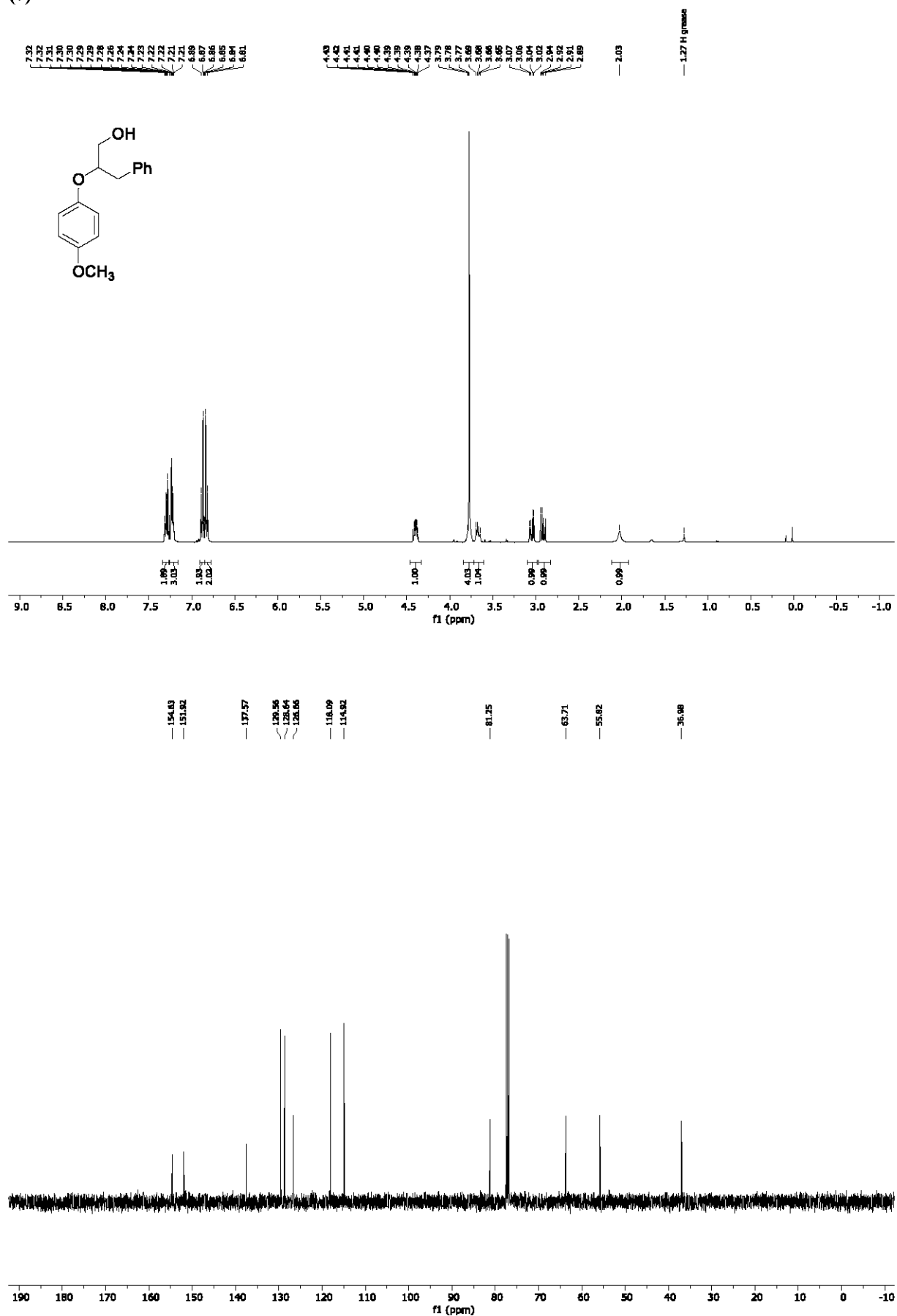
^1H NMR (400 MHz, CDCl_3) and ^{13}C NMR (100 MHz, CDCl_3); 2-(1*H*-indol-1-yl)-3-phenylpropan-1-ol (5)



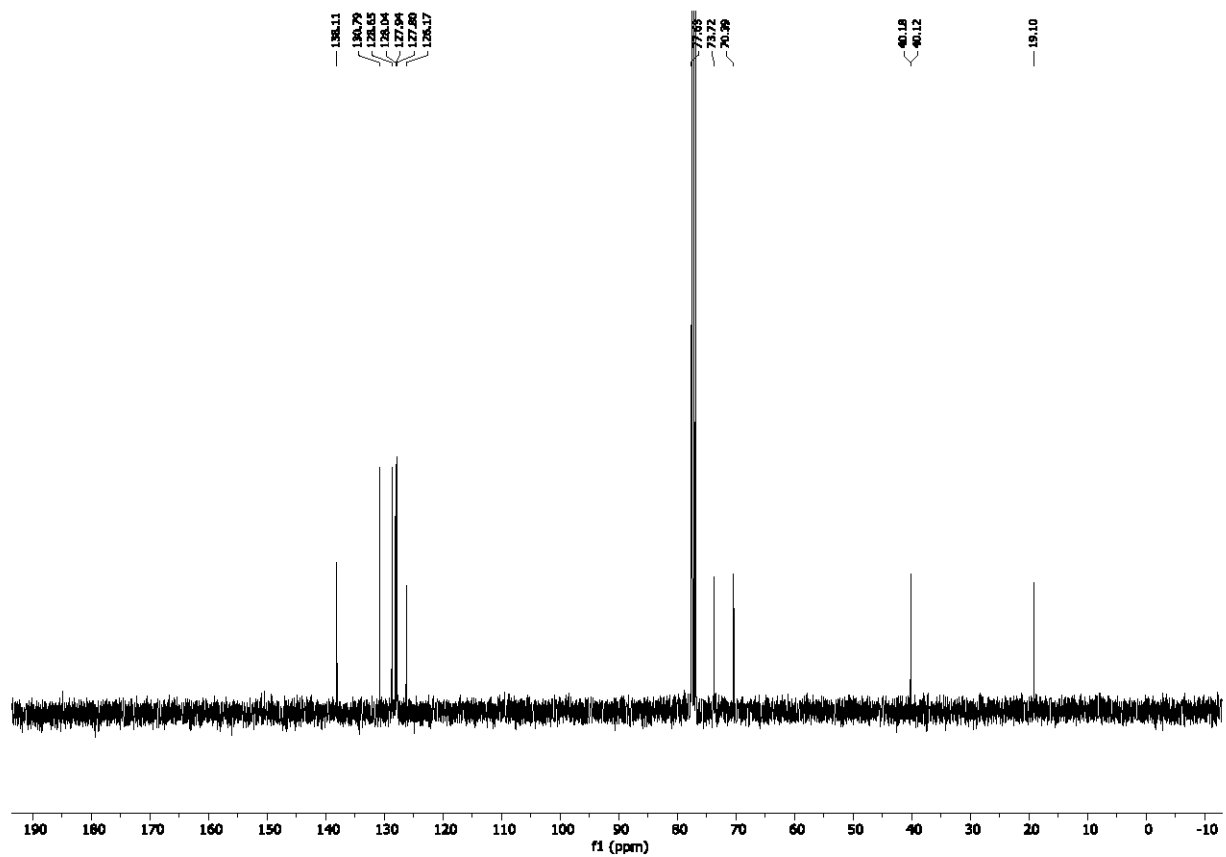
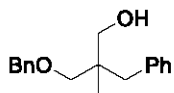
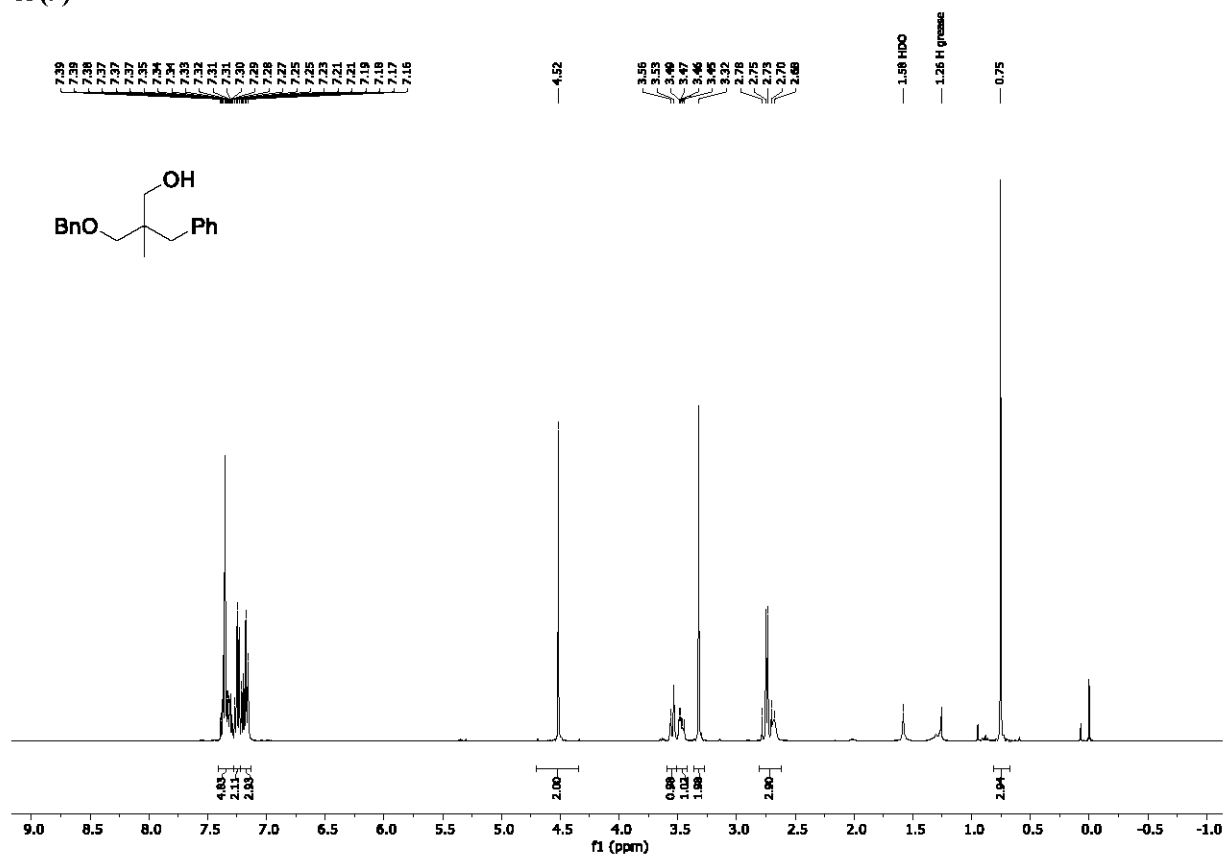
^1H NMR (400 MHz, CDCl_3) and ^{13}C NMR (100 MHz, CDCl_3); 2-(1-hydroxy-3-phenylpropan-2-yl)isoindoline-1,3-dione (6)



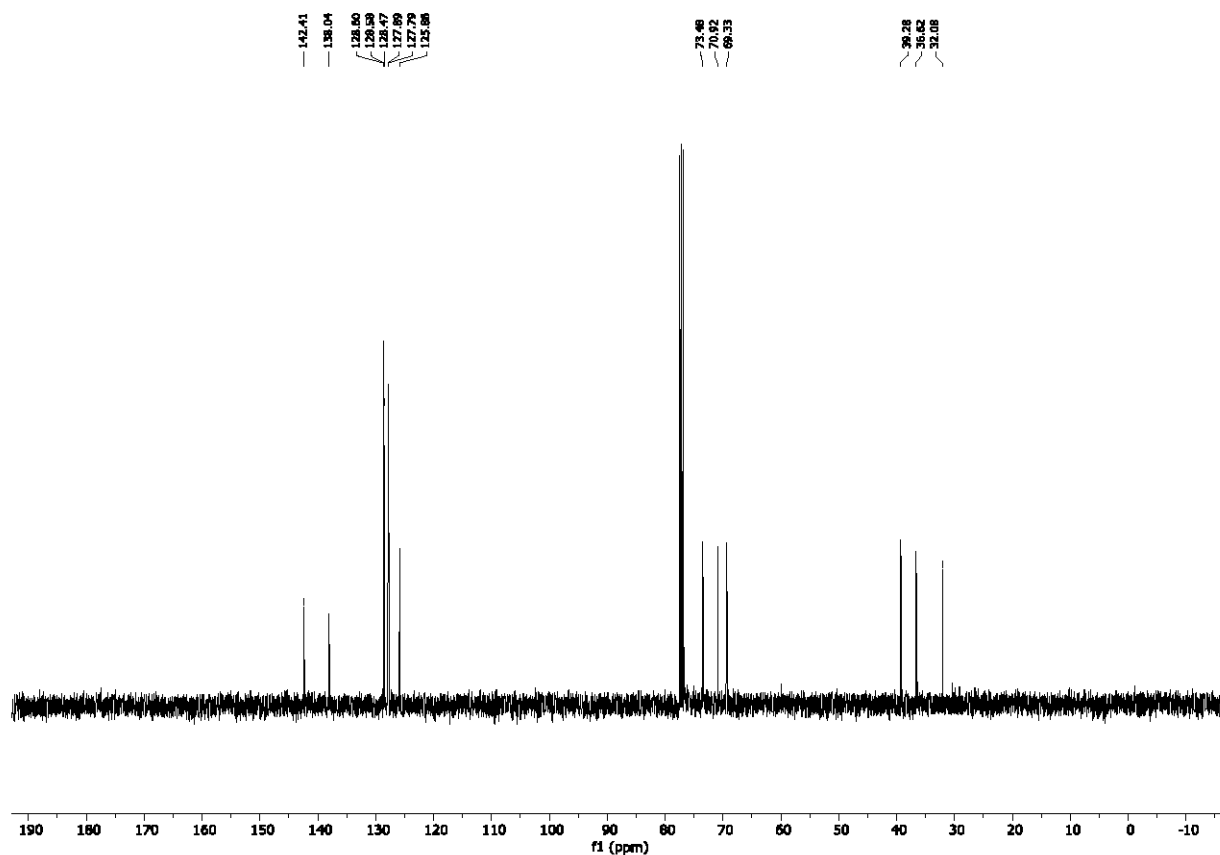
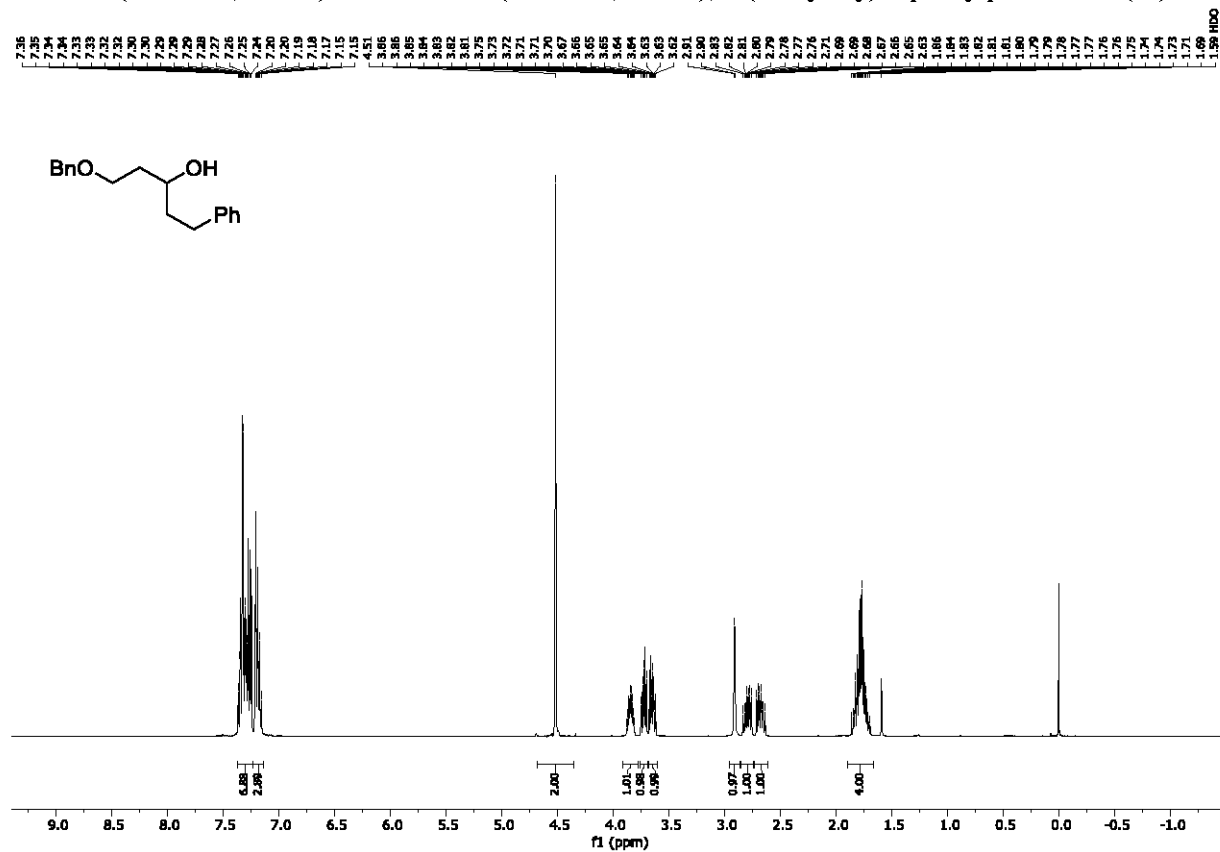
¹H NMR (400 MHz, CDCl₃) and ¹³C NMR (100 MHz, CDCl₃); 2-(4-methoxyphenoxy)-3-phenylpropan-1-ol
(7)



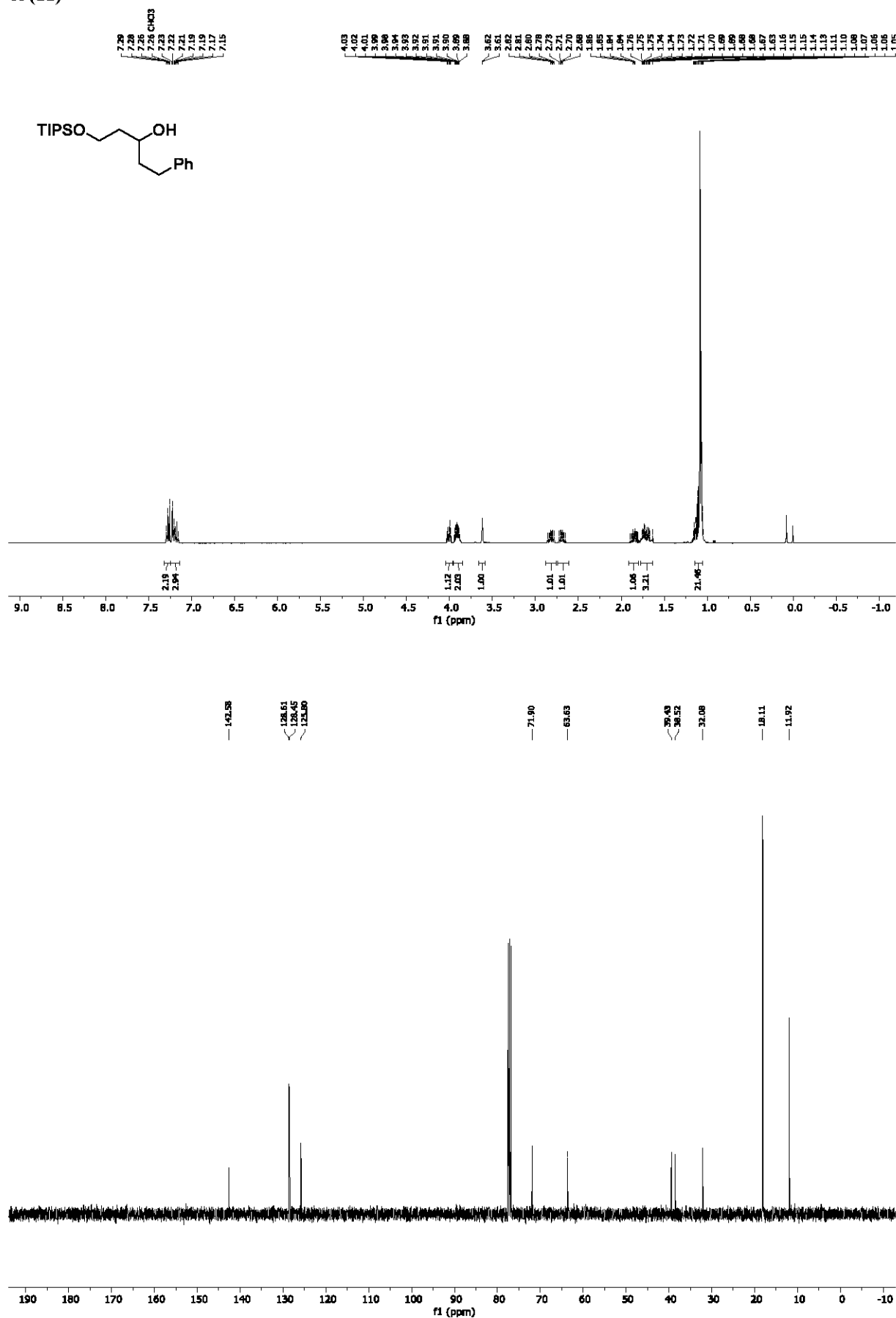
^1H NMR (400 MHz, CDCl_3) and ^{13}C NMR (100 MHz, CDCl_3); 2-benzyl-3-(benzyloxy)-2-methylpropan-1-ol (9)



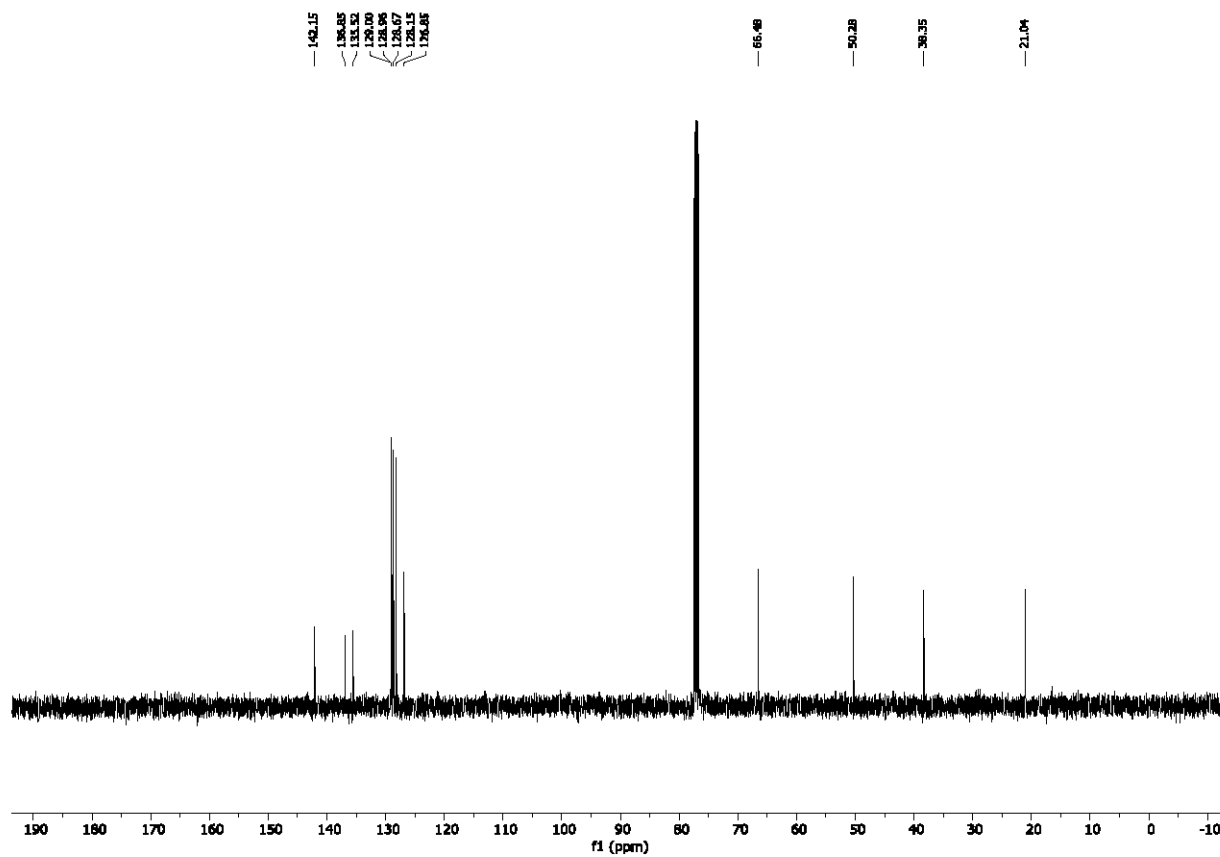
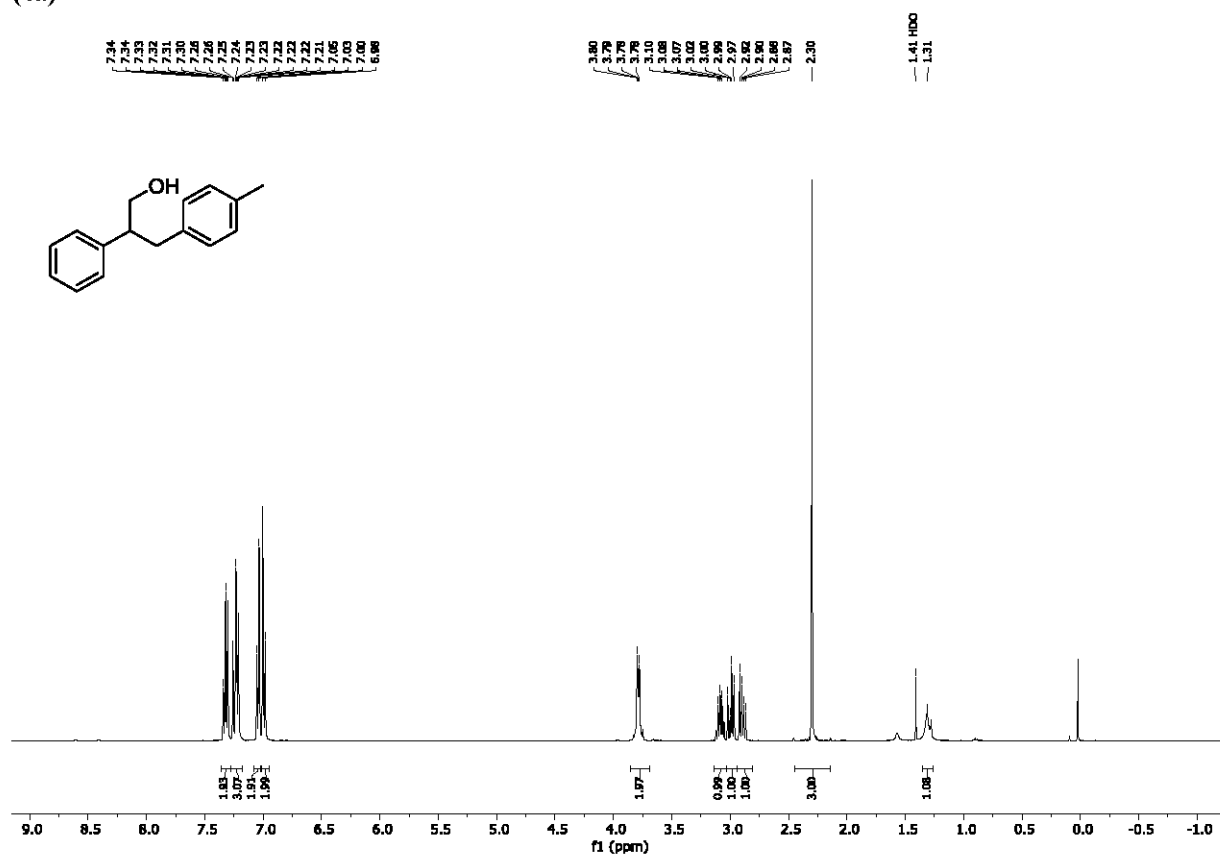
¹H NMR (400 MHz, CDCl₃) and ¹³C NMR (100 MHz, CDCl₃); 1-(benzyloxy)-5-phenylpentan-3-ol (10)



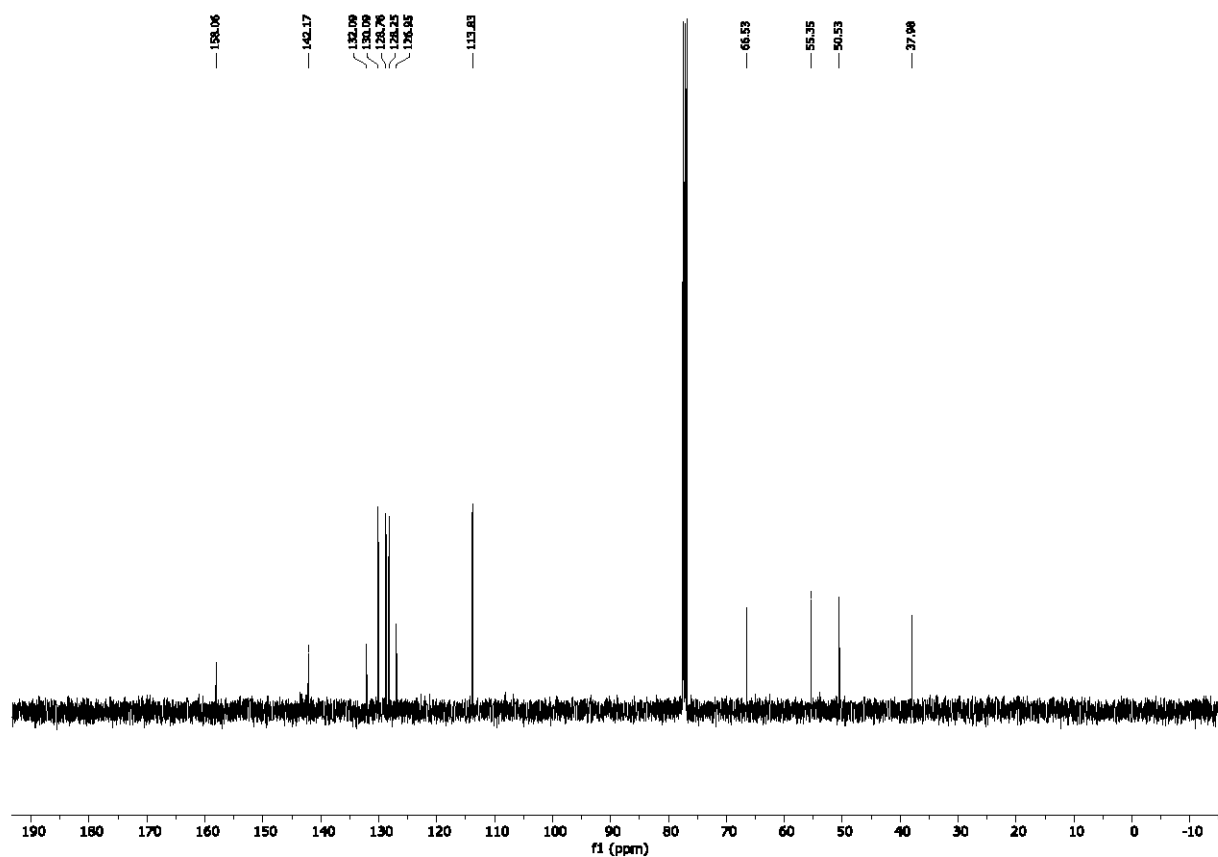
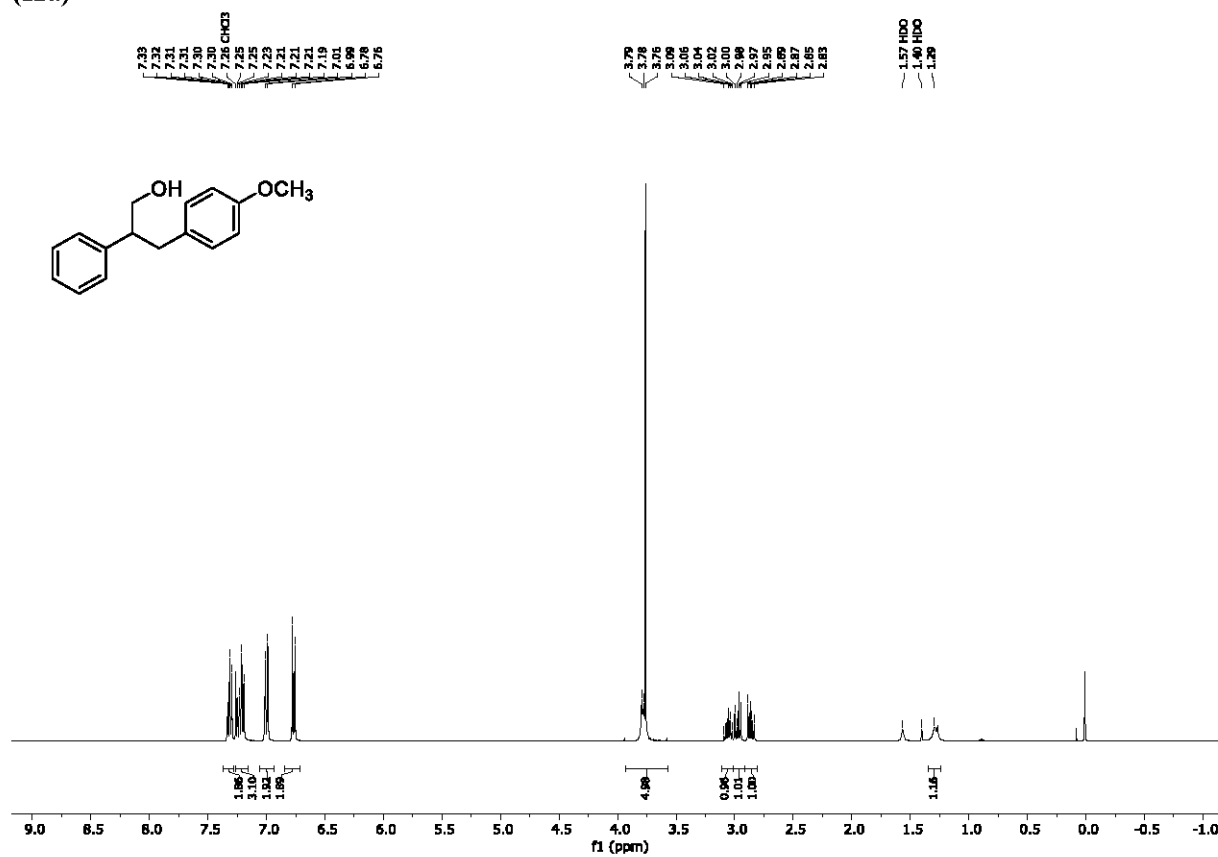
^1H NMR (400 MHz, CDCl_3) and ^{13}C NMR (100 MHz, CDCl_3); 1-phenyl-5-((triisopropylsilyl)oxy)pentan-3-ol (11)



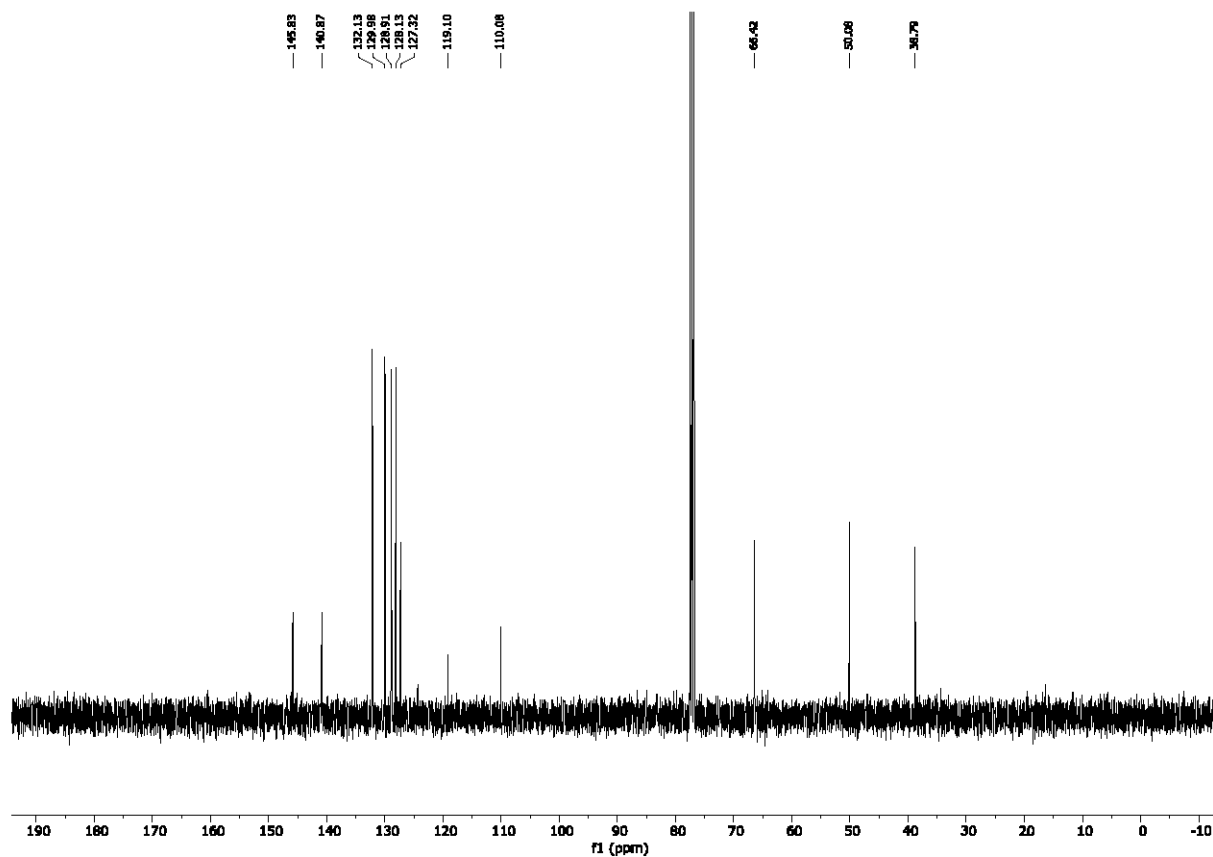
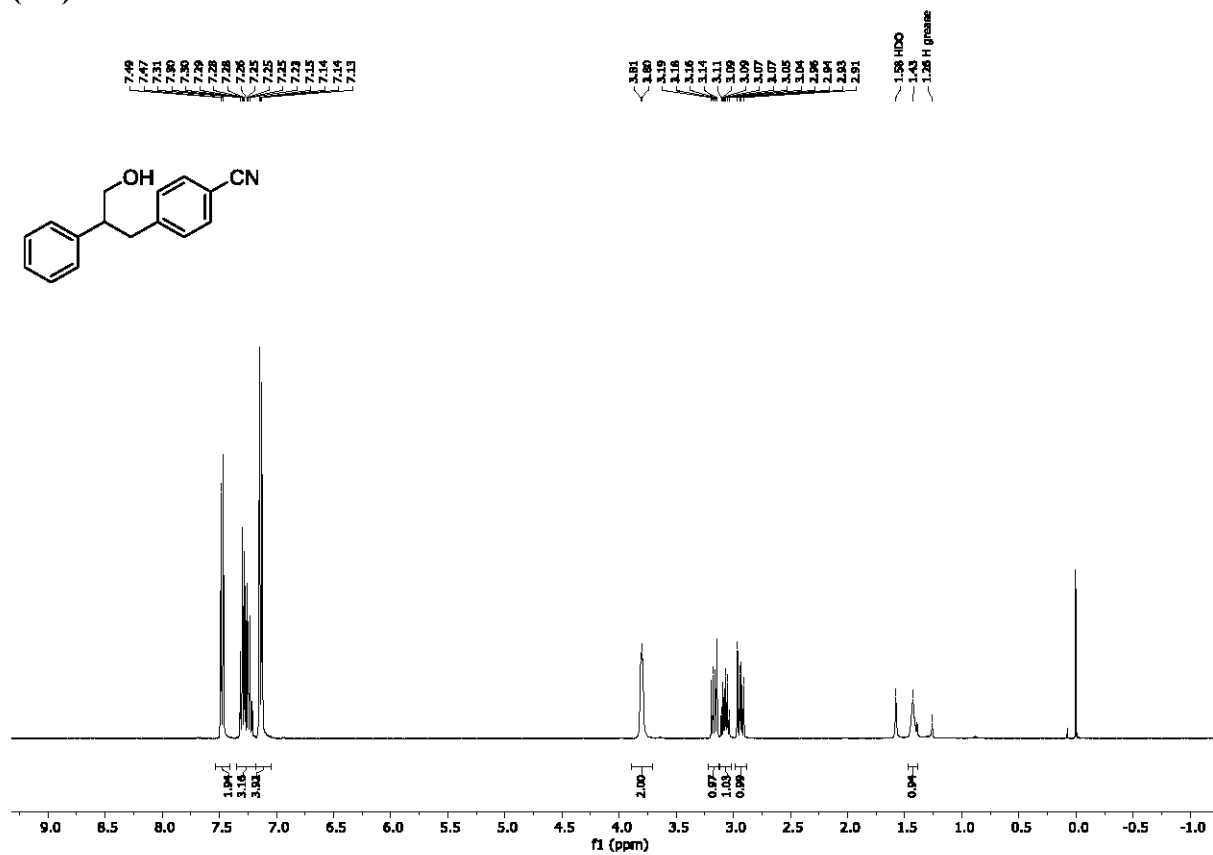
^1H NMR (400 MHz, CDCl_3) and ^{13}C NMR (100 MHz, CDCl_3); 2-phenyl-3-(4-methylphenyl)propan-1-ol (4a)



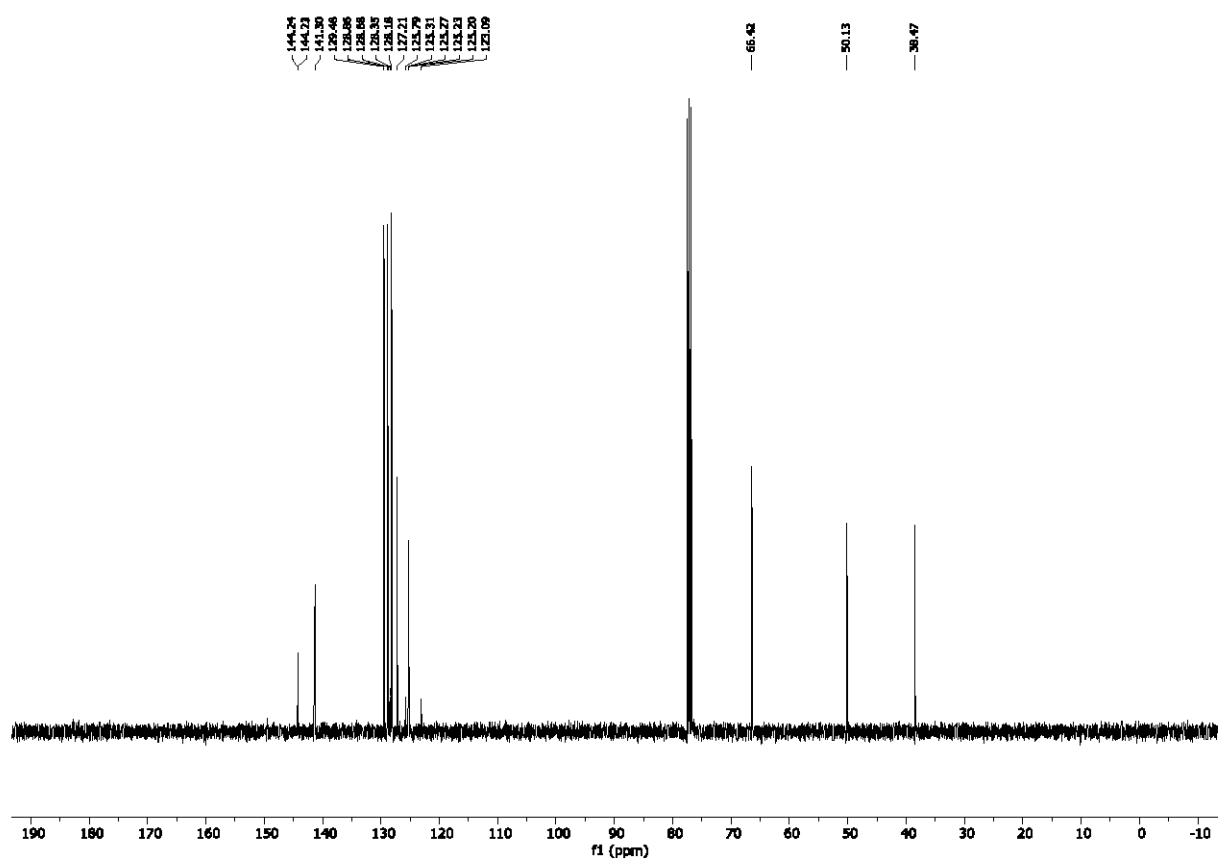
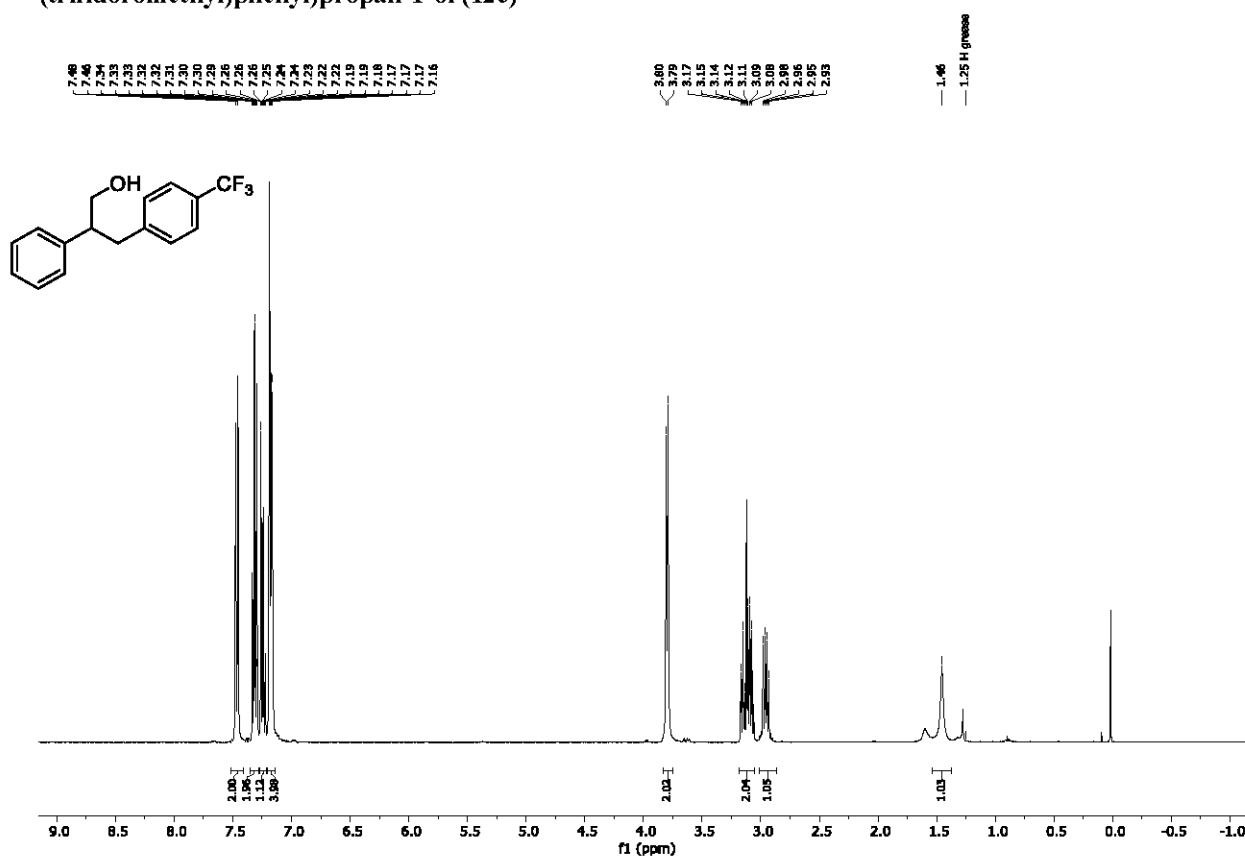
¹H NMR (400 MHz, CDCl₃) and ¹³C NMR (100 MHz, CDCl₃); 3-(4-methoxyphenyl)-2-phenylpropan-1-ol (12a)

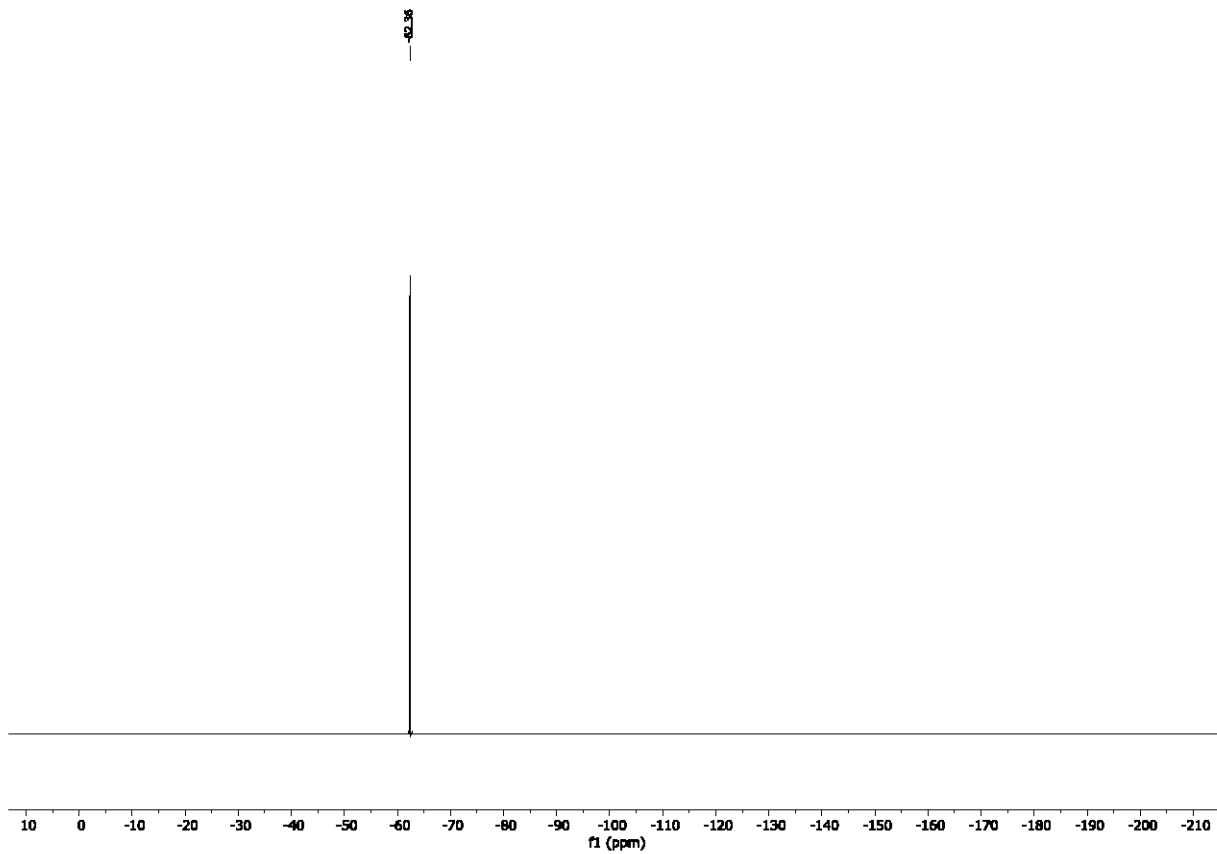


¹H NMR (400 MHz, CDCl₃) and ¹³C NMR (100 MHz, CDCl₃); 4-(3-hydroxy-2-phenylpropyl)benzonitrile (12b)

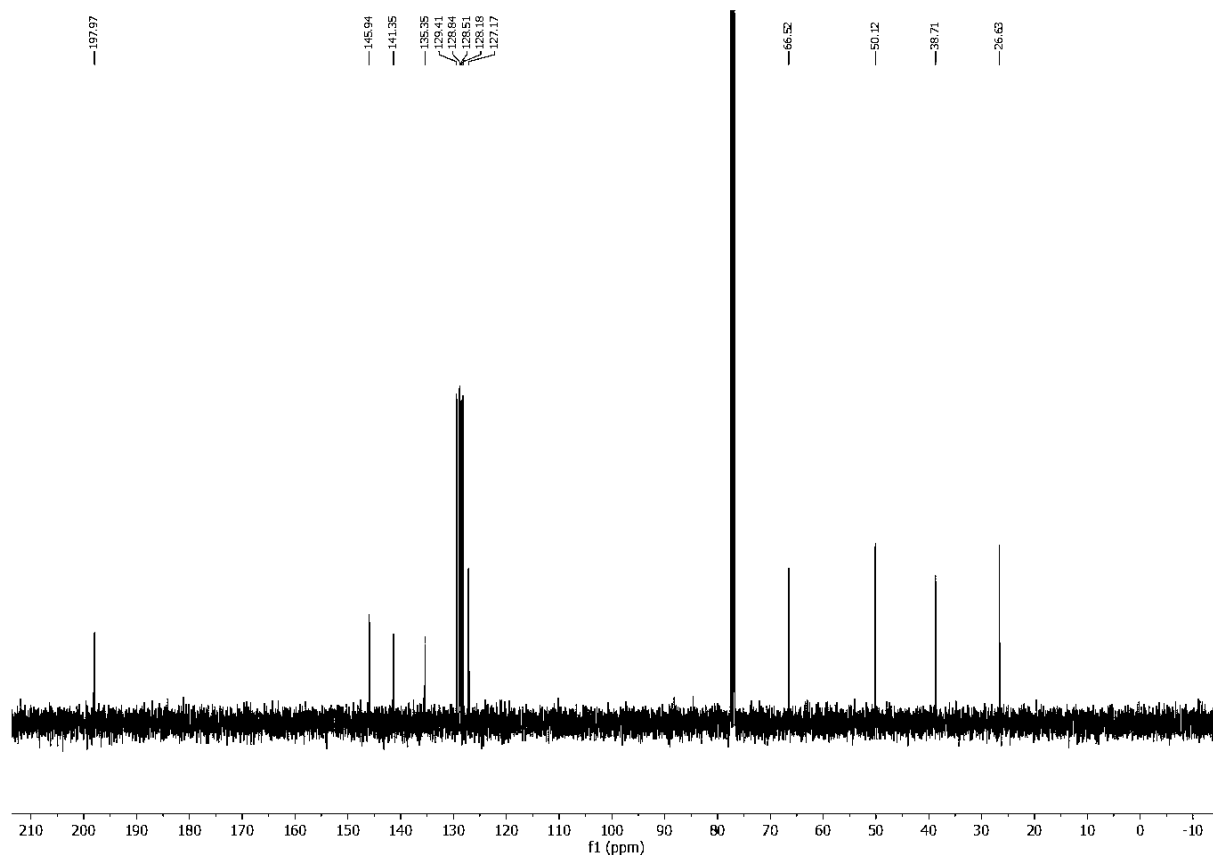
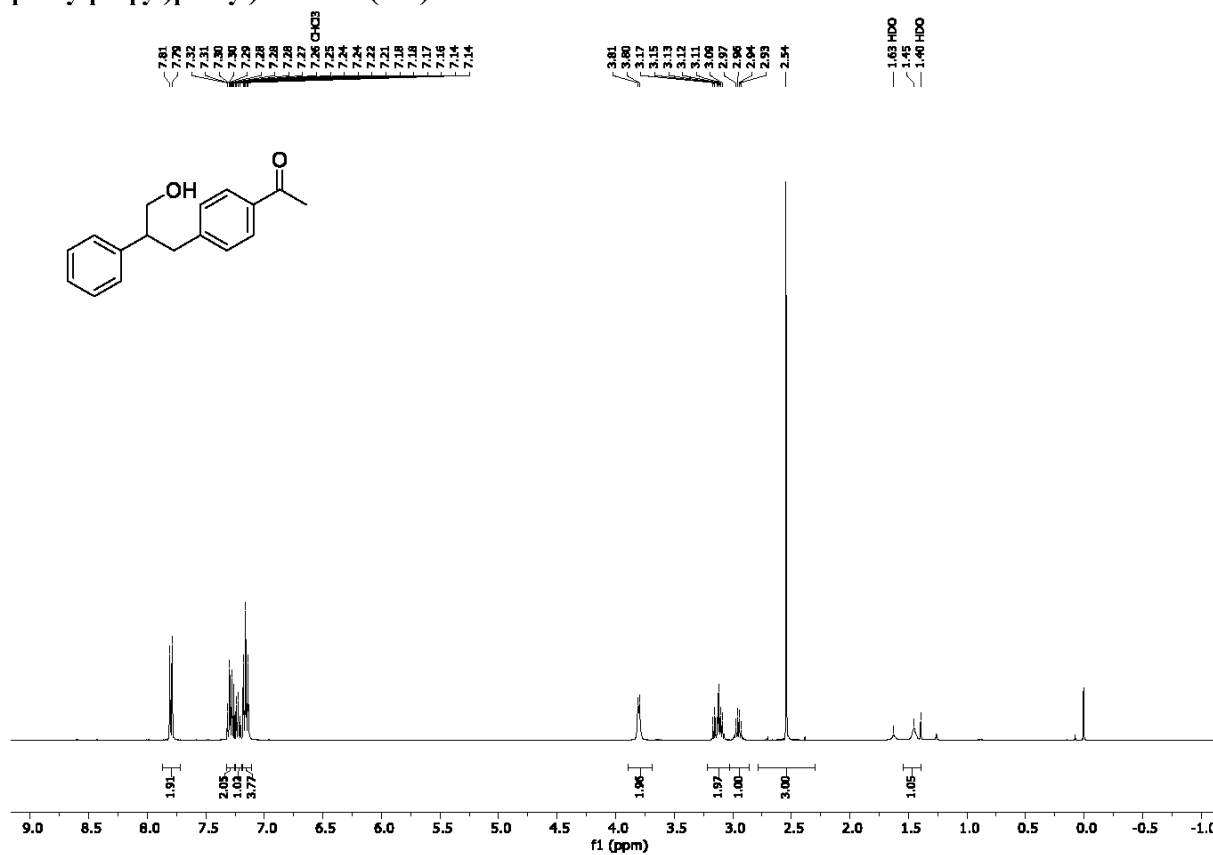


¹H NMR (400 MHz, CDCl₃), ¹³C NMR (100 MHz, CDCl₃) and ¹⁹F NMR (376 MHz, CDCl₃); 2-phenyl-3-(4-(trifluoromethyl)phenyl)propan-1-ol (12c)

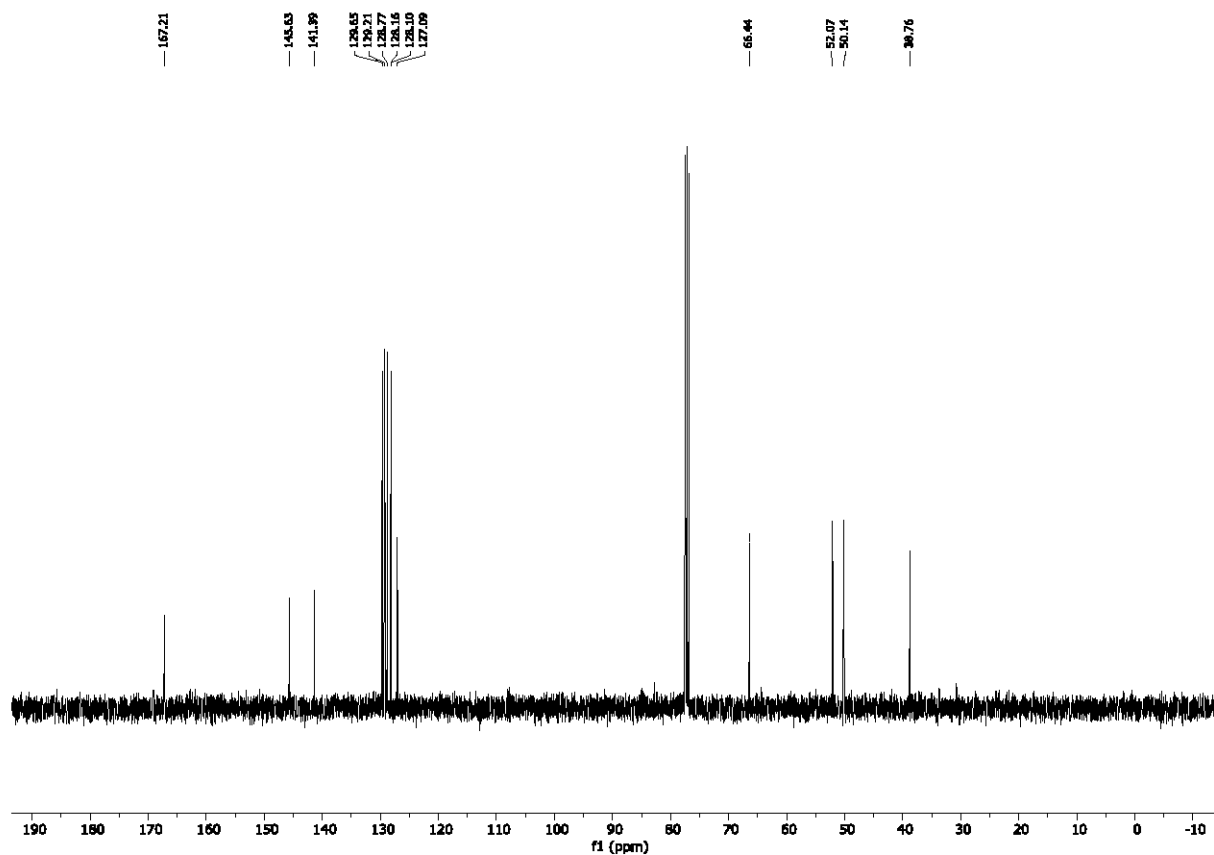
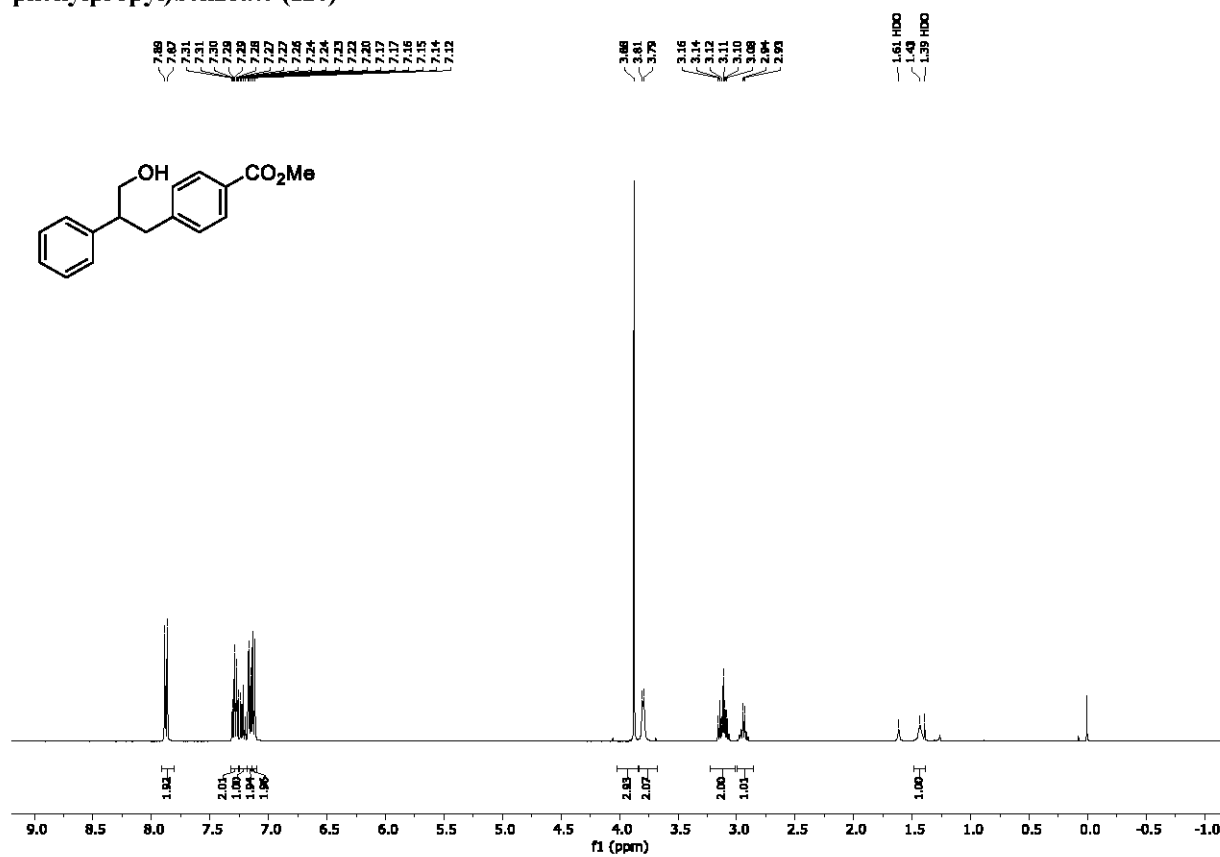




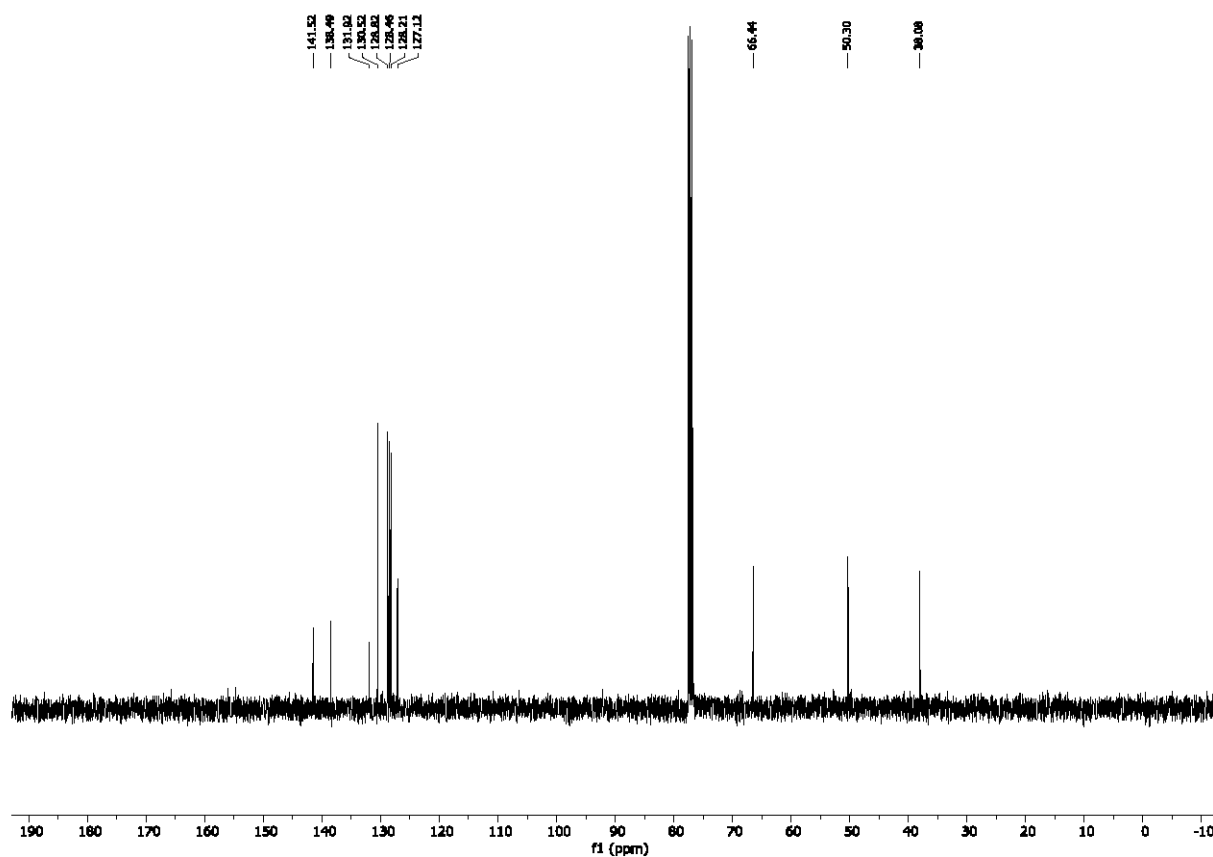
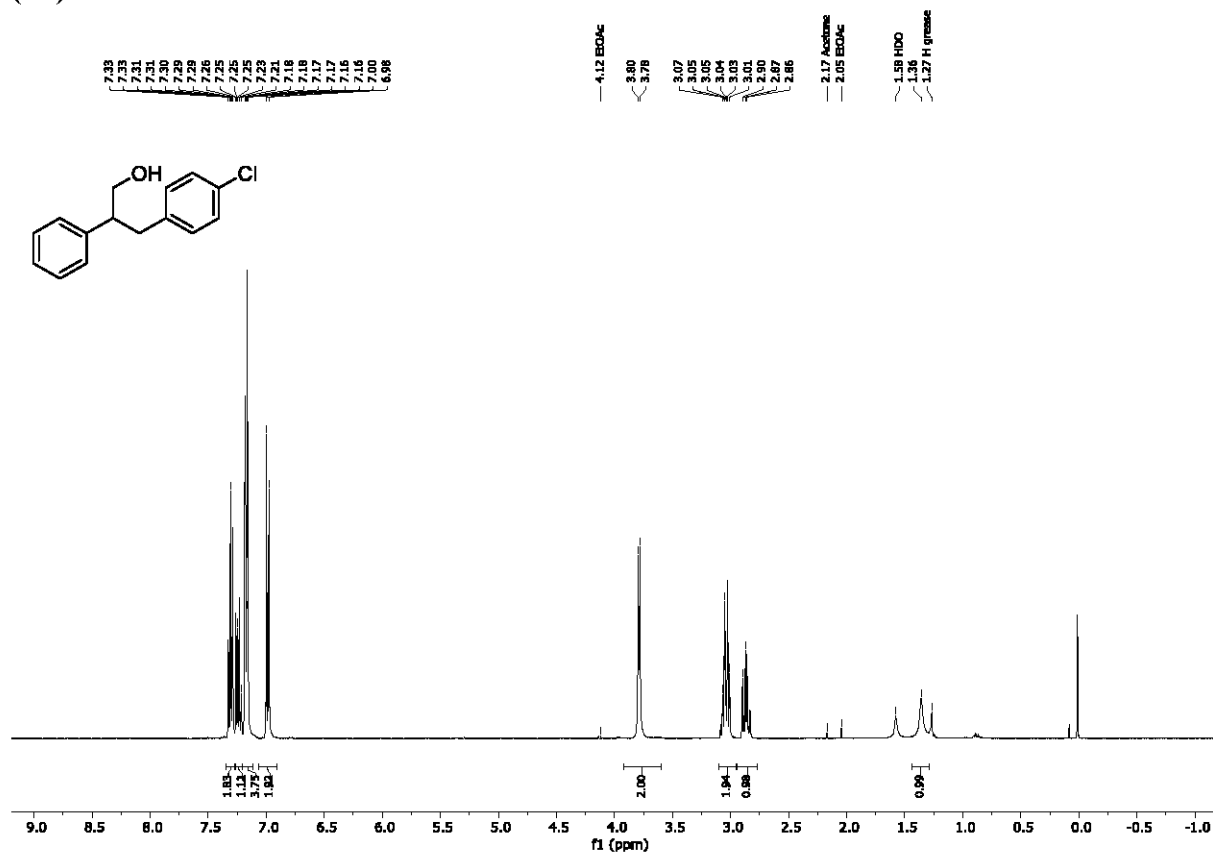
¹H NMR (400 MHz, CDCl₃) and ¹³C NMR (100 MHz, CDCl₃); 1-(4-(3-hydroxy-2-phenylpropyl)phenyl)ethanone (12d)



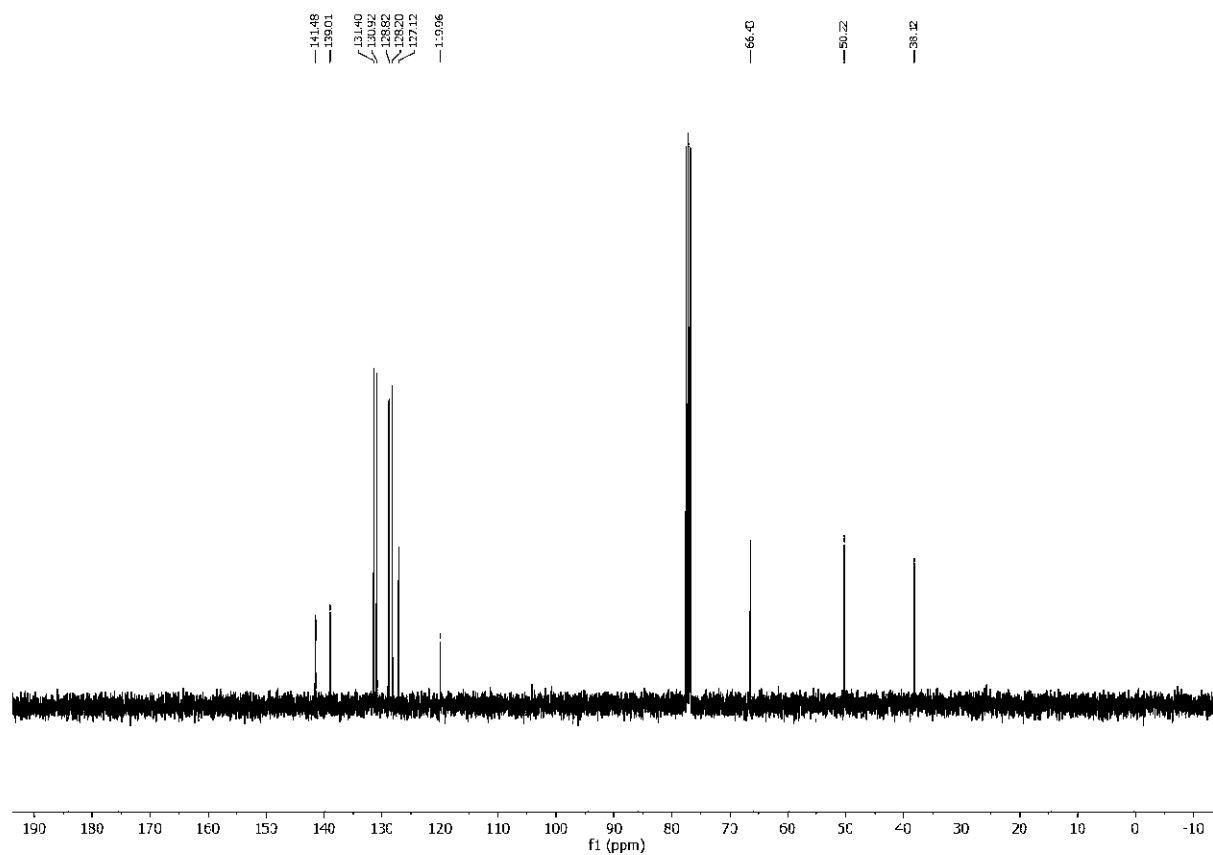
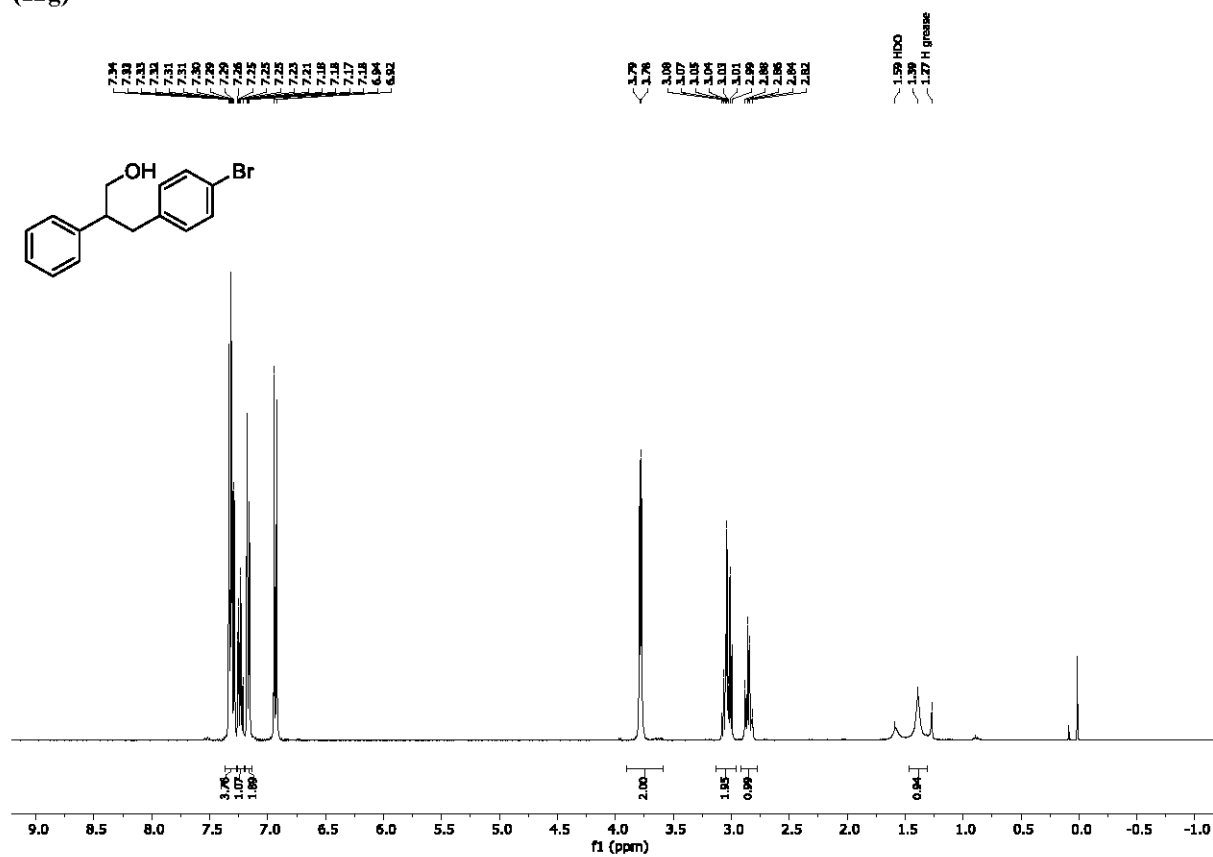
¹H NMR (400 MHz, CDCl₃) and ¹³C NMR (100 MHz, CDCl₃); methyl 4-(3-hydroxy-2-phenylpropyl)benzoate (12e)



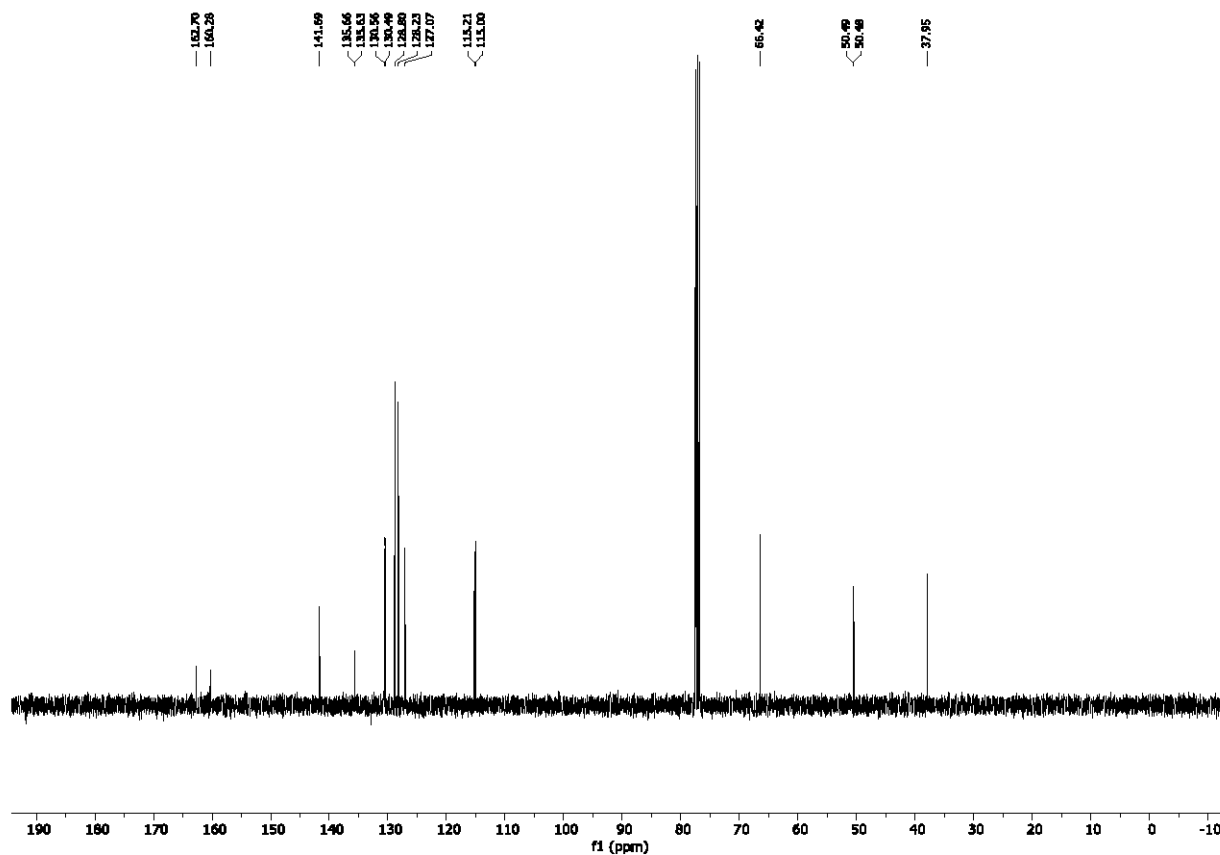
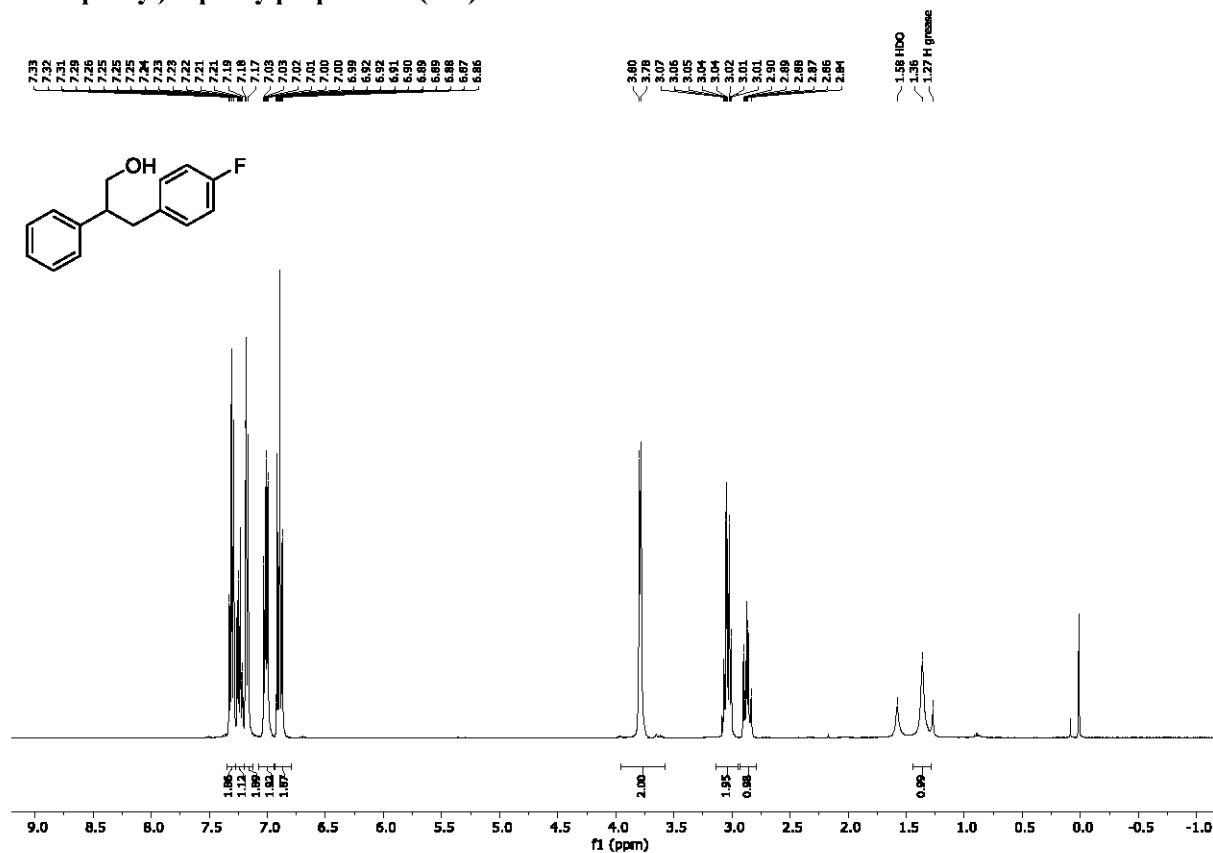
^1H NMR (400 MHz, CDCl_3) and ^{13}C NMR (100 MHz, CDCl_3); 3-(4-chlorophenyl)-2-phenylpropan-1-ol (12f)

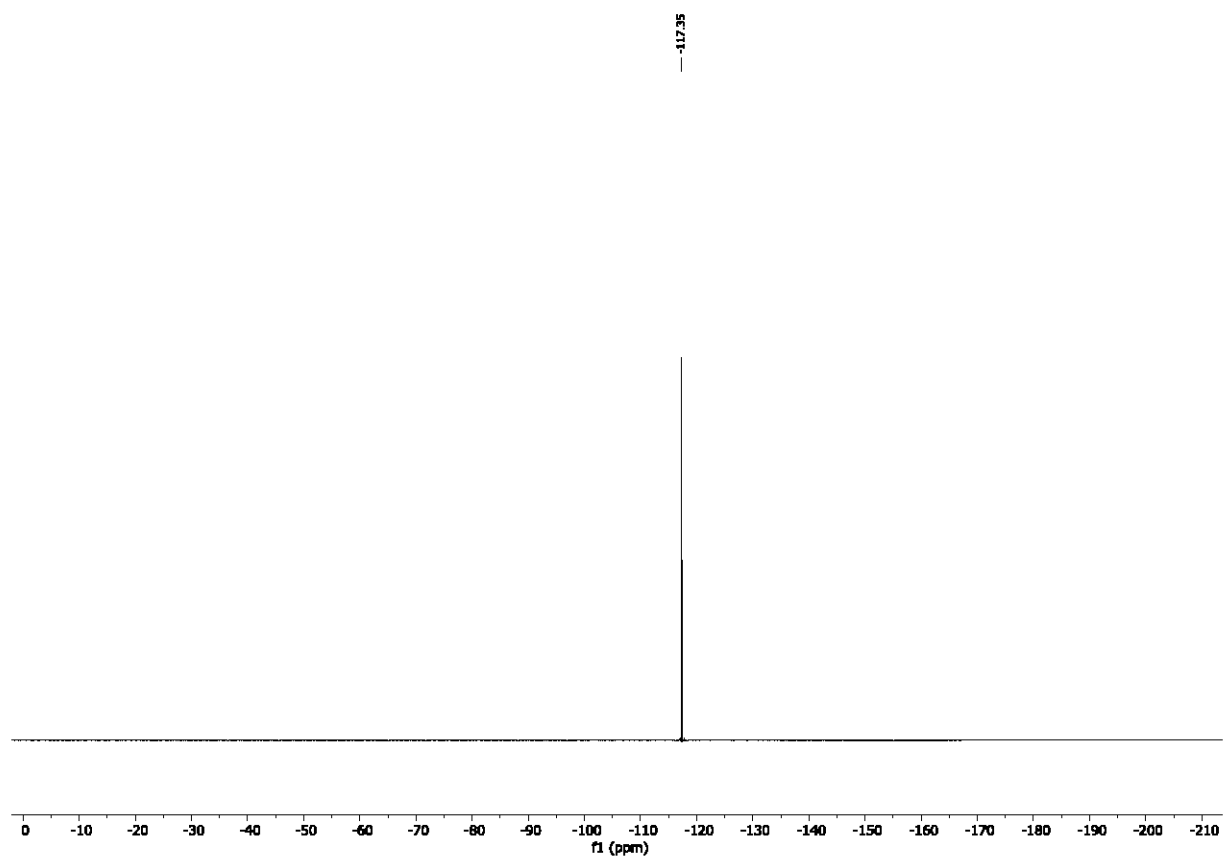


^1H NMR (400 MHz, CDCl_3) and ^{13}C NMR (100 MHz, CDCl_3); 3-(4-bromophenyl)-2-phenylpropan-1-ol (12g)

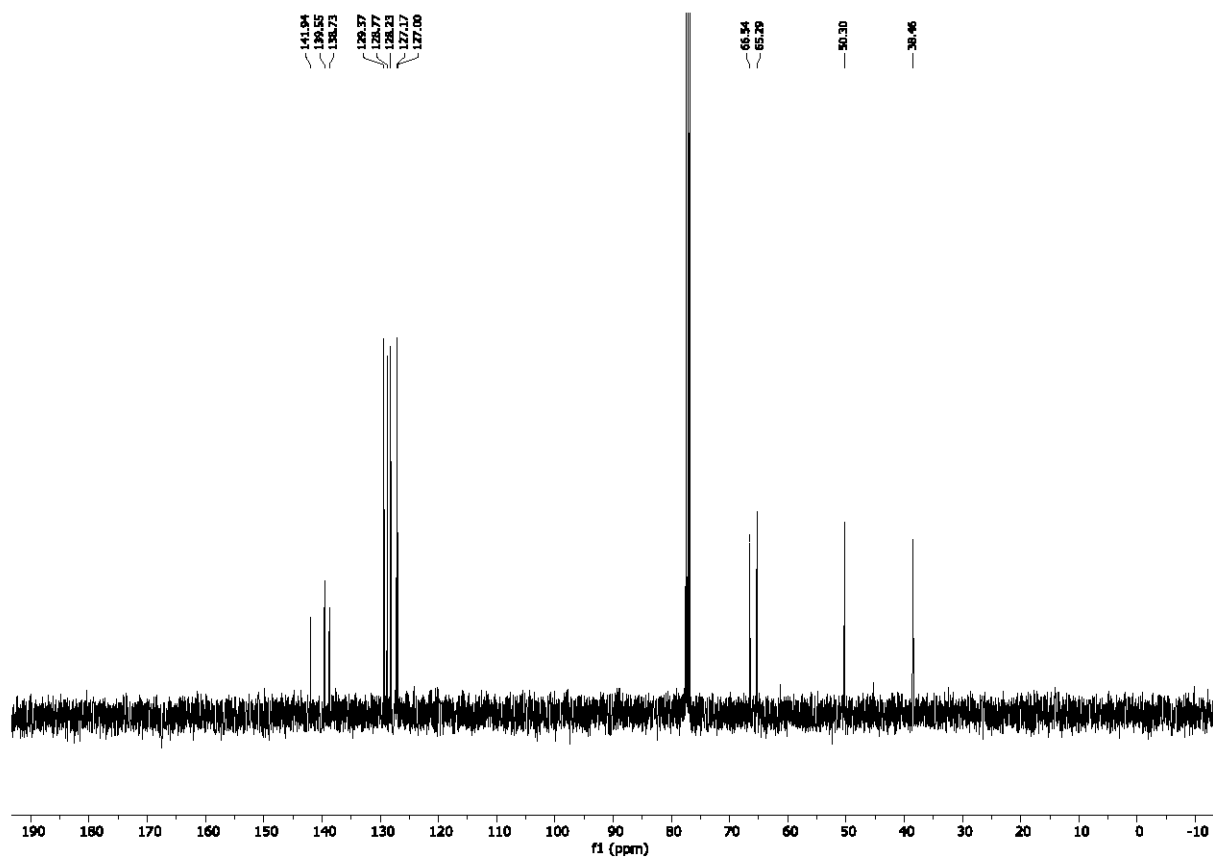
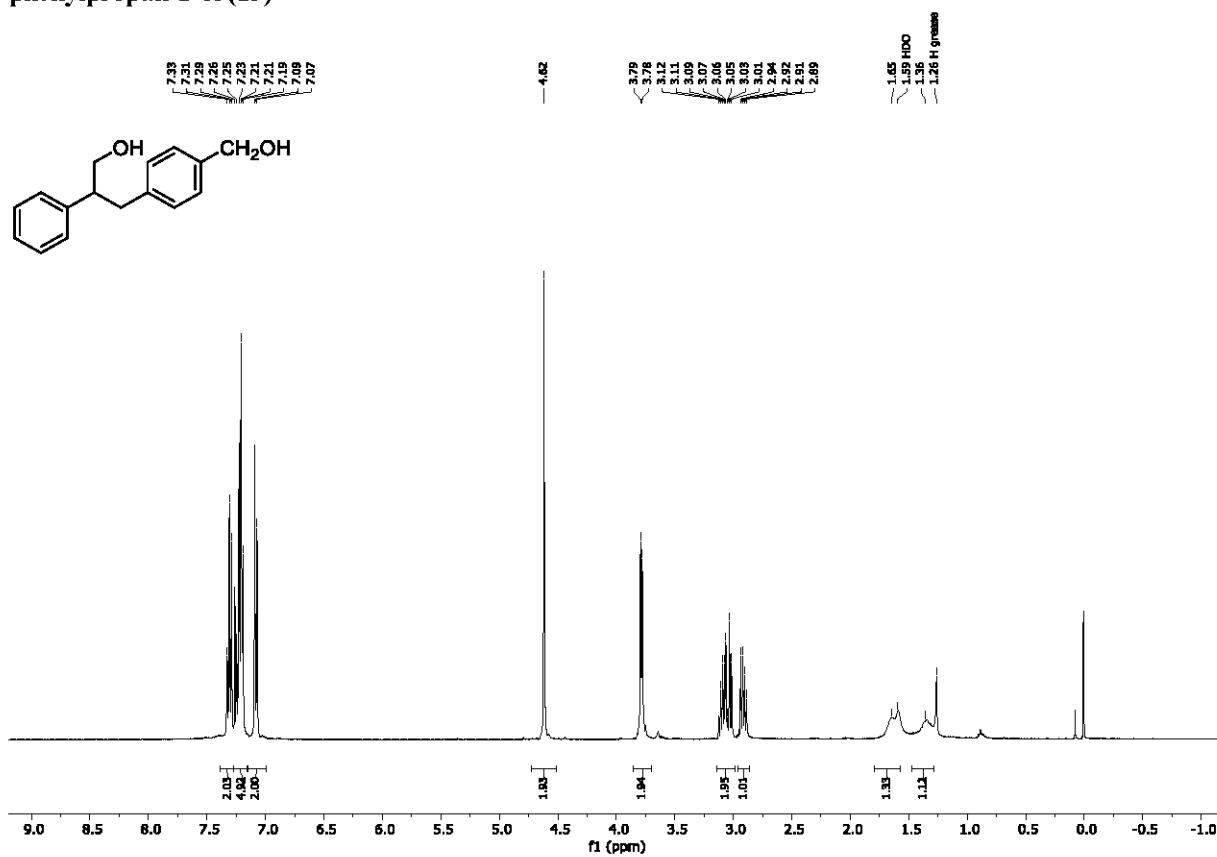


¹H NMR (400 MHz, CDCl₃), ¹³C NMR (100 MHz, CDCl₃) and ¹⁹F NMR (376 MHz, CDCl₃); 3-(4-fluorophenyl)-2-phenylpropan-1-ol (12h)

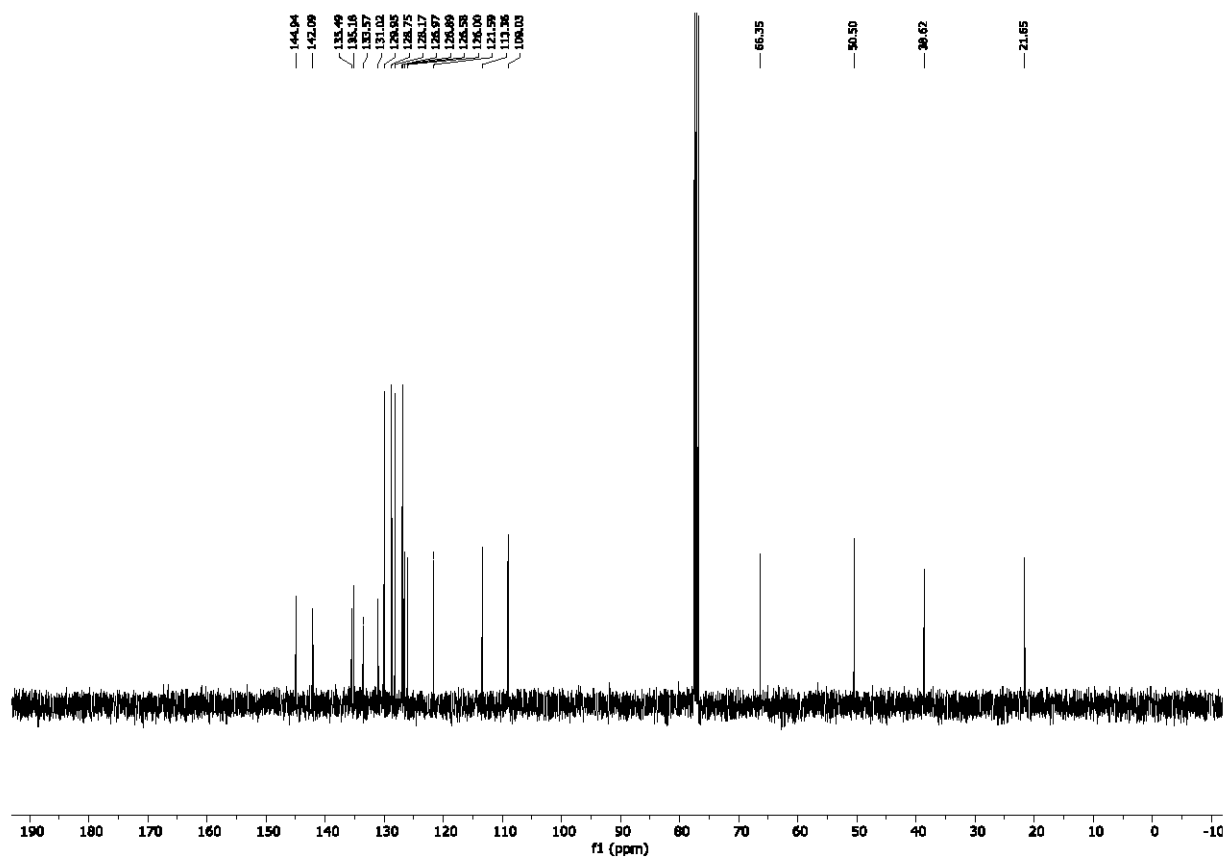
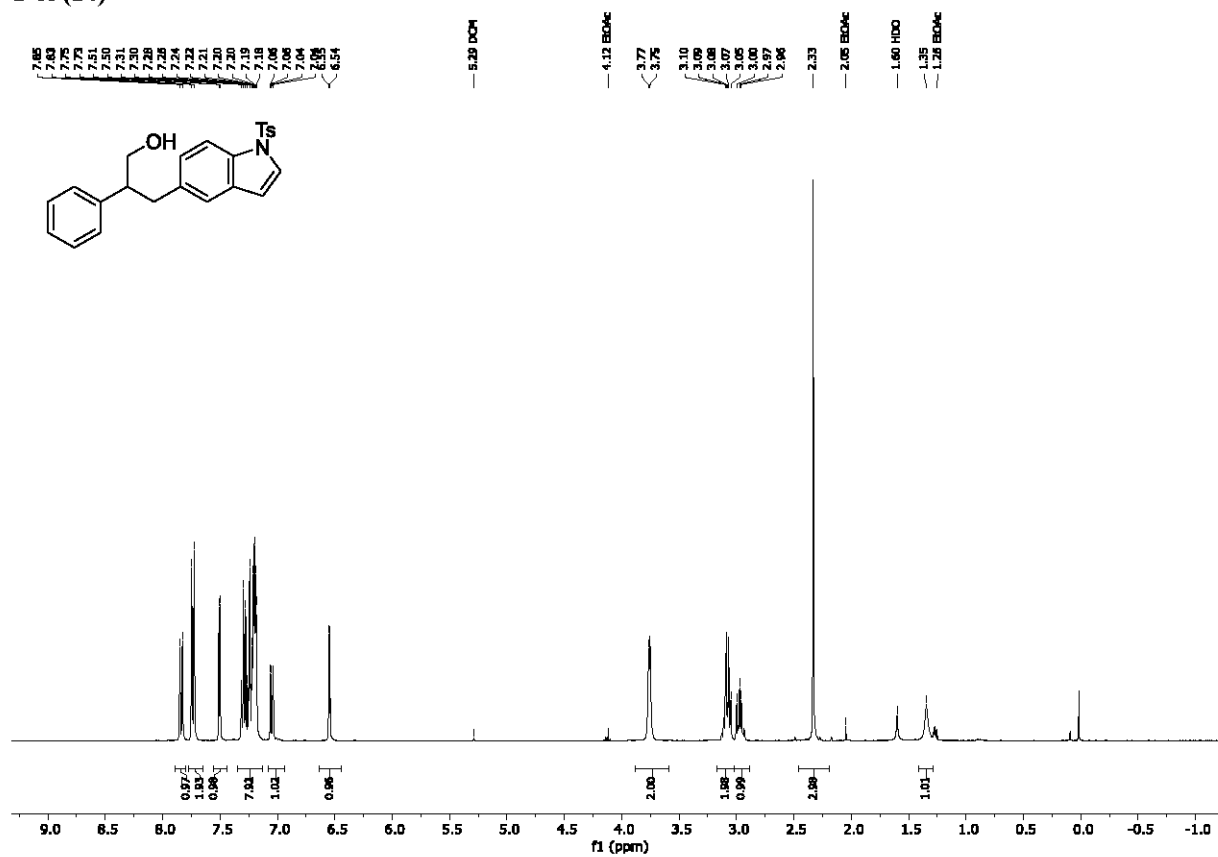




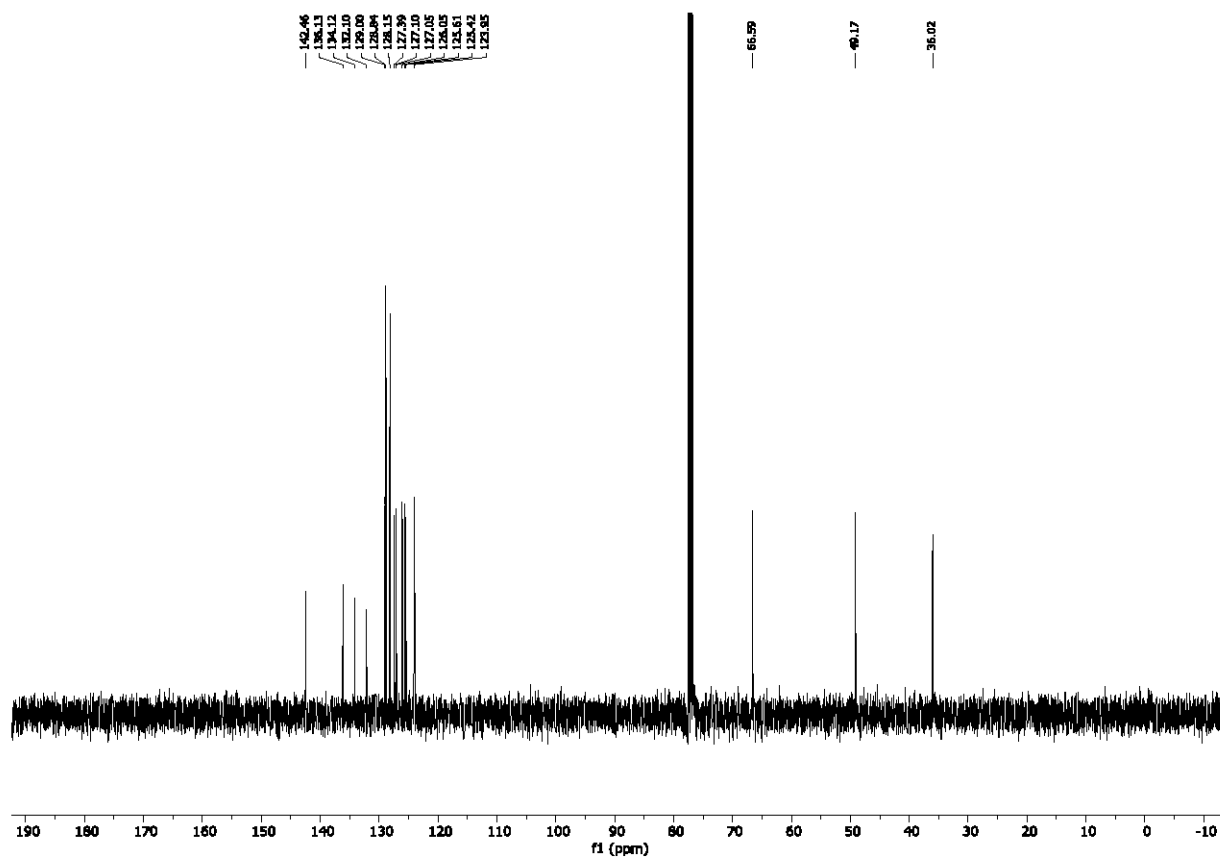
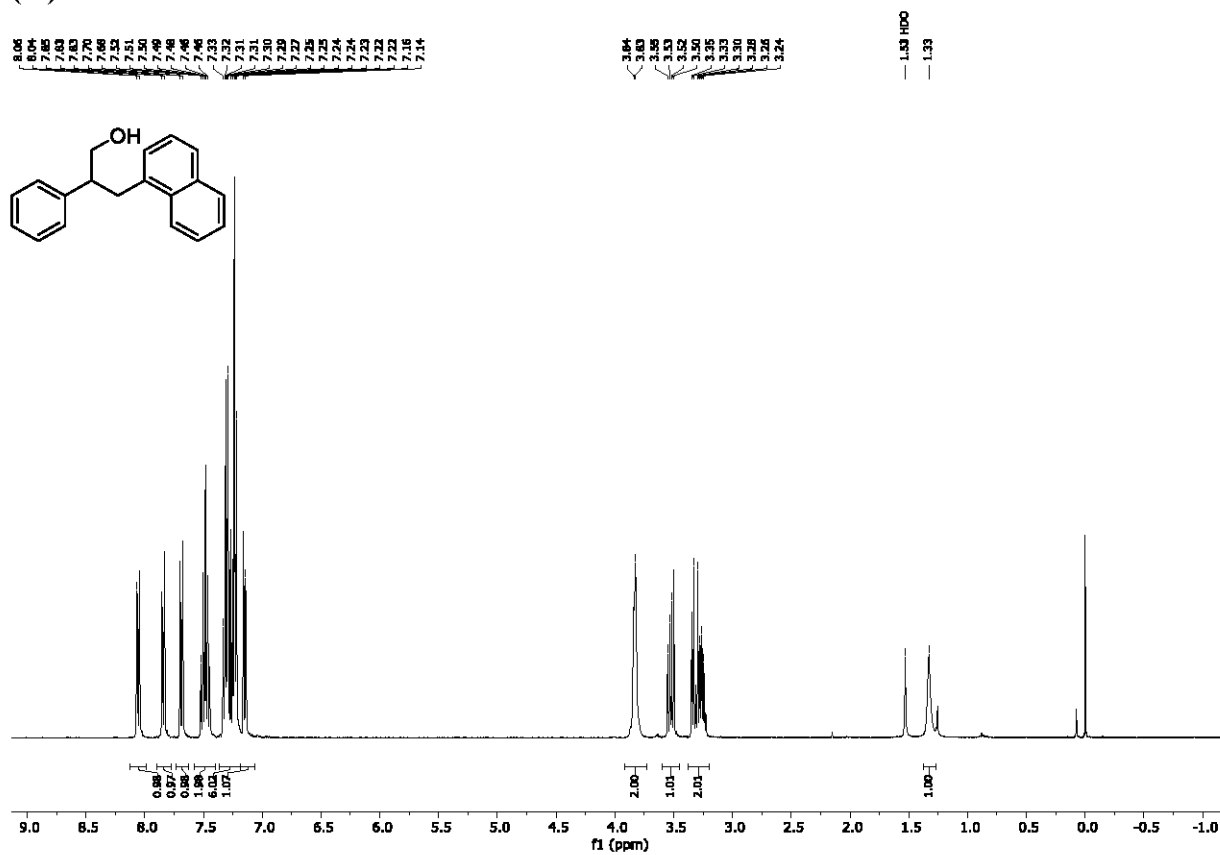
¹H NMR (400 MHz, CDCl₃) and ¹³C NMR (100 MHz, CDCl₃); 3-(4-(hydroxymethyl)phenyl)-2-phenylpropan-1-ol (13)



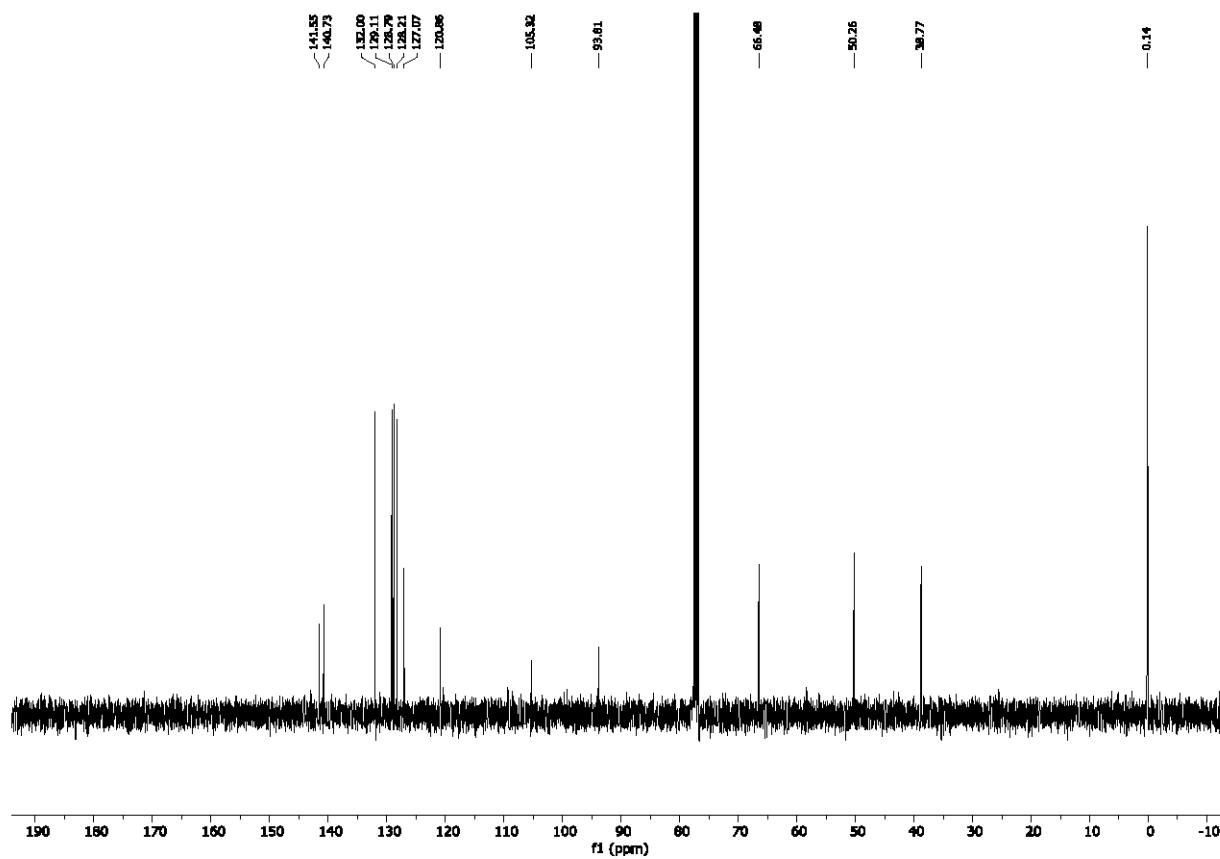
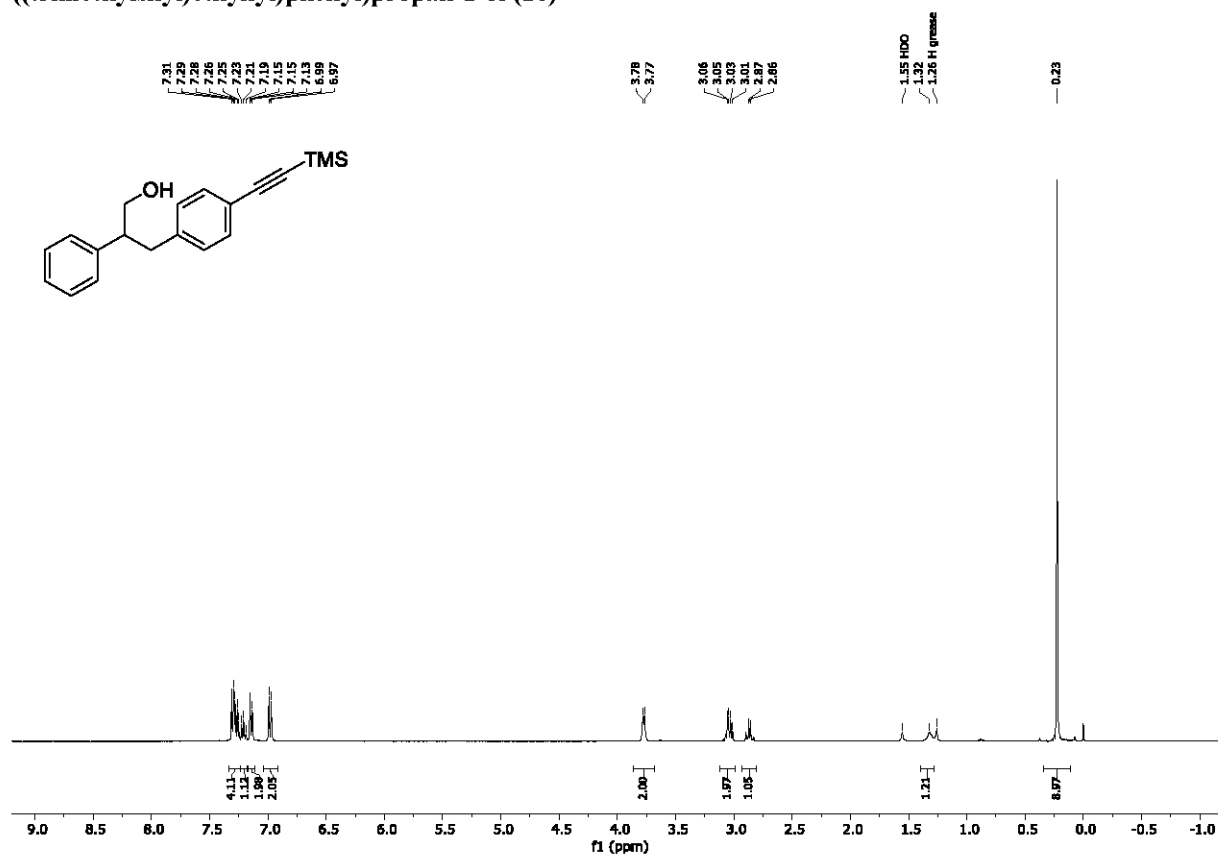
¹H NMR (400 MHz, CDCl₃) and ¹³C NMR (100 MHz, CDCl₃); 2-phenyl-3-(1-tosyl-1*H*-indol-5-yl)propan-1-ol (14)



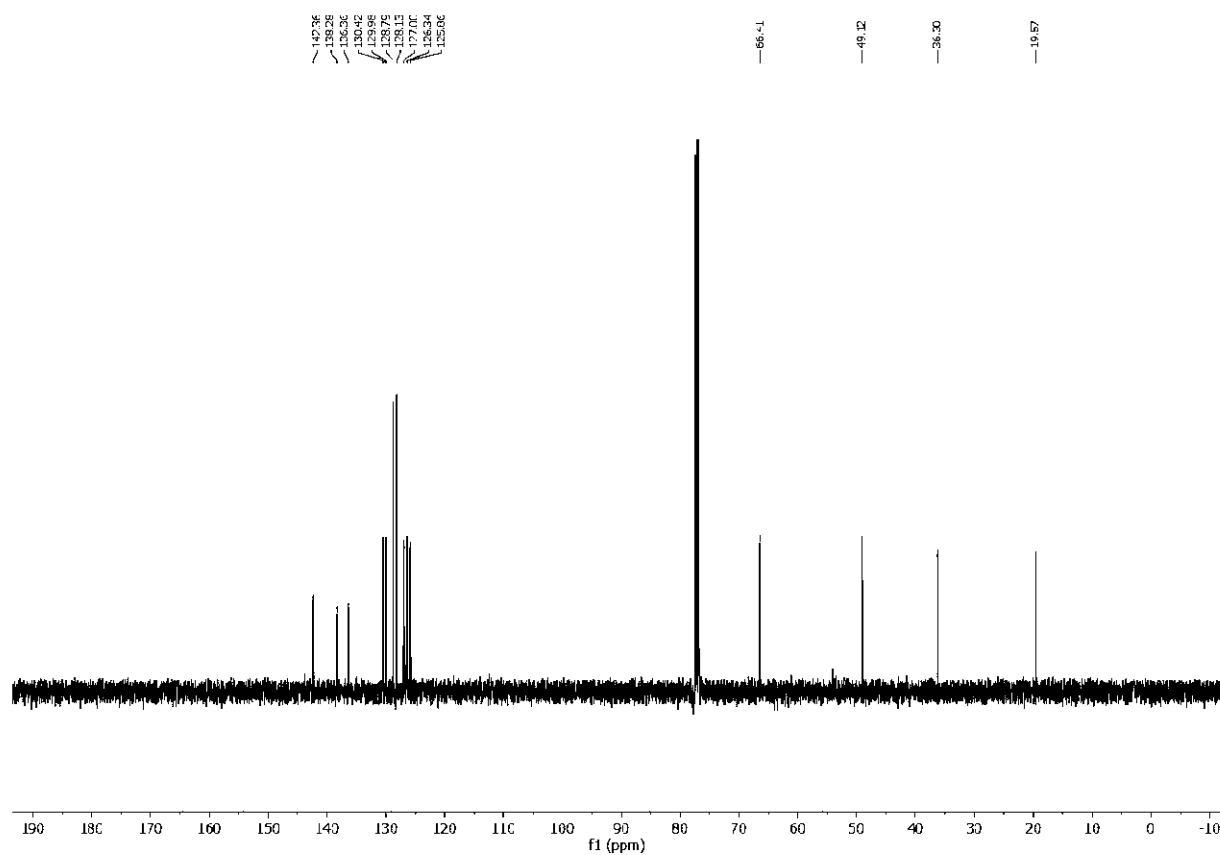
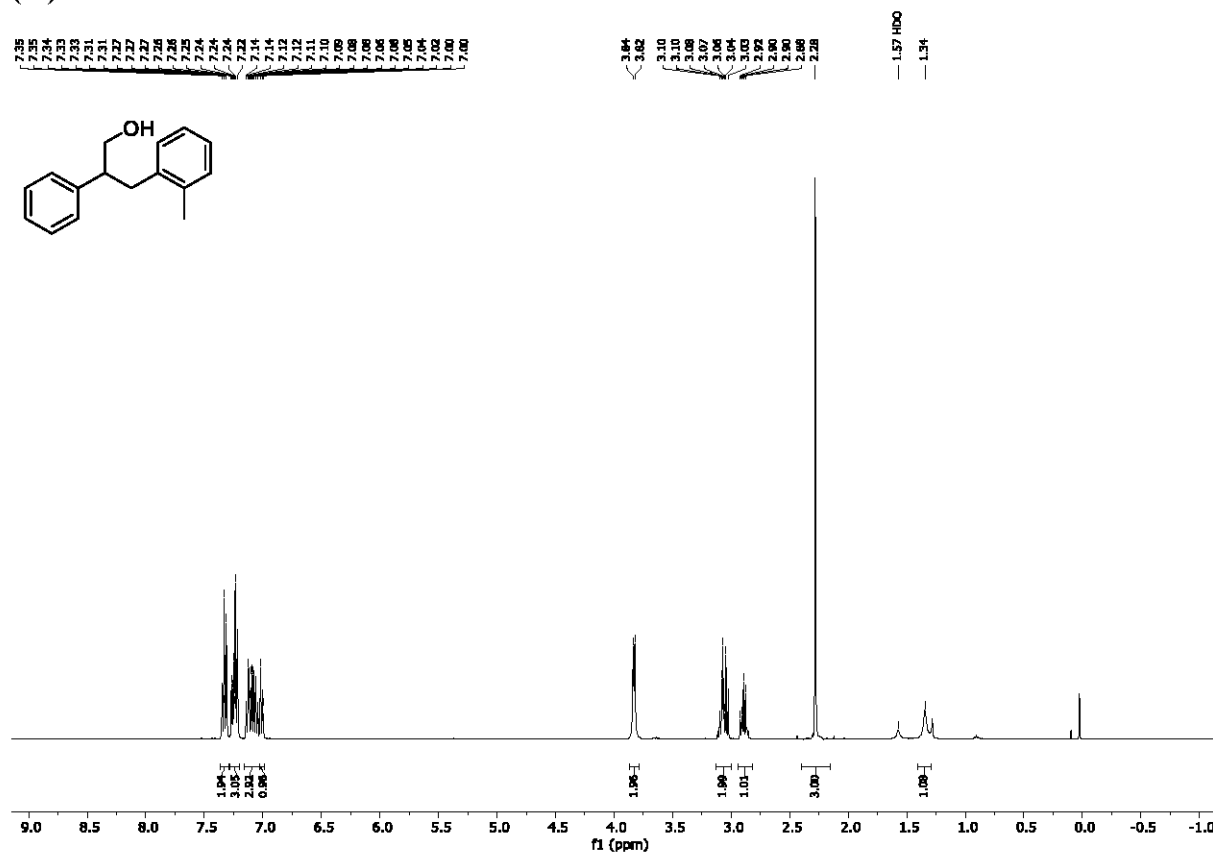
¹H NMR (400 MHz, CDCl₃) and ¹³C NMR (100 MHz, CDCl₃); 3-(naphthalen-1-yl)-2-phenylpropan-1-ol (15)



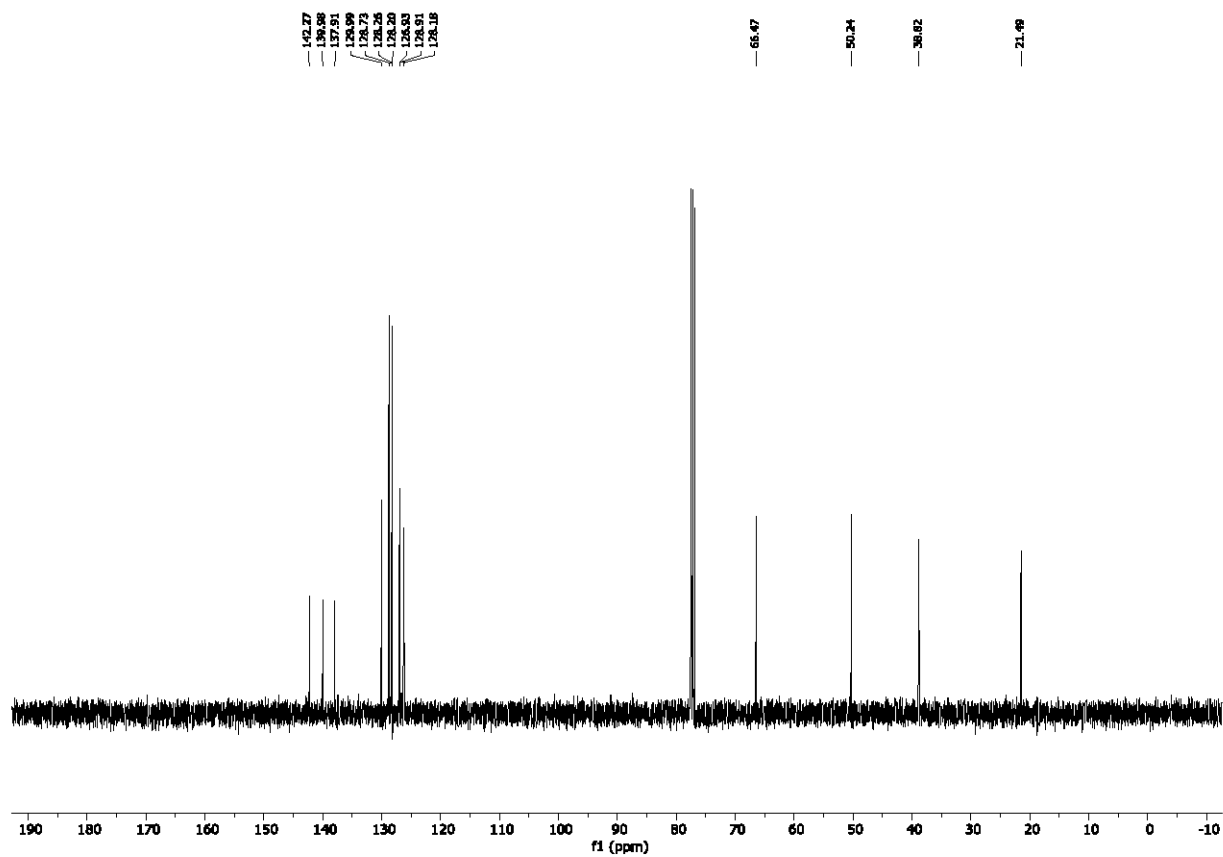
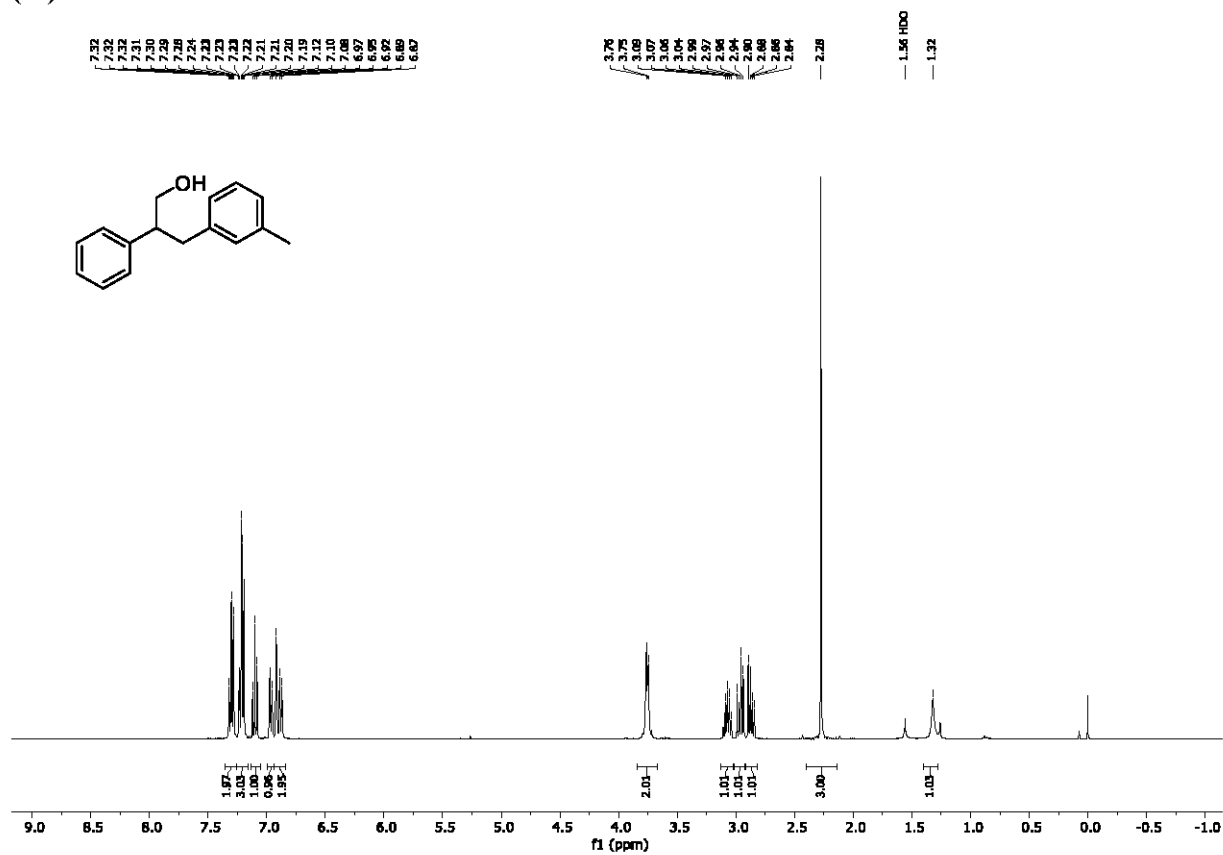
^1H NMR (400 MHz, CDCl_3) and ^{13}C NMR (100 MHz, CDCl_3); 2-phenyl-3-(4-((trimethylsilyl)ethynyl)phenyl)propan-1-ol (16)



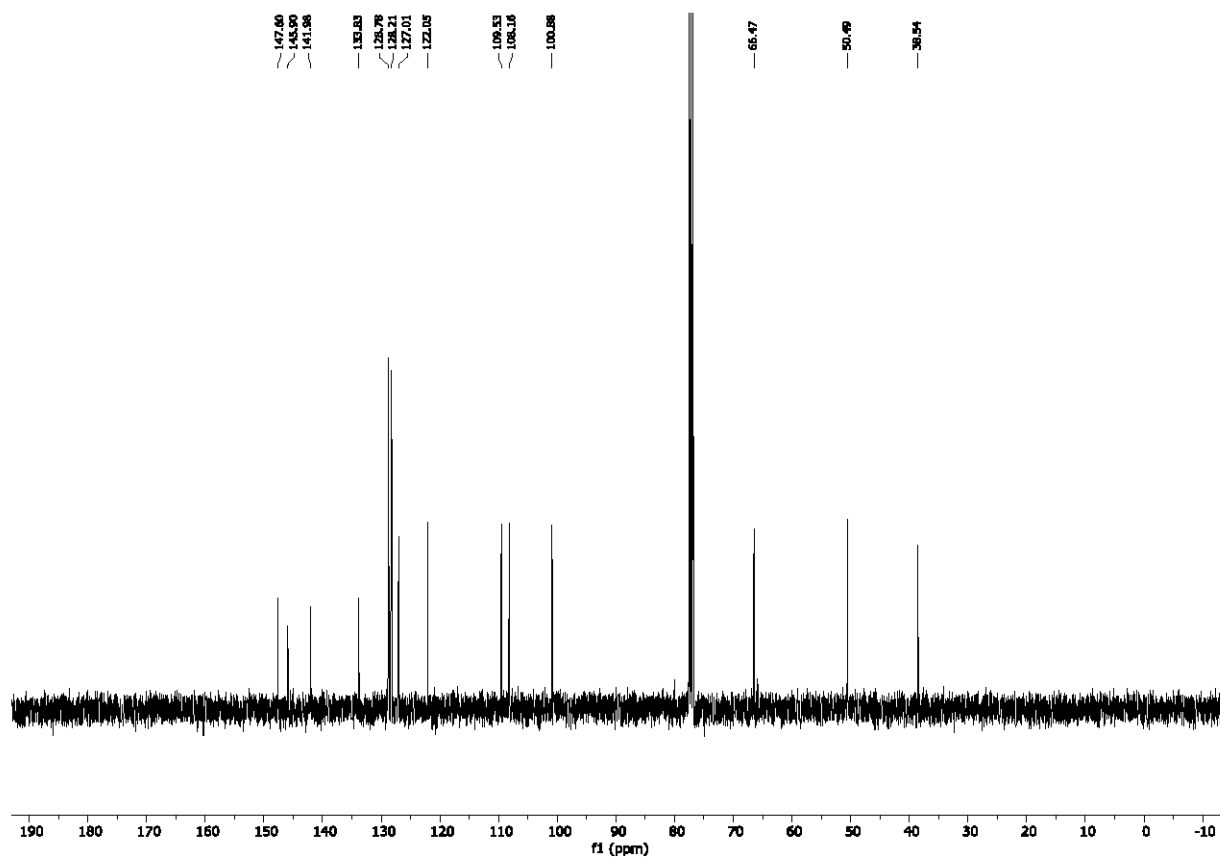
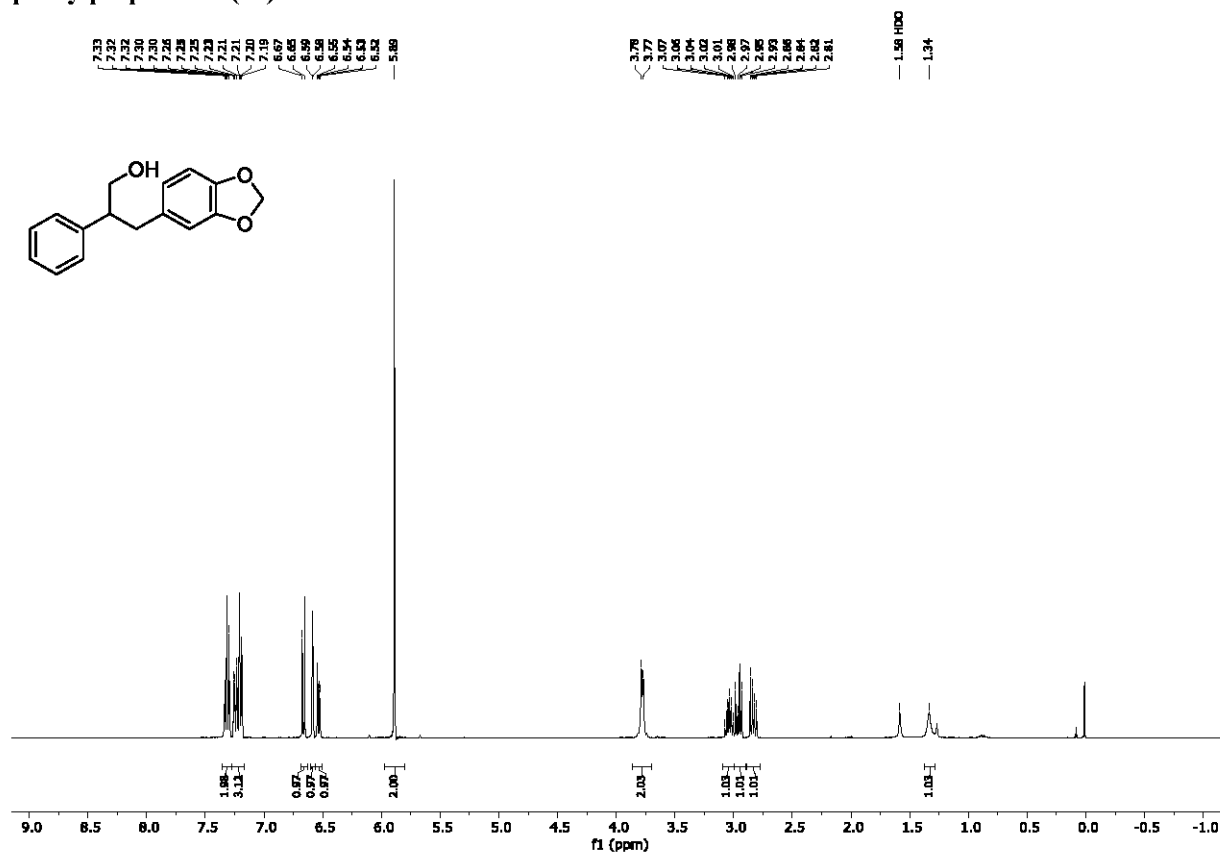
¹H NMR (400 MHz, CDCl₃) and ¹³C NMR (100 MHz, CDCl₃); 2-phenyl-3-(2-methylphenyl)propan-1-ol
(17)



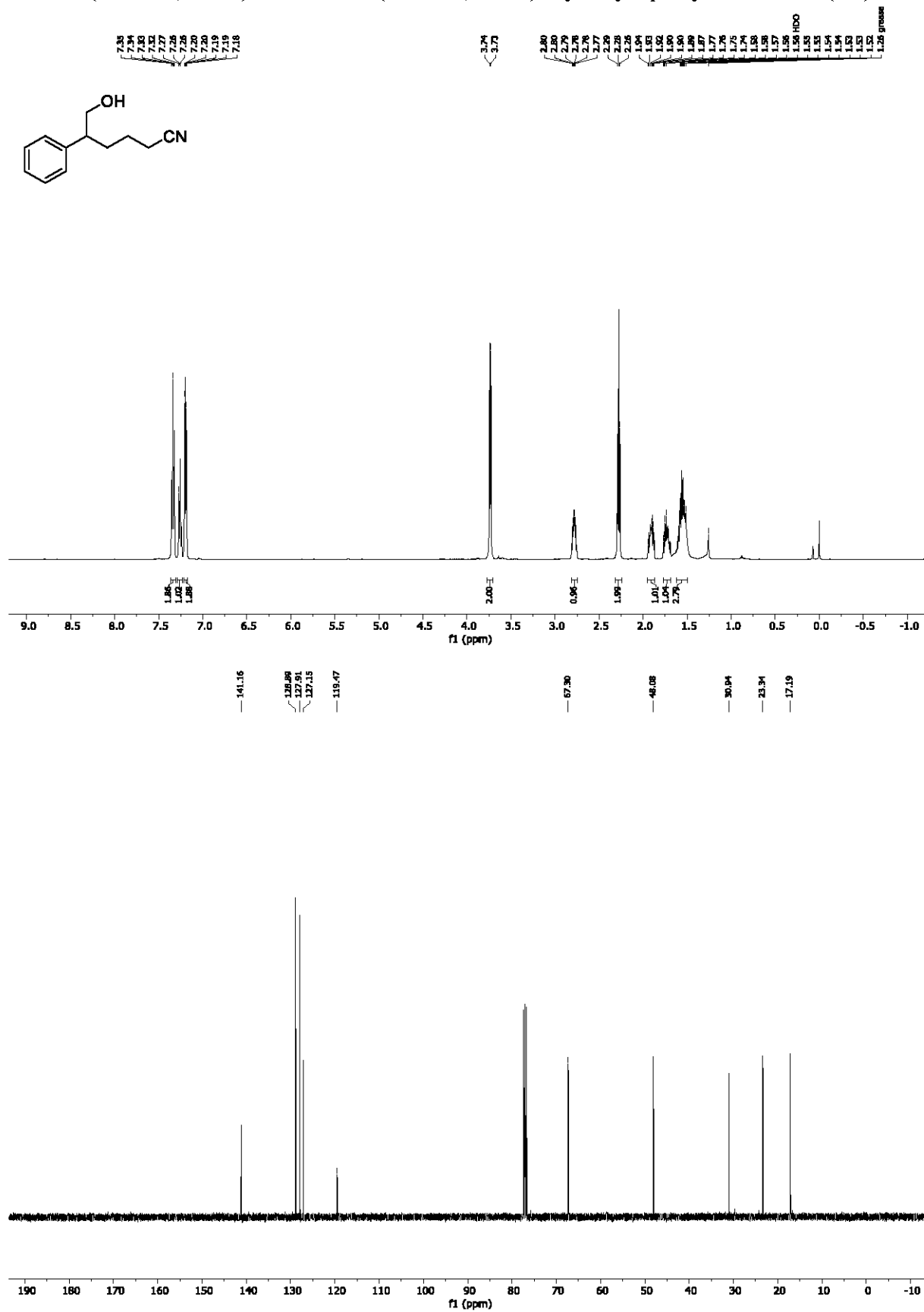
¹H NMR (400 MHz, CDCl₃) and ¹³C NMR (100 MHz, CDCl₃); 2-phenyl-3-(3-methylphenyl)propan-1-ol
(18)



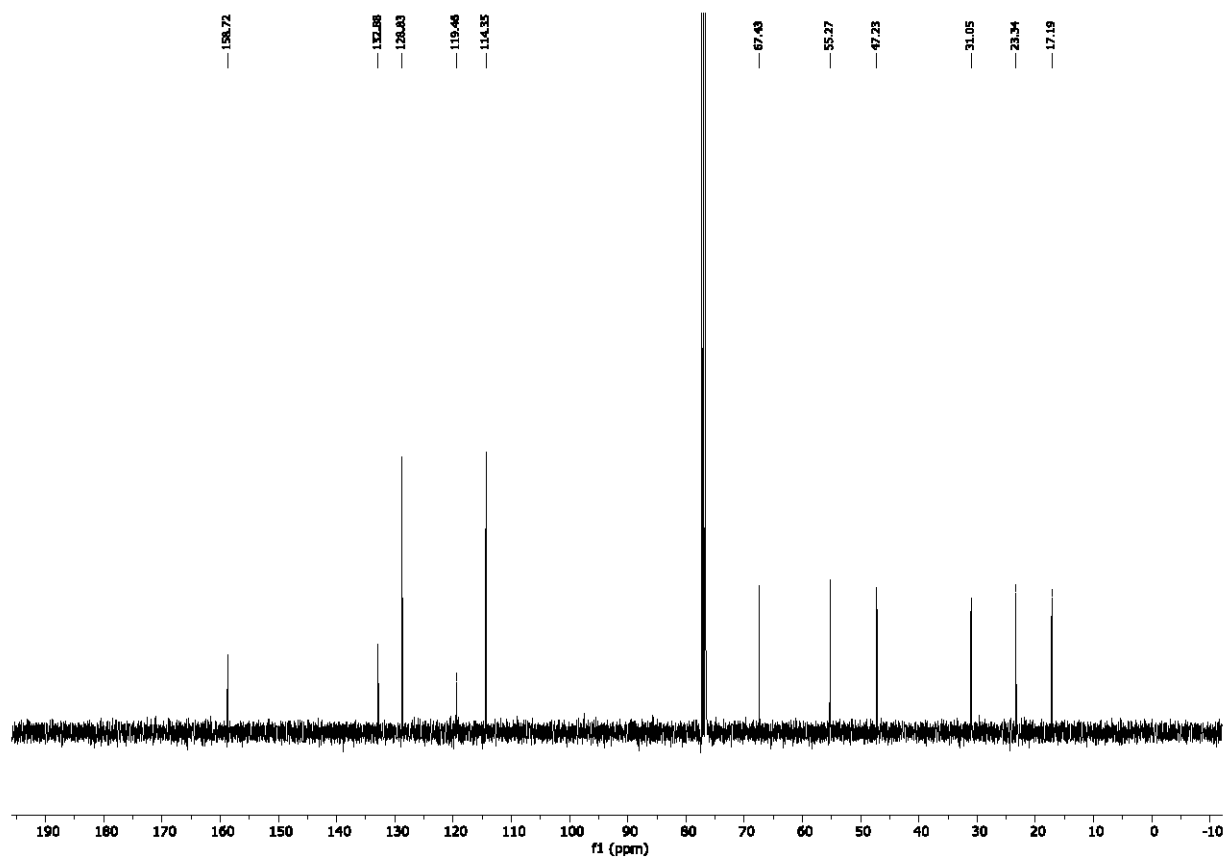
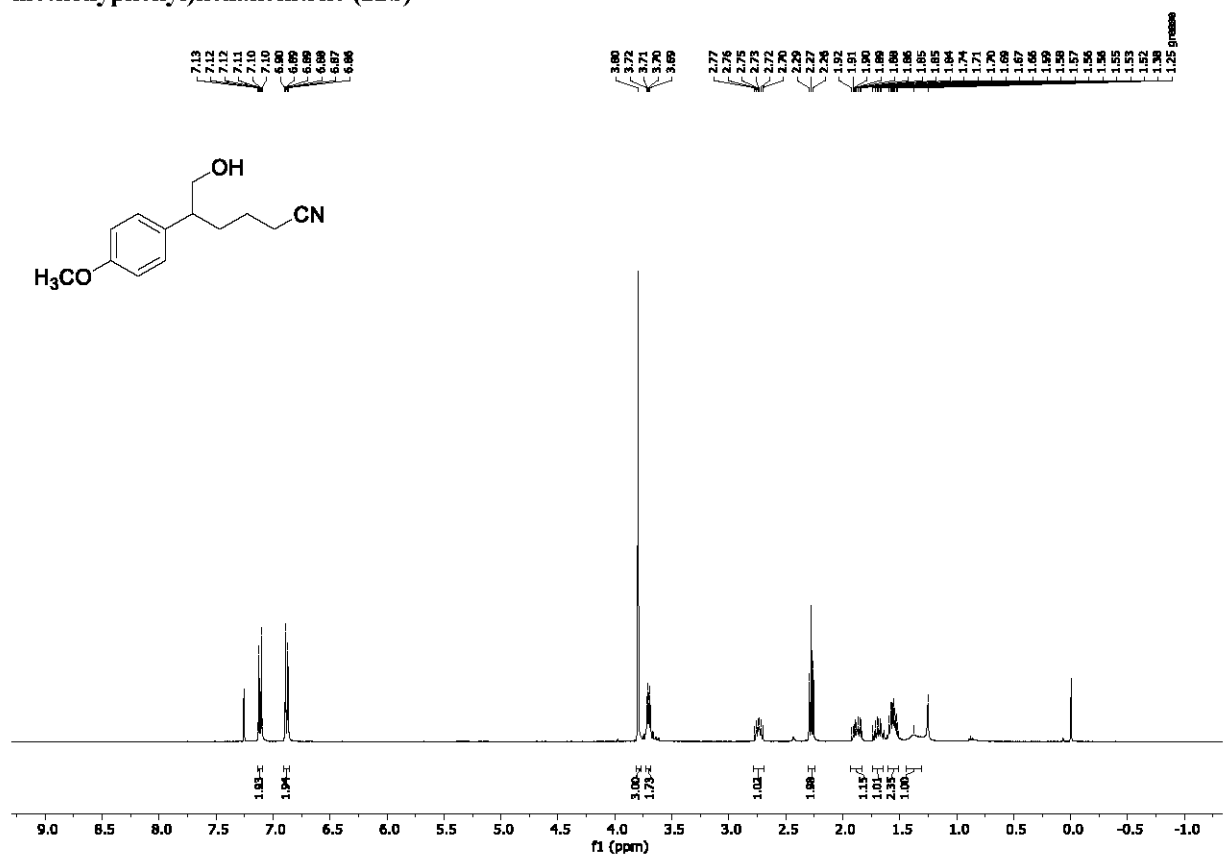
¹H NMR (400 MHz, CDCl₃) and ¹³C NMR (100 MHz, CDCl₃); 3-(benzo[d][1,3]dioxol-5-yl)-2-phenylpropan-1-ol (19)



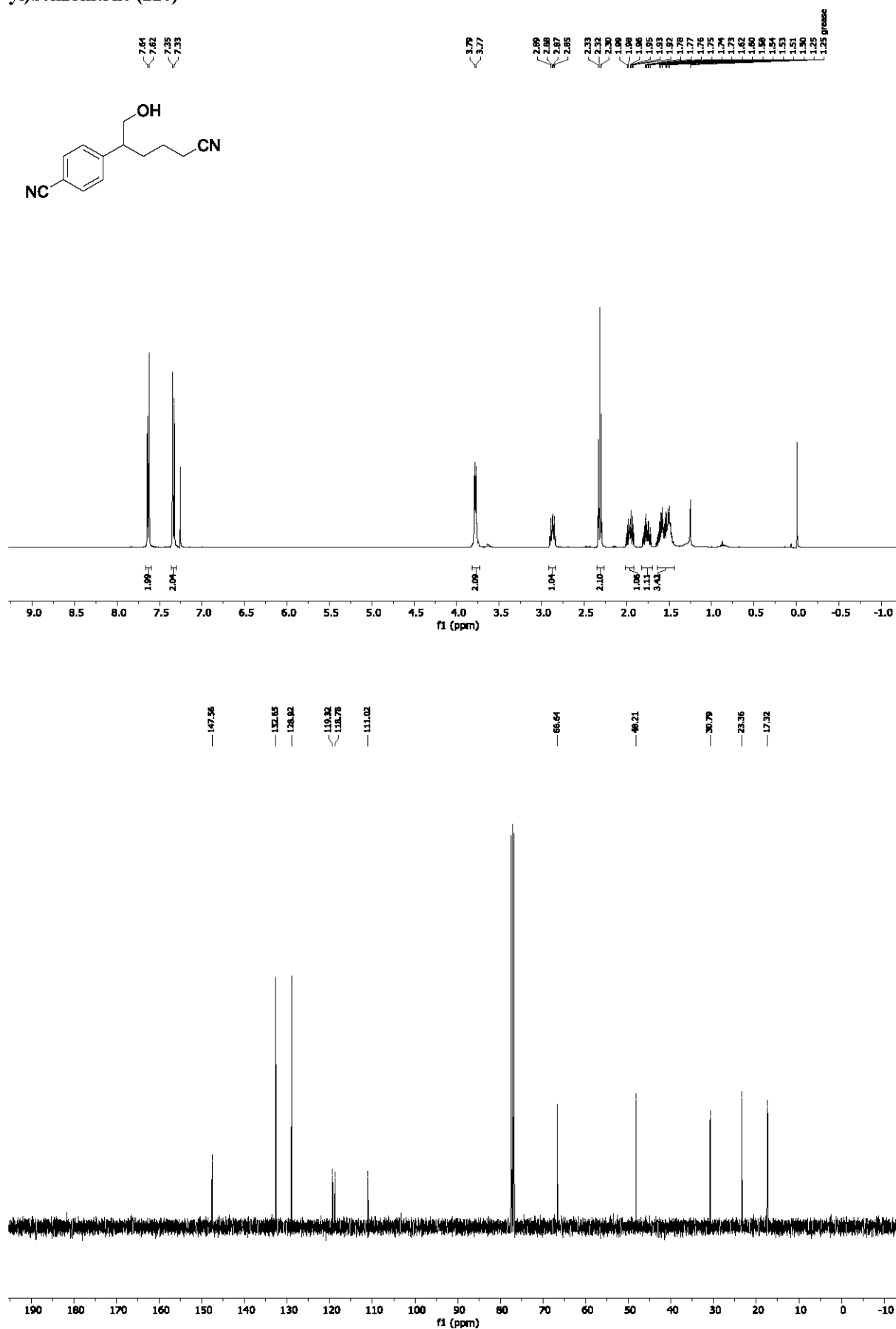
^1H NMR (500 MHz, CDCl_3) and ^{13}C NMR (125 MHz, CDCl_3) 6-hydroxy-5-phenylhexanenitrile (22a)



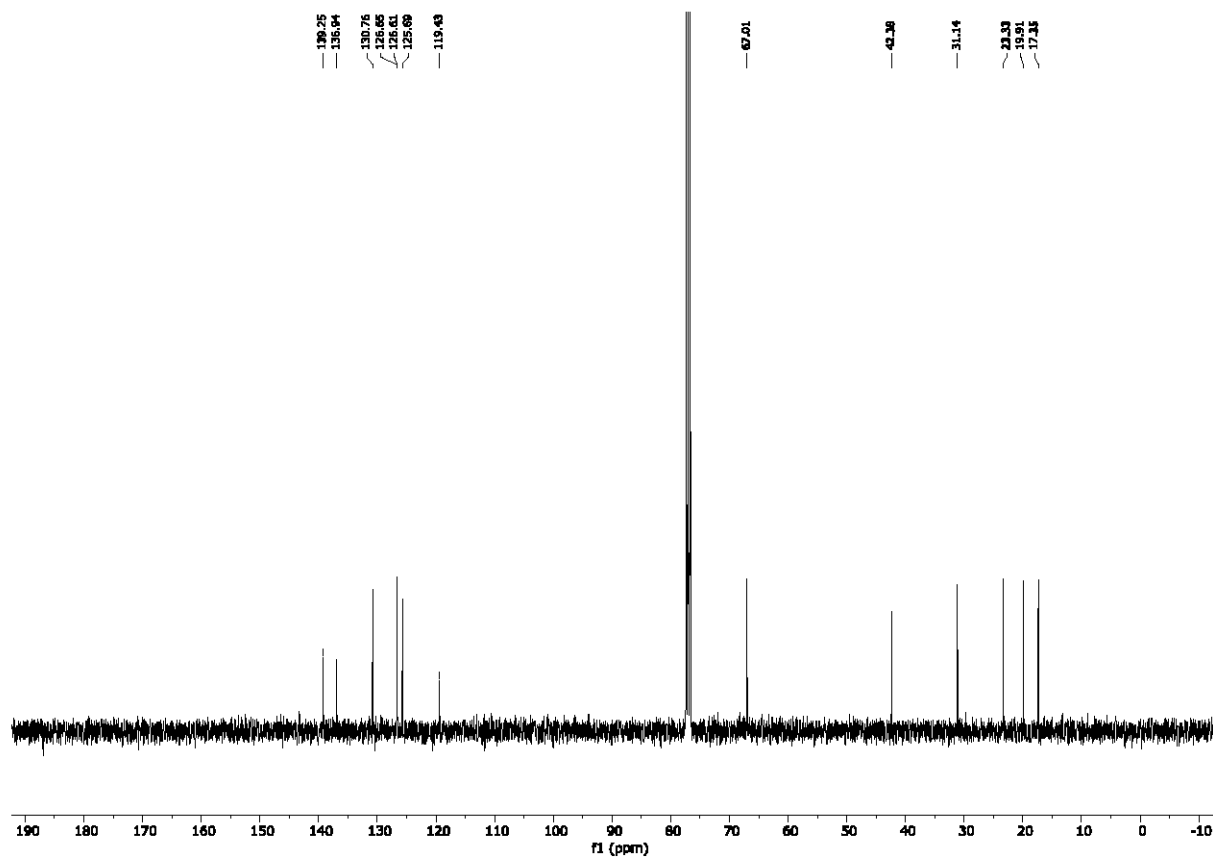
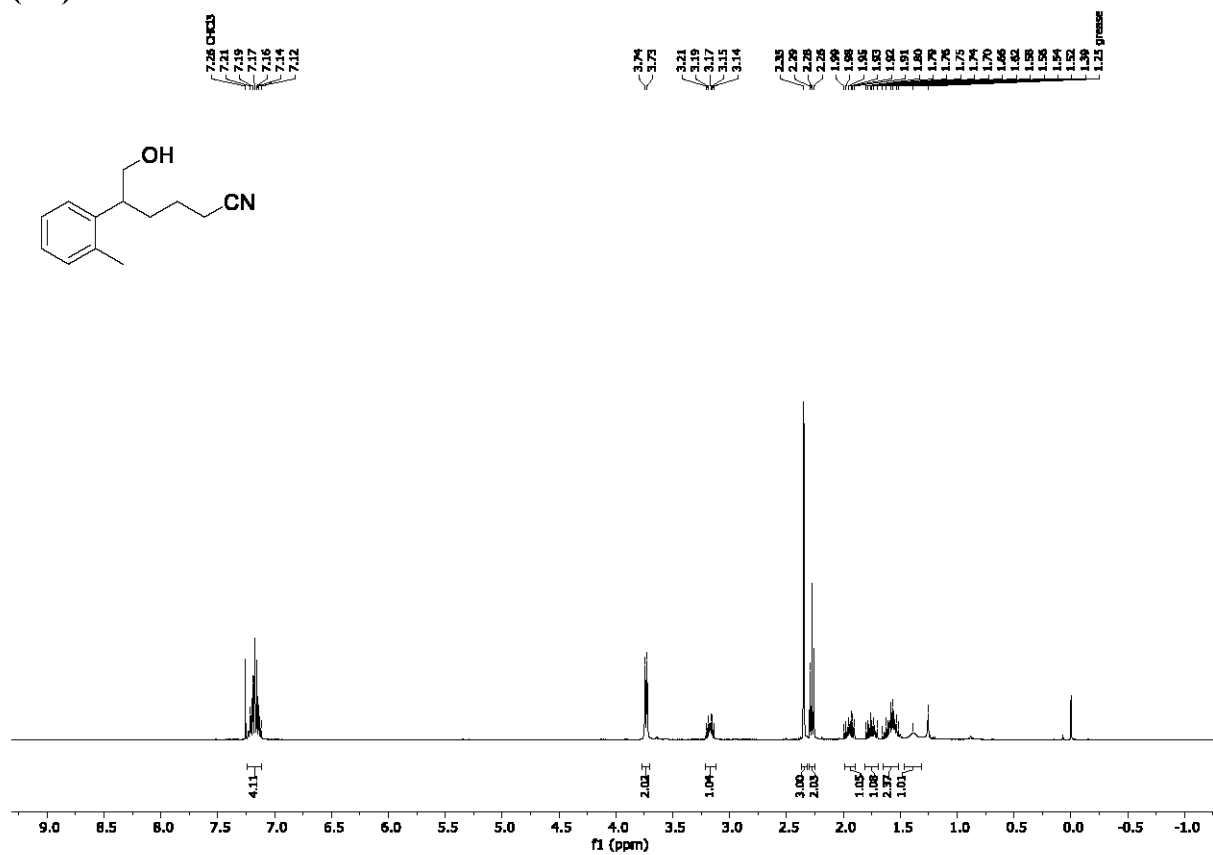
¹H NMR (400 MHz, CDCl₃) and ¹³C NMR (100 MHz, CDCl₃); 6-hydroxy-5-(4-methoxyphenyl)hexanenitrile (22b)



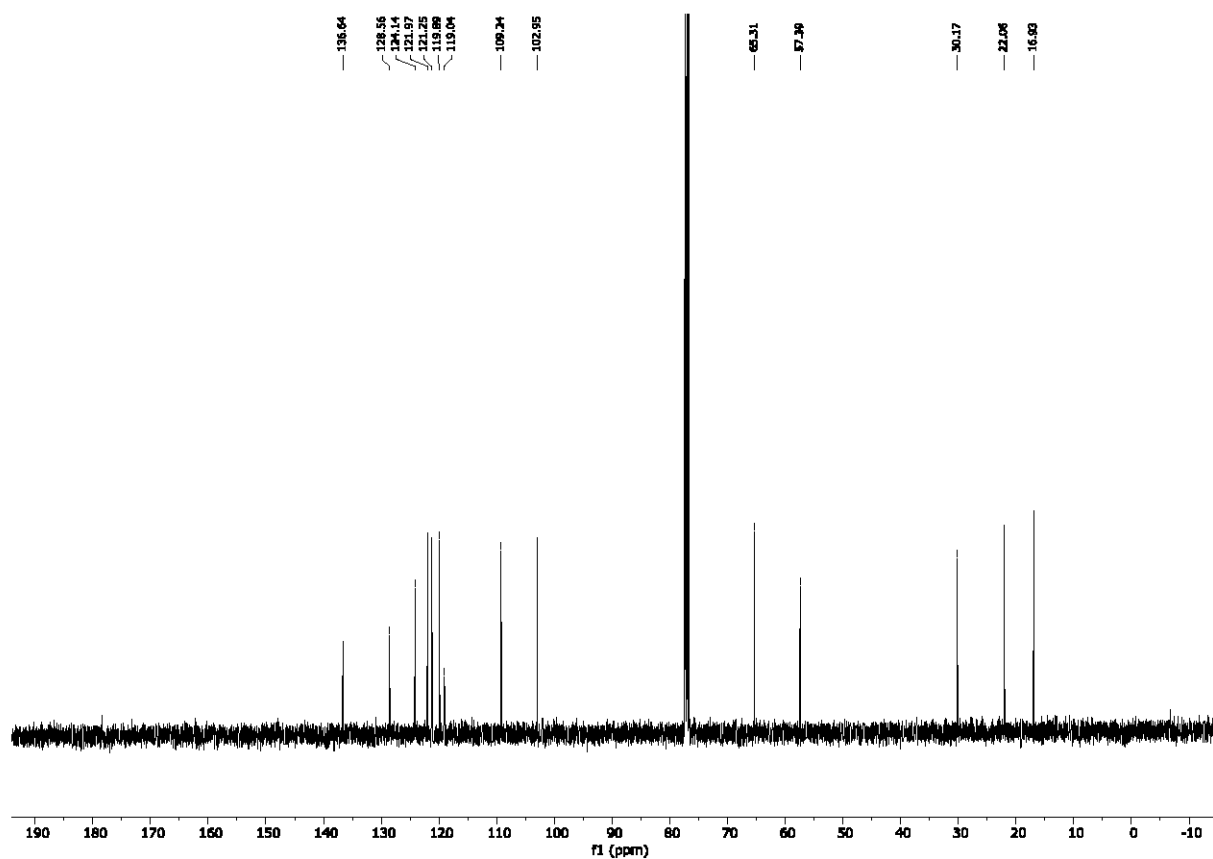
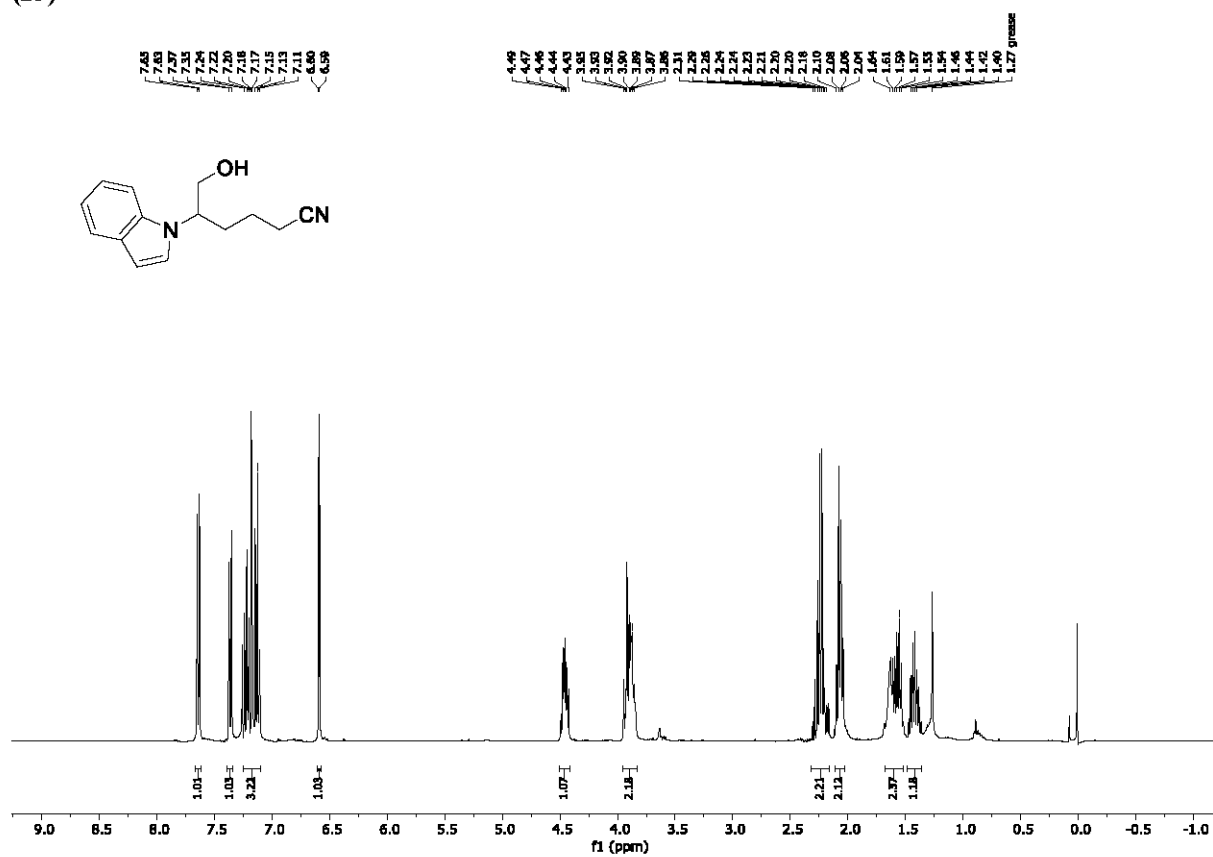
^1H NMR (400 MHz, CDCl_3) and ^{13}C NMR (100 MHz, CDCl_3); 4-(5-cyano-1-hydroxypentan-2-yl)benzonitrile (22c)



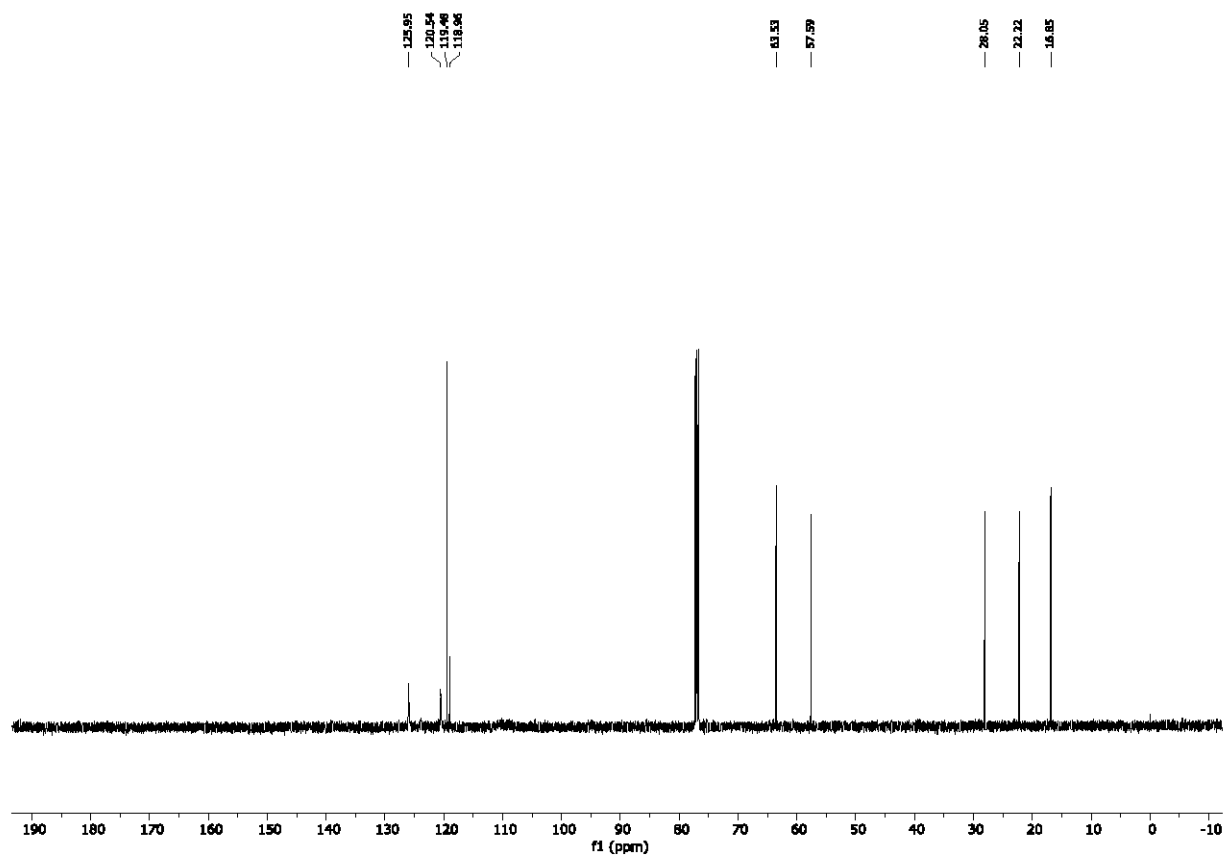
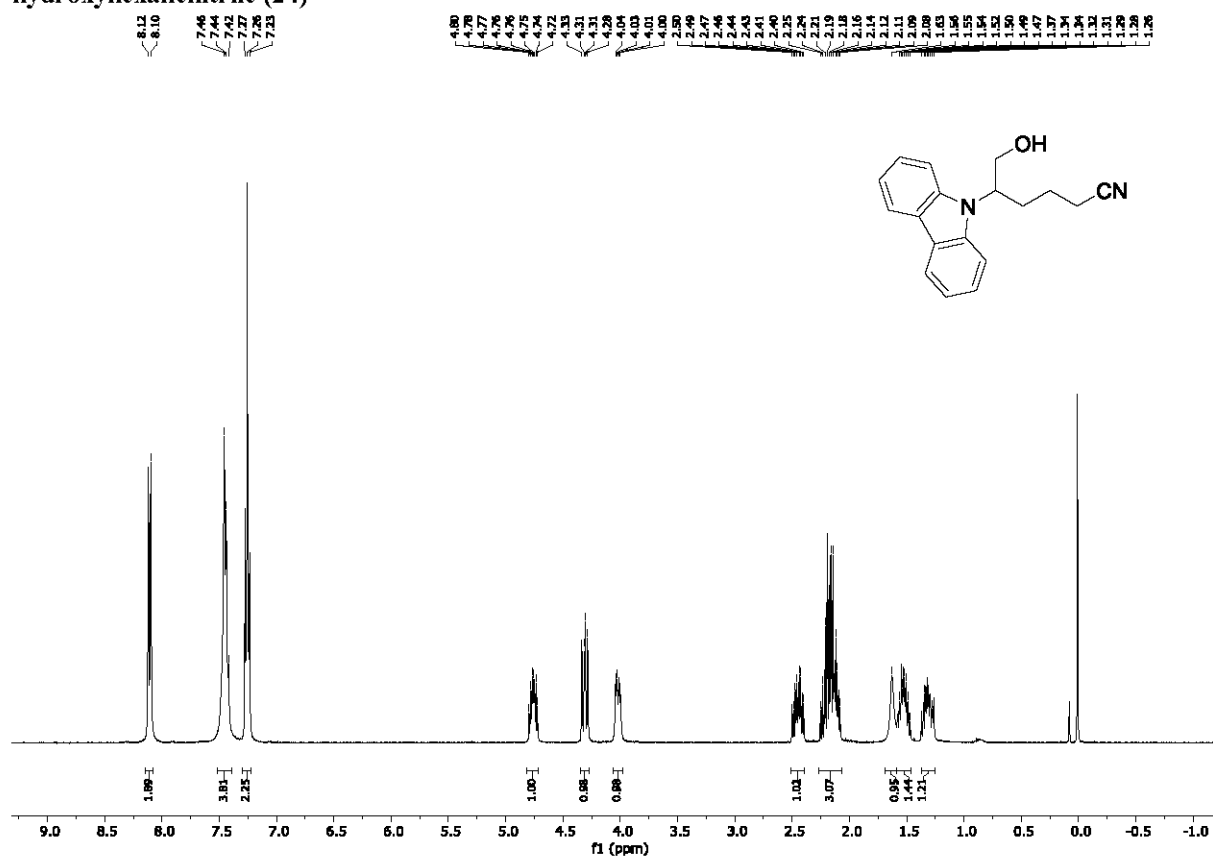
¹H NMR (400 MHz, CDCl₃) and ¹³C NMR (100 MHz, CDCl₃); 6-hydroxy-5-(2-methylphenyl)hexanenitrile (22d)



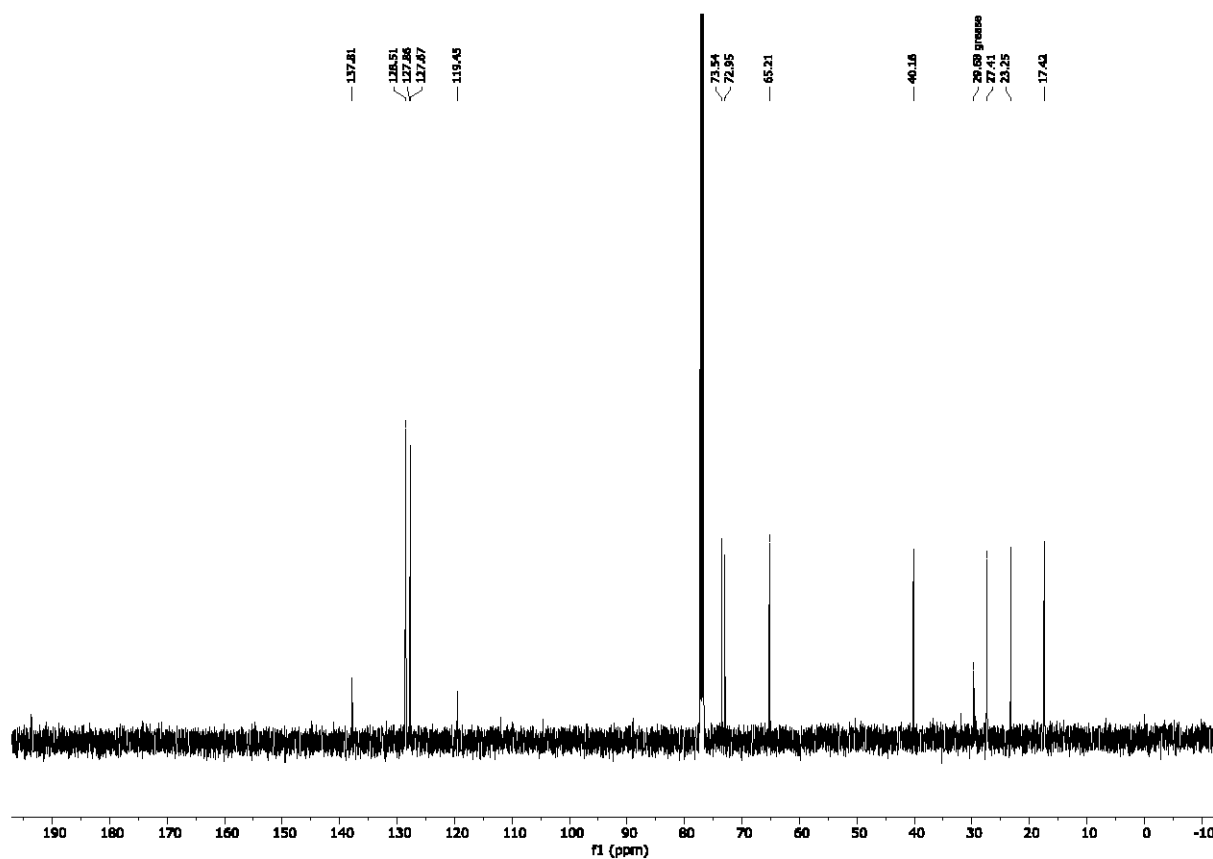
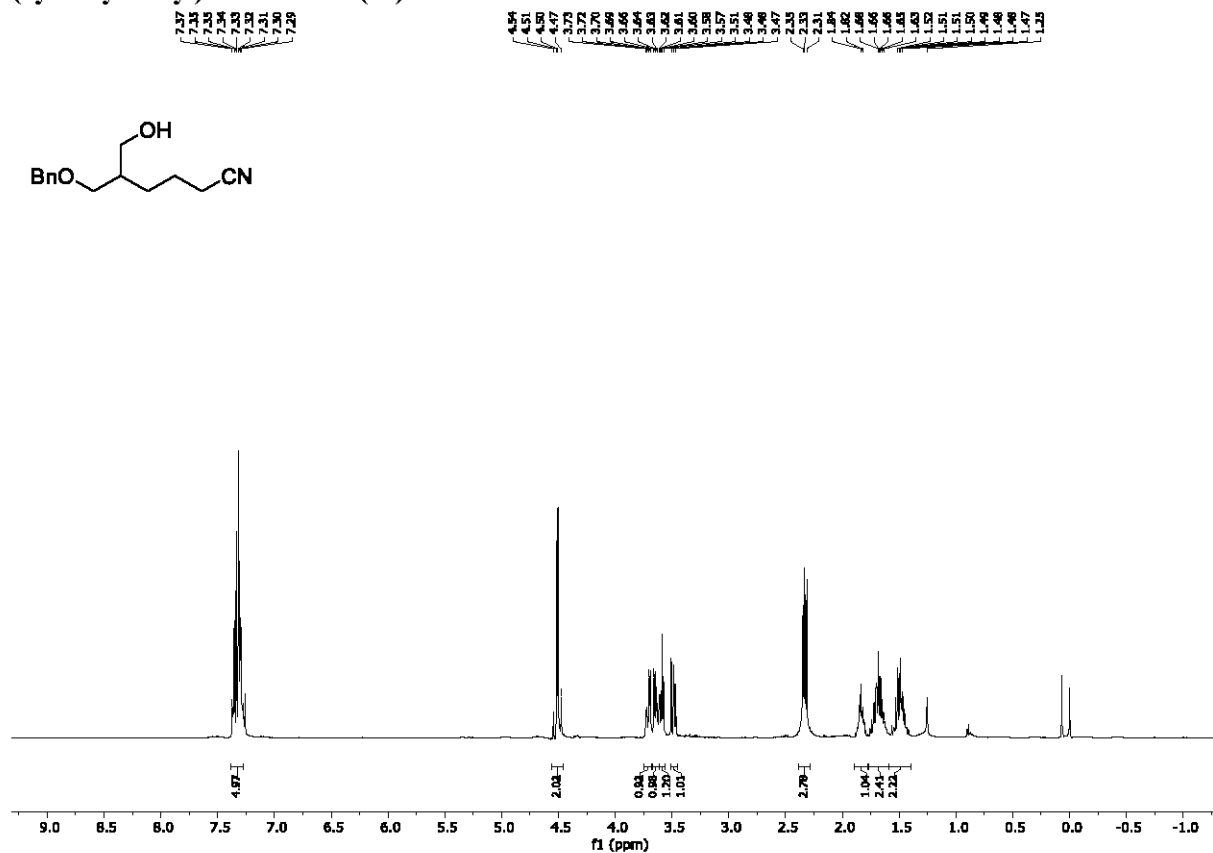
¹H NMR (400 MHz, CDCl₃) and ¹³C NMR (100 MHz, CDCl₃); 6-hydroxy-5-(1*H*-indol-1-yl)hexanenitrile (23)



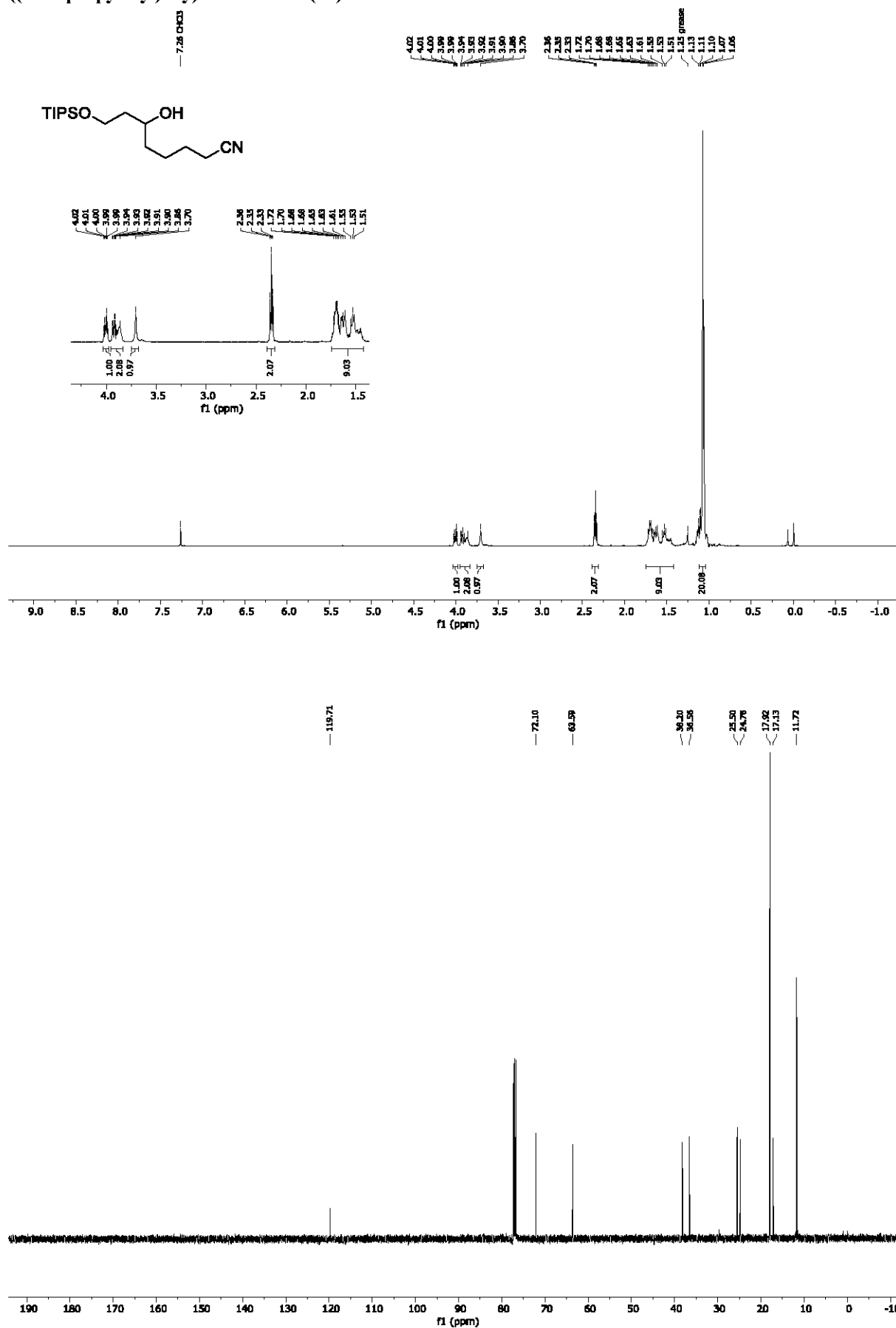
¹H NMR (500 MHz, CDCl₃) and ¹³C NMR (125 MHz, CDCl₃); 5-(9H-carbazol-9-yl)-6-hydroxyhexanenitrile (24)



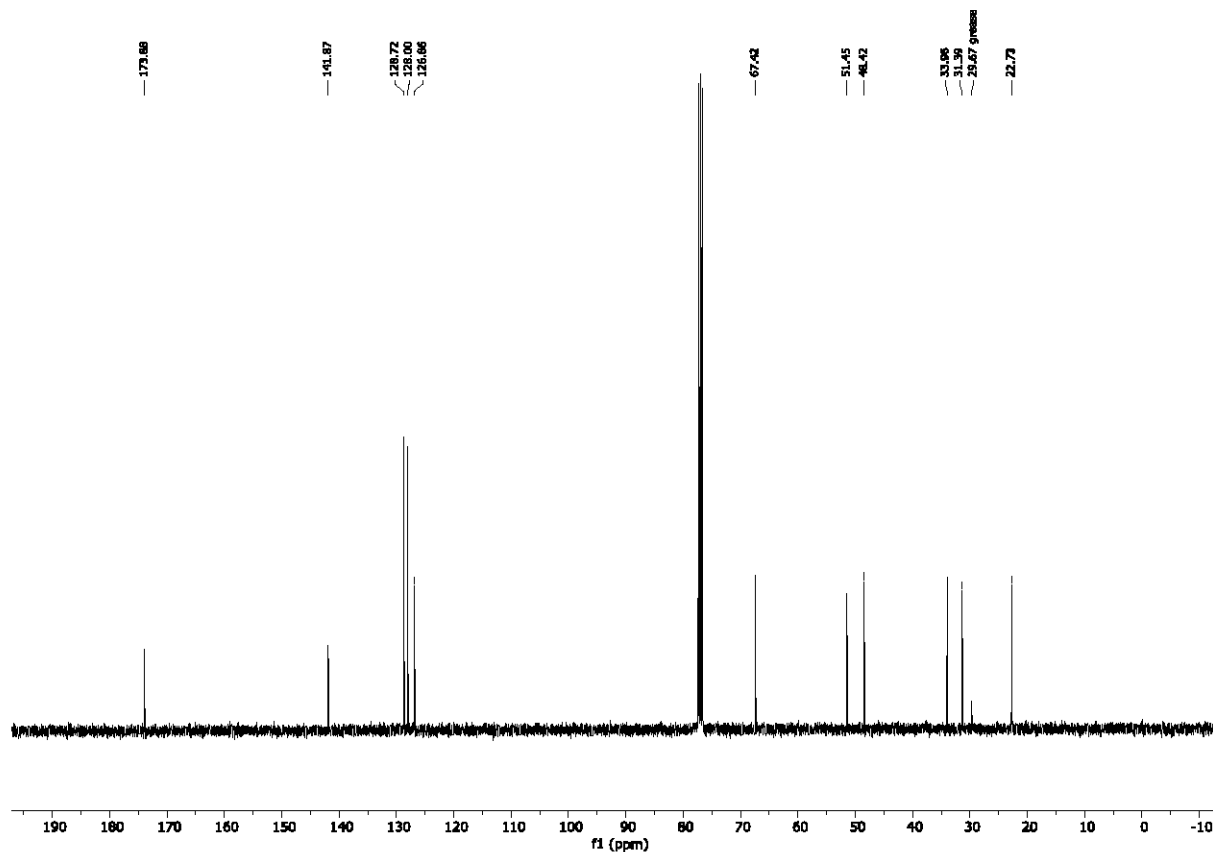
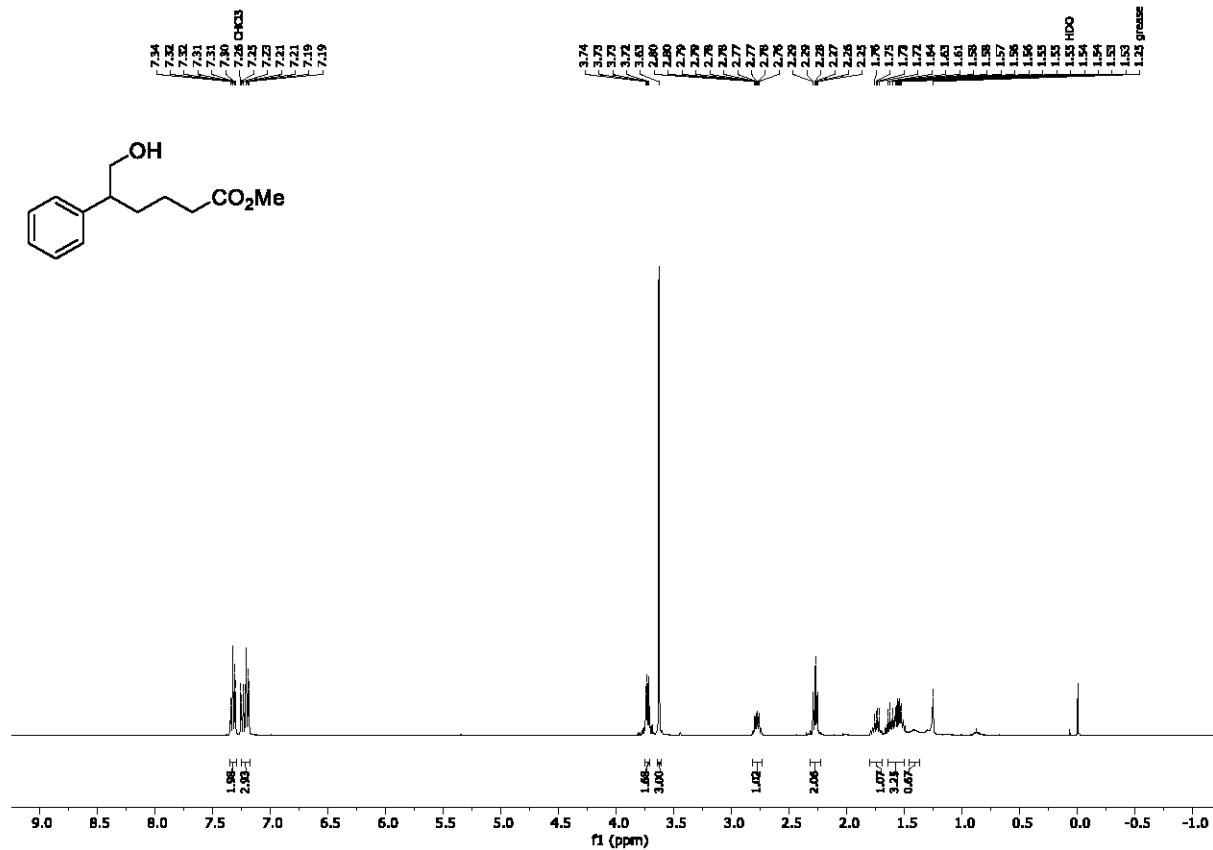
^1H NMR (400 MHz, CDCl_3) and ^{13}C NMR (125 MHz, CDCl_3); 6-(benzyloxy)-5-(hydroxymethyl)hexanenitrile (26)



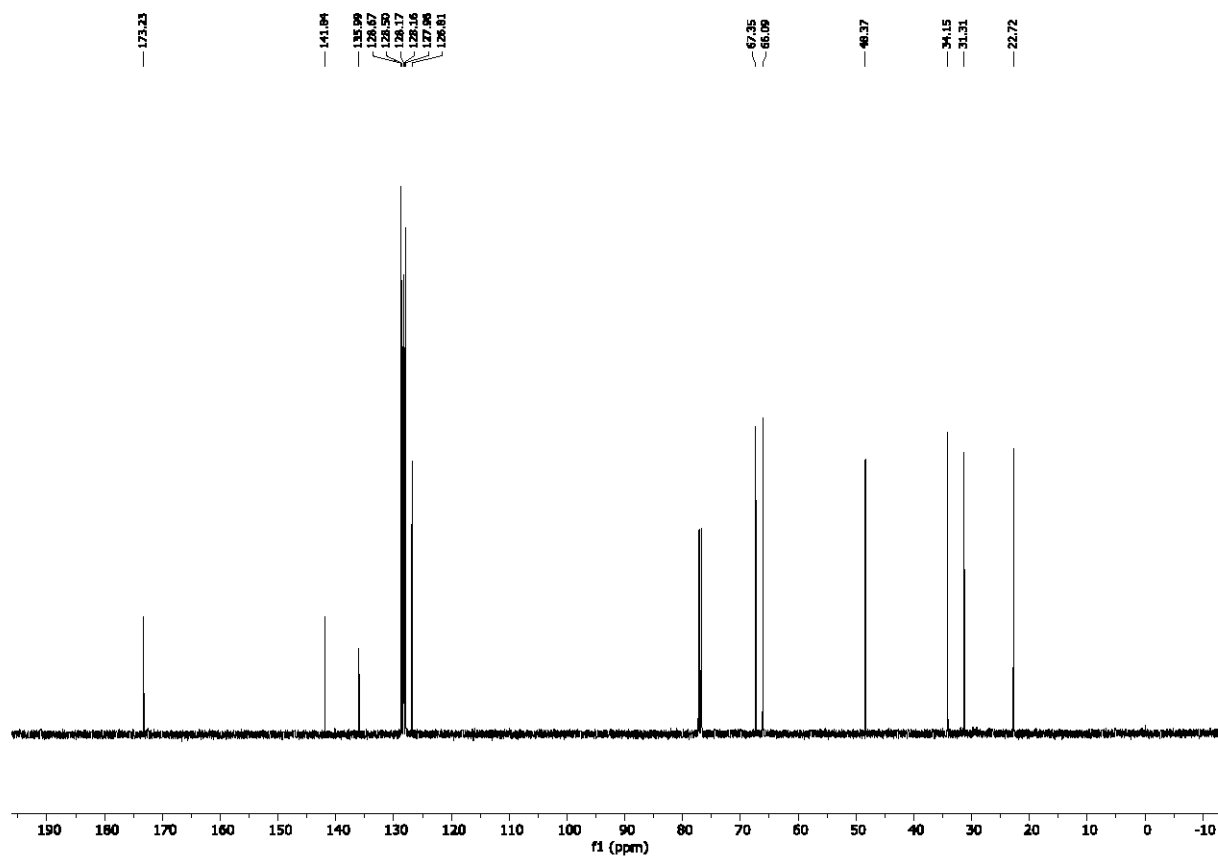
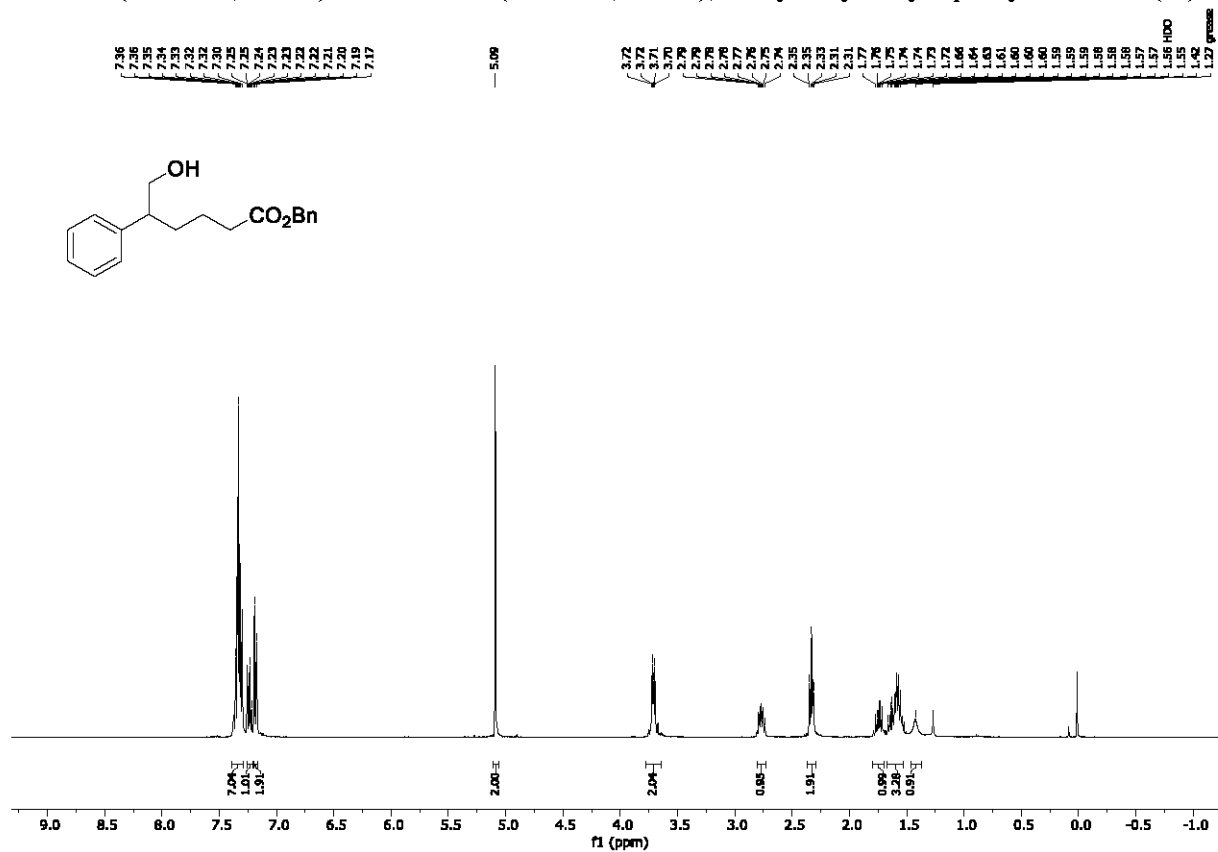
¹H NMR (500 MHz, CDCl₃) and ¹³C NMR (125 MHz, CDCl₃); 6-hydroxy-8-((triisopropylsilyloxy)octanenitrile (29)



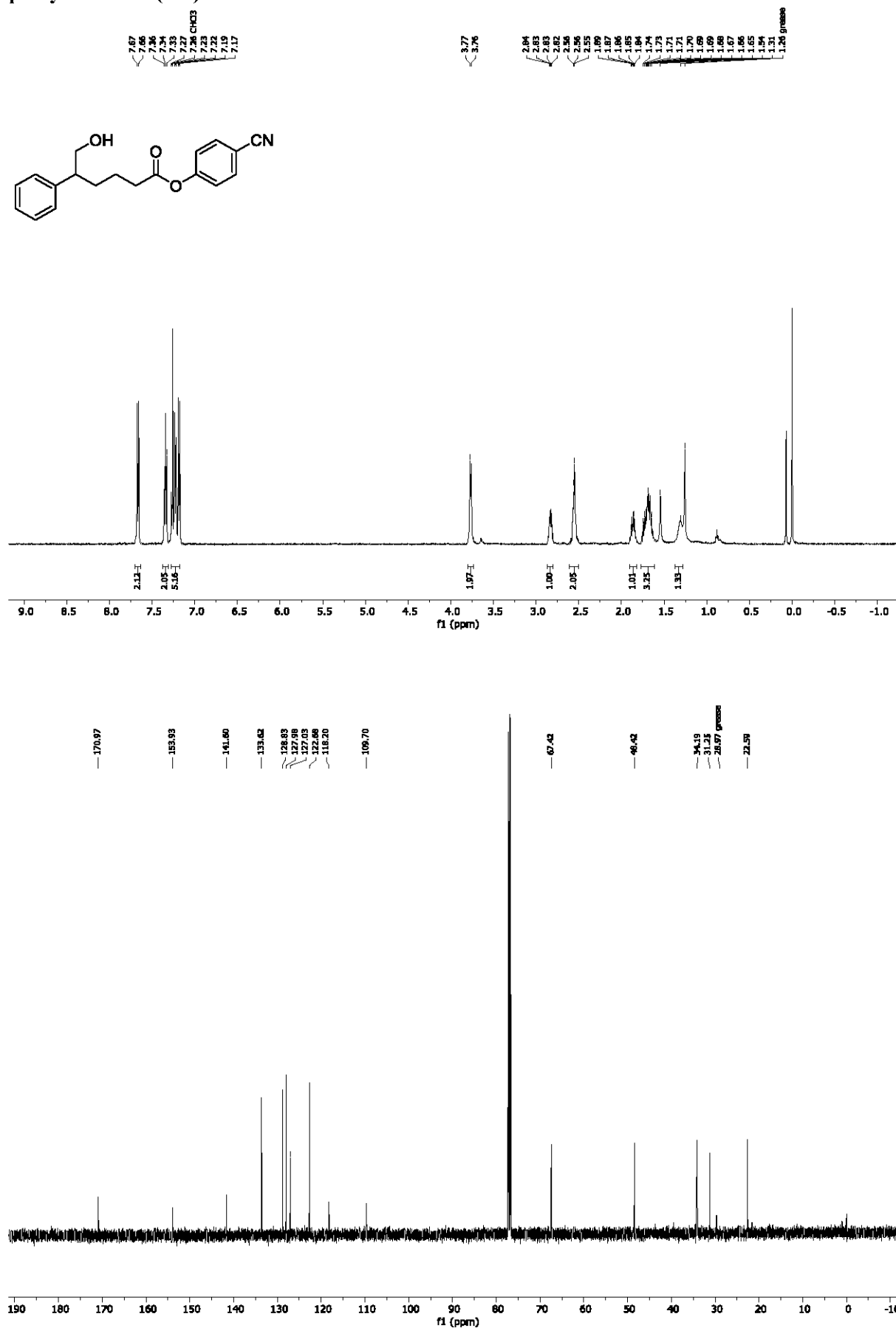
¹H NMR (400 MHz, CDCl₃) and ¹³C NMR (100 MHz, CDCl₃); methyl 6-hydroxy-5-phenylhexanoate (21)



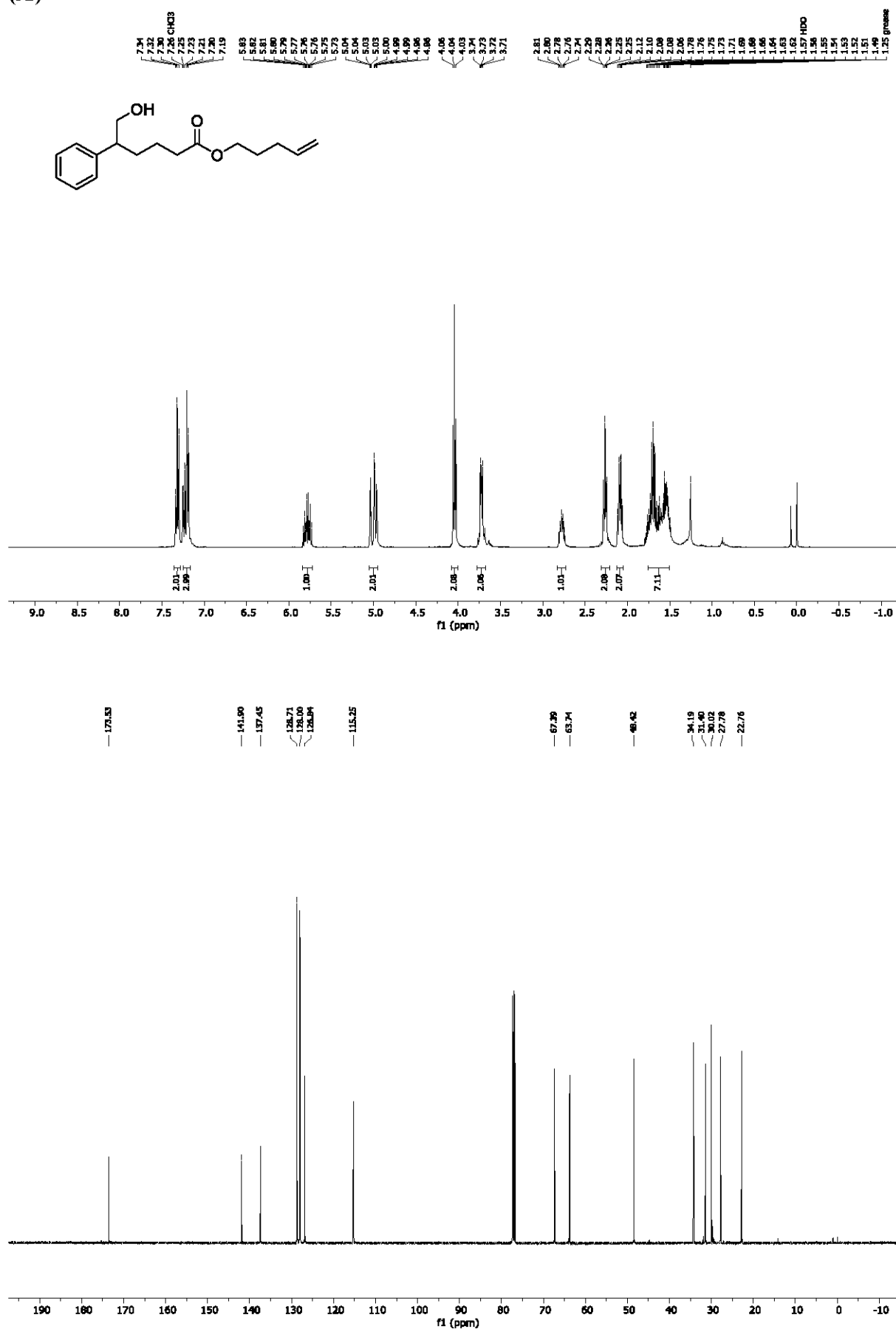
^1H NMR (400 MHz, CDCl_3) and ^{13}C NMR (125 MHz, CDCl_3); benzyl 6-hydroxy-5-phenylhexanoate (30)



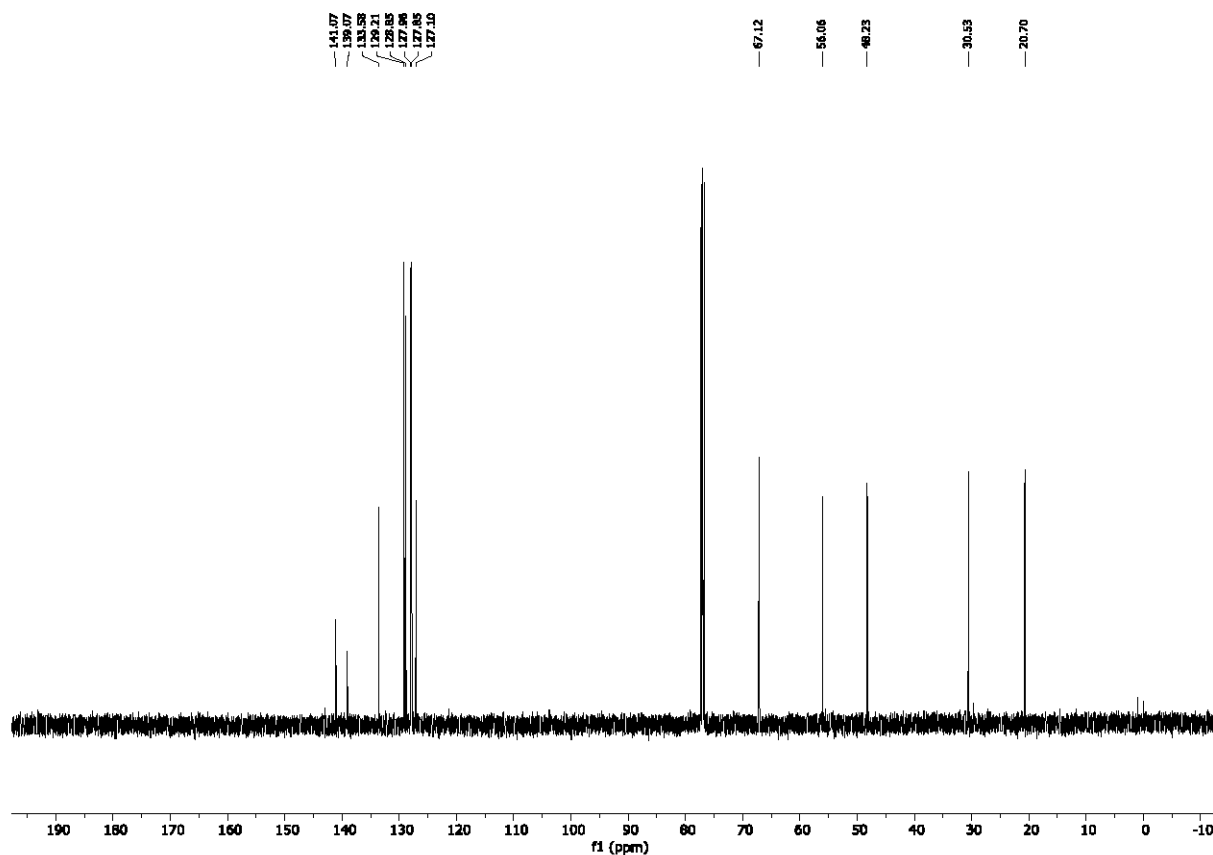
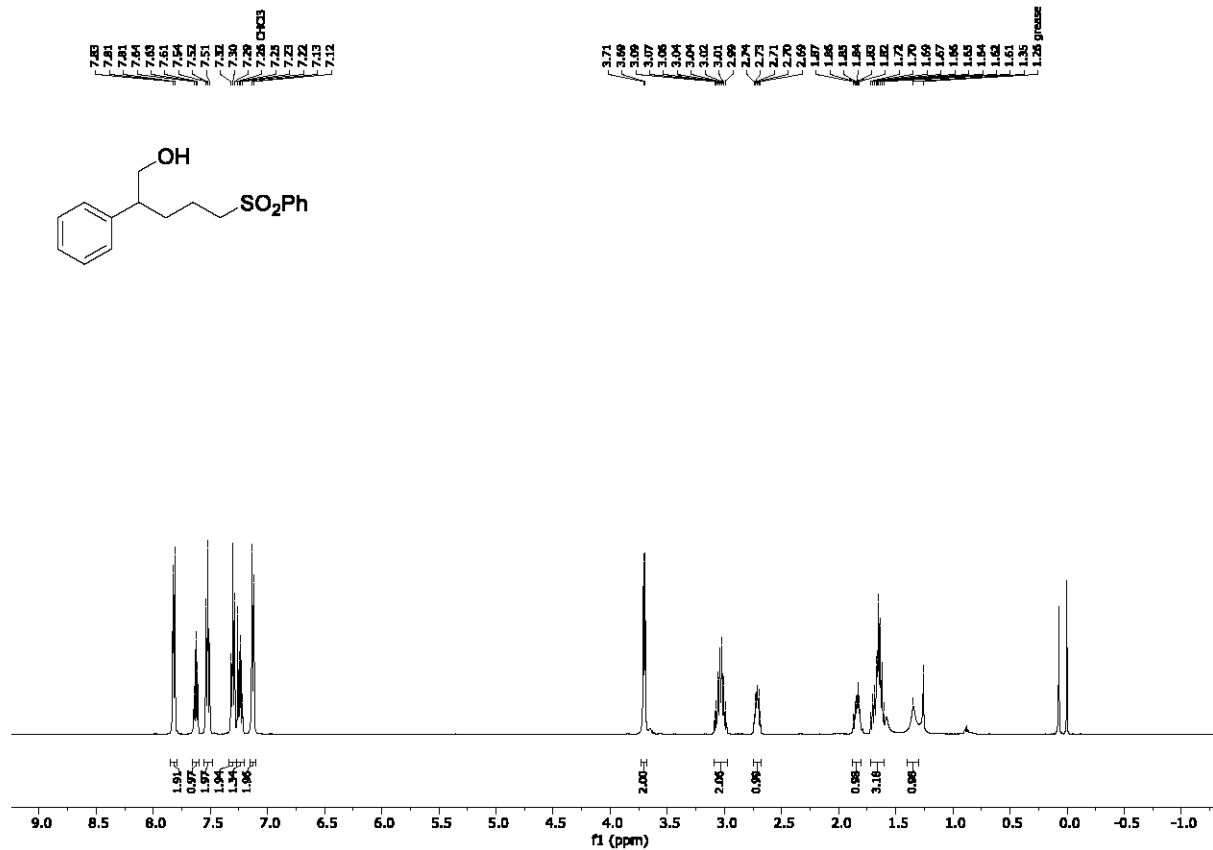
¹H NMR (500 MHz, CDCl₃) and ¹³C NMR (125 MHz, CDCl₃); 4-cyanophenyl 6-hydroxy-5-phenylhexanoate (31b)



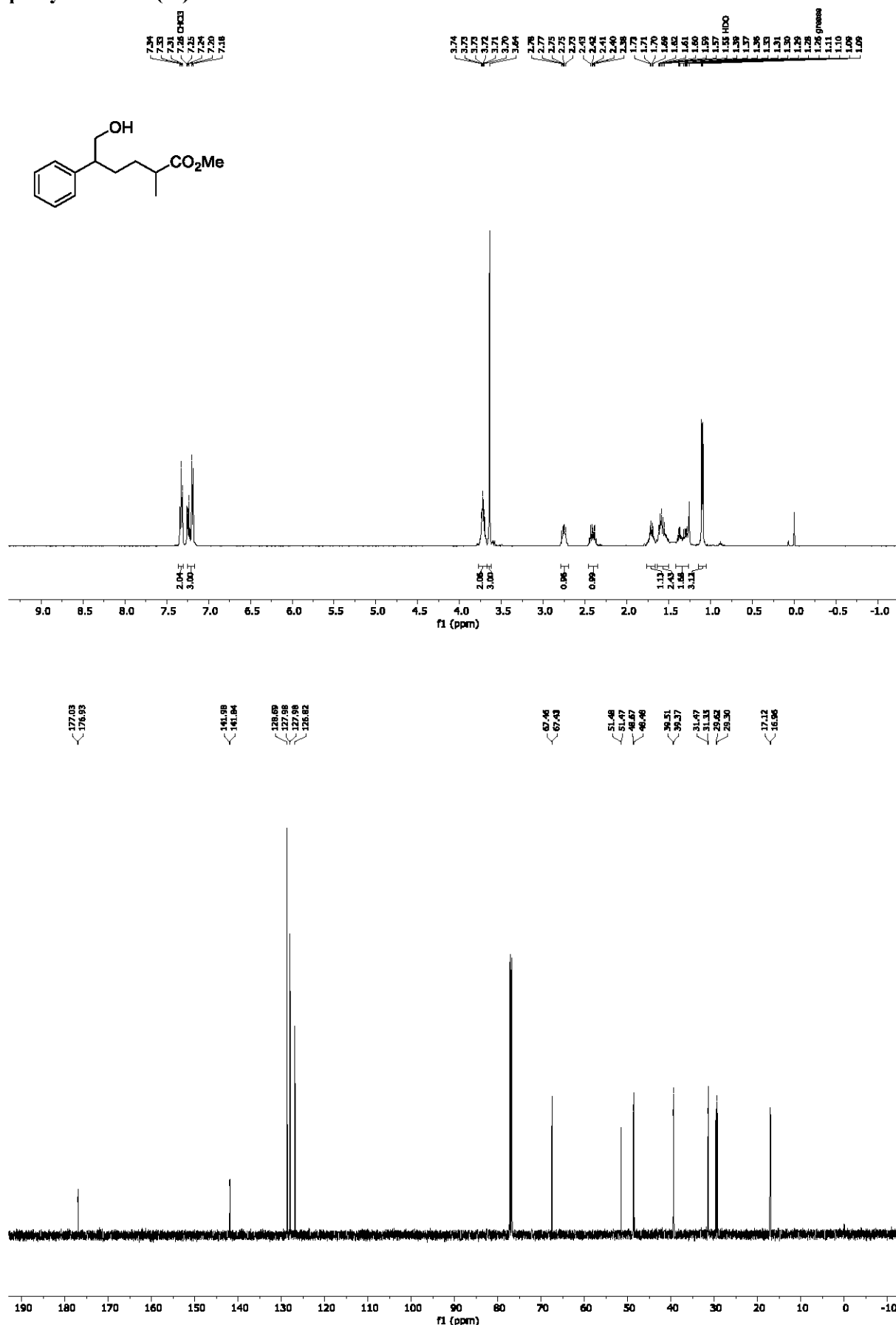
¹H NMR (400 MHz, CDCl₃) and ¹³C NMR (125 MHz, CDCl₃) pent-4-en-1-yl 6-hydroxy-5-phenylhexanoate (32)



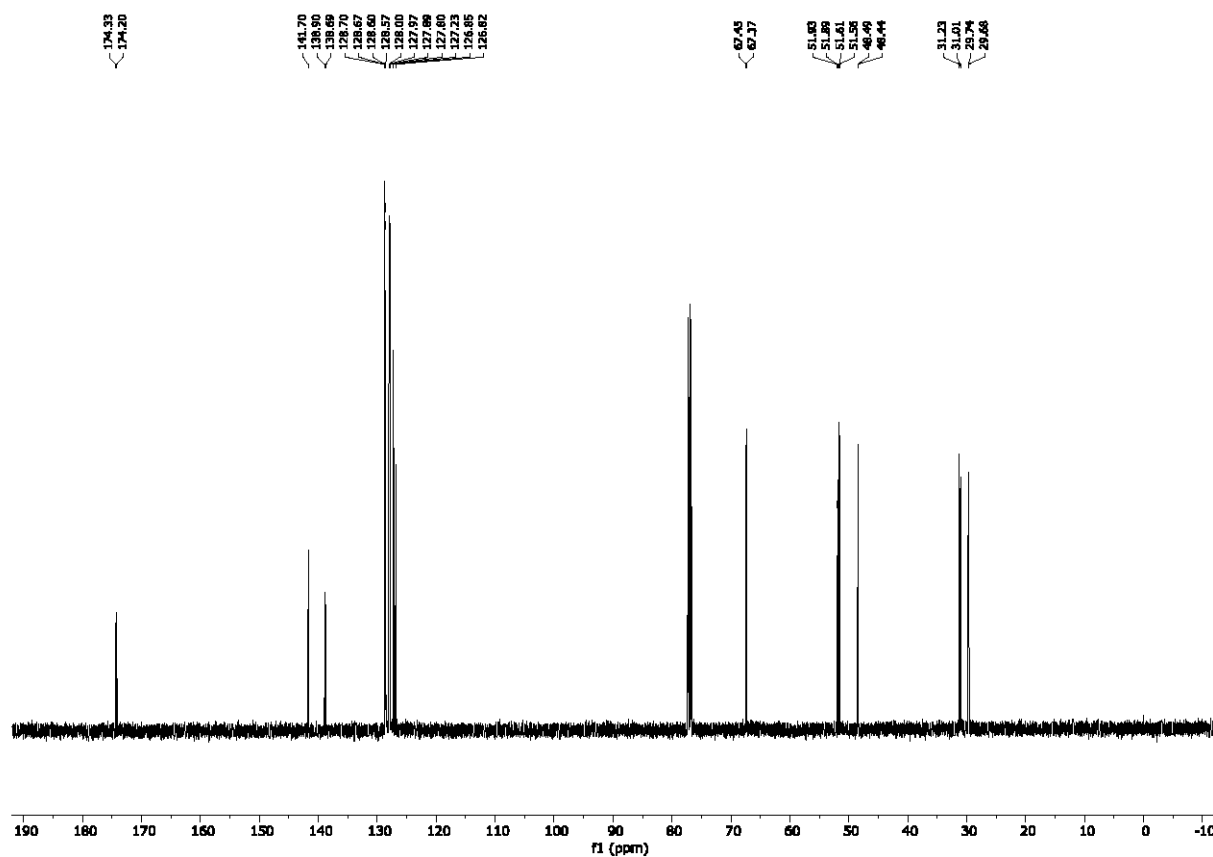
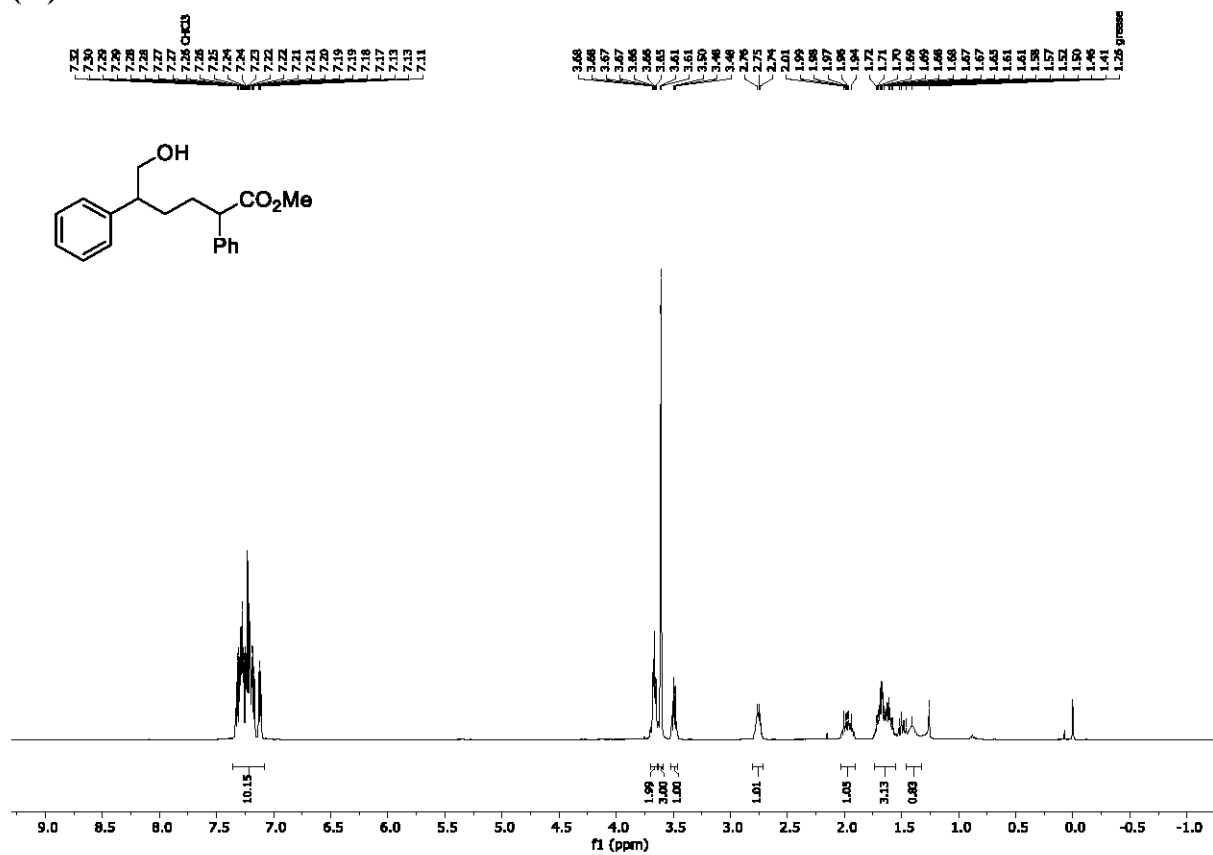
^1H NMR (500 MHz, CDCl_3) and ^{13}C NMR (125 MHz, CDCl_3); 2-phenyl-5-(phenylsulfonyl)pentan-1-ol (33)



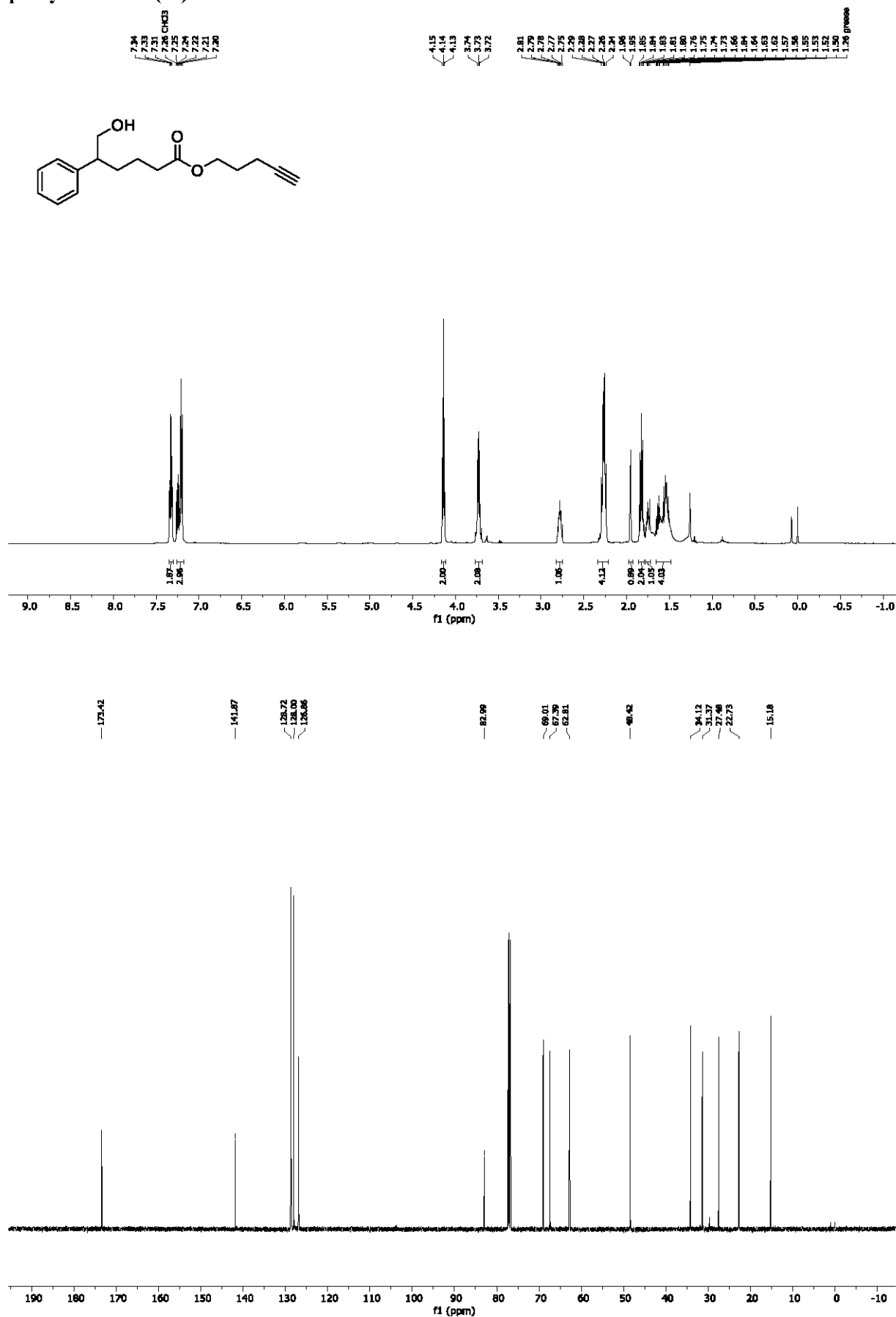
¹H NMR (500 MHz, CDCl₃) and ¹³C NMR (125 MHz, CDCl₃); methyl 6-hydroxy-2-methyl-5-phenylhexanoate (34)



¹H NMR (500 MHz, CDCl₃) and ¹³C NMR (125 MHz, CDCl₃); methyl 6-hydroxy-2,5-diphenylhexanoate (35)



^1H NMR (500 MHz, CDCl_3) and ^{13}C NMR (125 MHz, CDCl_3); pent-4-yn-1-yl 6-hydroxy-5-phenylhexanoate (36)



Co-Catalysis | *Very Important Paper* |**VIP** Vitamin B₁₂ Enables Consecutive Generation of Acyl and Alkyl Radicals from One ReagentAleksandra Potrząsaj,^[a] Michał Ociepa,^[a] Oskar Baka,^[a] Grzegorz Spólnik,^[a] and Dorota Gryko*^[a]

Abstract: Co complex – Cby(OMe)₇ - enables consecutive generation of alkyl and acyl radicals from adequately designed carboxylic acids possessing a halogen atom in their structures.

Mechanistic studies reveal that alkyl radicals form at much higher rate than the respective acyl derivatives enabling selective reactions with activated olefins.

DOSTĘP OGRANICZONY

DOSTĘP OGRANICZONY

DOSTĘP OGRANICZONY

DOSTĘP OGRANICZONY

DOSTĘP OGRANICZONY



Supporting Information

Vitamin B₁₂ Enables Consecutive Generation of Acyl and Alkyl Radicals from One Reagent

Aleksandra Potrzęsaj, Michał Ociepa, Oskar Baka, Grzegorz Spólnik,
and Dorota Gryko*

ejoc201901137-sup-0001-SupMat.pdf

Table of contents

1. General Information	3
2. General synthetic procedure	4
3. Optimization studies	4
4. Mechanistic considerations	7
4.1 Proposed mechanism	7
4.2 Experiments with deuterated reagents	8
4.3 Experiment with a radical trap	9
4.4 Mass Spectrometry	10
4.5 Kinetic studies	14
4.6 Electrochemical studies	17
5. Scope	18
6. References	27
7. Spectra data: ¹ H NMR and ¹³ C NMR	28
<i>S</i> -pyridin-2-yl 4-bromobutanethioate (4)	29
<i>S</i> -pyridin-2-yl 6-bromohexanethioate (5)	30
<i>S</i> -pyridin-2-yl 9-bromononanethioate (6)	31
<i>S</i> -pyridin-2-yl 11-bromoundecanethioate (7)	32
<i>S</i> -pyridin-2-yl 6-chlorohexanethioate (8)	33
<i>S</i> -pyridin-2-yl 5-bromodecanethioate (9)	34
<i>S</i> -pyridin-2-yl 4-(bromomethyl)benzothioate (10)	35
<i>S</i> -pyridin-2-yl 3-(chloromethyl)benzothioate (11)	36
<i>S</i> -pyridin-2-yl 2-(3-bromoadamantanyl)ethanethioate (12)	37
4-oxododecanedinitrile (14)	38
4-oxodecanedinitrile (18)	39
4-oxopentadecanedinitrile (19)	40
4-oxoheptadecanedinitrile (20)	41
4-oxo-8-pentylundecanedinitrile (21)	42
4-(3-(3-cyanopropyl)phenyl)-4-oxobutanenitrile (22)	43
4-oxo-4-(<i>p</i> -tolyl)butanenitrile (23)	44
5-(3-bromoadamantanyl)-4-oxopentanenitrile (24)	45
dimethyl 4-oxododecanedioate (25)	46
di- <i>tert</i> -butyl 4-oxododecanedioate (26)	47

1,10-bis(phenylsulfonyl)decan-3-one (27).....	48
---	----

1. General information

All solvents and chemicals used were of reagent grade and were used without further purification. Column chromatography was performed using Merck silica gel 60 (230-400 mesh). DCVC (dry column vacuum chromatography) was performed using Merck silica gel (200-300 mesh). Thin layer chromatography (TLC) was performed using Merck silica gel GF254, 0.20 mm thickness. High and low resolution ESI mass spectra were recorded on a Mariner and SYNAPT spectrometer. ^1H and ^{13}C NMR spectra were recorded at 25 °C on a Bruker 400 MHz or Varian 500 MHz instrument with TMS as an internal standard. Elemental analyses were performed on PERKIN-ELMER 240 Elemental Analyzer.

- ❖ ND_4Cl used in deuterium experiment contained 98 atom% of deuterium.
- ❖ CD_4CN used in deuterium experiment contained 99.8 atom% of deuterium.
- ❖ Photo-induced reactions were performed in a homemade photoreactor – made of 400 mL beaker covered on the inside with the LED tape and equipped with a cooling fan.

Characteristic of blue LEDs: 8 mm SMD3528 LED strip, 60 LED diodes/m; power consumption: 4.8 W/m; Blue light - $\lambda_{\text{max}} = 460 \text{ nm}$; 4.5 lm.
- ❖ Catalyst – heptamethyl cobyrinate ($(\text{CN})(\text{H}_2\text{O})\text{Cby}(\text{OMe})_7$) was prepared according to the reported procedure on 3 gram scale.^[1-3]
- ❖ Thioesters was synthesized according to the reported procedure.^{[1][4]}
- ❖ Before the reaction, zinc was activated by the following method: a) washing with 10% HCl, b) grinding, c) washing with H_2O , EtOH and Et_2O , d) drying in a vacuum.

2. General synthetic procedure



A glass tube (inner diameter = 18 mm) equipped with a magnetic stirrer was charged with heptamethyl cobyrate (14 mg, 5.0 mol%), activated Zn (48 mg, 0.75 mmol, 3 equiv.) and NH_4Cl (60.0 mg, 1.1 mmol, 4.5 equiv.) and sealed with a septum. Then MeCN (2.5 mL) was added and the reaction mixture was degassed by purging the solution with argon with simultaneous sonication in an ultrasonic bath (solution turned from red to dark green) for 15 min. Subsequently, an olefin (0.55 mmol, 1.0 equiv.) followed by a thioester (0.25 mmol, 0.45 equiv.) were added via syringe and the reaction mixture was irradiated with blue LED light ($\lambda = 460 \text{ nm}$) for 16 h at room temperature. It was then diluted with Et_2O , filtered through the cotton wool and concentrated *in vacuo*. A crude product was purified using column chromatography.

3. Optimization studies



3.1 Background reactions

Entry	Conditions	Yield [%]
1	no light	22
2	no catalyst	<5
3	no Zn	0
4	no NH_4Cl	15
5	no Zn and NH_4Cl	0

3.2 Catalyst loading

Entry	Catalyst[mol%]	Yield [%]
1	2.5	41
2	5.0	46
3	7.5	36

Reaction conditions: olefin (0.55 mmol, 1.0 equiv.), thioester (0.45 equiv.), catalyst: (CN)(H₂O)Cby(OMe)₇, Zn (3.0 equiv.), NH₄Cl (4.5 equiv.), MeCN (2.5 mL), 16 h, blue LEDs

3.3 Optimization of the substrates ratio

Entry	Thioester : Olefin (14:11)	Yield [%]
1	1.0 : 2.2	46
2	1.0 : 3.0	44
3	1.0 : 4.0	50
4	2.0 : 1.0	<10
5	3.0 : 1.0	<10

Reaction conditions: (CN)(H₂O)Cby(OMe)₇ (5 mol%), Zn (3.0 equiv.), NH₄Cl (1.5 equiv.), MeCN (2.5 mL), 16 h, blue LEDs

3.4 The influence of Zn and NH₄Cl amount

Entry	Zn [equiv.]	NH ₄ Cl [equiv.]	Yield [%]
1	3	1.5	46
2	6	1.5	29
3	1.5	1.5	traces
4	3	1	traces
5	3	3.4	51
6	3	4.5	64
7	3	6	55
8	4.5	4.5	58
9	4	6	55

Reaction conditions: Thioester (0.45 equiv.), olefin (0.55 mmol, 1.0 equiv.), catalyst (5 mol%), MeCN (2.5 mL), 16 h, blue LEDs

3.5 The influence of additives

Entry	Additive	Additive [equiv.]	Yield [%]
1	none	-	64
2	LiCl	3	traces
3	LiBF ₄	3	51
5	HFIP	5	35
6	DIPEA	2	25
7	Cs ₂ CO ₃	2	0
8	H ₂ O	5	52
9	Thiopyridine	1	43

Reaction conditions: Thioester (0.45 equiv.), olefin (0.55 mmol, 1.0 equiv.), Zn (3.0 equiv.), NH₄Cl (4.5 equiv.), catalyst (5 mol%), MeCN (2.5 mL), 16 h, blue LEDs

3.6 Optimization of a solvent

Entry	Solvent	Yield [%]
1	MeCN	64
2	THF	41
3	Aceton	45
4	AcOEt	43
5	MeCN (dry)	36
6	<i>i</i> -PrOH	0
7	DMF	0

Reaction conditions: Thioester (0.45 equiv.), olefin (0.55 mmol, 1.0 equiv.), Zn (3.0 equiv.), NH₄Cl (4.5 equiv.), catalyst (5 mol%), solvent (2.5 mL), 16 h, blue LEDs

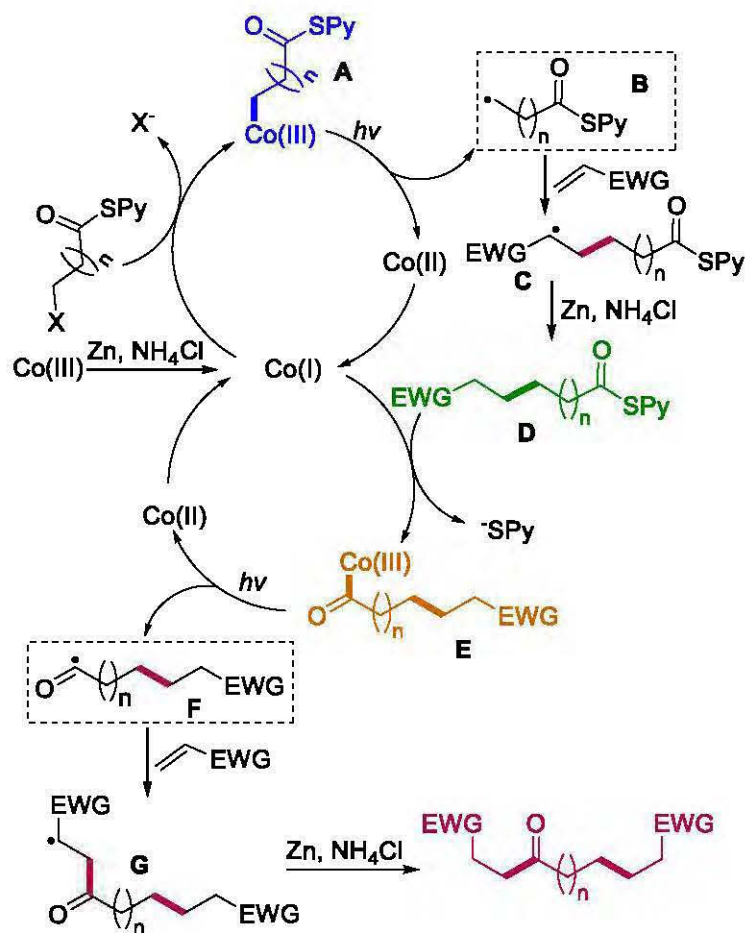
3.7 The influence of a light source

Entry	Light	Yield [%]
1	Blue LED	64
2	Green LED	34
3	White LED	61
4	Violet LED	65
5	Black LED	0

Reaction conditions: Thioester (0.45 equiv.), olefin (0.55 mmol, 1.0 equiv.), Zn (3.0 equiv.), NH₄Cl (4.5 equiv.), catalyst (5 mol%), MeCN (2.5 mL), 16 h

4. Mechanistic considerations

4.1 Proposed mechanism

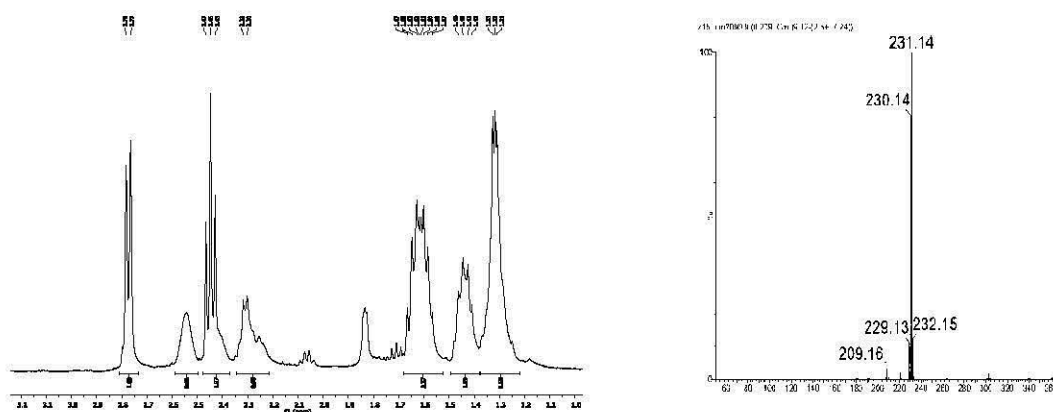


4.2 Experiments with deuterated reagents



Reaction conditions: Thioester (0.45 equiv.), olefin (0.55 mmol, 1 equiv.), Zn (3 equiv.), ND_4Cl (4.5 equiv.), catalyst (5 mol%), CD_3CN (2.5 mL), 16 h, blue LEDs

To prove the hypothesis of external proton incorporation at the α -position to the nitril group, the experiment with the deuterated ND_4Cl and CD_3CN was performed. The reaction was carried out according to the general procedure described in *Section 2*.



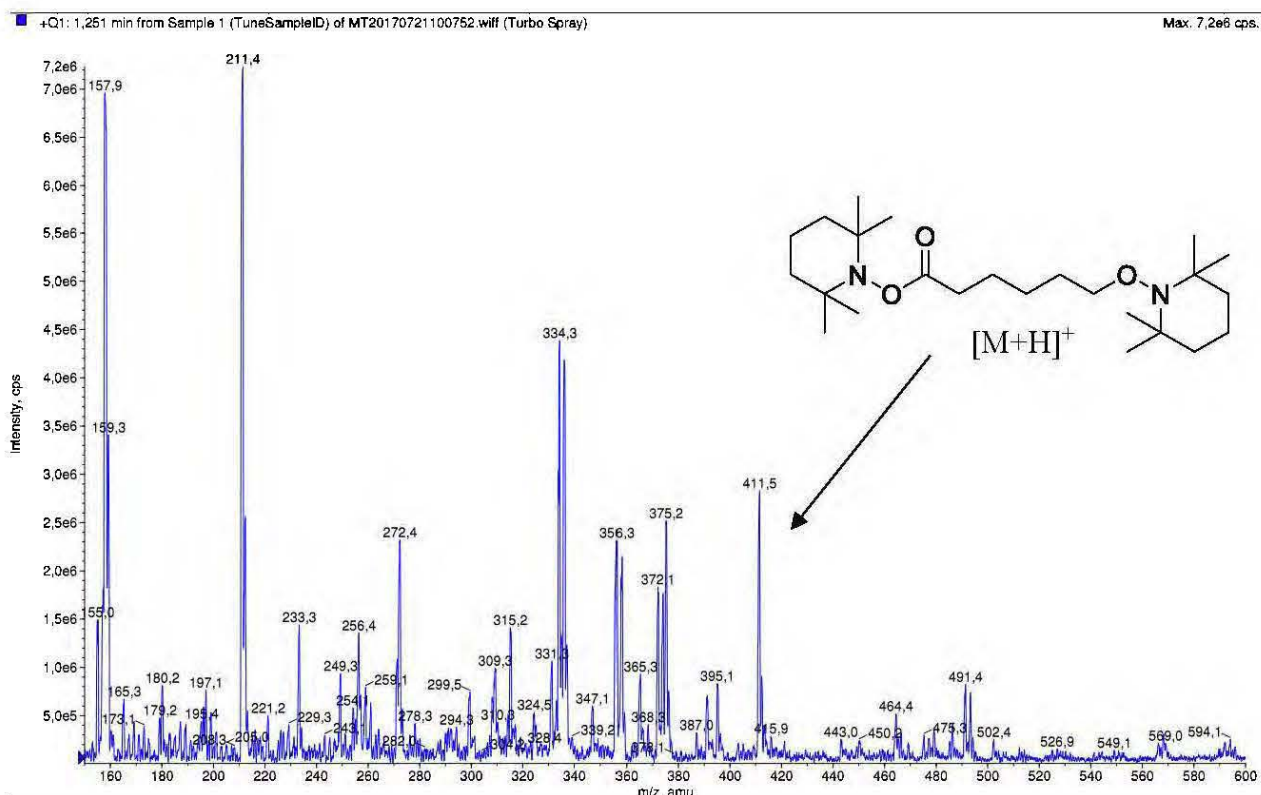
Scheme 1. Left) ^1H NMR fragment of a mixture of the products of deuterium incorporation experiment. Right) ESI MS spectrum of the reaction in deuterated conditions.

To confirm that NH_4Cl is a source of deuterium an additional experiments were performed:

- ❖ reaction with NH_4Cl and CD_3CN : there is no trace of a deuterated product **14b**, **14c**, **14d**.
- ❖ reaction with ND_4Cl and MeCN : deuterated product **14b**, **14c**, **14d** are observed

4.3 Radical trap experiment

The reaction was set up following the general procedure (see section 2). After 5 minutes 3.0 equiv. TEMPO was added. The product was confirmed by ESI MS.

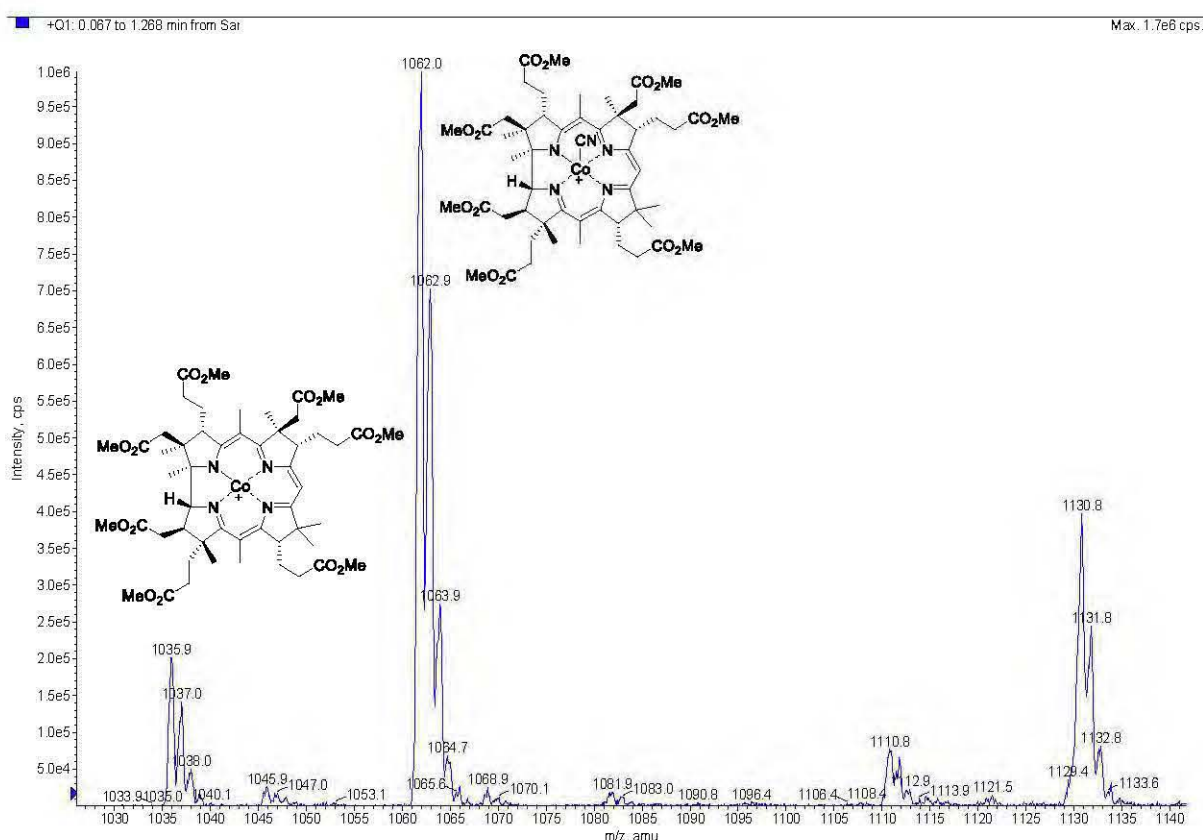


4.4 Mass Spectrometry studies



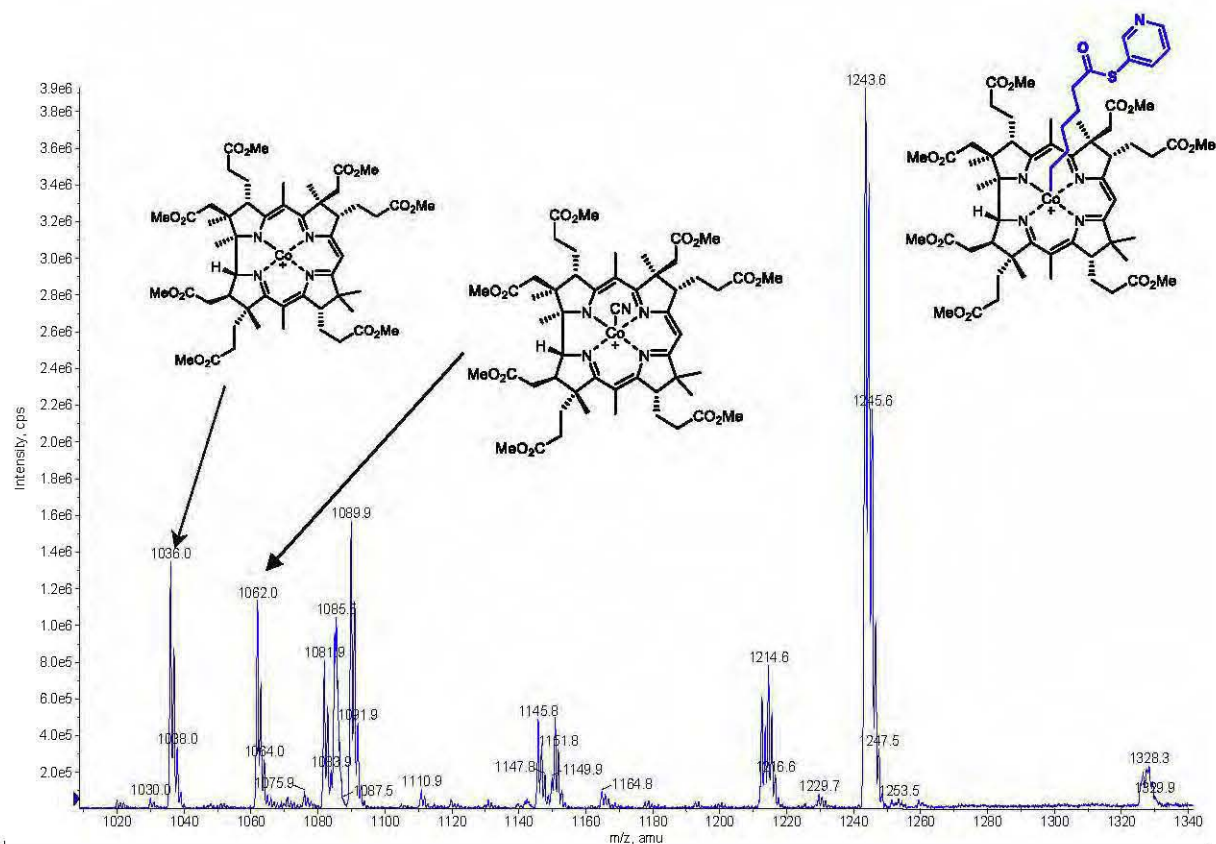
Reaction conditions: Thioester (0.45 equiv.), olefin (0.55 mmol, 1.0 equiv.), Zn (3.0 equiv.), NH_4Cl (4.5 equiv.), catalyst (5 mol%), MeCN (2.5 mL), 16 h, blue LEDs

4.4.1 Heptamethyl cobyrinate in MeCN



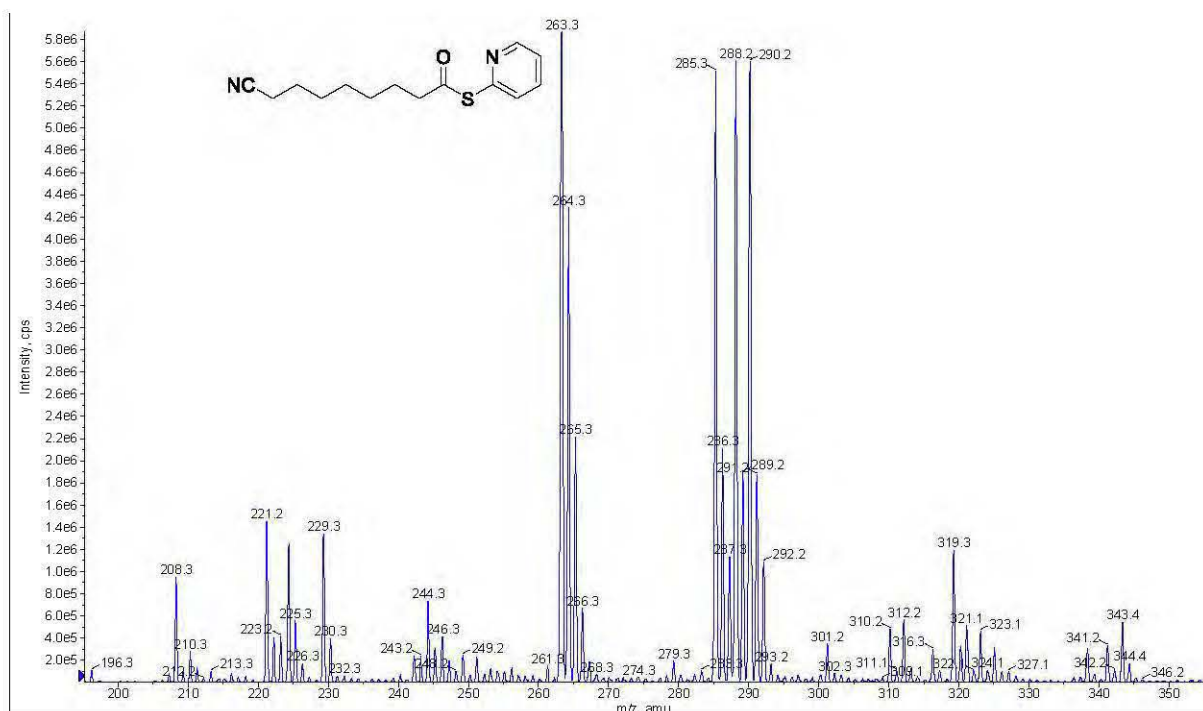
The LRMS spectrum of the catalyst $((\text{CN})(\text{H}_2\text{O})\text{Cby}(\text{OMe})_7)$ before the addition of the starting materials shows two peak that can be assigned as $[\text{M}-\text{CN}]^+$, $[\text{M}-\text{CN}, \text{H}_2\text{O}]$. The first group of signals corresponds to the mass of a catalyst lacking one axial ligand H_2O (peaks at m/z 1062.0). The second group of signals (peaks at m/z 1035.9) corresponds to a catalyst lacking both axial ligands: H_2O and CN^- .

4.4.2 The reaction before light irradiation



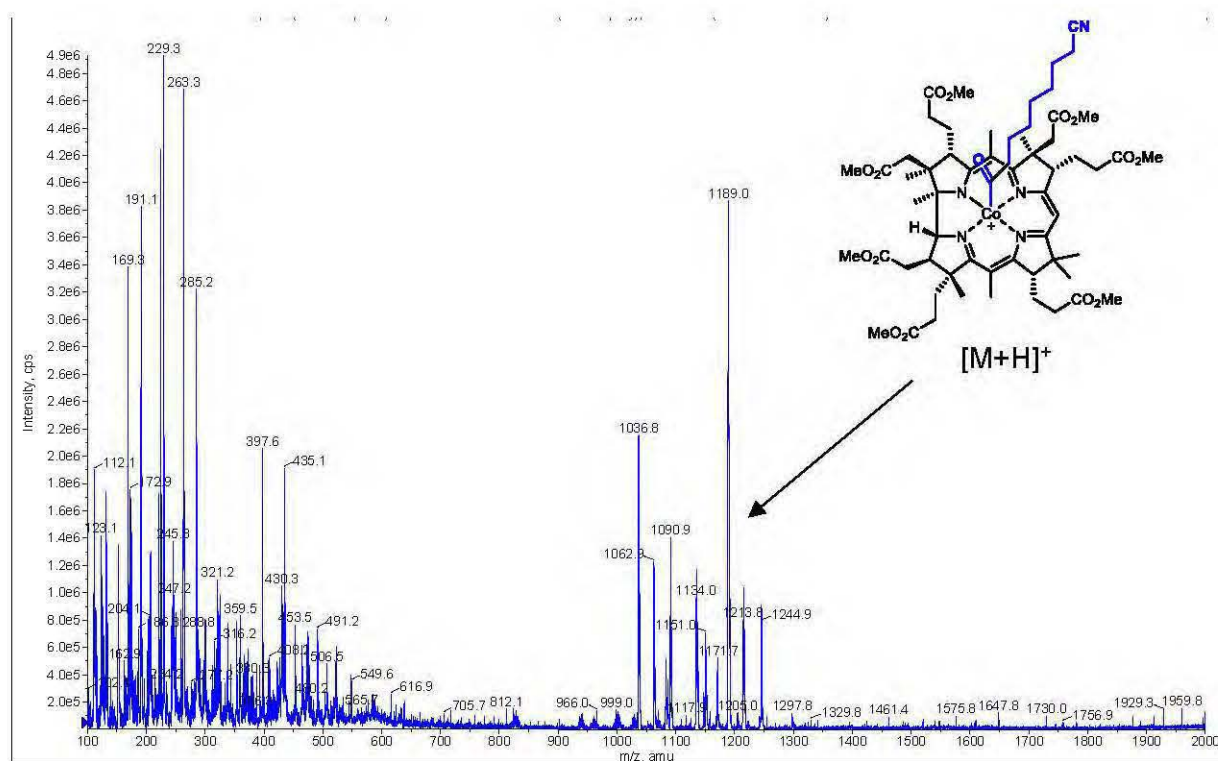
The LRMS spectrum of the reaction mixture recorded before light irradiation indicates the presence of an alkyl-cobalt complex A (peaks at m/z 1243.6). This result suggests that upon light irradiation an alkyl radical is generated prior to the formation of cobalt-acyl complex E.

4.4.3 The LRMS spectrum recorded after 15 minutes of light irradiation



After 15 minutes of light irradiation, adduct C is formed (peaks at m/z 263.3) confirming that alkyl radical generates prior acyl radical.

4.4.4 The LRMS spectrum recorded after 20 minutes of light irradiation



After 20 minutes of light irradiation, adduct **E** is formed (peaks at m/z 1189.0 [M+H]⁺).

4.5 Kinetic studies

The MS analyses were performed using LC-20 HPLC pump (Shimadzu, Japan) used as solvent delivery system and Rheodyne 7725i injection valve with 20 μ l sample loop. They were coupled with tandem mass spectrometer 4000 Q TRAP (AB SCIEX, USA) equipped with an electrospray ion source. At specified intervals accurately measured 100 μ l of the reaction mixture were transferred into vial filled with 5 ml of acetonitrile (ACN) using syringe, mixed and diluted 250 times. Immediately the sample loop was filled with the solution and sample was injected into the stream of MeCN pumped with the flow rate of 100 μ l/min.

The mass spectrometer operated in positive ion mode with the capillary voltage set to 5.5 kV. Declustering potential was set to 60 V. Desolvation temperature was 200 °C. Selected Ion Monitoring (SIM) scan type was used with the experiments programmed for measuring of signals intensities obtained for following ions: m/z 1062.5, m/z 1080.5, m/z 1036.5, m/z 1244.5 (compound **A**), m/z 1188.5 (compound **E**), m/z 263.0 (protonated ion of compound **C**), m/z 288.0 (protonated ion of compound **5**), m/z 229.0 (ion of compound **14**+Na). For the peaks that appeared on the counts per second (cps) vs. time graph the peak areas were quantified for individual ions (compounds). The peak area vs. time graphs (Figures 1 – 5) represent the changes of the concentration of the compounds in the reaction mixture. However, due to the inability of using standards the absolute concentration values could not be determined.

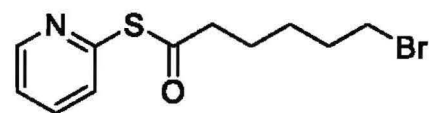
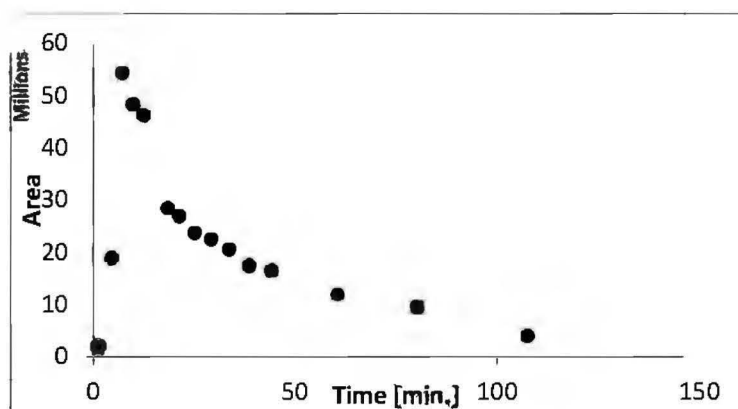


Figure 1.

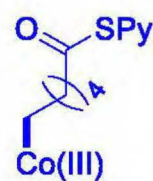
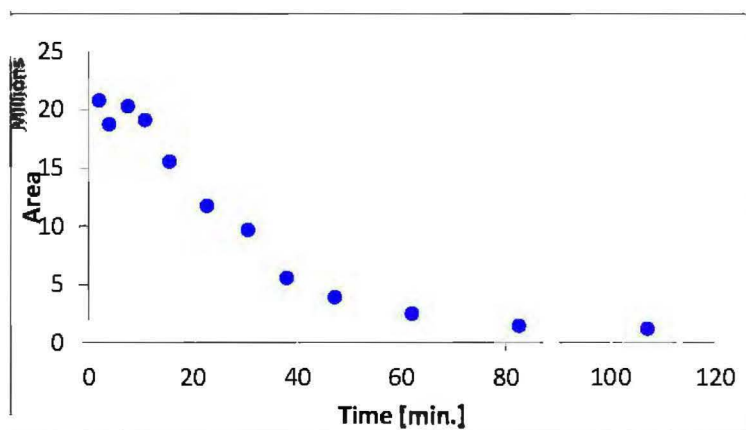


Figure 2.

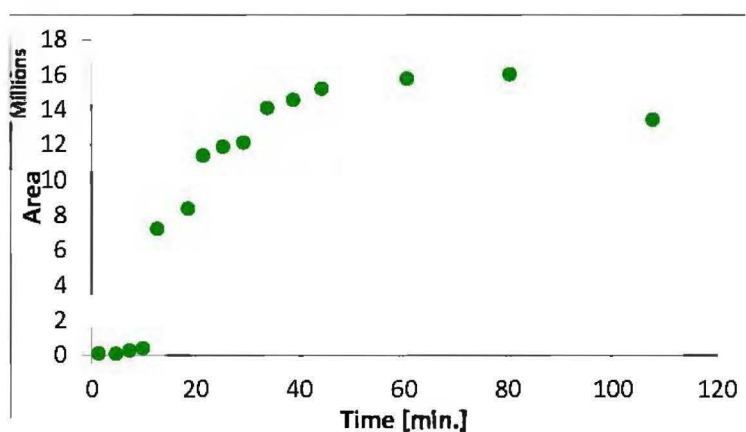


Figure 3.

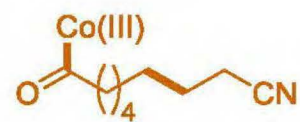
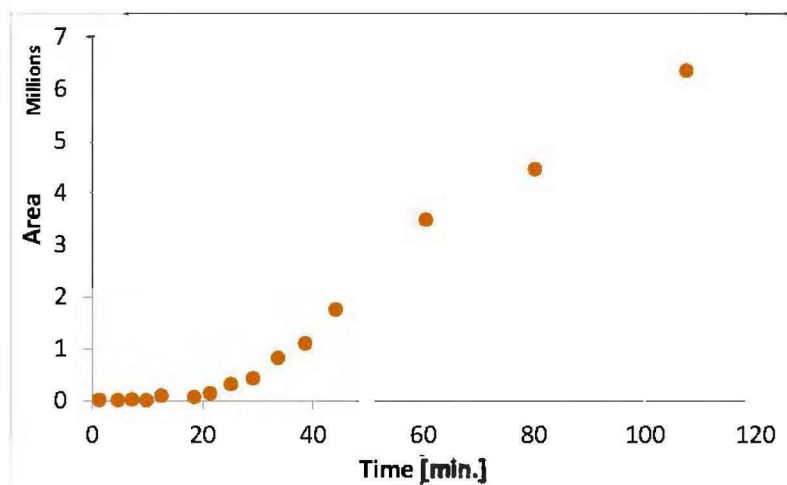


Figure 4.

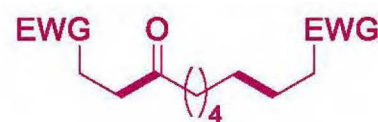
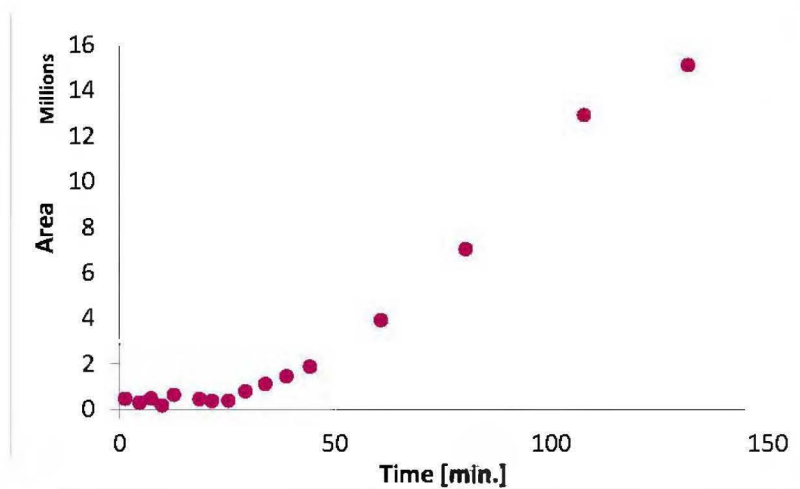


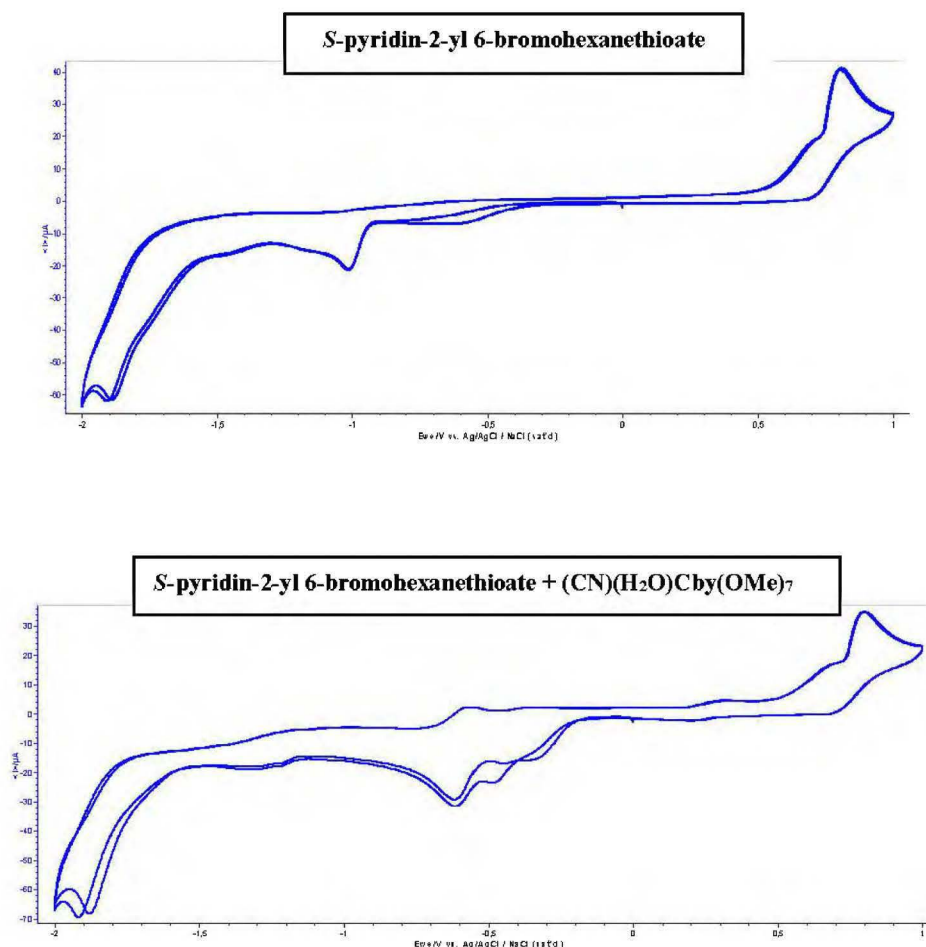
Figure 5.

4.6. Electrochemical studies

4.6.1 Measurements conditions

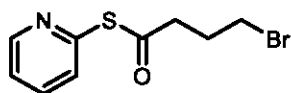
A cylindrical three-electrode cell was equipped with a glassy carbon working electrode, a 25 mm platinum wire as the counter electrode and an Ag/AgCl (3.0 M NaCl) electrode as the reference electrode. The scan rate for a typical experiment was $100 \text{ mV}\cdot\text{s}^{-1}$. The solution of thioester ($3.0\cdot 10^{-3} \text{ M}$) and $n\text{-Bu}_4\text{NClO}_4$ (0.1 M) in dry MeCN was deaerated by Ar gas bubbling before the measurement, and the cyclic voltammetry was carried out under an Ar gas atmosphere at room temperature. The $E_{1/2}$ value of the ferrocene–ferrocenium (Fc/Fc^+) in MeCN was +0.45 V vs. Ag/AgCl with this setup.

4.6.2 Cyclic Voltammograms



5. Scope and characterization of new compounds

S-pyridin-2-yl 4-bromobutanethioate (4)



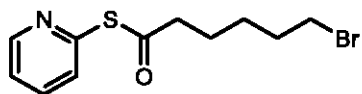
^1H NMR (400 MHz, CDCl_3 , 25 °C): δ 8.65 – 8.60 (m, 1H, Ar-H), 7.75 (td, $^3J_{\text{H-H}} = 7.7, 2.0$ Hz, 1H, Ar-H), 7.61 (dt, $^3J_{\text{H-H}} = 7.8, 1.0$ Hz, 1H, Ar-H), 7.30 (ddd, $^3J_{\text{H-H}} = 7.5, 4.9, 1.1$ Hz, 1H, Ar-H), 3.47 (t, $^3J_{\text{H-H}} = 6.4$ Hz, 2H, CH_2), 2.91 (t, $^3J_{\text{H-H}} = 7.1$ Hz, 2H, CH_2), 2.26 (p, $^3J_{\text{H-H}} = 6.7$ Hz, 2H, CH_2) ppm.

^{13}C NMR (100 MHz, CDCl_3 , 25 °C): δ 195.4, 151.1, 150.5, 137.2, 130.2, 123.6, 42.2, 32.1, 27.9 ppm.

HRMS (ESI): m/z calcd for $[\text{C}_9\text{H}_{10}\text{BrNOS}+\text{Na}]^+$: 281.9564 $[M+\text{Na}]^+$; found: 281.9550.

Hygroscopic compound.

S-pyridin-2-yl 6-bromohexanethioate (5)



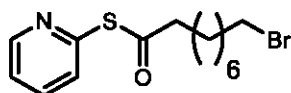
^1H NMR (400 MHz, CDCl_3 , 25 °C): δ 8.61 (ddd, $^3J_{\text{H-H}} = 4.8, 1.9, 0.8$ Hz, 1H, Ar-H), 7.72 (td, $^3J_{\text{H-H}} = 7.7, 1.9$ Hz, 1H, Ar-H), 7.60 (dt, $^3J_{\text{H-H}} = 7.9, 1.0$ Hz, 1H, Ar-H), 7.29 – 7.26 (m, 1H, Ar-H), 3.39 (t, $^3J_{\text{H-H}} = 6.7$ Hz, 2H, CH_2), 2.71 (t, $^3J_{\text{H-H}} = 7.4$ Hz, 2H, CH_2), 1.92 – 1.83 (m, 2H, CH_2), 1.79 – 1.71 (m, 2H, CH_2), 1.56 – 1.48 (m, 2H, CH_2) ppm.

^{13}C NMR (100 MHz, CDCl_3 , 25 °C): δ 196.2, 151.5, 150.4, 137.1, 130.1, 123.5, 43.9, 33.2, 32.3, 27.4, 24.5 ppm.

HRMS (ESI): m/z calcd for $[\text{C}_{11}\text{H}_{14}\text{BrNOS}+\text{Na}]^+$: 309.9877 $[M+\text{Na}]^+$; found 309.9865.

Elemental analysis calcd. (%) for $\text{C}_{11}\text{H}_{14}\text{BrNOS}$: C, 45.84, H, 4.90, N, 4.86; found: C, 46.07, H, 5.08, N, 4.90.

S-pyridin-2-yl 9-bromononanethioate (6)



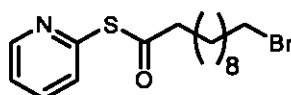
^1H NMR (400 MHz, CDCl_3 , 25 °C): δ 8.61 (ddd, $^3J_{\text{H-H}} = 4.9, 2.0, 0.9$ Hz, 1H, Ar-H), 7.73 (td, $^3J_{\text{H-H}} = 7.7, 2.0$ Hz, 1H, Ar-H), 7.61 (dt, $^3J_{\text{H-H}} = 8.0, 1.1$ Hz, 1H, Ar-H), 7.30 – 7.27 (m, 1H, Ar-H), 3.39 (t, $^3J_{\text{H-H}} = 6.8$ Hz, 2H, CH_2), 2.69 (t, $^3J_{\text{H-H}} = 7.4$ Hz, 2H, CH_2), 1.84 (p, $^3J_{\text{H-H}} = 7.0$ Hz, 2H, CH_2), 1.72 (p, $^3J_{\text{H-H}} = 7.5$ Hz, 2H, CH_2), 1.44 – 1.30 (m, 8H, CH_2) ppm.

^{13}C NMR (100 MHz, CDCl_3 , 25 °C): δ 196.5, 151.7, 150.4, 137.1, 130.1, 123.4, 44.2, 33.9, 32.7, 29.0, 28.8, 28.5, 28.1, 25.3 ppm.

HRMS (ESI): m/z calcd for $[\text{C}_{14}\text{H}_{20}\text{BrNOS}+\text{Na}]^+$: 352.0347 $[M+\text{Na}]^+$; found 352.0337.

Elemental analysis calcd. (%) for $\text{C}_{14}\text{H}_{20}\text{BrNOS}$: C, 50.91, H, 6.10, N, 4.24; found: C, 50.91, H, 6.26, N, 4.21.

S-pyridin-2-yl 11-bromoundecanethioate (7)



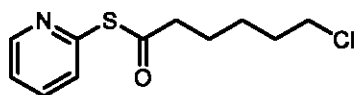
^1H NMR (400 MHz, CDCl_3 , 25 °C): δ 8.61 (dd, $^3J_{\text{H-H}} = 5.3, 1.3$ Hz, 1H, Ar-H), 7.73 (td, $^3J_{\text{H-H}} = 7.7, 1.9$ Hz, 1H, Ar-H), 7.62 – 7.60 (m, 1H, Ar-H), 7.30 – 7.26 (m, 1H, Ar-H), 3.39 (t, $^3J_{\text{H-H}} = 6.9$ Hz, 2H, CH_2), 2.69 (t, $^3J_{\text{H-H}} = 7.5$ Hz, 2H, CH_2), 1.84 (p, $^3J_{\text{H-H}} = 6.9$ Hz, 2H, CH_2), 1.72 (p, $^3J_{\text{H-H}} = 7.5$ Hz, 2H, CH_2), 1.29 (m-s, 12H) ppm.

^{13}C NMR (100 MHz, CDCl_3 , 25 °C): δ 196.5, 151.7, 150.3, 137.0, 130.1, 123.4, 44.2, 34.0, 32.8, 29.3, 29.2, 29.1, 28.9, 28.7, 28.1, 25.4 ppm.

HRMS (ESI): m/z calcd for $[\text{C}_{16}\text{H}_{24}\text{BrNOS}+\text{Na}]^+$: 380.0660 $[M+\text{Na}]^+$; found 380.0647.

Elemental analysis calcd. (%) for $\text{C}_{16}\text{H}_{24}\text{BrNOS}$: C, 53.63, H, 6.75, N, 3.91; found: C, 53.89, H, 6.85, N, 3.85.

S-pyridin-2-yl 6-chlorohexanethioate (8)



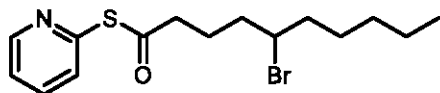
^1H NMR (400 MHz, CDCl_3 , 25 °C): δ 8.61 (ddd, $^3J_{\text{H-H}} = 4.8, 1.9, 0.9$ Hz, 1H, Ar-H), 7.73 (td, $^3J_{\text{H-H}} = 7.7, 1.9$ Hz, 1H, Ar-H), 7.60 (dt, $^3J_{\text{H-H}} = 7.9, 1.0$ Hz, 1H, Ar-H), 7.28 (ddd, $^3J_{\text{H-H}} = 7.5, 4.8, 1.2$ Hz, 1H, Ar-H), 3.53 (t, $^3J_{\text{H-H}} = 6.6$ Hz, 2H, CH_2), 2.72 (t, $^3J_{\text{H-H}} = 7.4$ Hz, 2H, CH_2), 1.84 – 1.70 (m, 4H), 1.58 – 1.48 (m, 2H, CH_2) ppm.

^{13}C NMR (100 MHz, CDCl_3 , 25 °C): δ 196.2, 151.5, 150.4, 137.1, 130.1, 123.5, 44.6, 43.9, 32.2, 26.2, 24.6 ppm.

HRMS (ESI): m/z calcd for $[\text{C}_{11}\text{H}_{14}\text{ClNOS}+\text{Na}]^+$: 266.0382 $[\text{M}+\text{Na}]^+$; found 266.0378.

Elemental analysis calcd. (%) for $\text{C}_{11}\text{H}_{14}\text{ClNOS}$: C, 54.20, H, 5.79, N, 5.75; found: C, 53.95, H, 5.89, N, 5.91.

S-pyridin-2-yl 5-bromodecanethioate (9)

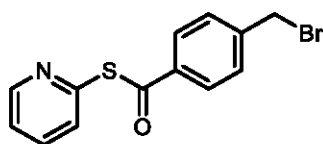


^1H NMR (400 MHz, CDCl_3 , 25 °C): δ 8.62 (ddd, $^3J_{\text{H-H}} = 4.8, 2.0, 0.9$ Hz, 1H, Ar-H), 7.74 (td, $^3J_{\text{H-H}} = 7.7, 1.9$ Hz, 1H, Ar-H), 7.61 (dt, $^3J_{\text{H-H}} = 7.9, 1.1$ Hz, 1H, Ar-H), 7.28 (ddd, $^3J_{\text{H-H}} = 7.6, 4.8, 1.2$ Hz, 1H, Ar-H), 4.04 – 3.96 (m, 1H), 2.78 – 2.68 (m, 2H), 2.06 – 1.96 (m, 1H), 1.92 – 1.75 (m, 5H), 1.52 – 1.55 (m, 1H), 1.44-1.40 (m, 1H), 1.34 – 1.25 (m, 4H), 0.89 (t, $^3J_{\text{H-H}} = 6.9$ Hz, 3H) ppm.

^{13}C NMR (100 MHz, CDCl_3 , 25 °C): δ 196.1, 151.5, 150.4, 137.1, 130.1, 123.5, 57.5, 43.3, 39.1, 38.0, 31.2, 27.2, 23.4, 22.5, 14.0 ppm.

HRMS (ESI): m/z calcd for $[\text{C}_{15}\text{H}_{23}\text{BrNOS}+\text{H}]^+$: 344.0684 $[\text{M}+\text{H}]^+$; found 344.0677.

S-pyridin-2-yl 4-(bromomethyl)benzothioate (10)



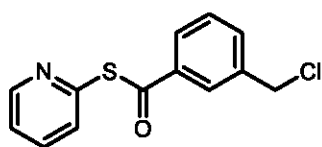
^1H NMR (400 MHz, CDCl_3 , 25 °C): δ 8.68 (dd, $^3J_{\text{H-H}} = 4.8, 1.0$ Hz, 1H, Ar-H), 7.99 (d, $^3J_{\text{H-H}} J = 8.3$ Hz, 2H, Ar-H), 7.79 (td, $^3J_{\text{H-H}} = 7.6, 1.9$ Hz, 1H, Ar-H), 7.73 – 7.71 (m, 1H, Ar-H), 7.51 (d, $^3J_{\text{H-H}} = 8.3$ Hz, 2H, Ar-H), 7.34 (ddd, $^3J_{\text{H-H}} = 7.4, 4.8, 1.3$ Hz, 1H, Ar-H), 4.51 (s, 2H, CH_2) ppm.

^{13}C NMR (100 MHz, CDCl_3 , 25 °C): δ 188.7, 151.2, 150.6, 143.7, 137.2, 136.4, 130.8, 129.5, 128.1, 123.7, 31.9 ppm.

HRMS (ESI): m/z calcd for $[\text{C}_{13}\text{H}_{10}\text{BrNOS}+\text{Na}]^+$: 329.9564 $[M+\text{Na}]^+$; found 329.9558.

Elemental analysis calcd. (%) for $\text{C}_{13}\text{H}_{10}\text{BrNOS}$: C, 50.66, H, 3.27, N, 4.54; found: C, 50.83, H, 3.41, N, 4.60.

S-pyridin-2-yl 3-(chloromethyl)benzothioate (11)



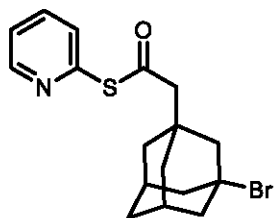
^1H NMR (400 MHz, CDCl_3 , 25 °C): δ 8.67 (ddd, $^3J_{\text{H-H}} = 4.9, 1.9, 0.9$ Hz, 1H, Ar-H), 8.03 – 8.01 (m, 1H, Ar-H), 7.99 – 7.96 (m, 1H, Ar-H), 7.79 (td, $^3J_{\text{H-H}} = 7.6, 1.9$ Hz, 1H, Ar-H), 7.74 – 7.71 (m, 1H, Ar-H), 7.76 – 7.74 (m, 1H, Ar-H), 7.50 (t, $^3J_{\text{H-H}} = 7.8$ Hz, 1H, Ar-H), 7.34 (ddd, $^3J_{\text{H-H}} = 7.4, 4.9, 1.3$ Hz, 1H, Ar-H), 4.64 (s, 2H, CH_2) ppm.

^{13}C NMR (100 MHz, CDCl_3 , 25 °C): δ 188.9, 151.1, 150.6, 138.4, 137.2, 137.09, 133.8, 130.8, 129.3, 127.5, 127.5, 123.7, 45.3 ppm.

HRMS (ESI): m/z calcd for $[\text{C}_{13}\text{H}_{10}\text{ClNOS}+\text{Na}]^+$: 286.0069 $[M+\text{Na}]^+$; found 286.0063.

Elemental analysis calcd. (%) for $\text{C}_{13}\text{H}_{10}\text{ClNOS}$: C, 59.20, H, 3.82, N, 5.31; found: C, 59.16, H, 3.90, N, 5.36.

***S*-pyridin-2-yl 2-(3-bromoadamantanyl)ethanethioate (12)**



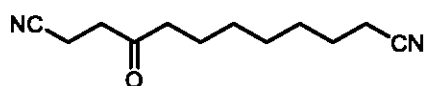
^1H NMR (500 MHz, CDCl_3 , 25 °C): δ 8.63 (dd, $^3J_{\text{H-H}} = 4.7, 1.1$ Hz, 1H, Ar-H), 7.75 (td, $^3J_{\text{H-H}} = 7.7, 2.0$ Hz, 1H, Ar-H), 7.62 – 7.61 (m, 1H, Ar-H), 7.29 (ddd, $^3J_{\text{H-H}} = 7.6, 4.8, 1.1$ Hz, 1H, CH), 2.52 (s, 2H CH_2), 2.25 – 2.32 (m-s, 6H, CH_2), 2.17 (m, 2H), 1.74 – 1.61 (m, 7H, CH_2) ppm.

^{13}C NMR (125 MHz, CDCl_3 , 25 °C): δ 193.8, 151.7, 150.4, 137.1, 130.0, 123.5, 64.6, 56.3, 53.4, 48.2, 40.3, 38.5, 34.5, 32.3 ppm.

HRMS (ESI): m/z calcd for $[\text{C}_{17}\text{H}_{21}\text{BrNOS}+\text{Na}]^+$: 388.0347 $[M+\text{Na}]^+$; found 388.0333.

Elemental analysis calcd. (%) for $\text{C}_{17}\text{H}_{20}\text{BrNOS}$: C, 55.74, H, 5.50, N, 3.82; found: C, 55.68, H, 5.46, N, 3.71.

4-oxododecanedinitrile (14)



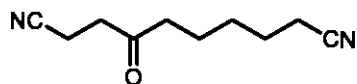
^1H NMR (400 MHz, CDCl_3 , 25 °C): δ 2.77 (t, $^3J_{\text{H-H}} = 7.1$ Hz, 2H, CH_2), 2.56 (t, $^3J_{\text{H-H}} = 7.1$ Hz, 2H, CH_2), 2.44 (t, $^3J_{\text{H-H}} = 7.4$ Hz, 2H, CH_2), 2.32 (t, $^3J_{\text{H-H}} = 7.1$ Hz, 2H, CH_2), 1.67 – 1.57 (m, 4H, CH_2), 1.48 – 1.39 (m, 2H, CH_2), 1.35 – 1.23 (m, 4H, CH_2) ppm.

^{13}C NMR (100 MHz, CDCl_3 , 25 °C): δ 206.0, 119.7, 119.0, 42.3, 37.7, 28.7, 28.5, 28.4, 25.2, 23.4, 17.1, 11.4. ppm.

HRMS (ESI): m/z calcd for $[\text{C}_{12}\text{H}_{18}\text{N}_2\text{O}+\text{Na}]^+$: 229.1317 $[M+\text{Na}]^+$; found 229.1314.

Elemental analysis calcd. (%) for $\text{C}_{12}\text{H}_{18}\text{N}_2\text{O}$: C, 69.87, H, 8.80, N, 13.58; found: C, 69.62, H, 8.73, N, 13.34.

4-oxodecanedinitrile (18)



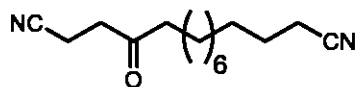
^1H NMR (400 MHz, CDCl_3 , 25 °C): δ 2.78 (t, $^3J_{\text{H-H}} = 7.1$ Hz, 2H, CH_2), 2.57 (t, $^3J_{\text{H-H}} = 7.1$ Hz, 2H, CH_2), 2.48 (t, $^3J_{\text{H-H}} = 7.2$ Hz, 2H, CH_2), 2.34 (t, $^3J_{\text{H-H}} = 7.1$ Hz, 2H, CH_2), 1.71 – 1.58 (m, 4H, CH_2), 1.50 – 1.39 (m, 2H, CH_2) ppm.

^{13}C NMR (100 MHz, CDCl_3 , 25 °C): δ 205.5, 119.5, 118.9, 41.9, 37.8, 28.0, 25.1, 22.6, 17.0, 11.4 ppm.

HRMS (ESI): m/z calcd for $[\text{C}_{10}\text{H}_{14}\text{N}_2\text{O}+\text{Na}]^+$: 201.1004 $[\text{M}+\text{Na}]^+$; found 201.1003.

Elemental analysis calcd. (%) for $\text{C}_{10}\text{H}_{14}\text{N}_2\text{O}$: C, 67.39, H, 7.92, N, 15.72; found: C, 67.28, H, 8.14, N, 15.65.

4-oxopentadecanedinitrile (19)



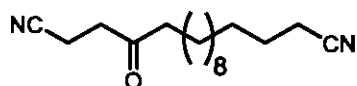
^1H NMR (400 MHz, CDCl_3 , 25 °C): δ 2.78 (t, $^3J_{\text{H-H}} = 7.2$ Hz, 2H, CH_2), 2.57 (t, $^3J_{\text{H-H}} = 7.2$ Hz, 2H, CH_2), 2.44 (t, $^3J_{\text{H-H}} = 7.4$ Hz, 2H, CH_2), 2.32 (t, $^3J_{\text{H-H}} = 7.1$ Hz, 2H, CH_2), 1.69 – 1.56 (m, 4H, CH_2), 1.48 – 1.39 (m, 2H, CH_2), 1.32 – 1.25 (m, 10H, CH_2) ppm.

^{13}C NMR (100 MHz, CDCl_3 , 25 °C): δ 206.2, 119.8, 119.0, 42.5, 37.7, 29.2, 29.2, 29.2, 29.0, 28.7, 28.6, 25.3, 23.6, 17.1, 11.4 ppm.

HRMS (ESI): m/z calcd for $[\text{C}_{15}\text{H}_{24}\text{N}_2\text{O}+\text{Na}]^+$: 271.1786 $[\text{M}+\text{Na}]^+$; found 271.1778.

Elemental analysis calcd. (%) for $\text{C}_{15}\text{H}_{24}\text{N}_2\text{O}$: C, 72.54, H, 9.74, N, 11.28; found: C, 72.40, H, 9.91, N, 11.01.

4-oxoheptadecanedinitrile (20)



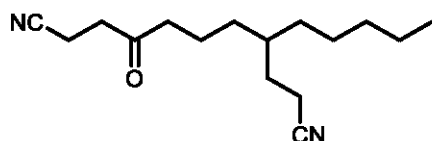
^1H NMR (400 MHz, CDCl_3 , 25 °C): δ 2.78 (t, $^3J_{\text{H-H}} = 7.2$ Hz, 2H, CH_2), 2.58 (t, $^3J_{\text{H-H}} = 7.1$ Hz, 2H, CH_2), 2.44 (t, $^3J_{\text{H-H}} = 7.4$ Hz, 2H, CH_2), 2.33 (t, $^3J_{\text{H-H}} = 7.1$ Hz, 2H, CH_2), 1.69 – 1.59 (m, 4H, CH_2), 1.48 – 1.39 (m, 2H, CH_2), 1.32 – 1.26 (m, 14H, CH_2) ppm.

^{13}C NMR (100 MHz, CDCl_3 , 25 °C): δ 206.3, 119.8, 119.0, 42.5, 37.6, 29.4, 29.4, 29.3, 29.3, 29.2, 29.1, 28.7, 28.6, 25.3, 23.7, 17.1, 11.4 ppm.

HRMS (ESI): m/z calcd for $[\text{C}_{17}\text{H}_{28}\text{N}_2\text{O}+\text{Na}]^+$: 299.2099 $[M+\text{Na}]^+$; found 299.2093.

Elemental analysis calcd. (%) for $\text{C}_{17}\text{H}_{28}\text{N}_2\text{O}$: C, 73.87, H, 10.21, N, 10.13; found: C, 73.97, 10.35, N, 9.98.

4-oxo-8-pentylundecanedinitrile (21)

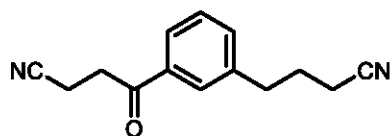


^1H NMR (500 MHz, CDCl_3 , 25 °C): δ 2.79 (t, $^3J_{\text{H-H}} = 7.1$ Hz, 2H), 2.58 (t, $^3J_{\text{H-H}} = 7.2$ Hz, 2H), 2.46 (t, $^3J_{\text{H-H}}$, $J = 7.2$ Hz, 2H), 2.36 – 2.28 (m, 2H), 1.64 – 1.58 (m, 4H), 1.51 – 1.44 (m, 1H), 1.31 – 1.23 (m, 10H), 0.91 – 0.86 (m, 3H) ppm.

^{13}C NMR (125 MHz, CDCl_3 , 25 °C): δ 205.8, 119.9, 118.91, 42.4, 37.8, 36.5, 32.6, 32.1, 32.06, 29.0, 26.0, 22.6, 20.2, 14.7, 14.0, 11.38 ppm.

HRMS (ESI): m/z calcd for $[\text{C}_{16}\text{H}_{26}\text{N}_2\text{O}+\text{Na}]^+$: 285.19439564 $[M+\text{Na}]^+$; found 285.1937.

4-(3-(3-cyanopropyl)phenyl)-4-oxobutanenitrile (22)



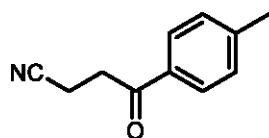
^1H NMR (400 MHz, CDCl_3 , 25 °C): δ 7.84 – 7.77 (m, 2H, Ar-H), 7.46 – 7.44 (m, 2H, Ar-H), 3.37 (t, $^3J_{\text{H-H}} = 7.2$ Hz, 2H, CH_2), 2.86 (t, $^3J_{\text{H-H}} = 8.0$ Hz, 2H, CH_2), 2.77 (t, $^3J_{\text{H-H}} = 7.2$ Hz, 2H, CH_2), 2.35 (t, $^3J_{\text{H-H}} = 7.0$ Hz, 2H, CH_2), 2.01 (p, $^3J_{\text{H-H}} = 7.1$ Hz, 2H, CH_2) ppm.

^{13}C NMR (100 MHz, CDCl_3 , 25 °C): δ 195.2, 140.8, 136.1, 134.0, 129.2, 127.8, 126.4, 119.1, 34.3, 26.7, 16.5, 11.8 ppm.

HRMS (ESI): m/z calcd for $[\text{C}_{14}\text{H}_{14}\text{N}_2\text{O}+\text{Na}]^+$: 249.1004 $[M+\text{Na}]^+$; found 249.1001.

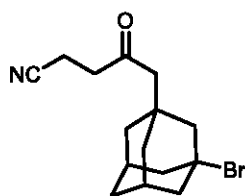
Elemental analysis calcd. (%) for $\text{C}_{14}\text{H}_{14}\text{N}_2\text{O}$: C, 74.31, H, 6.24, N, 12.38; found: C, 74.18, H, 6.15, N, 12.13.

4-oxo-4-(*p*-tolyl)butanenitrile (23)^[5]



^1H NMR (400 MHz, CDCl_3 , 25 °C): δ 7.84 (d, $^3J_{\text{H-H}} = 8.3$ Hz, 2H, Ar-H), 7.28 (d, $^3J_{\text{H-H}} = 8.0$ Hz, 2H, Ar-H), 3.34 (t, $^3J_{\text{H-H}} = 8.5$ Hz, 2H, CH_2), 2.75 (t, $^3J_{\text{H-H}} = 8.5$ Hz, 2H, CH_2), 2.42 (s, 3H, CH_3) ppm.

5-(3-bromoadamantanyl)-4-oxopentanenitrile (24)



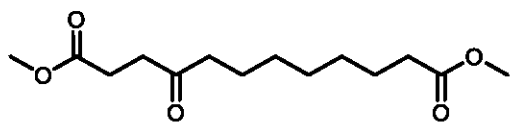
^1H NMR (400 MHz, CDCl_3 , 25 °C): δ 2.75 (t, $^3J_{\text{H-H}} = 7.1$ Hz, 2H, CH_2), 2.54 (t, $^3J_{\text{H-H}} = 7.1$ Hz, 2H, CH_2), 2.32 – 2.13 (m, 10H, CH_2), 1.69 – 1.56 (m, 6H, CH_2) ppm.

^{13}C NMR (100 MHz, CDCl_3 , 25 °C): δ 204.6, 118.9, 64.6, 54.0, 53.5, 48.3, 40.2, 40.2, 38.0, 34.6, 32.2, 11.3 ppm.

HRMS (ESI): m/z calcd for $[\text{C}_{15}\text{H}_{20}\text{BrNO}+\text{Na}]^+$: 332.0626 $[M+\text{Na}]^+$; found 332.0612.

Elemental analysis calcd. (%) for $\text{C}_{15}\text{H}_{20}\text{BrNO}$: C, 58.07, H, 6.50, N, 4.51; found: C, 58.30, H, 6.62, N, 4.47.

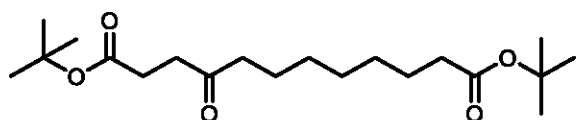
dimethyl 4-oxododecanedioate (25)^[6]



¹H NMR (500 MHz, CDCl₃, 25 °C): δ 3.66 (d, ³J_{H-H} = 4.1 Hz, 6H, CH₃), 2.70 (t, ³J_{H-H} = 6.5 Hz, 2H, CH₂), 2.57 (t, ³J_{H-H} = 6.5 Hz, 2H, CH₂), 2.43 (t, ³J_{H-H} = 7.4 Hz, 2H, CH₂), 2.28 (t, ³J_{H-H} = 7.5 Hz, 2H, CH₂), 1.61 – 1.52 (m, 4H, CH₂), 1.31 – 1.25 (m, 6H, CH₂) ppm.

¹³C NMR (125 MHz, CDCl₃, 25 °C): δ 208.9, 174.2, 173.3, 51.7, 51.4, 42.7, 37.0, 34.0, 28.98, 29.0, 28.9, 27.7, 24.9, 23.7 ppm.

di-tert-butyl 4-oxododecanedioate (26)



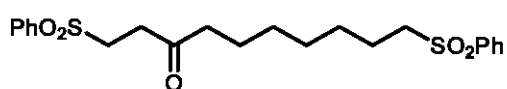
¹H NMR (400 MHz, CDCl₃, 25 °C): δ 2.64 (t, ³J_{H-H} = 6.6 Hz, 2H, CH₂), 2.47 (t, ³J_{H-H} = 6.8 Hz, 2H, CH₂), 2.41 (t, ³J_{H-H} = 7.5 Hz, 2H, CH₂), 2.17 (t, ³J_{H-H} = 7.5 Hz, 2H, CH₂), 1.61 – 1.48 (m, 4H, CH₂), 1.43 (s, 9H, CH₃), 1.42 (s, 9H, CH₃), 1.28 – 1.25 (m, 6H, CH₂) ppm.

¹³C NMR (100 MHz, CDCl₃, 25 °C): δ 209.2, 173.2, 172.0, 79.9, 42.7, 37.2, 35.5, 29.2, 29.0, 28.9, 28.1, 28.0, 25.0, 23.7 ppm.

HRMS (ESI): *m/z* calcd for [C₂₀H₃₅O₅+Na]⁺: 379.2460 [*M*+Na]⁺; found 379.2454.

Elemental analysis calcd. (%) for C₂₀H₃₅O₅: C, 67.38, H, 10.18; found: C, 67.24, H, 10.24.

1,10-bis(phenylsulfonyl)decan-3-one (27)



¹H NMR (500 MHz, CDCl₃, 25 °C): δ 7.87 (d, ³J_{H-H} = 8.0 Hz, 4H, Ar-H), 7.67 – 7.60 (m, 2H, Ar-H), 7.57 – 7.52 (m, 4H, Ar-H), 3.35 (t, ³J_{H-H} = 8.0 Hz, 2H, CH₂), 3.04 (t, ³J_{H-H} = 8.0 Hz, 2H, CH₂), 2.84 (t, ³J_{H-H} = 7.5 Hz, 2H, CH₂), 2.37 (t, ³J_{H-H} = 7.3 Hz, 2H, CH₂), 1.70 – 1.63 (m, 2H, CH₂), 1.51 – 1.43 (m, 2H, CH₂), 1.33 – 1.27 (m, 2H, CH₂), 1.23 – 1.18 (m, 4H, CH₂) ppm.

¹³C NMR (125 MHz, CDCl₃, 25 °C): ¹³C NMR (400 MHz, CDCl₃, 25 °C): δ 205.9, 139.3, 139.1, 133.9, 129.3, 128.0, 56.2, 50.6, 42.7, 34.9, 28.7, 28.0, 23.4, 22.5 ppm.

HRMS (ESI): *m/z* calcd for [C₂₂H₂₈O₅S₂+Na]⁺: 459.1276 [*M*+Na]⁺; found 459.1273.

Elemental analysis calcd. (%) for C₂₂H₂₈O₅S₂: C, 60.53, H, 6.46; found: C, 60.72, H, 6.39.

References

- [1] M. Ociepa, O. Baka, J. Narodowiec, D. Gryko, *Adv. Synth. Catal.* **2017**, *359*, 3560–3565.
- [2] M. Karczewski, M. Ociepa, K. Pluta, K. ó Proinsias, D. Gryko, *Chem. - A Eur. J.* **2017**, *23*, 7024–7030.
- [3] D. Pedersen, C. Rosenbohm, *Synthesis (Stuttg.)*. **2004**, *2001*, 2431–2434.
- [4] S. H. H. Zaidi, K. Muthukumaran, S. I. Tamaru, J. S. Lindsey, *J. Org. Chem.* **2004**, *69*, 8356–8365.
- [5] Y. Li, J. Q. Shang, X. X. Wang, W. J. Xia, T. Yang, Y. Xin, Y. M. Li, *Org. Lett.* **2019**, *21*, 2227–2230.
- [6] A. Charvieux, N. Duc Vu, N. Duguet, M. Lemaire, *European J. Org. Chem.* **2019**, *2019*, 1251–1256.

7. NMR Spectra

S-pyridin-2-yl 4-bromobutanethioate (4)

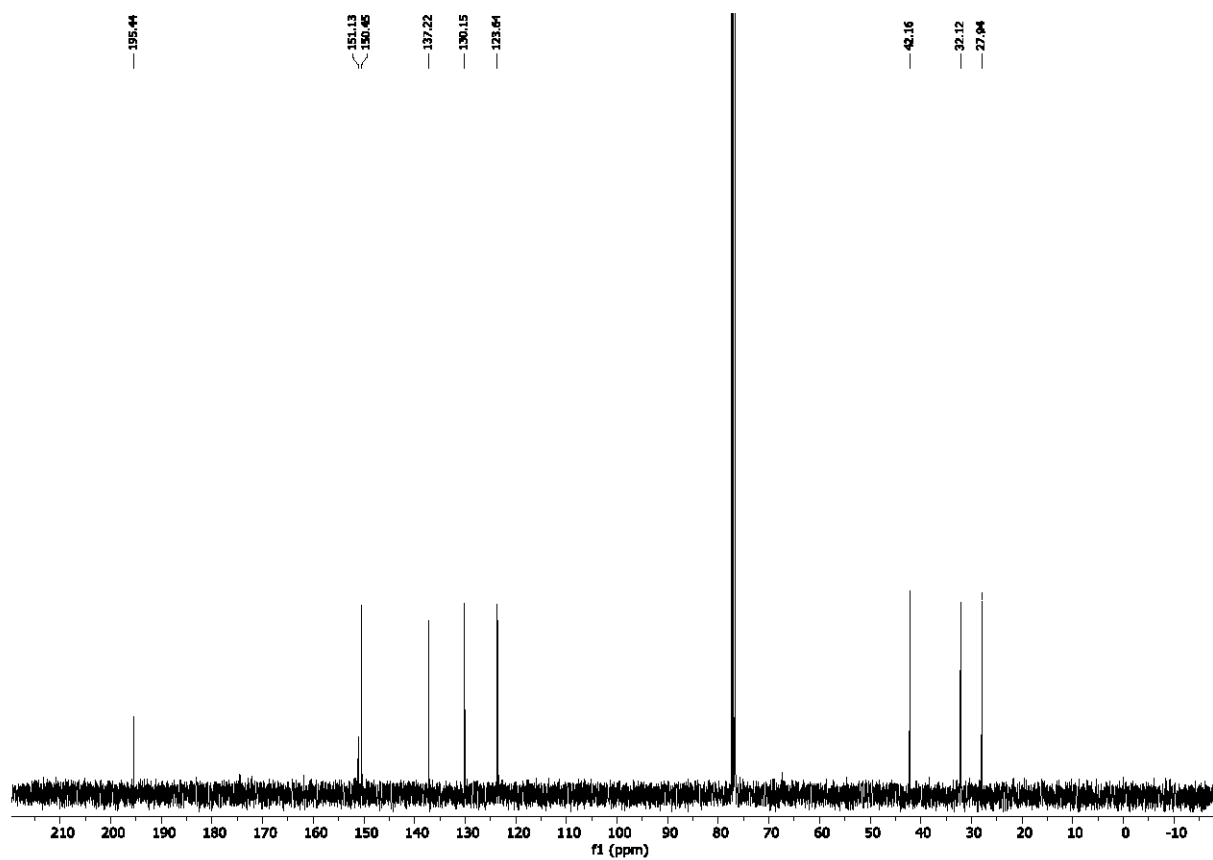
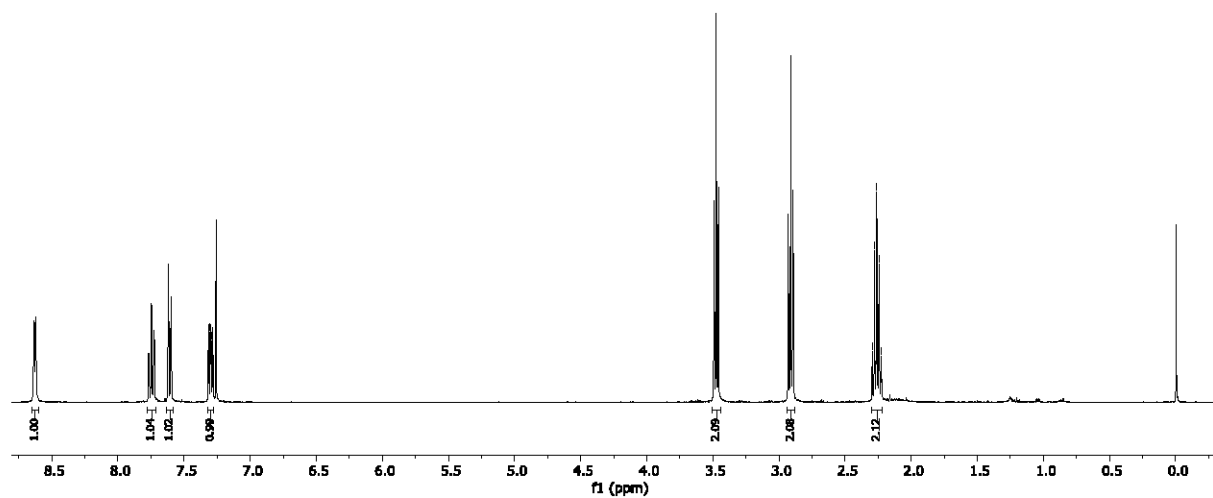
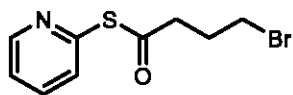
8.64
8.04
8.03
8.03
8.02
8.02

7.12
7.11
7.10
7.09
7.09
7.08
7.08

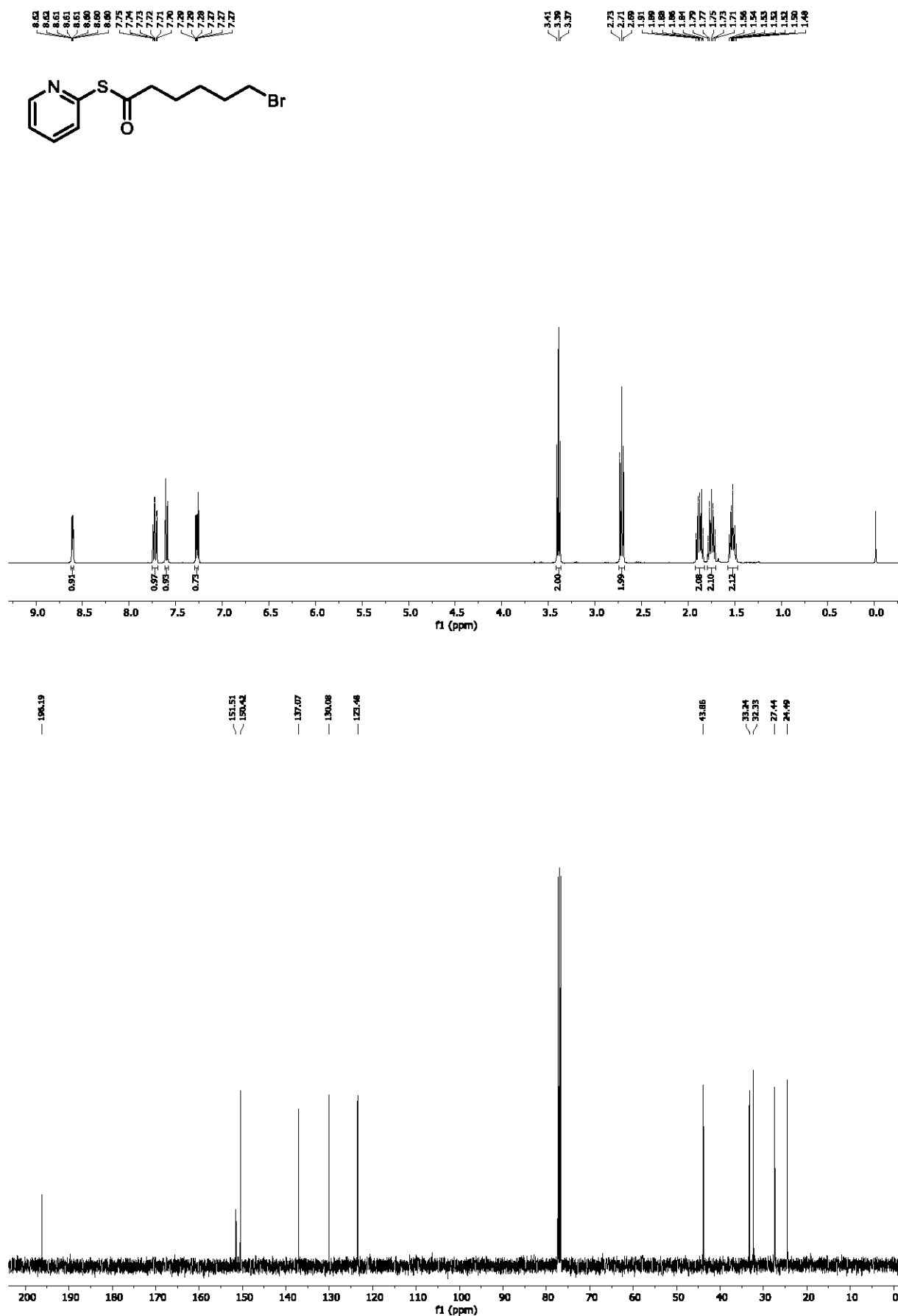
3.49
3.47
3.46

2.81
2.81
2.80

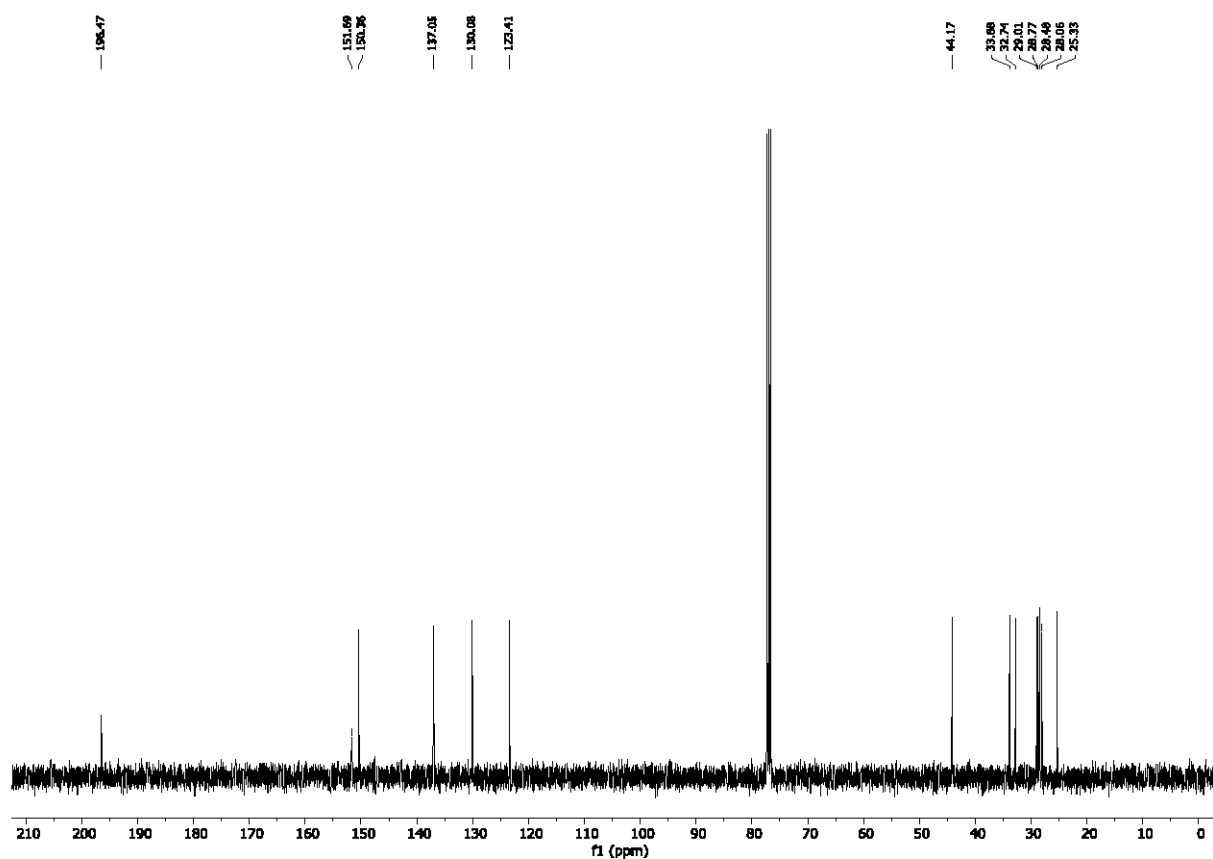
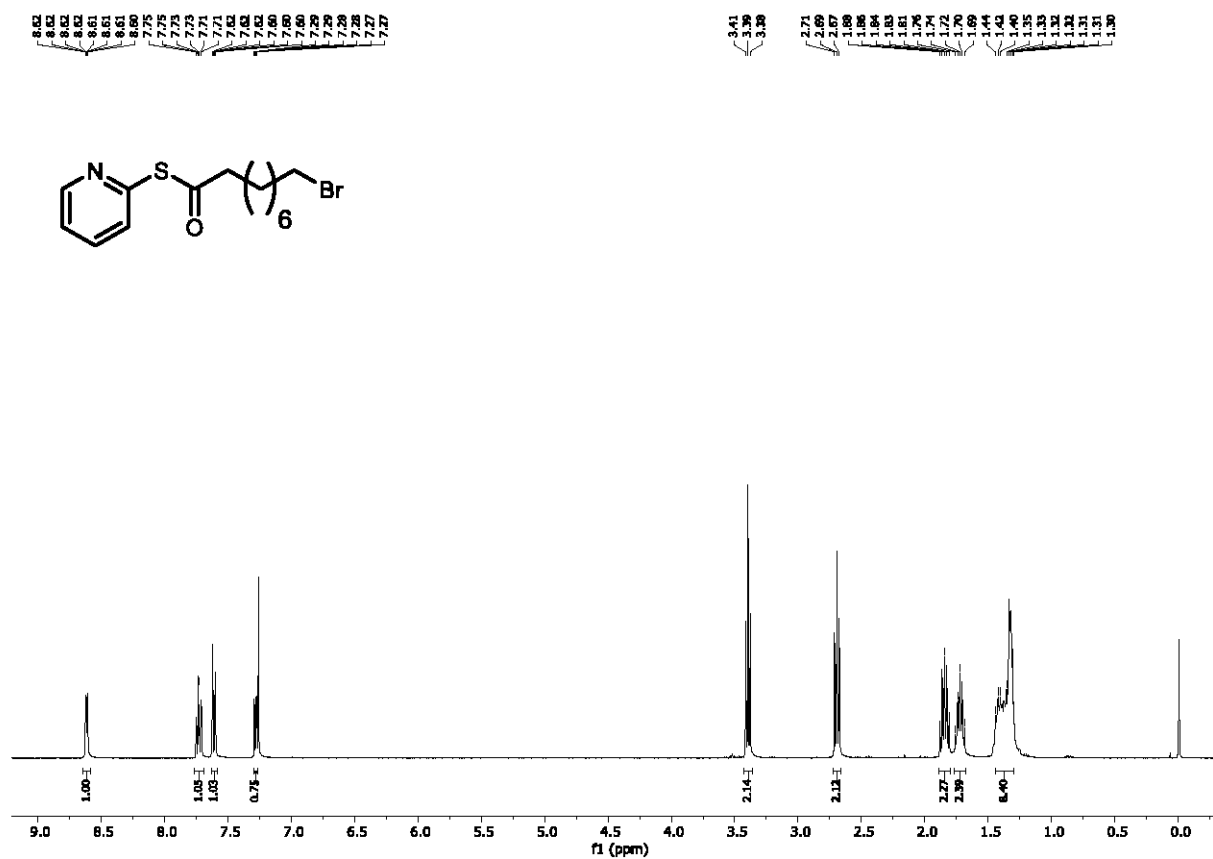
2.29
2.28
2.28
2.28
2.25



S-pyridin-2-yl 6-bromohexanethioate (5)



S-pyridin-2-yl 9-bromononanethioate (6)



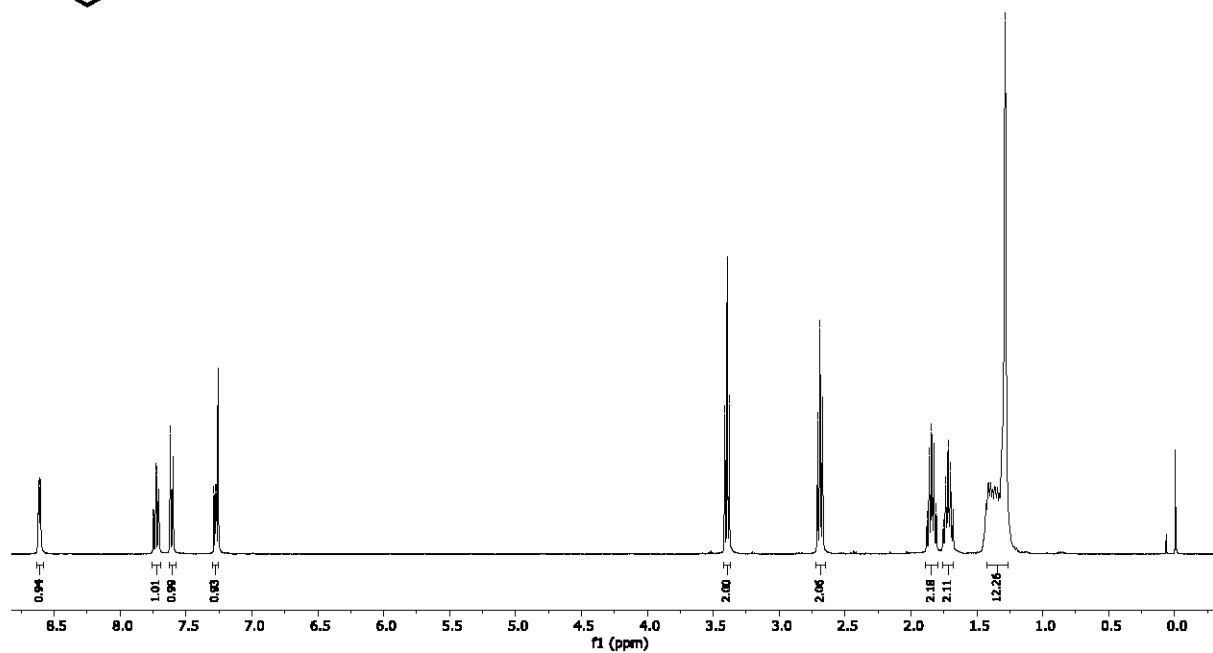
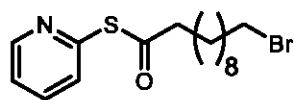
S-pyridin-2-yl 11-bromoundecanethioate (7)

8.02
8.02
8.01
7.75
7.74
7.73
7.72
7.71
7.68
7.68
7.29
7.27

3.41
3.39

2.71
2.69
2.67

1.88
1.86
1.84
1.82
1.81
1.79
1.77
1.75
1.73
1.71



196.51

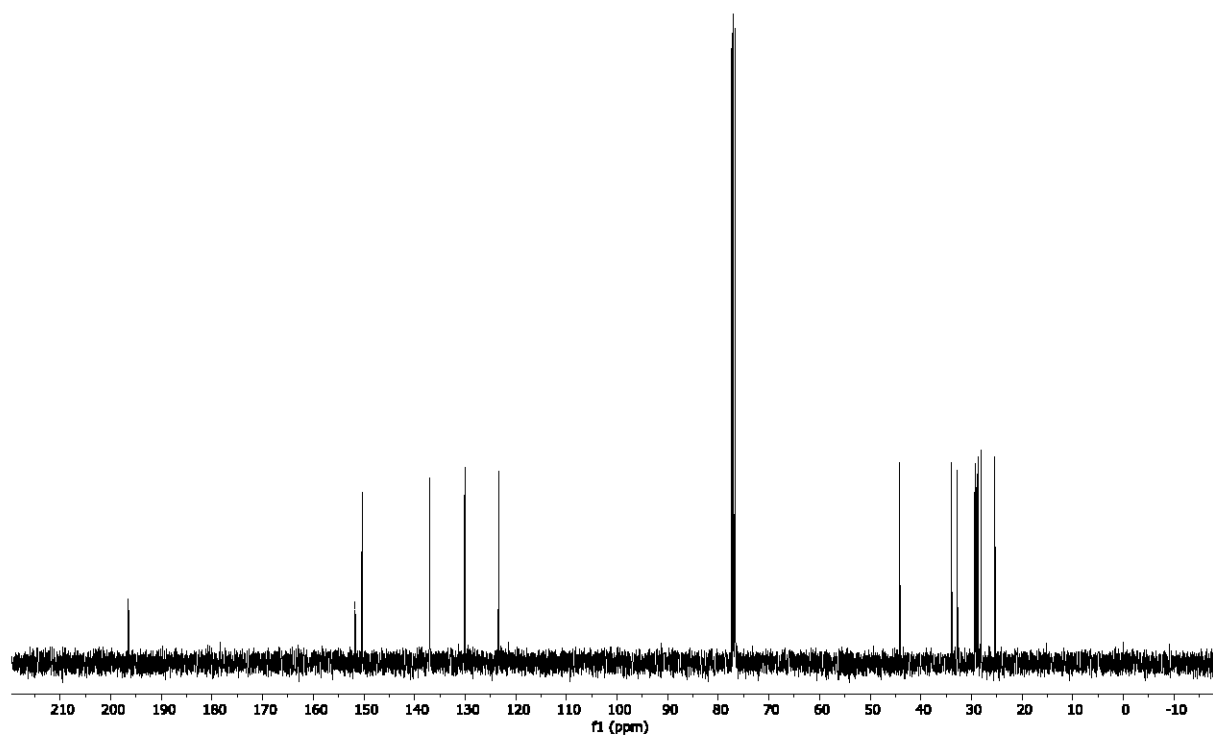
151.79
150.34

137.04

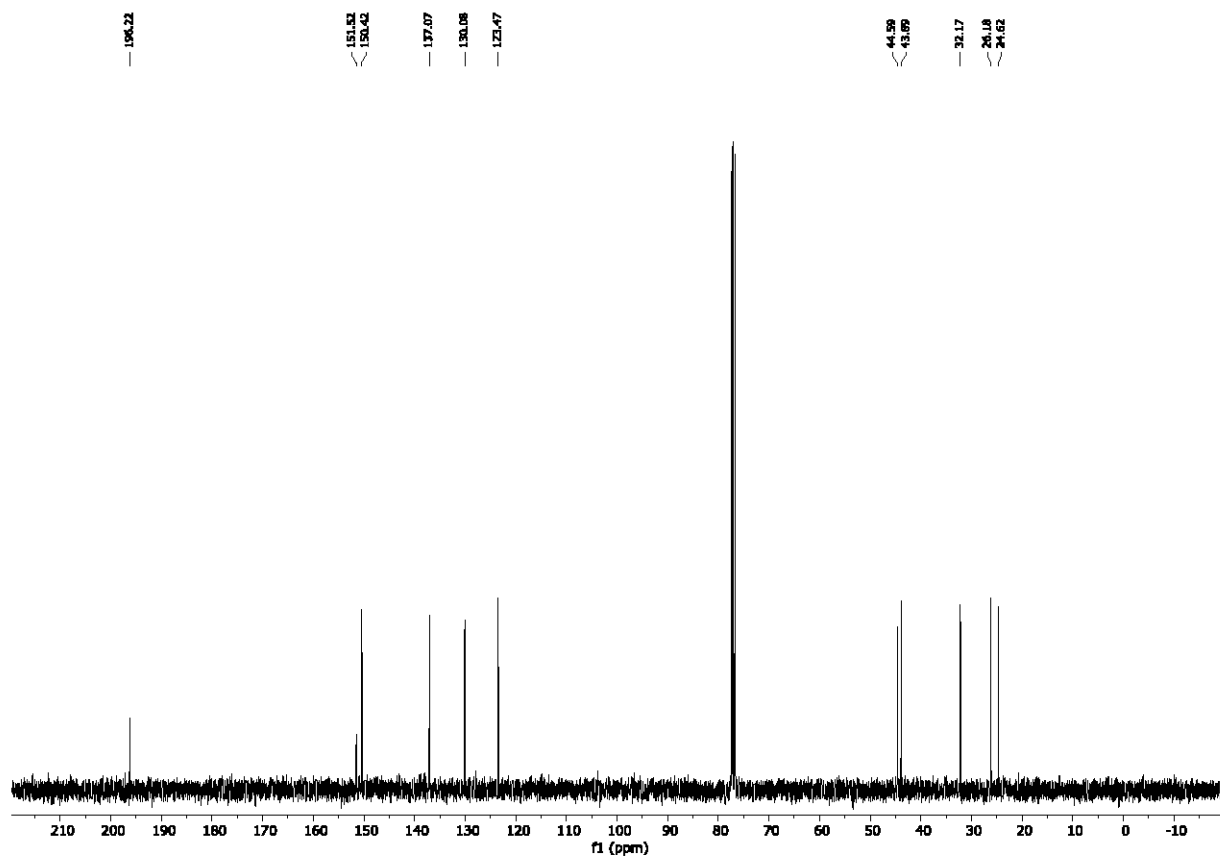
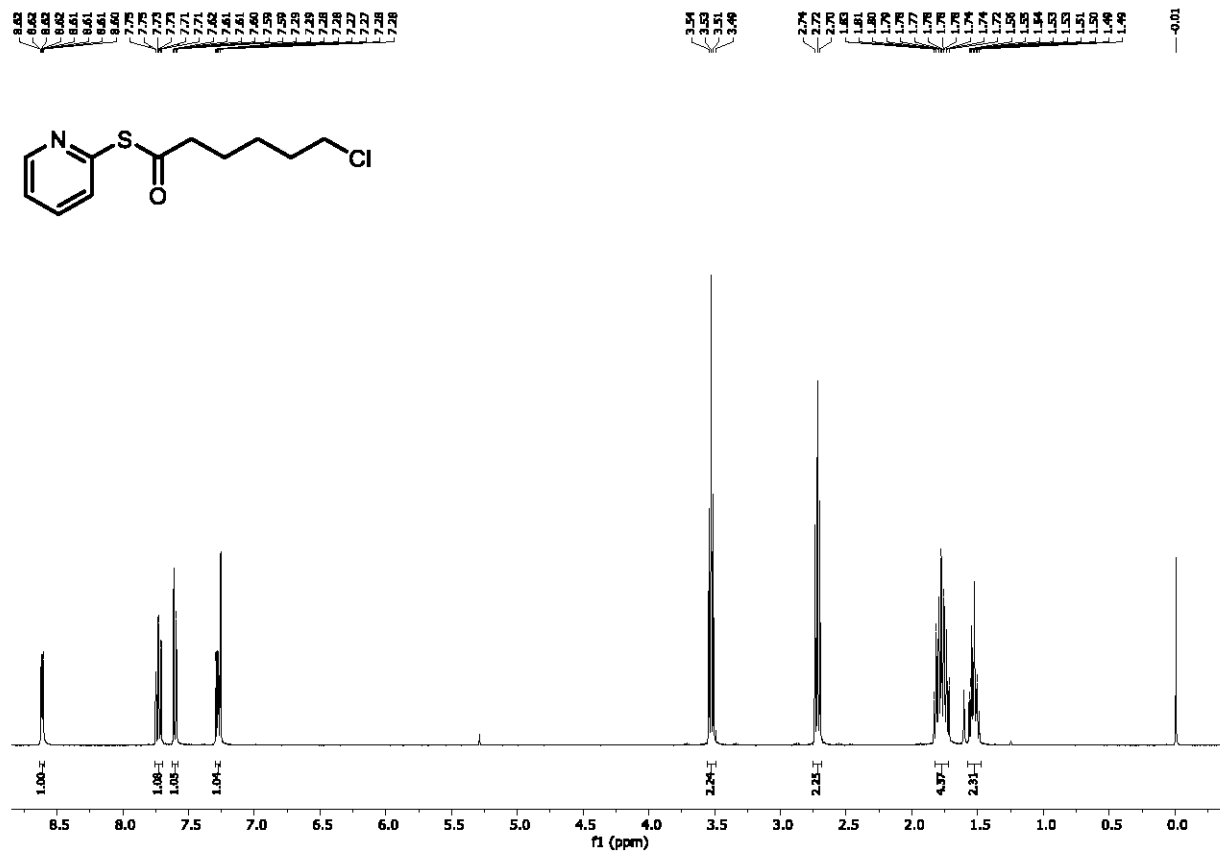
136.07

122.99

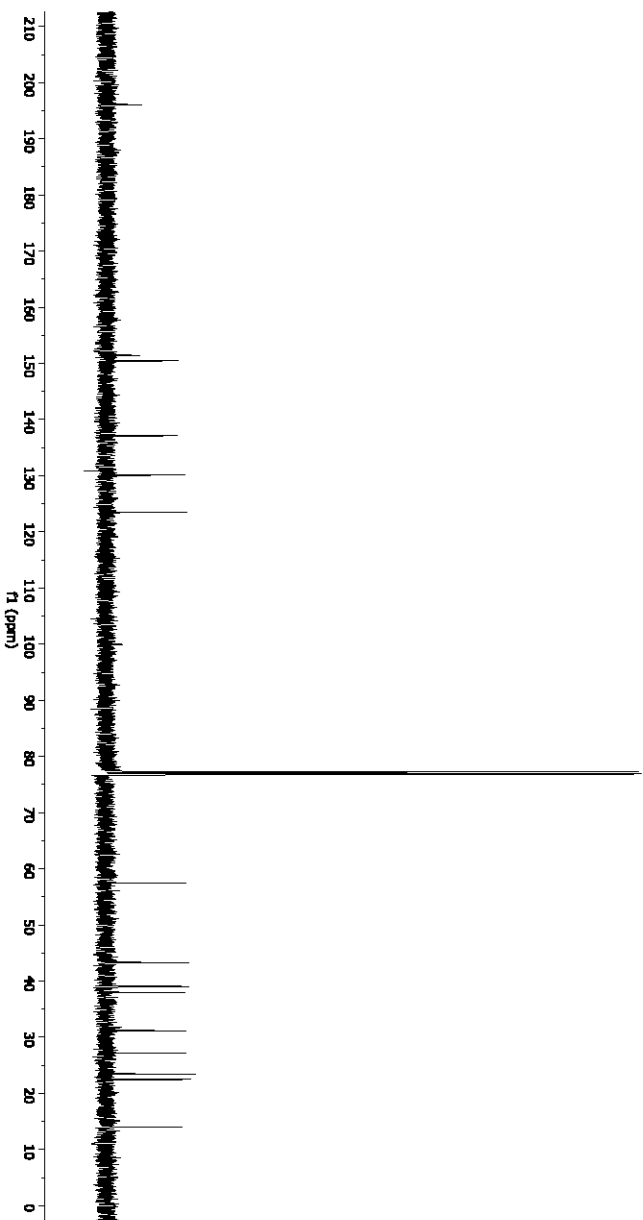
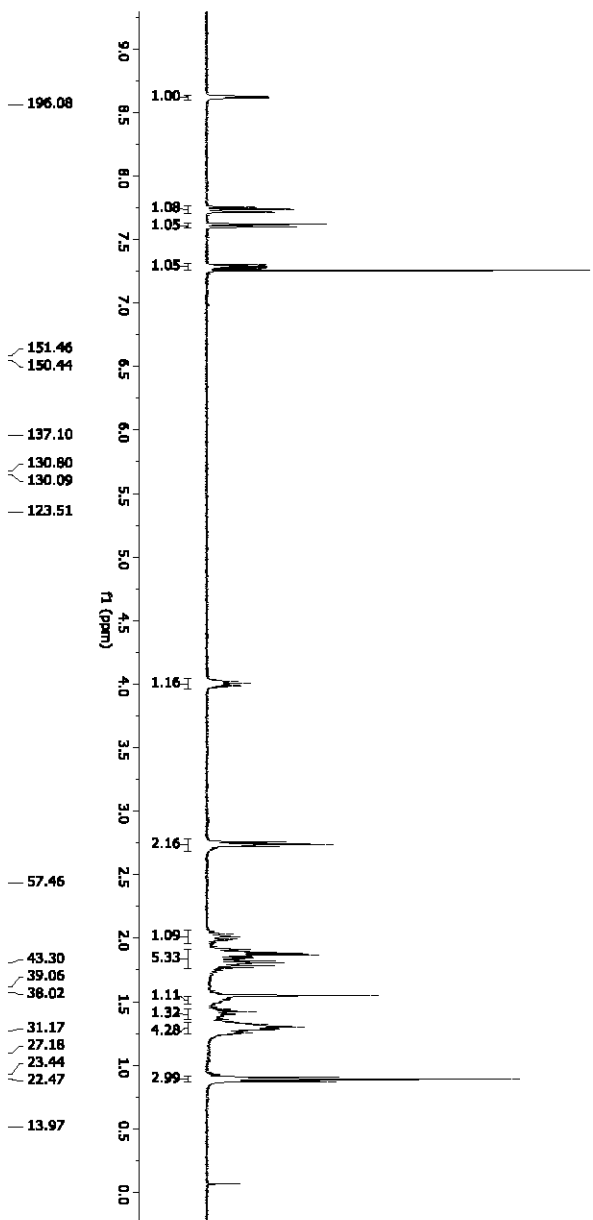
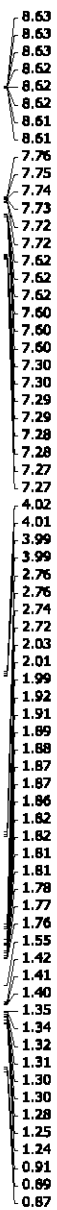
44.22
33.96
32.81
29.31
29.22
29.14
28.87
28.79
28.13
25.38



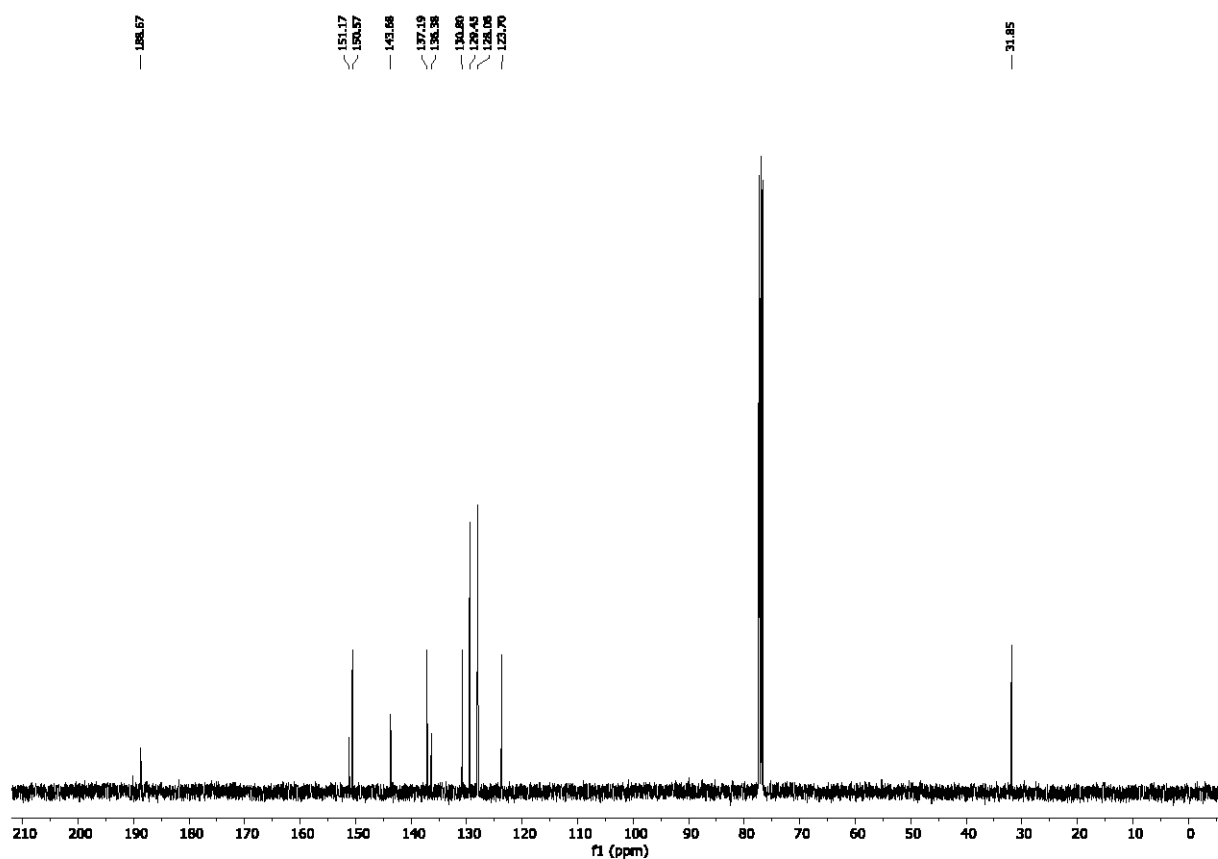
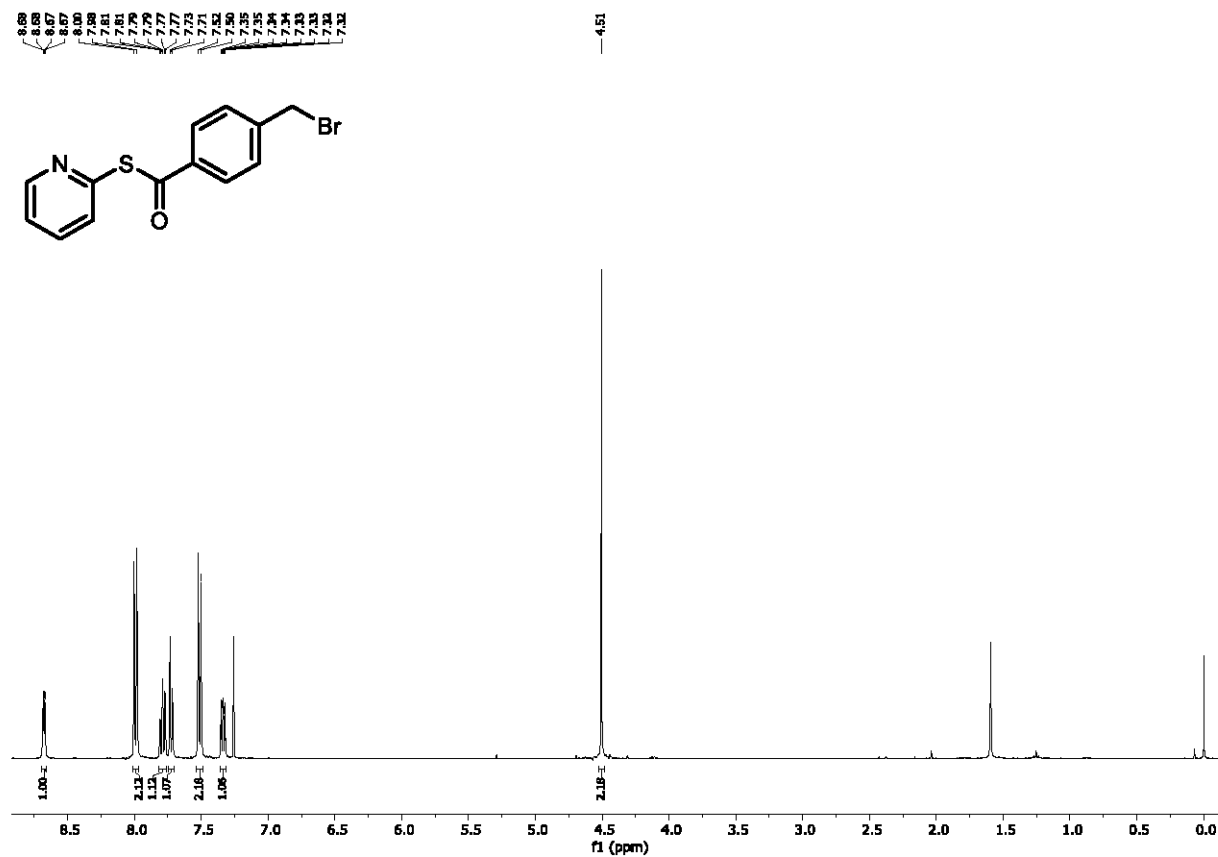
S-pyridin-2-yl 6-chlorohexanethioate (8)



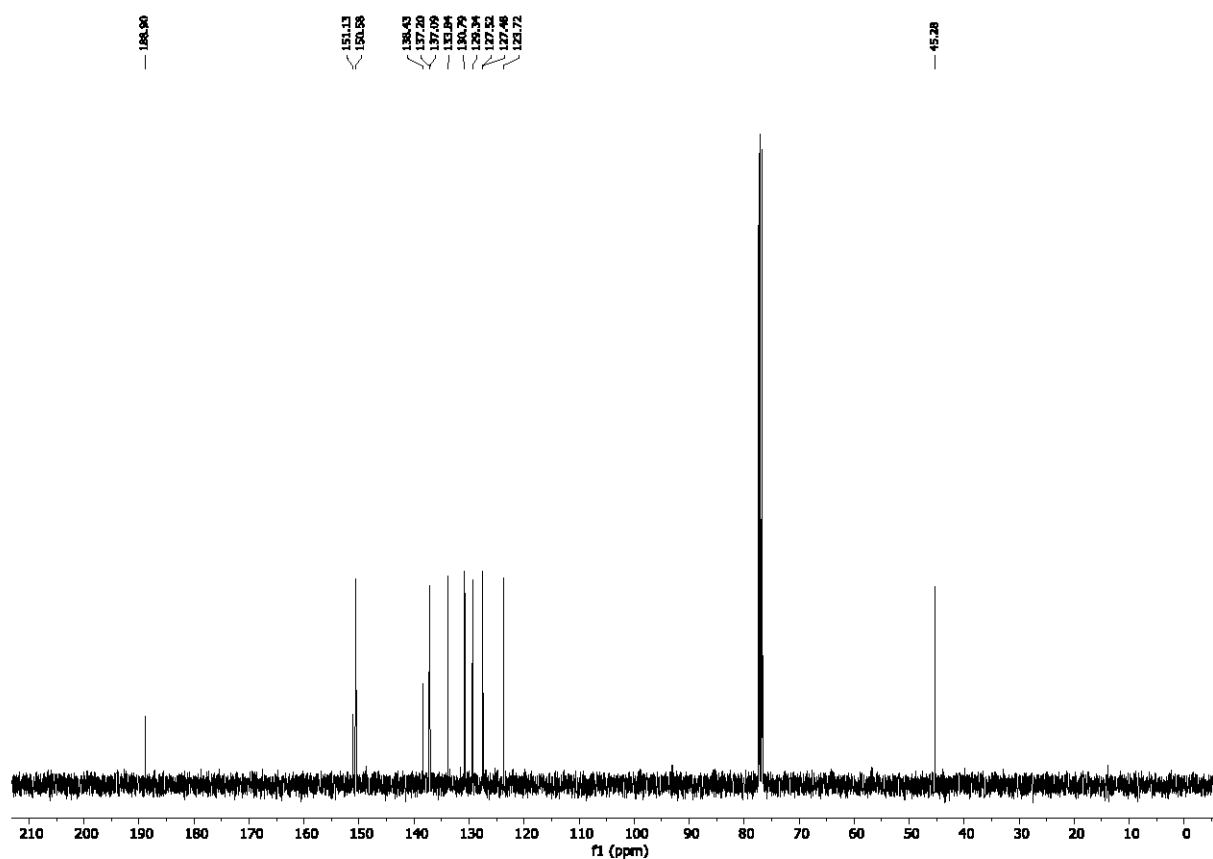
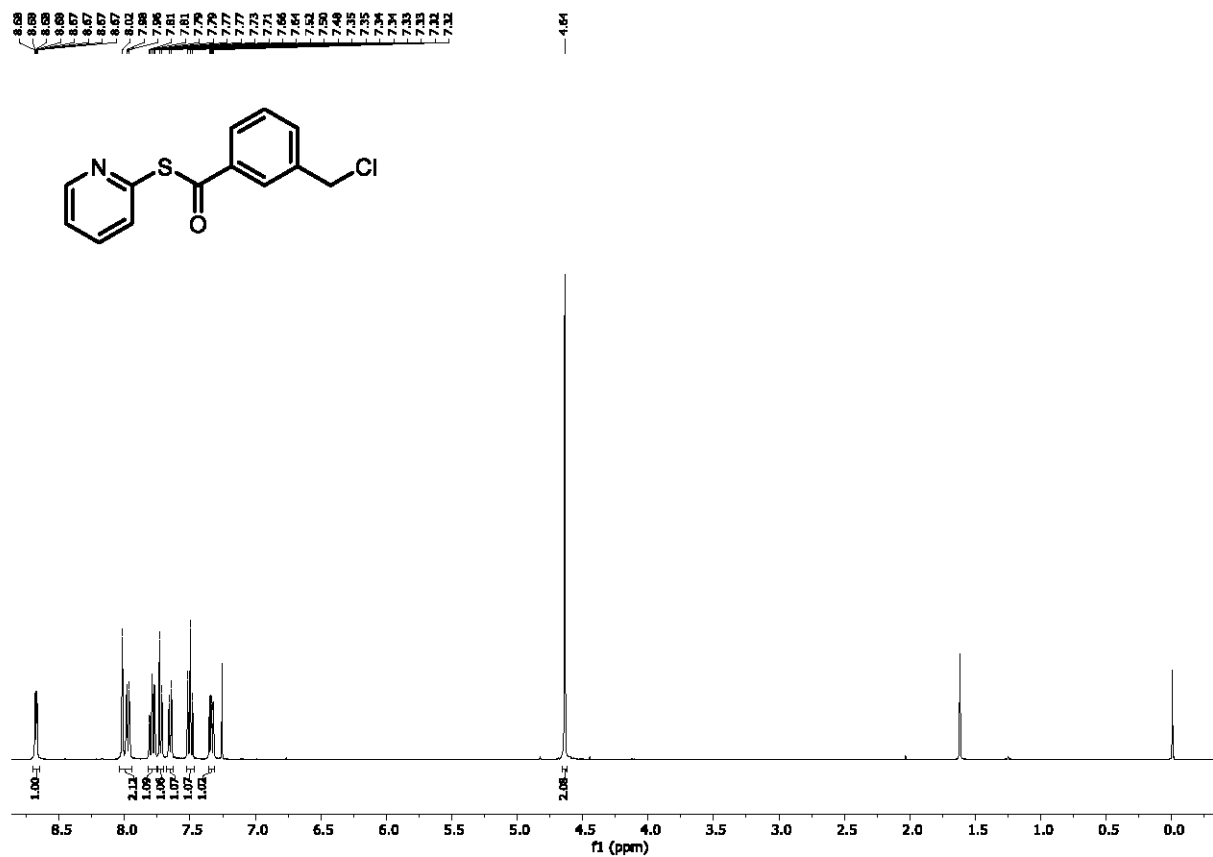
S-pyridin-2-yl 5-bromodecanethioate (9)



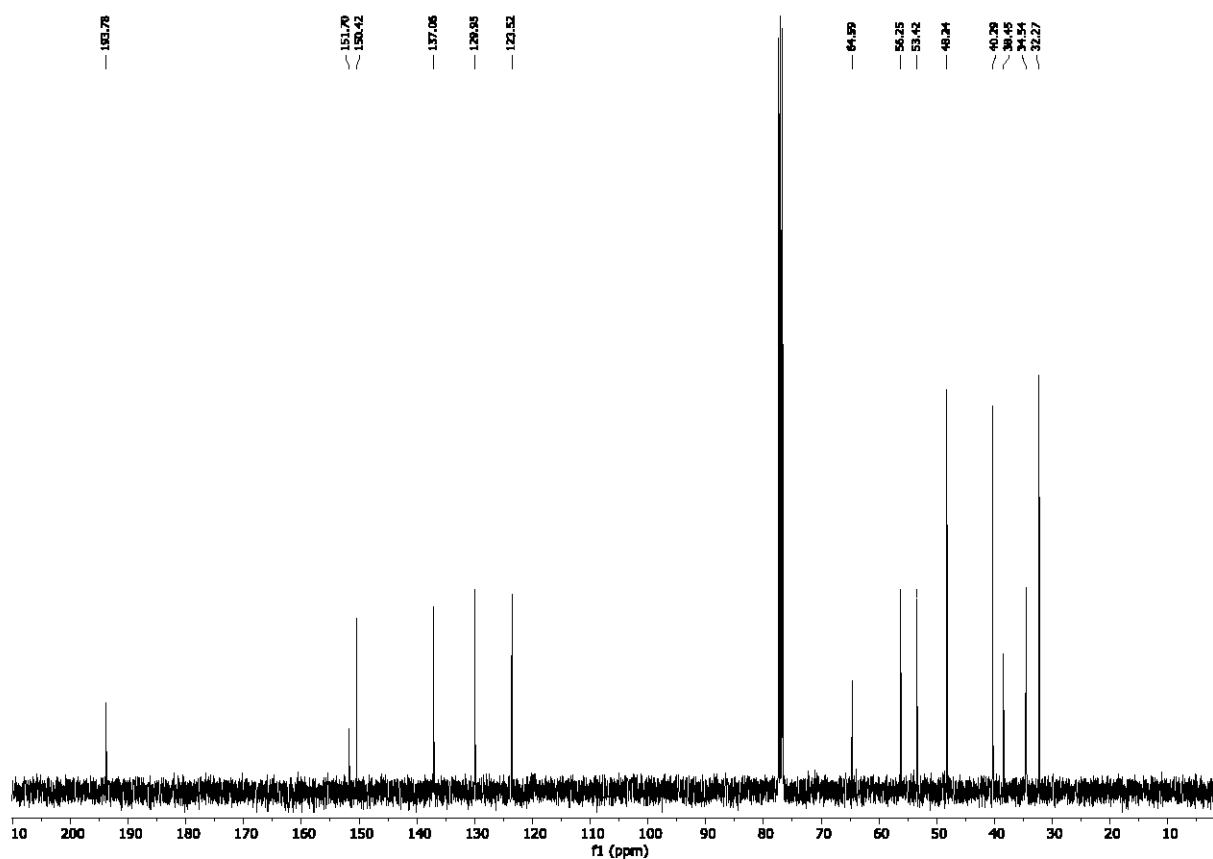
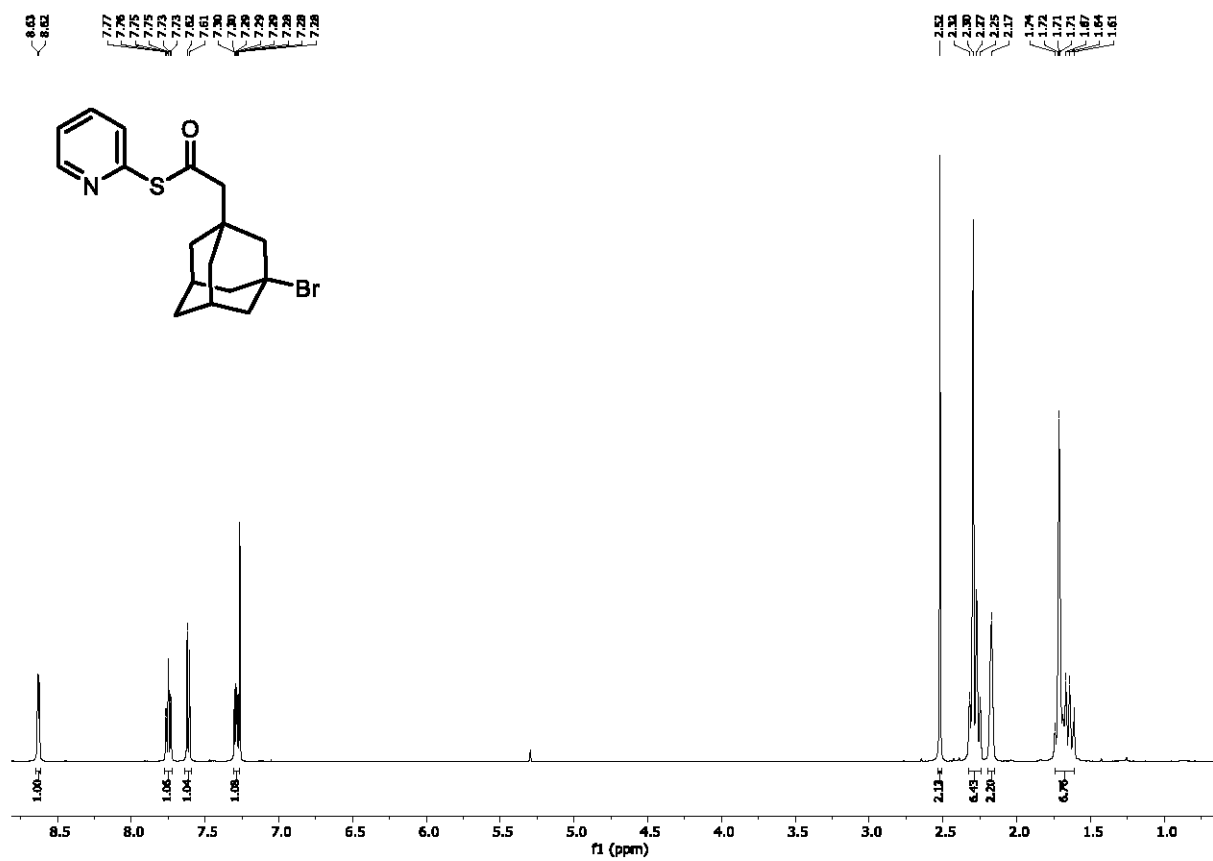
S-pyridin-2-yl 4-(bromomethyl)benzothioate (10)



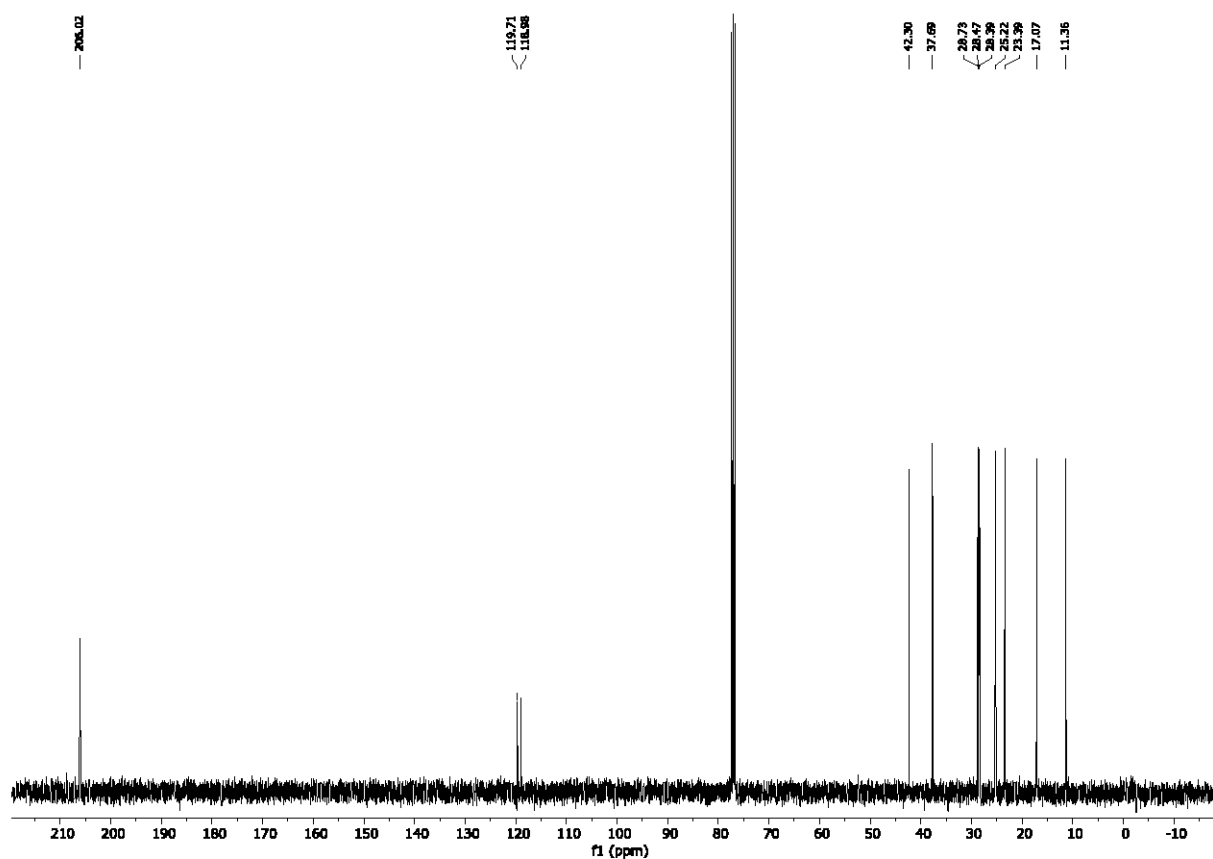
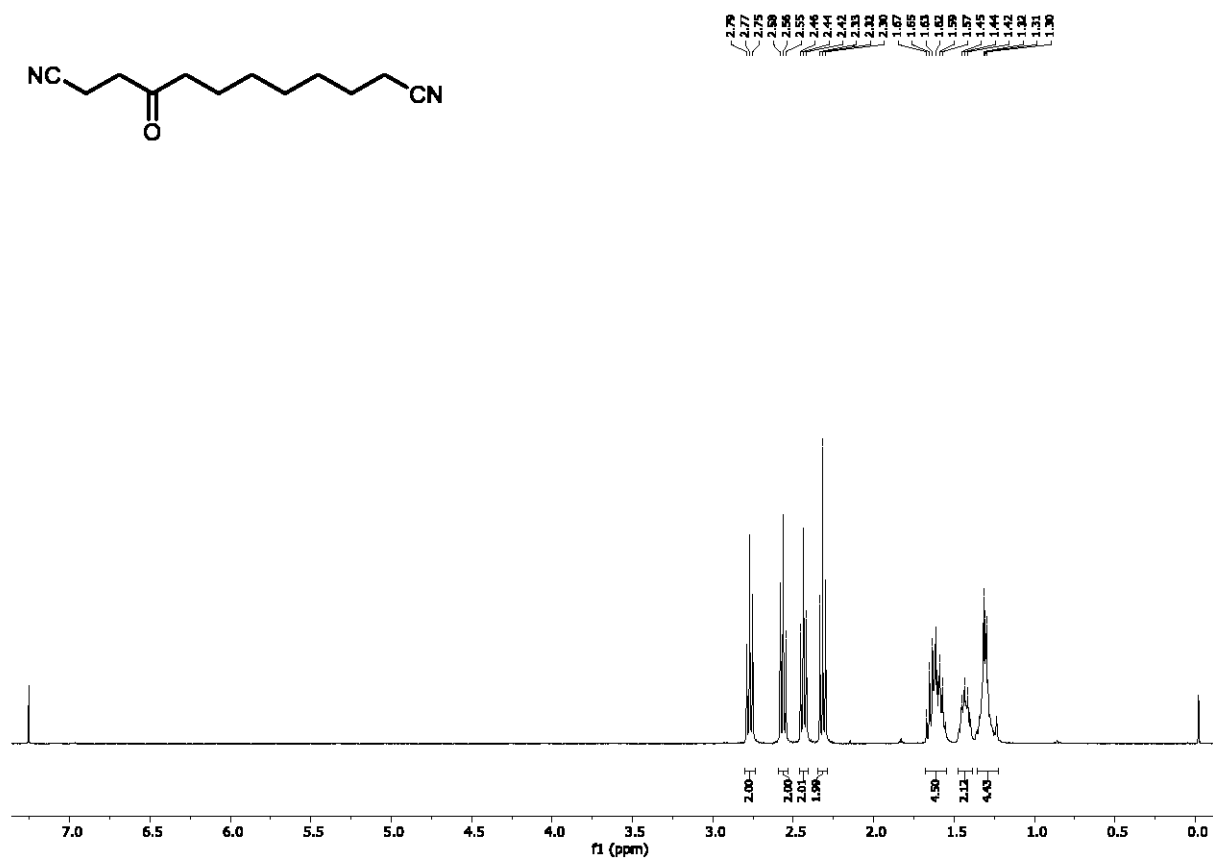
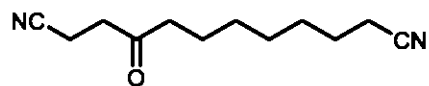
S-pyridin-2-yl 3-(chloromethyl)benzothioate (11)



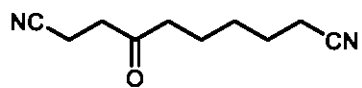
S-pyridin-2-yl 2-(3-bromoadamantan-1-yl)ethanethioate (12)



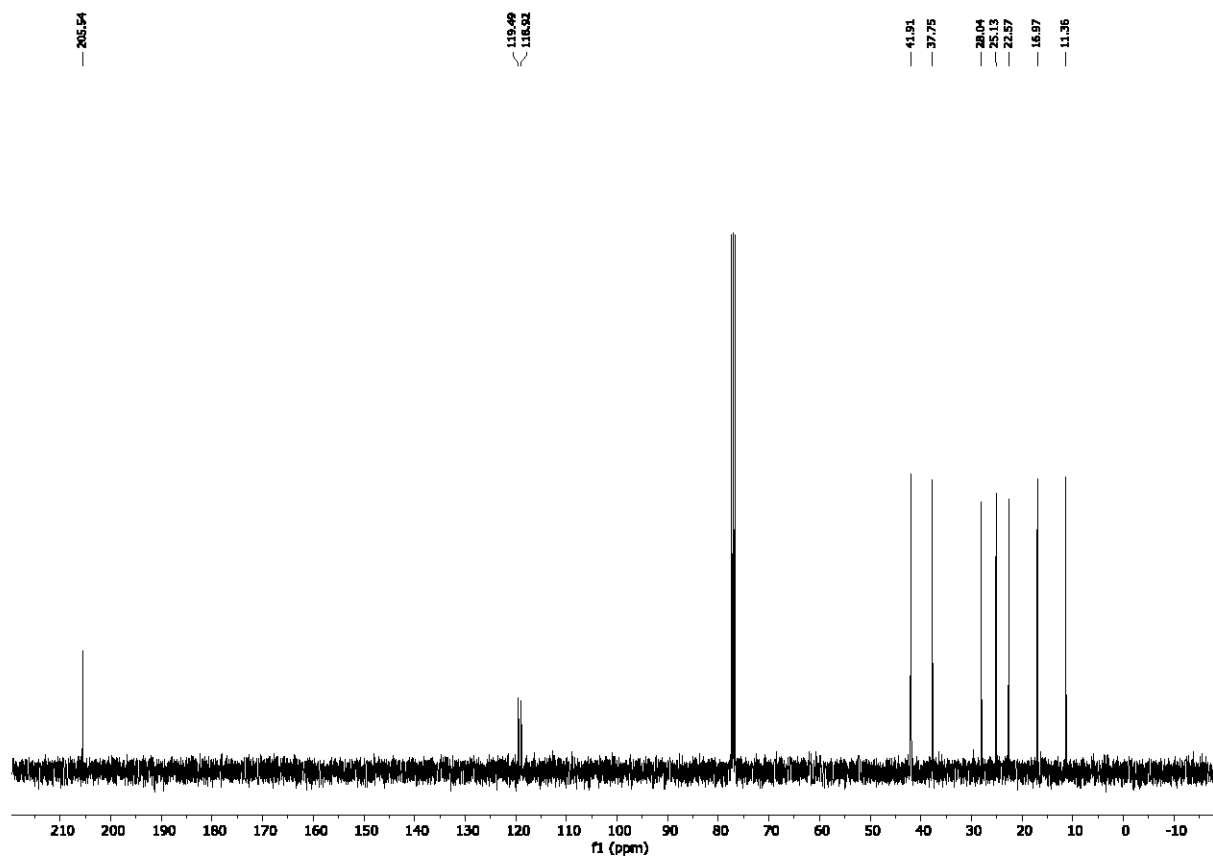
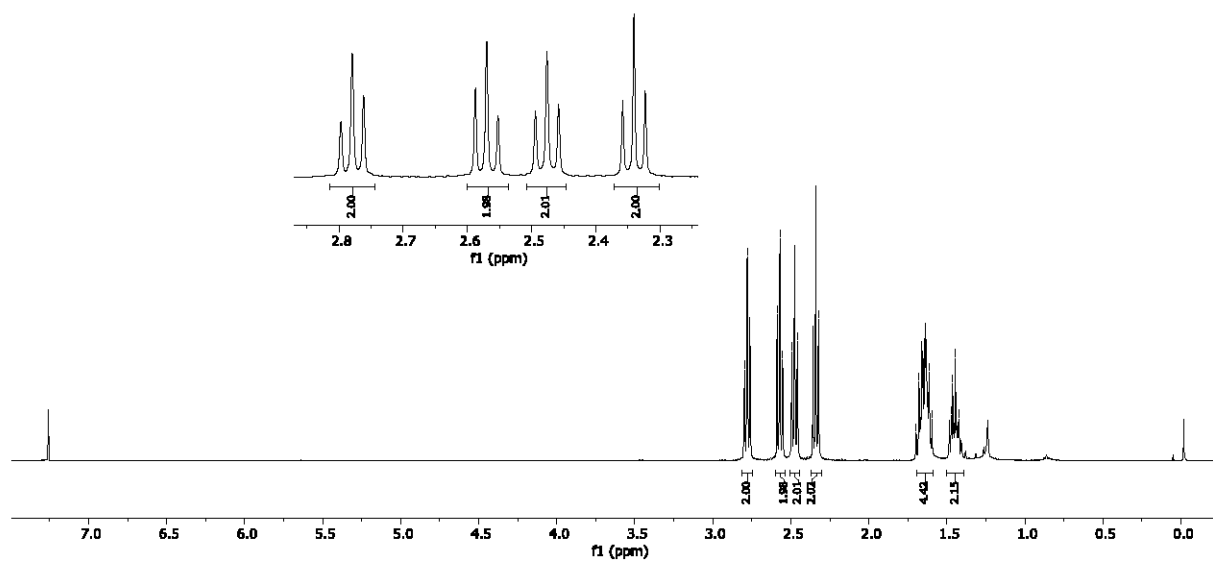
4-oxododecanedinitrile (14)



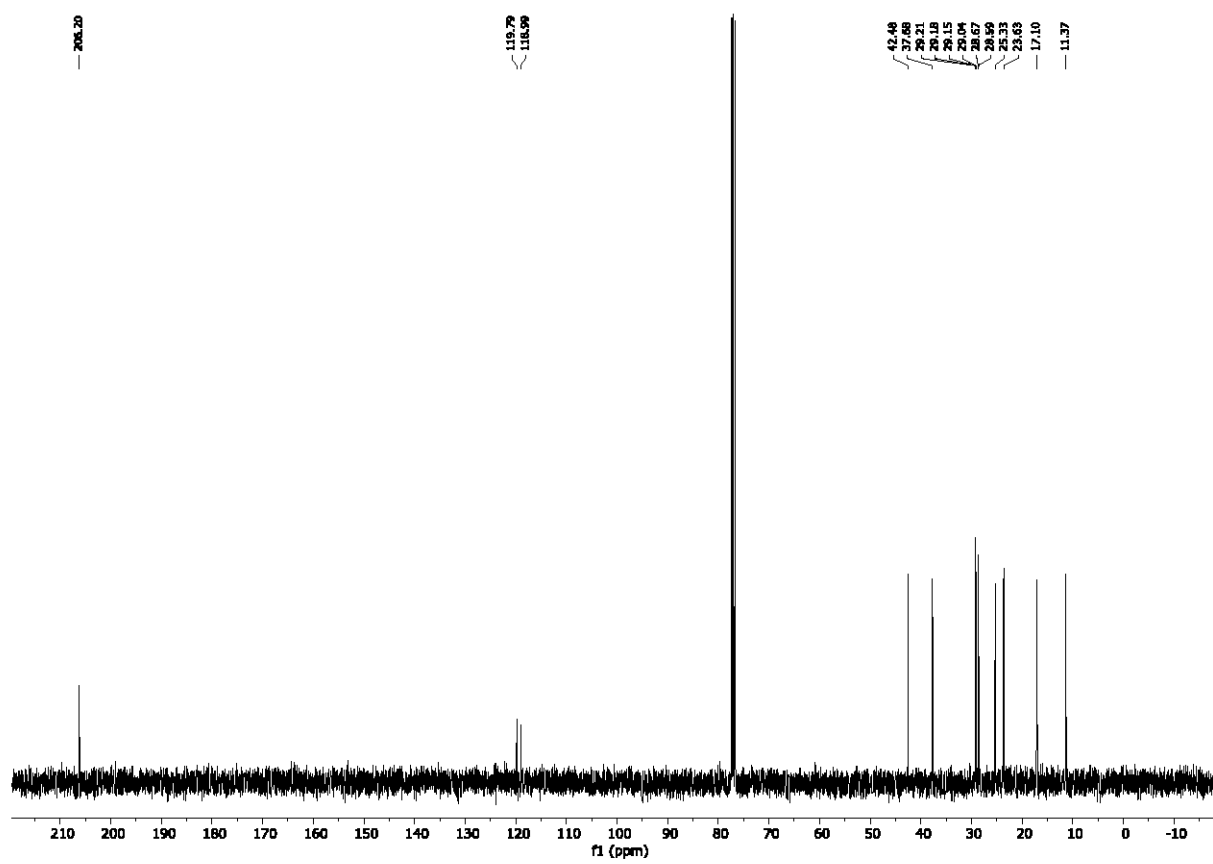
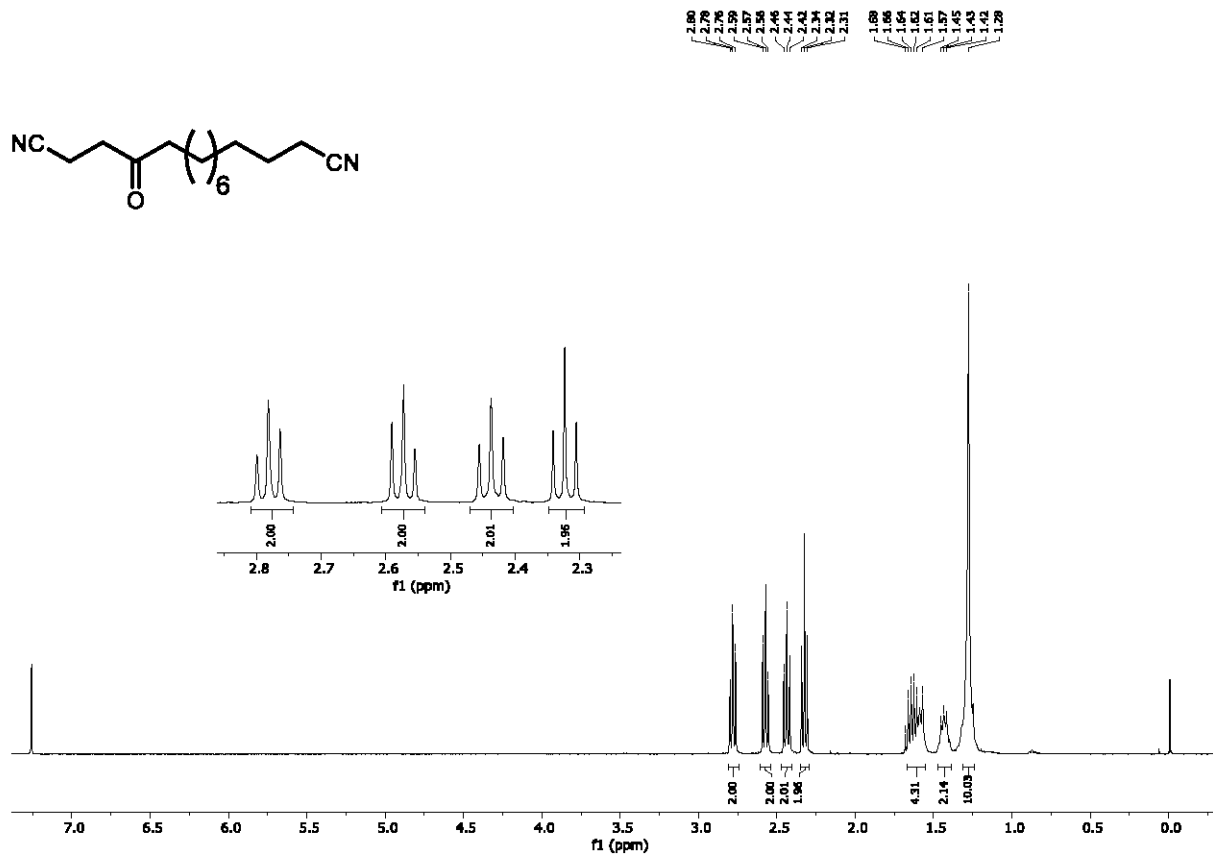
4-oxodecanedinitrile (18)



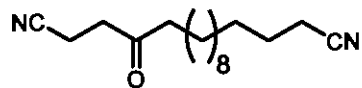
2.80
2.78
2.76
2.74
2.72
2.55
2.49
2.48
2.46
2.36
2.34
1.70
1.68
1.66
1.64
1.61
1.59
1.49
1.46
1.45
1.42



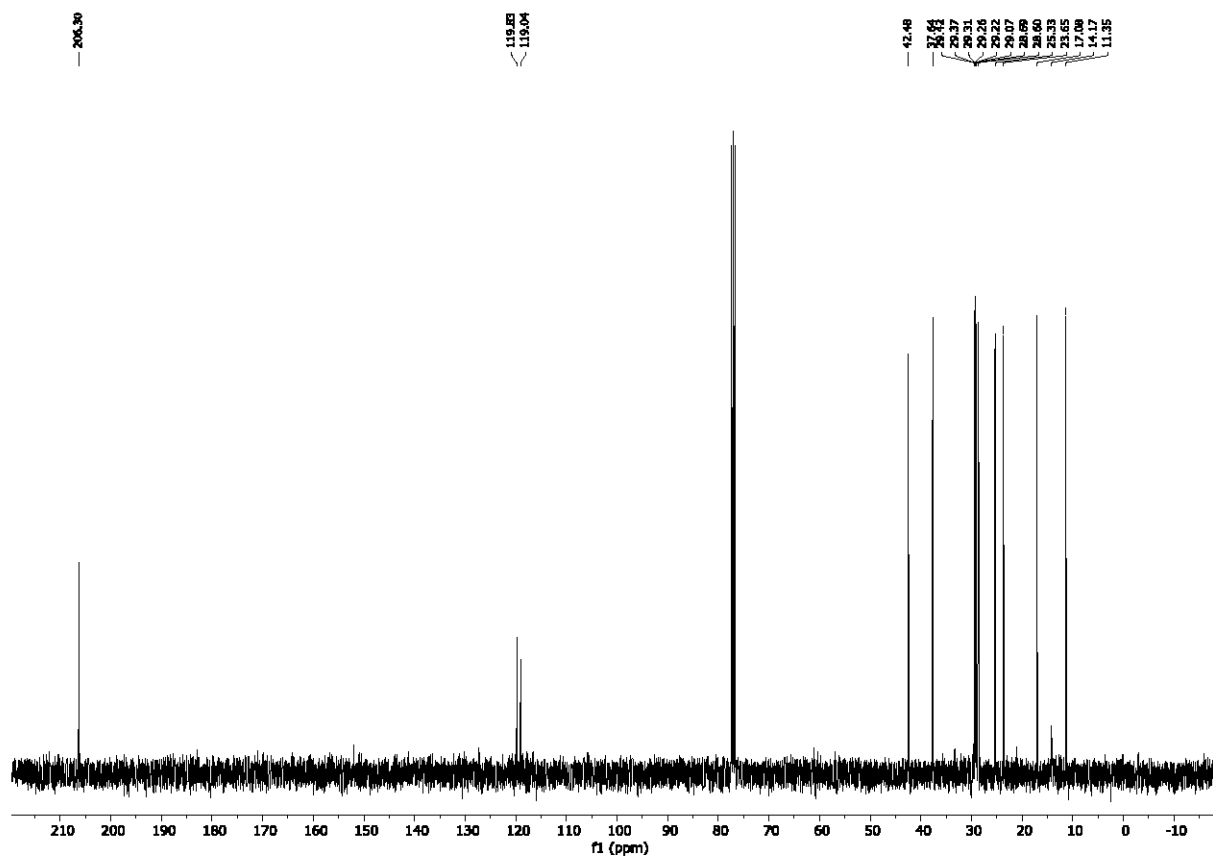
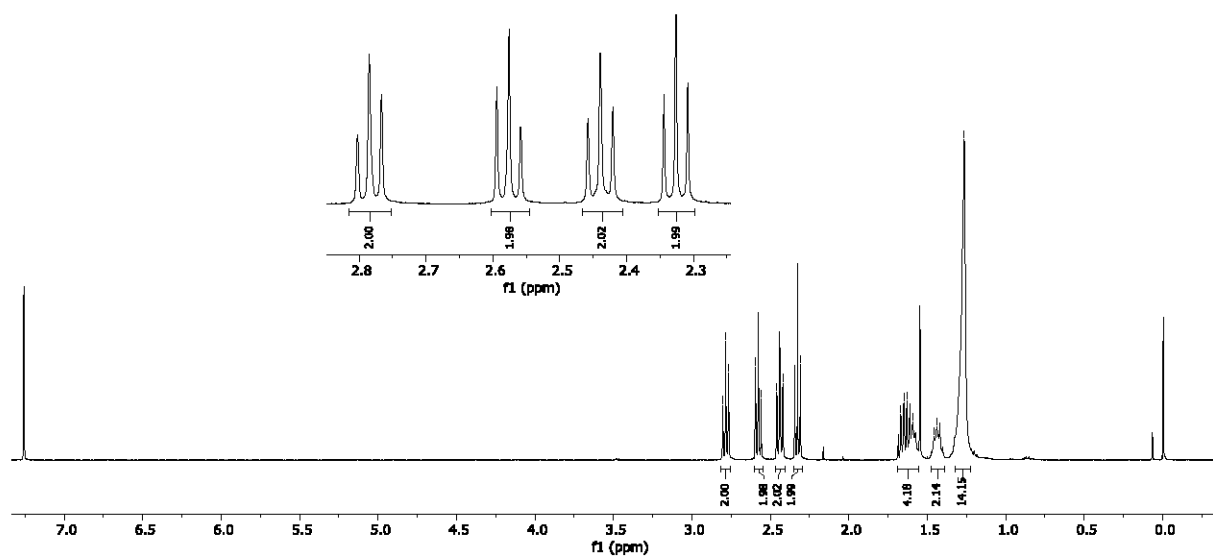
4-oxopentadecanedinitrile (19)



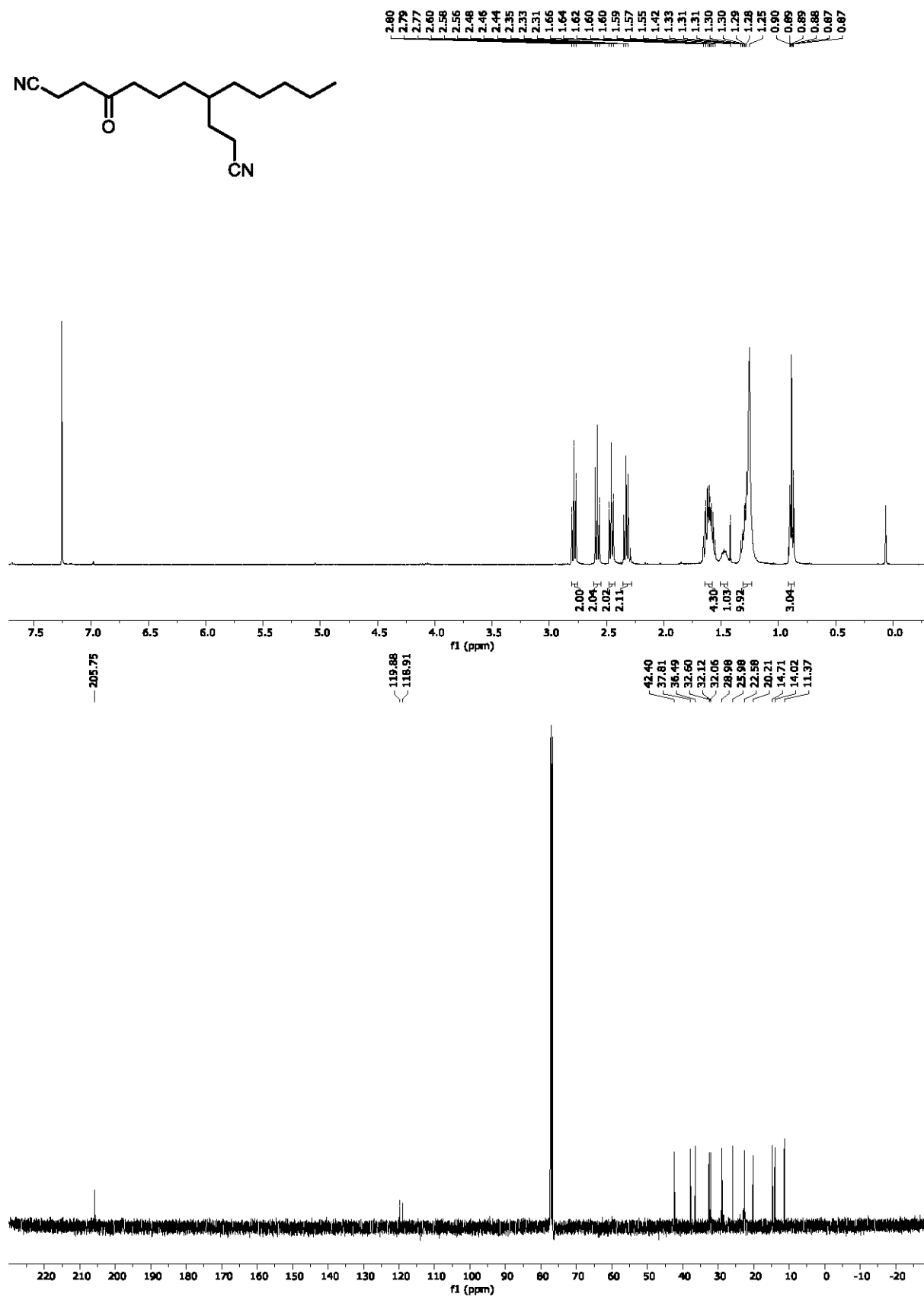
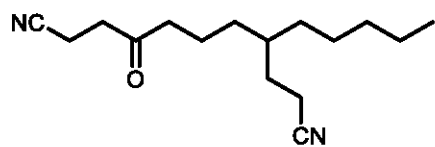
4-oxoheptadecanedinitrile (20)



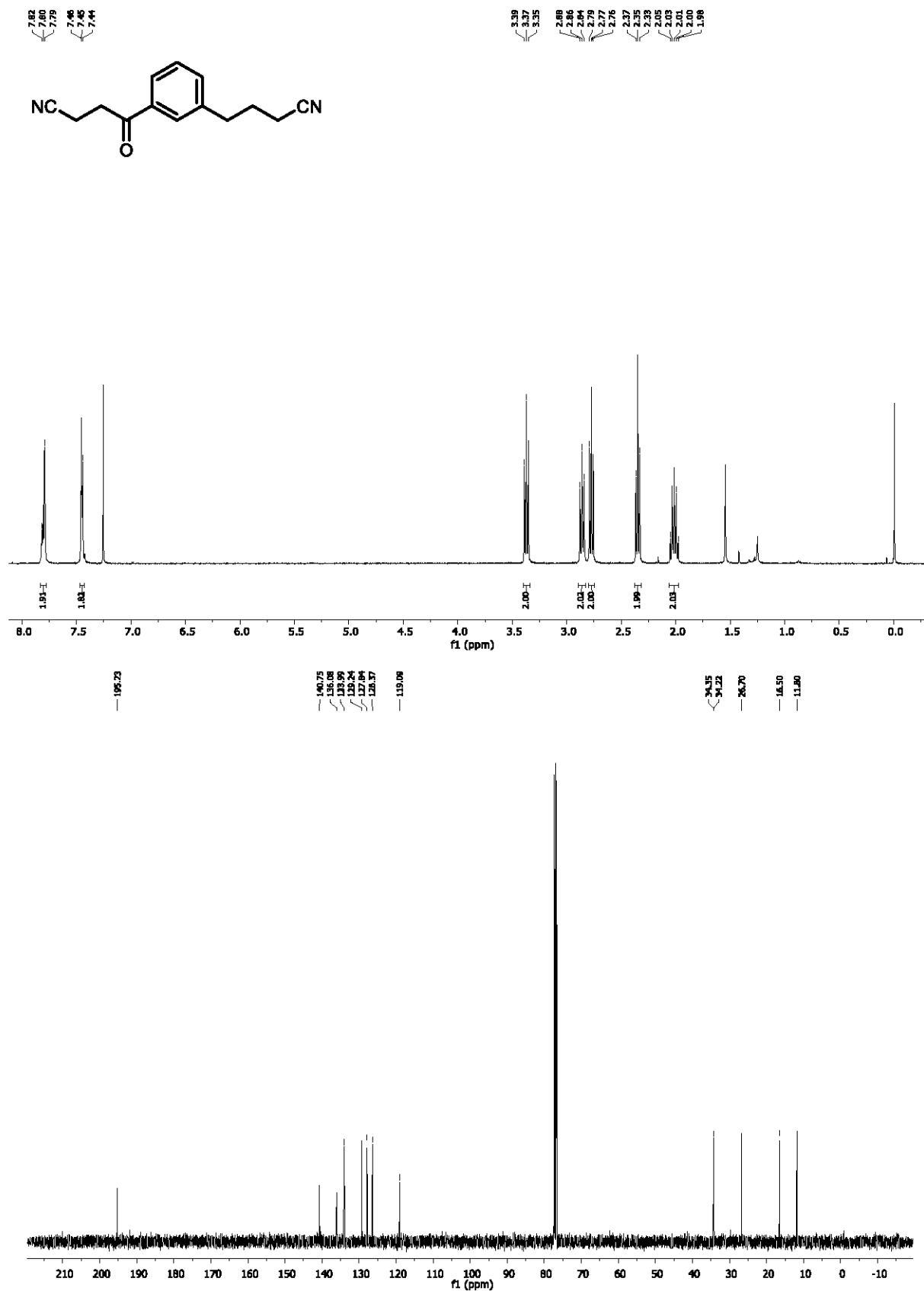
2.80
2.76
2.75
2.59
2.56
2.46
2.44
2.42
2.39
2.31
1.69
1.67
1.65
1.63
1.59
1.46
1.42
1.26



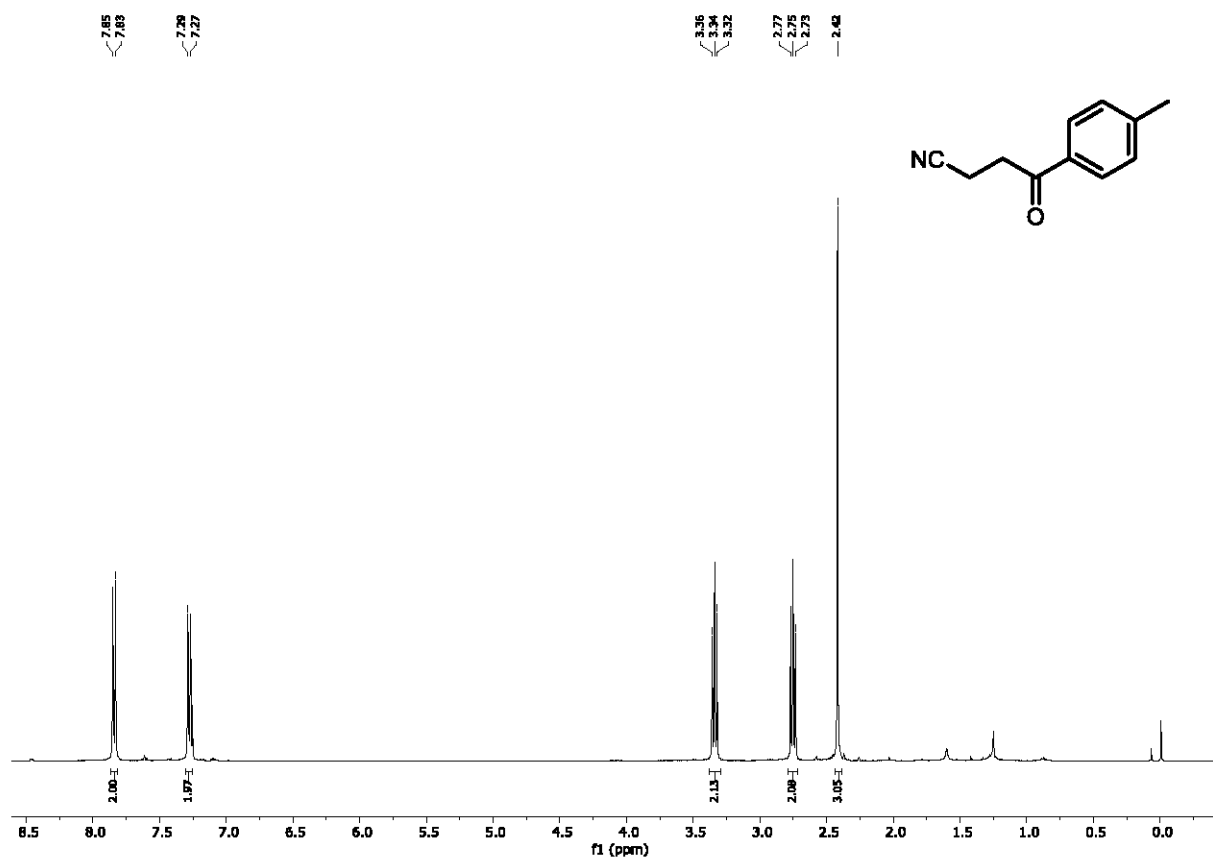
4-oxo-8-pentylundecanedinitrile (21)



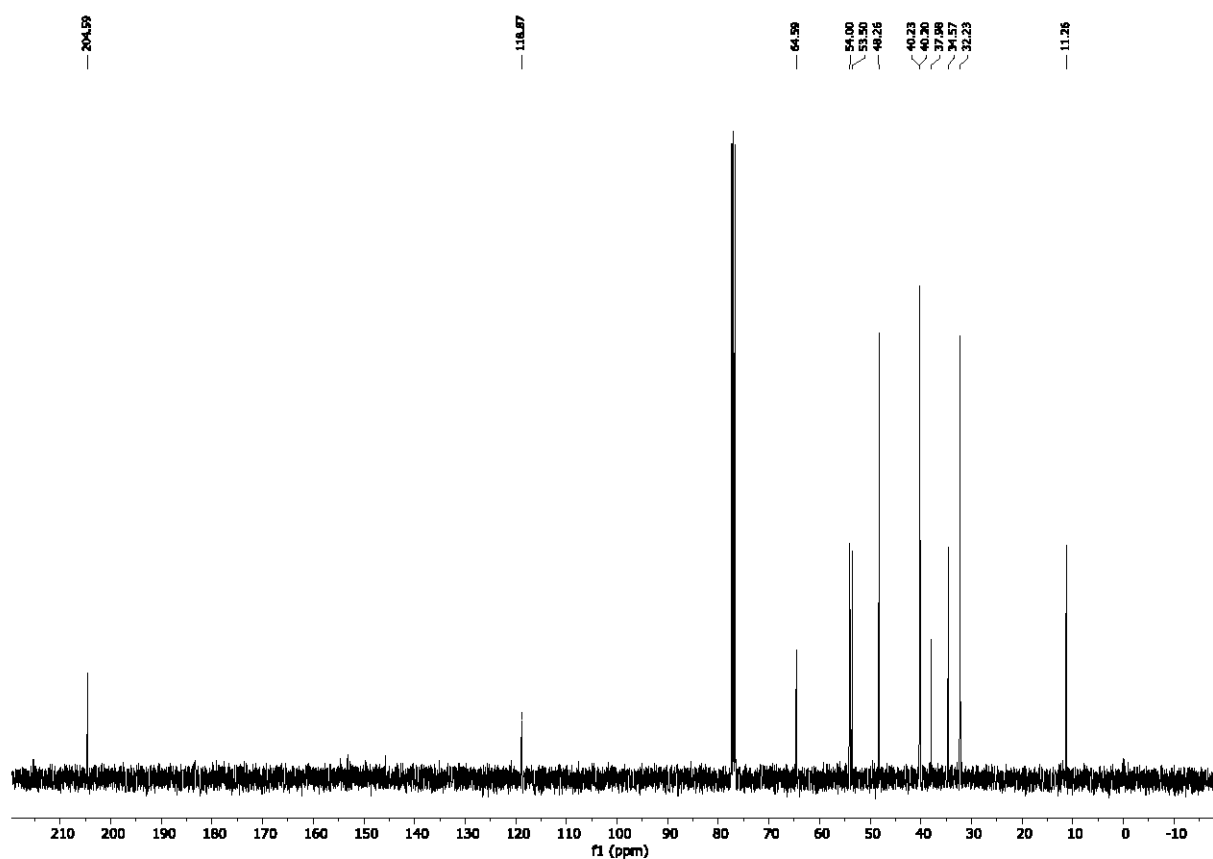
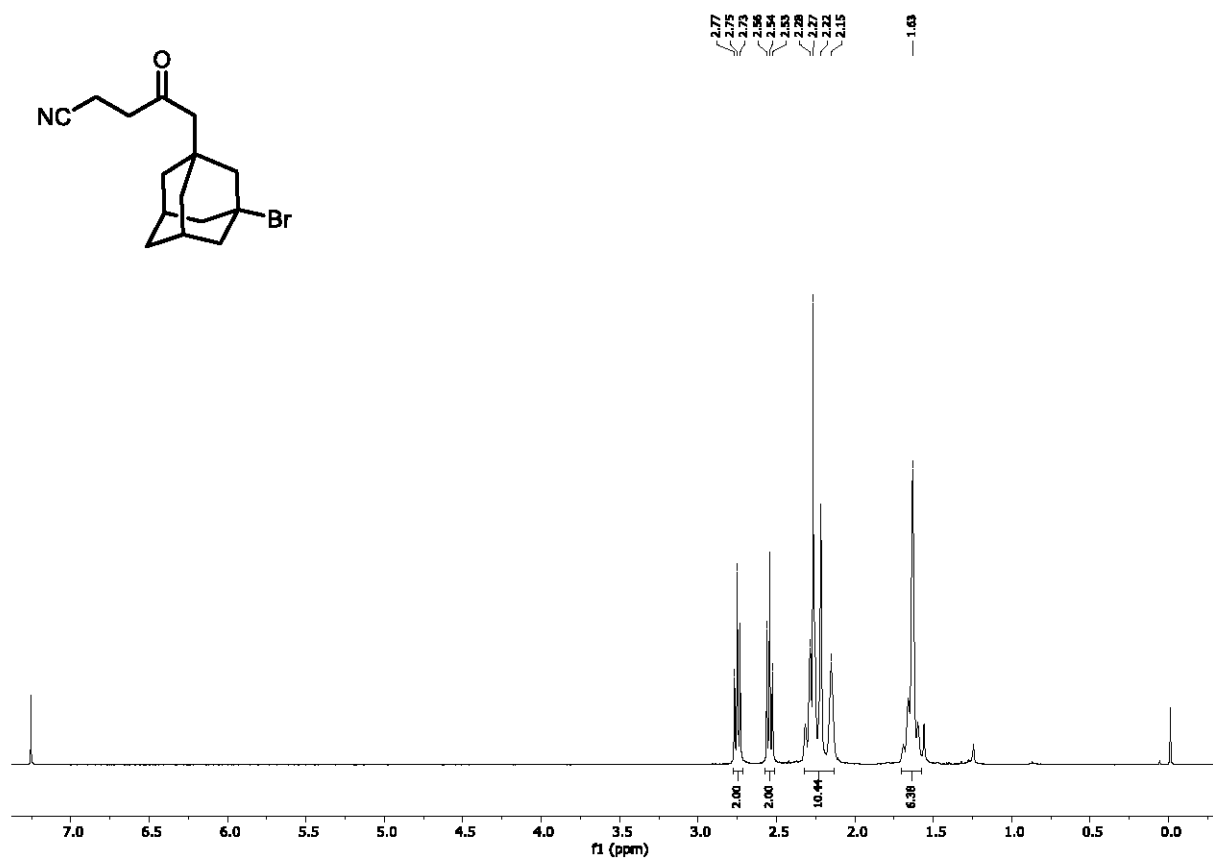
4-(3-(3-cyanopropyl)phenyl)-4-oxobutanenitrile (22)



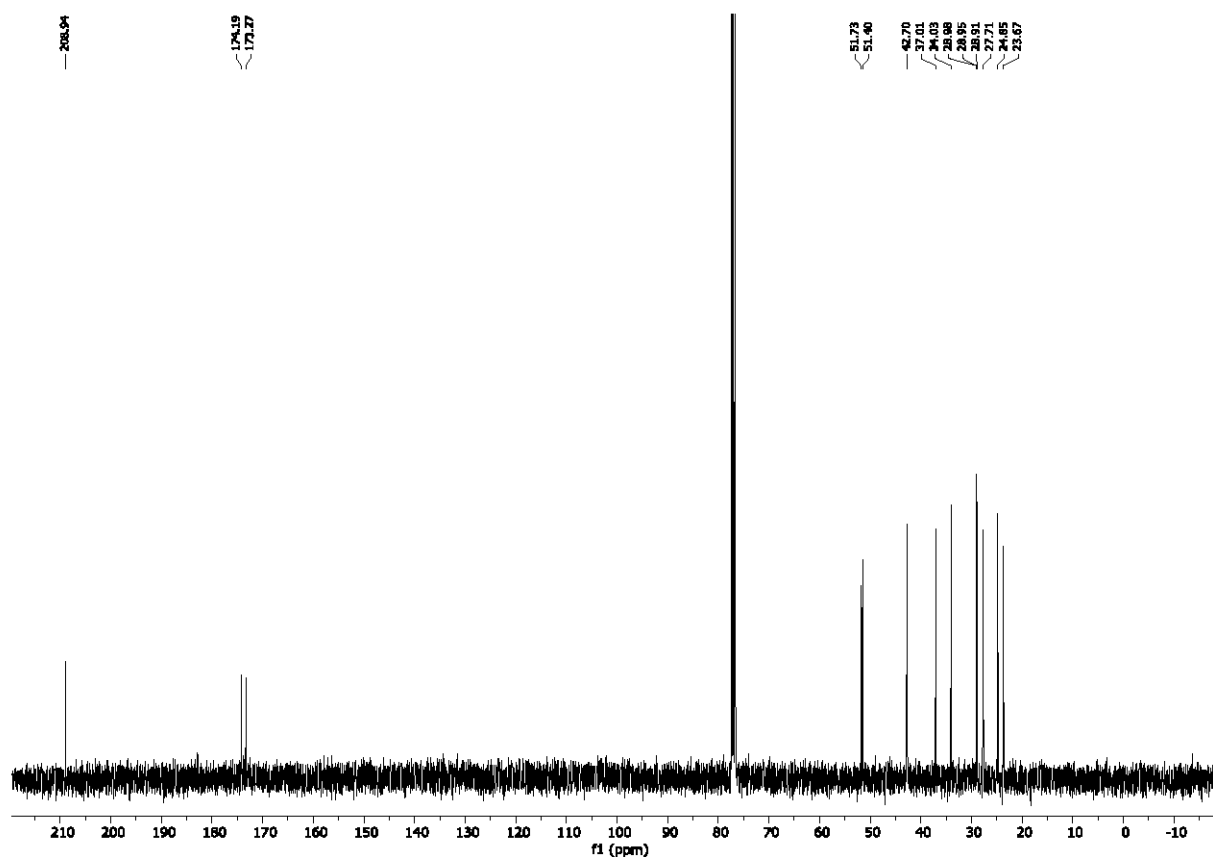
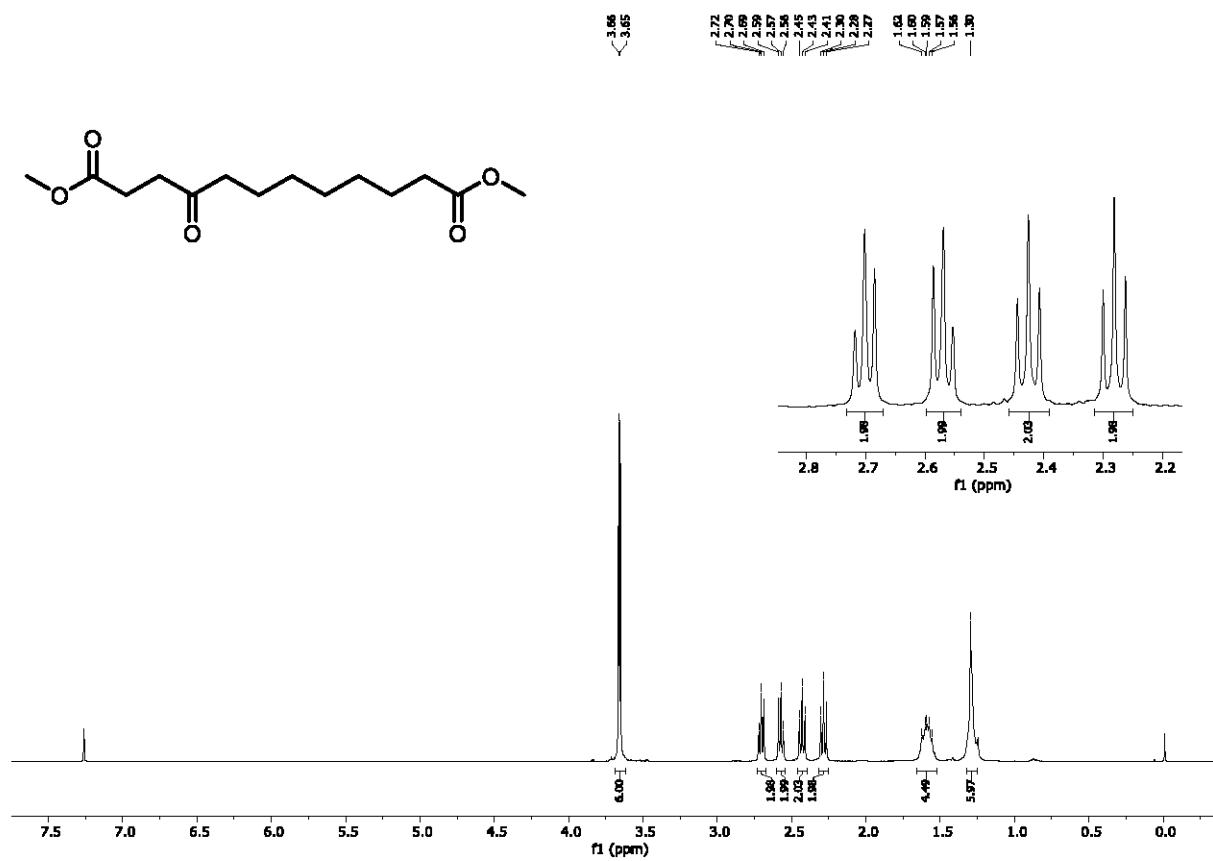
4-oxo-4-(*p*-tolyl)butanenitrile (23)



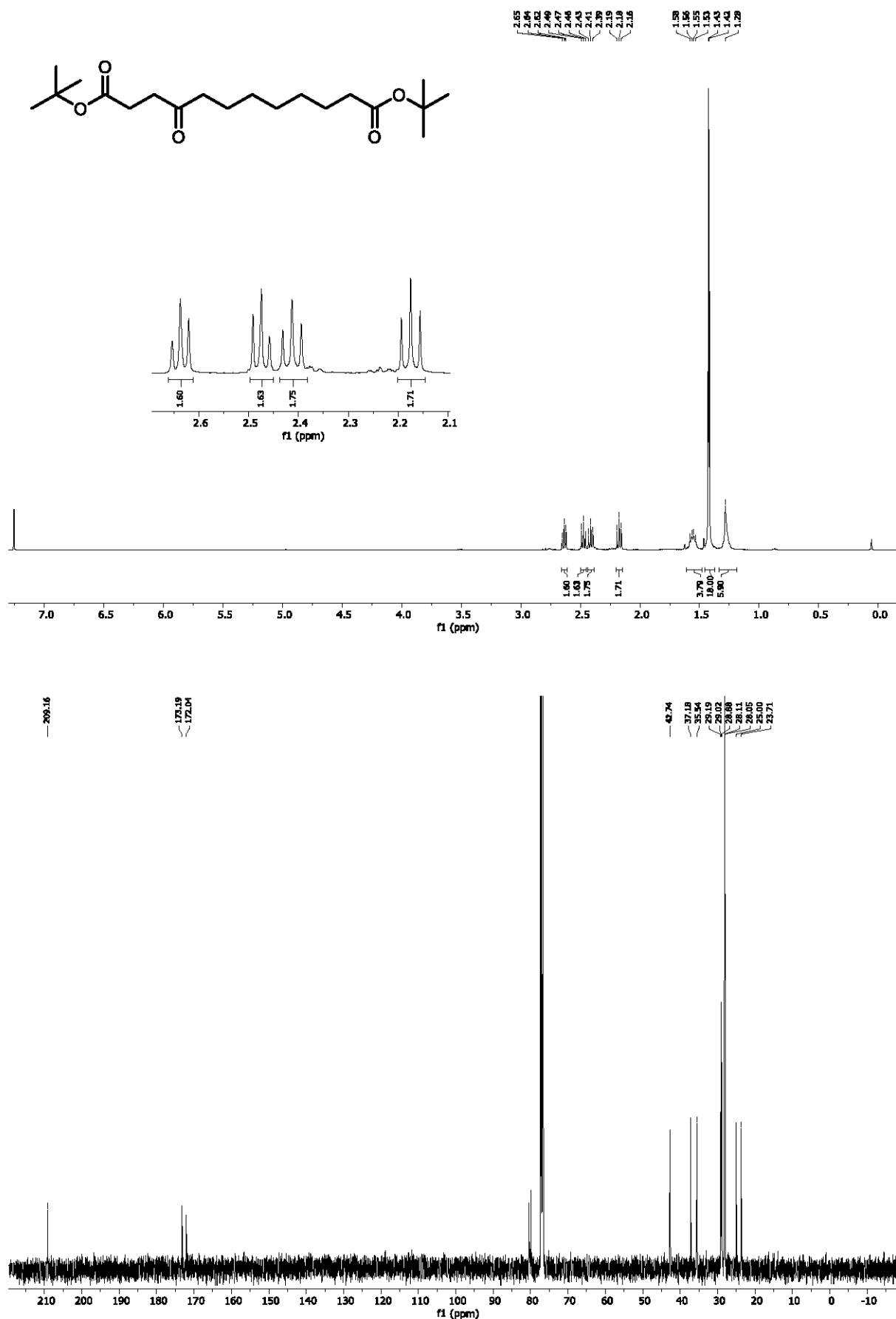
5-(3-bromoadamantan-1-yl)-4-oxopentanenitrile (24)



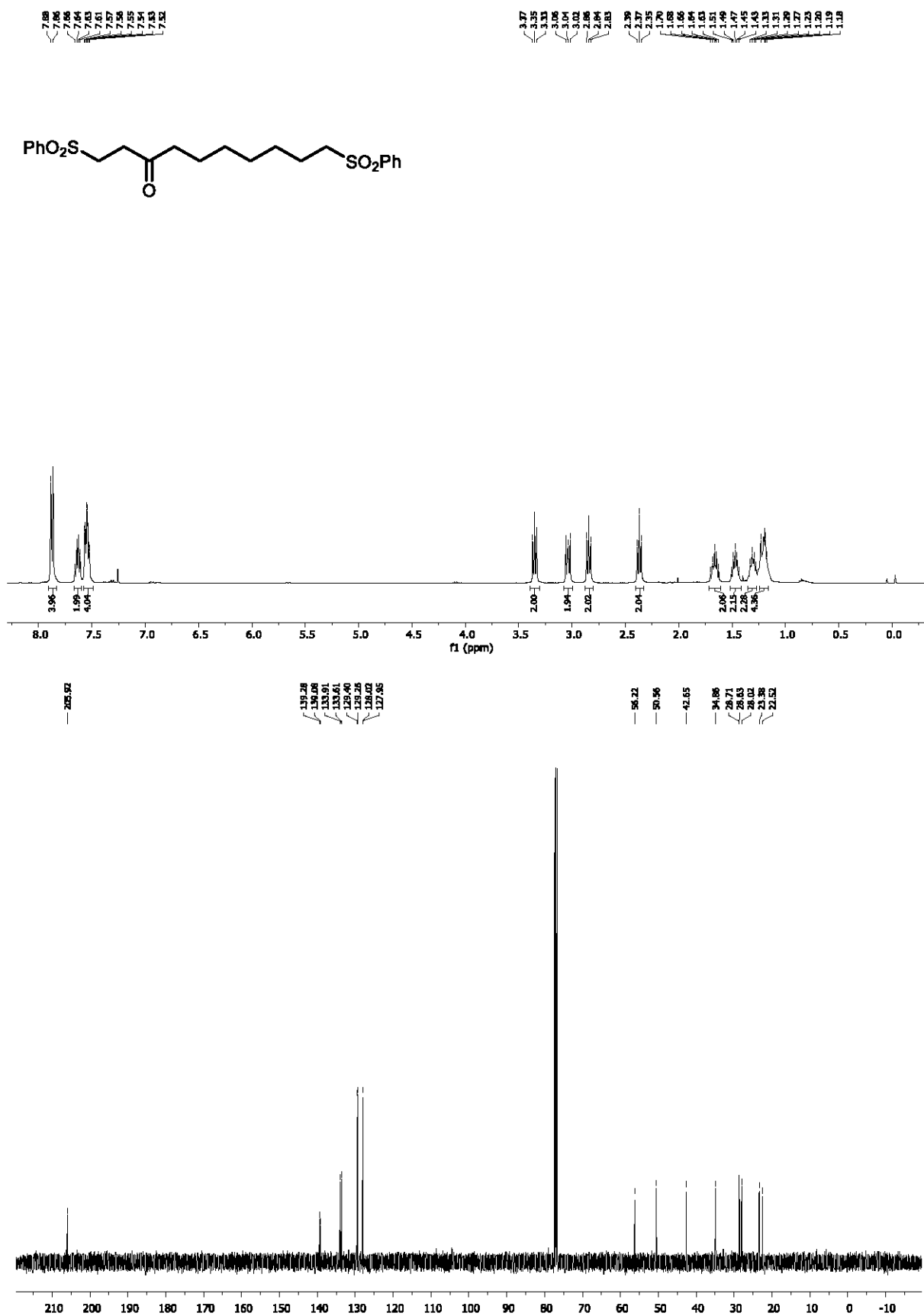
dimethyl 4-oxododecanedioate (25)



di-tert-butyl 4-oxododecanedioate (26)



1,10-bis(phenylsulfonyl)decan-3-one (27)



8. OŚWIADCZENIA AUTORÓW PUBLIKACJI



Instytut Chemii Organicznej PAN
ul. Kasprzaka 44/52
01-224 Warszawa, Polska

Warszawa, 31.03.2022r.

Oświadczam, że mój wkład w powstanie poniższych publikacji polegał na:

- › **A. Potrzasał**, M. Ociepa, O. Baka, G. Spólnik, D. Gryko, *Eur. J. Org. Chem*, **2020**, 1567-1571
Vitamin B₁₂ Enables Consecutive Generation of Acyl and Alkyl Radicals from One Reagent

współpracowaniu koncepcji badań oraz interpretacji wyników. Opracowałam i przeprowadziłam syntezę substratów **4-12** oraz dokonałam optymalizacji warunków reakcji modelowej. Wykonałam niezbędne eksperymenty mechanistyczne potwierdzające zaproponowany przeze mnie mechanizm, do których należały: reakcje z pułapką rodnikową oraz z deuterowanym odczynnikiem, powstałe w reakcji kompleksy kobalaminy potwierdziłam za pomocą spektrometrii mas (MS). W zoptymalizowanych warunkach sprawdziłam zakres stosowalności metody, otrzymując związki **14, 18-27**, które poddałam pełnej analizie chemicznej. Brałam udział w przygotowaniu manuskryptu.

- › **A. Potrzasał**, M. Musiejuk, W. Chaładaj, M. Giedyk, D. Gryko, *J. Am. Chem. Soc.*, **2021**, 143, 25, 9368-9376
Cobalt Catalyst Determines Regioselectivity in Ring Opening of Epoxides with Aryl Halides

współpracowaniu koncepcji badań i interpretacji wyników. Przeprowadziłam optymalizację warunków reakcji, a także sprawdziłam zakres stosowalności metody, otrzymując związki **7aa-7hl**, które poddałam pełnej analizie chemicznej. Wykonałam wszystkie eksperymenty mechanistyczne, które potwierdziły zaproponowany przeze mnie mechanizm reakcji. Określiłam profil kinetyczny epoksydów z podstawnikiem alifatycznym i cyklicznym. Uczestniczyłam w przygotowaniu manuskryptu.

- › **A. Potrzasał**, M. Ociepa, W. Chaładaj, D. Gryko, *Org. Lett*, **2022**, DOI: 10.1021/acs.orglett.2c00355
Bioinspired Co-Catalysis Enables Generation of Nucleophilic Radicals from Oxetanes

współpracowaniu koncepcji badań i interpretacji wyników. Przeprowadziłam optymalizację warunków reakcji typu Giesego, a także sprawdziłam zakres stosowalności metody, otrzymując związki **22a-38**, które poddałam pełnej analizie chemicznej. Wykonałam wszystkie eksperymenty mechanistyczne, które potwierdziły zaproponowany przeze mnie mechanizm reakcji. Uczestniczyłam w przygotowaniu manuskryptu.

Potwierdzam zgodność z prawdą
D. Gryko

Aleksandra Potrzasał



Instytut Chemii Organicznej PAN
ul. Kasprzaka 44/52
01-224 Warszawa, Polska

Warszawa, 28.03.2022r.

Oświadczam, że mój wkład w powstanie poniższych publikacji polegał na:

- › **A. Potrzęsaj**, M. Ociepa, O. Baka, G. Spólnik, D. Gryko, *Eur. J. Org. Chem*, **2020**, 1567-1571
Vitamin B₁₂ Enables Consecutive Generation of Acyl and Alkyl Radicals from One Reagent
współpracowaniu koncepcji badań, interpretacji wyników i przygotowaniu manuskryptu
- › **A. Potrzęsaj**, M. Musiejuk, W. Chaładaj, M. Giedyk, D. Gryko, *J. Am. Chem. Soc.*, **2021**, 143, 25,
9368–9376
Cobalt Catalyst Determines Regioselectivity in Ring Opening of Epoxides with Aryl Halides
współpracowaniu koncepcji badań, interpretacji wyników i przygotowaniu manuskryptu
- › **A. Potrzęsaj**, M. Ociepa, W. Chaładaj, D. Gryko, *Org. Lett*, **2022**, DOI: 10.1021/acs.orglett.2c00355
Bioinspired Co-Catalysis Enables Generation of Nucleophilic Radicals from Oxetanes
współpracowaniu koncepcji badań, interpretacji wyników i przygotowaniu manuskryptu

Dorota
Gryko

Digitally signed by
Dorota Gryko
Date: 2022.03.29
16:51:34 +02'00'



Instytut Chemii Organicznej
Polskiej Akademii Nauk

Dr Maciej Giedyk
Kierownik zespołu XVa
+48 22 343 21 15
maciej.giedyk@icho.edu.pl

Instytut Chemii Organicznej PAN
ul. Kasprzaka 44/52
01-224 Warszawa, Polska

Warszawa, 08.03.2022r.

Oświadczam, że mój wkład w powstanie poniższej publikacji polegał na:

- › **A. Potrzęsaj**, M. Musiejuk, W. Chaładaj, M. Giedyk, D. Gryko, *J. Am. Chem. Soc.*, **2021**, 143, 25, 9368–9376
Cobalt Catalyst Determines Regioselectivity in Ring Opening of Epoxides with Aryl Halides

współpracowaniu koncepcji badań, interpretacji wyników i przygotowaniu manuskryptu

Maciej Łukasz
Giedyk

Elektronicznie podpisany
przez Maciej Łukasz Giedyk
Data: 2022.03.10 10:34:12
+01'00'



Instytut Chemii Organicznej PAN
ul. Kasprzaka 44/52
01-224 Warszawa, Polska

Warszawa, 28.03.2022r.

Oświadczam, że mój wkład w powstanie poniższych publikacji polegał na:

- › **A. Potrzęsaj**, M. Musiejuk, W. Chaładaj, M. Giedyk, D. Gryko, *J. Am. Chem. Soc.*, **2021**, 143, 25, 9368–9376

Cobalt Catalyst Determines Regioselectivity in Ring Opening of Epoxides with Aryl Halides

przeprowadzeniu obliczeń DFT, oraz analizy i interpretacji otrzymanych danych

- › **A. Potrzęsaj**, M. Ociepa, W. Chaładaj, D. Gryko, *Org. Lett.*, **2022**, DOI: 10.1021/acs.orglett.2c00355
Bioinspired Co-Catalysis Enables Generation of Nucleophilic Radicals from Oxetanes

przeprowadzeniu obliczeń DFT, oraz analizy i interpretacji otrzymanych danych

Wojciech

Jan Chaładaj

Elektronicznie podpisany
przez Wojciech Jan Chaładaj
Data: 2022.03.28 14:37:53
+02'00'

San Diego, 28.03.2022

Oświadczam, że mój wkład w powstanie poniższych publikacji polegał na:

- **A. Potrząsaj**, M. Ociepa, O. Baka, G. Spólnik, D. Gryko, *Eur. J. Org. Chem*, **2020**, 1567-1571
Vitamin B₁₂ Enables Consecutive Generation of Acyl and Alkyl Radicals from One Reagent

współpracowaniu koncepcji badań oraz przeprowadzeniu wstępnej optymalizacji warunków reakcji

- **A. Potrząsaj**, M. Ociepa, W. Chaładaj, D. Gryko, *Org. Lett*, **2022**, DOI: 10.1021/acs.orglett.2c00355
Bioinspired Co-Catalysis Enables Generation of Nucleophilic Radicals from Oxetanes

współpracowaniu koncepcji badań, przeprowadzeniu optymalizacji warunków reakcji sprzężania krzyżowego oksetanów z jodkami aryłowymi, a także sprawdzeniu zakresu stosowalności opracowanej metody

Podpisano przez/ Signed by:
MICHĄŁ
OCIEPA
Data/ Date: 28.03.2022 19:35
 mSzofir

Michał Ociepa



Instytut Chemii Organicznej
Polskiej Akademii Nauk

dr Mateusz Musiejuk
mateusz.musiejuk@interia.eu

Instytut Chemii Organicznej PAN
ul. Kasprzaka 44/52
01-224 Warszawa, Polska

Warszawa, 26.02.2021r.

Oświadczam, że mój wkład w powstanie poniższej publikacji polegał na:

- › **A. Potrzęsaj**, M. Musiejuk, W. Chaładaj, M. Giedyk, D. Gryko, *J. Am. Chem. Soc.*, **2021**, 143, 25, 9368–9376
Cobalt Catalyst Determines Regioselectivity in Ring Opening of Epoxides with Aryl Halides

syntezie substratów



Instytut Chemii Organicznej
Polskiej Akademii Nauk

mgr Grzegorz Spólnik

Instytut Chemii Organicznej PAN
ul. Kasprzaka 44/52
01-224 Warszawa, Polska

Warszawa, 28.03.2022r.

Oświadczam, że mój wkład w powstanie poniższej publikacji polegał na:

-) A. Potrząsaj, M. Ociepa, O. Baka, G. Spólnik, D. Gryko, Eur. J. Org. Chem, 2020, 1567-1571
Vitamin B₁₂ Enables Consecutive Generation of Acyl and Alkyl Radicals from One Reagent

przeprowadzeniu niezbędnych pomiarów z wykorzystaniem techniki spektrometrii mas (MS)

Oskar Baka

Oświadczam, że mój udział w poniższej publikacji:

"Vitamin B₁₂ Enables Consecutive Generation of Acyl and Alkyl Radicals from One Reagent"

DOI: 10.1002/ejoc.201301134

polepać na wstępnej optymalizacji warunków reakcji.

Oskar Baka